Discovery and Development of Novel P,N Ligands for Selective Ethylene Oligomerisation Systems

JAMES EDWARD RADCLIFFE

Discovery and Development of Novel P,N Ligands for Selective Ethylene Oligomerisation Systems

Thesis submitted for the degree of Doctor of Philosophy

By

James Edward Radcliffe MSci

Department of Chemistry
Durham University

June 2015

Statement of Originality

This thesis is based on work conducted in the Department of Chemistry at Durham University between October 2011 and May 2015. All work was carried out by the author, unless stated otherwise, and has not been submitted for another degree at this, or any other University

Signed:_____ Date:_____

James E. Radcliffe

Abstract

Title: Discovery and Development of Novel P,N Ligands for Selective Ethylene Oligomerisation Systems

This thesis documents the design, discovery, and development of a range of P,N-type ligands and their application in selective ethylene oligomerisation processes. Two classes of ligand have been investigated, PNE ($Ph_2P(CH_2)_2NC_4H_8E$, E = NMe, O, CH_2) ligands, and iminophosphine ligands ($R(PR'_2)C{=}NAr$). The coordination chemistry of both these series of compounds has been investigated with various chromium species, and the behaviour of these molecules in ethylene oligomerisation systems probed.

Chapter 2 explores the application of PNE ligands to ethylene oligomerisation. The coordination chemistry of the PNE ligands with a selection of group VI starting materials has been investigated. It has been shown that both the PNO and PNC ligands form bidentate complexes upon reaction with $CrCl_3(THF)_3$ (*e.g.* $CrCl_3(THF)(PNO)$, **2.1**), while attempts to synthesise the PNN analogue proved unsuccessful. The coordination of PNE ligands with Cr(0) and Mo(0) has been studied, with the ligands exhibiting both mono- (*e.g.* $Cr(CO)_5(PNN)$ (**2.4**) and bi-dentate coordination (*e.g.* $Mo(CO)_4(PNN)$ (**2.7**)), dependant on the combination of metal and ligand used. Conversion of monodentate $Cr(CO)_5(\kappa^1\text{-PNN})$ (**2.4**) to bidentate $Cr(CO)_4(\kappa^2\text{-PNN})$ (**2.10**) is achieved on reaction with trimethylamine N-oxide. The application of PNE ligands to ethylene oligomerisation systems has been carried out. All of the catalytic systems tested gave primarily polymer products, with no selective ethylene oligomerisation occurring.

Chapter 3 describes the development of a modular synthetic route to novel iminophosphine compounds *via* reaction of imidoyl chlorides with trimethylsilyl phosphines. Using this synthetic process, a library of iminophosphines has been synthesised (**3.1**-**3.26**) with varying steric and electronic characteristics. The donor properties of the iminophosphines have been analysed by measurement of $|^1J_{Se\text{-}P}|$ couplings of the derivative phosphine selenides, with all the compounds demonstrating good phosphine donor properties. Finally, the *E*/*Z* isomerisation behaviour of the PCN compounds has been studied, revealing that P-aryl substituted iminophosphines exist as a mixture of the *E* and *Z* isomers in equilibrium in solution.

Chapter 4 details investigations into the coordination chemistry of iminophosphine ligands with chromium. A selection of ligands have been reacted with $CrCl_3(THF)_3$, forming a range of bidentate $Cr^{III}(\kappa^2\text{-PCN})$ complexes (*e.g.* $CrCl_3(THF)(Ph(PPh_2)C{=}NPh)$, **4.1**). The coordination of iminophosphine ligands with Cr(0) has shown that the ligands react with $Cr(CO)_6$ to yield both mono- and bi-dentate products (*e.g.* $Cr(CO)_4(Ph(P^iPr_2)C{=}N(2,6\text{-}^iPr_2C_6H_3))$ (**4.7**) and $Cr(CO)_5(Ph(P^iPr_2)C{=}N(2,6\text{-}^iPr_2C_6H_3))$ (**4.8**), respectively). The denticity of these $Cr(CO)_{(6\text{-}n)}(\kappa^n\text{-PCN})$ complexes can be controlled through the removal and addition of CO in the atmosphere.

Chapter 5 recounts the use of the novel iminophosphines as ligands in selective ethylene oligomerisation systems. A wide range of catalytic conditions were tested, including varying the chromium source, solvent, reaction temperature and pressure, the use of polymer reducing additives, and the dosing of O_2 into the reaction. It has been shown that a catalytic process using $Cr(2\text{-EH})_3$, 1 equivalent of iminophosphine **3.9**, 49 bar C_2H_4, in methylcyclohexane at 60 °C, with 0.66 ppm O_2 and 100 equivalents of $ZnEt_2$ yields a highly active and selective ethylene *tri*-/*tetra*-merisation process.

Acknowledgments

Firstly, I would like to thank my supervisor Dr Phil Dyer for all of his support and guidance throughout the last three and a half years. None of this work would have been possible without him, and this thesis would in all likelihood be twice the length it currently is without his eagle-eyed proofreading.

The other main contributor that must be thanked is Dr Martin Hanton, for his help with the catalytic testing carried out in this work in Sasol's laboratories. The weeks spent in St Andrews would not have been the same without David, John and William in the oligomerisation group. My experience of St Andrews, its endless golf courses and many bed and breakfasts will not be forgotten.

During my time in Durham I have had the pleasure of working with a long list of great PhD and Masters students in the Dyer group. Luke and Antonis were responsible for teaching me most of what I now know about lab work (and any bad habits I have picked up). For the past year and a half Anna, Ben, Jas and Michael have kept me company and amused with their shenanigans in the lab. Finally, thanks to Jack for being my "partner in crime" during my time in the Chemistry Department, and at many conferences.

All of the technical staff in the Chemistry Department must be thanked, in particular the NMR staff, the glassblowers, the electrical and mechanical workshops and Dr Andrei Batsanov for all of his crystallography work. All of the computational work I have done has been taught to me (with great patience) by Dr Mark Fox, and is greatly appreciated. The EPSRC and Sasol are thanked for their funding allowing me to undertake this work.

Thanks to all of the friends I have made while in Durham, in particular Andy and Dan for putting up with living with me for the majority of it. My family have been a great support throughout all of my work, thank you for everything.

Finally, thank you Emily for supporting me through all the ups and downs that a PhD throws at you, and reminding me that there is a big wide world out there beyond the chemistry lab!

Contents

List of Abbreviations

2-EH	2-ethylhexanoate
acac	Acetylacetone
Ar	Aryl
ASAP	Atmospheric Solid Analysis Probe
bp	Boiling Point
BP	British Petroleum
Bu	Butyl
COSY	Correlated Spectroscopy
Cy	Cyclohexyl
DCM	Dichloromethane
DEAC	Diethyl Aluminium Chloride
DFT	Density Functional Theory
DMAO	TMA-depleted MAO
dppe	1,2-bis(diphenylphosphino)ethane
dppm	bis(diphenylphosphino)methane
DSC	Differential Scanning Calorimetry
EPR	Electron Paramagnetic Resonance
Et	Ethyl
eq.	Equivalent(s)
GC-FID	Gas Chromatography - Flame Ionisation Detection
h	Hour(s)
HDPE	High Density Polyethene
HMBC	Heteronuclear Multiple-Bond Correlation
HOMO	Highest Occupied Molecular Orbital
HSQC	Heteronuclear Single Quantum Coherence
IR	Infra-Red
L	Generic 2 electron donor ligand
LAO	Linear Alpha Olefin
LUMO	Lowest Unoccupied Molecular Orbital
M	Generic Transition Metal (unless otherwise stated)
m-	*meta*-
m/z	Mass/charge ratio
MALDI	Matrix Assisted Laser Desorption/Ionisation
MAO	Methylaluminoxane
Me	Methyl
MMAO	Modified MAO
MW	Molecular Weight
NMR	Nuclear Magnetic Resonance
NPN	Diaminophosphine
o-	*ortho*-
ORTEP	Oak Ridge Thermal Ellipsoid Plot
PE	Polyethylene

p-	*para*-
Ph	Phenyl
PIBAO	Partially Hydrolysed Tri-isobutylaluminium
pip	Piperidine
PCN	Iminophosphine ligand
PMAO-IP	Polymethylaluminoxane – Improved Performance
PNC	piperidine-*N*-ethylene-diphenylphosphine
PNN	1-(2-diphenylphosphino-ethyl)-4-methyl-piperazine
PNNP	*bis*(diarylphosphino)dimethylhydrazine
PNO	1-(2-diphenylphosphino-ethyl)-morpholine
PNP	Diphosphinoamine
PNPN	Aminodiphosphinoamine
ppm	Parts per million
^{i}Pr	*iso*-Propyl
Py	Pyridyl
R	Generic alkyl, aryl group
SHOP	Shell Higher Olefin Process
SNS	Dithioamine
T	Temperature
TEA	Triethylaluminium
THF	Tetrahydrofuran
TM	Transition Metal
TMA	Trimethylaluminium
TMNO	Trimethylamine N-oxide
TMS	Trimethylsilyl
TON	Turn Over Number
T.S.	Transition State
UCC	Union Carbide Corporation
$\%V_{bur}$	Percentage buried volume
VT	Variable Temperature
wt	Weight
XAS	X-ray Absorption Spectroscopy
XPS	X-ray Photoelectron Spectroscopy
Xyl	$Me_2C_6H_4$
μ_B	Bohr Magneton
μ_{eff}	Effective Magnetic Moment

Chapter 1:

Introduction

1.1 General Background

Linear alpha olefins (LAOs) are vital products of the petrochemical industry with a wide variety of uses ranging from co-monomers in polymerisation processes (C_4-C_8), through to the production of lubricant additives (C_{14+}) (See Table 1.1).[1] The importance of these products is reflected in their total World production (2009) of 2.7 million tonnes, with a predicted market growth of 3% per annum.[2]

LAO chain length	**Application**
C_4-C_8	Comonomers in polyethylene manufacture
C_6-C_{10}	Used to produce plasticizers
C_{10}	Monomers in poly-α-olefin production
C_{10}-C_{20}	Production of detergents
C_{14+}	Lubricant additives

Table 1.1: Uses of LAOs in industry.[1]

The demand for individual LAO chain lengths varies greatly depending on their potential use in industry. This leads to some specific LAOs being far more valuable than others, with C_4-C_8 materials being particularly desirable due to their use as co-monomers in polyethylene production.[3] Despite the high demand for specific chain lengths most LAOs are still manufactured using traditional non-selective ethylene oligomerisation processes, such as the Sabic/Linde Alpha-Sablin® and Chevron Phillips (formerly Gulf) operations.[4] These oligomerisation processes operate *via* a Cossee-Arlman mechanism (Scheme 1.1),[5] leading to a statistical distribution of oligomer chain lengths (*e.g.* a Schulz-Flory distribution),[6,7] which are not tuneable to industry demands for specific LAO chain lengths. This lack of control over individual oligomer production inevitably leads to the production of lower value oligomers, and yields mixtures which require costly separation techniques to isolate specific olefins.

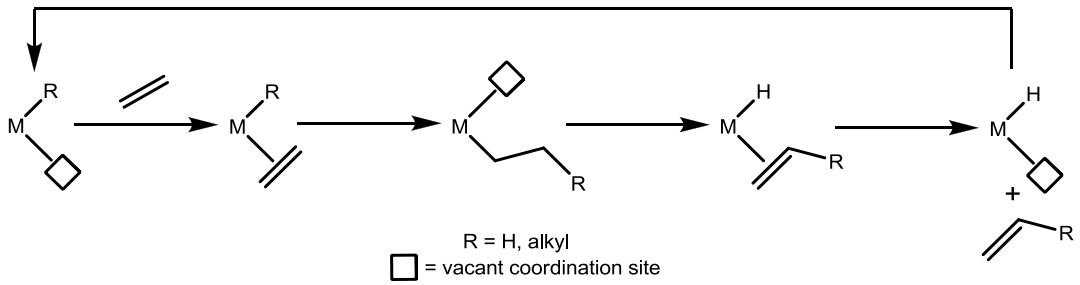

Scheme 1.1: The Cossee-Arlman mechanism of ethylene oligomerisation.[5]

In order to combat the disparity between production and demand for specific short chain LAOs, considerable effort has been put into discovering and developing selective ethylene

oligomerisation catalysts. In particular, research efforts have been focussed on *di-*, *tri-* and *tetra-*merisation processes utilising ethylene as a feedstock, due to the high value and importance of C_4-C_8 oligomers, and the ready availability of ethylene as a feedstock. If selective ethylene oligomerisation systems could be efficiently utilised in industry this would eliminate the need for costly product separation processes, reducing waste on a large scale, and ultimately allowing the production and supply of specific LAOs to be tailored to the demand from consumers.

Over the past ten years a number of excellent review articles have been published covering many aspects of selective ethylene oligomerisation chemistry, both from the open and the patent literature. The first of these was written by Dixon *et al.* and covers the progress in selective ethylene oligomerisation chemistry up to 2004, predominantly in the patent literature.[8] In 2007 Wass published a micro-review briefly introducing the explosion of literature in response to the publication of a novel ethylene trimerisation system by BP in 2002.[9] Possibly the most complete of all the reviews published in recent years is that of McGuinness, in which developments in metallacycle-based olefin oligomerisation processes are discussed primarily from 2004-2011.[10] van Leeuwen *et al.* also published a review concerning selective ethylene oligomerisation in 2011, which focused specifically on the recent advances in the selective production of 1-octene.[11] A review covering predominantly the mechanistic studies of chromium-based selective ethylene oligomerisation was also published in 2011.[12] Finally, in 2012 a review focussing very much on collating and reporting the data from various ethylene tetramerisation systems was published by Belov.[13] By way of introduction, Chapter 1 of this thesis aims to summarise aspects of these reviews, in particular giving a brief history and review of selective *tri-* and *tetra*-merisation chemistry from the open literature, as well as covering more recent advances in the field.

1.2 Selective Ethylene Trimerisation

1.2.1 A history of chromium-based selective ethylene oligomerisation

The first evidence of catalytic systems capable of delivering selectivity towards ethylene trimerisation was discovered by Manyik *et al.* in 1967 while working with the Union Carbide Corporation (UCC) on catalysts for polyethylene production. It was found that when Cr(III) 2-ethylhexanoate (Cr(III) 2-EH) was activated with partially hydrolysed *tri*-isobutylaluminium (PIBAO) not only does polymerisation occur, but a small amount of ethylene trimerisation takes place, yielding 1-hexene. This goes on to co-polymerise with ethylene to give a polymer with butyl side chains.[14] It was not until 10 years later that this discovery was published in the open literature. After further analysis, it was shown that the polymerisation reactions carried out by Manyik *et al.* produced unusually large amounts of C_4-C_{10} oligomers, in particular 1-hexene.[15] The UCC group also noticed that the reaction rate appeared to be second order with regard to ethylene, rather than a traditional first order polymerisation process, suggesting an alternative mechanism was responsible for this trimerisation activity. This difference in mechanism will be discussed in Section 1.2.2.1 of this report.

1.2.1.1 The Phillips trimerisation system

Following the publication of UCC's ethylene trimerisation discovery in 1977, it was not until the late 1980s that the first truly selective ethylene trimerisation systems were discovered and published. Workers from the Phillips Petroleum Company discovered that a series of chromium pyrrolyl complexes, activated with $AlEt_3$, were capable of catalysing ethylene trimerisation.[16] The precursors, $CrCl_2$ and $CrCl_3$, were reacted with varying amounts of sodium pyrrolide, yielding novel chromium pyrrolyl complexes, which upon activation with $AlEt_3$ and exposure to ethylene, demonstrated remarkable catalytic ethylene trimerisation activity, giving up to 99.1 % selectivity towards hexene formation in the liquid fraction, of which 83 % was 1-hexene.[17]

Building upon their discovery, the group at Phillips optimised their trimerisation system to utilise 2,5-dimethylpyrrole as a ligand precursor and Cr(III) 2-EH as the chromium source. It was found that the catalytic system could be generated by combining these new starting materials *in situ,* simplifying the process dramatically. It was also shown that the presence of a halide source (*e.g.* diethyl aluminium chloride) improved both the activity and selectivity of the system, for reasons not detailed in the patent.[18] After 10 years of research and development Phillips patented their best trimerisation system yet. Through the careful control of the molar ratio of starting materials and using a nitrogen purge to stir the reagents an optimised system

was developed, achieving a catalytic activity of 156,666 g/g Cr h^{-1} and an overall selectivity towards 1-hexene of 93 % (Scheme 1.2).[19]

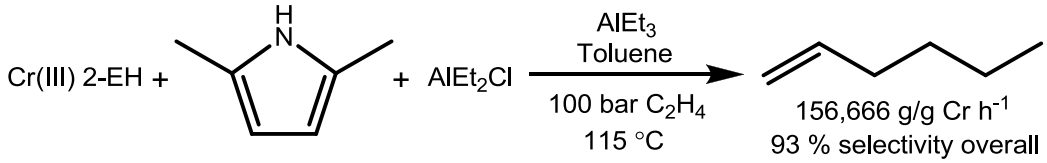

Scheme 1.2: The Phillips trimerisation system patented in 1999.[19]

Following publication of these patents by Phillips a range of other companies started work on developing their own ethylene trimerisation systems. All of the ensuing new patents were based around the established Phillips system, but with variations made to the ligand used, the aluminium activators and the catalytic protocol followed. Of the variants published, only one system greatly improved upon the Phillips system. The Mistubishi Chemical Corporation showed that by utilising hexachloroethane as a solvent and carefully controlling the ethylene:1-hexene ratio inside the reactor a process was developed that gave unprecedented activities of 3,780,000 g/g Cr h^{-1} along with an overall selectivity of 95.4 % towards 1-hexene (Scheme 1.3).[20] It is based on these modifications to their original catalytic system that Chevron-Phillips built the world's first selective ethylene trimerisation plant in 2003.

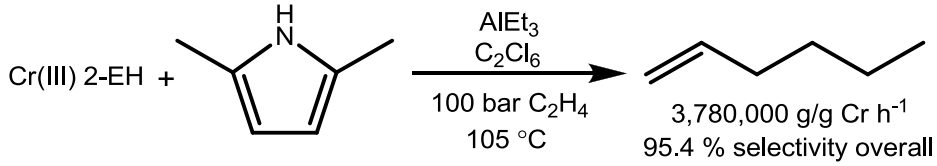

Scheme 1.3: The Phillips-Mitsubishi trimerisation system.[20]

Despite the ubiquity of the so-called Phillips trimerisation systems in the patent literature there have been very few experimental studies of Phillips-based systems published in the open literature over the last 20 years. In 2004 workers from Sasol published a theoretical study concerning Cr-pyrrolyl-based ethylene trimerisation systems, in which they proposed a metallacyclic mechanism (see Section 1.2.2.1) with catalysis proceeding *via* a Cr(II)/Cr(IV) redox couple (Scheme 1.4, *b*).[21] In this work it was also conjectured that the pyrrole ligand was able to alter its coordinate mode between η^1 and η^5, stabilising coordinatively unsaturated catalytic intermediates.

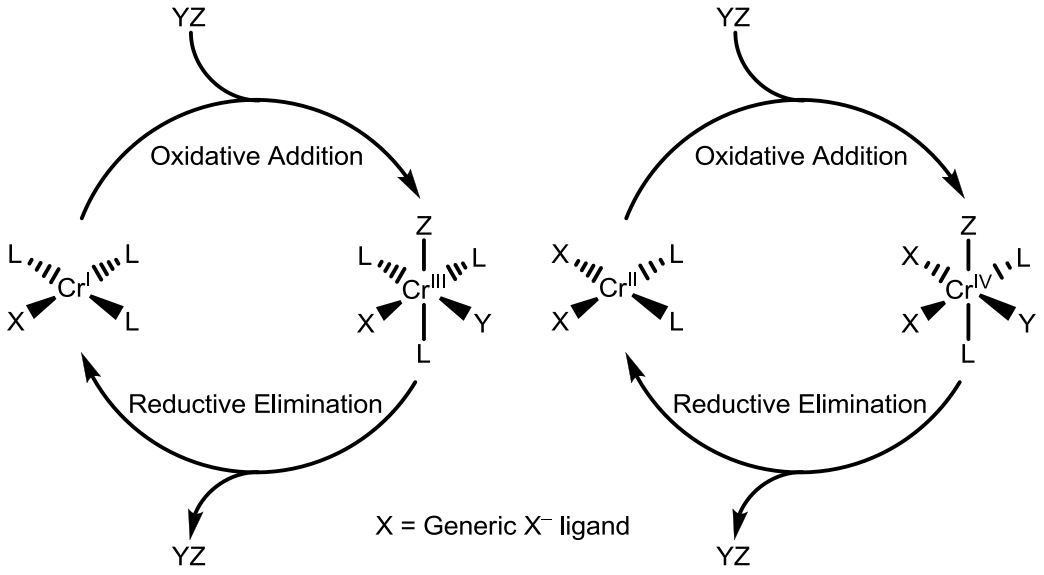

a) Cr(I)/(III) coupled system *b)* Cr(II)/(IV) coupled system

Scheme 1.4: The two possible Cr redox pathways suggested for ethylene trimerisation catalysis.

In order to experimentally probe the active catalytic species in the Phillips system Hu *et al.* carried out XPS analysis of wax-coated samples of active trimerisation catalysts.[22] The wax coating was found to render the catalyst relatively air stable, being able to retain 88 % of its catalytic activity after having been left for 24 hours under air. XPS analysis of these wax-encapsulated catalyst samples showed that the predominant chromium species was Cr^{3+}, leading the authors to conclude that this is the most likely candidate to be the active catalytic species. Based on an active Cr^{3+} species it is assumed, contrary to Sasol's theoretical study, that the catalytic cycle goes *via* a Cr(I)/Cr(III) coupled system (Scheme 1.4, *a*), with the Cr^{3+} species undergoing reductive elimination in the catalytic cycle to give a Cr^{+} complex. The argument for a Cr(I)/Cr(III) system was bolstered by two papers published by Gambarotta *et al.* investigating model Phillips systems.[23,24] In their two studies Gambarotta *et al.* isolated and characterised Cr(I) species, which were found to self-activate when put in contact with ethylene. Gambarotta suggested that these Cr(I) complexes undergo oxidative coupling of ethylene to give a Cr(I)/Cr(III) coupled cycle. More recently further experimental and theoretical studies have added further weight to the arguments for a Cr(I)/Cr(III) system. Talsi *et al.* used EPR spectroscopy to detect Cr(I) species, the concentration of which correlated with the catalytic activity of the system.[25] A pair of DFT studies published by Budzelaar[25] and Liu *et al.*[26] both provide additional theoretical evidence for a Cr(I)/Cr(III) system, supporting the experimental work previously mentioned. Currently, it appears that the most probable catalytic cycle for the Phillips trimerisation system involves a Cr(I)/Cr(III) redox coupling, but further work is required to provide definitive evidence for this.

1.2.1.2 Diphosphinoamine (PNP) ligands in trimerisation

Since the first discovery of ethylene trimerisation systems by Manyik,[14] a wide range of ligands and catalyst systems have been published, but very few of these give comparable activities and selectivities to the highly active Phillips-Mitsubishi trimerisation system previously discussed (Scheme 1.3, Section 1.2.1.1). However, in 2001 Wass *et al.* were working with a new class of ethylene polymerisation catalyst based on diphosphinoamine ligands bound to nickel.[26] In a related study the group from BP tested the effects of their PNP ligands with chromium species and discovered that this new system offered remarkable and unprecedented ethylene trimerisation behaviour with activities of 1,033,200 g/g Cr h^{-1} and an overall selectivity of 89.9 % towards hexene.[27,28] This novel trimerisation system used a combination of $CrCl_3(THF)_3$ and a PNP ligand with *o*-methoxy-substituted aryl groups on the phosphine donors, which was subsequently activated by MAO (Scheme 1.5). The greatest benefit of this new BP system was that the 1-hexene selectivity within the C_6 fraction of the products was 99.9 %, meaning that in an industrial setting the C_6 product stream could be used without the need for further purification.

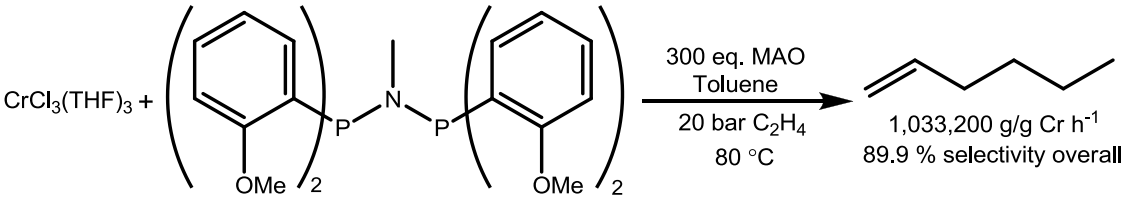

Scheme 1.5: The BP trimerisation system published in 2002.[28]

In their initial study Wass *et al.* proposed that the presence of the *ortho*-methoxy donor groups was vital to the catalytic activity of the system, based on results from their tests run with PNP ligands bearing alternatively-substituted aryl groups.[28] When *ortho*-ethyl or *para*-methoxy substituents were used, mimicking analogous steric and electronic properties of the $PNP^{o\text{-}OMe}$ ligand, respectively, the resulting systems were shown to be completely inactive. This dramatic difference in reactivity led the authors to conclude that the potential ability of the *ortho*-methoxy aryl groups to behave as pendant O-donors and bind to the Cr centre, was a crucial factor in creating an active ethylene trimerisation system. This discovery of a novel class of ligand for ethylene trimerisation opened a new avenue of research in the academic literature, and in the following years a plethora of papers have been published investigating the use of PNP ligands in *tri*- and *tetra*-merisation systems, and these will be discussed in the following sections.

1.2.1.3 The discovery of ethylene tetramerisation

Shortly after the publication of BP's novel trimerisation system, Sasol Technology began carrying out their own investigations into the properties of this novel process. The results of their testing of modified PNP ligands were highly surprising, and led to the discovery of an entirely new chemical reaction. Sasol demonstrated that using a PNP ligand with no *ortho*-substituents upon the aryl groups and an *iso*-propyl substituted N-backbone, in combination with $CrCl_3(THF)_3$ and MAO, gave an unprecedented selective ethylene tetramerisation system.[29,30]

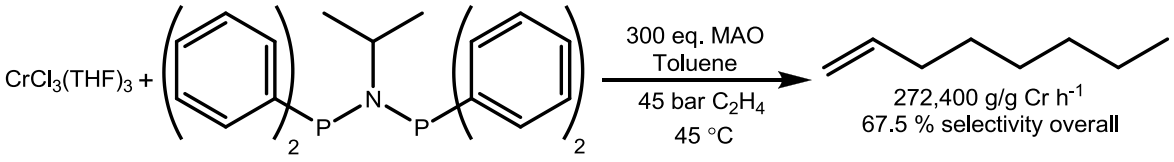

Scheme 1.6: The Sasol tetramerisation system published in 2004.[30]

This discovery of selectivity towards ethylene tetramerisation was a milestone for PNP ligands in metallacycle-based ethylene oligomerisation chemistry, as this reactivity had previously been ruled out by theoreticians due to limitations in forming the metallacyclononane intermediate required to give a selective tetramerisation system (see Section 1.2.2.1 for further detail).[31,32] Work continued at Sasol to improve on their initial tetramerisation system, and in 2009 Bollman and Wasserscheid *et al.* published results in which the process was run in a continuous tube reactor, giving rise to an unparalleled activity of 3,700,000 g/g Cr h^{-1} for a tetramerisation processes.[33] This remarkable result was achieved through the use of PNP ligands with branched N-alkyl substituents, which altered the steric parameters of the ligand. It is based on this work by Bollman and Wasserscheid *et al.* that Sasol have built and are commissioning the world's first ethylene tetramerisation plant in Louisiana, USA.

1.2.2 Mechanistic details of chromium-catalysed ethylene *tri*- and *tetra*-merisation

It is extremely important when developing a new catalytic system to understand the precise details of the mechanism by which the reaction occurs. If the precise pathway of a catalytic process can be fully elucidated, this makes optimisation and further development of the system considerably easier. Consequently, significant effort has been put into studying the details of the ethylene trimerisation process. The mechanism of traditional olefin poly- and oligo-merisation processes has long been understood, and it is generally accepted that a Cossee-Arlman mechanism is involved (Scheme 1.1). However, it is unlikely that such a process can deliver selective ethylene oligomerisation, and therefore a different pathway is assumed to be responsible for the reactivity seen in ethylene *tri*- and *tetra*-merisation systems. The details of this alternative mechanism, and an overview of the of the past 25 years of literature covering studies of ethylene *tri*- and *tetra*-merisation mechanisms will be discussed in this section. For further detail on this topic, an excellent review of mechanistic investigations into chromium-based ethylene oligomerisation was published in 2011 by Agapie.[12]

1.2.2.1 The metallacycle mechanism for selective ethylene oligomerisation

As part of the discovery of ethylene trimerisation by Manyik *et al.* it was noticed that the rates of reaction observed for the production of hexene did not conform to the kinetics predicted by a Cossee-Arlman mechanism.[15] After further investigation of the reaction it was found that the rate of 1-hexene formation was a second order in ethylene, rather than a first order process that would be expected for a non-selective oligomerisation reaction. This disparity led the authors to conclude that a different mechanism must have been responsible for the formation of 1-hexene, rather than a traditional linear chain growth process. It was not until 1989 that the first detailed mechanistic study of the ethylene trimerisation reaction was carried out, in which Briggs proposed that the oligomerisation goes *via* a metallacycle mechanism (Scheme 1.7).[34]

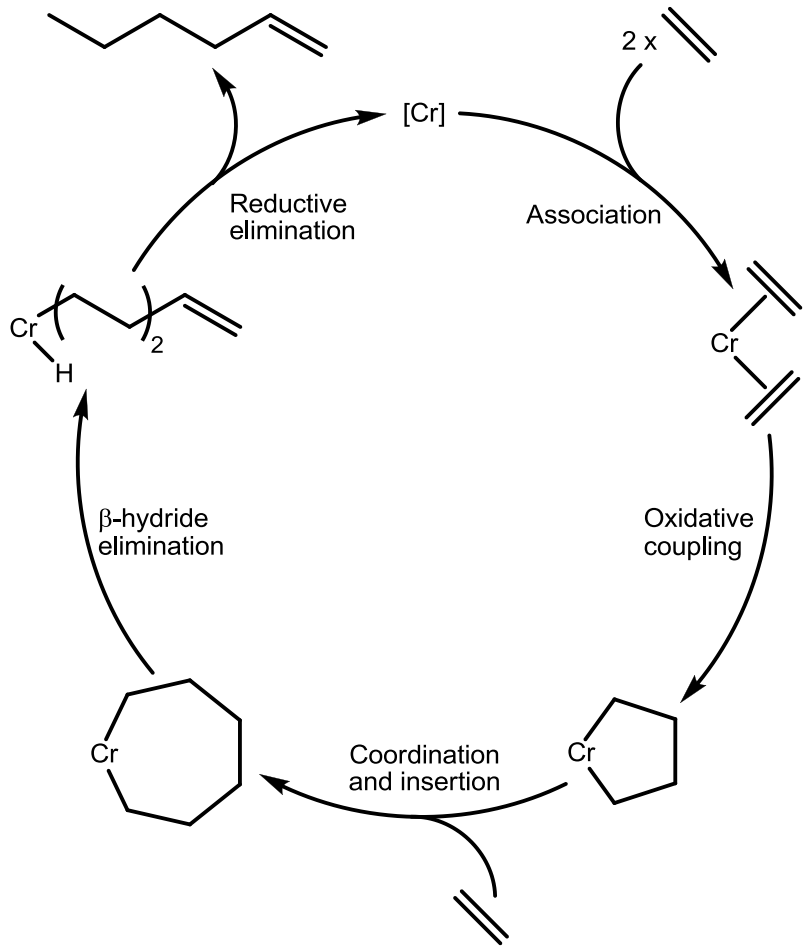

Scheme 1.7: The metallacycle mechanism of ethylene oligomerisation as proposed by Briggs.[34]

This metallacycle mechanism for selective ethylene oligomerisation will inherently give selectivity towards 1-hexene as long as: *a)* the rate of insertion of ethylene into the metallacyclopentane intermediate is faster than the decomposition of the metallacyclopentane and *b)* β-hydride elimination from the metallacycloheptane intermediate occurs faster than further ethylene insertion steps can occur. The relative rates of processes *a)* and *b)* are governed by the relative stabilities of the metallacyclopentane and metallacycloheptane rings. Whitesides *et al.* demonstrated the difference in stability between metallacyclo-pentane and –heptane rings by carrying out studies utilising model platinum metallacycle complexes, in which it was demonstrated that the flexibility of the metallacycloheptane species allowed facile β-hydride elimination, compared to the relative stability of the rigid metallacyclopentane species.[35] This observation was supported by a further study of chromacyclo-pentane and -heptane complexes by Jolly *et al.*, which yielded similar results, and concluded that the metallacyclopentane species synthesised were significantly more stable with regard to decomposition, compared to the analogous metallacycloheptane chromacycle.[36]

A detailed deuterium labelling study carried out by Bercaw *et al.* adds further weight to the argument for a metallacycle mechanism for olefin trimerisation. Here, catalytic trimerisation

tests were carried out using a 1:1 mixture of C_2H_4 and C_2D_4 as the feedstock. If a metallacyclic mechanism is operative, the hexene produced should retain all of the hydrogen atoms from the three constituent ethylene molecules, due to the hydrogen lost in the β-hydride elimination always being reincorporated in the following reductive elimination step (Scheme 1.7). This means that if a mixture of C_2H_4 and C_2D_4 is used as the feedstock, only products containing deuterons in multiples of four should be produced, *i.e.* C_6H_{12}, $C_6H_8D_4$, $C_6H_4D_8$ and C_6D_{12}, in a 1:3:3:1 ratio. Analysis of the resulting oligomeric products from Bercaw *et al.*'s trimerisation reaction showed the 1-hexene produced contained deuterons in multiples of four, matching that predicted by a metallacycle mechanism.[37] If a Cossee-Arlman mechanism had been operative (Scheme 1.1), scrambling of the deuterons would have occurred, leading to odd deuteron numbers in the products, but this was not observed. A later study by the Bercaw group investigating the cotrimerisation of ethylene and propylene yielded the same results.[38] In conclusion, it is now widely accepted that selective ethylene trimerisation follows a metallacyclic mechanism to yield 1-hexene in high selectivities.

1.2.2.1.1 Tetramerisation, a different metallacyclic mechanism to trimerisation?

The development of ethylene tetramerisation processes is highly desirable in industry, due to the high demand for 1-octene, primarily for use as a co-monomer in polyethylene production.[3] Before Sasol's discovery of ethylene tetramerisation in 2004 it was widely believed that this selective transformation of ethylene was not possible.[31,32] A group from Sasol carried out detailed mechanistic investigations to elucidate the pathway responsible for the tetramerisation of ethylene, and concluded that an extended metallacyclic mechanism including a second ethylene insertion step, was most likely responsible for the production of 1-octene (Scheme 1.8).[39] In order for this "extended metallacyclic" system to produce 1-octene, the metallacycloheptane intermediate must be stable enough to allow the insertion of a fourth ethylene unit, before undergoing β-hydride elimination to yield 1-octene as the product, something previously ruled out by theoretical studies.[31,32]

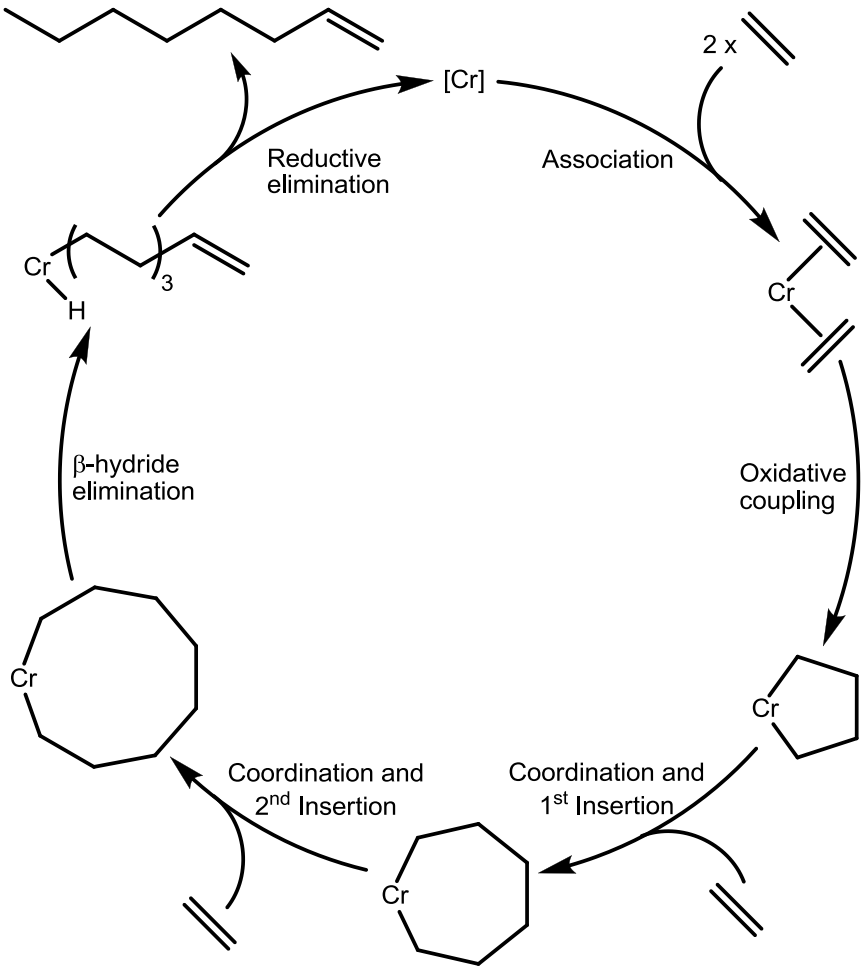

Scheme 1.8: Metallacyclic mechanism of ethylene tetramerisation proposed by Sasol (Overett *et al.*)[39]

Contrary to the "extended metallacyclic" mechanism published by Sasol, recent publications have proposed a modified metallacycle mechanism, based on computational studies suggesting that a single-centred extended metallacycle mechanism is unlikely due to the predicted instability of a metallacycloheptane intermediate.[31,32] In 2010 Rosenthal and Muller *et al.* published a paper postulating a new ethylene tetramerisation mechanism going *via* a bimetallic chromium-centred metallacyclic process (Scheme 1.9).[40] This suggested pathway involves a Cr-Cr bound bimetallic species as the active catalyst, and it is proposed that this bimetallic system is formed by the coupling of two separate metallacyclopentane moieties, which undergo a cooperative bimetallic reductive elimination to yield 1-octene as the product.

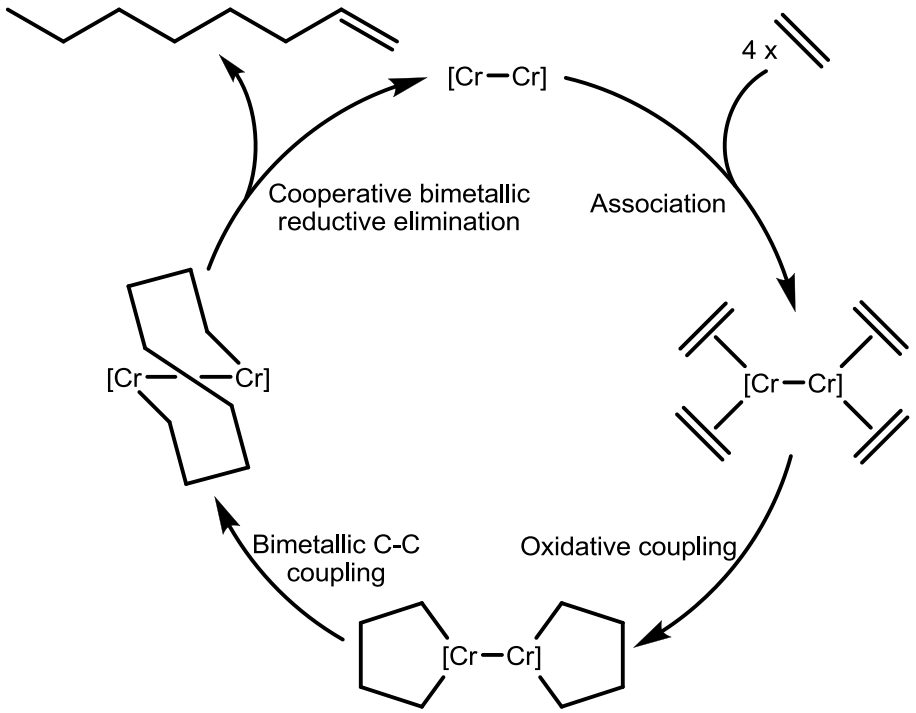

Scheme 1.9: A bimetallic metallacyclic ethylene tetramerisation mechanism proposed by Rosenthal and Muller *et al.*[40]

Rosenthal and Muller *et al.* base their proposed bimetallic tetramerisation mechanism on a suggested mechanism for the Cr-based Phillips ethylene polymerisation system. It has been conjectured that the Phillips polymerisation system reacts *via* a bimetallic mechanism involving the growth of metallacycles across Cr-O-Cr catalytic centres. This proposed pathway is supported by both experimental[41] and theoretical[42] evidence, in which ethylene inserts between two Cr atoms to yield a metallacycle, which grows through addition of further ethylene units (Scheme 1.10).[43]

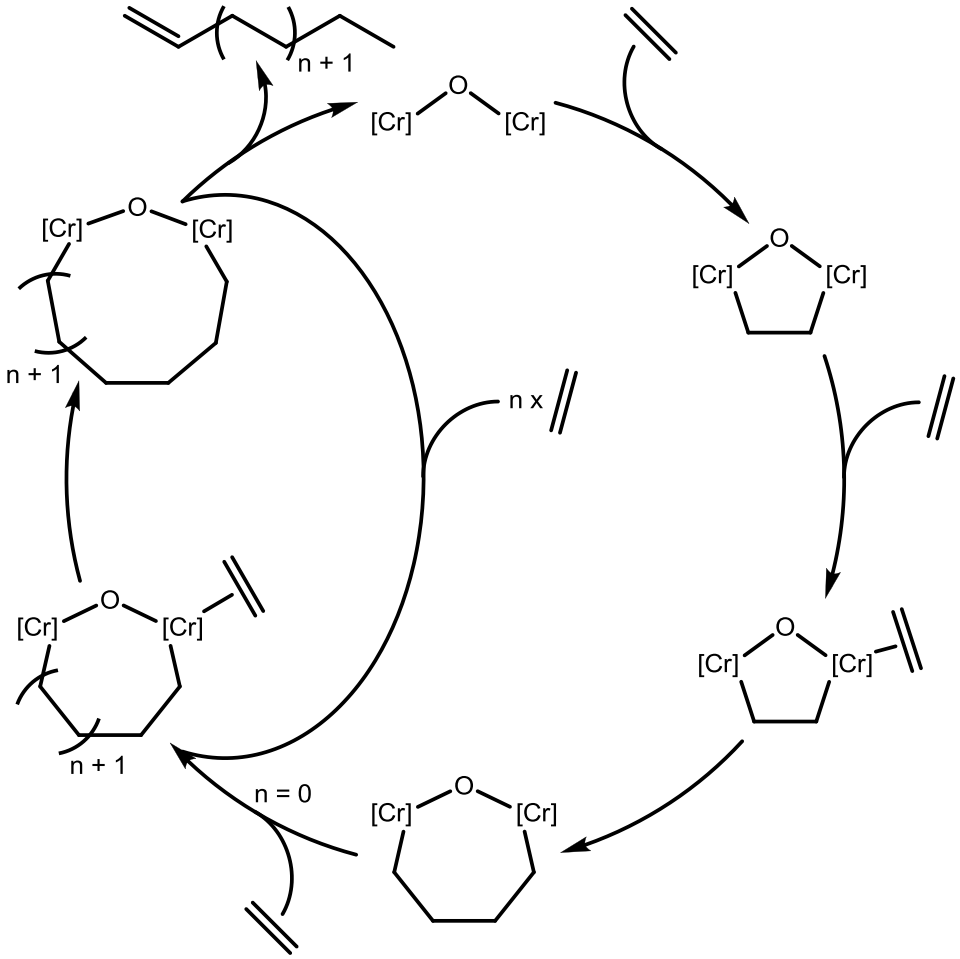

Scheme 1.10: A modified version of the mechanism for the Phillips polymerisation system proposed by Rebenstorf *et al.*[41]

Despite the suggestions by Rosenthal and Muller *et al.* of a bimetallic Cr-mediated tetramerisation mechanism[40] the only support for this in the literature comes from a paper by Gambarotta and Duchateau *et al.* in which they allude to this alternative mechanism for the production of 1-octene in high selectivities in their system.[44] At the time of writing there have been no studies to provide experimental evidence for this alternative ethylene tetramerisation mechanism, and it is evident that further studies are required before this bimetallic mechanism is widely accepted by the scientific community. However, these suggestions by Rosenthal and Muller *et al.* provide a plausible and interesting new avenue for investigation into ethylene tetramerisation chemistry.[40]

1.2.2.2 The oxidation state of chromium in ethylene tri- and tetra-merisation systems

Elucidation of the metal oxidation states in Cr-mediated ethylene *tri-* and *tetra-*merisation systems has presented researchers with a considerable challenge since the first discovery of ethylene trimerisation. The primary obstacle that is faced by researchers is the paramagnetic nature of Cr(I)/(II)/(III), which hinders traditional NMR spectroscopic studies. The presence of large amounts of aluminium activators also hinders investigation, as these have the

ability to change the metal oxidation state of any Cr starting materials used, and render the active catalyst highly air-sensitive. In order to overcome these difficulties in characterising the chromium oxidation state a wide range of ingenious studies have been carried out in attempts to define the catalytic chromium species responsible for ethylene *tri*- and *tetra*-merisation, which are discussed in this section. In this thesis the discussion will focus on PNP-based, and related systems, as the influence of oxidation state for Phillips pyrrole-based trimerisation systems has previously been covered (Section 1.2.1.1).

If it is assumed that a metallacyclic mechanism is responsible for the catalytic trimerisation of ethylene, then the metal centre must undergo a two-electron redox process in order for oxidative coupling and reductive elimination to take place, *i.e.* the metal is present in $M^{(n)+}$ and $M^{(n+2)+}$ oxidation states (Scheme 1.4). For the majority of PNP-based catalytic systems Cr(III) species are used as metal precursors, meaning that the active catalytic species must be generated from this starting point. Labinger and Bercaw *et al.* provided evidence of a Cr(I)/(III) system, starting from Cr(III), through the study of model Cr^{III}(PNP) complexes that underwent reductive elimination to give active trimerisation catalysts.[37,38] *Tri*- and *tetra*-merisation systems have also been discovered starting from Cr(I) species. Both Hanton *et al.* and Wass *et al.* succeeded in demonstrating that when $[Cr(CO)_4(PNP)]^+$ species were combined with a weakly coordinating anion they could be activated with $AlEt_3$ to give active ethylene *tri*- and *tetra*-merisation initiators, respectively (Scheme 1.11).[45,46] This led the authors of both papers to conclude that a Cr(I)/(III) system was responsible for the catalysis.

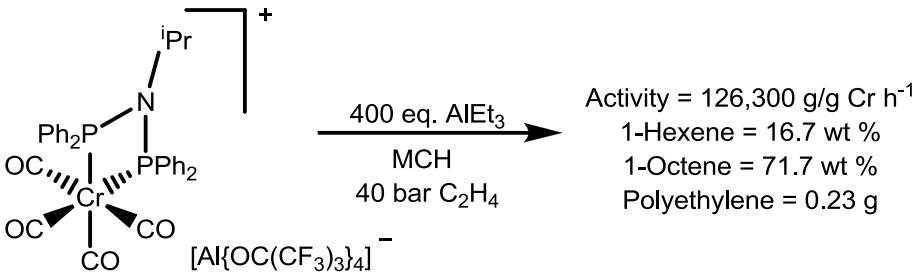

Scheme 1.11: An ethylene tetramerisation system utilising a Cr^{I}(PNP) precursor.[45]

In another paper by Bercaw and Labinger *et al.* $Cr(PNP^{OMe})Ph_3$ complexes were synthesised and their activities as catalyst precursors were investigated.[47] In this study only Cr(III) starting materials were used, but differences between neutral and charged complexes were noticed. It was demonstrated that cationic $[Cr(PNP^{OMe})Ph_2]^+$ gave trimerisation activity when exposed to ethylene, compared to the analogous neutral $Cr(PNP^{OMe})Ph_3$ complex, which was completely inactive (Scheme 1.12). Based on this evidence the authors reasoned that the active catalyst in this particular trimerisation system is most likely cationic.

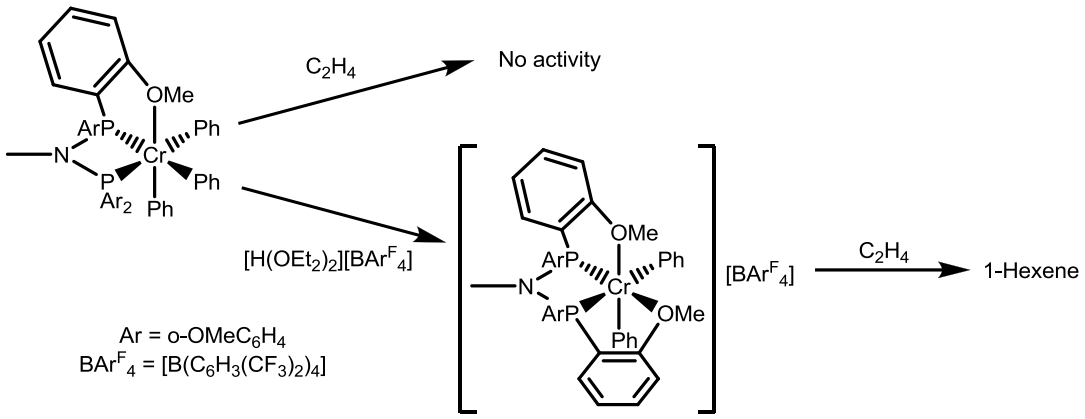

Scheme 1.12: Reaction of $CrPh_3$(PNP) complexes with ethylene, reported by Bercaw and Labinger *et al.*[47]

One analytical technique that is useful when studying paramagnetic species is electron paramagnetic resonance (EPR) spectroscopy. This has been used by a number of research groups to study ethylene *tri-* and *tetra*-merisation systems. One such study carried out by Bruckner *et al.* in 2008 found evidence for the reduction of Cr(III) to Cr(I) upon exposure to MMAO in PNP-based trimerisation systems, supporting the concept of a Cr(I)/(III) redox couple.[48] More recently, Bercaw and Labinger *et al.* carried out a range of detailed spectroscopic studies of $CrCl_3$(PNP) based ethylene trimerisation processes, including EPR spectroscopy. From their studies Bercaw *et al.* concluded that a small amount of a Cr(I) complex was most likely to be the active catalytic species, while the majority of the Cr present in the reaction resides as either inactive Cr(III) or an EPR silent Cr species.[49]

Studies of the oxidation state have also been carried out for Cr(SNS) (SNS = $RSCH_2CH_2N(H)CH_2CH_2SR$) trimerisation systems. Gambarotta and Duchateau *et al.* successfully demonstrated that Cr^{III}(SNS) species are stable and catalytically active for trimerisation, something that led them to conclude that SNS ligands support and stabilise the Cr(III) oxidation state.[50] The presence of a cationic Cr(III) species in trimerisation systems utilising tridentate 1,3,5-triazacyclohexanes as ligands has been proved by Kohn *et al.* through ^{19}F-NMR spectroscopy of their $[CrCl_3(1,3,5\text{-}R_3(C_3N_3H_6)(PhNMe_2H)][B(C_6F_5)_4]$ based catalysts, activated with Al^iBu_3 to yield active trimerisation systems.[51] In addition to the presence of Cr(III) Kohn *et al.* demonstrated that Cr(III) could easily be reduced to Cr(I), leading to the conclusion that a Cr(I)/(III) redox couple was most likely responsible for catalysis.

In a recent study Theopold *et al.* provided "unambiguous evidence" of an ethylene trimerisation catalytic cycle starting and ending in a Cr(I) state, using their $[(i\text{-}Pr_2Ph)_2nacnacCr]_2(\mu\text{–}\eta_2\text{:}\eta_2\text{-}N_2)$ ((*i*-$Pr_2Ph)_2$nacnac = 2,4-pentane-*N,N-bis*(2,6-diisopropylphenyl)-diketiminate)) complexes as catalyst precursors (Scheme 1.13). This activity of the Cr(I) complexes, coupled with the fact that the Cr(II) complexes synthesised in the same study

showed no catalytic activity, again leads to the conclusion that this catalytic system is the product of a Cr(I)/(III) redox couple.[52]

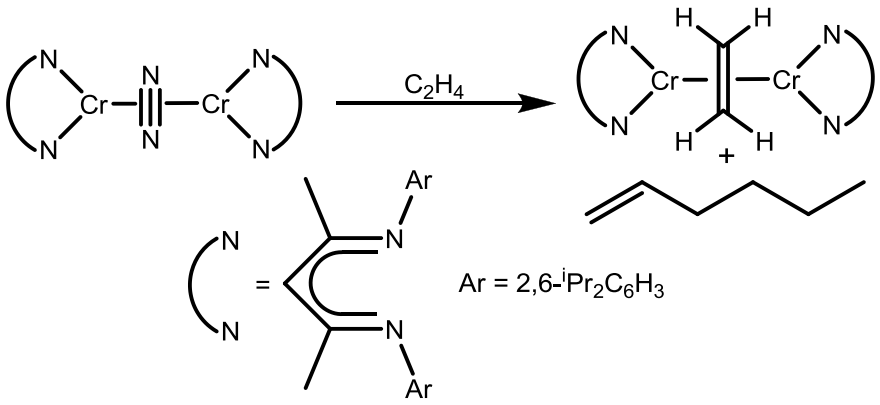

Scheme 1.13: A self-activating Cr(I) ethylene trimerisation system published by Theopold et *al.*[52]

Despite the large body of work supporting a Cr(I)/(III) coupled system, there is a wide range of literature suggesting that this is not the case, and that a Cr(II)/(IV) system is responsible for ethylene *tri*- and *tetra*-merisation reactions. In 2006 Gambarrota and Duchateau *et al.* reported the synthesis and isolation of a cationic Cr(II) complex that displayed trimerisation activity upon activation with $AlMe_3$, implying a Cr(II)/(IV) system may be the active catalyst.[53] The group of McGuinness *et al.* have investigated Cr(II)-PNP and Cr(II)-SNS trimerisation systems, finding that they offered catalytic activities comparable to that of analogous Cr(III) systems.[54] As part of this study magnetic susceptibility tests were carried out upon activated catalyst systems by NMR spectroscopic methods, confirming the presence of Cr(II) in solution and suggesting the operation of a Cr(II)/(IV)-based mechanism. These experimental results are backed up by computational studies by Mukhopadyay *et al.*, which suggest that a metallacyclic mechanism incorporating a Cr(II)/(IV) redox couple is the most favoured reaction pathway for ethylene trimerisation (Scheme 1.4, *b*).[55]

Work by Gambarotta and Duchateau *et al.* on $[(Ar)NPN(t\text{-}Bu)]_2Cr$ type complexes also showed that Cr(II) species are active trimerisation intiators (Scheme 1.14).[56] Despite this, the same research group published a second paper on the same $[(Ar)NPN(t\text{-}Bu)]_2Cr$ complexes, this time suggesting that it was unlikely for a divalent Cr(II) species to act as the active catalyst.[57] These contradicting results led the authors to propose that the divalent Cr(II) moiety was acting as a self-activating catalyst precursor. A similar conclusion was reached by Gambarotta and Duchateau *et al.* in their paper concerning Cr(SNS) systems, namely that both Cr(III) and Cr(II) species are likely to be precursors to the same active catalyst in the trimerisation system.[58]

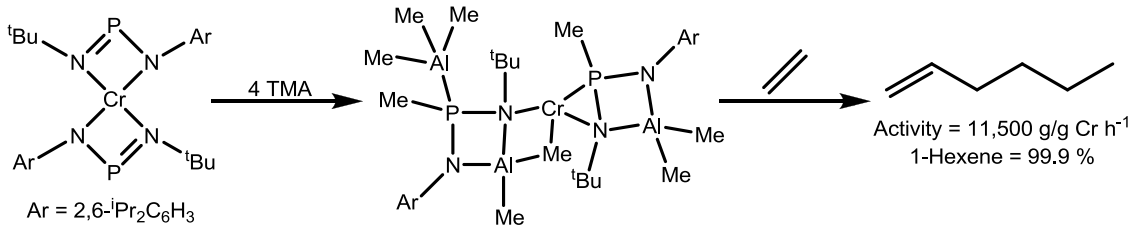

Scheme 1.14: The self-activating Cr(II)-based ethylene trimerisation system reported by Gambarotta and Duchateau *et al.*[56]

A recent study by Bruckner *et al.* involved monitoring Cr(PNP) ethylene tetramerisation systems under ethylene pressure by EPR and *in situ* X-ray absorption spectroscopy (XAS). Bruckner *et al.* found a $(PNP)Cr^{II}(CH_3)_2$ to be the most likely candidate as the active catalytic species, despite having used $Cr^{III}(acac)_3$ as the Cr precursor. This is, however, consistent with the observation that trivalent organochromium species readily and spontaneously reduce to Cr(II) species.[58] In addition to Cr(II), Bruckner also reported evidence for the presence of Cr(I), which was attributed to deactivation products in the reaction, further suggesting that the active catalytic cycle involves a Cr(II)/Cr(IV) cycle.[59]

Overall there is still considerable speculation as to the exact nature of the metal oxidation states present in chromium-based *tri-* and *tetra*-merisation systems. One possible reason for the wide variation of species described in the literature is that different types of ligand can support different specific oxidation states of chromium. There are also limitations of oxidation state formalism, as this gives little information as to the precise electronic configuration around the chromium centre, and it is possible that the varying electronic contributions from the ligands result in similar electron densities at Cr. Furthermore, it has been suggested by Agapie that alkyl aluminium reagents are able to partake in the oxidation chemistry occurring in the reaction, meaning that the oxidation state of the catalyst precursor may be significantly different to that isolated as a precatalyst.[12] Further discussion of the oxidation state of chromium in the catalytic systems investigated in this thesis is reported in Chapter 5 (Section 5.5.6).

1.2.2.3 The role of aluminium activators in ethylene oligomerisation systems

The use of alkyl aluminium activators is ubiquitous in the field of ethylene polymerisation and oligomerisation chemistry,[60] with selective ethylene oligomerisation being no exception. The vast majority of all ethylene *tri-* and *tetra*-merisation systems require the presence of alkyl aluminium species as co-catalysts, of which MAO, MMAO, $AlMe_3$ and $AlEt_3$ are the most common. However, recently a limited number of self-activating oligomerisation systems have been published,[52] but these do not offer catalytic activities comparable to traditional aluminium-activated systems.

In the open literature MAO or MMAO are generally the most commonly used activators in selective ethylene oligomerisation systems. The use of such partially hydrolysed alkyl aluminium species as olefin polymerisation activators was first hinted at in 1980, when it was revealed that if small amounts of water were added to Zr-based Ziegler-Natta polymerisation systems activated with $AlMe_3$, a dramatic increase in catalytic activity was observed.[61] The authors concluded that the increase in activity was due to the formation of alkyl aluminoxane species of the general formula $[Al(CH_3)O]_n$. Since the first discovery of MAO a large amount of time and effort has been dedicated to elucidating its precise structure in solution, but to no avail.[62] A number of oligomeric structures have been proposed, including rings, ladders and cages (Figure 1.1).[63]

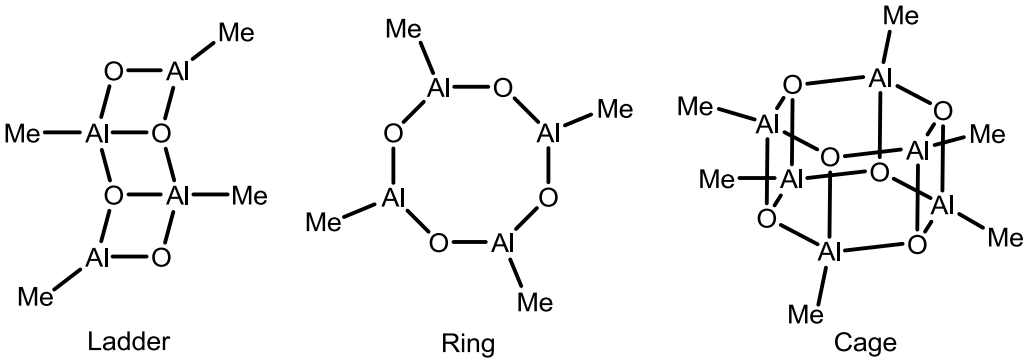

Figure 1.1: A selection of the proposed structures of MAO in solution.[63]

Computational studies carried out by van Rensburg *et al.* concerning MAO in selective ethylene oligomerisation systems found that it was energetically favourable for MAO to adopt a cage structure in solution.[64] In a more recent study using mass spectrometry the authors reported an upper MW limit on cage size of 3500 Da.[65] This calculated MW of MAO was verified by work from Stellbrink, Linnolahti and Bochmann *et al.* in which, after a thorough study of MAO was carried out using spectroscopic, neutron scattering and computational methods, it was found that each MAO cluster consisted of 30-60 aluminium atoms.[66] It is most likely that MAO exists in an equilibrium between various structures in solution, and this fluxional behaviour makes characterisation challenging. The precise structure and make-up of MAO is also thought to vary based on the various methods of producing MAO.[67] In many selective ethylene oligomerisation systems MMAO is used in preference to MAO due to MAO's poor solubility in non-polar solvents and its poor shelf-life. MMAO is prepared by the hydrolysis of a mixture of $AlMe_3$ and Al^iBu_3 which improves solubility in aliphatic solvents, and gives better stability for storage.[63]

Despite the difficulties in characterising the structure of MAO, the probable roles of MAO in oligomerisation systems have been deduced. The function of MAO is primarily two-fold,

to *a)* alkylate the chromium metal centre and *b)* behave as a Lewis acid and abstract an alkyl group to afford a cationic chromium species. The alkyl-abstracting behaviour of MAO has been studied compared to that of $AlMe_3$, and it has been found that MAO is much more Lewis acidic than $AlMe_3$, explaining the ease with which MAO abstracts alkyl groups.[68] It has also been suggested that MAO may be involved in the redox chemistry of activating the chromium centre, but this has proved difficult to study.[12]

Since the discovery of Cr(PNP)-based ethylene oligomerisation systems there has been a significant effort put into developing alternative activator systems to MAO. MAO is typically used in large excess with regard to the chromium source which is costly, wasteful and difficult to handle on a large scale, therefore finding a replacement activator is very attractive. One of the most successful alternative activation methods was first published by Overett *et al.* in which stoichiometric amounts of $B(C_6F_5)_3$ and $[Ph_3C][B(C_6F_5)_3]$ were used in conjunction with trialkylaluminiums to yield active ethylene *tri-*/*tetra*-merisation catalysts.[69] It was proposed that the alkylaluminium species is capable of alkylating the chromium centre, while the highly Lewis acidic borates can perform alkyl abstraction, thus replacing the functions of MAO. The downside to the use of borate activators was that while the liquid fraction selectivities remained comparable to MAO-activated systems, the activities were considerably lower. McGuinness and Tooze *et al.* were not deterred by this fact, and went on to study a whole range of weakly coordinating anions as potential co-catalysts. Studies of Krossing's anion, $[Al(OC(CF_3)_3)_4]^-$, were of particular interest, due to its extremely weakly coordinating nature, and considerable stability.[70] Their interest was well-founded, as the investigation revealed that when $AlEt_3$ and $[Ph_3C][Al(OC(CF_3)_3)_4]$ were combined and used as activators this gave a highly active ethylene tetramerisation system, 125,600 g/g Cr h^{-1}, 71.5 % overall 1-octene selectivity (Scheme 1.15).[71]

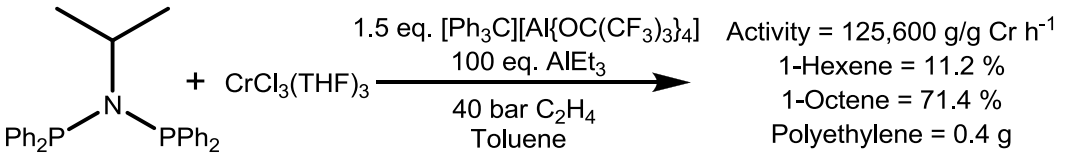

Scheme 1.15: Aluminate-activated ethylene tetramerisation system published by McGuinness and Tooze *et al.*[71]

Despite the development of novel catalyst activator packages for ethylene oligomerisation systems, MAO and its derivatives remain the most popular activators in the literature. In conclusion, it is clear that when designing a novel oligomerisation process care must be taken when choosing which activator system to use.

1.2.3 The effects of the ligand in ethylene *tri*- and *tetra*-merisation systems

As with any homogeneous catalytic system, the role of the ligand in supporting the active catalytic centre is vitally important, and has a direct effect on the behaviour of the catalyst. This means that understanding how the ligand behaves and how it interacts with other components of the system is necessary in order to develop and improve the performance of the catalysis. This section of the report will focus on the literature surrounding the developments and investigations carried out on the BP PNP-type ligands, as well as related *tri*- and *tetra*-merisation systems.

1.2.3.1 The effect of varying phosphine groups of PNP compounds

When the initial BP trimerisation system was published in 2002 the authors noted that the presence of aryl *ortho*-methoxy (Ar-o-OMe) groups was vital for the catalytic activity of the system. Ligands designed to mimic the steric effects (Ar-*o*-Et) and electronic effects (Ar-*p*-OMe) were both synthesised and tested for trimerisation activity, but Wass *et al.* found that neither gave catalytically active systems.[28] From these results it was concluded that the *ortho*-methoxy groups may behave as pendant donors in the catalytic cycle, displaying hemilabile coordinative properties. Subsequently, Blann *et al.* reported their own investigations into PNP ligands for ethylene trimerisation, and published results contradicting the findings of Wass *et al.*, demonstrating that PNP ligands bearing non-polar substituted aryl groups could be used to generate trimerisation-active systems.[72] In this work by Blann *et al.* it was also shown that the steric bulk of the ligands used had a direct effect on the 1-hexene/1-octene selectivity, with larger and more bulky *ortho*-aryl substituents favouring the production of 1-hexene (Scheme 1.16).

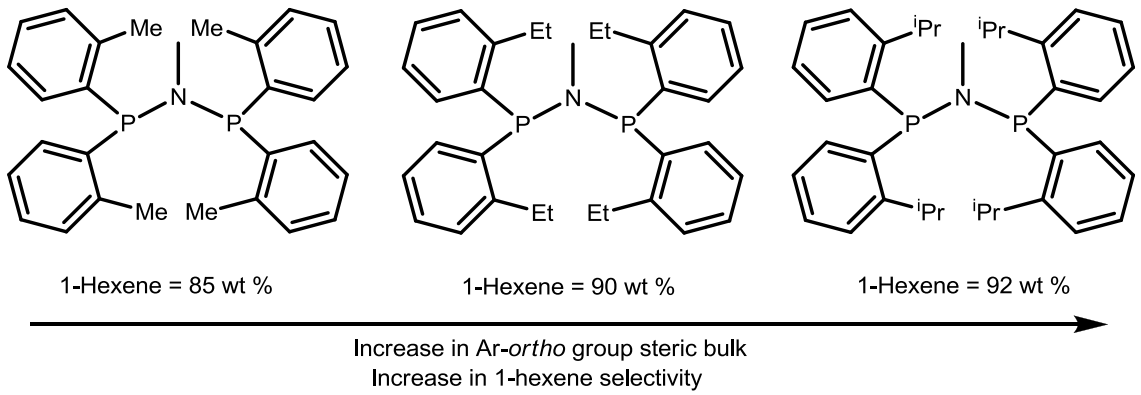

Scheme 1.16: Trend of increasing catalyst selectivity towards 1-hexene production with increasing PNP steric bulk observed by Blann *et al*.[72] Catalysis conditions: 0.033 mmol $Cr(acac)_3$, 2 eq. ligand, 300 eq. MAO, 100 mL toluene.

Another study conducted by Sasol focussed on the effect of polar-substituted aryl PNP ligands in which Overett *et al.* successfully demonstrated that Ar-*o*-OMe-substituted PNP ligands gave considerably higher activities than those of the *para*- or *meta*-substituted analogues, adding weight to the idea that Ar-*o*-OMe groups may behave as pendant donors.[73] This behaviour of Ar-*o*-OMe groups behaving as pendant donors was confirmed by Bercaw and Labinger *et al.* in their work on well-defined trimerisation initiator precursors.[74] In their study, Bercaw and co-workers succeeded in isolating Cr(PNP) complexes that showed structures displaying one Ar-*o*-OMe group coordinating to the metal centre, and the PNP ligand behaving as a tridentate species, proving that the Ar-*o*-OMe substituent can behave as a pendant donor. It is worth noting that when these Cr(PNP) molecular structures are studied in detail it is revealed that the Cr-O bond length is relatively long, at 2.1562(15) Å (compared to Cr-O = 1.939(2) Å, measured by Gambarotta and Duchateau *et al.* for a bidentate P,O ligand, Figure 1.2),[75] implying that this is a weak bond and is hence that the Ar-*o*-OMe oxygen coordination will be labile in solution.

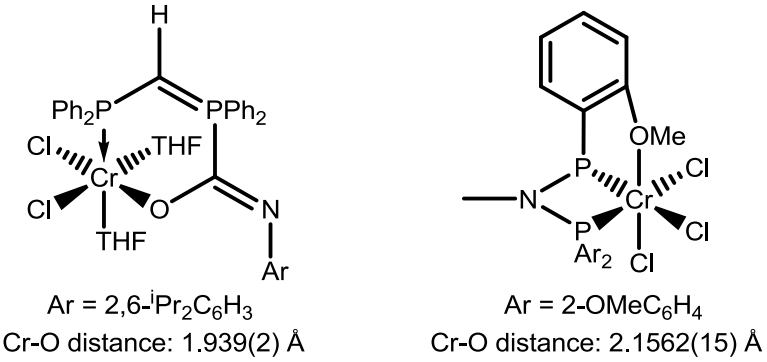

Figure 1.2: Comparison of a "traditional" bidentate Cr(κ^2-P,O) complex (left)[75] with the chromium PNP complex isolated by Bercaw and co-workers displaying pendant ether coordination (right).[74]

In a recent study by Wass *et al.* a series of PNP ligands have been synthesised bearing phosphole-substituted P donor groups. When applied to oligomerisation systems, these novel PNP ligands show moderate *tri*- and *tetra*-merisation activity (up to 28,600 g/g Cr h^{-1}), with the selectivity varying depending on the steric bulk of the phosphole group used (Figure 1.3).[76] It was found that more bulky, symmetrical phosphole-bearing PNP ligands gave a preference to 1-hexene formation, while the less bulky systems gave rise to 1-octene production. This trend matches previous results from Sasol's studies of bulky *ortho*-substituted PNP ligands,[72] which suggest that increasingly bulky PNP ligands hinder the formation of the larger metallacyclononane intermediate required for octene production, hence favouring ethylene trimerisation.

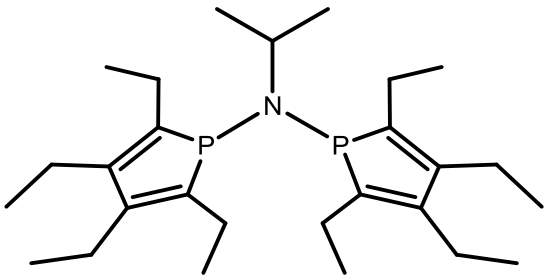

Activity = 21,900 g/g Cr h^{-1}
1-Hexene = 89.5 wt %
1-Octene = 2.5 wt %

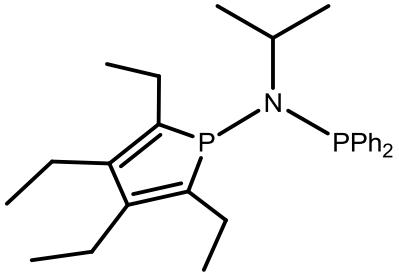

Activity = 28,600 g/g Cr h^{-1}
1-Hexene = 62.4 wt %
1-Octene = 30.8 wt %

Figure 1.3: Catalytic results from systems using two phosphole-based PNP ligands synthesised by Wass *et al.*[76] Catalysis conditions: 20 µmol $CrCl_3(THF)_3$, 1.2 eq. ligand, 300 eq. MAO.

1.2.3.2 The effect of varying the N-substituent of PNP compounds upon catalysis

The effect of changing the PNP ligand N-backbone group upon PNP-based oligomerisation systems has been studied by a number of research groups. One of the most important variations to be explored was the introduction of bulky aryl substituents at the N-group of the ligand by Bollmann *et al.*, something that gave the first ethylene tetramerisation systems (Figure 1.4).[30] In this work reported by Bollmann *et al.* it was shown that while the nitrogen substituent did not have a profound effect on the selectivity of the system, it played a vital role in controlling the catalytic activity.

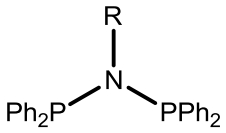

R = Methyl

Activity = 26,500 g/g Cr h^{-1}
C_6 = 24.8 wt %
C_8 = 59.0 wt %

R = *n*-Pentyl

Activity = 43,600 g/g Cr h^{-1}
C_6 = 24.9 wt %
C_8 = 58.1 wt %

R = *iso*-Propyl

Activity = 11,700 g/g Cr h^{-1}
C_6 = 32.7 wt %
C_8 = 60.6 wt %

Figure 1.4: A selection of PNP ligands synthesised and tested for selective ethlyene oligomerisation by Bollmann *et al*. Catalysis conditions: 33 µmol $CrCl_3(THF)_3$, 2 eq. ligand, 300 eq. MAO, 100 mL toluene.[30]

Work has also been carried out by Wasserscheid *et al.* investigating the effects of varying alkyl and cycloalkyl PNP ligand N-substituent groups, with the aim of reducing side-product formation.[77] A remarkable trend was found, showing that both the activity and α-olefin selectivity increased linearly with increasing cycloalkyl ring size, with the cyclododecane-substituted ligand variant giving an activity of 757,700 g/g Cr h^{-1} and an overall α-olefin selectivity of 84.9 wt % (Scheme 1.17). This result led the authors to conclude that the presence of bulky N-substituents is important for the reduction of high molecular weight by-products, and for the overall activity of the initiator.

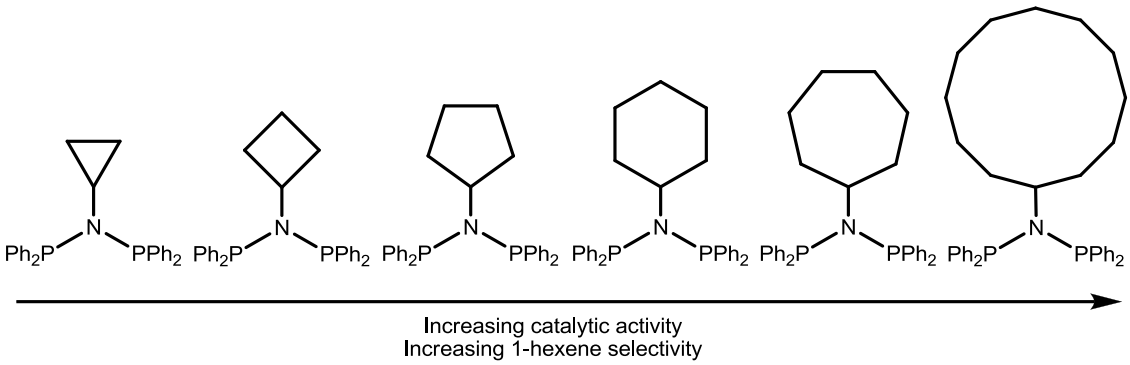

Scheme 1.17: Series of PNP ligands tested in oligomerisation systems by Wasserscheid *et al.*[77] Catalysis conditions: 5 µmol $Cr(acac)_3$, 1.5 eq. ligand, 270 eq. MMAO-3A.

Subsequently, Blann *et al.* published work detailing further improvements to the PNP-based oligomerisation system utilising bulky N-cycloalkyl-substituted groups to give a catalytic system with unprecedented activities of 3,200,00 g/g Cr h^{-1}.[78] It was found in this study that branching in the α-position of the N-alkyl substituent was vital in giving high selectivities for 1-octene. In a related investigation by another group from Sasol the effect of the electronic properties of the N-backbone substituents was investigated, revealing that when an electron-rich 4-^{t}Bu-Ph group was attached to the N-backbone the catalytic activity increased relative to that of the Ph-N analogue.[79] Conversely, the electron withdrawing 4-$(NO_2)C_6H_4$ substituted backbone led to a 9 % decrease in overall α-olefin selectivity relative to the Ph-N variant. A similar piece of work published by Jiang *et al.* using N-aryl substituted PNP ligands gave comparable results to those published by Sasol for their electron withdrawing PNP ligands, with even lower catalytic activities reported.[80]

A range of PNP ligands with backbone N-substituents containing donor-groups have been synthesised and investigated by a number of research groups, on the basis that any donor group may potentially be able to display the same hemi-labile coordination as Ar-*o*-OMe groups. Building on this idea, Weng and Hor *et al.* synthesised PNP ligands with ether and thioether pendant N-backbone groups, reporting that the presence of donor groups did increase the activity of the catalyst, and favoured tetramerisation over trimerisation.[81] Despite this improvement in catalyst performance, no direct evidence was found for coordination of the pendant donors. Bercaw *et al.* also published work detailing the synthesis of PNP ligands with pendant ether donor substituents on the N-backbone, and demonstrated that the presence of the ether groups did increase the activity of the catalytic system (Figure 1.5).[82]

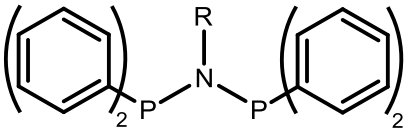

$R = (CH_2)_2OCH_3$

Figure 1.5: Example ligand bearing an N-ether pendant donor group reported by Bercaw *et al.*[82]

Bercaw's work again implies that there is some interaction of these donor ether groups with chromium in the catalytic cycle, but no concrete evidence was found. One more recent study undertaken by Wasserscheid and McGuinness *et al.* found that PNP ligands with N-pendant donor groups only gave catalytic activity when activated with MAO, and the same systems were inactive if $AlEt_3$ was used as an activator.[83] It is suggested by Wasserscheid and McGuinness *et al.* that this difference in reactivity observed between MAO and $AlEt_3$ may be due to the ability of $AlEt_3$ to coordinate to the pendant N-donor group, significantly altering the reactivity of the resulting catalytic species.

Overall, in the past 10 years it has been successfully demonstrated that by altering the N-backbone of PNP ligands the activities and selectivities of the resulting catalytic systems can be finely tuned. This has allowed for the development of incredibly highly active and selective PNP-based ethylene *tri-* and *tetra*-merisation systems, based on which Sasol have developed their industrial ethylene tetramerisation process.

1.2.3.3 Other chromium-diphosphine based scaffolds for selective ethylene oligomerisation

Shortly after the discovery of PNP ligands as ligands for ethylene trimerisation systems, work began on investigating the behaviour of a range of other simple bidentate diphosphine ligands in ethylene oligomerisation systems. In Bollmann *et al.*'s initial publication on ethylene tetramerisation systems both dppe and 1,2-diphosphinohydrazine (PNNP) ligands were tested and shown to give moderate tetramerisation activity.[30] In a later paper by workers from Sasol a series of carbon-bridged diphosphine ligands were tested for ethylene *tri-*/*tetra*-merisation activity, revealing that only a select few of the ligands offered activities and selectivities comparable to PNP systems.[84] Interestingly, the ligands that gave the worst performance were those with short carbon backbones, dppm and 1,1-*bis*(diphenylphosphino)ethylene. Naively these would be expected to yield the best catalytic systems, as they have the most similar bite-angle to that of PNP ligands when bound to a metal centre, and have similar steric properties to PNP ligands. If the inactivity of these two PCP-based systems is ignored, then Overett *et al.* found a general correlation between bite angle and C_8/C_6 ratio, with small bite angles offering the greatest tetramerisation selectivity (Figure 1.6). This preference matches that found in catalytic systems with tight bite angle PNP compounds, in which ligands with very small bite angles (~67 °) yield systems giving the highest octene:hexene product ratios.[30]

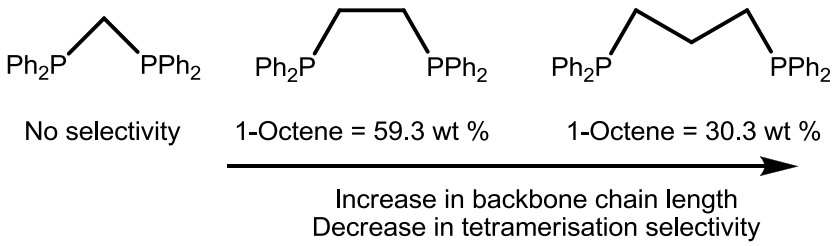

Figure 1.6: The selectivities of ethylene oligomerisation systems to 1-octene, utilising carbon-bridged diphosphine ligands with varying backbone lengths. Catalysis conditions: 5-30 µmol $[(Ph_2P(CH_2)_nPPh_2)CrCl_2(\mu\text{-}Cl)]_2$, 60 °C, 500 eq. MMAO-3A, 100 mL methylcyclohexane.[84]

A recent paper by Zhang *et al.* reports a class of carbon-bridged diphosphine ligands, with unsaturated $^tBuC{=}CH$ backbones, that offer remarkably high activities.[85] Their most active system gave an activity of 4,238,000 g/g Cr h^{-1} with reasonable selectivities (Figure 1.7). The work by Zhang *et al.* also demonstrates the trend that more bulky backbone substituents favour hexene production, and smaller substituents favouring octene production.

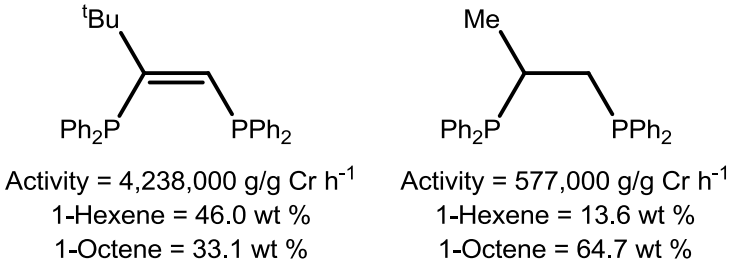

Figure 1.7: Carbon-bridged diphosphine ligands synthesised by Zhang *et al.* Catalysis conditions: 1 µmol precatalyst, 500 eq. MMAO-3A, 30 mL MeCy.[85]

In 2009 Le Floch *et al.* undertook a study of $R'N(CH_2PR_2)_2$ (PCNCP) ligands for ethylene trimerisation.[86] Initial coordination studies proved that the ligands bound to chromium in a κ^2-P,P-bidentate fashion, with no interaction of the central nitrogen with the metal centre. Ethylene oligomerisation tests showed the complexes of the ligands were modestly active (up to 9800 g/g Cr h^{-1}) with regard to trimerisation, but gave good selectivities to 1-hexene (up to 97 % overall selectivity to 1-hexene). More recently, in 2012, Gambarotta and Duchateau *et al.* published work discussing a new highly selective tetramerisation catalyst using a novel $Ph_2PN(R)(CH_2)_nN(R)PPh_2$ ligand framework (Scheme 1.18).[87]

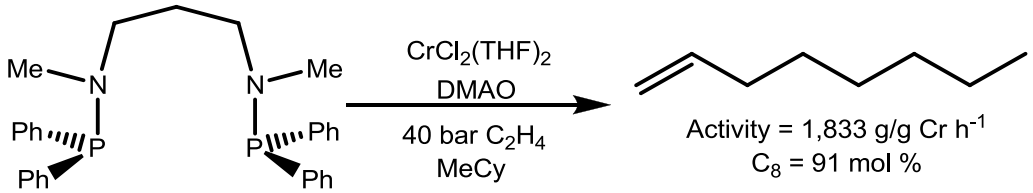

Scheme 1.18: A highly selective ethylene tetramerisation system published by Gambarotta and Duchateau *et al.*[87]

This novel tetramerisation system reported by the Gambarotta and Duchateau group gives very high selectivities towards octene production, but at the expense of catalytic activity. All of the systems reported by Gambarotta and Duchateau *et al.* that yield high selectivity towards 1-hexene or 1-octene display very low catalytic activities, suggesting that there may be room for optimisation of these systems in the future. Nevertheless, these highly selective systems demonstrate that it is possible to create processes that produce solely octene as the oligomer product, rather than octene-rich mixtures of 1-hexene and 1-octene as displayed by other ethylene tetramerisation systems (*e.g.* Sasol's PNP system).[29]

1.2.3.4 Tri- and tetra-merisation systems based on P,N ligands

In recent years a number of new classes of *tri-* and *tetra*-merisation ligands have been developed and published in the open literature based around ligands combining P and N donor groups. One system that has been thoroughly investigated is the PNPN ligand scaffold initially published by Rosenthal *et al.* in 2010.[88] In this communication they report the first synthesis and initial catalytic testing of their novel ligand, which was demonstrated to give an activity of 27,000 g/g Cr h^{-1}, and excellent selectivities with an overall C_6 selectivity of 90 %, of which 99.3 % was 1-hexene (Scheme 1.19). In their study Rosenthal *et al.* found that their PNPN ligand could bind in either a P,P or a P,N fashion depending on the metal precursor and conditions used.

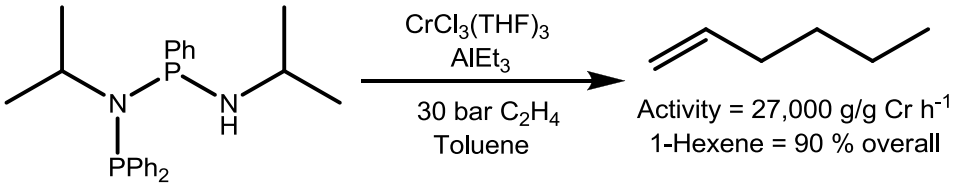

Scheme 1.19: A novel PNPN trimerisation system published by Rosenthal *et al.*[88]

Another paper from the Rosenthal group reported the tethering of the PNPN ligand to a solid polystyrene support, giving a solid-state catalyst with low activities of only 324 g/g Cr h^{-1}, but with selectivities comparable to that of the untethered system.[89] The great advantage of this supported system is the authors reported the catalysis to be indefinitely stable, with catalytic runs carried out over 40 hours. In the following years a number of papers have been published by the Rosenthal group, covering the coordination and metalation chemistry of the PNPN ligands,[90,91] kinetic studies of the PNPN ligands in *tri-*/*tetra*-merisation reactions,[92,93] and studies investigating the effect of changing the various substituent groups on the PNPN backbone.[94,95] In the recent studies concerning the effect of ligand substituents on catalytic activity it has been demonstrated that the efficacy of the PNPN ligand complexes is considerably less sensitive to variations at the central N atom than Sasol's PNP tetramerisation system, suggesting that these PNPN systems are never likely to offer the very high activities of traditional

PNP systems. Nevertheless, these compounds are a promising new class of trimerisation ligand due to the high purity of the 1-hexene produced and their remarkable stability.

In 2008 Gambarotta and Duchateau *et al.* published a pair of papers detailing a series of complexes based around anionic NPN ligands. In the first of these reports a divalent Cr(II) precursor was prepared and found to predominantly catalyse ethylene polymerisation and oligomerisation, under various conditions, but one system utilising $Al^{i}Bu_3$ as an activator gave an active ethylene trimerisation catalyst (Scheme 1.20).[57] In the second of the two publications the system was optimised to give systems with activities up to 11,500 g/g Cr h^{-1} that yielded up to 99.9 % hexene products.[56]

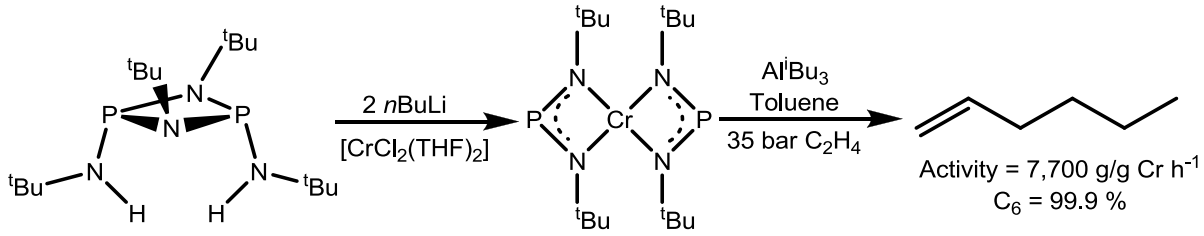

Scheme 1.20: NPN-based catalytic ethylene trimerisation system published by Gambarotta and Duchateau *et al.*[57]

In more recent work Gambarotta, Duchateau and co-workers synthesised novel ligands based around an anionic $[dppm]^-$ centre, incorporating both N and O donor groups.[75] This novel ligand scaffold, has the potential to bind to a metal centre in a number of different coordination modes with four potential donor groups, but it was found that when reacted with $CrCl_3(THF)_3$ the ligand adopted a bidentate P,O coordination mode (Scheme 1.21). When these ligands were tested as precursors in ethylene oligomerisation systems it was found that the process could be optimised to give only hexene and octene within the liquid product fraction, but along with the production of large amounts of polyethylene wax, leading to the conclusion that these systems cannot truly be described as selective ethylene oligomerisation catalysts.

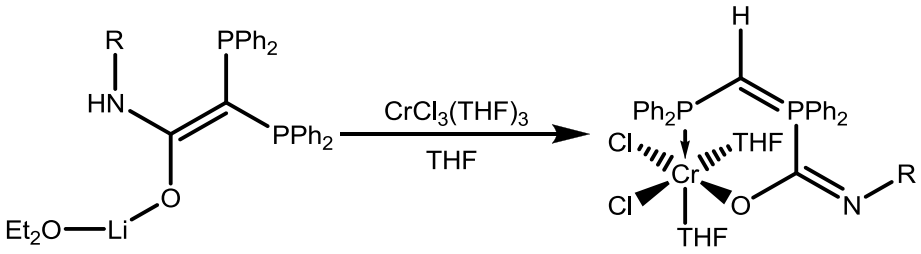

Scheme 1.21: Coordination of Gambarotta and Duchateau *et al.*'s novel anionic P,O ligand with Cr(III)[75]

The Gambarotta group have also recently published the results of their investigations into a selection of new aminophosphine ligands based around a $Ph_2PN(Me)(CH_2)_2$-X (X = NMe_2, PPh_2, Py) framework and the synthesis of well-defined catalyst precursor complexes with Cr(III).[96]

When tested for ethylene oligomerisation activity both the PNN and PNPy variants displayed low activities (12,500 g/g Cr h^{-1} and 4,500 g/g Cr h^{-1}, respectively), but reasonable selectivities to *tri*- and *tetra*-merisation (Figure 1.8). Surprisingly the PNP variant showed no selective ethylene oligomerisation behaviour, giving a Schulz-Flory distribution of oligomers, unlike other carbon-bridged diphosphine ligands discussed earlier in this report (Section 1.2.3.3).

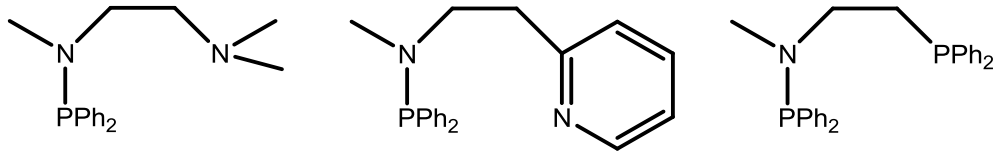

Activity: 12,500 g/g Cr h-1
1-Hexene = 11 %
1-Octene = 89 %
Polyethylene = 2.6 g

Activity: 4,500 g/g Cr h-1
1-Hexene = 25 %
1-Octene = 75 %
Polyethylene = 1.3 g

Activity: 6,700 g/g Cr h-1
1-Hexene = 39 %
1-Octene = 32 %
Polyethylene = 1.0 g

Figure 1.8: Ethylene oligomerisation results from Gambarotta *et al.*'s aminophosphine based ligand systems. Catalysis conditions: 30 µmol precursor complex, 500 eq. DMAO, 100 mL MeCy.[96]

In a follow-up to their 2012 paper Gambarotta and Duchateau *et al.* reported a study of pyridine-phosphine ligands, describing the synthesis, coordination chemistry and ethylene oligomerisation studies carried out (Figure 1.9). Two ligands were investigated with differing backbone chain lengths, and it was found that these gave very different results with regard to ethylene oligomerisation activity. The presence of an extra carbon spacer in the ligand backbone was found to completely switch off the *tri*- and *tetra*-merisation behaviour of the ligand in catalysis, giving predominantly polymer as product. Despite this the authors concluded that this class of pyridine-phosphine ligand still has potential for further research. [97]

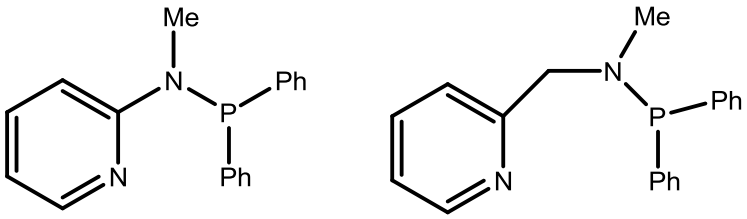

Activity: 22,300 g/g Cr h^{-1}
C_6 = 61 %
C_8 = 31 %
Polyethylene = 5 wt %

Activity: 4,900 g/g Cr h^{-1}
C_6 = 36 %
C_8 = 58 %
Polyethylene = 80 wt %

Figure 1.9: Catalytic activities of pyridine-phosphine ligand-based ethylene oligomerisation systems tested by Gambarotta and Duchateau *et al.* Catalysis conditions: 10 µmol catalyst precursor, 500 eq. MAO, 100 mL MeCy.[97]

The potential for compounds containing P-N bonds to behave as ancillary ligands in ethylene *tri*-/*tetra*-merisation systems has been investigated by Duchateau *et al.* for a series of molecules. Out of the selection tested, only one showed any reasonable *tri*-/*tetra*-merisation activity in combination with Cr(III), and this was *N*-pyrrolyldiphenylphosphine, with an activity

of 11,200 g/g Cr h^{-1} and good selectivities to hexene (37 mol %) and octene (58.3 mol %).[98] *N*-Pyrrolyldiphenylphosphine is an interesting ligand to choose in a system containing chromium, as it has been recently proved that P-N bonds are capable of being broken in selective ethylene oligomerisation systems by Gambarotta *et al.*[99] This demonstrates that it may be possible for the P-N linkage in *N*-pyrrolyldiphenylphosphine to be broken, yielding pyrrole and diphenylphosphine, to give a system remarkably similar to the Phillips trimerisation system (see Section 1.2.1.1). If this P,N breakage does occur, then it is perhaps unsurprising that an active ethylene *tri*-/*tetra*-merisation system is formed.

One of the most notable recent discoveries vis-á-vis P,N ligands in selective ethylene oligomerisation chemistry is the catalytic activity of systems using P-imine based ligands. The first investigation into imine-based trimerisation systems was published by Bluhm *et al.* on their tridentate imine ligands combined with N, P, O and S donor atoms.[100] Of the ligands synthesised, Bluhm reported their P,N,P donor ligand to give only ethylene trimerisation products from catalysis (97 % overall selectivity to 1-hexene), but this system gave very low activities of only 25 g/g Cr h^{-1} (Scheme 1.22). All of the other systems tested gave higher catalytic activities, but at the expense of hexene selectivity.

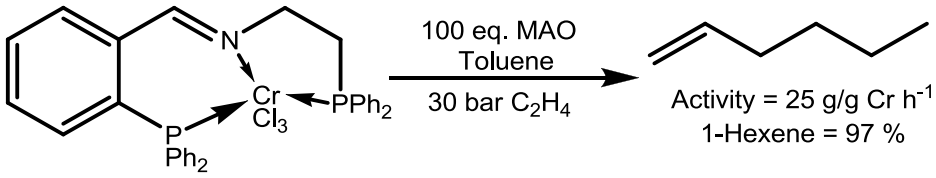

Scheme 1.22: Selective ethylene trimerisation system based on phosphine-imine ligands reported by Bluhm *et al*.[100]

Workers from Chevron Phillips published a very similar system to that of Bluhm *et al.*, based on *N*-phosphinoamidine ligands bound to Cr(III) centres. It was shown that a handful of these complexes performed excellently as selective ethylene oligomerisation precursors, with the best system giving activities up to 1,052,000 g/g Cr h^{-1} with an overall selectivity of 93 % to 1-hexene, comparable to the best reported PNP-based systems (Figure 1.10).[101,102] Through modification of the steric parameters of the ligand it was possible to switch the selectivity of the system to produce up to 45 % 1-octene.

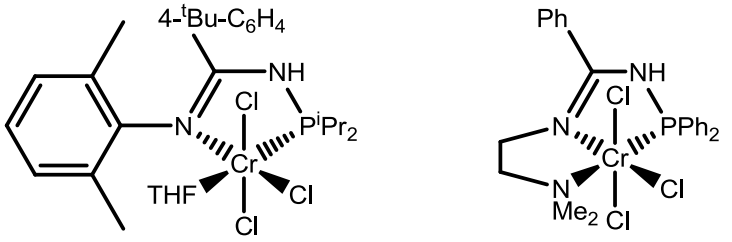

Activity = 1,052,000 g/g Cr h^{-1}
1-Hexene = 93.6 wt %
1-Octene = 0.9 wt %
Polyethylene = trace

Activity = 0 g/g Cr h^{-1}
1-Hexene = 0 wt %
1-Octene = 0 wt %
Polyethylene = 1.2 g

Figure 1.10: Bidentate vs. tridentate phosphinoamidine based ethylene trimerisation systems.[101]

Interestingly, when a third donor moiety was added to the Chevron Phillips phosphinoamidine compound to give a tridentate ligand, this was found to shut down the catalytic activity of the system entirely, despite the potential for the tertiary amine group to behave as a pendant donor as seen in previous PNP-based systems (such as the first BP Cr(PNP) trimerisation system[28]). The authors concluded that the abstraction of THF from the bidentate κ^2-P,N bound complex is a vital step in the catalytic cycle (Scheme 1.23), hence the tridentate analogue was inactive due to the lack of THF to be abstracted and leaving a vacant coordination site.

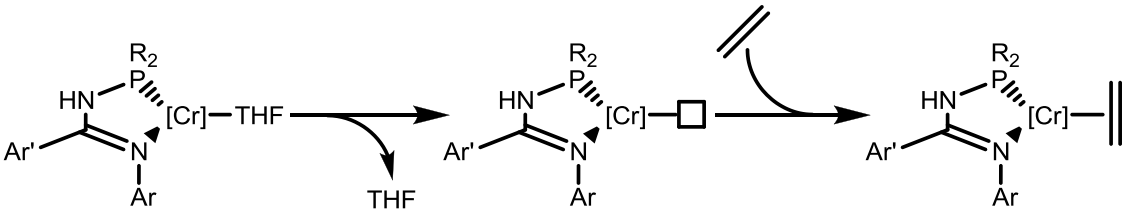

Scheme 1.23: Suggested catalyst activation pathway for the Chevron Phillips phosphinoamidine-based oligomerisation system, going *via* a THF abstraction step.[101]

1.3 P,N Ligands

As is obvious from Section 1.2, the field of *tri*- and *tetra*-merisation systems based on PNP ligands is relatively mature and has been thoroughly investigated by both the academic and industrial communities. It is therefore of interest to establish new systems based on an alternative class of ligand for selective ethylene oligomerisation. To this end, the investigations in this thesis will focus on developing novel ligands based on a P,N framework, which is a relatively new field in chromium-based *tri*- and *tetra*-merisation chemistry.

1.3.1 Heteroditopic ligands

The use of phosphine-based ligands containing functional groups that are also donor atoms is a very attractive proposal for many areas of research in homogeneous catalysis. This approach of using heteroditopic ligands in coordination chemistry means that different donor properties of varying donor groups can be combined into one species to create a “hybrid” ligand that can adopt a variety of coordination modes with a metal centre (Figure 1.11).

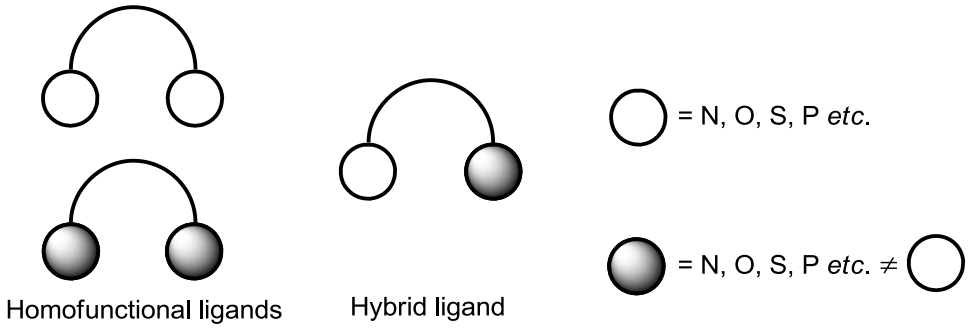

Figure 1.11: Homo- and bi-functional bidentate ligands.

A combination of both hard and soft donor groups into a single ligand can give rise to a system in which partial dissociation of one of the Lewis basic moieties can occur in solution, opening a vacant coordination site at the metal centre. This so-called “hemi-labile” nature of these ligands has significance in catalysis, as vacant coordination sites on a metal centre are vital to allow the coordination of a substrate species, to form an active catalytic species.

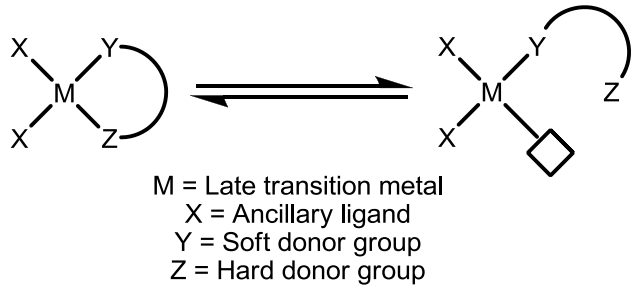

Scheme 1.24: A reversible "hemi-labile" dissociation/association process.

Pearson's "hard-soft-acid-base" theory predicts that a soft polarisable phosphine group will bind strongly to large, soft late-transition metals, in comparison to a hard amine group which will coordinate strongly to harder early transition metal centres.[103] On this basis heteroditopic ligands can be designed that incorporate a phosphine "tether", to bind strongly to soft metal centres, while containing N- or O-donor groups with weaker coordination properties that allow for dissociation in solution.

1.3.2 Heteroditopic ligands and their uses in catalysis

Possibly the most famous use of heteroditopic ligands in industrial catalysis is in the Shell Higher Olefin Process (SHOP), in which a P,O donor ligand is used in combination with nickel to yield an ethylene oligomerisation catalyst precursor (Scheme 1.25).[104-106] Since the discovery and commercialisation of SHOP technology in the 1970s a huge amount of research has been carried out investigating many facets of the oligomerisation system involved.

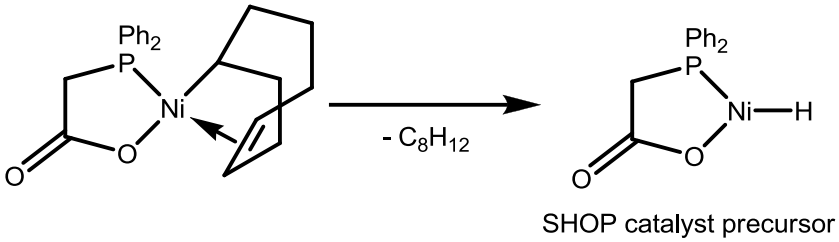

Scheme 1.25: Postulated formation of SHOP catalyst precursor.[104]

The potential for SHOP-type P,O-based ligands to possess hemi-labile character in other transition metal complexes is well documented in the literature, one example being published by Braunstein *et al.* in 1987 using model palladium complexes to investigate the coordination chemistry of their β-phosphinoketonate ligands.[107] It was demonstrated that upon the dissolution of a single isomer of their Pd(P,O) complex in CD_2Cl_2 isomerisation was observed, yielding a 1:1 mixture of the two possible product isomers (Scheme 1.26). From this observation the authors concluded that the mechanism for this transformation must involve the dissociation and rotation of the P,O ligand around the Pd-P bond.

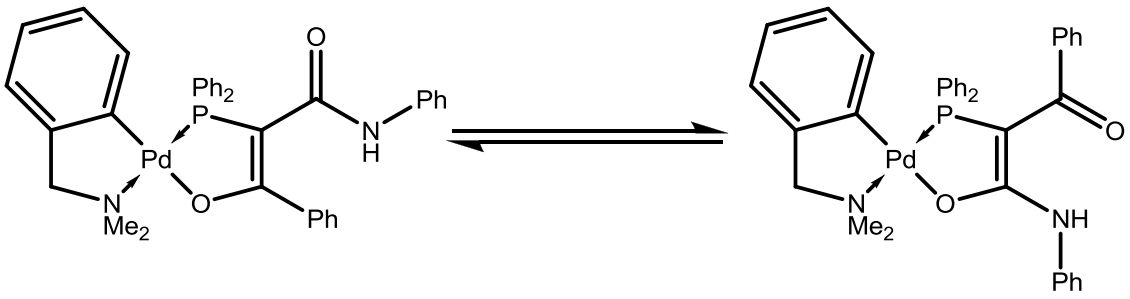

Scheme 1.26: Isomerisation of a Pd(P,O) complex synthesised by Braunstein *et al.*[107]

Keim *et al.* investigated the use of a similar class of heteroditopic P,O ligand with palladium for the co-dimerisation of ethylene and styrene, as well as the co-oligomerisation of ethylene and carbon monoxide. In this study both mono- and bi-dentate coordination complexes were successfully isolated and characterised, and the monodentate complex was easily converted to the bidentate species through oxidation of the palladium using $AgSbF_6$.[108] The bidentate complexes were shown to offer far better performance in the catalytic systems tested than the monodentate equivalents, leading the authors to speculate that the dissociation of the Pd-O bond is an important step in the formation of an active catalytic species.

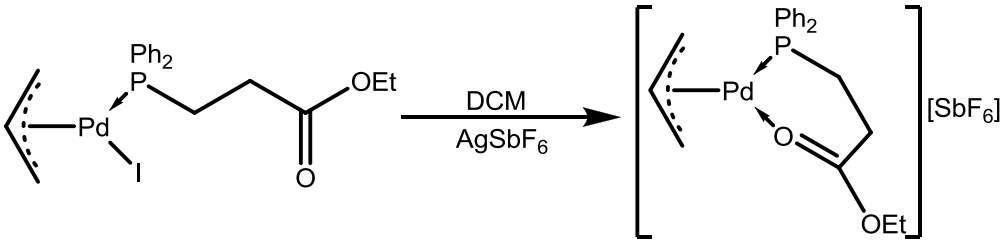

Scheme 1.27: Conversion of a mono- to bi-dentate Pd(P,O) complex.[108]

More recently Cavell *et al.* have published work concerning palladium complexes of OPN phosphine ligands and their application in catalytic reactions of carbon monoxide with alkenes and alkynes.[109] In their three-donor systems they successfully isolated bidentate planar P,N-bound complexes (Scheme 1.28), but also report tentative indications of the ligand binding to palladium in a tridentate O,P,N planar fashion. Unfortunately, the data to indicate the presence of a planar tridentate species could only be gathered by NMR spectroscopy at low temperatures, and so the species could not be fully characterised.

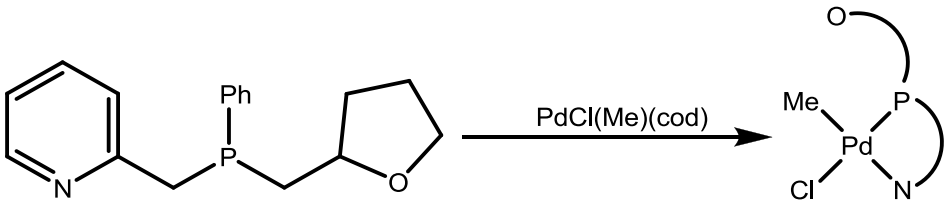

Scheme 1.28: Complexation of Cavell *et al.*'s OPN ligand with palladium.[109]

Heteroditopic P,N-type ligands have also been used in a range of catalytic applications, including hydrogenation,[*e.g.*110] Diels-Alder,[111] and oligomerisation processes.[*e.g.*112] One such example is the class of phosphine-oxazoline P,N ligands investigated by Braunstein *et al.* for use in transfer hydrogenation catalysis.[113] It was demonstrated that upon coordination of the P-oxazoline compound with palladium, two C=N vibrations were observed in the solution state IR spectrum of the complex. It was concluded that these two signals correspond to the κ^1-P-mono- and κ^2-P,N-bi-dentate complexes interconverting in solution due to the hemi-labile nature of the ligand.

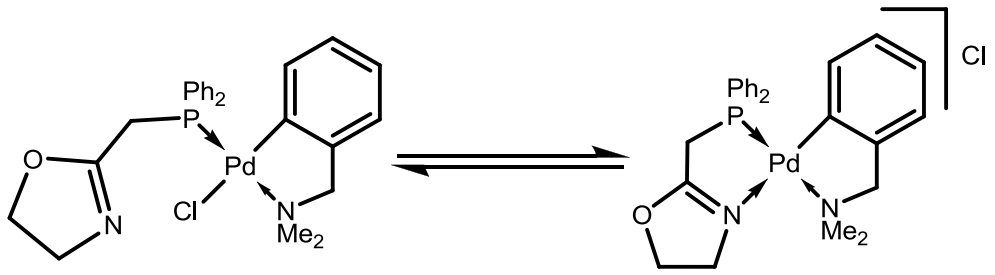

Scheme 1.29: Hemi-labile behaviour displayed by a P-oxazoline ligand reported by Braunstein *et al.*[113]

Overall it is clear that hemi-labile ligands have a wide range of uses in modern chemistry, especially with regard to catalysis. The concept of hemi-labile ligands has previously been touched upon in this thesis with regard to the coordinative properties of BP's PNP$^{o\text{-OMe}}$ ligand for selective ethylene oligomerisation. In the first report concerning this ligand by Wass *et al.* it was suggested that the ability of the pendant OMe donor group to reversibly coordinate to the chromium centre was vital in creating an active catalytic system,[28] with further weight added to this argument by Bercaw and Labinger *et al.* and the publication of their Cr(κ^3-P,P,O-((*o*-OMeC$_6$H$_4$)$_2$PNP(*o*-OMeC$_6$H$_4$)$_2$)Cl$_3$ complex.[37] It is hoped that by applying the principles of heteroditopic and hemi-labile ligand design to the synthesis of novel P,N ligand scaffolds new selective ethylene oligomerisation systems can be developed, to match the high activities and selectivities of existing literature systems.

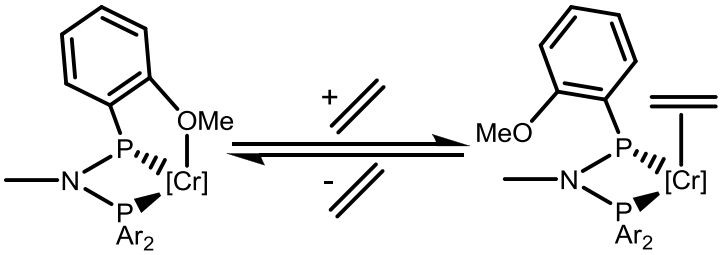

Scheme 1.30: Suggested variable coordination behaviour of the BP Cr(PNP) trimerisation catalyst.

1.4 Thesis Aims and Objectives

This thesis aims to report and discuss the search for, and development of, new catalytic selective ethylene oligomerisation systems based around P,N-type ligands. Studies of two classes of ligand will be reported. The first of these will be a series of PNE-type ligands that have previously been synthesised by Dyer *et al.* (Figure 1.12), which will be reported in Chapter 2.[114]

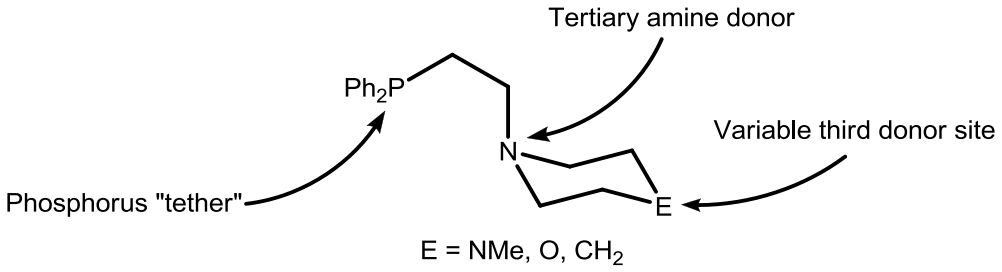

Figure 1.12: PNE ligand synthesised by Dyer *et al.*[114] to be investigated in this thesis.

The coordination of these PNE ligands with late transition metals has previously been investigated, but no work has been done regarding their coordination properties with early transition metals or studying their behaviour as precursors in ethylene oligomerisation systems. To this end, the coordinative properties of PNE ligands with a variety of group VI metal complexes will be scrutinised. In combination with Cr(III) species, the potential for PNE ligands to act as selective ethylene oligomerisation precursors will be tested using conditions comparable to those found in the literature.

The second ligand class to be investigated will be based around an iminophosphine (PCN) framework. It is proposed that PCN ligands may mimic the structure of PNP ligands when bound to chromium, and therefore promote selective ethylene oligomerisation in catalytic systems (Figure 1.13).

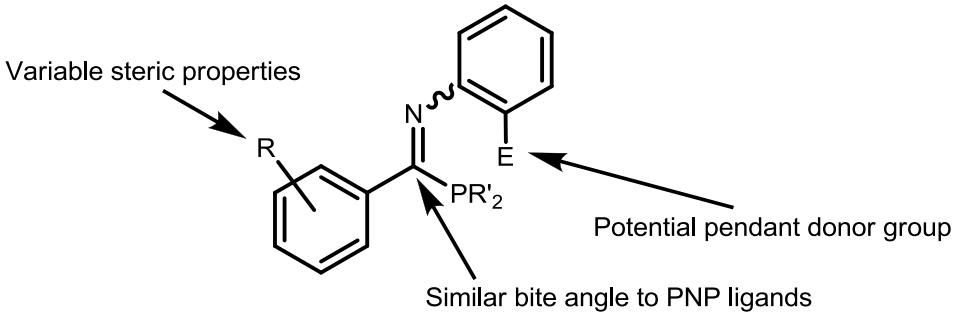

Figure 1.13: The target PCN ligand framework for this investigation

This class of PCN compound is not well represented in the literature, and very few examples of their synthesis have been reported. In order for these PCN ligands to be thoroughly investigated a new synthetic route to compounds bearing an iminophosphine backbone must

be developed, which will be discussed in Chapter 3 of this thesis. The method should preferably be modular, easily scalable, and utilise starting materials that are affordable and readily available. Once a synthetic route has been optimised, the coordination chemistry with chromium species will be investigated, which will be reported in Chapter 4. The synthesis of model Cr(PCN) complexes will be carried out in order to probe both the ligand structure and the coordinative properties of these novel complexes.

Finally, in Chapter 5, the PCN ligands synthesised will be tested as catalyst precursors in selective ethylene oligomerisation systems. From these catalytic data it is hoped that trends and relationships between ligand structure and catalytic activity/selectivity can be drawn to aid the design of future PCN ligands for use in ethylene *tri*- and *tetra*-merisation systems.

1.5 References

(1) Vogt, D. *Applied Homogeneous Catalysis with Organometallic Compounds Vol. 1*; 2nd ed.; Wiley VCH: Weinheim, 2002; p 242.

(2) Camara Greiner, E. O.; Inoguchi, Y.; CEH Marketing Research Report "*Linear Alpha Olefins*", **2010**.

(3) Forestière, A.; Olivier-Bourbigou, H.; Saussine, L. *Oil Gas Sci. Technol. Rev. IFP* **2009**, *64*, 649.

(4) Plains, W.; Nexant Chem Systems: New York, USA, 2008.

(5) Arlman, E. J.; Cossee, P. *J. Catal.* **1964**, *3*, 99.

(6) Schulz, G. V. *Z. Naturforsch., B: Chem. Sci.* **1935**, *30*, 379.

(7) Flory, P. J. *J. Am. Chem. Soc.* **1940**, *62*, 1561.

(8) Dixon, J. T.; Green, M. J.; Hess, F. M.; Morgan, D. H. *J. Organomet. Chem.* **2004**, *689*, 3641.

(9) Wass, D. F. *Dalton Trans.* **2007**, 816.

(10) McGuinness, D. S. *Chem. Rev.* **2011**, *111*, 2321.

(11) van Leeuwen, P. W. N. M.; Clément, N. D.; Tschan, M. J.-L. *Coord. Chem. Rev.* **2011**, *255*, 1499.

(12) Agapie, T. *Coord. Chem. Rev.* **2011**, *255*, 861.

(13) Belov, G. P. *Petrol. Chem.* **2012**, *52*, 139.

(14) Manyik, R. M.; Walker, W. E.; Wilson, T. P.; US 3300458 (Union Carbide Corporation), January 24, **1967**.

(15) Manyik, R. M.; Walker, W. E.; Wilson, T. P. *J. Catal.* **1977**, *47*, 197.

(16) Reagan, W. K. *Symp. Prepr. Conv. Light Olefins, Div. Pet. Chem., Am. Chem. Soc.* **1989**, *34*.

(17) Reagan, W. K.; EP 0417477 (Phillips Petroleum Company), March 20, **1991**.

(18) W.K. Reagan, J.W. Freeman, B.K. Conroy, T.M. Pettijohn, E.A. Benham, EP 0608447 (Phillips Petroleum Company), August 3, **1994**

(19) J.W. Freeman, J.L. Buster, R.D. Knudsen, US 5,856,257 (Phillips Petroleum Company), January 5, **1999**.

(20) Y. Araki, H. Nakamura, Y. Nanba, T. Okanu, US 5,856,612 (Mitsubishi Chemical Corporation), January 5, **1999**.

(21) van Rensburg, W. J.; Grové, C.; Steynberg, J. P.; Stark, K. B.; Huyser, J. J. Steynberg, P. J. *Organometallics* **2004**, *23*, 1207.

(22) Fang, Y. Q.; Liu, Y. X.; Ke, Y. C.; Guo, C. Y.; Zhu, N.; Mi, X.; Ma, Z.; Hu, Y. L. *Appl. Catal. A* **2002**, *235*, 33.

(23) Jabri, A.; Mason, C. B.; Sim, Y.; Gambarotta, S.; Burchell, T. J.; Duchateau, R. *Angew. Chem. Int. Ed.* **2008**, *47*, 9717.

(24) Vidyaratne, I.; Nikiforov, G. B.; Gorelsky, S. I.; Gambarotta, S.; Duchateau, R.; Korobkov, I. *Angew. Chem. Int. Ed.* **2009**, *48*, 6552.

(25) Skobelev, I. Y.; Panchenko, V. N.; Lyakin, O. Y.; Bryliakov, K. P.; Zakharov, V. A.; Talsi, E. P. *Organometallics* **2010**, *29*, 2943.

(26) Cooley, N. A.; Green, S. M.; Wass, D. F.; Heslop, K.; Orpen, A. G.; Pringle, P. G. *Organometallics* **2001**, *20*, 4769.

(27) D.F. Wass, WO 02/04119 (BP Chemicals Ltd), January 17, **2002**.

(28) Carter, A.; Cohen, S. A.; Cooley, N. A.; Murphy, A.; Scutt, J.; Wass, D. F. *Chem. Commun.* **2002**, 858.

(29) Blann, K.; Bollmann, A.; Dixon, J. T.; Neveling, A.; Morgan, D. H.; Maumela, H.; Killian, E.; Hess, F.; Otto, S.; Pepler, L.; Mahomed, H.; Overett, M. WO 04056479A1 (Sasol Technology), **2004**

(30) Bollmann, A.; Blann, K.; Dixon, J. T.; Hess, F. M.; Killian, E.; Maumela, H.; McGuinness, D. S.; Morgan, D. H.; Neveling, A.; Otto, S.; Overett, M.; Slawin, A. M. Z.; Wasserscheid, P.; Kuhlmann, S. *J. Am. Chem. Soc.* **2004**, *126*, 14712.
(31) Yu, Z. X.; Houk, K. N. *Angew. Chem. Int. Ed.* **2003**, *42*, 808.
(32) Blok, A. N. J.; Budzelaar, P. H. M.; Gal, A. W. *Organometallics* **2003**, *22*, 2564.
(33) Kuhlmann, S.; Paetz, C.; Hägele, C.; Blann, K.; Walsh, R.; Dixon, J. T.; Scholz, J.; Haumann, M.; Wasserscheid, P. *J. Catal.* **2009**, *262*, 83.
(34) Briggs, J. R. *J. Chem. Soc., Chem. Commun.* **1989**, 674.
(35) McDermott, J. X.; White, J. F.; Whitesides, G. M. *J. Am. Chem. Soc.* **1976**, *98*, 6521.
(36) Emrich, R.; Heinemann, O.; Jolly, P. W.; Krüger, C.; Verhovnik, G. P. J. *Organometallics* **1997**, *16*, 1511.
(37) Agapie, T.; Schofer, S. J.; Labinger, J. A.; Bercaw, J. E. *J. Am. Chem. Soc.* **2004**, *126*, 1304.
(38) Agapie, T.; Labinger, J. A.; Bercaw, J. E. *J. Am. Chem. Soc.* **2007**, *129*, 14281.
(39) Overett, M. J.; Blann, K.; Bollmann, A.; Dixon, J. T.; Haasbroek, D.; Killian, E.; Maumela, H.; McGuinness, D. S.; Morgan, D. H. *J. Am. Chem. Soc.* **2005**, *127*, 10723.
(40) Peitz, S.; Aluri, B. R.; Peulecke, N.; Mueller, B. H.; Woehl, A.; Mueller, W.; Al-Hazmi, M. H.; Mosa, F. M.; Rosenthal, U. *Chem. Eur. J.* **2010**, *16*, 7670.
(41) Rebenstorf, B.; Larsson, R. *J. Mol. Catal.* **1981**, *11*, 247.
(42) Espelid, O.; Borve, K. J. *J. Catal.* **2002**, *206*, 331.
(43) Theopold, K. H. *Eur. J. Inorg. Chem.* **1998**, *1998*, 15.
(44) Licciulli, S.; Thapa, I.; Albahily, K.; Korobkov, I.; Gambarotta, S.; Duchateau, R.; Chevalier, R.; Schuhen, K. *Angew. Chem. Int. Ed.* **2010**, *49*, 9225.
(45) Rucklidge, A. J.; McGuinness, D. S.; Tooze, R. P.; Slawin, A. M. Z.; Pelletier, J. D. A.; Hanton, M. J.; Webb, P. B. *Organometallics* **2007**, *26*, 2782.
(46) Bowen, L. E.; Haddow, M. F.; Orpen, A. G.; Wass, D. F. *Dalton Trans.* **2007**, 1160.
(47) Schofer, S. J.; Day, M. W.; Henling, L. M.; Labinger, J. A.; Bercaw, J. E. *Organometallics* **2006**, *25*, 2743.
(48) Brückner, A.; Jabor, J. K.; McConnell, A. E. C.; Webb, P. B. *Organometallics* **2008**, *27*, 3849.
(49) Do, L. H.; Labinger, J. A.; Bercaw, J. E. *ACS Catal.* **2013**, *3*, 2582.
(50) Temple, C.; Jabri, A.; Crewdson, P.; Gambarotta, S.; Korobkov, I.; Duchateau, R. *Angew. Chem. Int. Ed.* **2006**, *45*, 7050.
(51) Köhn, R. D.; Smith, D.; Mahon, M. F.; Prinz, M.; Mihan, S.; Kociok-Köhn, G. *J. Organomet. Chem.* **2003**, *683*, 200.
(52) Monillas, W. H.; Young, J. F.; Yap, G. P. A.; Theopold, K. H. *Dalton Trans.* **2013**, *42*, 9198.
(53) Jabri, A.; Crewdson, P.; Gambarotta, S.; Korobkov, I.; Duchateau, R. *Organometallics* **2006**, *25*, 715.
(54) McGuinness, D. S.; Brown, D. B.; Tooze, R. P.; Hess, F. M.; Dixon, J. T.; Slawin, A. M. Z. *Organometallics* **2006**, *25*, 3605.
(55) Bhaduri, S.; Mukhopadhyay, S.; Kulkarni, S. A. *J. Organomet. Chem.* **2009**, *694*, 1297.
(56) Albahily, K.; Al-Baldawi, D.; Gambarotta, S.; Duchateau, R.; Koç, E.; Burchell, T. J. *Organometallics* **2008**, *27*, 5708.
(57) Albahily, K.; Koç, E.; Al-Baldawi, D.; Savard, D.; Gambarotta, S.; Burchell, T. J.; Duchateau, R. *Angew. Chem. Int. Ed.* **2008**, *47*, 5816.
(58) Jabri, A.; Temple, C.; Crewdson, P.; Gambarotta, S.; Korobkov, I.; Duchateau, R. *J. Am. Chem. Soc.* **2006**, *128*, 9238.

(59) Rabeah, J.; Bauer, M.; Baumann, W.; McConnell, A. E. C.; Gabrielli, W. F.; Webb, P. B.; Selent, D.; Brückner, A. *ACS Catal.* **2013**, *3*, 95.
(60) Kaminsky, W. *Macromolecules* **2012**, *45*, 3289.
(61) Sinn, H.; Kaminsky, W.; Vollmer, H.-J.; Woldt, R. *Angew. Chem. Int. Ed.* **1980**, *19*, 390.
(62) Chen, E. Y.; Marks, T. J. *Chem. Rev.* **2000**, *100*, 1391.
(63) Zijlstra, H. S.; Harder, S. *Eur. J. Inorg. Chem.* **2015**, *1*, 19.
(64) Janse van Rensburg, W.; van den Berg, J.-A.; Steynberg, P. J. *Organometallics* **2007**, *26*, 1000.
(65) Trefz, T. K.; Henderson, M. A.; Wang, M. Y.; Collins, S.; McIndoe, J. S. *Organometallics* **2013**, *32*, 3149.
(66) Ghiotto, F.; Pateraki, C.; Tanskanen, J.; Severn, J. R.; Luehmann, N.; Kusmin, A.; Stellbrink, J.; Linnolahti, M.; Bochmann, M. *Organometallics* **2013,** *32*, 3354.
(67) Reddy, S. S.; Sivaram, S. *Prog. Polym. Sci.* **1995**, *20*, 309.
(68) Pasynkiewicz, S.; Boleslawski, M.; Sadownik, A. *J. Organomet. Chem.* **1976**, *113*, 303.
(69) McGuinness, D. S.; Overett, M.; Tooze, R. P.; Blann, K.; Dixon, J. T.; Slawin, A. M. Z. *Organometallics* **2007**, *26*, 1108.
(70) Krossing, I. *Chem. Eur. J.* **2001**, *7*, 490.
(71) McGuinness, D. S.; Rucklidge, A. J.; Tooze, R. P.; Slawin, A. M. Z. *Organometallics* **2007**, *26*, 2561.
(72) Blann, K.; Bollmann, A.; Dixon, J. T.; Hess, F. M.; Killian, E.; Maumela, H.; Morgan, D. H.; Neveling, A.; Otto, S.; Overett, M. J. *Chem. Commun.* **2005**, 620.
(73) Overett, M. J.; Blann, K.; Bollmann, A.; Dixon, J. T.; Hess, F.; Killian, E.; Maumela, H.; Morgan, D. H.; Neveling, A.; Otto, S. *Chem. Commun.* **2005**, 622.
(74) Agapie, T.; Day, M. W.; Henling, L. M.; Labinger, J. A.; Bercaw, J. E. *Organometallics* **2006**, *25*, 2733.
(75) Kulangara, S. V.; Mason, C.; Juba, M.; Yang, Y.; Thapa, I.; Gambarotta, S.; Korobkov, I.; Duchateau, R. *Organometallics* **2012**, *31*, 6438.
(76) Stennett, T. E.; Hey, T. W.; Ball, L. T.; Flynn, S. R.; Radcliffe, J. E.; McMullin, C. L.; Wingad, R. L.; Wass, D. F. *ChemCatChem* **2013**, *5*, 2946.
(77) Kuhlmann, S.; Blann, K.; Bollmann, A.; Dixon, J. T.; Killian, E.; Maumela, M. C.; Maumela, H.; Morgan, D. H.; Prétorius, M.; Taccardi, N.; Wasserscheid, P. *J. Catal.* **2007**, *245*, 279.
(78) Blann, K.; Bollmann, A.; de Bod, H.; Dixon, J. T.; Killian, E.; Nongodlwana, P.; Maumela, M. C.; Maumela, H.; McConnell, A. E.; Morgan, D. H.; Overett, M. J.; Prétorius, M.; Kuhlmann, S.; Wasserscheid, P. *J. Catal.* **2007**, *249*, 244.
(79) Killian, E.; Blann, K.; Bollmann, A.; Dixon, J. T.; Kuhlmann, S.; Maumela, M. C.; Maumela, H.; Morgan, D. H.; Nongodlwana, P.; Overett, M. J.; Pretorius, M.; Höfener, K.; Wasserscheid, P. *J. Mol. Catal. A: Chem.* **2007**, *270*, 214.
(80) Jiang, T.; Zhang, S.; Jiang, X.; Yang, C.; Niu, B.; Ning, Y. *J. Mol. Catal. A: Chem.* **2008**, *279*, 90.
(81) Weng, Z.; Teo, S.; Andy Hor, T. S. *Dalton Trans.* **2007**, 3493.
(82) Elowe, P. R.; McCann, C.; Pringle, P. G.; Spitzmesser, S. K.; Bercaw, J. E. *Organometallics* **2006**, *25*, 5255.
(83) Suttil, J. A.; Wasserscheid, P.; McGuinness, D. S.; Gardiner, M. G.; Evans, S. J. *Catal. Sci. Tech.* **2014**, *4*, 2574.
(84) Overett, M. J.; Blann, K.; Bollmann, A.; de Villiers, R.; Dixon, J. T.; Killian, E.; Maumela, M. C.; Maumela, H.; McGuinness, D. S.; Morgan, D. H. *J. Mol. Catal. A: Chem.* **2008**, *283*, 114.

(85) Zhang, J.; Wang, X.; Zhang, X.; Wu, W.; Zhang, G.; Xu, S.; Shi, M. *ACS Catal.* **2013**, 2311.
(86) Klemps, C.; Payet, E.; Magna, L.; Saussine, L.; Le Goff, X. F.; Le Floch, P. *Chem. Eur. J.* **2009**, *15*, 8259.
(87) Shaikh, Y.; Albahily, K.; Sutcliffe, M.; Fomitcheva, V.; Gambarotta, S.; Korobkov, I.; Duchateau, R. *Angew. Chem. Int. Ed.* **2012**, *51*, 1366.
(88) Peitz, S.; Peulecke, N.; Aluri, B. R.; Hansen, S.; Müller, B. H.; Spannenberg, A.; Rosenthal, U.; Al-Hazmi, M. H.; Mosa, F. M.; Wöhl, A.; Müller, W. *Eur. J. Inorg. Chem.* **2010**, *2010*, 1167.
(89) Peulecke, N.; Müller, B. H.; Peitz, S.; Aluri, B. R.; Rosenthal, U.; Wöhl, A.; Müller, W.; Al-Hazmi, M. H.; Mosa, F. M. *ChemCatChem* **2010**, *2*, 1079.
(90) Aluri, B. R.; Peulecke, N.; Peitz, S.; Spannenberg, A.; Müller, B. H.; Schulz, S.; Drexler, H.-J.; Heller, D.; Al-Hazmi, M. H.; Mosa, F. M.; Wöhl, A.; Müller, W.; Rosenthal, U. *Dalton Trans.* **2010**, *39*, 7911.
(91) Peitz, S.; Peulecke, N.; Aluri, B. R.; Muller, B. H.; Spannenberg, A.; Rosenthal, U.; Al-Hazmi, M. H.; Mosa, F. M.; Wohl, A.; Muller, W. *Organometallics* **2010**, *29*, 5263.
(92) Müller, W.; Wöhl, A.; Peitz, S.; Peulecke, N.; Aluri, B. R.; Müller, B. H.; Heller, D.; Rosenthal, U.; Al-Hazmi, M. H.; Mosa, F. M. *ChemCatChem* **2010**, *2*, 1130.
(93) Wöhl, A.; Müller, W.; Peitz, S.; Peulecke, N.; Aluri, B. R.; Müller, B. H.; Heller, D.; Rosenthal, U.; Al-Hazmi, M. H.; Mosa, F. M. *Chem. Eur. J.* **2010**, *16*, 7833.
(94) Härzschel, S.; Kühn, F. E.; Wöhl, A.; Müller, W.; Al-Hazmi, M. H.; Alqahtani, A. M.; Müller, B. H.; Peulecke, N.; Rosenthal, U. *Catal. Sci. Tech.* **2015**, *5*, 1678.
(95) Heinig, S.; Wöhl, A.; Müller, W.; Al-Hazmi, M. H.; Müller, B. H.; Peulecke, N.; Rosenthal, U. *ChemCatChem* **2013**, *5*, 3107.
(96) Shaikh, Y.; Gurnham, J.; Albahily, K.; Gambarotta, S.; Korobkov, I. *Organometallics* **2012**, *31*, 7427.
(97) Yang, Y.; Gurnham, J.; Liu, B.; Duchateau, R.; Gambarotta, S.; Korobkov, I. *Organometallics* **2014**, *33*, 5749.
(98) Yang, Y.; Liu, Z.; Liu, B.; Duchateau, R. *ACS Catal.* **2013**, 2353.
(99) Alzamly, A.; Gambarotta, S.; Korobkov, I. *Organometallics* **2014**, *33*, 1602.
(100) Bluhm, M. E.; Walter, O.; Döring, M. *J. Organomet. Chem.* **2005**, *690*, 713.
(101) Sydora, O. L.; Jones, T. C.; Small, B. L.; Nett, A. J.; Fischer, A. a.; Carney, M. J. *ACS Catal.* **2012**, *2*, 2452.
(102) Sydora, O. L.; Carney, M. J.; Small, B. L.; Hutshison, S.; Gee, J. C.; WO 2011/082192 (Chevron Phillips Chemical Company LP), December 29, 2011.
(103) Pearson, R. G. *J. Am. Chem. Soc.* **1963**, *85*, 3533.
(104) Keim, W. *Angew. Chem. Int. Ed.* **1990**, *29*, 235.
(105) Mol, J. C. *J. Mol. Catal. A: Chem.* **2004**, *213*, 39.
(106) Keim, W. *Angew. Chem. Int. Ed.* **2013**, *52*, 12492.
(107) Bouaoud, S.-E.; Braunstein, P.; Grandjean, D.; Matt, D.; Nobel, D. *J. Chem. Soc., Chem. Commun.* **1987**, 488.
(108) Britovsek, G. J. P.; Keim, W.; Mecking, S.; Sainz, D.; Wagner, T. *J. Chem. Soc., Chem. Commun.* **1993**, 1632.
(109) Green, M. J.; Cavell, K. J.; Edwards, P. G.; Tooze, R. P.; Skelton, B. W.; White, A. H. *Dalton Trans.* **2004**, 3251.
(110) Pàmies, O.; Andersson, P. G.; Diéguez, M. *Chem. Eur. J.* **2010**, *16*, 14232.
(111) Takahashi, K.; Nakano, H.; Fujita, R. *Chem. Commun.* **2007**, 263.
(112) Weng, Z.; Teo, S.; Hor, T. S. A. *Organometallics* **2006**, *25*, 4878.
(113) Braunstein, P.; Naud, F.; Rettig, S. J. *New J. Chem.* **2001**, *25*, 32.

(114) Anderson, C. E.; Apperley, D. C.; Batsanov, A. S.; Dyer, P. W.; Howard, J. A. K. *Dalton Trans.* **2006**, 4134.

Chapter 2:

The Coordination Chemistry of PNE Ligands and Their Potential Role in Ethylene Oligomerisation Systems

2.1 Introduction

The use of multidentate ligands in ethylene oligomerisation and polymerisation catalysis chemistry is well established.[1] Multidentate ligands offer a multitude of advantages over their monodentate counterparts, due to their increased control over metal coordination number, improved influence of metal stereochemistry and greater steric effects when bound to a metal centre.[2] Heteroditopic ligands are of particular interest due to the ease with which the reactivity of the compounds can be altered. By individually altering the differing donor groups of heteroditopic ligands, greater control of the electronic properties of the resulting metal complexes can be achieved. The advantages and selected uses of heteroditopic and hemi-labile ligands in catalysis are briefly detailed in Section 1.3.2.

One such example of a novel class of heteroditopic ligand was reported by Dyer *et al.* in 2006, concerning a difunctionalized phosphine ligand based around a PNE framework ($Ph_2P(CH_2)_2NC_4H_8E$, E = NMe, O, S). These PNE ligands were all synthesised *via* the base-catalysed Michael addition of diphenylvinyl phosphine to the relevant heterocyclic secondary amine (Scheme 2.1).

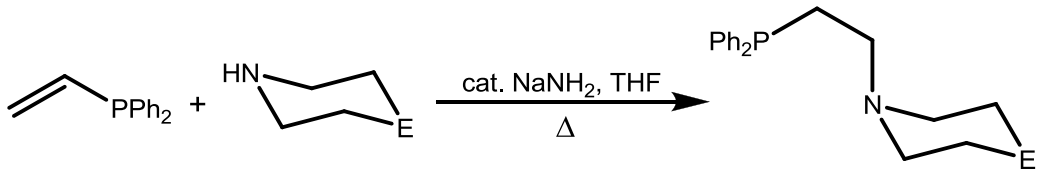

Scheme 2.1: The synthesis of PNE (E = NMe, O, CH_2) ligands reported by Dyer *et al.*[3]

It has been demonstrated that this type of PNE ligand is capable of displaying both bi- and tri-dentate coordination modes with palladium.[3] In their publication Dyer *et al.* reported that the cyclic tertiary amine backbone is highly flexible, allowing the group to adopt either a chair or boat configuration, hence enabling the PNE ligands to adopt both *fac*- and *mer*-tridentate coordination modes when bound to a metal centre (Figure 2.1).

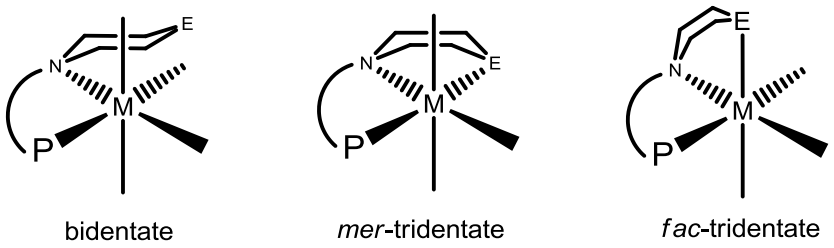

Figure 2.1: The varying coordination modes of PNE ligands synthesised by Dyer *et al.*[3]

The coordination mode adopted by these PNE ligands studied was shown to vary depending on the metal fragment used, with the nature of the ligand coordination also being

strongly affected by the *trans*-effect of other ligands present on the starting metal fragment. Dyer *et al.* proved the lability of the third *N*Me donor group through the addition of $Cy_2PC_2H_4NMe_3Cl$ to a [PdCl(κ^3-PNN)][Cl] complex, causing the displacement of the *N*Me donor with the phosphine, yielding the bidentate [PdCl($Cy_2PC_2H_4NMe_3$)(κ^2-PNN)][Cl_2] product (Scheme 2.2).

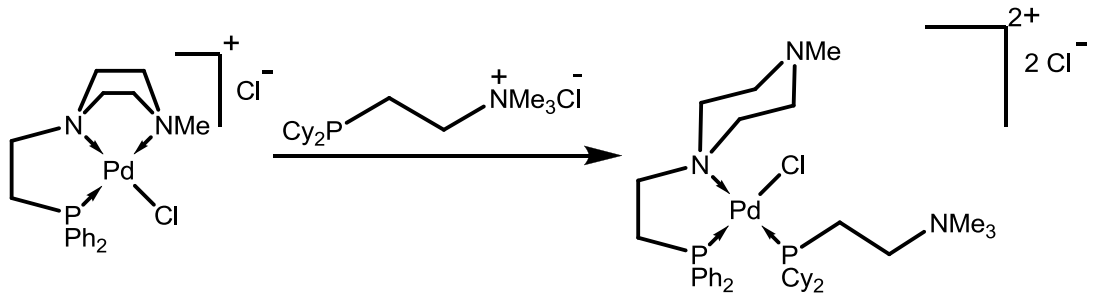

Scheme 2.2: Conversion of a tridentate Pd(κ^3-PNN) to a bidentate Pd(κ^2-PNN) complex reported by Dyer *et al.*[3]

In recent years a number of P,N ligand scaffolds bearing structural similarities with PNE ligands have been developed for use in ethylene *tri*- and *tetra*-merisation systems. One example of particular relevance are the aminophosphine compounds reported by Gambarotta *et al.* (*e.g.* Figure 2.2) which have been shown to promote ethylene tetramerisation when used in combination with a Cr(III) source.[4]

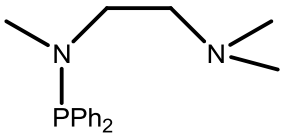

Figure 2.2: An example of a P,N ligand developed by Gambarotta *et al*. for use in ethylene tetramerisation systems.[4]

While these catalytic systems reported by Gambarotta *et al.* did not display very high activities (only 12,500 g/g Cr h^{-1}), the catalysts did display excellent selectivity towards tetramerisation, with the $Ph_2PN(Me)C_2H_4NMe_2$ aminophosphine (Figure 2.2) system producing up to 89 wt % 1-octene, within the oligomer product fraction.[4] It is the success of systems such as these described by Gambarotta using P,N ligands that highlight the potential of PNE ligands as promising scaffolds for use in novel ethylene oligomerisation systems.

So far no study of the coordination chemistry of PNE ligands with early transition metals has been carried out. The use of early transition metals is ubiquitous in the field of selective ethylene oligomerisation chemistry, with chromium-based systems being particularly prevalent in the literature. Therefore, it is proposed that, in combination with chromium, the variable coordination properties exhibited by PNE ligands may give rise to interesting behaviour in ethylene oligomerisation systems. Consequently, this chapter will report and discuss the

synthesis of a range of complexes of group VI metals with three PNE ligands (E = NMe, O, CH_2), as well as detailing the effects of using these ligands in ethylene oligomerisation systems.

2.2 Reactions of $CrCl_3(THF)_3$ with PNE Ligands

It has already been mentioned in Section 1.2.2.2 of this thesis that Cr(III) complexes are the most commonly used chromium sources in ethylene *tri*- and *tetra*-merisation initiator systems. In particular, the use of $CrCl_3(THF)_3$ is ubiquitous in ethylene oligomerisation chemistry, with the highly active BP PNP-based trimerisation system being a notable example.[5]

Based upon this, the synthesis of model complexes from PNE ligands and $CrCl_3(THF)_3$ starting materials is of interest, as any resulting complexes should have structures similar to that of potential catalyst precursors. A number of oligomerisation systems published in the literature have also been demonstrated to display significantly different catalytic behaviour when well defined, pre-formed $CrCl_3(L_2)(THF)$ (L_2 = bidentate P,P or P,N ligand) are used as catalyst precursors, compared to the use of the analogous *in situ* formed complexes.[6] A disadvantage of using Cr(III) complexes as precursors is the paramagnetic nature of the species, which rules out the use of NMR spectroscopy to characterise products formed, complicating the elucidation of the structure and subsequent reactivity of the complexes. Although the magnetic susceptibility of such complexes can be determined, this alone does not allow for the identity of the products to be assigned. In this investigation elemental analysis has been used as the primary tool for characterisation of the compounds synthesised.

2.2.1 Reaction of $CrCl_3(THF)_3$ with the PNN ligand $Ph_2P(CH_2)_2NC_4H_8NMe$

The complexation of the $Ph_2P(CH_2)_2NC_4H_8NMe$ ligand (PNN) with $CrCl_3(THF)_3$ was attempted, initially employing reaction conditions similar to those used by Bollmann *et al.* to synthesise their $[Cr(PNP)Cl_2(\mu\text{-}Cl)]_2$ complexes, in which a solution of the starting materials in toluene was heated to 80 °C for 16 hours .[7] (Scheme 2.3). Upon mixing a solution of the PNN ligand toluene with a solution of $CrCl_3(THF)_3$ the reaction mixture turned a deep blue, indicating complexation had occurred. A pale blue powder precipitated from solution and was isolated from the reaction by filtration. Solubility testing of the product with a range of polar and non-polar solvents showed the blue powder to be highly insoluble. This lack of solubility significantly hindered the growth of crystals for X-ray diffraction analysis.

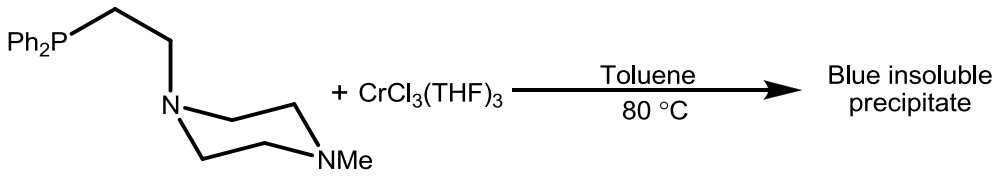

Scheme 2.3: Coordination of PNN ligand $Ph_2P(CH_2)_2NC_4H_8NMe$ with $CrCl_3(THF)_3$.

Mass spectrometric analysis was attempted of the product, and due to the lack of solubility of the complex the solid phase ASAP technique was used. However, problems were

encountered due to the lack of volatility of the Cr-containing material. At temperatures and ionisation voltages sufficiently high to vaporise and subsequently ionise the product, extensive fragmentation occurred and hence no useful data could be obtained. Elemental analysis was also attempted, but yielded results that did not match with any expected product.

The complexation reaction was attempted again utilising different conditions, namely DCM as a solvent and triturating the resulting blue solid with hexane before the solid was dried under vacuum. Again, similar problems were encountered, with the resulting product found to be insoluble, hindering any purification. It is proposed that the insoluble nature of the reaction products may be due to oligomeric $[CrCl_3(THF)(PNN)]_n$ species forming (Figure 2.3). It is conceivable that the PNN ligand, with multiple donor sites, may be able to bridge between multiple metal centres, to create insoluble oligomeric materials. Unfortunately though, no successful characterisation has been achieved to support this hypothesis.

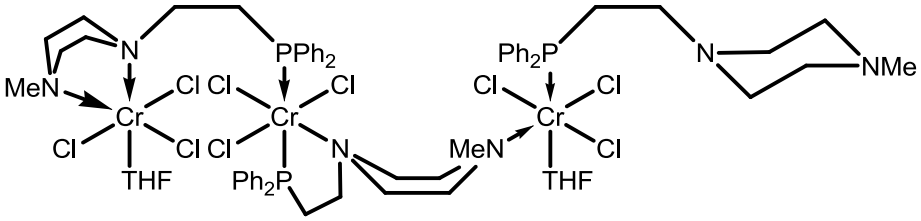

Figure 2.3: A proposed example of a $CrCl_3(THF)(PNN)$ oligomeric species structure.

2.2.2 Synthesis of $CrCl_3(THF)(PNO)$ (2.1)

The reaction of $CrCl_3(THF)_3$ with the $Ph_2P(CH_2)_2NC_4H_8O$ ligand (PNO) was carried out utilising a modified version of the method initially reported in Section 2.2.1, albeit without heating the reaction mixture (Scheme 2.4). The starting materials were dissolved in toluene and mixed, resulting in the formation of a blue precipitate. This solid was isolated by filtration to yield the reaction product as a pale green/blue powder (73 % yield). Elemental analysis verified that the isolated product was the expected $CrCl_3(THF)(PNO)$ (**2.1**) complex. Attempts were made to grow crystals suitable for X-ray diffraction, but after numerous attempts only amorphous solids could be obtained. Analysis of the product by IR spectroscopy was attempted, but no characteristic absorptions were observed, meaning no characterisation was achieved.

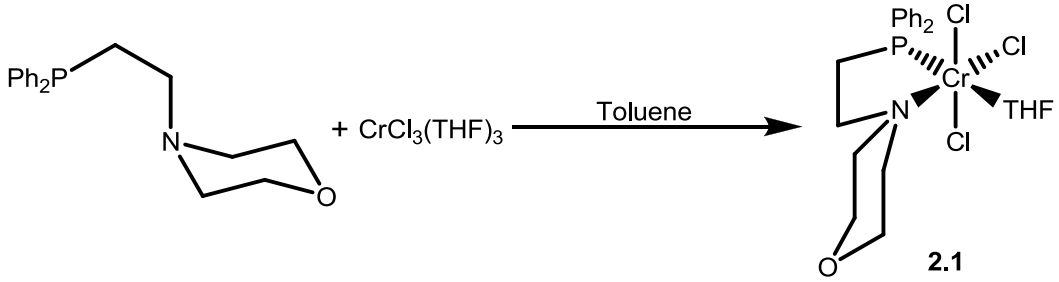

Scheme 2.4: Synthesis of complex **2.1**.

It is possible for the THF ligand to be positioned *trans*- to either the P- or N-donor groups in the complex **2.1**. Work published by Gambarotta and Duchateau *et al.* on a series of P,N pyridine-phosphine ligands showed that their ligands bound to the Cr centre with the THF group *trans*- to P, rather than N.[8] Due to the similarity of the PNO ligand with these previously reported P,N ligands, it is highly likely that complex **2.1** will adopt a similar structure to the complexes described by Gambarotta and Duchateau *et al.*

2.2.3 Synthesis of $CrCl_3$(THF)(PNC) (2.2)

As well as the $CrCl_3$(THF)(PNO) complex (**2.1**) synthesised, it was decided to investigate how PNE ligands with only two (P and N) donor groups bound to Cr(III) species. It is hoped that the lack of a third donor group (*i.e*. N or O) will limit the ability of the ligand to form oligomeric complexes, such as those for the suggested $[CrCl_3(THF)(PNN)]_x$ species (Figure 2.3). To this effect, the complexation of the PNC ligand $Ph_2P(CH_2)_2NC_5H_{10}$ with $CrCl_3(THF)_3$ was carried out.

The reaction of $CrCl_3(THF)_3$ with the ligand $Ph_2P(CH_2)_2NC_5H_{10}$ (PNC) was carried out utilising a modified version of a method initially reported by Labinger and Bercaw *et al.* used for the synthesis of their $CrCl_3(\kappa^3\text{-}PNP^{o\text{-}OMe})$ complexes (Scheme 2.5).[9] Upon mixing of the chromium precursor and ligand solutions in DCM an instantaneous colour change to blue/turquoise was observed. On removal of the solvent *in vacuo* complex **2.2** was isolated as a turquoise solid (72 % yield). Attempts to grow crystals suitable for X-ray diffraction proved to be fruitless, and mass spectrometry did not give any useful data. Elemental analysis did, however, confirm the expected composition of the product. The structure proposed in Scheme 2.5 shows the PNC ligand binding to Cr with P *trans* to THF, for the same reasoning as given in Section 2.2.2.

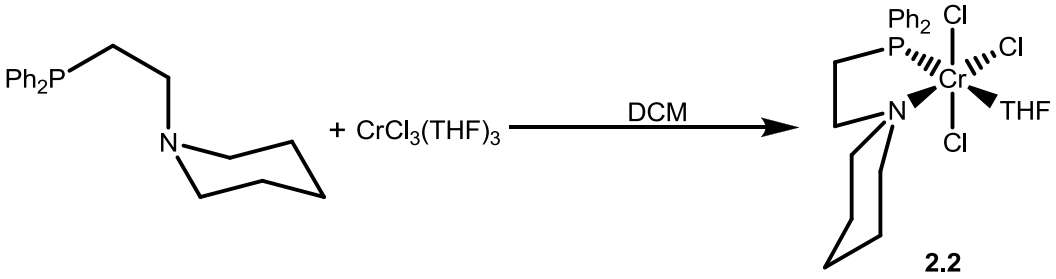

Scheme 2.5: Synthesis of complex **2.2**.

2.2.4 Synthesis of $[CrCl_4(PNO)][HNEt_3]$ (2.3)

Due to the problems encountered in acquiring crystals of the products of reactions of $CrCl_3(THF)_3$ with PNE-type ligands suitable for X-ray diffraction studies, a new approach was taken to synthesising model complexes. Work published in 2003 by Kohn *et al.* reported the isolation and crystallisation of $[(triazacyclohexane)CrCl_3)][HNR_3]$ complexes obtained by reaction of $[(triazacyclohexane)CrCl_3)]$ starting materials with the ammonium salt $[PhNMe_2H][B(C_6F_5)_4]$.[10] Based on this, a similar method was employed to prepare ammonium salts of Cr^{III}(PNO) complexes (Scheme 2.6).

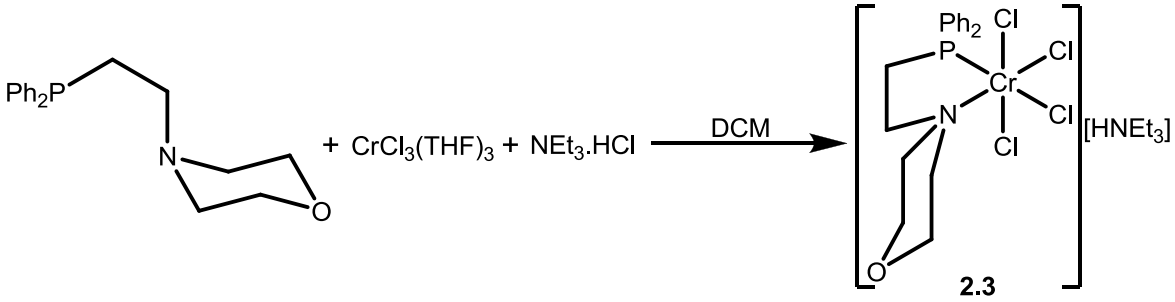

Scheme 2.6: Synthesis of complex **2.3**.

Upon mixing the starting materials in DCM, the solution instantly turned a deep blue/purple colour and, shortly after, dark blue crystals suitable for X-ray crystallographic analysis formed from the reaction mixture. The molecular structure was successfully determined by X-ray diffraction (Figure 2.4) revealing that the complex consists of the expected anionic chromium centre displaying a distorted octahedral coordination sphere, comprising four chloride ligands and a bidentate κ^2-PN bound PNO ligand, with a bite angle of 82.9°. A selection of important bond lengths and angles is given in Table 2.1.

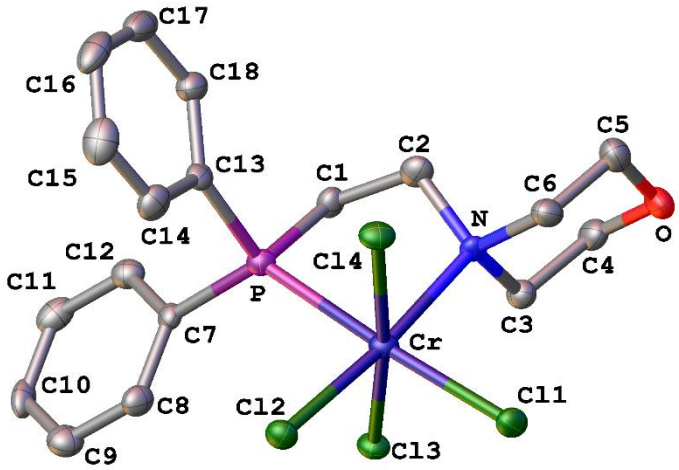

Figure 2.4: ORTEP representation of the molecular structure determined for complex **2.3** (anion only), with thermal ellipsoids set at 50 % probability level (the $[HNEt_3]^+$ cation is omitted for clarity).

$[CrCl_4(PNO)][HNEt_3]$, 2.3		
Bond Lengths (Å)	Cr – P	2.4588(12)
	Cr – N	2.262(3)
	Cr – Cl(1)	2.3526(11)
	Cr – Cl(2)	2.3416(11)
	Cr – Cl(3)	2.3452(11)
	Cr – Cl(4)	2.3075(11)
Bond Angles (°)	N-Cr-P	82.90(8)

Table 2.1: Selected bond lengths (Å) and angles (°) determined for complex **2.3**

The data displayed in Table 2.1 show the N-Cr-P bite angle to be relatively large when compared to other 5-membered Cr(P,N) chelate rings such as those reported by Wong and Wong *et al.* for their $Ph_2PN(H)C(Ph)=N(SiMe_3)$ ligands (79.7(2)°),[11] and Edwards *et al.* with their $CrCl[N(CH_2CH_2PMe_2)_2)]$ complexes (80.4(1)°).[12] This large bite-angle is thought to be due to the flexibility of the saturated CH_2CH_2 backbone of the PNO ligand.

Unfortunately, due to the air sensitive nature of the complex no analysis beyond X-ray crystallography was successfully carried out. Both mass spectrometry and elemental analysis were attempted, but both yielded inconclusive results. Consequently, no firm conclusions can be drawn regarding the identity of the bulk sample. The molecular structure determined indicates that the target complex has been produced, but the purity and yield of the product cannot be commented upon due to the lack of other data.

2.2.5 Reaction of PNN with $CrCl_3(THF)_3$ and $HNEt_3Cl$

Following the successful synthesis of complex **2.3** an analogous reaction was attempted with the PNN ligand $Ph_2P(CH_2)_2NC_4H_8NMe$. Initially the reaction proceeded as expected, giving a deep blue/purple solution in DCM. Upon cooling the product remained in solution, indicating a significant difference in solubility to that of complex **2.3**. Even after prolonged standing at −30 °C no precipitation occurred. Subsequently, the solvent was removed under vacuum and a blue powder was isolated. Multiple attempts at recrystallization failed to yield crystals suitable for X-ray diffraction, and elemental analysis and mass spectrometry failed to give satisfactory data. Disappointingly, no conclusion as to the identity of the complex formed in this reaction can be drawn.

2.3 Complexation of PNE Ligands with $M(CO)_6$ (M = Cr, Mo) Complexes

Group VI metal carbonyl complexes of PNE ligands are of interest to this study for a number of reasons. Firstly, unlike Cr(III) species, $Cr(CO)_6$ and $Mo(CO)_6$ are not paramagnetic, therefore allowing NMR spectroscopic analysis of the complexes. Additionally, the electronic properties of the PNE ligands may be probed by IR spectroscopic analysis of the chromium carbonyl complexes. Finally, these types of $Cr(CO)_{(6-n)}(\kappa^n\text{-PNE})$ complexes may serve as precursors to catalytic ethylene *tri-* and *tetra*-merisation systems, as exemplified by the use of $[Cr(CO)_4(PNP)]$ complexes as precursors to catalytically active Cr(I) species in combination with weakly coordination anions (Scheme 2.7).[13]

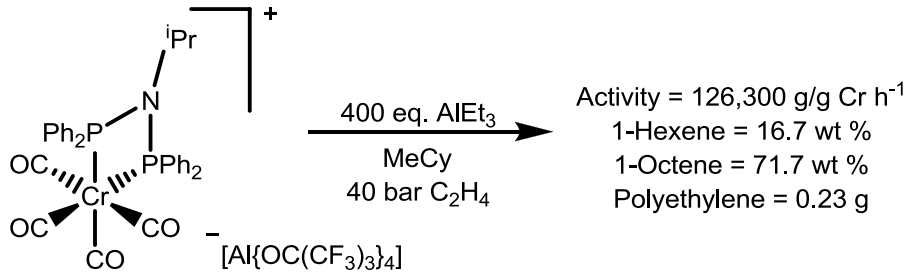

Scheme 2.7: An ethylene tetramerisation system utilising a $[Cr^{I}(CO)_4(PNP)]^+$ precursor.[13]

2.3.1 Preparation of $[Cr(CO)_{(6-n)}(\kappa^n\text{-PNE})]$ complexes (2.4-2.6)

Complexes **2.4** ($Cr(CO)_5$(PNN)) and **2.5** ($Cr(CO)_5$(PNO)) were synthesised by the reaction of the PNN and PNO ligands, respectively, with $Cr(CO)_6$, following the methods reported by Wass *et al.* for their PNP ligands.[14] The starting materials were heated at reflux in a toluene solution for 16 hours, to give a yellow solution that was subsequently filtered, and the solvent removed *in vacuo*. Both complexes **2.4** and **2.5** were initially isolated as yellow oils in good yields (74 and 96 %, respectively) which subsequently solidified upon scraping. The compounds were both fully characterised by NMR and IR spectroscopies, and mass spectrometry. The reactions require high temperatures (110 °C) and relatively long reaction times (24 hours) to displace the carbonyl groups with the chosen PNE ligand. The reactions are easily followed by ^{31}P NMR spectroscopy due to the characteristic change in chemical shift from $\delta \approx -19$ ppm of the starting ligands to $\delta \approx 43$ ppm of the complex. For each ligand, analysis of the crude reaction mixtures by ^{31}P NMR spectroscopy showed only a single product formed in the reactions.

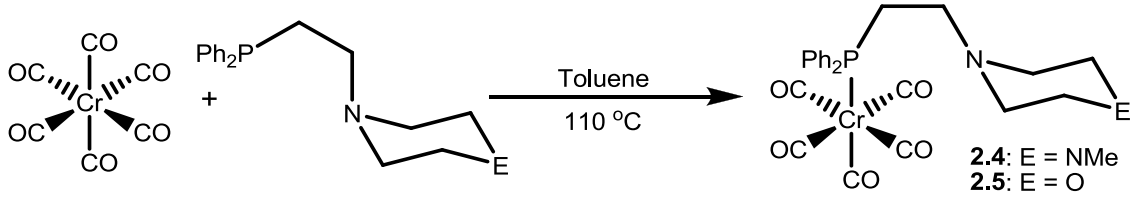

Scheme 2.8: The synthesis of complexes **2.4** and **2.5**.

It was discovered that complexes **2.4** and **2.5** are highly soluble, even in non-polar solvents such as pentane and hexane, which created challenges with regard to purification of the products. Despite this, crystals of **2.4** were grown by leaving a concentrated solution of the complex in pentane to stand for one hour. The resulting crystals were subject to analysis by X-ray diffraction, and the molecular structure of **2.4** successfully determined (Figure 2.5, Table 2.2).

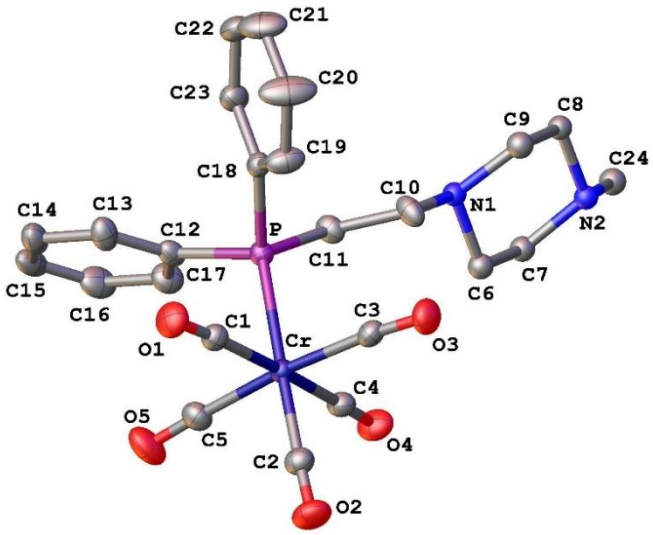

Figure 2.5: ORTEP representation of the molecular structure determined for complex **2.4** with thermal ellipsoids set at 50 % probability level.

	$Cr(CO)_5(\kappa^1$-P-PNN), 2.4	
Bond Lengths (Å)	Cr – P	2.3841(4)
	Cr – C(1)	1.8944(13)
	Cr – C(2)	1.8783(14)
	Cr – C(3)	1.8980(14)
	Cr – C(4)	1.9004(14)
	Cr – C(5)	1.9004(15)
	O(1) – C(1)	1.1468(17)
	O(2) – C(2)	1.1427(18)
	O(3) – C(3)	1.1408(17)
	O(4) – C(4)	1.1448(17)
	O(5) – C(5)	1.1411(18)
Bond Angles (°)	C(11)-P-Cr	116.52(4)
	C(12)-P-Cr	111.83(4)
	C(18)-P-Cr	119.49(4)

Table 2.2: Selected bond lengths (Å) and angles (°) determined for complex **2.4**.

The molecular structure of complex **2.4** reveals that the PNN ligand is bound to the chromium centre in a monodentate fashion (κ^1-P), leaving the methylpiperazine ring uncoordinated. Due to the similarities in the NMR spectra of complexes **2.4** and **2.5** it is believed that **2.5** shares this monodentate ligation mode. It is thought that the highly soluble and oily nature of complex **2.4** and **2.5** is due to this alkyl moiety's flexibility. Unfortunately, despite multiple attempts crystals suitable for X-ray diffraction of **2.5** could not be grown. Analysis of the complexes by ^{13}C NMR spectroscopy reveals that both complexes **2.4** and **2.5** display a pair of doublets in the region $\delta \approx$ 200-230 ppm, indicative of CO groups in two separate environments. This observation supports the structure determined by X-ray crystallography for complex **2.4**.

The effect of the *trans* influence on the bond length of the C-O groups is apparent in Table 2.2, with the Cr-C(2) bond, *trans* to the phosphine, being shorter than the other Cr-C bonds in the complex. The short Cr-C bond *trans* to the phosphine is due to the weak *trans* influence of the P-donor relative to that of the CO ligands, therefore the Cr-C bonds *trans* to the CO ligands are lengthened to a greater extent than the Cr-C bond *trans* to phosphorus. The data from the IR spectra of **2.4** and **2.5** are reported in Table 2.3. Complexes **2.4** and **2.5** both show the three expected IR absorption bands in the carbonyl region of the spectrum, as predicted by group theory for a complex with a C_{4v} point group. The IR spectra for both **2.4** and **2.5** display C-O absorptions with very similar stretching frequencies, suggesting both PNN and PNO ligands have similar electronic donor properties as would be expected.

Complex	**ν C≡O[a] (cm^{-1})**		
2.4	2062	1982	1935
2.5	2063	1982	1938
[a] Spectra recorded in DCM solution			

Table 2.3: The carbonyl stretching frequencies for complexes **2.4** and **2.5**.

The monodentate binding of the PNN and PNO ligands determined for complexes **2.4** and **2.5** contrasts with the coordination determined for complex **2.3**, in which the PNO ligand is bound to the Cr(III) centre in a bidentate κ^2-P,N-fashion. This demonstrates that the PNE ligands discussed so far are capable of adopting both mono- and bi-dentate coordination modes with chromium, and suggests that the ligands may have the potential to behave as hemi-labile species when bound to chromium. It is thought that this difference in PNE ligand binding with Cr(0) and Cr(III) centres may be due to a difference in "hardness" of the metals, as described by Pearson's hard-soft-acid-base theory.[15] The Cr(III) centre is harder than Cr(0), and would be expected to bind more strongly to a hard nitrogen donor group, hence bidentate P,N-

coordination of PNE ligands with Cr(III) is observed, but only monodentate complexation occurs with Cr(0).

Alongside the traditional solution-phase thermal method used for the synthesis of complex **2.4**, a synthetic process was developed involving the use of a microwave reactor to heat the reaction solution. A solution of the PNN ligand and $Cr(CO)_6$ in toluene was sealed in a crimp-cap microwave reactor vessel before being heated to 140 °C for four hours[*]. The microwave reaction was found to be very clean as demonstrated by the ^{31}P NMR spectrum of the crude product only displaying one signal corresponding to the product. By comparison, the crude product solution from the traditional "reflux method" of synthesis exhibited an impurity signal in the ^{31}P NMR spectrum at δ = 57.6 ppm. Following work-up the desired product (complex **2.4**) was isolated in an almost quantitative yield of 96 %, much improved upon the yield of 76 % isolated using the traditional solution-phase thermal synthesis method. It is suggested that the short reaction time employed (4 hours microwave vs. 16 hours reflux) in the microwave synthesis avoids the formation of side products.

The complexation of the PNC (piperadine-*N*-ethylene-diphenylphosphine) ligand with $Cr(CO)_6$ was also carried out, using a method that was the same as that used for the preparation of **2.4** and **2.5**, but surprisingly gave different results. After heating a mixture of the ligand PNC and $Cr(CO)_6$ at reflux for 24 hours in toluene, ^{31}P NMR spectroscopic analysis of the crude reaction mixture showed three new singlet resonances, suggesting three products had formed, rather than one product, as is seen with the analogous PNN and PNO ligands. One of these three products was found to be insoluble in hexane, and hence could be separated by washing. This insoluble product was isolated by crystallisation from a concentrated solution in DCM layered with hexane in a low yield (19 %). These crystals were suitable for X-ray crystallography, and the structure was determined to be that of the octahedral complex $Cr(CO)_4$(PNC) (**2.6**) (Figure 2.6). Complex **2.6,** was fully characterised by NMR and IR spectroscopies and mass spectrometry.

[*] A Biotage Initiator microwave reactor was used, set to retain a constant reaction temperature.

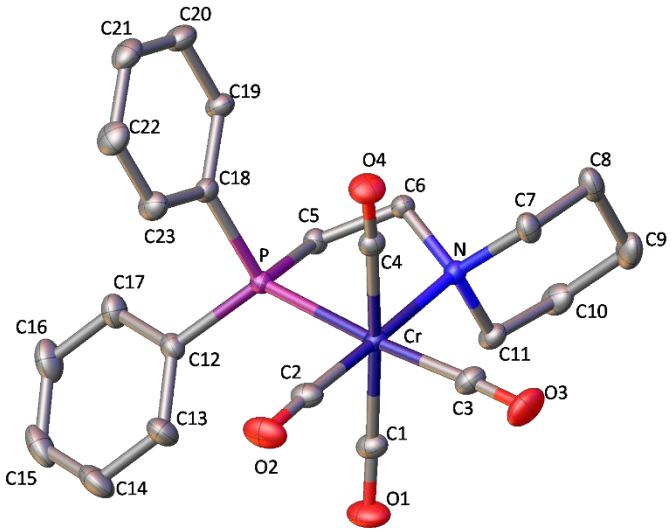

Figure 2.6: ORTEP representation of the molecular structure determined for complex **2.6**, with thermal ellipsoids set at 50% level.

	$Cr(CO)_4(\kappa^2$-P,N-PNC) (4)	
Bond Lengths (Å)	Cr – P	2.3419(3)
	Cr – N	2.2724(7)
	Cr – C(1)	1.8854(9)
	Cr – C(2)	1.8258(9)
	Cr – C(3)	1.8588(9)
	Cr – C(4)	1.8958(9)
	O(1) – C(1)	1.1534(12)
	O(2) – C(2)	1.1644(12)
	O(3) – C(3)	1.1534(12)
	O(4) – C(4)	1.1474(11)
Bond Angles (°)	N-Cr-P	82.54(2)

Table 2.4: A selection of bond lengths (Å) and angles (°) determined for complex **2.6**.

The molecular structure of complex **2.6** contrasts with that of the PNN analogue, **2.4**. In complex **2.6** the PNC ligand binds to the chromium centre in a κ^2-P,N-bidentate fashion, to give $Cr(CO)_4$(PNC), with the chromium centre adopting a distorted octahedral geometry and the ligand displaying a P-Cr-N bite angle of 82.54(2)°. A selection of relevant bond lengths and angles are given in Table 2.4. The Cr-C bond lengths measured reflect the differences in *trans*-influence between the phosphine and amine donor groups. As expected, the Cr-C(2) bond length, *trans* to the amine group, is shorter than the Cr-C(3) bond *trans* to the phosphine due to the weaker

trans influence of the amine donor, relative to that of the phosphine donor *trans* to the Cr-C(3) bond. This matches the observations of Dobson and Bernal *et al.* for their $Cr(CO)_4(Ph_2PCH_2CH_2NEt_2)$ complex, in which the Cr-C bond length *trans* to the amine donor was measured at 1.73(4) Å, shorter than the other Cr-C bond distances measured.[16]

It is apparent from ^{31}P NMR spectroscopic analysis of the crude products following the reaction of $Cr(CO)_6$ with the PNC ligand that the low yield of complex **2.6** is due to the formation of a number of side products. Of the three ^{31}P NMR spectroscopic signals observed, one appeared at δ = 42.5 ppm, which is very similar to the chemical shifts displayed by complexes **2.4** and **2.5** (δ ≈ 43 ppm). This suggests that this resonance at δ = 42.5 ppm may be due to the formation of the monodentate $Cr(CO)_5$(PNC) complex. Unfortunately, due its high solubility, this species could not be isolated and no further analysis could be carried out.

The IR spectrum of complex **2.6** should display four carbonyl absorption bands, however, the spectrum measured in solution only exhibits three carbonyl absorptions bands (Table 2.5). One of these absorptions is non-Gaussian in shape, suggesting that the band may consist of overlapping absorptions. Deconvolution of the IR spectrum obtained for complex **2.6** showed that the broad absorption band consists of two bands (Figure 2.7).

Complex	**ν C≡O[a] (cm^{-1})**			
2.6	2006	1899[b]	1882[b]	1840
[a] Spectra obtained in DCM solution [b] Peaks acquired by deconvolution of raw data				

Table 2.5: The carbonyl absorption frequencies measured for complex **2.6**.

It is apparent that the PNC ligand prefers to coordinate differently to the PNN and PNO ligands, but the precise reason for this behaviour is not clear. It is suggested that presence of an N or O atom in the six-membered ring of the ligand significantly alters the inversion of the tertiary amine group, hence altering the coordination behaviour of the amine.

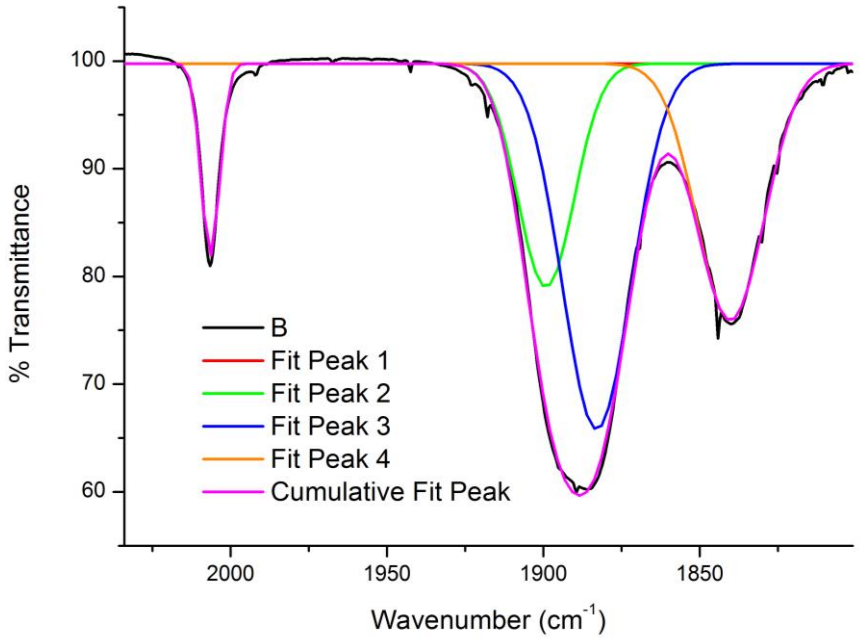

Figure 2.7: Deconvolution of the IR spectrum measured for complex **2.6** (DCM).

2.3.2 Preparation of $Mo(CO)_4$(PNE) complexes (E = N, O, C) (2.7-2.9)

In order to further investigate the binding properties of PNE ligands with group VI metals, complexation reactions were carried out with $Mo(CO)_6$. These reactions utilised the same experimental method as used in Section 2.3.1, *i.e.* heating a solution of $Mo(CO)_6$ and the relevant PNE ligand in toluene at reflux for 24 hours; in each case ^{31}P NMR spectroscopic analysis revealed the reactions had given complete conversion to the products, with all three displaying characteristic shifts of δ ≈ 37 ppm. Subsequently, complexes **2.7**-**2.9** were isolated as yellow crystalline solids in moderate yields (38 - 49 %) and were successfully characterised by NMR spectroscopy, mass spectrometry and X-ray crystallography. IR spectroscopy was also used to characterise complexes **2.7**-**2.9**.

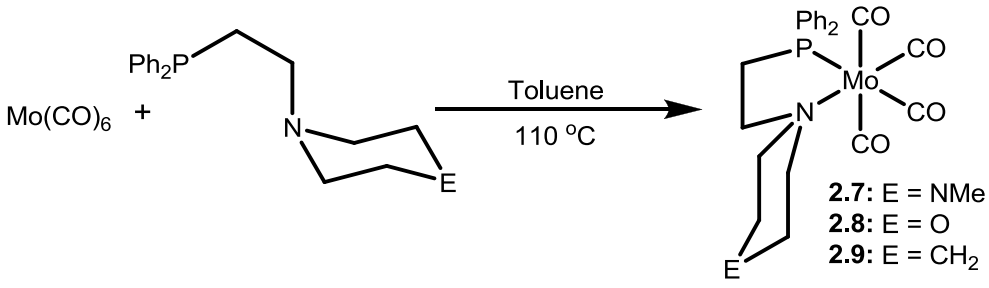

Scheme 2.9: The synthesis of complexes **2.7**-**2.9**.

Both complexes **2.7** and **2.8** show significant differences to their chromium-containing counterparts, **2.4** and **2.5**. Both of the molybdenum complexes **2.7** and **2.8** are insoluble in hexane making their purification and crystallisation considerably easier than that of **2.4** and **2.5**.

Crystals of all three $Mo(CO)_4$(PNE) complexes suitable for X-ray diffraction were successfully grown and their structures determined (Figure 2.8). The molecular structures determined for complexes **2.7**-**2.9** all show the PNE ligands binding in a bidentate fashion to the molybdenum centre, in contrast to complexes **2.4** and **2.5**, both of which display monodentate coordination. All three of the complexes **2.7**-**2.9** are shown to adopt a distorted octahedral geometry with respect to the molybdenum centre, as expected. A selection of relevant bond lengths and angles for complexes **2.7**-**2.9** are presented in Table 2.6. The crystallographic data for complexes **2.7**-**2.9** reveal all three have very similar Mo-P, Mo-N and Mo-C bond lengths, and the ligands display similar bite angles. The impact of the differing *trans* influences of the phosphine and amine groups on the relevant Mo-C and C-O bonds can be seen, and matches the observations made previously for the analogous Cr complexes. The Mo-C bond *trans* to the amine donor has the shortest of the Mo-C bond lengths, with the group *trans* to the phosphine donor being slightly longer. These trends support the observations of Dobson and Bernal *et al.* for their similar $Mo(CO)_4(Ph_2PCH_2CH_2NEt_2)$ complex.[16]

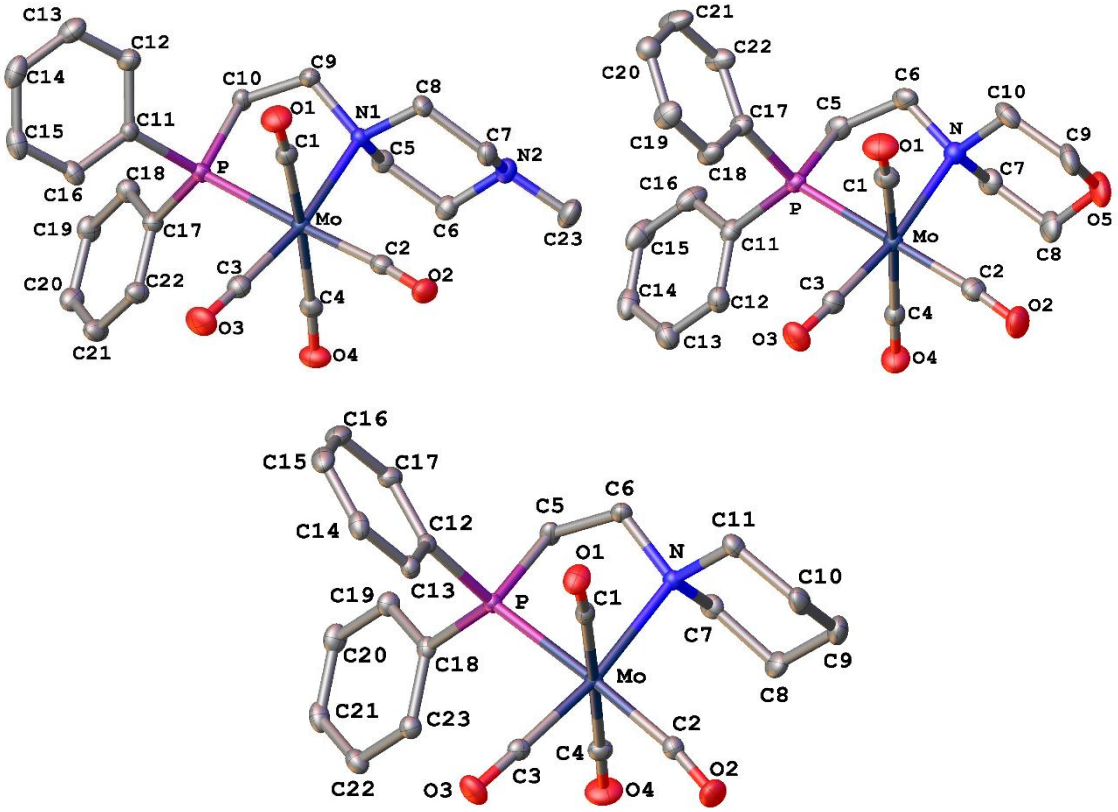

Figure 2.8: ORTEP representations of the molecular structures determined for complexes **2.7** (top left) **2.8** (top right) and **2.9** (bottom), with thermal ellipsoids set at 50 % probability.

	$Mo(CO)_4$(PNN) (2.7)		**$Mo(CO)_4$(PNO) (2.8)**		**$Mo(CO)_4$(PNC) (2.9)**	
Bond Lengths (Å)	Mo – P	2.5008(6)	Mo – P	2.4916(5)	Mo – P	2.4933(5)
	Mo – N(1)	2.4264(18)	Mo – N	2.424(3)	Mo – N	2.424(1)
	Mo – C(1)	2.033(2)	Mo – C(1)	2.053(2)	Mo – C(1)	2.050(1)
	Mo – C(2)	1.999(2)	Mo – C(2)	1.991(2)	Mo – C(2)	2.002(2)
	Mo – C(3)	1.954(2)	Mo – C(3)	1.9534(19)	Mo – C(3)	1.937(1)
	Mo – C(4)	2.041(2)	Mo – C(4)	2.0281(19)	Mo – C(4)	2.021(1)
	O(1) – C(1)	1.152(3)	O(1) – C(1)	1.155(2)	O(1) – C(1)	1.166(2)
	O(2) – C(2)	1.154(3)	O(2) – C(2)	1.143(2)	O(2) – C(2)	1.140(2)
	O(3) – C(3)	1.160(3)	O(3) – C(3)	1.157(2)	O(3) – C(3)	1.153(2)
	O(4) – C(4)	1.148(3)	O(4) – C(4)	1.141(2)	O(4) – C(4)	1.148(2)
Bond Angles (°)	N(1)-Mo-P	77.93(4)	N-Mo-P	79.64(7)	N-Mo-P	79.39(3)

Table 2.6: A selection of bond lengths (Å) and angles (°) determined for complexes **2.7**-**2.9**.

Solution phase ^{13}C NMR spectroscopy was used to analyse complexes **2.7**-**2.9**, with all three displaying three sets of doublets in the carbonyl region (δ ≈ 200 - 230 ppm) corresponding to three unique carbonyl environments, supporting the bidentate coordination mode exhibited in the solid molecular structures. The ^{1}H NMR spectrum of complex **2.7** shows that the methylpiperazine ring is fluxional, which causes broadening of the ring proton signals, matching with earlier reports of similar behaviour of these ligands.[17] Low temperature VT ^{1}H NMR spectroscopy was carried out, but this did not aid assignment of the spectrum.

IR spectroscopy was also used to analyse complexes **2.7-2.9**; the spectroscopic data are displayed in Table 2.7. It is predicted that the carbonyl region of the IR spectrum should exhibit four absorption bands, but initial analysis of the solution-state IR spectra of **2.7-2.9** only show three absorptions.

Complex		**ν C≡O [a] (cm^{-1})**		
2.7	2018	1909[b]	1889[b]	1846
2.8	2018	1909[b]	1888[b]	1848
2.9	2017	1908[b]	1888[b]	1844

[a] Spectra obtained in DCM solution
[b] Peaks acquired by deconvolution of raw data

Table 2.7: The IR carbonyl absorption frequencies measured for complexes **2.7**-**2.9**.

One of these three bands is considerably larger than the other two and does not fit a Gaussian distribution as would be expected, implying that this band consists of two smaller overlapping absorptions. Deconvolution was carried out upon the measured IR spectra of **2.7**-**2.9** to calculate the positions of these two smaller absorptions (Figure 2.9). These IR spectroscopic data correspond with that found for complex **2.6**, in which the ligand also adopted a κ^2-P,N bidentate coordination mode.

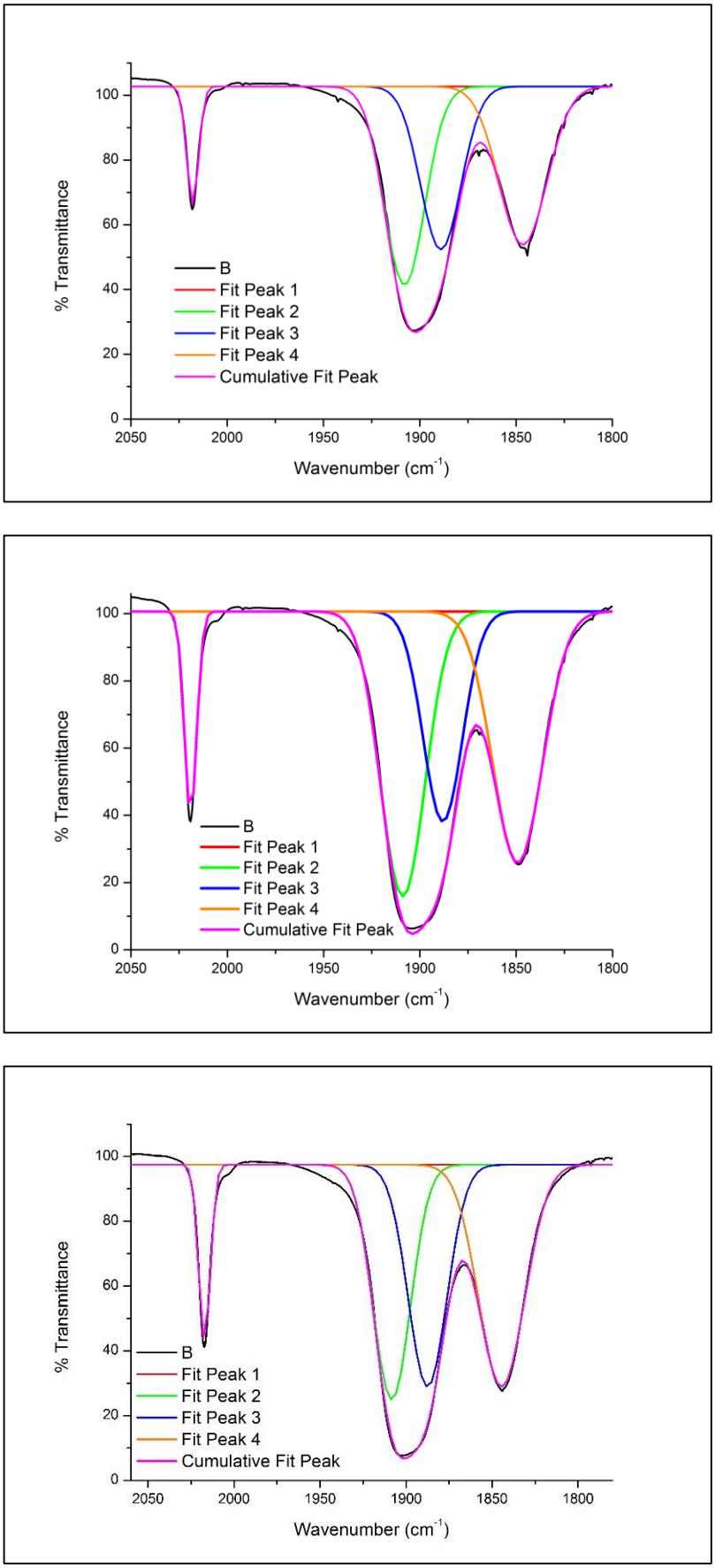

Figure 2.9: Deconvolution of the IR spectra of complexes **2.7** (top), **2.8** (middle) and **2.9** (bottom).

In conclusion, it has been demonstrated that PNE ligands form coordination complexes with Cr(0) and Mo(0) centres, and are capable of adopting both mono- and bi-dentate coordination modes. Unfortunately, no evidence of tridentate coordination of PNE ligands with chromium or molybdenum has been observed. This lack of κ^3-coordination with Cr and Mo is in contrast to the reactivity of PNE ligands with late transition metals reported by Dyer *et al.*[3] It is suggested that this may be due to the smaller size of the group VI metal centres, compared to palladium, hindering coordination of the sterically demanding PNE ligand.

2.4 Decarbonylation of $Cr(CO)_5$(PNN)

It has been suggested by Hanton *et al.* that in order for $[Cr^{I}(CO)_4(PNP)]^+$ complexes to become active ethylene trimerisation catalysts they must firstly undergo decarbonylation to create a vacant coordination site for catalysis to occur.[18] It is therefore important to investigate whether $[Cr(CO)_{(6-n)}(\kappa^n\text{-PNE})]$ complexes are able to undergo decarbonylation, something that is likely to be accompanied by alteration of the PNE ligand's coordination mode. So far it has been shown that PNE ligands can adopt both mono- and bi-dentate coordination modes, but in order for PNE ligands to be labelled as truly hemi-labile it should be shown that Cr(PNE) complexes can alter their coordination mode on one chromium species.

2.4.1 Decarbonylation of complex 2.4 with TMNO to $Cr(CO)_4$(PNN) (2.10)

Decarbonylation of metal carbonyls using trimethylamine N-oxide (TMNO) is well established in the literature, and this method was chosen to decarbonylate complex **2.4**.[19] The complex **2.4** and TMNO were heated at reflux in toluene for 54 hours and the reaction was followed by ^{31}P NMR spectroscopy (Scheme 2.10). At the end of this time the ^{31}P NMR spectrum showed three major products were formed by the reaction, of which one (complex **2.10**) was subsequently successfully isolated as a yellow solid in a low yield (10 mg, 7 %) through washing the crude product mixture with hexane. The isolated product **2.10** displayed a single resonance in the ^{31}P NMR spectrum, with a chemical shift of δ = 55.8 ppm, but the ^{1}H NMR spectrum showed significant line broadening making full characterisation difficult. ^{13}C NMR spectroscopy reveals three signals in the carbonyl region, suggesting that the complex **2.10** contains the PNN ligand bound in a bidentate fashion to the Cr centre, consistent with decarbonylation having taken place and the PNN ligand having changed its coordination from κ^1-P to κ^2-P,N.

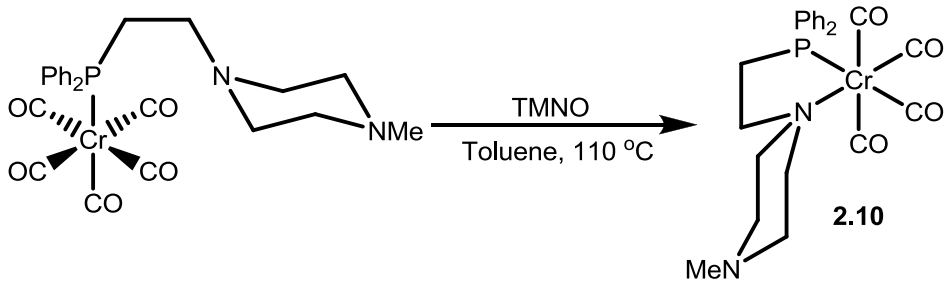

Scheme 2.10: The synthesis of complex **2.10**.

A concentrated solution of complex **2.10** in DCM was layered with hexane, subsequently affording crystals suitable for X-ray crystallography, allowing the molecular structure to be determined (Figure 2.10). The resulting structure shows the PNN ligand in complex **2.10** to be adopting a bidentate κ^2-P,N coordination mode, supporting initial conclusions drawn from the ^{13}C NMR spectroscopic data.

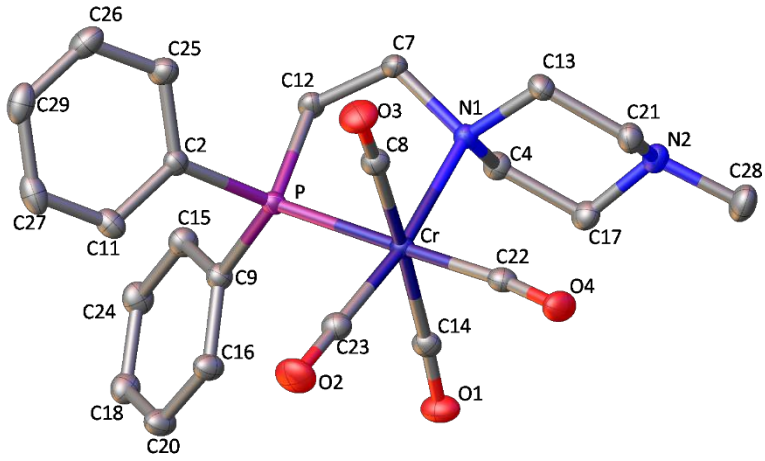

Figure 2.10: ORTEP representation of the molecular structure determined for complex **2.10**, with thermal ellipsoids set at 50 % level.

A selection of relevant bond angles and lengths for complex **2.10** are displayed in Table 2.8. The data show that complex **2.10** exhibits a distorted octahedral geometry around the Cr centre as expected. From these data the effect of the amine and phosphine *trans* influences on the CO moieties can be seen. The Mo-C bonds *trans* to both the amine and phosphine donors are shorter than the Mo-C bonds *trans* to the CO groups, with the Mo-C bond *trans* to the amine being the shortest, as predicted by theory, and matching the previous observations for $Cr(CO)_4$(PNC) (**2.6**) in this thesis, and those of Dobson and Bernal *et al.* for their $Cr(CO)_4(Ph_2PCH_2CH_2NEt_2)$ complex.[16]

$Cr(CO)_4$(PNN) (2.10)		
Bond Lengths (Å)	Cr – P	2.3603(4)
	Cr – N	2.306(1)
	Cr – C(8)	1.893(1)
	Cr – C(14)	1.897(1)
	Cr – C(22)	1.860(1)
	Cr – C(23)	1.831(1)
	O(1) – C(14)	1.155(2)
	O(2) – C(23)	1.163(2)
	O(3) – C(8)	1.150(2)
	O(4) – C(22)	1.161(2)
Bond Angles (°)	N-Cr-P	80.86(3)

Table 2.8: A selection of bond lengths (Å) and angles (°) determined for complex **2.10**.

It is thought that the low yield of the product resulting from the decarbonylation is likely to be due to a side reaction occurring between the TMNO and the PNN ligand. It is suggested that TMNO is capable of oxidising the phosphine group of the PNN ligand, causing the starting complex to decompose rather than react in the desired manner. Despite this, it can be concluded that the PNN ligand can adopt both mono- and bi-dentate coordination modes with a Cr(0) centre, and can be forced to convert from κ^1- to κ^2-coordination with Cr(0).

2.4.2 Control Reaction of TMNO with the PNN ligand

The suggestion that the low yield of complex **2.10** (Section 2.4.1) is caused by the oxidation of the PNN ligand by TMNO was investigated by carrying out an NMR-scale reaction with TMNO and free PNN. The starting materials were heated to reflux at 70 °C in DCM for 24 hours and the reaction was followed by ^{31}P NMR spectroscopy. It was found that the major product of the reaction detected by ^{31}P NMR spectroscopy matched the major impurity signal (δ = 28.2 ppm) observed in the decarbonylation reaction of $Cr(CO)_5$(PNN). It is suggested that this side product is $Ph_2P(O)(CH_2)_2NC_4H_8NMe$, *i.e.* the oxidised PNN ligand. This result demonstrates that the side products, and therefore low yield, observed in Section 2.3.1 are most probably due to a reaction occurring between TMNO and the PNN ligand. This observation of phosphine decomposition caused by TMNO may also explain the low yields of other TMNO-based decarbonylation studies utilising phosphines as ligands, such as that reported by Coville *et al.*[20]

2.5 Catalytic Ethylene Oligomerisation Testing Using PNE Ligand-based Systems

All three of the PNE ligands (PNN, PNO and PNC) synthesised as part of this investigation were tested for their performance as ligands in chromium-based ethylene *tri-* and *tetra-*merisation systems. The testing was carried out using conditions widely used in the field of ethylene *tri-* and *tetra*-merisation catalysis, namely chlorobenzene as the solvent and 500 equivalents of MMAO-3A as the aluminium activator run at 60 °C with 40 bar ethylene pressure.[21]

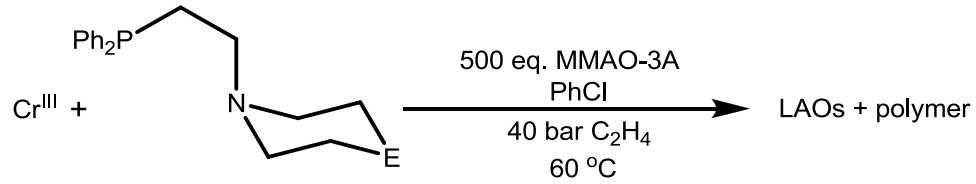

Scheme 2.11: The reaction conditions used for ethylene oligomerisation testing.

As part of the investigation of PNE-based ethylene oligomerisation systems two different catalyst activation methods were tested. Previous work from Chevron Phillips regarding their phosphinoamidine-based ethylene oligomerisation systems has demonstrated that the catalyst activation method employed can have a major effect upon the behaviour of the resulting catalyst system.[22] The two activation protocols tested were:

- Method **A** involved activating the catalyst *in situ* by charging the autoclave with the chromium and ligand starting materials, before adding MMAO-3A to activate the catalyst and subsequently pressurising the vessel with ethylene.
- Method **B** used a preactivated catalyst, in which the desired ligand and chromium source were stirred for five minutes to pre-form the initiator precursor, before adding MMAO-3A to activate the catalyst; the resulting initiator solution was then transferred to the autoclave, which was subsequently pressurised with ethylene.

The catalytic tests used a semi-batch process in a 250 mL steel autoclave. For both activation methods (**A** and **B**) the ethylene uptake of the reaction was monitored through the use of a mass-flow meter, allowing for the uptake of ethylene by the reaction to be monitored. The use of a mass-flow meter also meant that the point at which the catalyst had "died" was readily apparent, and the reaction could be terminated once the ethylene uptake had stopped. For all tests undertaken in this thesis the activity of the catalyst systems is reported as the amount of ethylene consumed by the reaction, per mole of chromium, per hour (mol/mol Cr h^{-1}). Unfortunately, due to the time-consuming nature of the catalytic testing

carried out repeat runs could not be run, and so accurate error bars cannot be generated for comparison of the data collected. Extensive testing within Sasol has shown that the error of the equipment used for the catalytic runs is ± 5 %, and it is assumed that the error is the same for the testing reported in this investigation. All of the catalyst testing carried out for this report was undertaken in collaboration with Dr M. J. Hanton at Sasol Technology UK. The results of the catalytic testing of the PNE ligands are displayed in Table 2.9.

Run	Pre-catalyst	Time (mins)	TON (mol C_2H_4 /mol Cr)	Activity (mol C_2H_4 /mol Cr/h)	Liquid (wt %)	PE (wt %)	Total (g)	C_4 (wt %)	C_6 (wt %) (1-C_6)[d]	C_8 (wt %) (1-C_8)[d]	C_{10-14} (wt %)	C_{15+} (wt %)
1	$Cr(acac)_3$ + PNN[b]	5	968	11,614	24.5	75.5	0.27	19.9	58.2 (45.4)	21.9 (74.7)	0.0	0.0
2	$Cr(acac)_3$ + PNO[b]	5	1,100	13,196	27.1	72.9	0.31	25.8	51.2 (84.7)	23 (75.2)	0.0	0.0
3	$Cr(acac)_3$ + PNN[c]	5	979	11,747	22.1	77.9	0.28	19.3	53.4 (56.4)	27.3 (72.6)	0.0	0.0
4	$Cr(acac)_3$ + PNO[c]	5	1,105	13,262	24.2	75.8	0.31	22.5	50.8 (60.8)	26.7 (74.4)	0.0	0.0
5	$Cr(acac)_3$[b]	8	6,891	49,514	5.0	95.0	1.93	22.4	42.3 (74.2)	20.9 (59.2)	14.4	0.0
6	$CrCl_3(THF)_3$[b]	6	52,829	539,533	0.5	99.5	14.82	12.0	33.3 (16.8)	11 (41.2)	27.8	15.9
7	$CrCl_3(THF)_3$ + PNN[c]	8	5,114	40,886	1.9	98.2	1.44	17.1	54.9 (0.0)	28 (0.0)	0.0	0.0
8	$CrCl_3(THF)_3$ + PNO[c]	10	9,380	56,303	2.3	97.7	2.63	20.5	56.5 (30.9)	23 (49.8)	0.0	0.0
9	$CrCl_3(THF)_3$ + PNC[b]	10	25,785	154,710	1.0	99.0	7.23	12.3	44.1 (19.8)	16.1 (34.8)	21.1	6.4
10	$CrCl_3(THF)_3$ + PNC[c]	10	29,341	168,669	1.0	99.0	8.23	13.8	25.4 (26.2)	13.9 (32.0)	36.0	10.9

[a] General conditions: 10 µmol Cr, 12 µmol ligand, 500 eq MMAO-3A used in all runs; 40 bar ethene; 60 °C; 70 mL PhCl (solvent). [b] *In situ* catalyst activation (Method **A**). [c] Catalyst pre-activation (Method **B**) [d] Selectivity to α-olefin within carbon length fraction

Table 2.9: Ethylene oligomerisation results using PNE ligands in catalysis.

From the catalyst testing undertaken (Table 2.9) the various PNE-based ethylene oligomerisation systems show no selectivity towards ethylene *tri*- or *tetra*-merisation. All of the catalytic systems tested gave predominantly polymer as the product (73-99 %), along with mainly butene, hexene and octenes within the liquid fraction. The overall product distributions given by all the catalyst systems show a mathematical distribution of chain lengths rather than selectivity to one specific chain length. Despite this, a number of trends can be drawn from the data that offer insight into how the PNE ligands may influence the chromium-mediated oligomerisation of ethylene.

The first comparison to be made is that between the two activation methods employed (**A** and **B**). The data in Graph 2.1 demonstrates that any difference in catalytic activity between the two activation methods is negligible, and within the estimated error of the system. The trend that is obvious from these data is the difference in catalytic activity between the PNN- and PNO-based systems, as with both methods of activation the PNO system demonstrates a higher activity (up to 13,282 mol/mol Cr h^{-1}). From this observation it is concluded that the method of catalyst activation has no effect upon the formation of the active catalytic species, and therefore further testing was carried out using Method **A**, namely *in situ* catalyst activation, due to the greater ease of using this method.

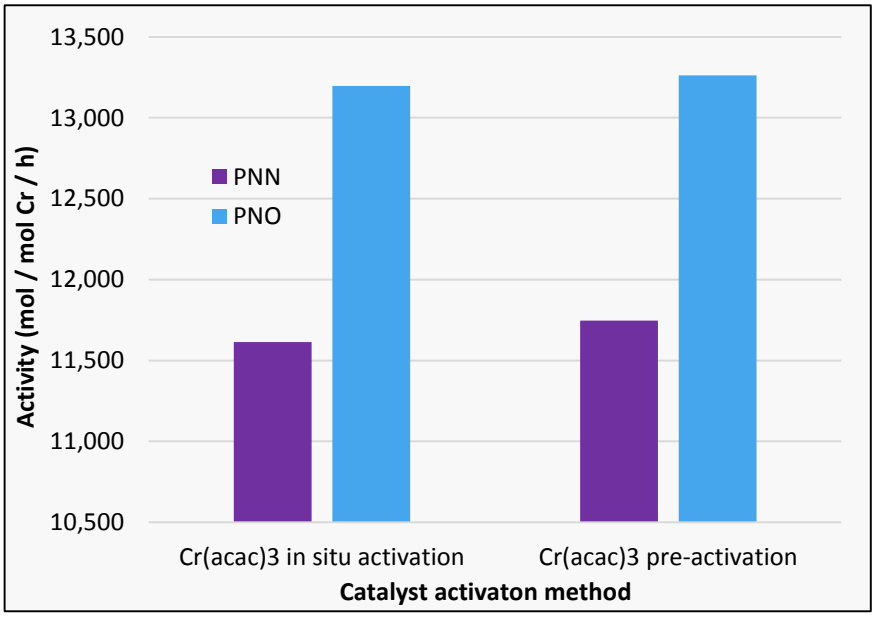

Graph 2.1: A comparison of the effect of *in situ* activation (Method **A**) versus pre-activation (Method **B**) methods on ethylene oligomerisation catalysis, using the PNN and PNO ligands.

The influence of chromium source upon the catalytic system was investigated by comparing systems utilising $Cr(acac)_3$ and $CrCl_3(THF)_3$ as precursors with both PNN and PNO ligands (Graph 2.2). These tests reveal that although there is a significant increase in activity when $CrCl_3(THF)_3$ is used, selectivity towards to the oligomer fraction is lost. The systems

utilising $Cr(acac)_3$ in combination with the PNN and PNO ligands produced between 73-76 % polymer, compared to use of $CrCl_3(THF)_3$, which gave a higher selectivity towards polymer formation of 98-99 % (Graph 2.3).

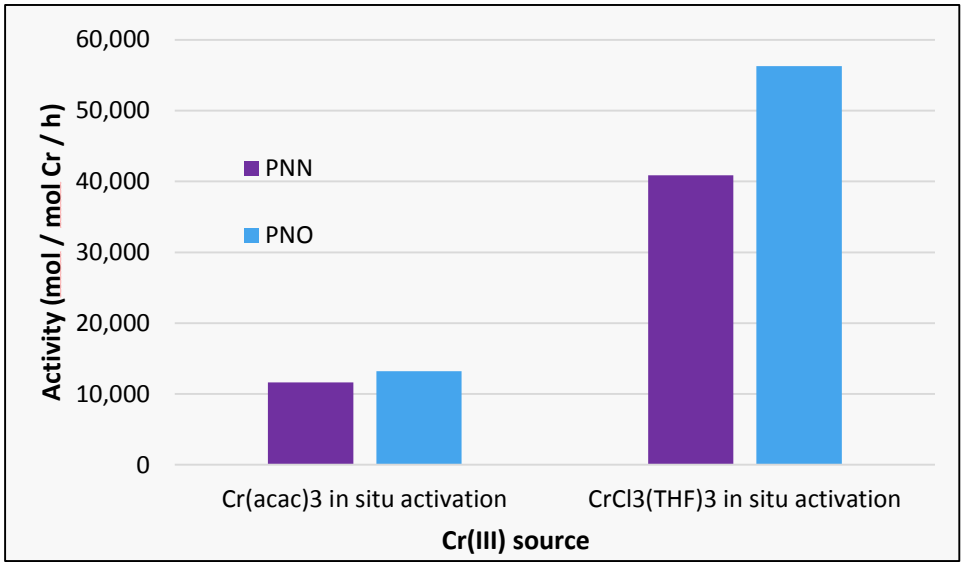

Graph 2.2: Comparison of catalytic activities for ethylene oligomerisation systems using $Cr(acac)_3$ and $CrCl_3(THF)_3$ as the Cr(III) source, with PNN and PNO ligands. Activation Method **A** used.

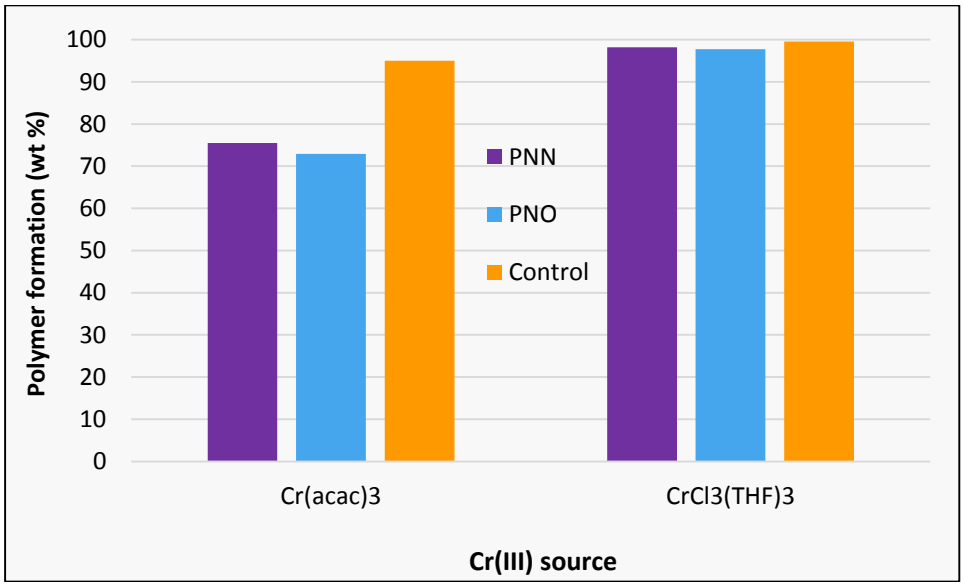

Graph 2.3: Comparison of polymer formation for ethylene oligomerisation systems using $Cr(acac)_3$ and $CrCl_3(THF)_3$ as the Cr(III) source, with PNN and PNO ligands, and a "blank" control run (using 10 µmol Cr(III) and no ligand present). Activation Method **A** used.

It can also be seen from the data in Graph 2.3 that the control run carried out with only the $Cr(acac)_3$ metal precursor (in the absence of PNE ligand) and aluminium activator present gave notably more polymer than the analogous system with a PNE ligand present. Unfortunately, no comparable trend can be drawn for the $CrCl_3(THF)_3$ systems as the extent of polymer formation is too similar to separate from the error of the system. This observation that

PNE ligands inhibit polymerisation activity in the catalytic systems suggests that the PNE ligands favour the formation of oligomer-forming catalytic species, with low activities.

A series of test runs was carried out for each of the three PNE (PNN, PNO, PNC) ligands, and a "blank" control run with only $CrCl_3(THF)_3$ for comparison, all using MMAO-3A as an activator. The data obtained show that the control run gives a much higher activity than the ligand-containing systems (Graph 2.4). Unfortunately, all of the systems using $CrCl_3(THF)_3$ gave very high levels of polymer formation (98-99 %), all of which lie within the estimated error of the system. This means that no conclusions can be drawn from the polymerisation behaviour of the $CrCl_3(THF)_3$-based systems. Despite this, the drop in activity observed when the PNE ligands are present in the catalytic system suggest that the ligands act to inhibit the polymerisation activity of the catalytic system.

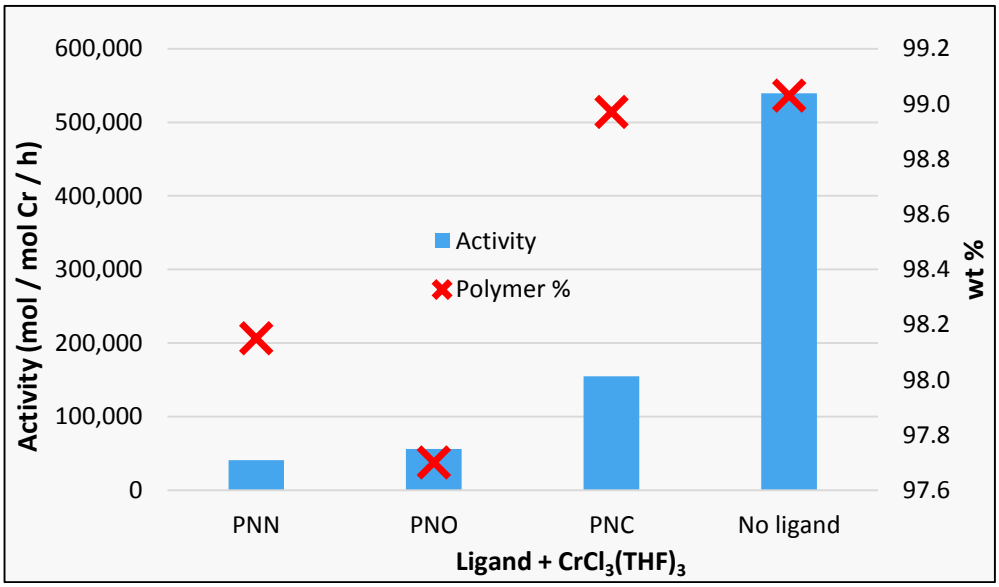

Graph 2.4: Comparison of catalytic activities and extents of polymer formation for $CrCl_3(THF)_3$ based catalytic systems using the PNN, PNO, and PNC ligands, as well as a "blank" control run. Activation Method **A** used.

Arguably the most interesting trend observed from the data compared in Graph 2.4 is the difference between the two PNE systems with E = NMe, O and the PNC ligand. It is clear that the PNC system gives somewhat higher catalytic activities than the PNN and PNO systems. The catalytic activity data show that the presence of a third donor group on the PNE ligand (*i.e.* NMe, O) affects the catalytic activity of the system, if only to inhibit the activity. This effect of the third donor group gives tantalising evidence to suggest that the third donor group may reversibly coordinate during catalysis, and hence limit the formation of highly active polymer producing catalytic chromium centres.

Overall, it can be concluded that the PNO ligand gives the slightly better ethylene oligomerisation behaviour when combined with $Cr(acac)_3$ in an oligomerisation system. It is

hypothesised that the difference between the PNO and PNN-based catalytic systems is due to the different coordinative properties of the N and O donor groups. The fact that Cr(PNO) complexes behave as better ethylene oligomerisation promoters is interesting when compared back to the structure of the first BP PNP trimerisation ligand (Ar_2PNPAr_2, Ar = *o*-$OMeC_6H_4$), containing the all-important *ortho*-methoxy aryl groups.[5] It is tempting to suggest that the ether donor group of the PNO ligand in this study may behave in a similar fashion to that found in the BP PNP system (see Section 1.2.1.2 for details for the BP system), leading to improved ethylene oligomerisation properties (Scheme 2.12).

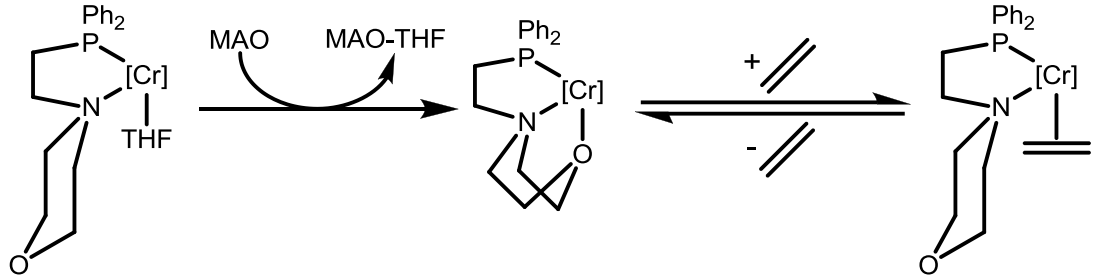

Scheme 2.12: The hypothesised variable bi-/tri-dentate coordination of the PNO ligand with Cr(III) in an ethylene oligomerisation system.

2.6 Summary and Conclusions

In this chapter a small library of PNE (E = NMe, O, CH_2) ligands has been synthesised according to literature procedures, their coordination chemistry with Cr(0), Mo(0) and Cr(III) has been investigated, and they have been tested as ancillary ligands in Cr-based catalytic ethylene oligomerisation systems. The complexation reactions with chromium and molybdenum yielded a series of complexes demonstrating that PNE ligands can adopt either κ^1-mono- or κ^2-bi-dentate coordination modes. All three PNE ligands were reacted with $CrCl_3(THF)_3$ with the aim of synthesising and characterising $CrCl_3$(THF)(PNE) complexes, which may serve as precursors for use in ethylene *tri*- and *tetra*-merisation systems. The complexes $CrCl_3$(THF)(PNO) (**2.1**) and $CrCl_3$(THF)(PNC) (**2.2**) were synthesised and characterised by elemental analysis, but the analogous Cr^{III}(PNN) complex could not be isolated. Due to the paramagnetic nature of the complexes, coupled with their lack of volatility, no further definitive characterisation could be achieved. The ammonium salt of a Cr^{III}(PNO) complex ([$CrCl_4$(PNO)][$HNEt_3$], **2.3**) was successfully synthesised, and X-ray crystallographic analysis revealed the complex exhibits κ^2-bidentate coordination to the chromium centre through the P and N donor groups.

The PNE ligands synthesised were also complexed with $Cr(CO)_6$ and $Mo(CO)_6$ to give complexes demonstrating the various coordination modes of the ligands. Six complexes were synthesised and characterised (**2.4**-**2.9**) and the molecular structures of five of these (**2.4**, **2.6**-**2.9**) were determined. These solid-state studies demonstrate that the PNE ligands can adopt both κ^1-mono- and κ^2-bi-dentate coordination modes, with the P donor group acting as a "permanent tether". The structure of complex **2.4** shows the PNN ligand bound to a chromium as a κ^1-monodentate species, while the structures of **2.6**-**2.9** all show PNE ligands bound to chromium and molybdenum in κ^2-bidentate coordination modes. It has been shown that the monodentate complex **2.4** can be converted to its bidentate analogue, complex **2.10** through decarbonylation of the metal centre. Upon removal of CO with TMNO, the PNN ligand fills the vacant coordination site, a κ^2-P,N-bidentate coordination mode.

Finally, the performance of the PNE ligands as metal scaffolds for selective ethylene oligomerisation was investigated. In combination with an activator (MMAO-3A) and Cr(III) sources the PNE ligands gave low activities and no selectivity towards *tri*- or *tetra*-merisation of ethylene. All of the tests carried out demonstrated a preference for polymerisation (72-99 wt %), although primarily C_4, C_6 and C_8 olefins were found within the product liquid fraction. The systems tested using PNC as a ligand gave more polymer than both PNN and PNO systems, suggesting that the third donor group in the ligand is important for disfavouring polymerisation, and there is likely to be some form of interaction of the third donor group with the metal centre

occurring in the oligomerisation catalytic cycle. It was found that the $Cr(acac)_3$-PNO-based catalyst system gave the best activities and selectivities towards ethylene oligomerisation of all the tests carried out. When compared to other P,N-based ethylene oligomerisation systems, such as those reported by Gambarotta *et al.*,[4] it is clear that PNE-based catalytic systems perform poorly in ethylene *tri*- and *tetra*-merisation processes. Therefore it was concluded that efforts should be made into the development of a new P,N ligand scaffold, which is described in the following chapters of this thesis.

2.7 References

(1) Britovsek, G. J. P.; Gibson, V. C.; Wass, D. F. *Angew. Chem. Int. Ed.* **1999**, *38*, 428.
(2) Helmchen, G.; Pfaltz, A. *Acc. Chem. Res.* **2000**, *33*, 336.
(3) Anderson, C. E.; Apperley, D. C.; Batsanov, A. S.; Dyer, P. W.; Howard, J. A. K. *Dalton Trans.* **2006**, 4134.
(4) Shaikh, Y.; Gurnham, J.; Albahily, K.; Gambarotta, S.; Korobkov, I. *Organometallics* **2012**, *31*, 7427.
(5) Carter, A.; Cohen, S. A.; Cooley, N. A.; Murphy, A.; Scutt, J.; Wass, D. F. *Chem. Commun.* **2002**, 858.
(6) Sydora, O. L.; Jones, T. C.; Small, B. L.; Nett, A. J.; Fischer, A. a.; Carney, M. J. *ACS Catal.* **2012**, *2*, 2452.
(7) Bollmann, A.; Blann, K.; Dixon, J. T.; Hess, F. M.; Killian, E.; Maumela, H.; McGuinness, D. S.; Morgan, D. H.; Neveling, A.; Otto, S.; Overett, M.; Slawin, A. M. Z.; Wasserscheid, P.; Kuhlmann, S. *J. Am. Chem. Soc.* **2004**, *126*, 14712.
(8) Yang, Y.; Gurnham, J.; Liu, B.; Duchateau, R.; Gambarotta, S.; Korobkov, I. *Organometallics* **2014**, *33*, 5749.
(9) Agapie, T.; Day, M. W.; Henling, L. M.; Labinger, J. A.; Bercaw, J. E. *Organometallics* **2006**, *25*, 2733.
(10) Köhn, R. D.; Smith, D.; Mahon, M. F.; Prinz, M.; Mihan, S.; Kociok-Köhn, G. *J. Organomet. Chem.* **2003**, *683*, 200.
(11) Wai-Kwok, W.; Tao, J.; Kwong, D. W. J.; Wing-Tak, W. *Polyhedron* **1995**, *14*, 1695.
(12) Al-Soudani, A.-R. H.; Batsanov, A. S.; Edwards, P. G.; Howard, J. A. K. *J. Chem. Soc., Dalton Trans.* **1994**, 987.
(13) Bowen, L. E.; Haddow, M. F.; Orpen, A. G.; Wass, D. F. *Dalton Trans.* **2007**, 1160.
(14) Bowen, L. E.; Charernsuk, M.; Hey, T. W.; McMullin, C. L.; Orpen, A. G.; Wass, D. F. *Dalton Trans.* **2010**, *39*, 560.
(15) Pearson, R. G. *J. Am. Chem. Soc.* **1963**, *85*, 3533.
(16) Dobson, G. R.; Bernal, I.; Reisner, G. M.; Dobson, B.; Mansour, S. E. *J. Am. Chem. Soc.* **1985**, *107*, 525.
(17) Anderson, C. E., PhD Thesis, University of Durham, **2007**.
(18) Rucklidge, A. J.; McGuinness, D. S.; Tooze, R. P.; Slawin, A. M. Z.; Pelletier, J. D. A.; Hanton, M. J.; Webb, P. B. *Organometallics* **2007**, *26*, 2782.
(19) Chen, H.; Johnson, B. F. G.; Lewis, J.; Braga, D.; Parisini, E.; Ciamician, C. G.; Selmi, V. *J. Chem. Soc., Dalton Trans.* **1991**, *4*, 215.
(20) Ingham, W. L.; Coville, N. J. *Inorg. Chem.* **1992**, *31*, 4084.
(21) Elowe, P. R.; McCann, C.; Pringle, P. G.; Spitzmesser, S. K.; Bercaw, J. E. *Organometallics* **2006**, *25*, 5255.
(22) Sydora, O. L.; Carney, M. J.; Small, B. L.; Hutshison, S.; Gee, J. C.; WO 2011/082192 (Chevron Phillips Chemical Company LP), December 29, **2011**.

Chapter 3:

Synthesis of and Characterisation of Iminophosphine Compounds

3.1 Introduction

Since their discovery in 2002,[1] PNP-based selective ethylene oligomerisation systems have become ubiquitous in the field of ethylene *tri-* and *tetra*-merisation chemistry.[2] The effects of the PNP ligand structure on the activity and selectivity of ethylene oligomerisation systems have been studied in great detail,[3] with three main factors having been shown to have the greatest impact (Figure 3.1):

a) The steric bulk and branching of the N-backbone substituent.[4]

b) The steric bulk and potential donor properties of the P-aryl groups.[5]

c) The bite angle of the bidentate PNP donor.[6]

Consequently, it is suggested that the design of any new ligand to be used in ethylene *tri-* and *tetra*-merisation systems should aim to include attributes of these three features.

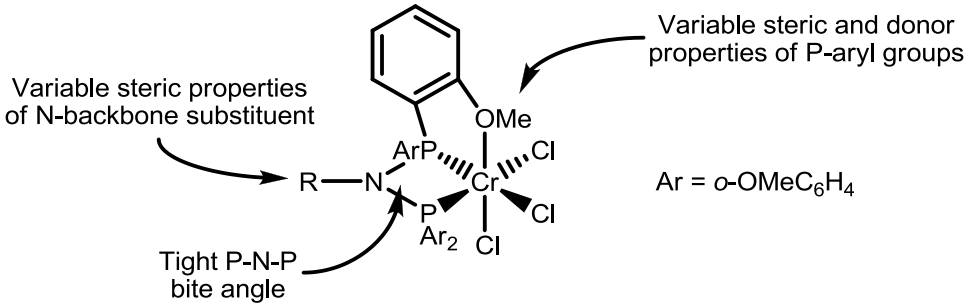

Figure 3.1: A chromium PNP complex isolated by Bercaw *et al.* demonstrating the structural features important for *tri-* / *tetra*-merisation activity.[7]

Due to the saturation of both the open and patent literature with PNP ligands in recent years, a number of research groups have begun the development of novel ligand scaffolds that avoid the PNP structure. One such example comes from workers from Chevron Phillips, in which ligands utilising a combination of phosphine and imine donors have been used as components in chromium-mediated ethylene oligomerisation systems (Figure 3.2).[8]

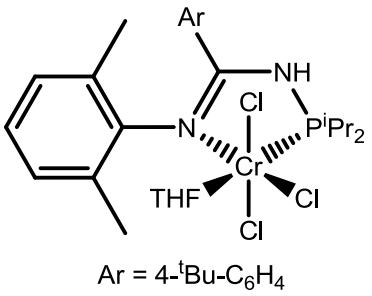

Figure 3.2: A highly active ethylene oligomerisation precursor chromium-iminophosphine complex developed workers from Chevron Phillips.[8]

These novel metal/ligand combinations reported by Chevron Phillips, remarkably, give selectivities and activities comparable to those of traditional PNP-based processes, giving rise

to activities of up to 1,052,000 g/g Cr h^{-1} and selectivities of up to 94 wt % towards 1-hexene. The literature surrounding selective ethylene oligomerisation chemistry contains no other examples of highly active P-imine based ethylene *tri*- or *tetra*-merisation systems, and therefore this paper has opened new avenues of research to be explored.

Due to the notable success of the phosphinoamidine-based oligomerisation system reported by Chevron Phillips it would be of great interest to develop a novel class of iminophosphine ligands utilising the principles governing the activity and selectivity of PNP-systems. With this in mind, this chapter reports the development of novel iminophosphine ligands with a PCN framework (Figure 3.3), incorporating ideas from both the design of PNP ligands and the phosphinoamidine ligands described by the Chevron Phillips group.

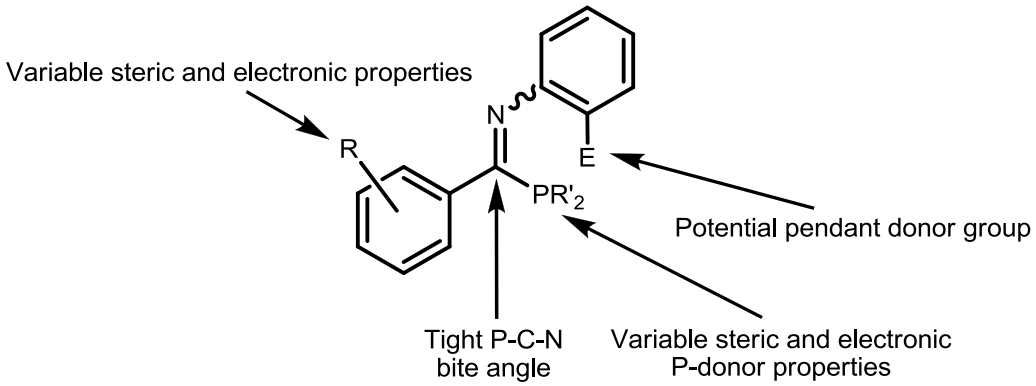

Figure 3.3: Target PCN ligand framework.

The proposed PCN ligand framework displayed in Figure 3.3 can be easily modified, allowing for a library of compounds to be synthesised covering a wide range of ligand properties.* Through the use of different alkyl- and aryl-substituents at phosphorus the steric and donor properties of the phosphine component of these new metal scaffolds can be controlled. The synthesis of PCN compounds bearing a range of N-aryl groups will also be possible. In the future this will hopefully allow for correlations to be drawn between ligand structure and efficacy in Cr-mediated ethylene oligomerisation systems (Chapter 5).

* The iminophosphines synthesised may be able to adopt both *E* and *Z* configurations around the imine bond, a phenomena that will be discussed in Section 3.4. For simplicity and consistency, all iminophosphines will be drawn as the *Z* isomer in this thesis, unless stated otherwise.

3.2 Preliminary Investigations into Iminophosphine Synthesis

This section will discuss investigations into using previously reported methods for the synthesis of the iminophosphine target ligands. A search of the literature for synthetic routes to iminophosphines yields only a few reports. The first reported synthesis of PCN ligands comes from the work of Issleib *et al.* who described reactions of imidoyl chlorides with alkaline metal phosphides, ultimately reporting the synthesis of two iminophosphine compounds (Figure 3.4).[9]

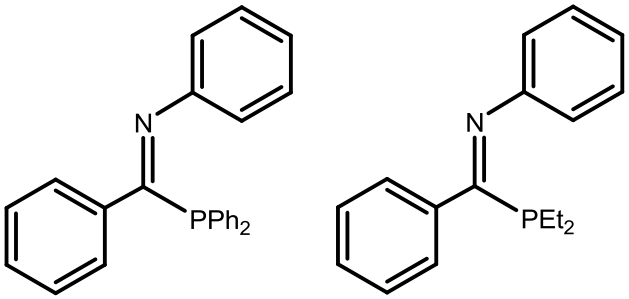

Figure 3.4: The two iminophosphine compounds synthesised by Issleib *et al.*[9]

The disadvantage of Issleib's reported method is the use of alkaline metal phosphides, which are highly reactive and often difficult to isolate, something hindering the development of any modular ligand synthetic procedure. Despite its limitations, a similar phosphide-based route was more recently reported by Cui *et al.*, yielding their iminophosphine product as a white crystalline solid (Scheme 3.1).[10] While this synthetic method has proven to be reliable in the literature, it was not investigated in this thesis due to the limitations in isolating the starting materials required for the reaction.

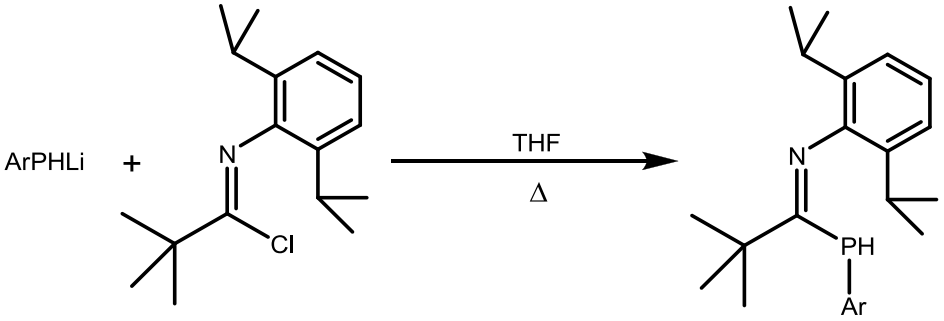

Scheme 3.1: Iminophosphine synthesis reported by Cui *et al.*[10]

3.2.1 Reactions of aldimines with phosphines

Due to the problems isolating the intermediates in Issleib's synthetic route, alternative methods for the synthesis of iminophosphine compounds were investigated in this thesis. In 1988 Abd-Ellah *et al.* reported the synthesis of phosphorus derivatives of Schiff bases, using chlorophosphine and aldimine starting reagents, both of which are stable and easy to manipulate.[11] In their work Abd-Ellah and co-workers propose that this reaction proceeds by attack of the aldimine nitrogen at the phosphine, followed by a rearrangement to yield the PCN iminophosphine product (Scheme 3.2). Due to the apparent ease of the synthesis reported by Abd-Ellah *et al.*, a synthetic methodology based on this approach was used in attempts to prepare iminophosphine ligands, and is reported below.

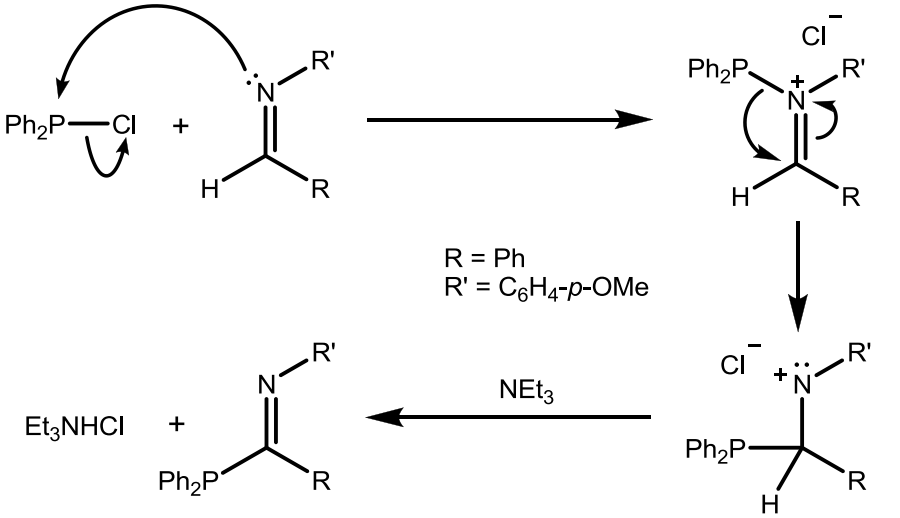

Scheme 3.2: The aldimine-chlorophosphine reaction mechanism proposed by Abd-Ellah *et al.*[11]

3.2.1.1 Attempts to reproduce the synthesis of iminophosphines reported by Abd-Ellah et al.

In an attempt to repeat the synthesis reported by Abd Ellah *et al.*,[11] a solution of the aldimine (C_6H_4-*o*-OMe)N=C(H)Ph and chlorophosphine Ph_2PCl, was heated in toluene to 80 °C. The reaction progress was monitored by ^{31}P NMR spectroscopy but, after 18 hours, no reaction was observed to have taken place. This observation brings into question the reproducibility and generality of the iminophosphine synthesis reported by Abd-Ellah *et al.* Under the conditions used in this thesis it is suggested that this reaction does not proceed as reported due to the chlorophosphine moiety not being reactive enough to attack the imine group.

On the basis of chlorophosphines not being susceptible to attack by aldimines under the conditions used in the current investigation, it was proposed that a more reactive phosphorus species might be more amenable to this reaction sequence. Consequently, an alternative strategy was devised in which the more reactive lithium diphenylphosphide was reacted with the aldimine (C_6H_4-*o*-OMe)N=C(H)Ph. Here, a solution of (C_6H_4-*o*-OMe)N=C(H)Ph and lithium

diphenylphosphide in THF was heated at reflux, and the reaction progress monitored periodically by ^{31}P NMR spectroscopy. After 20 hours at reflux no reaction was observed to have taken place, again leading to the conclusion that this synthetic route is impractical. No further attempts were made to investigate the reaction of phosphines or phosphides with aldimines.

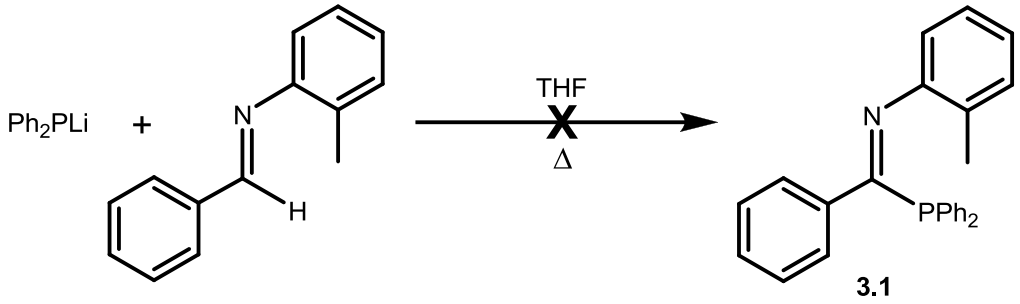

Scheme 3.3: The attempted reaction of diphenylphosphide with a secondary aldimine.

3.2.2 Production of iminophosphines from nitrilium salts

Recent work by Slootweg and Lammertsma *et al.* has shown that it is possible to synthesise iminophosphines from nitrilium salts.[12] Their work shows that nitrilium triflates can be easily synthesised by the reaction of chloroimines with TMSOTf at low temperatures (–78 °C), which can subsequently be reacted with phosphines to yield iminophosphine products in good yields (Scheme 3.4). It is reported that these nitrilium salts are easily isolable, and stable (albeit at –80 °C), making them promising candidates for a modular synthetic route to iminophosphines. To this end, it was attempted to repeat the iminophosphine synthesis reported by Slootweg and Lammertsma *et al.*

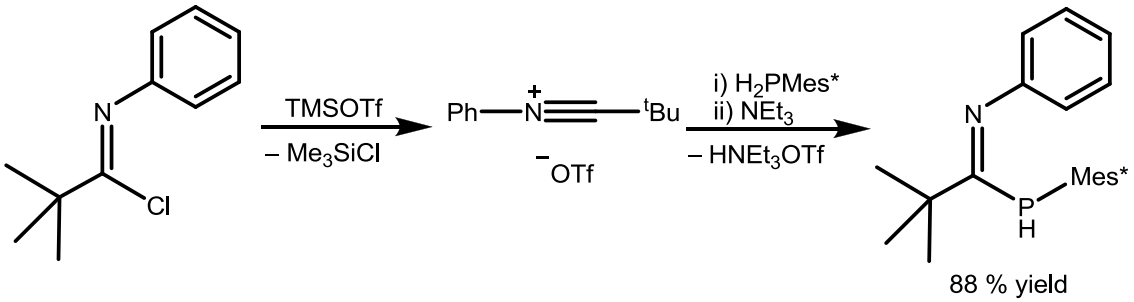

Scheme 3.4: Synthesis of an iminophosphine from a nitrilium salt reported by Slootweg and Lammertsma *et al.*[12]

3.2.2.1 Attempted synthesis of an iminophosphine from a nitrilium salt

A synthetic route to create iminophosphines was explored using the nitrilium salt route reported by Slootweg and Lammertsma *et al*.[12] Initially, the benzimidoyl chloride (C_6H_4-*o*-Me)N=C(Ph)Cl was converted to its nitrilium salt, before pyridine was added to stabilise this

highly reactive species as a pyridinium salt. This salt was then reacted with Ph_2PH, to yield a crude product as an oil (Figure 3.5).

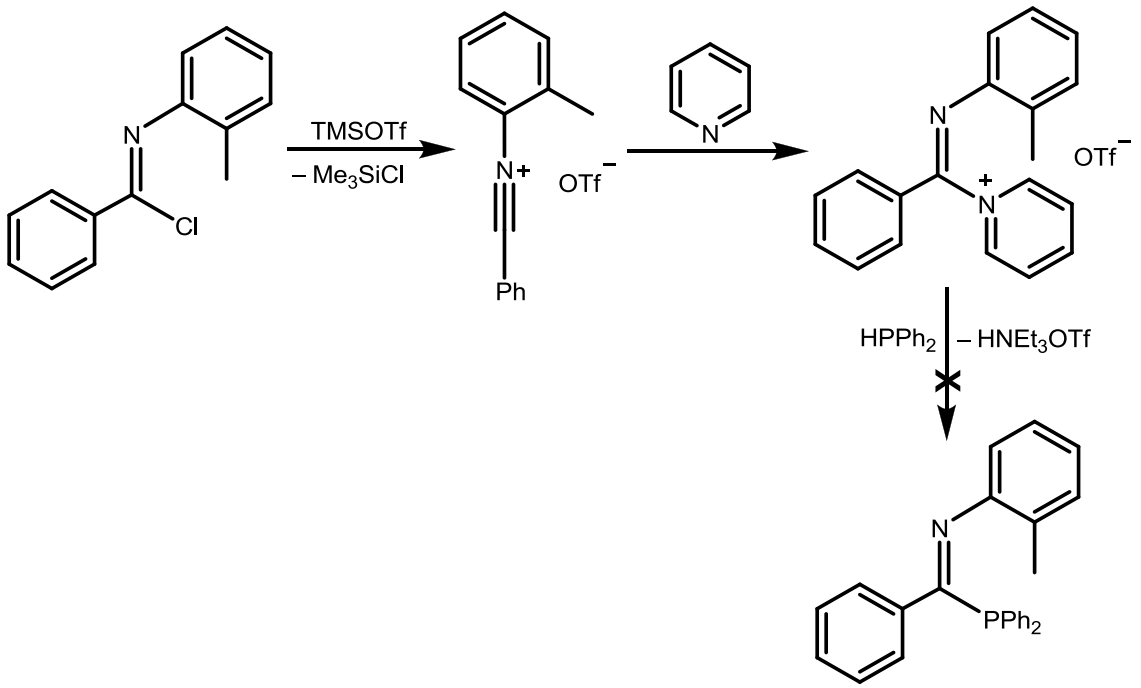

Figure 3.5: Attempted synthesis of an iminophosphine from a nitrilium salt carried out in this investigation.

Analysis of the oil by ^{31}P NMR spectroscopy showed that the reaction had formed a large number of products (11 separate resonances), with one major product (~ 50 % by integration). Unfortunately, the complex and highly soluble nature of the product mixture precluded all attempts at purification. It is proposed that the lack of success of this reaction is due to the highly reactive nature of the starting nitrilium salt, which can easily undergo a range of side reactions with the phosphine. Again, this led to the conclusion that the nitrilium-based synthetic route to iminophosphines is of limited use in developing a modular synthesis to create a library of iminophosphines. As a result, no further investigations into this route to iminophosphines was undertaken.

3.2.3 Synthesis of iminophosphine ligands from the reaction of chloroimines and trimethylsilylphosphines

Due to the lack of success encountered with the synthetic strategies attempted to yield the iminophosphine target, an alternative method was sought. To this end, it was found that there are a limited number of examples in the literature of the reaction of trimethylsilylphosphines with imidoyl chlorides that eliminate TMSCl to yield the desired iminophosphine product. The first of these publications came from Issleib *et al.* demonstrating

the potential of this silyl-transfer reaction.[13] Citing Issleib's work, in 2003 Walther *et al.* published their synthesis of a range of novel 2,3-*bis*(diarylphosphanyl)-1,4-diazadiene ligands, containing a P-C=N iminophosphine motif, using the same type of silyl transfer reactions.[14] In this work the reaction of an α-chloroimine with a silylated phosphine was shown to generate the desired iminophosphine containing fragment (Scheme 3.5) in reasonable yields (~ 65 %).

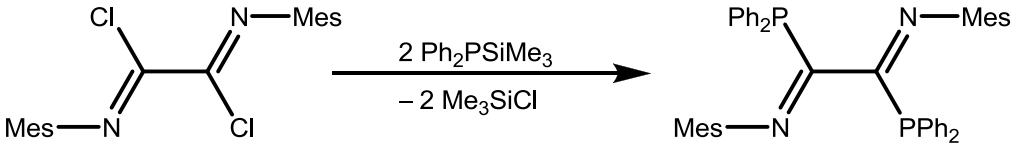

Scheme 3.5: The synthesis of 2,3-*bis*(diarylphosphanyl)-1,4 dimesityl-1,4-diazadiene reported by Walther *et al.*[14]

This silyl transfer reaction pathway demonstrates a number of advantages over the previously discussed routes to iminophosphines. The starting materials are easily synthesised on a large scale, are stable, and can be stored for extended periods of time. Another major advantage is that the side product of the reaction (TMSCl) is volatile and can be easily removed from the product under reduced pressure. Together, these features make this silyl-transfer route to iminophosphines highly attractive for investigation.

3.3 Synthesis and Characterisation of Iminophosphine Ligands

3.3.1 First synthesis of iminophosphine ligands

Building on the work reporting the synthesis of di-iminophosphines by Walther *et al.*,[14] a successful synthetic route was developed to give the related mono-iminophosphine compounds (Scheme 3.6). Initially the synthesis of these iminophosphines was carried out by heating a solution of benzimidoyl chloride with the relevant trimethylsilyl phosphine at reflux in toluene for 5-16 hours.

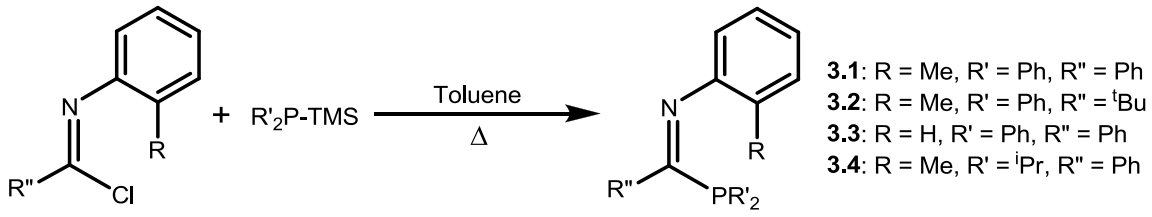

Scheme 3.6: New synthetic route to iminophosphine ligands, used to synthesise ligands **3.1** – **3.4**.

The first iminophosphine to be prepared (**3.1**) was synthesised from trimethylsilyl(diphenyl)phosphine, which was generated *in situ* before addition of the imidoyl chloride. The reaction was subsequently heated at reflux and its progress monitored by ^{31}P NMR spectroscopy. Upon completion, the volatile components were removed *in vacuo* to yield the crude product as a yellow oil. Subsequently, the product was purified by re-crystallisation from hot hexane to yield **3.1** as a yellow crystalline solid in good yield (76 %). The iminophosphine product was fully characterised by NMR spectroscopy, elemental analysis and mass spectrometry. Interestingly, upon analysis of iminophosphine **3.1** by ^{31}P NMR spectroscopy, two broad resonances are observed. It is suggested that these are due to the imine isomerising in solution, displaying both *E* and *Z* isomers. This *E*/*Z* isomerism behaviour is discussed in detail in Section 3.4.

The synthetic method described in Scheme 3.6 was used for the synthesis of iminophosphines **3.2-3.4**, albeit using pre-formed trimethylsilyl phosphines and imidoyl chlorides. Both compounds **3.2** and **3.3** were isolated as yellow crystalline solids in good yields (~85 %) by crystallisation from hot hexane and fully characterised by NMR spectroscopy, elemental analysis and mass spectrometry. Single crystals of what was thought to be **3.2** were obtained *via* recrystallization from hot hexane, and analysed by X-ray crystallography (Figure 3.6). However, the molecular structure showed the crystals contained a mixture of oxidised iminophosphine (90 %) in addition to the target P(III) derivative (10 %), suggesting that **3.2** had been exposed to air during recrystallization. Crystallographic analysis showed the crystal to contain both P(V) and P(III) centres as a "solid solution", meaning only the P(V) iminophosphine-

oxide structure was determined. Table 3.1 shows selected bond lengths and angles determined for the P-oxide of **3.2**. NMR spectroscopic analysis of the bulk iminophosphine sample showing no evidence of phosphine oxidation, confirming that the oxidation of compound **3.2** had occurred during crystallisation.

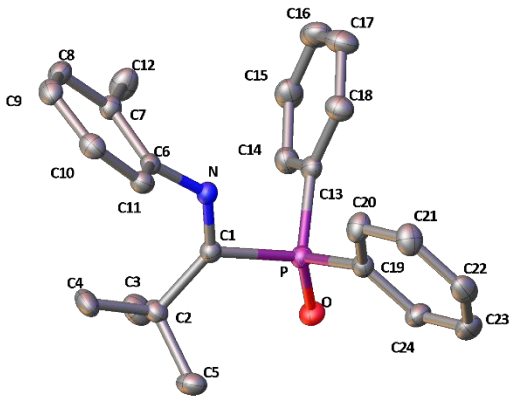

Figure 3.6: ORTEP representation of the molecular structure determined for the P-oxide of **3.2** with thermal ellipsoids at the 50% probability level.

^{t}Bu(OPPh$_2$)C=N(*o*-MeC$_6$H$_4$), (3.2 P-oxide)		
Bond Lengths (Å)	N – C(1)	1.270(2)
	P – C(1)	1.864(1)
	C(1) – C(2)	1.530(2)
Bond Angles (°)	P-C(1)-N	108.41(8)
	Angles around C(1)	360

Table 3.1: Selected bond lengths (Å) and angles (°) determined for the P-oxide of **3.2**

Interestingly, analysis of the bulk-sample of iminophosphine **3.2** by ^{31}P NMR spectroscopy in solution shows only one phosphorus resonance (δ = –0.2 ppm), compared to two observed for the analogous compound, **3.1** (see Table 3.2). This result suggests that compound **3.2** is locked in, presumably, the *E* configuration (by reference to the molecular structure of the oxidised iminophosphine) in solution, most likely as a result of the ^{t}Bu backbone group being sufficiently bulky to make the *Z* isomer unfavourable.

Upon analysis of iminophosphine **3.3** (Ph(PPh$_2$)C=NPh) by ^{31}P NMR spectroscopy two phosphorus environments are observed, comparable to compound **3.1**. This similarity between the ^{31}P NMR spectra of **3.3** and **3.1** is perhaps unsurprising, as the steric bulk of the substituents of both compounds is very similar. Unfortunately due to the complexity of the ^{1}H and ^{13}C NMR spectra of **3.3** not all the resonances could be assigned. Selected NMR and IR spectroscopic data

for compounds **3.1**, **3.2**, **3.3** and *N*-(2,2-dimethyl-1-(phenylphosphino)propylidene)aniline[12] (^{t}Bu(PHPh)C=NPh, **A**) are shown in Table 3.2. It can be seen that all three compounds synthesised in this study display a characteristic doublet in their ^{13}C NMR spectra at δ ≈ 177 - 180 ppm, indicative of the imine carbon signal, which exhibits coupling to phosphorus. The C=N-*C ipso*-carbon also give rise to a resonance at a characteristic ^{13}C NMR chemical shift of δ ≈ 149 - 152 ppm for all of the compounds.

Spectroscopic technique		**3.1**	**3.2**	**3.3**	**A**[12]
^{13}C NMR (ppm) [a]	*C*=N-C	177.1	180.0	178.5	185.4
	C=N-*C*	150.4	149.4	152.2	152.1
^{31}P NMR (ppm) [a]	*P*	8.2, –2.2	–0.2	8.5, –3.2	–64.7
IR (cm^{-1}) [b]	C=N stretch	1588	1611	1587	1595

[a]NMR spectroscopy carried out in $CDCl_3$. ^{13}C NMR 176 MHz, ^{31}P NMR 283 MHz
[b]IR spectra measured in the solid state as a Nujol mull

Table 3.2: A comparison of selected spectroscopic data for compounds **3.1**, **3.2**, **3.3** and ^{t}BuC(PHPh)=NPh (**A)**.

In contrast to the previous iminophosphines synthesised in this investigation (namely compounds **3.1**-**3.3**), the bulk sample of compound **3.4** could not be isolated as a solid, and could only be acquired as an oil. Therefore the crude product was purified by vacuum distillation (0.2 mbar, 119 - 124 °C), however this did not remove traces (~ 10 %) of the chloroimine starting material. Despite the oily nature of the bulk sample of **3.4**, small samples of the purified product did crystallise upon standing to give crystals suitable for X-ray crystallographic analysis; the structure is shown in Figure 3.7. A selection of bond lengths and angles are presented in Table 3.3.

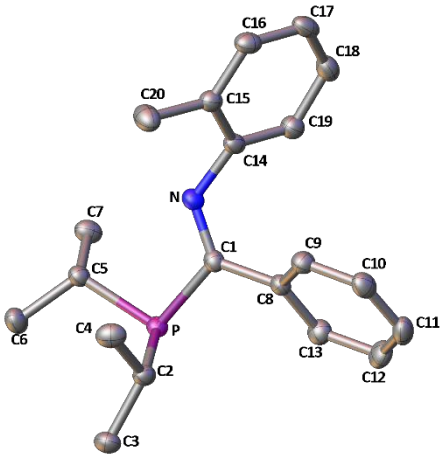

Figure 3.7: ORTEP representation of the molecular structure determined for **3.4** with thermal ellipsoids at the 50 % probability level.

	Ph(P^iPr_2)C=N(*o*-MeC_6H_4), (3.4)	
Bond Lengths (Å)	N – C(1)	1.2832(16)
	P – C(1)	1.8553(12)
	C(1) – C(8)	1.4936(17)
Bond Angles (°)	P-C(1)-N	118.41(9)
	Angles around C(1)	360

Table 3.3: Selected bond lengths (Å) and angles (°) determined for **3.4**.

The molecular structure of **3.4** is as expected for this type of iminophosphine. Interestingly, the C(1)-C(8) bond distance is the shortest C-C bond in iminophosphine **3.4**, suggesting there is a partial conjugation between the imine and phenyl backbone groups. Again, as with compound **3.2**, the structure of iminophosphine **3.4** adopts an *E* conformation about the imine double bond in the solid state, similar to that found for **3.2**. The ^{31}P NMR spectrum of **3.4** shows only one signal, suggesting the imine is fixed in the *E* conformation in solution on the NMR timescale at ambient temperature, as well as in the solid state.

Attempts were also made to synthesise and purify (Ph-*o*-OMe)N=C(Ph)PPh_2, but the compound was found to have a very high boiling point (~180 °C, 0.3 mbar), which prevented purification. Consequently, the product could not be fully characterised, although analysis of the crude mixture by ^{31}P NMR spectroscopy showed two resonances (δ = 8.2, –0.9) indicative of both *E* and *Z* isomers being present in solution (see Section 3.4).

3.3.2 Further Developments to the Silyl-transfer Synthesis of PCN Compounds

The synthesis of iminophosphine ligands, as detailed in Scheme 3.6, was found to work well when using diphenyl- and diisopropyl-phosphines, but when reactions were attempted using trimethylsilyl-*bis*(*tert*-butyl)phosphine the reaction was found to be very slow at best, and at worst, impossible to reach completion. For example, when the imidoyl chloride PhN=C(Ph)Cl was heated at reflux in toluene with trimethylsilyl-*bis*(*tert*-butyl)phosphine for 48 hours, subsequent analysis by ^{31}P NMR spectroscopy showed the reaction had only achieved 45 % conversion of the starting phosphine to product, indicating a much lower rate of reaction than for the analogous trimethylsilyl(diphenyl)phosphine syntheses (Section 3.3.1). It was therefore speculated that the toluene solvent may not be polar enough to aid the nucleophilic phosphine attacking the imine carbon, especially when using the bulky and weakly nucleophilic di-*tert*-butylphosphine. McMurry describes the effect of polar aprotic solvents upon S_N2 reactions, and the increase in reaction rate caused by increasingly polar solvent.[15] Consequently, based on the hypothesis that the target reaction does indeed proceed *via* an S_N2 mechanism, the more polar solvent chlorobenzene was used in place of toluene. When PhN=C(Ph)Cl was treated with trimethylsilyl-*bis*(*tert*-butyl)phosphine and heated to reflux in chlorobenzene, it was found that the reaction went to completion within 16 hours. Based upon this result, chlorobenzene was used as a solvent in synthesising all of the remaining compounds in the PCN ligand library (**3.6**-**3.26**, see Figure 3.8), starting with ligand **3.6** (Scheme 3.7).

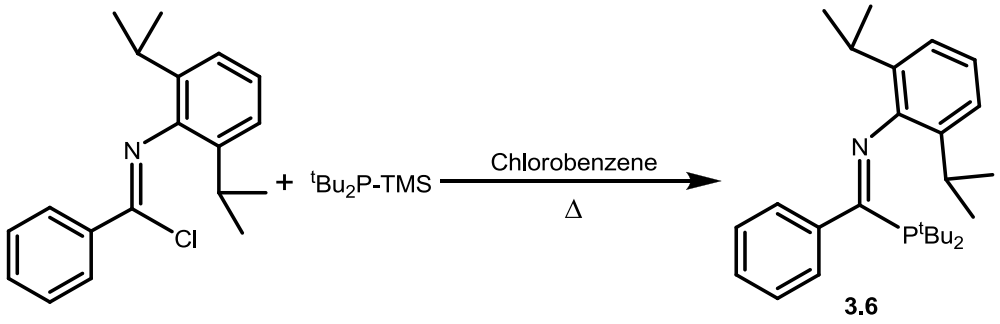

Scheme 3.7: Synthetic procedure for iminophosphine synthesis in chlorobenzene, using **3.6** as an example.

Assuming that the reaction of trimethylsilyphosphines with imidoyl chlorides does occur *via* an S_N2 mechanism, it is suggested that the mechanism is analogous to the formation of amides by the substitution of acyl chlorides with amines, as described by Clayden *et al.* (Scheme 3.8).[16] It is therefore thought that the iminophosphine formation follows a similar pathway, undergoing elimination of TMSCl, rather than the formation of an ammonium salt in the amide forming reaction (Scheme 3.9).

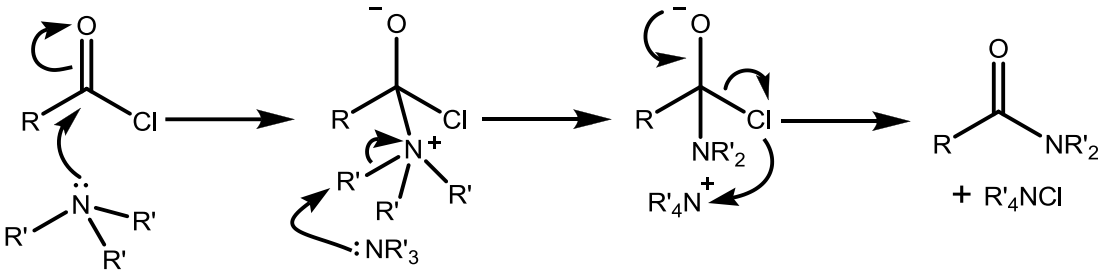

Scheme 3.8: Mechanism of amide formation from acyl chlorides and tertiary amines as described by Clayden *et al.*[16]

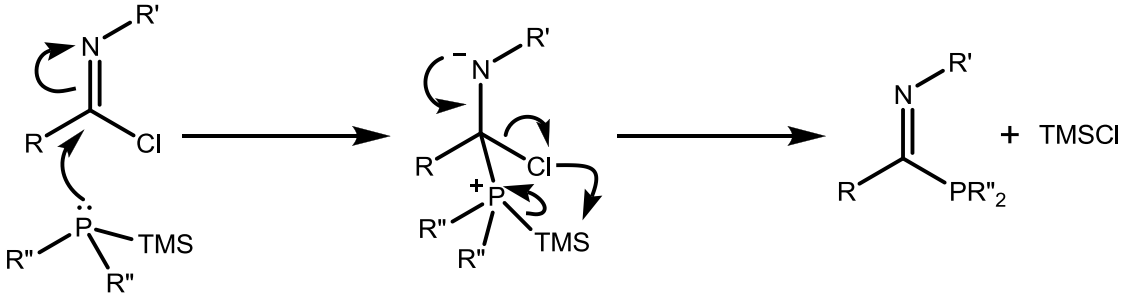

Scheme 3.9: Proposed mechanism for the formation of iminophosphines from trimethylsilyphosphines and imidoyl chlorides.

In a small number of the iminophosphine synthesis reactions carried out (*e.g.* **3.5, 3.6, 3.9, 3.10, 3.16, 3.18**) the formation of a secondary phosphine side-product was observed by ^{31}P NMR spectroscopy. This side reaction leads to the presence of unreacted imidoyl chloride, and so additional trimethylsilyphosphine starting material was added to these reactions, to compensate for this effect. The amount of phosphine added was based on the percentage of the secondary phosphine formed, relative to the desired product, as measured by integration of the ^{31}P NMR spectrum of the crude reaction mixture. The secondary phosphine side products were easily removed *in vacuo* along with the other volatile reaction components. It is thought that the formation of the secondary phosphines may have been due to the reaction of the relevant trimethylsilyphosphine with HCl, present in small amounts from hydrolysis of the imidoyl chloride (Scheme 3.10). It is thought that this hydrolysis of the imidoyl chlorides occurred after the purification of the compounds, while transferring the product oils from a Kugelrohr vacuum distillation setup (in air), into a flask under an inert atmosphere.

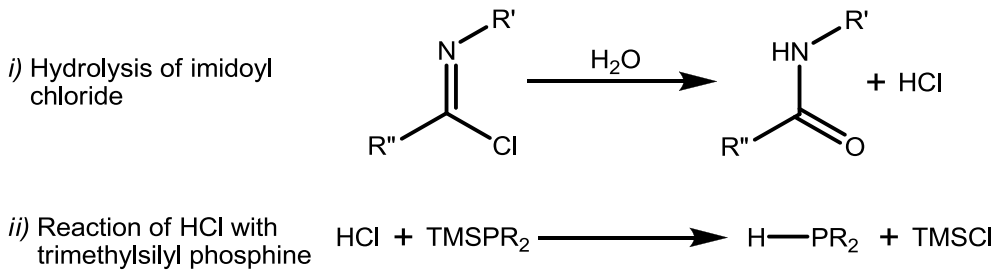

Scheme 3.10: Proposed route of HCl formation, and the subsequent reaction of HCl with trimethylsilyphosphines.

Once established, the chlorobenzene-based synthetic route was used to synthesise a library of PCN ligands. This was made possible due to the modular nature of the synthetic route used, meaning a large number of ligand variants could be synthesised from a relatively small number of starting materials, all of which were easily produced on reasonable to large scales (2 - 50 g). The full library of PCN ligands synthesised is shown in Figure 3.8, and the relevant ^{31}P NMR spectroscopic data and isolated yields for the compounds is displayed in Table 3.4.

Iminophosphine	Isolated Yield (%)	^{31}P NMR δ (ppm)[a]
3.1	76	8.2, –2.2
3.2	84	–0.2
3.3	87	8.5, –3.2
3.4	65	26.7
3.5	80	45.0
3.6	59	49.5
3.7	87	9.3, –5.0
3.8	81	8.8, 1.0
3.9	64	27.1
3.10	76	26.9
3.11	40	–12.1, –24.7
3.12	80	48.7
3.13	79	45.0
[a] ^{31}P NMR 283 MHz		

Iminophosphine	Isolated Yield (%)	^{31}P NMR δ (ppm) [a]
3.14	67	18.5
3.15	45	18.8
3.16	82	27.8
3.17	84	2.8
3.18	60	–8.1
3.19	42	–15.8
3.20	59	15.5
3.21	65	13.7
3.22	81	26.6
3.23	51	31.5
3.24	46	9.3, –19.1
3.25	70*	34.1
3.26	76	2.5
[a] ^{31}P NMR 283 MHz		

Table 3.4: The isolated yields and ^{31}P NMR spectroscopic data for iminophosphines **3.1**-**3.26**.

* Approximate yield, not all of the product could be removed from flask due to the highly viscous nature of the compound.

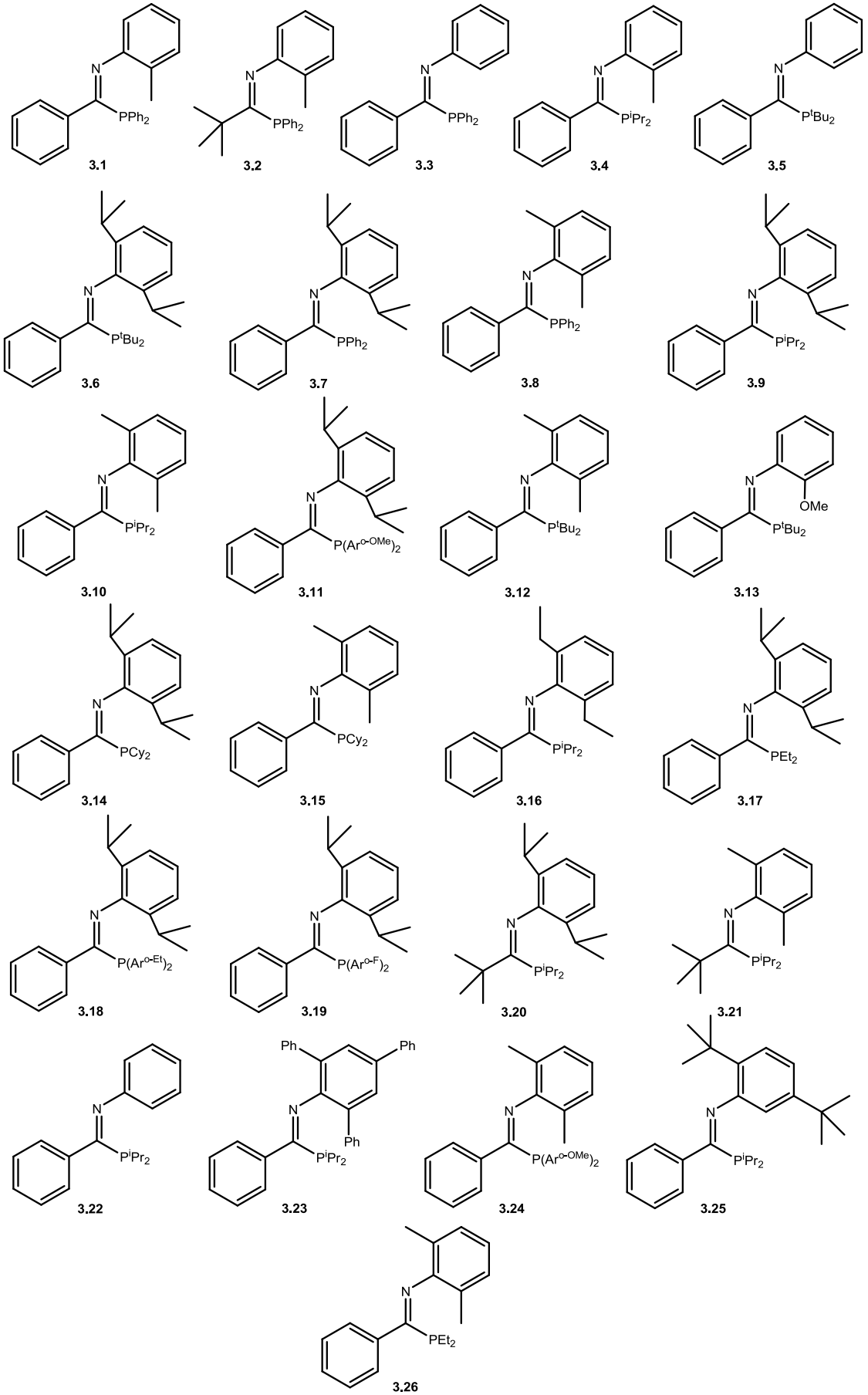

Figure 3.8: The library of iminophosphine ligands **3.1**-**3.26** synthesised in this investigation

The PCN ligands synthesised (**3.1**-**3.26**) were selected in order to cover a wide range of steric and electronic properties, with a view to probing their efficacy in Cr-mediated ethylene oligomerisation (Chapter 5). The three functional groups that were varied were: *a)* the carbon backbone substituent (Figure 3.9, R'''); *b)* the N-aryl substituent (Figure 3.9, R and R'); and *c)* the aryl/alkyl phosphine substituent (Figure 3.9, R''). For simplicity of synthesis the iminophosphines were prepared with either a phenyl or a *tert*-butyl backbone, as these groups do not contain α-protons and hence cannot undergo imine tautomerization.

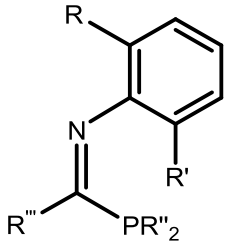

Figure 3.9: The PCN scaffold used in this investigation.

A selection of different N-aryl substituents were used in preparing the PCN compounds, covering a wide range of steric parameters, with phenyl being the smallest, through to 2,4,6-triphenyl-benzene and 2,5-di-*tert*-butyl-benzene being the most sterically demanding. It is difficult to precisely quantify the differences in steric bulk of the N-aryl groups bearing various alkyl substituents, but it has been assumed that N-aryl groups with large substituents in the 2,6 position (*e.g.* 2,6-$^{i}Pr_2C_6H_3$) offer greater steric protection of the imine group than unsymmetrically substituted N-aryl groups with small substituents (*e.g.* 2-MeC_6H_4). As well as N-aryl groups bearing alkyl substituents, a ligand bearing a pendant ether donor (N-C_6H_4-*o*-OMe) has been synthesised in order to probe any potential hemi-labile donor effects, similar to those demonstrated by Bercaw *et al.* for PNP ligands.[7]

Finally, the phosphine substituents have been varied on the iminophosphine compounds. Alkyl groups ranging from ethyl to *tert*-butyl and aryl groups with a range of different electronic and steric properties have been utilised (*e.g.* 2-FC_6H_4, 2-EtC_6H_4), as the steric bulk of phosphines is one of the key factors affecting the reactivity of these functional groups. The characterisation of the steric bulk of the iminophosphine ligands will be further discussed in Section 3.3.3.1.

All of the PCN compounds synthesised in this investigation are listed in Figure 3.8, and each derivative was fully characterised by NMR spectroscopy, mass spectrometry and elemental analysis. Due to the number of iminophosphine variants prepared, the synthesis and characterisation of each individual compound will not be discussed separately, rather a selection of general examples will be covered in detail. Each of the examples detailed below has

been chosen to demonstrate properties and themes that are observed across the whole range of ligands synthesised in this thesis.

3.3.2.1 Synthesis and characterisation of iminophosphine Ph(P^{i}Pr$_2$)C=N(2,6-^{i}Pr$_2$C$_6$H$_3$) (3.9)

The compound Ph(P^{i}Pr$_2$)C=N(2,6-^{i}Pr$_2$C$_6$H$_3$) (**3.9**) was synthesised using the standard chlorobenzene-based synthetic procedure outlined in Section 3.3.2 for iminophosphines. The crude product **3.9** was isolated as a yellow oil that spontaneously crystallises, and was further purified by crystallisation from a concentrated hot hexane solution, which was left to cool slowly and to stand for 16 hours. This crystallisation process was carried out multiple times in order to maximise the recovered yield. The final product was isolated as a yellow crystalline solid in a reasonable yield (64 %). Analysis by NMR spectroscopy, mass spectrometry and elemental analysis confirmed the structure as shown in Scheme 3.11.

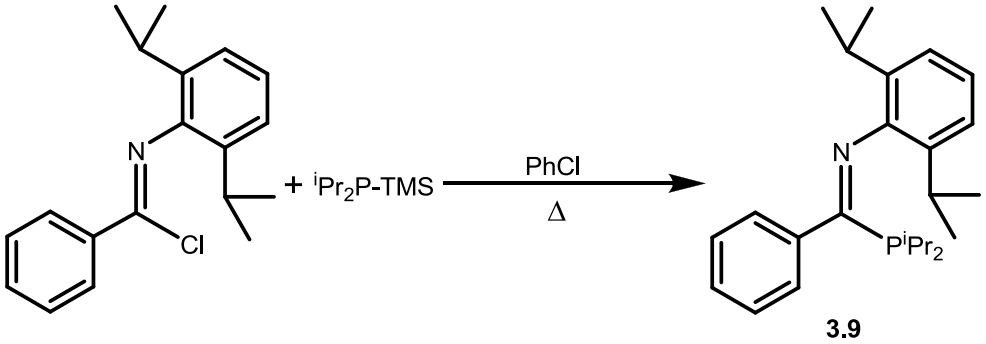

Scheme 3.11: Synthesis of iminophosphine **3.9.**

The ^{31}P NMR spectrum of **3.9** shows one sharp resonance at δ = 27.1 ppm, characteristic of the diisopropylphosphine-substituted iminophosphine ligands synthesised in this investigation. Both the ^{1}H and ^{13}C NMR spectra gave sharp peaks, which were fully assigned, aided by 2D HMBC and HSQC NMR spectroscopic experiments.

IR spectroscopy was also carried out, revealing a C=N stretching frequency of 1583 cm^{-1}. This can be compared to the data gathered by Hessen *et al.* for the related imidoyl chloride, ((2,6-^{i}Pr$_2$C$_6$H$_3$)N=C(Ph)Cl), giving a C=N absorption of 1665 cm^{-1}.[17] Thus, addition of the phosphine group results in a lowering of the C=N stretching frequency, indicating a weaker C=N bond in the PCN compound, relative to that for the analogous imidoyl chloride. It is proposed that this C=N bond weakening is caused by the electron donation from the phosphine lone pair group into C=N anti-bonding orbitals (Figure 3.10), hence altering the electronic donor character on the imine nitrogen.

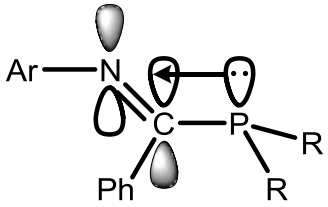

Figure 3.10: Hypothesised electron donation from phosphorus into a π* imine anti-bonding orbital.

3.3.2.2 Synthesis and characterisation of iminophosphine Ph(P(C$_6$H$_4$-o-OMe)$_2$)C=N(2,6-^{i}Pr$_2$C$_6$H$_3$) (3.11)

It has been demonstrated by Wass *et al.* that the presence of *o*-methoxy-substituted phosphine groups upon PNP ligands (*o*-MeOC$_6$H$_4$)$_2$PN(Me)P(*o*-MeOC$_6$H$_4$)$_2$) dramatically increased the activity of PNP-based ethylene trimerisation systems.[1] Based on this, it is of interest to synthesise iminophosphine ligands bearing a P(*o*-MeOC$_6$H$_4$)$_2$ phosphine group, in this case ^{i}Pr$_2$C$_6$H$_3$)N=C(Ph)P(C$_6$H$_4$-o-OMe)$_2$ (**3.11**) (Figure 3.11). The standard chlorobenzene-based synthetic method outlined in Section 3.3.2 was used to synthesise compound **3.11**.

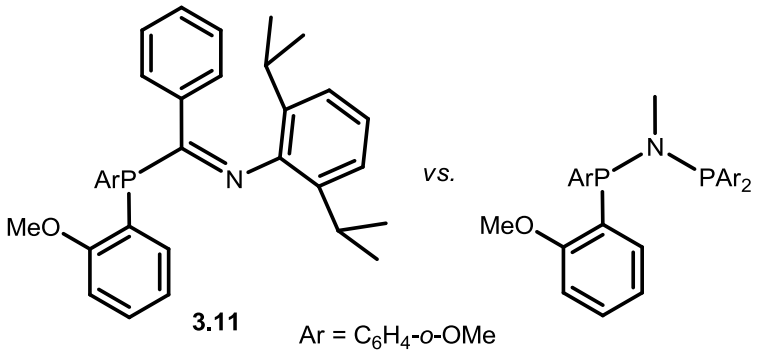

Figure 3.11: Comparison of the structure of **3.11** and the PNP$^{o\text{-OMe}}$ ligand reported by Wass *et al.*, used in highly active ethylene trimerisation systems.[1]

Pure samples of compound **3.11** were isolated by crystallisation of the crude product from hot hexane, yielding the iminophosphine as a yellow solid in a moderate yield (40 %). The compound **3.11** was successfully characterised by NMR spectroscopy, mass spectrometry and elemental analysis. The ^{31}P NMR spectrum of compound **3.11** displayed two signals, indicative of both *E* and *Z* isomers of the imine present in solution.

Both the ^{1}H and ^{13}C NMR spectra display line broadening, indicative of the compound being fluxional in solution on the NMR timescale. In order to aid the assignment of the ^{1}H NMR spectrum, VT NMR spectroscopic experiments were carried out between 25 - 50 °C. Upon increasing the temperature of the NMR spectroscopic experiments the broad signals observed at room temperature sharpened, suggesting an increase in fluxionality of the groups relating to these signals at higher temperatures (α-δ, Figure 3.12).

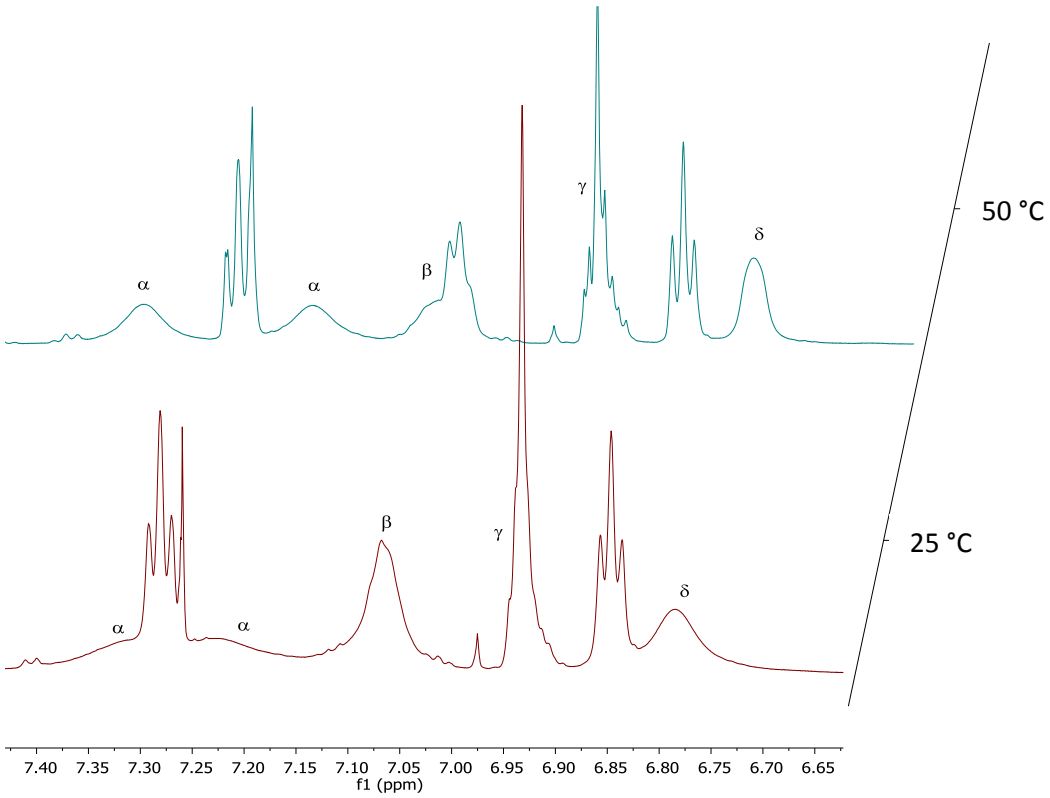

Figure 3.12: ^{1}H (700 MHz, $CDCl_3$) VT NMR spectra of **3.11**.

The use of 2D HMBC, HSQC and COSY NMR spectroscopic experiments allows the assignment of these broad peaks (α-δ) as the di(*ortho*-methoxy-aryl)phosphine aryl protons, suggestive of the line broadening displayed at room temperature being caused by the hindered rotation of these aryl groups (Scheme 3.12). Unfortunately a precise assignment of the signals to individual aryl protons is not possible, even at increased temperature, due to the line broadening.

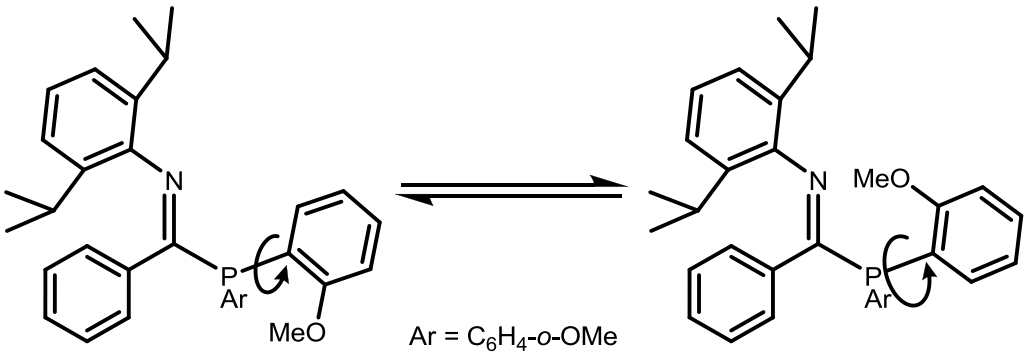

Scheme 3.12: Illustration of the proposed aryl group rotation thought to be cause of the line broadening observed in the ^{1}H and ^{13}C NMR spectra of **3.11**.

Interestingly, upon raising the temperature of acquisition of the ^{31}P NMR spectroscopic experiments, the phosphorus signals were seen to broaden, rather than sharpen as observed in the ^{1}H NMR spectra (Figure 3.13). This broadening is indicative of an increased rate of interconversion between the two phosphorus species, although at a different rate to the

fluxionality displayed in the ^{1}H NMR spectrum. This supports the suggestion that the two phosphorus signals are caused by separate *E* and *Z* isomers, and this phenomenon will be further discussed in Section 3.4.2. The ^{13}C NMR spectrum of compound **3.11** shows similar line broadening to the ^{1}H NMR spectrum, but VT experiments were not carried out due to the length of time required to run the experiment at high temperatures.

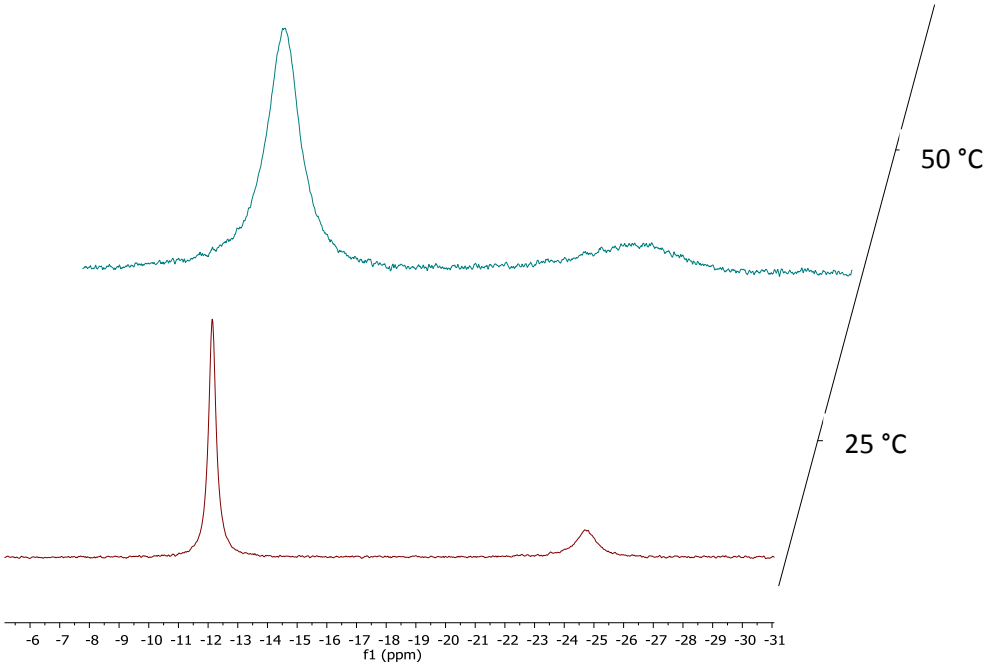

Figure 3.13: ^{31}P (283 MHz, $CDCl_3$) VT NMR spectra of iminophosphine **3.11**.

3.3.2.3 Synthesis and characterisation of iminophosphine Ph(P(o-MeOC$_6$H$_4$)$_2$)C=N(2,6-Me$_2$C$_6$H$_3$) (3.24)

The iminophosphine (2,6-$Me_2C_6H_3$)N=C(Ph)P(*o*-OMe-C_6H_4)$_2$ (**3.24**) was synthesised following the synthetic procedure reported in Section 3.3.2. The pure product was isolated by crystallisation from a mixture of hot hexane (~100 mL) and a small amount of acetonitrile (1 mL) which gave yellow crystals of the title compound in moderate yield (46 %). The crystals grown were of suitable quality for X-ray crystallographic analysis, allowing the molecular structure of compound **3.24** to be determined (Figure 3.14). The compound was fully characterised by NMR spectroscopy, elemental analysis and mass spectrometry, analyses that were in agreement with the molecular structure determined (Figure 3.14).

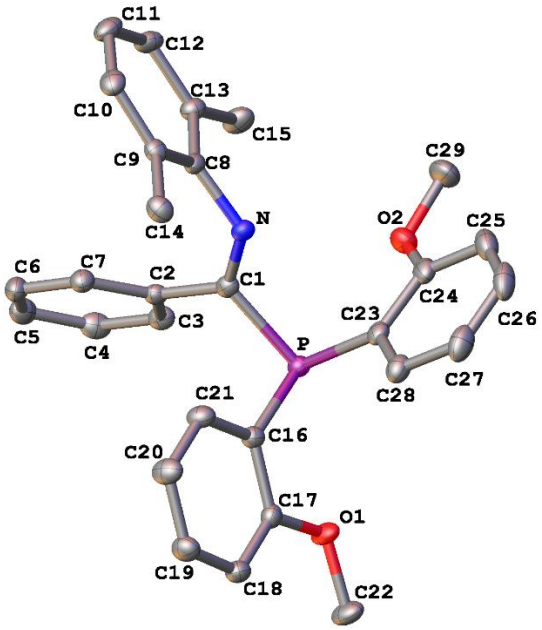

Figure 3.14: ORTEP representation of the molecular structure determined for **3.24**, with thermal ellipsoids set at the 50 % probability level.

The molecular structure depicted in Figure 3.14 exhibits the imine group of **3.24** adopting an *E* configuration, comparable to that of the previous structure determined for the iminophosphine **3.4** (Ph(P^{i}Pr$_2$)C=N(*o*-MeC$_6$H$_4$)). The key bond lengths and angles also match with those reported for **3.4**, and are shown in Table 3.5.

	Ph(P(*o*-OMeC$_6$H$_4$)$_2$)C=N(o-Xyl) (3.24)	
Bond Lengths (Å)	N – C(1)	1.277(2)
	P – C(1)	1.866(2)
	C(1) – C(2)	1.502(2)
Bond Angles (°)	P-C(1)-N	119.7(1)
	Angles around C(1)	360

Table 3.5: Selected bond lengths (Å) and angles (°) determined for iminophosphine **3.24**.

Analysis of compound **3.24** by ^{31}P NMR spectroscopy shows two phosphorus resonances in a 3:2 ratio, suggesting that the iminophosphine is present as both the *E* and *Z* isomer in solution. Further in-depth analysis of the isomerisation behaviour of compound **3.24** is discussed in Section 3.4. Analysis of iminophosphine **3.24** by ^{1}H and ^{13}C NMR spectroscopy at room temperature gives spectra with a number of broad resonances, which hamper the characterisation of the compound. These broad resonances are thought to be due to the hindered rotation of the C-phenyl and P-anisyl groups on the NMR spectroscopic timescale,

similar to those observed for the compound **3.11** (Section 3.3.2.2). To aid the assignment of the ^{1}H and ^{13}C NMR spectra of compound **3.24**, a series of VT NMR spectroscopic experiments were carried out, including 2D experiments to aid the assignment of the spectra. Upon increasing the acquisition temperature of the NMR spectroscopic experiments the broad resonances were found to sharpen to give distinct signals suitable for assignment in both the ^{1}H and ^{13}C NMR spectra; examples these high temperature VT ^{1}H NMR spectra are displayed in Figure 3.15.

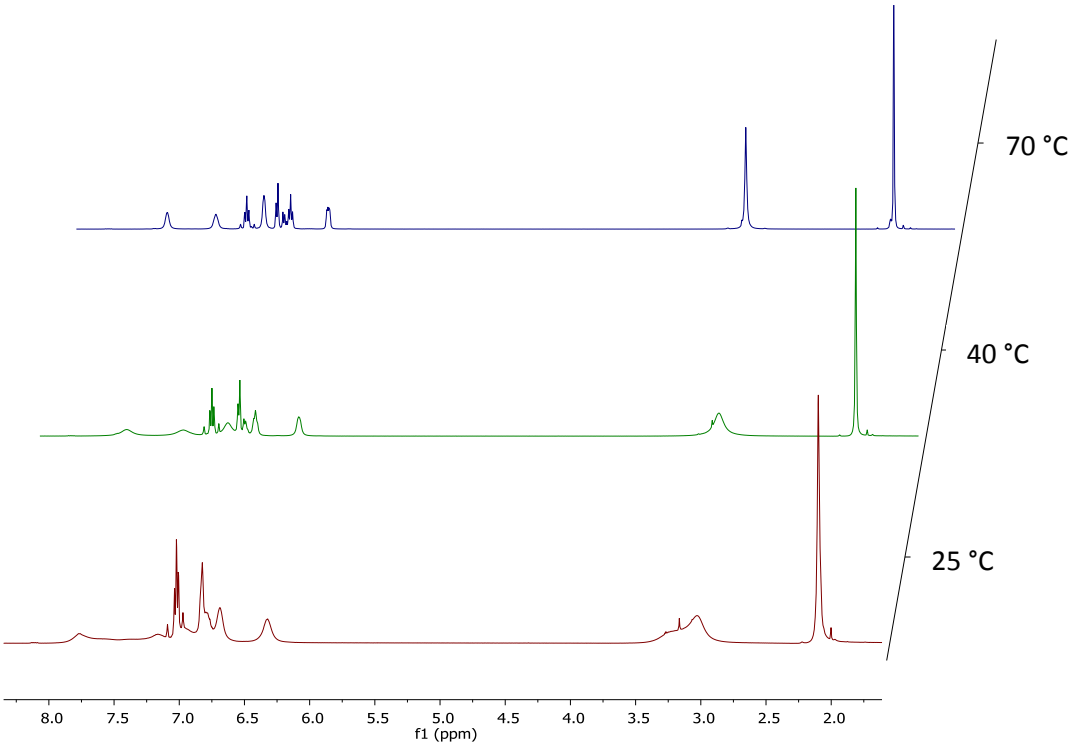

Figure 3.15: Selected high-temperature ^{1}H (500 MHz, d_8-toluene) NMR spectra of iminophosphine **3.24.**

Low temperature NMR spectroscopy experiments were also carried out for compound **3.24**. Upon lowering the temperature to –30 °C each of the broad ^{1}H NMR resonances were observed to separate into two distinct signals, suggesting that the broadening of the signals at room temperature is due to the fast interconversion of two species. It is suggested that this interconversion is due to imine *E* and *Z* isomerisation of the iminophosphine (Scheme 3.13).

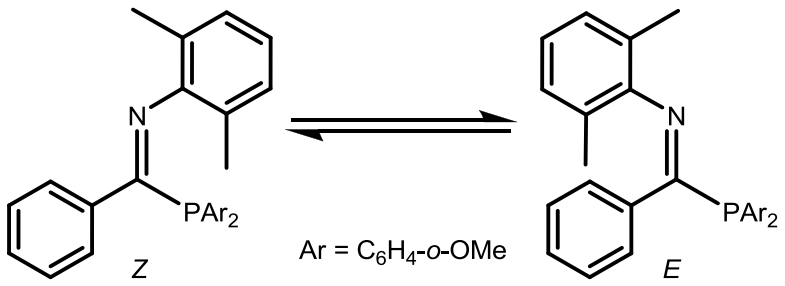

Scheme 3.13: Suggested interconversion between the *E* and *Z* isomers of iminophosphine **3.24**.

In order to prove this hypothesis, the integrals of the new pairs of resonances were measured, and these were shown to give the same 3:2 ratio as displayed by the signals in the ^{31}P NMR spectrum (Figure 3.16). This leads to the conclusion that origins for the observation of the pairs of signals in the ^{1}H NMR spectrum (α, β, γ) at –30 °C and the pair of signals shown in the ^{31}P NMR spectrum are the same, *i.e.* the presence of both *E* and *Z* imine isomers in solution.

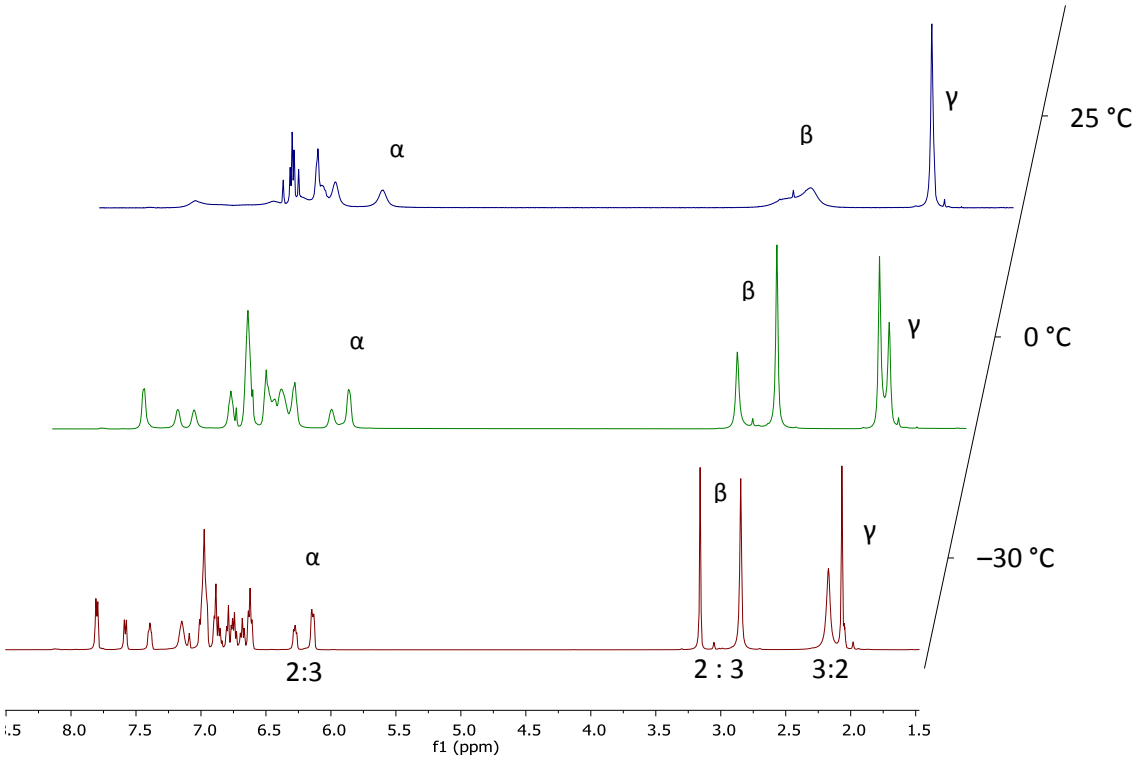

Figure 3.16: Selected low-temperature ^{1}H (500 MHz, d_8-toluene) VT NMR spectra of iminophosphine **3.24**.

3.3.2.4 Synthesis and characterisation of Ph(PEt$_2$)C=N(2,6-Me$_2$C$_6$H$_3$) (3.26)

The compound Ph(PEt$_2$)C=N(2,6-Me$_2$C$_6$H$_3$) (**3.26**) was synthesised following the synthesis reported in Section 3.3.2. The crude product was isolated as a brown oil, which was subsequently distilled under vacuum (0.1 mbar, 130 - 135 °C), yielding the title compound as a yellow oil in good yield (76 %). Analysis of compound **3.26** by NMR spectroscopy, mass spectrometry and elemental analysis confirmed the structure shown in Figure 3.8. However, the ^{1}H and ^{13}C NMR spectra of **3.26** also showed the presence of significant amounts of imidoyl chloride starting material present in the sample (≈ 20 %), which can be assigned based on the NMR spectra collected for the relevant starting material (Figure 3.17).

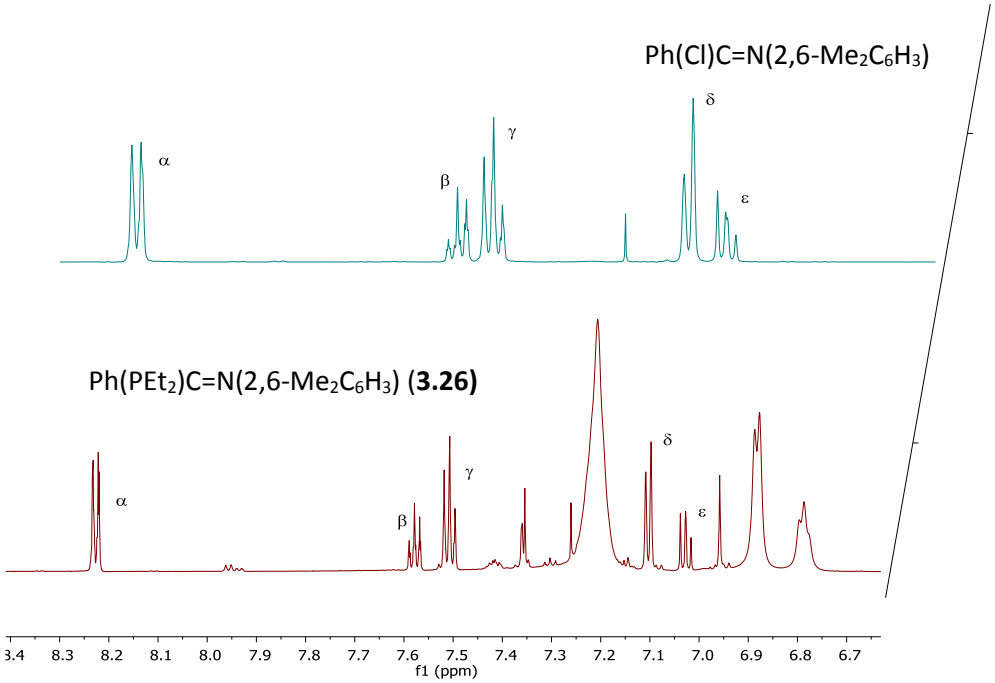

Figure 3.17: A section of the ^{1}H (400 MHz, $CDCl_3$) NMR spectra of Ph(Cl)C=N(2,6-$Me_2C_6H_3$) (top) and Ph(PEt_2)C=N(2,6-$Me_2C_6H_3$) (**3.26)** (bottom)

The NMR spectra in Figure 3.17 show all the peaks α-ε observed in the spectrum of compound **3.26** correspond to signals indicative of the imidoyl chloride starting material (2,6-$Me_2C_6H_3$)N=C(Ph)Cl. It is thought that the vacuum distillation carried out to purify **3.26** also transferred the imidoyl chloride along with the product, which is almost unavoidable due to a very small difference in boiling point of the two compounds (both in the range 130-135 °C).

3.3.3 Characterisation of PCN ligands

As well as the usual characterisation of the novel compounds reported in this thesis, a series of further investigations have been carried out in order to allow for more detailed conclusions regarding the properties of the iminophosphines to be drawn. Three primary features of the PCN compounds have been studied: the overall steric bulk, the C=N bond strength, and the phosphine donor characteristics. The discussion of these studies are reported below.

3.3.3.1 Quantifying the steric bulk of iminophosphines

The steric bulk of phosphines is one of the key factors affecting the reactivity and coordination chemistry of such compounds. In the past, a number of methods to quantify the steric bulk of phosphines have been developed, with the most well-known being the Tolman cone angle, giving rise to the parameter θ.[18,19] The Tolman cone angle is calculated from empirical bond length data and the van der Waals radii for the phosphorus substituents, creating an imaginary cone, which it is assumed the ligand occupies. The angle between the two edges of the cone is described as the Tolman cone angle, θ (Figure 3.18).

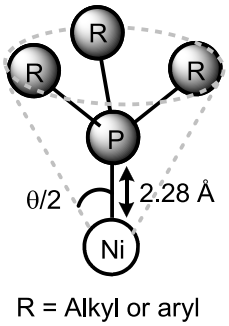

Figure 3.18: Determination of the Tolman cone angle, θ, for a tertiary phosphine; the circles represent the van der Waals radii of the substituents.[18]

The Tolman cone angle is successful at quantifying the steric bulk of monodentate phosphines, but issues arise when the model is applied to bidentate systems.[20] Recently, a new method of assessing steric demand in such multidentate systems has been developed, which calculates the "percent buried volume" ($\%V_{bur}$) in order to measure steric bulk of unsymmetrical ligands.[21] The $\%V_{bur}$ concept was first developed for use with N-heterocyclic carbenes, and has since been modified for use with both mono- and bi-dentate phosphines.[22] The use of $\%V_{bur}$ to quantify steric bulk of ligands, unlike Tolman cone angle, does not rely upon the ligand being symmetrical, hence is of use for ligands such as the iminophosphines in this investigation.

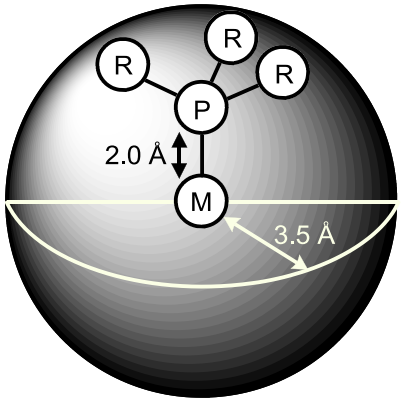

Figure 3.19: Determination of the Percentage Buried Volume (% V_{bur}) for a tertiary phosphine, assuming a fixed M-P distance of 2.0 Å and a sphere radius of 3.5 Å.[21]

The %V_{bur} can be calculated from crystallographic or computational data of the relevant ligand, and is defined as "the percentage of the total volume of a sphere occupied by a ligand",[22] when measured at a fixed metal-ligand bond distance. A series of example %V_{bur} values for tertiary phosphines calculated by Nolan *et al.* is displayed in Table 3.6.[22] The percentage buried volume of tertiary phosphines has been shown to correlate well with the Tolman cone angle calculated for a series of AuCl(PR_3) complexes, suggesting that % V_{bur} is a reliable method of quantifying the steric bulk of phosphines.[22]

PR_3	**Percentage Buried Volume (% V_{bur})**	**Tolman Cone Angle, θ (°)**
PMe_3	26	118
PEt_3	33	132
P^nPr_3	31	132
P^nBu_3	30	132
PPh_3	35	145
$P(p\text{-Tol})_3$	33	145
P^iPr_3	38	160
PCy_3	37	170
P^tBu_3	42	182
$P(C_6F_5)_3$	43	184
$P(o\text{-Tol})_3$	47	194
$PMes_3$	53	212

Table 3.6: Selected percentage buried volume (%V_{bur}) values for tertiary phosphines, calculated for [AuCl(PR_3)] complexes with a fixed Au-P bond distance of 2.00 Å, along with calculated Tolman Cone Angles (θ) for comparison.[22]

The technique for calculating %V_{bur} values for phosphines has been applied to a selection of the iminophosphine compounds synthesised in this investigation, in order to

quantify the steric bulk of the various PCN ligands prepared. The $\%V_{bur}$ values for a series of iminophosphine ligands have been calculated based on computationally-optimised structures of the molecules. Compounds of the general formula $Ph(PR_2)C=N(o\text{-Xyl})$ (R = phenyl, alkyl, Figure 3.20) were used as representative examples of all the iminophosphines synthesised, and the results are collated in Table 3.7. The general structure $Ph(PR_2)C=N(o\text{-Xyl})$ was chosen due to the relative simplicity of the N-Xyl group allowing for the computational optimisations to be carried out easily.

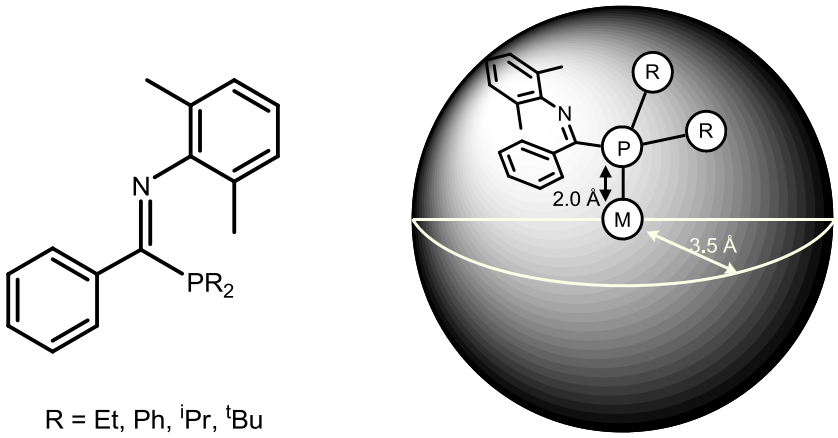

Figure 3.20: The general PCN structure used to calculate representative % V_{bur} values (left) and schematic of how the % V_{bur} is calculated for iminophosphines in this investigation (right).

The $\%V_{bur}$ values for iminophosphines **3.26**, **3.8**, **3.10** and **3.12** were calculated from computationally-optimised (DFT, B3LYP 6-31G+ basis) structures of the compounds, while the Cartesian-coordinate files of these structures were processed using SambVca© software.[21] In order to verify the validity of these computationally-derived ligand structures, the $\%V_{bur}$ value for ligand **3.10** while bound to $Cr(CO)_5$ (**4.8**, see Chapter 4) was calculated, starting from the experimentally-derived molecular structure. The same procedure as previously described was followed. The $\%V_{bur}$ values from this experimentally-determined structure and that from a purely computationally-derived system show reasonable agreement (33.0 $\%V_{bur}$ (**4.8**) vs. 37.0 $\%V_{bur}$ (**3.10**), respectively), suggesting that the computational structure optimisations carried out are representative of the actual molecular structures.

Iminophosphine	P-substituent	Percentage Buried Volume ($\%V_{bur}$)
$(Xyl)N=C(Ph)PEt_2$ (**3.26**)	Et	34.5
$(Xyl)N=C(Ph)PPh_2$ (**3.8**)	Ph	36.5
$(Xyl)N=C(Ph)P^iPr_2$ (**3.10**)	^{i}Pr	37.0
$(Xyl)N=C(Ph)P^tBu_2$ (**3.12**)	^{t}Bu	37.0
$(Xyl)N=C(Ph)P^iPr_2$ (**4.8**) (complex)	^{i}Pr	33.0

Table 3.7: Percentage buried volume ($\%V_{bur}$) values calculated for a selection of iminophosphines.

The data in Table 3.7 show that the $\%V_{bur}$ values for **3.26**, **3.8**, **3.10** and **3.12** follow the expected trend of ^{t}Bu > ^{i}Pr, Ph > Et. However, the difference between the calculated $\%V_{bur}$ values for compounds **3.8**, **3.10** and **3.12** is small, suggesting that the bulk of the phosphine group only has a relatively small effect upon the overall steric demands of the ligand. It is based on these $\%V_{bur}$ data that trends between the steric bulk of the phosphine-substituents on PCN ligands, and the catalytic properties of iminophosphine-based ethylene oligomerisation systems will be drawn in Chapter 5.

3.3.3.2 Analysis of the C=N stretching frequency of iminophosphines 3.1-3.26 by IR spectroscopy

All of the iminophosphines synthesised in this investigation were analysed by IR spectroscopy (Table 3.9). Imine C=N bonds are known to give characteristic absorptions in the IR spectrum at around 1600 cm^{-1}, with variations depending upon the strength of the C=N bond.[23] The C=N absorptions for the imidoyl chloride starting materials used in this investigation have been measured for comparison with the iminophosphine products, and are listed in Table 3.8.

Compound Formula	**C=N ν (cm^{-1})[a]**
PhC(Cl)=N(2-Me-C_6H_4)	1661
^{t}BuC(Cl)=NPh(o-Me)	1694
PhC(Cl)=NPh	1653
PhC(Cl)=NPh(2-(OMe)Ph)	1654
PhC(Cl)=N(2,6-$^{i}Pr_2$Ph)	1663
PhC(Cl)=N(2,6-Me_2Ph)	1668
PhC(Cl)=N(2,6-Et_2Ph)	1656
PhC(Cl)=N(2,4,6-$Ph_3C_6H_2$)	1640
^{t}BuC(Cl)=N(2,6-$^{i}Pr_2C_6H_3$)	1692
^{t}BuC(Cl)=N(2,6-$Me_2C_6H_3$)	1699
^{i}PrC(Cl)=N(2,6-$^{i}Pr_2$Ph)	1695
PhC(Cl)=NPh(2,5-$^{t}Bu_2C_6H_3$)	1663
[a]IR spectra measured using an ATR cell	

Table 3.8: IR spectroscopic data of C=N stretching frequencies for the imidoyl chloride starting materials used in this investigation.

The iminophosphines **3.1**-**3.26** all display C=N absorptions in the region 1549-1636 cm^{-1}, somewhat lower than a series of C=N stretching frequencies reported by Sandorfy (*e.g.* Ph(H)C=N($CH_2CH(CH_3)_2$, 1640 cm^{-1}) , and is indicative of conjugation of the aryl groups with the C=N bond.[23] The C=N stretches exhibited by the PCN compounds also appear at lower frequency

than their imidoyl chloride starting materials (Table 3.8), suggesting that the phosphine group also conjugates with the C=N bond (as previously discussed in Section 3.3.2.1). The iminophosphines with aliphatic C backbone-substituents (*i.e.* C-^{t}Bu groups) all demonstrate the highest C=N stretch frequencies, hence the least conjugation of the C=N bond within the compound. Other than this observation regarding C-^{t}Bu substituted iminophosphines, no general trend in the C=N absorptions is discernable, suggesting that the link between C=N bond strength and the iminophosphine substituents is complex.

Iminophosphine	Compound Formula	C=N ν (cm^{-1})[a]
3.1	$PhC(PPh_2)=N(2\text{-}MeC_6H_4)$	1588
3.2	$^tBuC(PPh_2)=N(2\text{-}MeC_6H_4)$	1611
3.3	$PhC(PPh_2)=NPh$	1587
3.5	$PhC(P^tBu_2)=NPh$	1582
3.6	$PhC(P^tBu_2)=N(2,6\text{-}^iPr_2C_6H_3)$	1580
3.7	$PhC(PPh_2)=N(2,6\text{-}^iPr_2C_6H_3)$	1602
3.8	$PhC(PPh_2)=N(2,6\text{-}Me_2C_6H_3)$	1605
3.9	$PhC(P^iPr_2)=N(2,6\text{-}^iPr_2C_6H_3)$	1583
3.10	$PhC(P^iPr_2)=N(2,6\text{-}Me_2C_6H_3)$	1587
3.11	$PhC(P(2\text{-}OMe\text{-}C_6H_4)_2)=N(2,6\text{-}^iPr_2C_6H_3)$	1584
3.12	$PhC(P^tBu_2)=NPh(2,6\text{-}Me_2C_6H_3)$	1583
3.13	$PhC(P^tBu_2)=NPh(2\text{-}OMe\text{-}C_6H_4)$	1602
3.14	$PhC(PCy_2)=N(2,6\text{-}^iPr_2C_6H_3)$	1585
3.15	$PhC(PCy_2)=N(2,6\text{-}Me_2C_6H_3)$	1586
3.16	$PhC(P^iPr_2)=N(2,6\text{-}Et_2C_6H_3)$	1584
3.17	$PhC(PEt_2)=N(2,6\text{-}^iPr_2C_6H_3)$	1585
3.18	$PhC(P(2\text{-}Et\text{-}C_6H_4)_2)=N(2,6\text{-}^iPr_2C_6H_3)$	1584
3.19	$PhC(P(2\text{-}F\text{-}C_6H_4)_2)=N(2,6\text{-}^iPr_2C_6H_3)$	1597
3.20	$^tBuC(P^iPr_2)=N(2,6\text{-}(2,6\text{-}^iPr_2C_6H_3)$	1630
3.21	$^tBuC(P^iPr_2)=N(2,6\text{-}Me_2C_6H_3)$	1636
3.22	$PhC(P^iPr_2)=NPh$	1587
3.23	$PhC(P^iPr_2)=N(2,4,6\text{-}Ph_3C_6H_2)$	1586
3.24	$PhC(P(2\text{-}OMe\text{-}C_6H_4)_2)=N(2,6\text{-}Me_2C_6H_3)$	1585
3.25	$PhC(P^iPr_2)=N(2,5\text{-}^tBu_2C_6H_3)$	1549
3.26	$PhC(PEt_2)=N(2,6\text{-}Me_2C_6H_3)$	1588
[a]IR spectra measured using an ATR cell		

Table 3.9: IR spectroscopic data of C=N stretching frequencies for iminophosphines **3.1**-**3.26.**

In conjunction with the experimental measurement of the C=N stretching vibrations of iminophosphine ligands, a preliminary computational study was carried out to calculate the C=N stretching frequencies of a small selection of compounds (**3.9**, **3.10** and **3.24**). The three structures were optimised, before frequency calculations were run using gaussian09 and a B3LYP/6-31G+ basis set. In order to make the calculated frequency values comparable with experimental measurements a scaling factor must be applied to the results. For the

B3LYP/6-31G+ basis set used in this investigation a scaling factor of 0.96 was applied, based on values from the Computational Chemistry Comparison and Benchmark Database (CCCBDB).[24] The calculated data, along with the measured C=N stretching values are given in Table 3.10 for comparison.

Iminophosphine	Formula	Calculated C=N stretch (cm^{-1})[a]		Calculated C=N stretch, with scaling factor (cm^{-1})[d]		Average calculated, scaled C=N stretch (cm^{-1})[e]	Measured C=N stretch (cm^{-1})[b]
N-(phenylethylidene) aniline	Ph(Me)C=NPh	1685		1618		1618	1627[c]
3.10	$Ph(P^iPr_2)C=N(2,6\text{-}Me_2C_6H_3)$	1656	1636	1590	1571	1583	1587
3.9	$Ph(P^iPr_2)C=N(2,6\text{-}^iPr_2C_6H_3)$	1653	1634	1587	1569	1580	1583
3.24	$Ph(P(2\text{-}MeOC_6H_4)_2)C=N(2,6\text{-}Me_2C_6H_3)$	1661	1636	1595	1571	1585	1585
[a] Calculated using DFT B3LYP/6-31G+ basis set in the gas phase, [b] Measured in the solid state, [c] Reported by Sandorfy,[23] [d] Scaling factor from CCCBDB.[24] [e] Weighted average, based upon the calculated absorption intensities						**Scaling Factor[d]**	
						0.96	

Table 3.10: Theoretical and experimentally derived C=N stretching values for iminophosphines **3.10**, **3.9** and **3.24**.

The frequency calculations carried out (B3LYP/6-31G+, gas phase) upon iminophosphines **3.9**, **3.10** and **3.24** show that the all three compounds exhibit two C=N stretching modes. This differs from the experimental data, in which only one broad C=N stretch was observed. The single C=N absorption in the experimentally determined IR spectra of the PCN compounds is a weighted average (based on the calculated absorption intensities) of the calculated frequencies, therefore a weighted average of the theoretically derived frequencies was calculated, in order to make the two data sets comparable. It is shown that the theoretically derived C=N stretching frequencies match remarkably well with the experimentally measured frequencies (all values within 0.6 %). Based upon this excellent match, it is suggested that the B3LYP/6-31G+ basis set used in this calculation is a good choice for carrying out further computational studies of iminophosphine ligands, and will be used for investigation of the *E*/*Z* isomerisation behaviour of the PCN compounds later in this chapter (Section 3.4.3).

3.3.3.3 Assessing the donor properties of phosphines: Synthesis of selenophosphine derivatives of iminophosphines

It is well known that, as well as the steric bulk of donor phosphine groups (Section 3.3.2.1), the electronic donor properties of phosphines have a major effect upon the coordination of such ligands.[25] In 1981 Allen *et al.* first reported the use of the NMR spectroscopic analysis of phosphine selenides to "measure" the electronic properties of phosphines.[26,27] This is possible due to ^{77}Se having a nuclear spin of ½ and a natural abundance of 7.5 %, meaning that phosphine selenides will display ^{31}P NMR spectroscopic signals with characteristic satellites, due to $^{1}J_{Se\text{-}P}$ coupling. It is known that the magnitude of the $^{1}J_{Se\text{-}P}$ coupling constant is proportional to the degree of s-character of the phosphorus lone-pair on the parent phosphine.[28] This means that it can be inferred that a phosphine selenide that displays a large $^{1}J_{Se\text{-}P}$ coupling constant has a lone-pair with poor s-character, and therefore is likely to be poorly donating, and weakly Lewis basic. In contrast, a small $^{1}J_{Se\text{-}P}$ coupling constant is indicative of an electron-rich, strongly Lewis basic phosphine. A selection of $^{1}J_{Se\text{-}P}$ coupling constants reported in the literature are displayed in Table 3.11.[29-31]

Se=PR$_3$, R =	**$\lvert^{1}J_{P\text{-}Se}\rvert$ (Hz)[a]**	**^{31}P δ (ppm)**
OPh	1027	58.6
OMe	963	77.5
NMe_2	805	81.2
Ph	736	34.1
o-$OMeC_6H_4$	720[b]	20.5
o-MeC_6H_4	705[b]	29.0
^{t}Bu	693[c]	93.3
^{i}Pr	692[c]	70.6
Me	684	8.0
[a] Spectra recorded at 162 MHz, $CDCl_3$; [b] 121 MHz, $CDCl_3$; [c] CD_2Cl_2		

Table 3.11: Representative $\lvert^{1}J_{P\text{-}Se}\rvert$ and ^{31}P δ values for a selection of phosphine selenides.[29-31]

To probe the electronic properties of the P-donor component of the iminophosphines synthesised in this thesis, the corresponding phosphine selenide derivatives were prepared. From these PCN-selenides the phosphine donor properties can be inferred by measuring the $^{1}J_{P\text{-}Se}$ couplings. The phosphine selenides **3.1(Se)-3.26(Se)** were all synthesised on an NMR scale by the reaction of the parent iminophosphine with grey selenium in $CDCl_3$ solvent in NMR tubes fitted with J. Young's taps (Scheme 3.14).

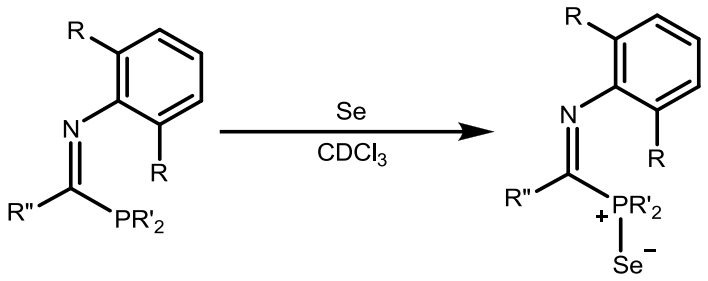

Scheme 3.14: General reaction of an iminophosphine with selenium

The reaction starting materials were placed in a Young's tap NMR tube, to which $CDCl_3$ was added, before the resulting mixture was sonicated for at least 30 minutes. All of the phosphine selenide reactions were observed to reach at least 60 % conversion after sonication, as measured by integration of the ^{31}P NMR spectra. The reaction mixture was then analysed by ^{31}P NMR spectroscopy, from which the $|^1J_{P\text{-}Se}|$ coupling constant was determined (Table 3.12).

Label	Compound	$\lvert^1J_{P\text{-}Se}\rvert$ (Hz)[a]	^{31}P δ (ppm)
3.1(Se)	$PhC(SePPh_2)=N(2\text{-}MeC_6H_4)$	740	36.5
3.2(Se)	$^tBuC(SePPh_2)=N(2\text{-}MeC_6H_4)$	731[b]	34.6
3.3(Se)	$PhC(SePPh_2)=NPh$	742	36.4
3.5(Se)	$PhC(SeP^tBu_2)=NPh$	715	76.5
3.6(Se)	$PhC(SeP^tBu_2)=N(2,6\text{-}^iPr_2C_6H_3)$	705	77.3
3.7(Se)	$PhC(SePPh_2)=N(2,6\text{-}^iPr_2C_6H_3)$	740	36.0
3.8(Se)	$PhC(SePPh_2)=N(2,6\text{-}Me_2C_6H_3)$	738	36.2
3.9(Se)	$PhC(SeP^iPr_2)=N(2,6\text{-}^iPr_2C_6H_3)$	711	64.4
3.10(Se)	$PhC(SeP^iPr_2)=N(2,6\text{-}Me_2C_6H_3)$	710	64.1
3.11(Se)	$PhC(SeP(2\text{-}MeOC_6H_4)_2)=N(2,6\text{-}^iPr_2C_6H_3)$	719	21.4
3.12(Se)	$PhC(SeP^tBu_2)=NPh(2,6\text{-}Me_2C_6H_3)$	708	77.5
3.13(Se)	$PhC(SeP^tBu_2)=NPh(2\text{-}MeOC_6H_4)$	711	76.4
3.14(Se)	$PhC(SePCy_2)=N(2,6\text{-}^iPr_2C_6H_3)$	709	56.2
3.15(Se)	$PhC(SePCy_2)=N(2,6\text{-}Me_2C_6H_3)$	706	56.2
3.16(Se)	$PhC(SeP^iPr_2)=N(2,6\text{-}Et_2C_6H_3)$	709	63.9
3.17(Se)	$PhC(SePEt_2)=N(2,6\text{-}^iPr_2C_6H_3)$	703	43.0
3.18(Se)	$PhC(SeP(2\text{-}Et\text{-}C_6H_4)_2)=N(2,6\text{-}^iPr_2C_6H_3)$	708	30.1
3.19(Se)	$PhC(SeP(2\text{-}F\text{-}C_6H_4)_2)=N(2,6\text{-}^iPr_2C_6H_3)$	750	23.8
3.20(Se)	$^tBuC(SeP^iPr_2)=N(2,6\text{-}(2,6\text{-}^iPr_2C_6H_3)$	701	61.1
3.21(Se)	$^tBuC(SeP^iPr_2)=N(2,6\text{-}Me_2C_6H_3)$	702	60.2
3.22(Se)	$PhC(SeP^iPr_2)=NPh$	715	66.2
3.23(Se)	$PhC(SeP^iPr_2)=N(2,4,6\text{-}Ph_3C_6H_2)$	712	64.1
3.24(Se)	$PhC(SeP(2\text{-}MeOC_6H_4)_2)=N(2,6\text{-}Me_2C_6H_3)$	721	22.3
3.25(Se)	$PhC(SeP^iPr_2)=N(2,5\text{-}^tBu_2C_6H_3)$	707	65.5
3.26(Se)	$PhC(SePEt_2)=N(2,6\text{-}Me_2C_6H_3)$	701	43.3

[a]162 MHz, $CDCl_3$; [b]81 MHz, $CDCl_3$

Table 3.12: Iminophosphine selenide compounds synthesised *in situ* in this investigation and their ^{31}P NMR spectroscopic data.

From the data in Table 3.12 it can be seen that all of the iminophosphine selenides show moderately small $^1J_{P\text{-}Se}$ coupling constants, indicative of the parent phosphines being relatively strong Lewis bases, with good donor properties as would be expected. The magnitudes of the $^1J_{P\text{-}Se}$ coupling constants for all of the iminophosphine selenides are similar to that of PPh_3. The compounds displaying the smallest $^1J_{P\text{-}Se}$ coupling constants are **3.17(Se)**, **3.20(Se)**, **3.21(Se)** and

3.26(Se). Both **3.17(Se)** and **3.26(Se)** have ethyl-substituted phosphines, suggesting there is a correlation between the bulk of the alkyl substituents and the phosphine donor properties, something that is mirrored by tertiary phosphines (*e.g.* PMe_3 $^1J_{P\text{-}Se}$ = 684 Hz). This correlation between phosphine s-character and steric bulk of the alkyl groups can be explained by applying the "Walsh Correlation Diagram Analysis" to the PR_3 fragment (Figure 3.21).[32,33] A highly pyramidal phosphine, with small alkyl substituents, will have a large s-donor character, due to stabilisation this configuration offers to the $2a_1$ HOMO. Conversely, a phosphine with sterically demanding alkyl substituents (*e.g*. *t*-butyl) is forced to adopt a more planar configuration, hence giving the lone pair a greater p-character and less s-character.

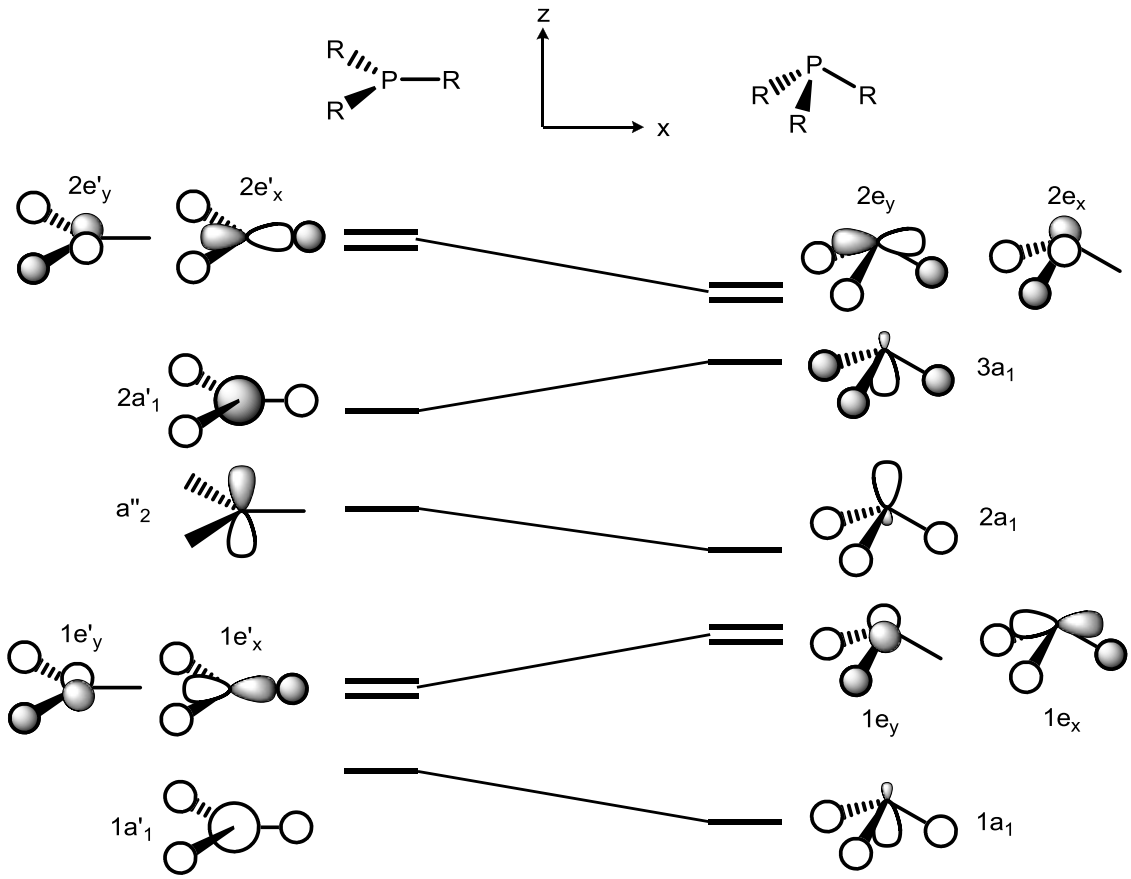

Figure 3.21: The correlation between the molecular orbitals of planar (left) and pyramidal (right) PR_3 fragments, modified from Gilheany.[33]

The compounds **3.20(Se)** (^{t}BuC(SeP^{i}Pr$_2$)=N(2,6-(2,6-^{i}Pr$_2$C$_6$H$_3$)) and **3.21(Se)** (^{t}BuC(SeP^{i}Pr$_2$)=N(2,6-Me$_2$C$_6$H$_3$)) have *iso*-propyl-substituted phosphine groups, but have *tert*-butyl substituted C-backbones, which has a significant effect on the basicity of the phosphine (*e.g.* comparing **3.20(Se)** with **3.9(Se)**). From this we can conclude that iminophosphines with alkyl-substituted phosphines and *tert*-butyl C-substituted backbones display the strongest donor characteristics as would be anticipated.

At the other end of the scale, **3.19(Se)** (PhC(SeP(2-$FC_6H_4)_2$)=N(2,6-$^{i}Pr_2C_6H_3$)) exhibits the largest magnitude of $^1J_{P\text{-}Se}$ coupling. This is due to the electron-withdrawing nature of the Ar-*o*-F phosphine substituents. All of the iminophosphine selenides with PPh_2 groups, and phenyl-substituted C-backbones give $|^1J_{P\text{-}Se}|$ coupling values remarkably similar to those of triphenylphosphine ($^1J_{P\text{-}Se}$ = 736 Hz), suggesting that the N-substituent group has very little effect on the donor properties of the phosphine. This lack of influence by the N-substituent is observed across the whole range of iminophosphine selenides prepared here. From all of the $|^1J_{P\text{-}Se}|$ coupling constants measured for the iminophosphine selenides synthesised it can be concluded that the donor properties of the phosphine group can be tuned by altering both the phosphine and C-backbone substituents to give good to moderate P-donor electronic characteristics.

3.4 Analysis of the *E/Z* Isomerisation Behaviour of Iminophosphines

It has been previously mentioned (Section 3.3.1) that a number of the iminophosphine compounds synthesised in this investigation display two ^{31}P NMR spectroscopic resonances, which is thought to be due to the C=N imine bond existing in both the *E* and *Z* configurations in solution. This matches the conclusions of Slootweg and Lammerstma *et al.*, who reported that one of their iminophosphines displayed both *E* and *Z* isomers in solution in a 3:2 ratio, measured by integration of the ^{31}P NMR spectroscopic resonances (Figure 3.22).[12] In other iminophosphine compounds synthesised, Slootweg and Lammertsma *et al.* reported that these adopted only the *E* configuration based on crystallographic and computational studies, suggesting that the conformation of the imine bond is easily affected by the steric bulk of the molecule. Despite these findings, Slootweg and Lammertsma *et al.* gave no suggestion of the mechanism of isomerisation in their report.

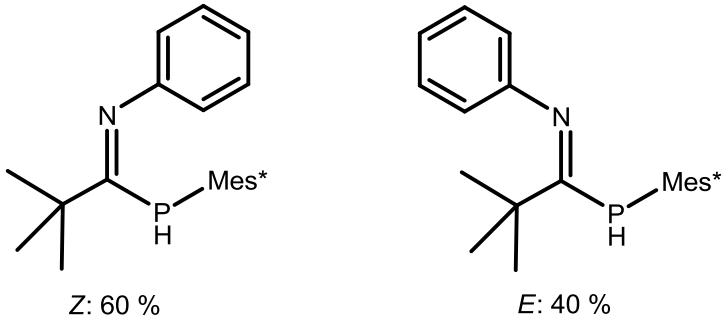

Z: 60 % *E*: 40 %

Figure 3.22: *E* and *Z* isomers of an iminophosphine compound synthesised by Slootweg and Lammertsma *et al.*[12]

The first suggestions of possible mechanisms for the isomerisation of imines were made by Huckel in 1930,[34] with further work being carried out in the 1960s to investigate this phenomena.[35,36] Based on these other publications, two possible pathways were proposed: *a)* "Torsional motion", rotation around the C-N bond *via* an ylide transition state, or *b)* "Lateral shift", the shift of the N-substituent in the plane of the molecule, *via* a linear transition state (Scheme 3.15).[37]

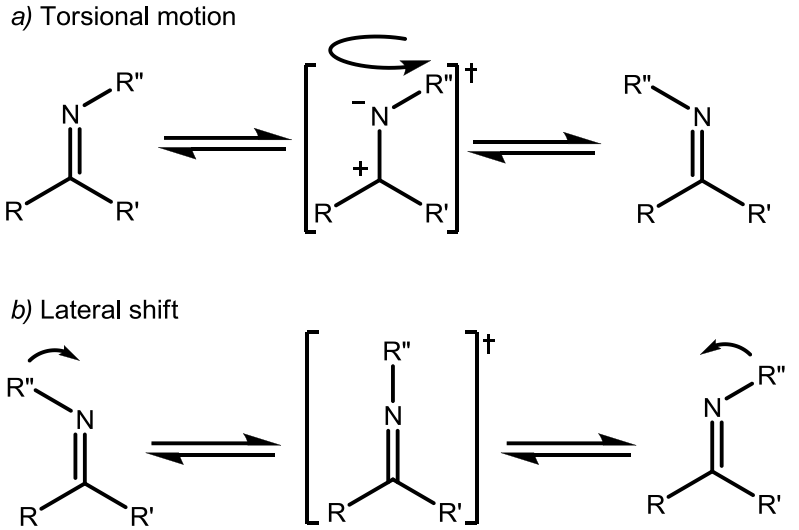

Scheme 3.15: The possible mechanisms for imine isomerisation reported by Ostrogovich *et al.*[37]

Ostrogovich *et al.* reported that the most likely mechanism for the isomerisation of imines is *b)*, the "Lateral shift" pathway, based upon a series of computations carried out investigating the relative energies required for both transformations *a)* and *b)*. It is based on this lateral shift pathway that the studies into the *E*/*Z* isomerisation behaviour of the iminophosphines synthesised in this investigation have been carried out.

The ability of iminophosphines to undergo *E*/*Z* isomerisation is vital for the coordination properties of the PCN compounds, as it is conceivable that the *Z* isomer of a PCN ligand could not bind to a metal centre, due to the lone pair of the nitrogen being incorrectly orientated (Scheme 3.16). In order to investigate this a series of crystallographic, NMR spectroscopic and theoretical studies have been conducted in order to attempt to elucidate the factors affecting the *E*/*Z* isomerism displayed by iminophosphines.

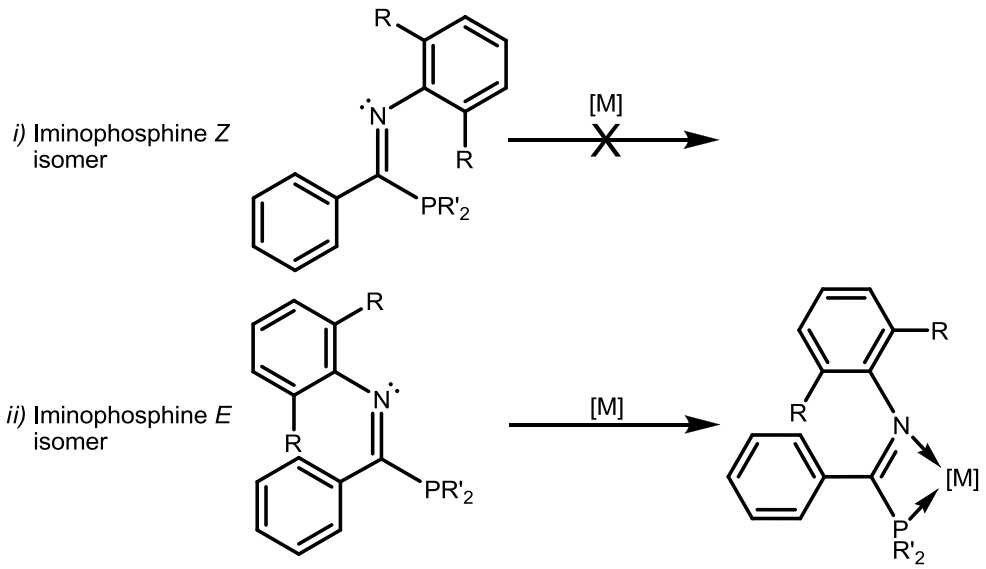

Scheme 3.16: Comparison of the coordination abilities of *E* and *Z* iminophosphine isomers.

3.4.1 Crystallographic studies of iminophosphine *E/Z* isomers

Over the course of the synthesis of the iminophosphine library in this thesis some of the compounds were successfully crystallised and subsequently analysed by X-ray crystallography. The solid-state structures of **3.4** (Figure 3.7) and **3.24** (Figure 3.14) were determined, and both the compounds exist as the *E* isomer. The molecular structure of the P-oxide of **3.2** (Figure 3.6) was also determined, displaying the iminophosphine in the *E* configuration. The P(V) structure of the oxidised iminophosphine **3.2** may have a major effect upon the steric parameters of the phosphine, hence this structure is of limited use when drawing conclusions about the structure of the parent phosphine. Overall, based on the crystallographic data gathered for compounds **3.4**, **3.24** and **3.2** it can be concluded that the *E* configuration is the more stable in the solid state for these iminophosphines.

3.4.2 NMR spectroscopic studies of iminophosphine *E/Z* isomerisation

A number of the iminophosphine compounds synthesised (**3.1**, **3.3**, **3.7**, **3.8**, **3.11** and **3.24**) display two resonances in their solution-state ^{31}P NMR spectra, indicative of both the *E* and *Z* isomers of the products being present in solution. All of the systems demonstrating this feature are linked by the fact that they either have phenyl- or *ortho*-anisyl-substituted phosphine groups, suggesting that the -PPh_2 and -$P(Ar^{o\text{-}OMe})_2$ groups are responsible for favouring the presence of both imine *E* and *Z* isomers in solution. For compounds bearing either of these substituents the conversion of the two iminophosphine isomers is slow on an NMR timescale, hence the presence of two phosphorus resonances in the ^{31}P NMR spectra of these iminophosphines. In order to further probe the *E*/*Z* isomerisation of the iminophosphines VT NMR studies were conducted on **3.24**. The compound **3.24** was chosen due to both of the isomers being present in similar amounts (3:2 ratio) at room temperature. Initially, high-temperature VT NMR spectroscopic experiments were carried out to investigate the behaviour of the two iminophosphine isomers at increased temperatures (Figure 3.23). These high-temperature NMR spectroscopic experiments demonstrated that at 40 °C the two ^{31}P resonances start to coalesce, a process which is essentially complete at 80 °C, when only one signal is observed (δ = –14.5 ppm). This demonstrates that at 80 °C the rate of isomerisation between the *E* and *Z* isomers has increased to become fast on an NMR timescale, and at lower temperatures the two isomers are likely to be present in equilibrium. On cooling, the presence of two resonances was re-established.

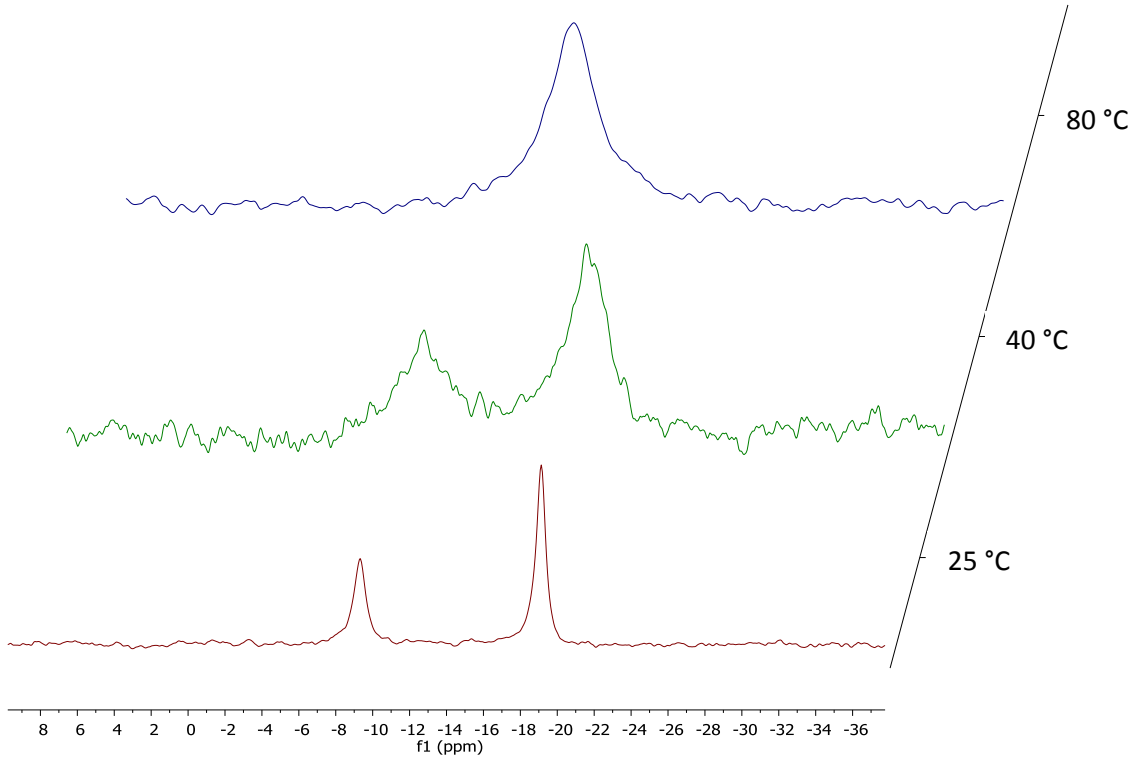

Figure 3.23: High-temperature ^{31}P NMR (202 MHz, toluene-d_8) spectra of **3.24**.

The equilibrium between the *E* and *Z* isomers of iminophosphine **3.24** was also investigated at low temperatures, by NMR spectroscopy. Experiments were carried out at range of temperatures from 10 - –80 °C. Upon lowering the temperature to –30 °C the two ^{31}P NMR spectroscopic signals sharpened, but maintained their 3:2 integral ratio observed at room temperature, indicative of no interchange occurring between the two isomers. When the temperature was lowered further to –60 °C it was observed that the signal at lower frequency started to broaden. Upon lowering the temperature again to –80 °C the resonance at lower frequency split into two new, unique signals (Figure 3.24).

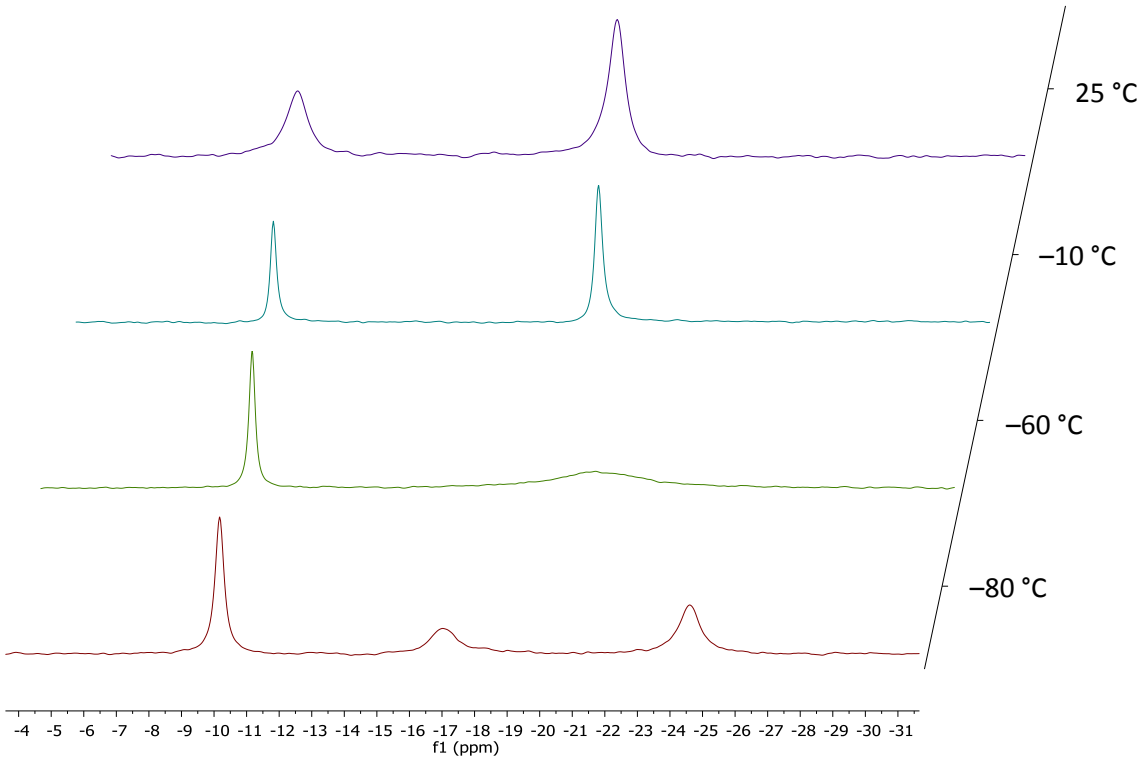

Figure 3.24: Selected low-temperature ^{31}P NMR (202 MHz, toluene-d_8) spectra of **3.24**

It is thought that these two new signals (δ = –17.0, –24.6 ppm) observed at –80 °C are due to two rotamers of the P($Ar^{o\text{-}OMe}$)$_2$ groups being frozen out at this low temperature (Figure 3.25). This theory was tested by carrying out low-temperature NMR spectroscopic experiments on compound **3.8** (Ph(PPh_2)C=N(2,6-$Me_2C_6H_3$)), which is identical to iminophosphine **3.24** except for possessing P-phenyl substituents, rather than P-anisyl. Due to the symmetry of the P-phenyl substituents, it should not be possible to observe unique rotamers of the PPh_2 group. The NMR spectra measured at –80 °C for iminophosphine **3.8** showed no separation of either of the two phosphorus signals that were observed at ambient temperature, indicating that the division of signals seen in compound **3.24** is caused by rotamers of the P-anisyl groups freezing their positions on an NMR timescale.

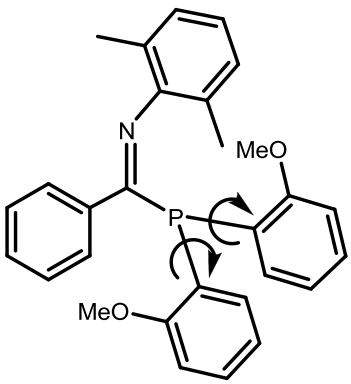

Figure 3.25: Rotation around P-C bonds of **3.24**, which is thought be slowed at –80 °C.

Solution-state NMR spectroscopic analysis of compound **3.24** has demonstrated that both *E* and *Z* isomers of the compound are present in solution, but they do not interconvert at room temperature on the NMR timescale. Contrary to this, X-ray crystallographic studies have shown that the compound **3.24** crystallises as solely the *E* isomer. In order to investigate this apparent contradiction, solid state NMR spectroscopy was carried out of a ground solid sample of the bulk of compound **3.24**. The solid-state ^{31}P NMR spectrum displayed only one resonance (δ = –12.8 ppm) with the associated spinning sidebands, indicative of only one isomer of the iminophosphine being present in the bulk sample. It is assumed that this is the *E* isomer, based on the molecular structure determined by X-ray crystallography. It is therefore demonstrated that the imine *E* and *Z* isomers must interconvert in solution, in order for the entire sample of **3.24** to crystallise as the same isomer.

The ^{31}P NMR spectra of all the iminophosphines synthesised bearing alkyl-substituted phosphine groups only display one resonance in solution, but with NMR spectroscopy alone no conclusions can be drawn as to which isomer is present. In order to further probe the *E*/*Z* isomerisation behaviour of the iminophosphines, a series of computational calculations were carried out to determine the relative energies of the *E* and *Z* isomers for a selection of the PCN compounds (Section 3.4.3)

3.4.3 Computational DFT studies of iminophosphine *E*/*Z* isomerisation

Computational studies of a selection of the iminophosphine compounds synthesised in this investigation have been carried out. The use of theoretical calculations allows for the prediction of the relative energies of the *E* and *Z* isomers of iminophosphines, and can probe the energies of potential transition states on the isomerisation pathways. Computational chemistry can also be used to calculate structures for theoretical molecular conformations that cannot be isolated experimentally, and these can be compared with energies of molecules that have been successfully synthesised.

The calculations carried out in this thesis have utilised DFT methods and employed a B3LYP/6-31G+ basis set. The structures calculated were based around the “lateral shift” imine isomerisation mechanism (Section 3.4), in which the P-C=N-C moiety remains planar and the C-N-C angle is varied (Scheme 3.17). Energies were calculated for a series of structures with imine unit (P-C=N-C) fixed as planar and the C-N-C angle varied in 10 ° intervals. This allows the calculated energies to be plotted against the C-N-C angle (θ), to give a potential energy surface for the isomerisation pathway. As expected, the imine cannot adopt a linear C-N-C configuration (*i.e.* a C-N-C angle of 180 °) and calculations cannot be carried out for this structure, therefore

the “transition state” structures were calculated with a C-N-C angle of 179 ° to avoid this problem.

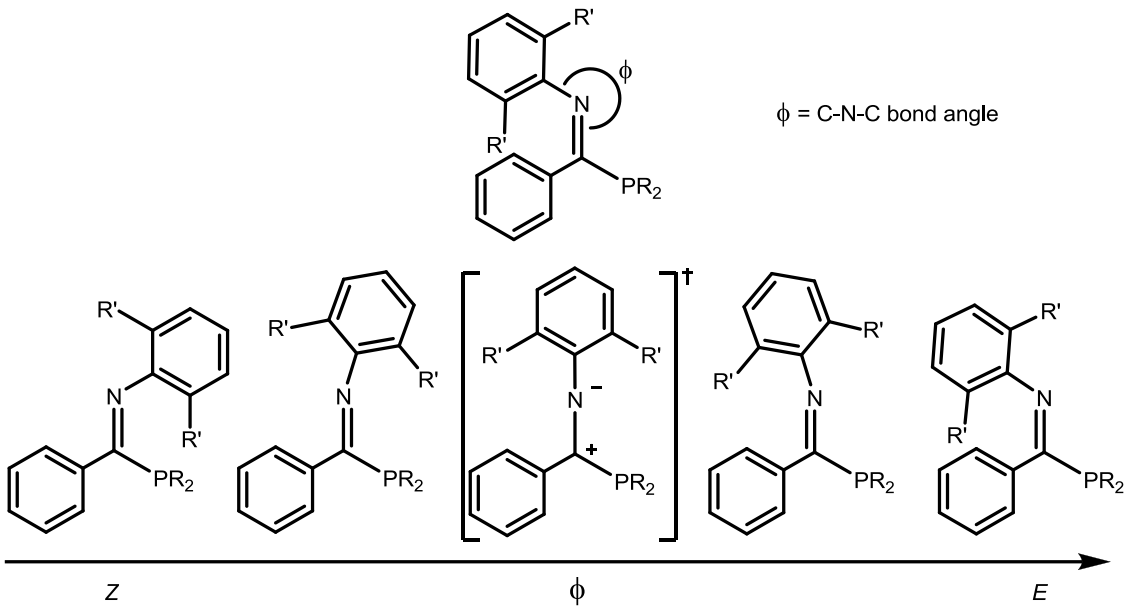

Scheme 3.17: A schematic displaying the methodology used in in calculating the energy of the imine isomerisation mechanism pathway, in which the C-N-C bond angle (ϕ) is varied transform the *Z* isomer (left) through to the *E* isomer (right).

In the process of calculating optimised structures of some iminophosphines (*e.g.* compounds **3.8** and **3.24**) it was found that the orientation of the pyramidal P-(aryl)$_2$ moiety has a significant effect on the minimum energy of the structures optimised. Different minima were found for the P-(aryl)$_2$ groups in either the “A” (with the phosphorus lone pair *anti*, with respect to the nitrogen) or the “B” conformation (with the phosphorus lone pair *syn* with respect to the nitrogen) (Figure 3.26). Details of these conformational differences are discussed in detail for iminophosphines for which it was found to effect the energy minima of the relevant iminophosphines (*e.g.* compounds **3.8** and **3.24**).

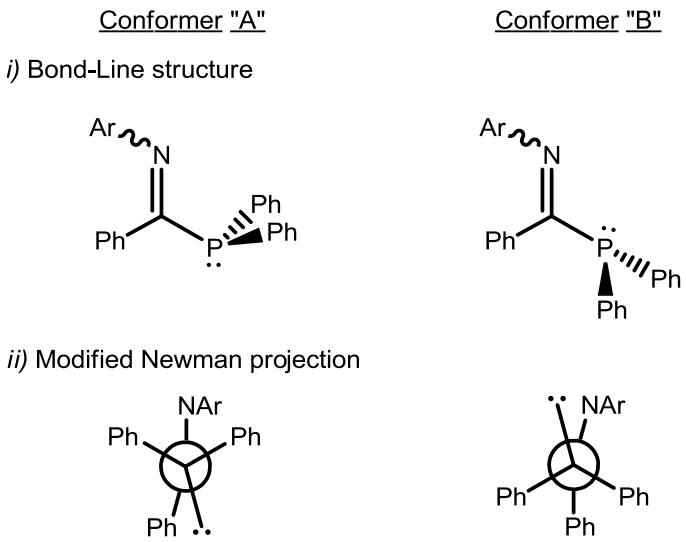

Figure 3.26: The two potential conformer structures found by DFT calculations of iminophosphine **3.8**.

In order to investigate the isomerisation process for different compounds, the calculations were carried out for a range of iminophosphines, including those that display two isomers by ^{31}P NMR spectroscopy in solution, and those with only one observed isomeric form. The data from the calculations are presented in Table 3.13 for comparison, and the findings discussed below.

Compound	C-N-C bond angle, ϕ (°)	Isomer	Calculated Energy (Hartrees)	Favoured Isomer	*E* vs. *Z* energy (kcal mol^{-1})
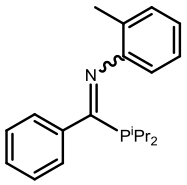 **3.4**	133	*Z*	–1173.680524		
	233	*E*	–1173.685118	*E*	2.9
	179	T.S.	–1173.664648		
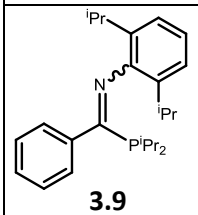 **3.9**	135	*Z*	–1370.196161		
	232	*E*	–1370.204455	*E*	5.2
	179	T.S.	–1370.186498		
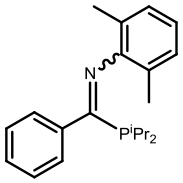 **3.10**	136	*Z*	–1212.983126		
	232	*E*	–1212.991538	*E*	5.3
	179	T.S.	–1212.973508		
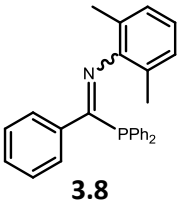 **3.8**	129	*Z*	–1439.169138		
	231	*E*	–1439.170453	*E*	0.8
	179	T.S.	–1439.156207		
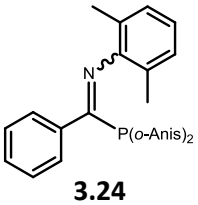 **3.24**	129	*Z*	–1668.144687		
	231	*E*	–1668.143098	*Z*	1.0
	179	T.S	–668.129191		

Table 3.13: Summary of calculated (B3LYP/6-31G+) optimised C-N-C bond angles (ϕ) and energies for selected iminophosphines.

The first calculations were carried out on iminophosphine **3.4**, using the molecular structure previously determined (Figure 3.7) as a starting point for the optimisations. The results are displayed in Graph 3.1.

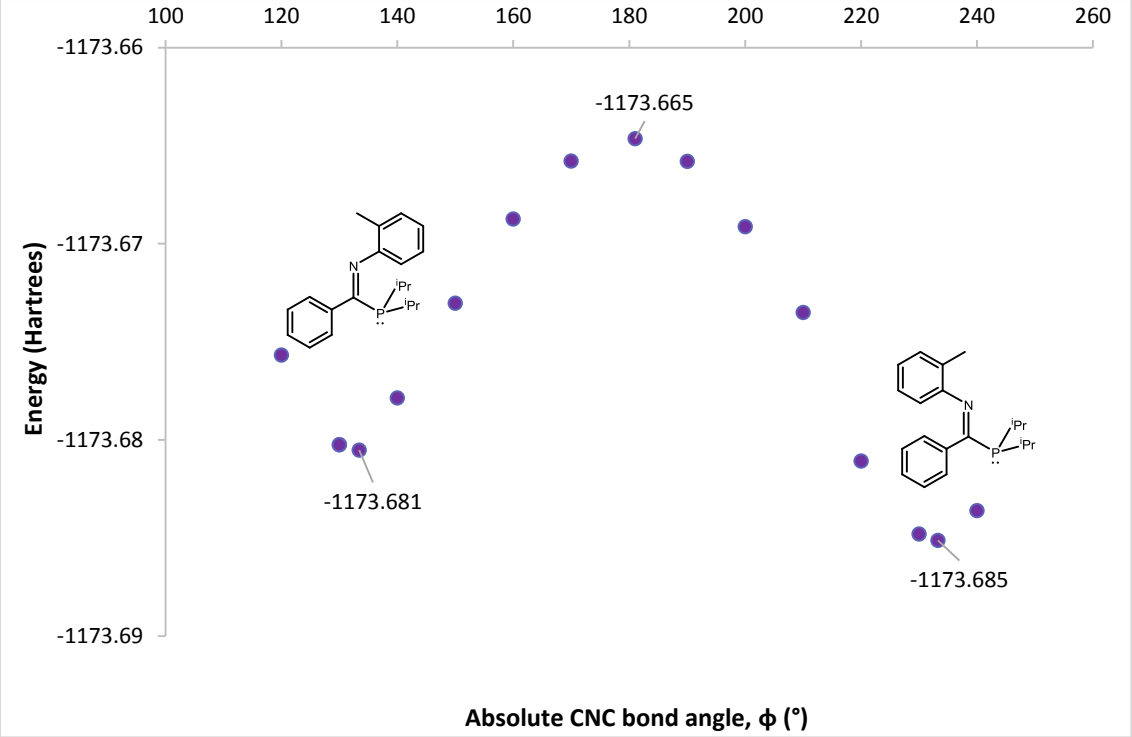

Graph 3.1: The energies of optimised structures of **3.4** plotted against the C-N-C bond angle, ϕ

The data presented in Graph 3.1 show that the *E* isomer of compound **3.4** is calculated to be lower in energy, and therefore more stable. This matches with the molecular structure determined for **3.4** in the solid-state by X-ray crystallography that shows the imine adopting an *E* configuration, suggesting that the computational methodology used is valid.* From the computation it is calculated that the difference in energy between the *E* and *Z* isomer is 2.9 kcal mol^{-1} and this, combined with the knowledge that only one isomer is observed by ^{31}P NMR spectroscopy in solution, indicates that this energy difference is enough to favour only the *E* isomer in solution. Slootweg and Lammerstma *et al.* reported observing only a single isomer of their iminophosphine compounds, which were calculated to have an energy difference of 2.2 kcal mol^{-1}, matching the results observed and calculated for the *E* and *Z* isomers of iminophosphine **3.4**.[12]

Analogous calculations were carried out for compounds **3.9** and **3.10** in order to probe the effect of varying the N-aryl substituent on the relative energies of the *E* and *Z* iminophosphine isomers. Both compounds **3.9** and **3.10** showed a stronger preference to the *E* isomer (5.2 kcal mol^{-1} and 5.3 kcal mol^{-1}, respectively) than **3.4**, suggesting that the increased steric bulk of the N-aryl substituent favours the imine *E* configuration. Based on these results it is concluded that both iminophosphines **3.9** and **3.10** exist solely as the *E* isomers in solution.

* For further validation of the computational methods used, see Section 3.3.3.2 for the comparison of measured and simulated IR C=N stretching frequencies.

This concurs with the solution-state ^{31}P NMR spectra of these compounds, which both only exhibit one signal. Therefore, it is likely that all of the iminophosphines synthesised with P-alkyl substituents adopt the *E* configuration in solution.

Computations were also carried out to investigate the differences in energy of the *E* and *Z* isomers of iminophosphines **3.8** and **3.24**, both of which display two ^{31}P NMR spectroscopic resonances in solution, indicating the presence of both isomers in solution. Both of these compounds display significant energy differences between the P-aryl rotational conformers ("A" and "B", Figure 3.26), and the results are discussed below.

The ^{31}P NMR spectrum of compound **3.8** shows two resonances present in a 6:1 ratio, indicating that one of the isomeric forms is more favoured in solution. DFT calculations show that the energy difference between the optimised structures for the *E* and *Z* isomers of **3.8** is 0.8 kcal mol^{-1}, with the *E* isomer being lower in energy (Graph 3.2). It is also shown that for the *E* isomer of **3.8,** the "A" conformer is significantly lower in energy than its counterpart "B", in comparison to the *Z* isomer in which both the "A" and "B" conformers have very similar energies. From these results it can be concluded that the signal with the larger integral at δ = 8.8 ppm in the ^{31}P NMR spectrum of **3.8** represents the *E* iminophosphine isomer, and the smaller resonance at δ = 0.9 ppm is due to the higher energy *Z* isomer.

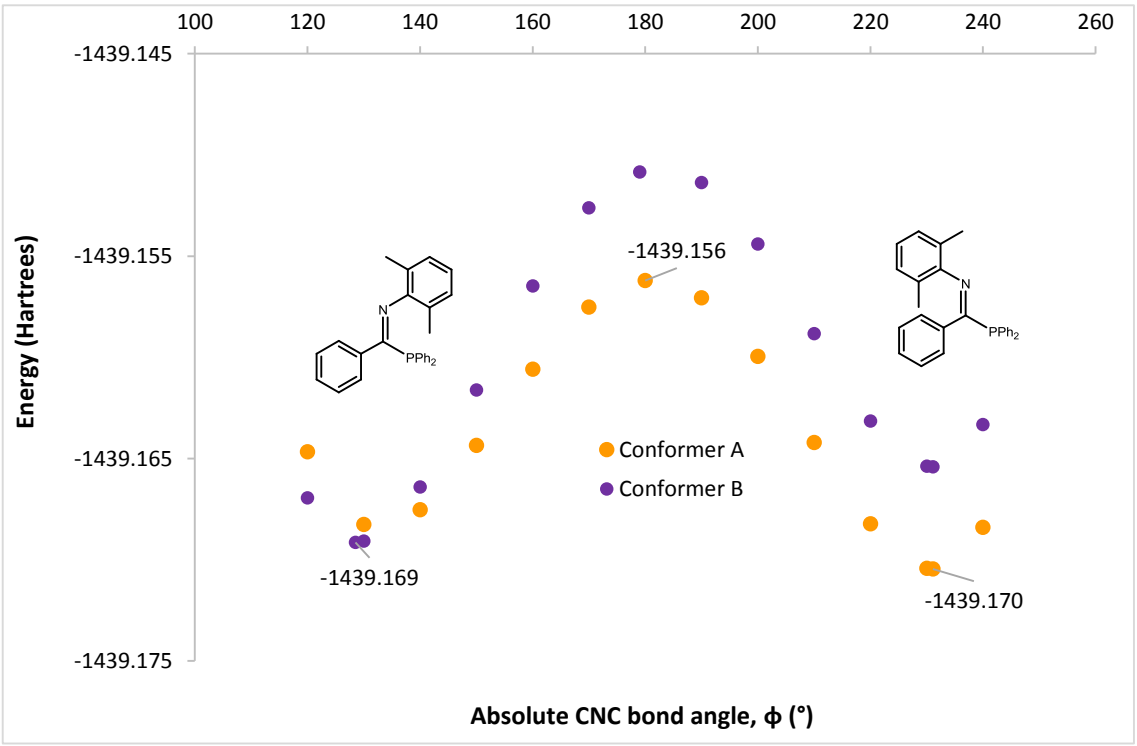

Graph 3.2: The energies of optimised structures of **3.8** plotted against the C=N-C bond angle, ϕ.

The final iminophosphine to be studied computationally was compound **3.24** (Ph(P(2-$MeOC_6H_4)_2$)C=N(2,6-$Me_2C_6H_3$)). The ^{31}P NMR spectrum of **3.24** is interesting due to the signal of

larger integration appearing at a lower frequency than the signal with a smaller integral, which is the opposite to all of the other iminophosphines synthesised. This is indicative of the *Z* isomer being the predominant species in solution, based on the previous NMR spectroscopic experiments and theoretical calculations carried out, and so further calculations were carried out in order to add weight to this argument. Again, as with compound **3.8**, it was found that the rotation of the P-aryl group had a significant effect on the energy minima calculated for the *E* and *Z* isomers. It was demonstrated that the "B" conformer was far higher in energy for the *E* isomer, while the *Z* isomer displayed a significantly lower energy structure for the "B" conformer. This difference in conformation leads to the *Z* isomer of **3.24** having a marginally lower calculated energy than the *E* isomer, with a difference of 1.0 kcal mol^{-1}. This small difference is almost negligible, but matches with the ^{31}P NMR spectroscopic measurements that suggest the *Z* isomer is favoured in solution, and it therefore can be concluded that the *Z* configuration of **3.24** is the primary isomer in solution.

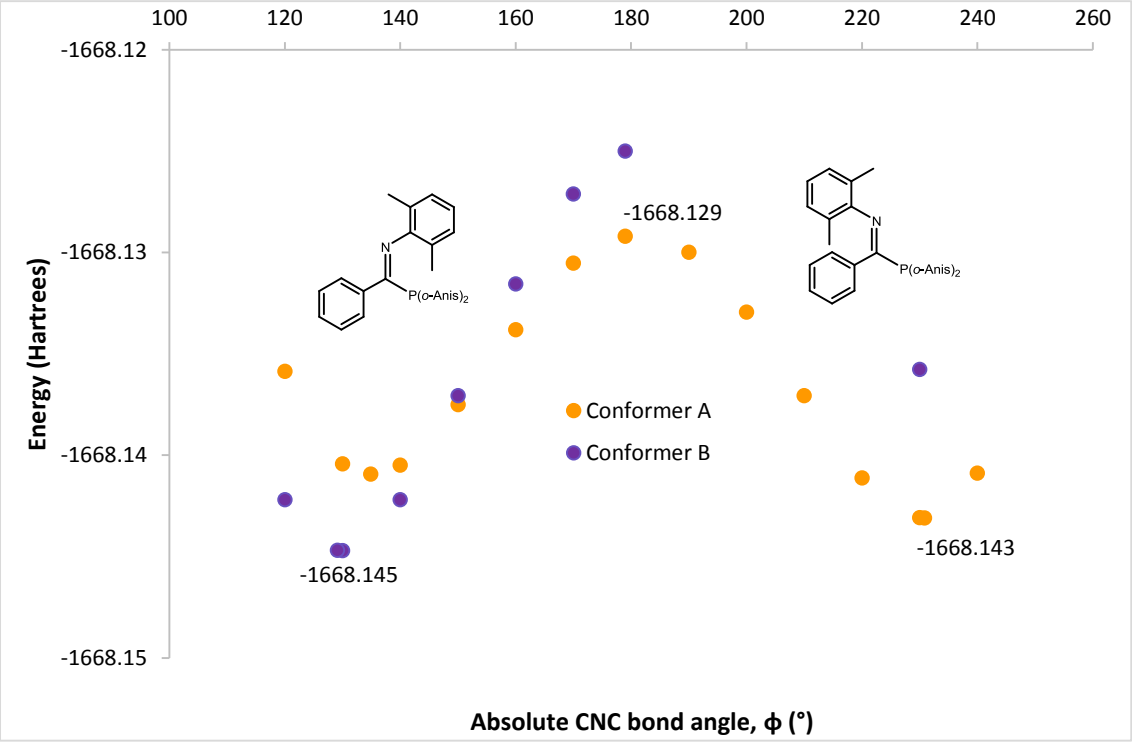

Graph 3.3: The energies of optimised structures of **3.8** plotted against the C=N-C bond angle, ϕ.

From the series of DFT calculations carried out on iminophosphine ligands in this thesis, it can be concluded that the majority of the compounds studied exist primarily as the iminophosphine *E* isomer. Nevertheless, it remains possible to synthesise iminophosphines that exist as the *Z* isomer in solution through tuning of the N-aryl- and phosphine-substituents, as demonstrated by **3.24**, and compounds reported by Slootweg and Lammerstma *et al*.[12]

3.5 Reactions of Iminophosphines with Trialkylaluminium Species

The use of MAO and other alkylaluminoxane derivatives as ethylene oligomerisation activators is ubiquitous in the field of ethylene polymerisation and oligomerisation.[38] However, the high cost, and large activator:transition metal ratio required by catalytic systems means that the development of other activator packages is highly desirable. In 2007 Overett *et al.* reported a novel method of activating Cr/PNP-based ethylene *tri-*/*tetra*-merisation systems utilising alkyl aluminiums in combination with weakly coordinating alkyl-abstracting agents.[39] These alternative catalyst activation methods, using trialkyl aluminiums, have a number of advantages over the traditional use of MAO including lower cost, requiring lower aluminium:chromium ratios, and the resulting catalytic systems often produce less polymer, compared to MAO-activated systems. It is therefore worthwhile investigating the reactivity of iminophosphines with alkyl aluminium species to attempt to shed light upon any ligand-aluminium interactions that may occur in any potential catalytic process. For example, a recent publication by Gambarotta *et al.* has demonstrated that alkyl aluminium reagents are capable of cleaving P-N bonds of P,N-based ligands (Scheme 3.18).[40] Based upon this report it is likely that alkyl aluminium species used in the catalyst activation process may undergo similar reactions with iminophosphine ligands, hence highlighting the importance of carrying out such studies.

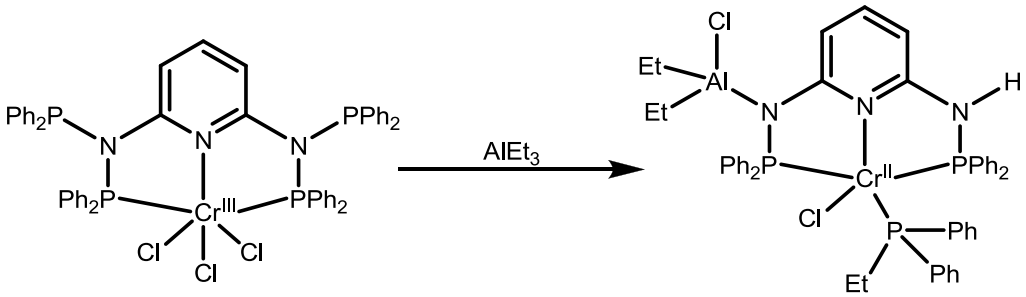

Scheme 3.18: P-N bond cleavage of a pyridine-phosphine ligand by $AlEt_3$ reported by Gambarotta *et al.* [40]

3.5.1 Reaction of $Ph(P^iPr_2)C{=}N(2,6\text{-}^iPr_2C_6H_3)$ (3.9) with 1 equivalent of $AlMe_3$

The reaction of $Ph(P^iPr_2)C{=}N(2,6\text{-}^iPr_2C_6H_3)$ (**3.9**) and $AlMe_3$ was carried out using a modified version of the method reported by Rosenthal, Mosa and Muller *et al.*[41] A sample of iminophosphine **3.9** was dissolved in toluene before one equivalent of $AlMe_3$ (2M in toluene) was added and the reaction mixture then stirred for one hour at room temperature (Scheme 3.19). Analysis of the reaction by ^{31}P NMR spectroscopy demonstrated a new product had been formed (δ = 18.3 ppm), displaying a lower frequency resonance than the iminophosphine starting material **3.9** (δ = 27.1 ppm). This change of ^{31}P NMR spectroscopic signal caused by reaction of the iminophosphine **3.9** with $AlMe_3$ suggests that the phosphine is likely to have

coordinated with the aluminium. Upon attempting to crystallise the product from hot hexane the product decomposed into a new phosphorus-containing species, as well as starting material (δ = 52.0, 47.4, 42.9, 27.1 ppm). Unfortunately no products could be isolated and purified from the reaction due to the highly reactive and unstable nature of the species.

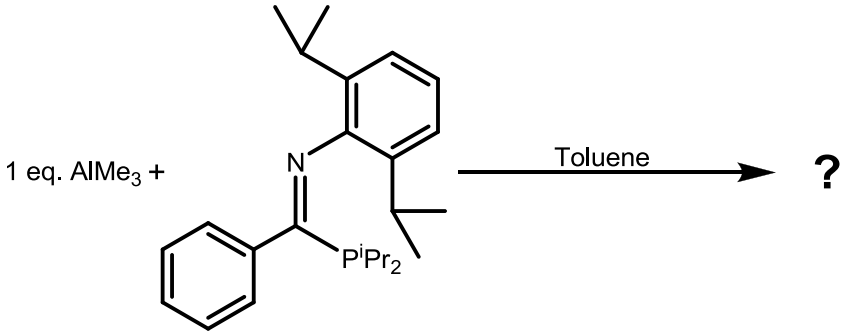

Scheme 3.19: Reaction carried out of 1 equivalent of $AlMe_3$ with compound **3.9**.

The reaction was repeated (a second time), but this time the crude product solution was concentrated under vacuum and stored at –30 °C in an attempt to crystallise the product. Unfortunately no precipitate formed and despite further concentration and cooling of the solution, still no product could be isolated. The solution was subsequently layered with pentane and, after slow diffusion, a yellow oil separated out of solution. The oil was isolated and analysed by ^{1}H and ^{31}P NMR spectroscopy; the phosphorus spectrum showed the first product formed (δ = 18.3 ppm) had decomposed to yield two new signals (δ = 52.0, 42.9 ppm), again all at a higher frequency than the starting material (**3.9**) phosphorus resonance (δ = 27.1 ppm). The ^{1}H NMR spectrum did not display any signals characteristic of $AlMe_3$ binding to either the P or N donor groups, and it was found that the product was not pure enough to allow definitive characterisation. Ultimately, no pure product could be isolated from the reaction, and it was concluded that the primary product of the reaction was not stable enough to be isolated.

3.5.2 Reaction of Ph(P^{i}Pr$_2$)C=N(2,6-^{i}Pr$_2$C$_6$H$_3$) (3.9) with 2 equivalents of AlMe$_3$

Rosenthal, Mosa and Muller *et al.* have reported that upon reaction of their PNPN ligands with two equivalents of trialkylaluminium (AlMe$_3$ or AlEt$_3$) that a series of reactions occured, starting with the dimetallation of the ligand (Scheme 3.20, *a*) followed by a rearrangement to yield a monometallic NPPN species (Scheme 3.20, *b*).[41] Based upon this observation by Rosenthal, Mosa and Muller *et al.*, it was of interest to explore the reactivity of iminophosphine **3.9** with two equivalents of AlMe$_3$ and reactions were carried out in order to investigate the possibility of similar differences occurring with iminophosphine ligands.

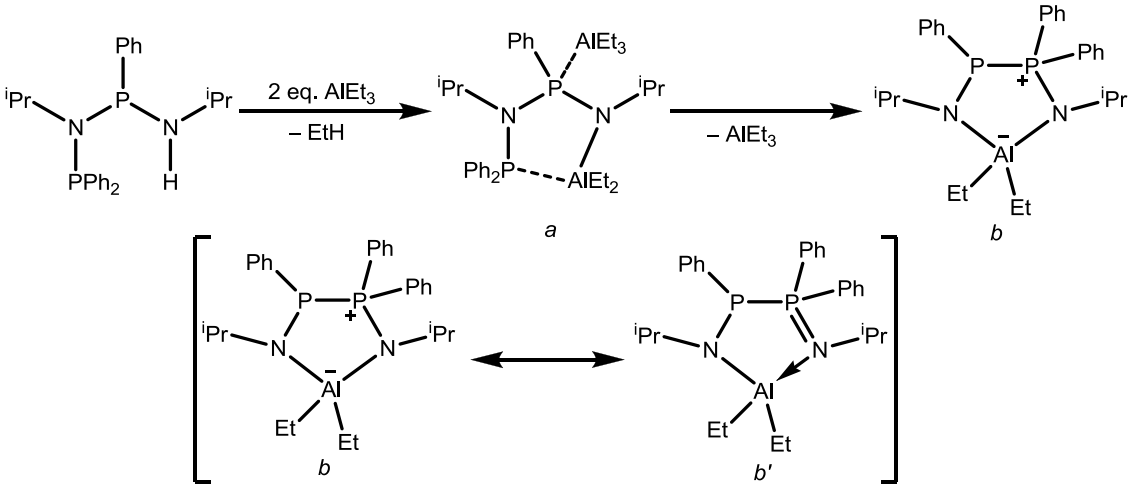

Scheme 3.20: Reaction of a PNPN ligand with 2 equivalents of AlEt$_3$ as reported by Rosenthal, Mosa and Muller *et al*.[41]

To this end, two equivalents of AlMe$_3$ (2M in toluene) were added to a sample of Ph(P^{i}Pr$_2$)C=N(2,6-^{i}Pr$_2$C$_6$H$_3$) (**3.9**) dissolved in toluene (Scheme 3.21). The resulting reaction mixture was left to stir for 16 hours. The solution was then analysed by ^{31}P NMR spectroscopy, revealing a new phosphorus species had formed (δ = 15.7 ppm), different to that observed in the analogous reaction with one equivalent of AlMe$_3$ (δ = 18.3 ppm). The crude reaction mixture was concentrated under vacuum and stored at –30 °C for 16 hours, but no precipitate formed. The solution was concentrated further, and again stored at –30 °C for another 16 hours, but still no precipitate formed. As a consequence all of the solvent was removed under vacuum to yield a yellow oil. Analysis of this crude product by ^{1}H and ^{31}P NMR spectroscopy showed that the product was impure and could not be identified or characterised.

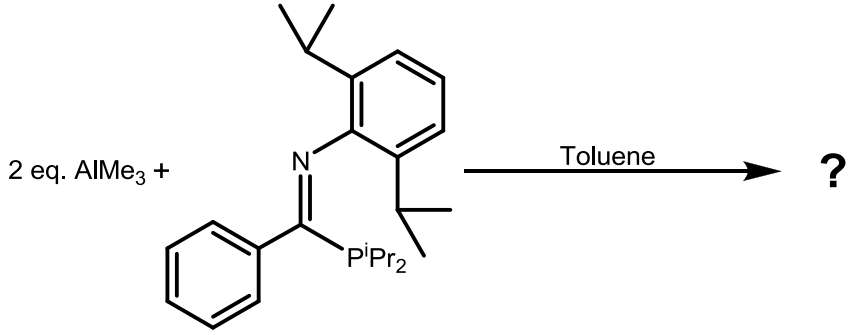

Scheme 3.21: Reaction carried out between 2 equivalents of $AlMe_3$ with compound **3.9**.

In conclusion, it has been demonstrated that iminophosphines react with $AlMe_3$, but the identity of the products formed is currently unknown. The reactions carried out in this investigation suggest that the reaction of iminophosphine ligands with one or two equivalents of $AlMe_3$ form different products, but neither of these products are stable out of solution. It is clear that the species formed by the reaction of $AlMe_3$ with iminophosphines are highly reactive, and therefore cannot be easily isolated and characterised. Further work is required on this subject if any further conclusions are to be drawn on the reactivity of iminophosphines with alkyl aluminium species.

3.6 Attempts to Reduce Iminophosphines to Phosphinoamines

So far in this chapter both the synthesis and characterisation of iminophosphine compounds has been discussed in great detail, and attempts have been made to investigate their reactivity with trialkylaluminium reagents. During the reaction of the iminophosphines with $AlMe_3$ (Section 3.5) it was assumed that the ligand would coordinate to the aluminium centre, while retaining the iminophosphine structure, but no products could be isolated from the reactions. However, it has previously been reported that trialkylaluminium reagents are capable of reducing imines, rather than coordinating to them. Gibson *et al.* published work detailing the reduction of their 2,6-*bis*(imino)pyridine ligands by $AlMe_3$, to yield an *N,N,N*-pyridyliminoamide ligand, bound to an aluminium centre (Scheme 3.22).[42] Further work reported by Gibson *et al.* utilises this imine reduction by $AlMe_3$, followed by removal of the aluminium by reaction with water, to yield 2,6-*bis*(arylamino-methyl)pyridine ligands.[43]

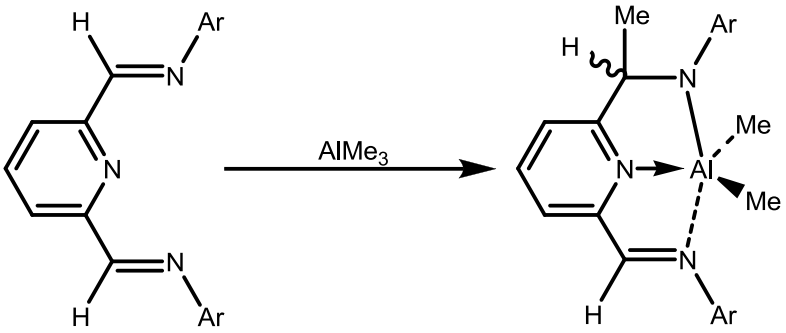

Ar = 2,6-$^{i}Pr_2$-C_6H_3

Scheme 3.22: The reduction of a 2,6-*bis*(imino)pyridine compound to an *N,N,N*-pyridyliminoamide, reported by Gibson *et al.*[42]

Both of Gibson *et al.*'s reports concerning their 2,6-*bis*(imino)pyridine ligands indicate that alkyl aluminium species may be capable of reacting with the imine functional group present in the iminophosphine compounds synthesised in this investigation. It is therefore possible that the use of aluminium activators (*e.g.* MAO) in iminophosphine-based ethylene oligomerisation systems may lead to the reduction of the imine donor group, forming aminophosphines. In order to prove that chromium-iminophosphine complexes are ethylene oligomerisation promoters, rather than aminophosphine derivatives of iminophosphines that are formed during the necessary activation process, it is desirable to synthesise some of these potential ligands and explore their behaviour. Based on this suggestion, reactions were carried out in order to attempt to synthesise aminophosphines by the reduction of their parent iminophosphines, which are detailed below.

3.6.1 Attempted reduction of $Ph(P^iPr_2)C=N(2,6\text{-}^iPr_2C_6H_3)$ (3.9) with $LiAlH_4$

It has previously been reported that imines are easily reduced to amines using $LiAlH_4$.[44,45] Consequently, $LiAlH_4$ was used to attempt to reduce **3.9** ($Ph(P^iPr_2)C=N(2,6\text{-}^iPr_2C_6H_3)$) to its phosphinoamine derivative (Scheme 3.23). Initially a 1 M solution of $LiAlH_4$ in diethyl ether was added to an ethereal solution of **3.9**, but analysis by ^{31}P NMR spectroscopy revealed no reaction occurred. Subsequently the reaction was heated at reflux for 16 hours, after which time NMR spectroscopic analysis again showed that no reaction has taken place. In order to rule out the possibility of the $LiAlH_4$ solution having decomposed, solid $LiAlH_4$ was added to the reaction, and the reaction mixture was again heated at reflux for 16 hours. Analysis by ^{31}P NMR spectroscopy once again showed no reaction had occurred. Based on these results it was concluded that $LiAlH_4$ does not have the capacity to reduce these iminophosphines to their related phosphinoamine derivatives.

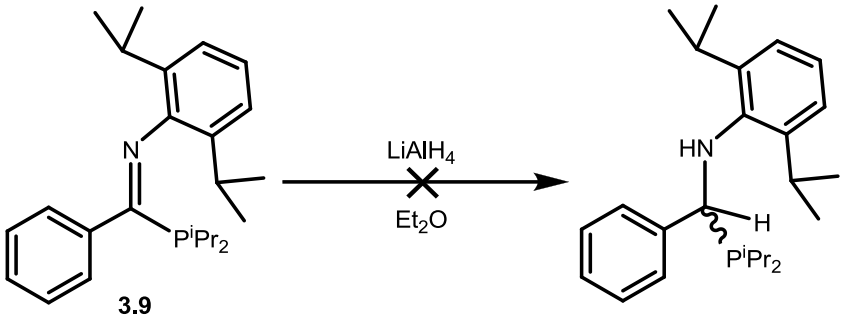

Scheme 3.23: Attempted reduction of iminophosphine **3.9** with $LiAlH_4$.

3.6.2 Attempted reduction of $Ph(P^iPr_2)C=N(2,6\text{-}^iPr_2C_6H_3)$ (3.9) with H_2 over Pd/C

After the failure of $LiAlH_4$ to reduce the iminophosphine compound, it was decided that the reaction should be attempted with an alternative reducing reagent. Imines are known to be reduced under mild conditions by H_2 over a Pd/C catalyst,[46] so consequently, the reduction of **3.9** was attempted using these conditions. A solution of **3.9** ($Ph(P^iPr_2)C=N(2,6\text{-}^iPr_2C_6H_3)$) in hexane was stirred for 16 hours over a catalytic amount of Pd/C under H_2 at atmospheric pressure (Scheme 3.24). Subsequent analysis of the reaction mixture by ^{31}P NMR spectroscopy showed that no reaction of the iminophosphine had occurred.

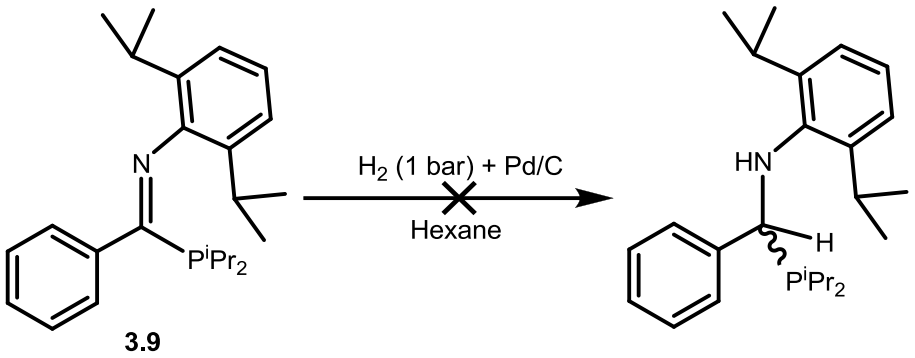

3.9

Scheme 3.24: Attempted reduction of iminophosphine **3.9** with H_2 over Pd/C at ambient pressure.

Based on the initial unsuccessful reductions described above it was concluded that more forcing conditions are required to reduce bulky iminophosphines such as **3.9**. In order to further investigate potential methods of reducing iminophosphines to imines, it was decided to probe the reactivity of compound **3.10** with Wilkinson's Catalyst, and to then undertake a Rh-catalysed hydrogenation.

3.6.3 Attempted reaction of $Ph(P^iPr_2)C{=}N(2,6\text{-}Me_2C_6H_3)$ with Wilkinson's Catalyst, $RhCl(PPh_3)_3$

Wilkinson's Catalyst is a well-known reagent for use in hydrogenation catalysis,[47,48] and it is easily conceivable that this rhodium complex may be capable of reducing the iminophosphine ligands described in this thesis. In order to investigate this possibility, the reaction of $RhCl(PPh_3)_3$ with iminophosphine **3.10** was attempted prior to the addition of hydrogen, since compound **3.10** bears a phosphine group capable of coordinating to Rh (Scheme 3.25).

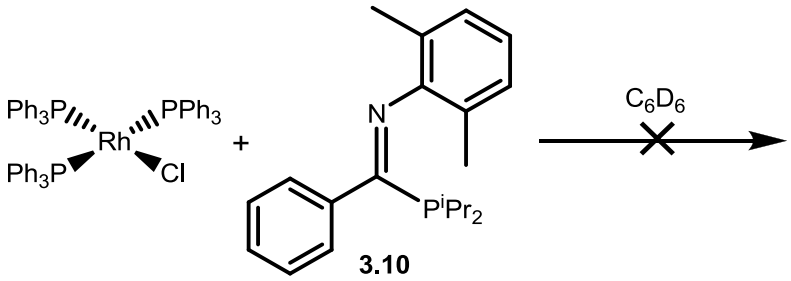

3.10

Scheme 3.25: Attempted reaction of iminophosphine **3.10** with Wilkinson's Catalyst.

Initially, a 1:1 (Rh:PCN) mixture of $RhCl(PPh_3)_3$ and iminophosphine **3.10** in C_6D_6 was heated to 60 °C for four hours, after which time the mixture was analysed by $^{31}P\{^1H\}$ NMR spectroscopy. The spectrum showed that no reaction had taken place, and the reaction mixture was subsequently left to stand for one month. After this time further $^{31}P\{^1H\}$ NMR spectroscopic analysis revealed that all of the starting iminophosphine remained present in the reaction. Prior to the reaction it was expected that the iminophosphine ligand should bind to the rhodium

centre of Wilkinson's Catalyst, either *via* the phosphine or imine moieties, but this has found not to be the case in the reaction carried out.

Based upon the lack of reaction between $RhCl(PPh_3)_3$ and compound **3.10** it is assumed that Wilkinson's catalyst is not a good candidate as a catalyst capable of hydrogenating iminophosphines. The choice of further hydrogenation catalysts for testing must be made carefully, due to ability of certain reducing agents (*e.g.* Raney Nickel)[46] to reduce aromatic groups, such as the phenyl functional groups in iminophosphine **3.9**.

Recently, a novel transfer hydrogenation system has been reported by Oestreich *et al.* using catalytic amounts of $B(C_6F_5)_3$ and 1,4-cyclohexadiene as a hydrogen source, that has been demonstrated to give excellent conversion of imines to amines.[49] Based on this work it is suggested that the imine hydrogenation system reported by Oestreich *et al.* could be used in the to hydrogenate the bulky iminophosphines reported in this thesis, but due to the lack of time, this reduction could not be carried out as part of this investigation.

Overall, the lack of imine hydrogenation observed using both $LiAlH_4$ and H_2 over Pd/C, and the lack of reaction with Wilkinson's Catalyst suggests that the iminophosphine ligands synthesised in this thesis cannot by readily reduced to their phosphinoamine counterparts. It is therefore presumed that when placed under catalytic ethylene oligomerisation conditions, the iminophosphines will retain their structure, rather than being reduced to phosphinoamines.

3.7 Summary and Conclusions

In this chapter a new modular synthetic route to iminophosphine compounds has been reported, which has been utilised to synthesise a library of novel iminophosphines. A range of synthetic routes have been attempted, and a number of the reported literature procedures carried out have been found not to be easily reproducible. A total of 26 novel PCN compounds have been synthesised, with various functional groups in order to give compounds with a wide variety of steric and electronic properties, to enable a wide-ranging catalytic screening to be undertaken. It has been demonstrated that PCN compounds can be easily synthesised from the reaction of imidoyl chlorides with trimethylsilylphosphines to yield the desired iminophosphine products in good yields. It is suggested that the reaction mechanism proceeds by nucleophilic attack of the phosphine at the imidoyl chloride, based on the observation that there is an increase in rate of reaction upon use of polar solvents in comparison to less-polar solvents. All of the iminophosphine compounds synthesised have been fully characterised using a variety of NMR spectroscopic techniques, as well as mass spectrometry and elemental analysis. The C=N stretching frequencies were also measured for all the iminophosphines by IR spectroscopy. The C=N stretching frequencies measured for the iminophosphines were lower than those of their imidoyl chloride starting materials, indicating conjugation between the phosphine and the C=N imine bond.

Theoretical calculations of the percentage buried volume ($\%V_{bur}$) have been carried out on a series of the iminophosphines synthesised (**3.26, 3.8, 3.10 and 3.12**) in an attempt to quantify the steric demands of the various phosphine groups used. It was found that the $\%V_{bur}$ increased with larger P-alkyl substituents, as expected. In order to elucidate the phosphine electronic donor characteristics of the compounds synthesised, the derivative phosphine selenides of the iminophosphines were made and ^{31}P NMR spectroscopy was used to measure $^{1}J_{P\text{-}Se}$ coupling constants. The $|^{1}J_{P\text{-}Se}|$ couplings measured revealed the PCN compounds to have relatively good donor properties, comparable to that of alkyl phosphines through to PPh_3, depending on the functional groups present.

A detailed study of the *E*/*Z* isomerisation behaviour of the various iminophosphine compounds has been carried out. X-Ray crystallographic analysis and solid state NMR spectroscopy were used to determine the isomers present in the solid state, while VT NMR spectroscopic experiments were used to probe the solution state behaviour of a selection of PCN compounds. A series of computational calculations were carried out in order to probe the mechanism of isomerisation. From these investigations into the *E*/*Z* isomerisation of iminophosphines it was concluded that iminophosphines bearing P-alkyl substituents favour the

E isomers in both the solution- and solid-states. It has been shown that iminophosphines with P-aryl groups can exist as both *E* and *Z* isomers in solution, in varying proportions, dependant on the steric effects of the functional groups. The only compound found to exist primarily as the *Z* isomer in solution is **3.24**, which possesses P-anisyl phosphine substituents.

Attempts have been made to reduce the iminophosphine compounds synthesised (**3.9**) to their phosphinoamine counterparts. Two methods were undertaken, using $LiAlH_4$ and atmospheric H_2 over Pd/C as reducing agents. Neither of these reagents were shown to be capable of reducing iminophosphines under the conditions attempted.

A final set of reactions were carried out to investigate the reactivity of iminophosphines with alkylaluminium species. It was found that upon reaction of ligand **3.9** with one equivalent of $AlMe_3$ a new product was observed by ^{31}P NMR spectroscopy (δ = 18.3 ppm), but the species was found to be highly reactive, and therefore could not be isolated and characterised. An analogous reaction of compound **3.9** with two equivalents of $AlMe_3$ was also carried out, which resulted in another new product being observed by ^{31}P NMR spectroscopy (δ = 15.7 ppm). Unfortunately again, this was found to be a yellow oil that could not be purified and characterised. It is concluded that iminophosphines do react with $AlMe_3$, but not to give stable and isolable products that can be easily characterised.

The next step in the investigation of the iminophosphines synthesised as potential ligands for use in ethylene oligomerisation systems is to synthesise Cr(PCN) complexes, in order to study the coordination chemistry of the compounds. This will allow for the structure and electronic effects of the ligands to be probed further. This extra information on the coordination chemistry of the ligands can then be applied to the development of selective ethylene oligomerisation catalysis systems.

3.8 References

(1) Carter, A.; Cohen, S. A.; Cooley, N. A.; Murphy, A.; Scutt, J.; Wass, D. F. *Chem. Commun.* **2002**, 858.
(2) Wass, D. F. *Dalton Trans.* **2007**, 816.
(3) McGuinness, D. S. *Chem. Rev.* **2011**, *111*, 2321.
(4) Kuhlmann, S.; Blann, K.; Bollmann, A.; Dixon, J. T.; Killian, E.; Maumela, M. C.; Maumela, H.; Morgan, D. H.; Prétorius, M.; Taccardi, N.; Wasserscheid, P. *J. Catal.* **2007**, *245*, 279.
(5) Agapie, T.; Day, M. W.; Henling, L. M.; Labinger, J. A.; Bercaw, J. E. *Organometallics* **2006**, *25*, 2733.
(6) Overett, M. J.; Blann, K.; Bollmann, A.; de Villiers, R.; Dixon, J. T.; Killian, E.; Maumela, M. C.; Maumela, H.; McGuinness, D. S.; Morgan, D. H. *J. Mol. Catal. A: Chem.* **2008**, *283*, 114.
(7) Agapie, T.; Schofer, S. J.; Labinger, J. A.; Bercaw, J. E. *J. Am. Chem. Soc.* **2004**, *126*, 1304.
(8) Sydora, O. L.; Jones, T. C.; Small, B. L.; Nett, A. J.; Fischer, A. a.; Carney, M. J. *ACS Catal.* **2012**, *2*, 2452.
(9) Issleib, K.; Low, O. *Z. Anorg. Allg. Chem.* **1966**, *346*, 241.
(10) Li, X.; Song, H.; Cui, C. *Dalton Trans.* **2009**, 9728.
(11) Abdellah, I.; Ibrahim, E.; Farag, R. *Gazz. Chim. Italia* **1988**, *118*, 141.
(12) van Dijk, T.; Burck, S.; Rong, M. K.; Rosenthal, A. J.; Nieger, M.; Slootweg, J. C.; Lammertsma, K. *Angew Chem Int Ed Engl* **2014**, *53*, 9068.
(13) Issleib, K.; Schmidt, H.; Meyer, H. *J. Organomet. Chem.* **1978**, *160*, 47.
(14) Walther, D.; Liesicke, S.; Fischer, R.; Görls, H.; Weston, J.; Batista, A. *Eur. J. Inorg. Chem.* **2003**, *2003*, 4321.
(15) McMurry, J. *Organic Chemistry*; 1st ed.; Brooks/Cole: Belmont, California, USA, 1984, p 303.
(16) Clayden, J. P.; Greeves, N.; Warren, S.; D., W. P. *Organic Chemistry*; Oxford University Press: New York, USA, 2001, p 284.
(17) Nijhuis, C. A.; Jellema, E.; Sciarone, T. J. J.; Meetsma, A.; Budzelaar, P. H. M.; Hessen, B. *Eur. J. Inorg. Chem.* **2005**, *2005*, 2089.
(18) Tolman, C. A. *J. Am. Chem. Soc.* **1970**, *92*, 2956.
(19) Tolman, C. A. *Chem. Rev.* **1977**, *77*, 313.
(20) Tolman, C. A.; Seidel, W. C.; Gosser, L. W. *J. Am. Chem. Soc.* **1974**, *96*, 53.
(21) Poater, A.; Cosenza, B.; Correa, A.; Giudice, S.; Ragone, F.; Scarano, V.; Cavallo, L. *Eur. J. Inorg. Chem.* **2009**, *2009*, 1759.
(22) Clavier, H.; Nolan, S. P. *Chem. Commun.* **2010**, *46*, 841.
(23) Sandorfy, C. In *Carbon–Nitrogen Double Bonds (1970)*; John Wiley & Sons, Ltd.: 2010, p 37.
(24) NIST Computational Chemistry Comparison and Benchmark Database, NIST Standard Reference Database Number 101 Release 16a, August 2013, Editor: Russell D. Johnson III, http://cccbdb.nist.gov/
(25) Gillespie, J. A.; Zuidema, E.; van Leeuwen, P. W. N. M.; Kamer, P. C. J. In *Phosphorus(III) Ligands in Homogeneous Catalysis: Design and Synthesis*; John Wiley & Sons, Ltd: 2012, p 7.
(26) Allen, D. W.; Taylor, B. F. *J. Chem. Res.-S* **1981**, 220.
(27) Allen, D. W.; Taylor, B. F. *J. Chem. Soc., Dalton Trans.* **1982**, 51.
(28) Pinnell, R. P.; Megerle, C. A.; Manatt, S. L.; Kroon, P. A. *J. Am. Chem. Soc.* **1973**, *95*, 977.
(29) Dyer, P. W.; Fawcett, J.; Hanton, M. J.; Kemmitt, R. D. W.; Padda, R.; Singh, N. *Dalton Trans.* **2003**, 104.

(30) Hrib, C. G.; Ruthe, F.; Seppälä, E.; Bätcher, M.; Druckenbrodt, C.; Wismach, C.; Jones, P. G.; du Mont, W.-W.; Lippolis, V.; Devillanova, F. A.; Bühl, M. *Eur. J. Inorg. Chem.* **2006**, *2006*, 88.
(31) Muller, A.; Otto, S.; Roodt, A. *Dalton Trans.* **2008**, 650.
(32) Gilheany, D. G. In *The Chemistry of Organophosphorus Compounds*; Hartley, F. R., Ed.; John Wiley & Sons, Inc.: 1990, p 9.
(33) Gilheany, D. G. *Chem. Rev.* **1994**, *94*, 1339.
(34) Huckel, E. *Z. Physik* **1930**, *60*, 423.
(35) Curtin, D. Y.; Hausser, J. W. *J. Am. Chem. Soc.* **1961**, *83*, 3474.
(36) Curtin, D. Y.; Grubbs, E. J.; McCarty, C. G. *J. Am. Chem. Soc.* **1966**, *88*, 2775.
(37) Kerek, F.; Simon, Z.; Ostrogov.G *J. Chem. Soc. B - Phys. Org.* **1971**, 541.
(38) Baier, M. C.; Zuideveld, M. a.; Mecking, S. *Angew. Chem. Int. Ed.* **2014**, *53*, 9722.
(39) McGuinness, D. S.; Overett, M.; Tooze, R. P.; Blann, K.; Dixon, J. T.; Slawin, A. M. Z. *Organometallics* **2007**, *26*, 1108.
(40) Alzamly, A.; Gambarotta, S.; Korobkov, I. *Organometallics* **2014**, *33*, 1602.
(41) Peitz, S.; Peulecke, N.; Aluri, B. R.; Hansen, S.; Muller, B. H.; Spannenberg, A.; Rosenthal, U.; Al-Hazmi, M. H.; Mosa, F. M.; Wohl, A.; Muller, W. *Eur. J. Inorg. Chem.* **2010**, *2010*, 1167.
(42) Bruce, M.; Gibson, V. C.; Redshaw, C.; Solan, G. A.; White, A. J. P.; Williams, D. J. *Chem. Commun.* **1998**, 2523.
(43) Britovsek, G. J. P.; Gibson, V. C.; Mastroianni, S.; Oakes, D. C. H.; Redshaw, C.; Solan, G. A.; White, A. J. P.; Williams, D. J. *Eur. J. Inorg. Chem.* **2001**, *2001*, 431.
(44) Howe, R. K. *J. Org. Chem.* **1968**, *33*, 2848.
(45) Dyer, P. W.; Fawcett, J.; Griffith, G. A.; Hanton, M. J.; Olivier, C.; Patterson, A. R.; Suhard, S. *Chem. Commun.* **2005**, 3835.
(46) Augustine, R. L. *Catalytic hydrogenation: techniques and applications in organic synthesis*; M. Dekker, 1965, p 102.
(47) Osborn, J. A.; Wilkinson, G.; Young, J. F. *Chem. Commun.* **1965**, 17.
(48) Jardine, F. H. In *Prog. Inorg. Chem.*; John Wiley & Sons, Inc.: 1981; Vol. 28, p 63.
(49) Chatterjee, I.; Oestreich, M. *Angew. Chem. Int. Ed.* **2015**, *54*, 1965.

Chapter 4:

Coordination Chemistry of Iminophosphine Compounds

4.1 Introduction

Since the vast majority of selective catalytic ethylene oligomerisation systems utilise chromium,[1] chromium-based catalysts are therefore the obvious first choice for developing new oligomerisation processes. For many studies investigating the mechanism of ethylene *tri*- and *tetra*-merisation the first port of call is to synthesise discrete chromium-ligand complexes.[2] The synthesis of model complexes is useful in order to study a wide range of features of the ligand, including the coordination chemistry,[3] electronic effects of the ligand,[4] and the structures of potentially catalytically active species.[5]

Alternatively, pre-formed chromium complexes can be used as catalytic precursors in ethylene oligomerisation systems, and it has been found with some *tri*- and *tetra*-merisation systems that the use of pre-formed chromium-ligand complexes gives a significantly better activity and selectivity than allowing Cr-ligand complexes to form *in situ*. In a patent from Chevron Phillips it was reported that a series of chromium-phosphinoamidine complexes were precursors to highly active ethylene *tri*- and *tetra*-merisation systems (Scheme 4.1, *a*).[6] Interestingly, the Chevron Phillips group found that upon generation of their catalytic precursors *in situ*, the catalytic system was rendered entirely inactive towards *tri*- and *tetra*-merisation, suggesting that pre-formation of the chromium precursor complex is vital to yield an active catalyst (Scheme 4.1, *b*).

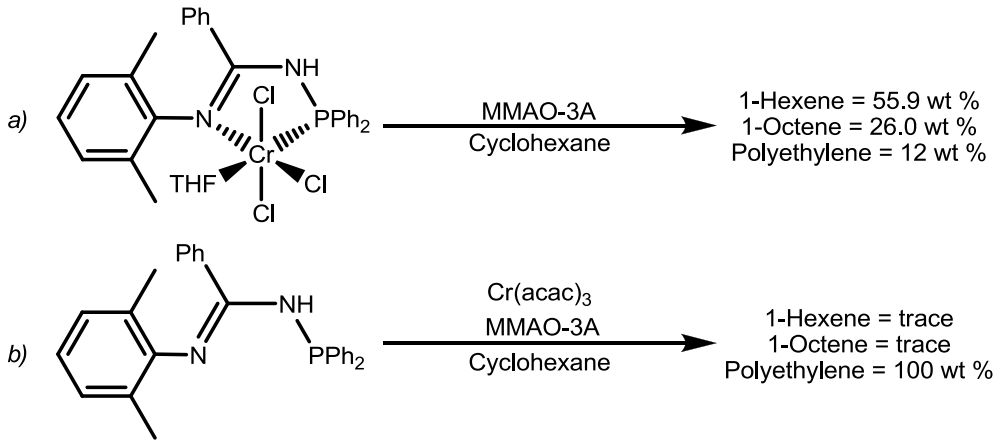

Scheme 4.1: Comparing the catalytic selectivity of pre-formed versus *in situ* formed Cr(III) complexes reported by Sydora *et al.*[6]

As well as Cr(III) complexes, it has been demonstrated that Cr(I) species can be used as precursors for ethylene oligomerisation catalysis. In a pair of reports concerning $Cr(CO)_4$(PNP) complexes, Wass *et al.* and Hanton *et al.* both demonstrated that ethylene *tri*- and *tetra*-merisation systems can be generated from pre-formed Cr(I) complexes.[5,7] In these investigations using Cr(I) pre-catalysts it was found that $Cr(CO)_4$(PNP) complexes could be easily oxidised using

silver salts to give $[Cr(CO)_4(PNP)]^+$ species, which when subsequently activated with trialkylaluminiums yielded active ethylene *tri*- and *tetra*-merisation systems.

It is based on the above ideas and concepts that the synthesis of a range of chromium-iminophosphine complexes was carried out as part of this thesis. The coordination of iminophosphine ligands with Cr(III) will be investigated, and the resulting Cr^{III}(PCN) complexes will be tested as precursors in ethylene oligomerisation systems (catalytic testing detailed in Chapter 5). Complexation reactions of Cr(II) with iminophosphine ligands have also been carried out, following on from work by McGuinness *et al.*, in which Cr^{II}(PNP) complexes were used as ethylene oligomerisation precursors.[8] Finally, the complexation of iminophosphine ligands with Cr(0) species will be investigated, allowing for more detailed characterisation of Cr(PCN) complexes to be carried out, due to the diamagnetic nature of Cr(0) making NMR spectroscopic analysis possible.

4.2 Coordination of Iminophosphines with Cr(III)

The synthesis and characterisation of Cr(III)-iminophosphine complexes is desirable due to the potential application of the resulting systems as well-defined catalytic precursors for selective ethylene oligomerisation. Unfortunately, the characterisation of any Cr(III) complexes synthesised is hindered by their paramagnetic nature. The highly air-/moisture-sensitive nature of the complexes synthesised has also caused problems with mass spectrometric analysis, further hampering characterisation of the products. This means that the primary method of characterisation of the Cr(III) complexes synthesised has been elemental analysis, along with X-ray crystallographic studies where possible.

4.2.1 Synthesis of $CrCl_3(THF)(PhC(PPh_2)=NPh)$ (4.1)

The complex **4.1** was synthesised by reaction of $CrCl_3(THF)_3$ with a slight excess (1.1 equivalents) of iminophosphine **3.3** in toluene (Scheme 4.2), a method derived from that reported by Bollmann *et al.*[9] Subsequently, the complex $CrCl_3(THF)(PhC(PPh_2)=NPh)$ (**4.1**) was isolated as a blue solid in a reasonable yield (64 %), with elemental analysis confirming the identity and purity of the product.

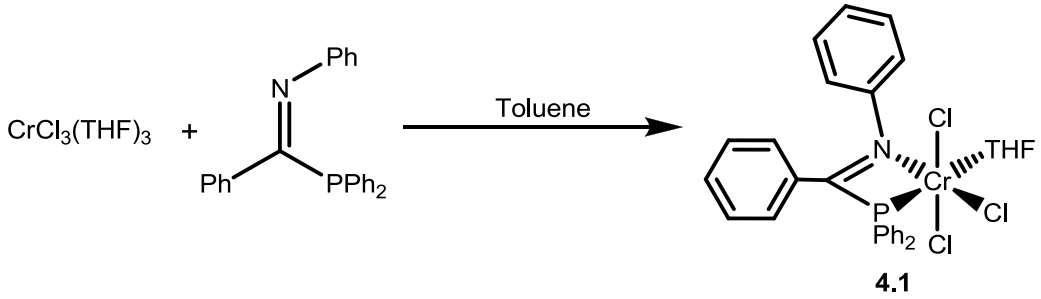

4.1

Scheme 4.2: Synthesis of $CrCl_3(THF)(PhC(PPh_2)=NPh)$ **4.1** by the reaction of $CrCl_3(THF)_3$ with ligand **3.3**.

Crystals of complex **4.1** suitable for X-ray crystallographic analysis were grown by slow diffusion of hexane into a concentrated solution of **4.1** in DCM. The resulting molecular structure revealed that **4.1** adopts a distorted octahedral structure about chromium, with the iminophosphine coordinating in a bidentate fashion as anticipated (Figure 4.1).

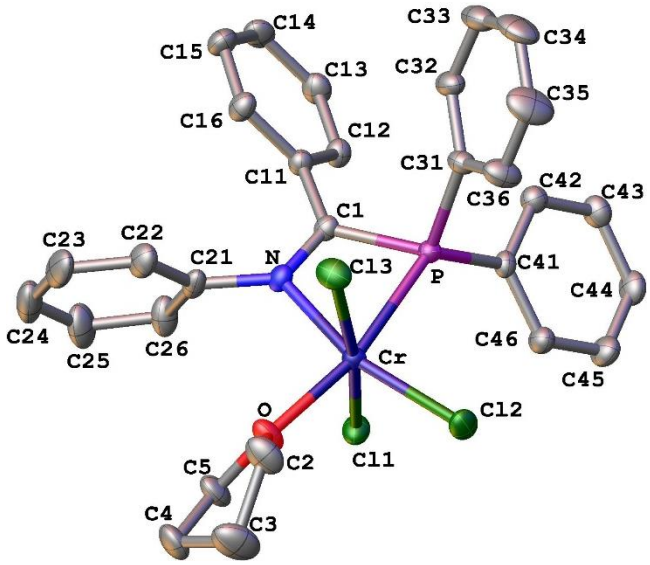

Figure 4.1: ORTEP representation of the molecular structure determined for **4.1**, with thermal ellipsoids set at 50 % probability level.

From the molecular structure of **4.1** it can be seen that the iminophosphine binds with the THF ligand *trans* to the phosphine donor group, matching the *trans* P-Cr-THF configuration displayed by the chromium-(pyridine-phosphine) complexes reported by Gambarotta and Duchateau *et al.*[10] The molecular structure adopted by **4.1** takes up the configuration predicted by the *trans* influence principle, with the phosphine (strongest *trans* influence) binding *trans* to the THF ligand (weakest *trans* influence).[11] The effect of the weak *trans* influence of nitrogen (relative to the Cl and P donors) can also be seen in the three Cr-Cl bond lengths, with the Cr-Cl bond *trans* to the nitrogen being the shortest (Table 4.1).

$CrCl_3(THF)(PhC(PPh_2)=NPh)$ (4.1)		
Bond Lengths (Å)	Cr – P	2.4284(6)
	Cr – N	2.1101(18)
	Cr – Cl(1)	2.3181(6)
	Cr – Cl(2)	2.2876(6)
	Cr – Cl(3)	2.2981(7)
	Cr – O	2.0554(17)
Bond Angles (°)	N – Cr – P	66.48(6)
	P – C – N	103.89(15)

Table 4.1: Selected bond lengths (Å) and angles (°) determined for complex **4.1**.

The tight P-C-N angle of **4.1** (~104 °) is noteworthy, being more acute than any of the P-C-N angles measured for free iminophosphine ligands (118 - 120 °), and is more closely comparable to the P-N-P angles of $[CrCl_3(PNP)]_2$ complexes measured by Overett *et al.* of 106 ° (Figure 4.2),[12] indicating that the four-membered chelate ring of Cr(PCN) complexes is similar to that of Cr(PNP) complexes. This is of interest, as it has been previously suggested that ligands with a tight bite angle give better selectivities towards ethylene trimerisation when used in oligomerisation systems.[13]

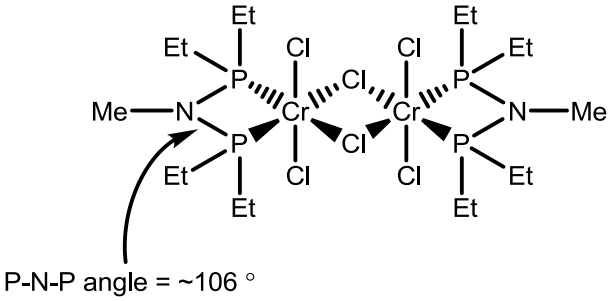

Figure 4.2: The $[CrCl_3(PNP)]_2$ complex synthesised by Overett *et al.*[12]

In order to further confirm the identity of **4.1** the magnetic susceptibility of this paramagnetic Cr(III) species was measured using the NMR spectroscopic Evans' method.[14,15] The Evans' method of measuring magnetic susceptibility of paramagnetic compounds exploits the ability of paramagnetic species to cause a shift in NMR spectroscopic signals of the solvent the complex is dissolved in. This shift in the NMR frequency of the solvent can be measured, relative to an external solvent sample, hence allowing the magnetic susceptibility of the desired paramagnetic complex to be deduced. For this investigation the paramagnetic complexes were dissolved in d_2-DCM, with a sealed d_2-DCM-filled capillary placed in the NMR tube along with the sample. Using this approach, the magnetic susceptibility (μ_{eff}) of complex **4.1** was determined to be 3.9 μ_B, which is comparable to the value of μ_{eff} = 3.8 μ_B reported by Labinger and Bercaw *et al.* for their $CrPh_3(PNP^{OMe})$ complex.[16]

4.2.2 Synthesis of $CrCl_3(THF)(PhC(PPh_2)=N(2\text{-}MeC_6H_4))$ (4.2)

The Cr(III) complex **4.2** ($CrCl_3(THF)(PhC(PPh_2)=N(2\text{-}MeC_6H_4))$) was synthesised using an analogous procedure to that used to prepare $CrCl_3(THF)(PhC(PPh_2)=NPh)$ **(4.1)**. Complex **4.2** was successfully isolated as a green powder in a relatively low yield (30 %). The identity of the product and its purity were confirmed by elemental analysis. A concentrated solution of **4.2** in DCM was layered with hexane and allowed to slowly diffuse, giving crystals suitable for X-ray crystallography and allowing the molecular structure of **4.2** to be determined (Figure 4.3).

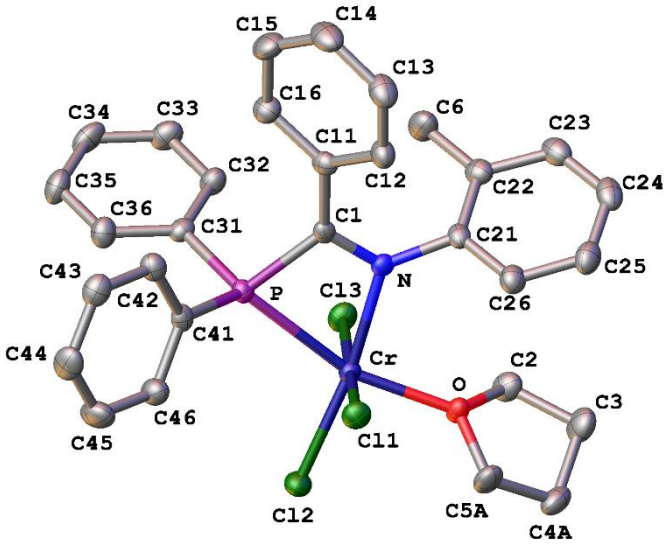

Figure 4.3: ORTEP representation of the molecular structure determined for **4.2**, with thermal ellipsoids at 50 % probability level.

The molecular structure adopted by **4.2** reveals the iminophosphine ligand binding to the chromium centre in a bidentate fashion, giving rise to a distorted octahedral structure about the Cr centre. As seen with complex **4.1**, the phosphine donor occupies the coordination site *trans* to the THF ligand, as predicted by the *trans* influence. The Cr-Cl bond *trans* to the nitrogen donor is the shortest of the three Cr-Cl bonds, again due to the weak *trans* influence of the nitrogen donor (Table 4.2).

$CrCl_3(THF)(Ph(PPh_2)C{=}N(2\text{-}MeC_6H_4))$ (4.2)		
Bond Lengths (Å)	Cr – P	2.4869(7)
	Cr – N	2.1160(18)
	Cr – Cl(1)	2.3251(7)
	Cr – Cl(2)	2.2845(7)
	Cr – Cl(3)	2.2953(7)
	Cr – O	2.0387(15)
Bond Angles (°)	N – Cr – P	65.42(5)
	P – C(1) – N	104.03(15)

Table 4.2: Selected bond lengths (Å) and angles (°) determined for complex **4.2**.

The Evans' NMR spectroscopic method was again used to measure the magnetic susceptibility of complex **4.2.** The complex was dissolved in d_2-DCM, and the spectrum was

measured at 600 MHz. The magnetic moment was determined to be 3.6 μ_B, which is comparable to that measured for **4.1** (μ_{eff} = 3.8 μ_B), consistent with the analogous structure of complex **4.2**.

4.2.3 Synthesis of $CrCl_3(Ph(PPh_2)C{=}N(2\text{-}MeOC_6H_4)$ (4.3)

An analogous procedure to that used in the synthesis of $CrCl_3(THF)(Ph(PPh_2)C{=}NPh)$ (**4.1**) was employed to prepare complex ($CrCl_3(Ph(PPh_2)C{=}N(2\text{-}MeOC_6H_4)$)) **4.3**. Upon addition of the ligand solution to a solution of $CrCl_3(THF)_3$ the reaction mixture turned dark green, and subsequently the solution was concentrated under vacuum. A brown solid precipitated out of the solution, which was isolated by filtration, washed with diethyl ether (3 × 5 mL) and dried under vacuum to yield the product as a brown solid in a relatively low yield (30 %) (Scheme 4.3). Initially it was assumed, based on the structures of the comparable complexes **4.1** and **4.2**, that the iminophosphine had adopted a bidentate P,N coordination mode, but elemental analysis revealed this not to be the case. Instead CHN analyses were consistent with the tridentate $CrCl_3(\kappa^3\text{-}Ph(PPh_2)C{=}N(2\text{-}MeOC_6H_4)$ complex, **4.3**. Unfortunately, crystals suitable for X-ray crystallographic analysis could not be grown, meaning a definitive molecular structure has not been determined. IR spectroscopy was attempted to aid the characterisation of the complex, but no characteristic signals were observed to identify the compound.

The magnetic susceptibility of **4.3** was measured by Evans' NMR spectroscopic method. The complex **4.3** was dissolved in d_2-DCM, and the magnetic moment was determined to be 3.8 μ_B. This matches with the values found for the other Cr(III) complexes synthesised in this investigation, based on the assumption that the diamagnetic correction of the *o*-OMe donor group is the same as that of a THF donor, as found in the other complexes in this thesis. Unfortunately, this doesn't give any more information as to the coordination mode of iminophosphine ligand with the chromium centre, but based on all of the data gathered for **4.3** it is proposed that the structure is that of the title compound, $CrCl_3(Ph(PPh_2)C{=}N(C_6H_4\text{-}o\text{-}OMe)$.

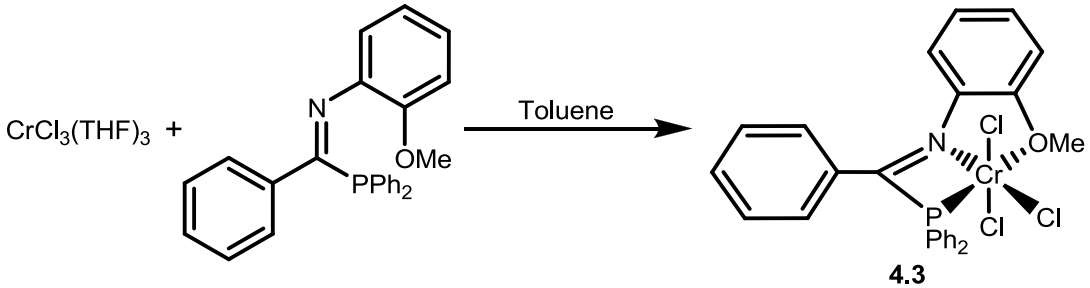

4.3

Scheme 4.3: Synthesis of $CrCl_3(Ph(PPh_2)C{=}N(2\text{-}MeOC_6H_4))$ (**4.3**) by reaction of $CrCl_3(THF)_3$ with $Ph(PPh_2)C{=}N(C_6H_4\text{-}o\text{-}OMe)$.

Since the molecular structure for complex **4.3** could not be obtained, it is not known whether the tridentate ligand binds to the chromium in a *fac*- or *mer*-coordination mode. In

order to probe this, a computational study was carried out, based upon the experimentally determined structure of **4.2** ($CrCl_3(THF)(Ph(PPh_2)C=N(2\text{-}MeC_6H_4))$). The N-*o*-Me-$C_6H_4$ group of complex **4.2** was replaced with an N-*o*-OMe-C_6H_4 group, and the THF group removed, to yield a theoretical structure of $CrCl_3(Ph(PPh_2)C=N(C_6H_4\text{-}o\text{-}OMe)$ (**4.3**). Subsequently, the N-aryl group was rotated around the N-C *ipso* bond (while retaining all other geometric parameters as determined experimentally for **4.2**). It was found that the closest approach of the Cr and O atoms was 2.8 Å, when the ligand was in a pseudo-*mer* coordination position (Figure 4.4). Based on this analysis it is easily conceivable that the donor OMe group could coordinate to the Cr centre, yielding the tridentate $CrCl_3(THF)(mer\text{-}\kappa^3\text{-}Ph(PPh_2)C=N(C_6H_4\text{-}o\text{-}OMe)$ complex displayed in Scheme 4.3.

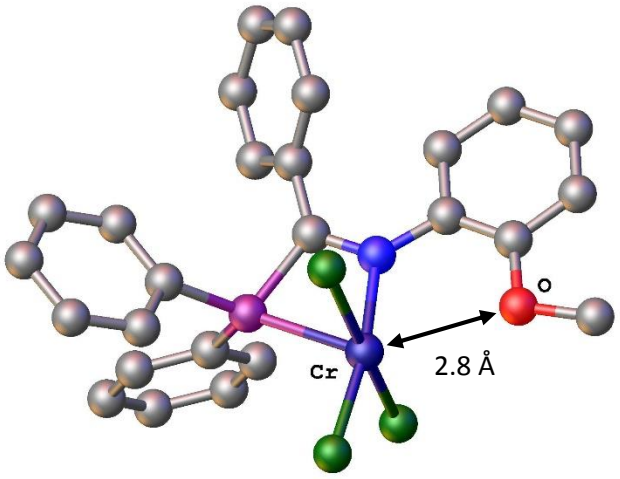

Figure 4.4: Ball and stick representation of a computationally-derived structure of complex **4.3**, based on the experimentally derived structure of **4.2**, displaying the closest approach of the *o*-OMe-C_6H_4 group to the Cr centre.

4.2.4 Synthesis of $CrCl_3(THF)(Ph(P^iPr_2)C=N(2\text{-}MeC_6H_4))$ (4.4), $CrCl_3(THF)(Ph(P^iPr_2)C=N(2,6\text{-}Me_2C_6H_3))$ (4.5) and $CrCl_3(THF)(Ph(P^iPr_2)C=N(2,6\text{-}^iPr_2C_6H_3))$ (4.6)

Complexes **4.4**, **4.5** and **4.6** were all synthesised using modifications of a method reported by Labinger and Bercaw *et al*.[3] A slight excess of the chosen iminophosphine ligand (1.1 equivalents) in DCM was added to a DCM solution of $CrCl_3(THF)_3$ and stirred for 1 hour. Subsequently the solvent was removed under vacuum before the resulting products were triturated with hexane and dried under vacuum to yield the desired products. All of the three product complexes **4.4**, **4.5** and **4.6** were successfully characterised by elemental analysis, and their magnetic susceptibilities measured by Evans' NMR spectroscopic method. The magnetic susceptibility, yield and results of the CHN analyses for each complex are reported in Table 4.3.

Complex	**4.4**	**4.5**	**4.6**
Proposed Structure	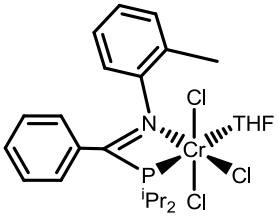	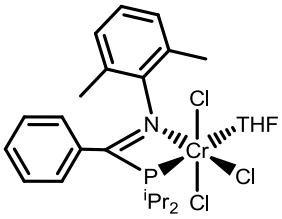	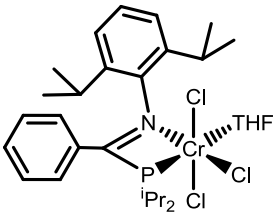
Yield	66 %	90 %	81 %
Magnetic susceptibility (μ_B)	3.7	3.8	3.7
CHN analysis	$C_{24}H_{34}Cl_3CrNOP$	$C_{25}H_{36}Cl_3CrNOP$	$C_{29}H_{44}Cl_3CrNOP$
Calc.	C, 53.20; H, 6.32; N, 2.58	C, 54.02; H, 6.53; N, 2.52	C, 56.91; H, 7.25; N, 2.29
Found	C, 53.04; H, 6.15; N, 2.63	C, 53.97; H, 6.66; N, 2.43	C, 56.84; H, 7.34; N, 2.35

Table 4.3: Experimental data from complexes **4.4**, **4.5** and **4.6**

4.3 Attempted Coordination of Iminophosphines with Cr(II)

It has been reported previously that Cr(II) complexes can be used as initiators in selective ethylene oligomerisation systems with SNS ligands,[17] and a number of studies have suggested that Cr(II) may play an important role in the mechanism of ethylene *tri*- and *tetra*-merisation (see Section 1.2.2.2).[8,18] With this in mind, an investigation into the reactivity of iminophosphine ligands with Cr(II) species was undertaken.

4.3.1 Reaction of $CrCl_2$ with $Ph(P^iPr_2)C{=}N(2,6\text{-}Me_2C_6H_3)$ (3.10)

Based upon work reported by Bouachir *et al.*,[19] the synthesis of a $CrCl_2(\kappa^2\text{-}Ph(P^iPr_2)C{=}N(2,6\text{-}Me_2C_6H_3))$ complex was attempted (Scheme 4.4, *a*). Initially a sample of $CrCl_2$ in THF was heated at reflux for 16 hours, in order to generate $CrCl_2(THF)_2$.[20] Subsequently, after all of the solid $CrCl_2$ had dissolved it was assumed that complete conversion of $CrCl_2$ to $CrCl_2(THF)_2$ had occurred, so a solution of ligand **3.10** was then added to the reaction, and the resulting mixture was heated at reflux. After 2 hours the solution was concentrated under vacuum and, after standing at room temperature for 72 hours, purple crystals formed. Analysis by X-ray crystallography showed that the crystals comprised of $CrCl_3(THF)_3$. The crystallisation process was repeated, again yielding crystals of $CrCl_3(THF)_3$. The formation of $CrCl_3(THF)_3$ suggests that the Cr(II) starting material must have been oxidised during the reaction to Cr(III). This oxidation may be explained by the disproportionation of Cr(II) in the reaction, yielding a dimer of $Cr(\mu\text{-}Cl)_2$(**3.10**)$_4$ and two equivalents of $CrCl_3(THF)_3$ (Scheme 4.4, *b*). Unfortunately, despite a number of attempts no products other than $CrCl_3(THF)_3$ could be isolated. As a result, the true course of the reaction remains unknown. Due to the difficulties encountered in isolating the products of the reaction between $CrCl_2$ and ligand **3.10** no further investigations were carried out regarding the complexation of iminophosphines with Cr(II) species.

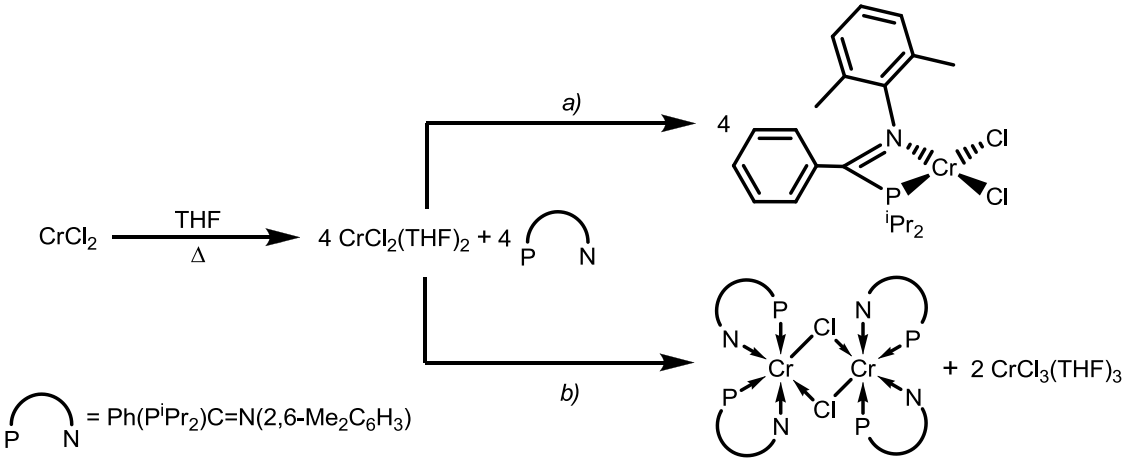

Scheme 4.4: Potential reactions of $CrCl_2$ with $Ph(P^iPr_2)C{=}N(2,6\text{-}Me_2C_6H_3)$ (**3.10**).

4.4 Coordination of Iminophosphines with Cr(0)

It has been shown previously that Cr(0)-ligand complexes are useful to probe both the electronic and structural characteristics of the ligand in question (Section 4.1). Working with Cr(0) is significantly easier than Cr(III) complexes, due to Cr(0) being diamagnetic, facilitating the use of NMR spectroscopy. Furthermore, the synthesis of $Cr(CO)_{(6-n)}(\kappa^n\text{-L})$ (L = ligand, denticity *n*) complexes allows the CO stretching frequencies to be measured by IR spectroscopy, giving both structural (based on the symmetry of the complex) and electronic information about the complex, and hence the ligand.[4] The synthesis of Cr(0)-ligand complexes is of particular interest with regard to *tri*- and *tetra*-merisation systems, as these are known catalyst precursors. A number of studies have also shown that $Cr(CO)_4(PNP)$ complexes can be oxidised to $[Cr(CO)_4(PNP)]^+$ species, which can in turn be used as ethylene *tri*- and *tetra*-merisation precursors, in the presence of TEA.[5,7] In order to use the above methods to explore the properties of iminophosphine ligands, studies were carried out to synthesise Cr(0) complexes of the ligands **3.9** and **3.10**.

4.4.1 Synthesis of $Cr(CO)_4(Ph(P^iPr_2)C{=}N(2,6\text{-}^iPr_2C_6H_3))$ (4.7) and $Cr(CO)_5(Ph(P^iPr_2)C{=}N(2,6\text{-}^iPr_2C_6H_3))$ (4.8)

The complexes $Cr(CO)_5(Ph(P^iPr_2)C{=}N(2,6\text{-}^iPr_2C_6H_3))$ (**4.8**) and $Cr(CO)_4(Ph(P^iPr_2)C{=}N(2,6\text{-}^iPr_2C_6H_3))$ (**4.7**) were both synthesised in the same reaction, using a modified version of the method reported by Krishnamurthy *et al.*[21] A solution of the starting materials, $Cr(CO)_6$ and ligand **3.9**, was heated at reflux in toluene for 72 hours, resulting in the formation of a deep purple coloured solution (Scheme 4.5). Analysis of the crude reaction mixture by ^{31}P NMR spectroscopy revealed that two products had formed; these were further analysed and found to be the mono- and bi-dentate Cr(0)-iminophosphine complexes, **4.8** and **4.7**, respectively. The solvent was removed from the reaction mixture to yield the crude product as a purple residue. Hexane was added to the residue, forming a yellow solution and leaving a purple solid, which were subsequently separated by filtration.

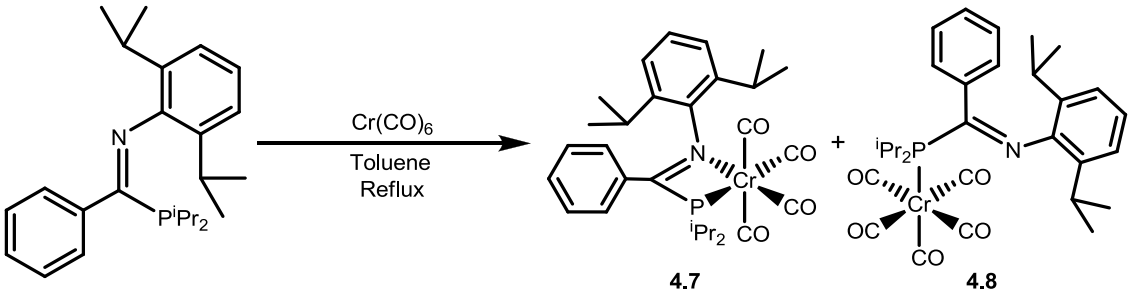

Scheme 4.5: Synthesis of **4.7** and **4.8** from iminophosphine **3.9** and $Cr(CO)_6$ in toluene

4.4.1.1 Characterisation of $Cr(CO)_4(Ph(P^iPr_2)C=N(2,6\text{-}^iPr_2C_6H_3))$ (4.7)

A concentrated DCM solution of the purple solid was layered with hexane and stored at 0 °C for 16 hours, during which time purple crystals, suitable for X-ray diffraction, formed. The crystals of complex **4.7** were isolated in a low yield (8 %). The product was successfully characterised by NMR spectroscopy and X-ray crystallography. However, despite a number of attempts, both elemental analyses and mass spectrometric analysis yielded inconclusive results. The bidentate coordination of the iminophosphine displayed by complex **4.7** is interesting when compared to the $Cr(CO)_5$(PNN) (**2.4**) complex isolated (Section 2.3.1) which adopted a monodentate coordination mode. It is suggested that this difference is due to the superior donor properties of the imine group, relative to that of the tertiary amine donor in the PNN ligand.

The molecular structure of **4.7** determined by X-ray crystallographic analysis is shown in Figure 4.5, with complex **4.7** being found to adopt a distorted octahedral geometry about Cr, with the iminophosphine ligand binding to the chromium centre in a bidentate fashion. The variation in the Cr-C bond distances is consistent with the relative *trans* influences of the P- and N-donor components of the ligand **3.9** (Table 4.4). The Cr-C bond *trans* to the imine donor is the shortest of the four Cr-C bonds, due to the weak *trans* influence of the imine, while the Cr-C bond *trans* to the phosphine is shorter than the Cr-C(2) and Cr-C(4) bond lengths, due to the phosphine *trans* influence.[11]

The molecular structure of the bidentate complex **4.7** displays the ligand bound to Cr with a bite angle very similar to that found for complex **4.2** ($CrCl_3(THF)(Ph(PPh_2)C=N(2\text{-}MeC_6H_4))$) (65.79(2) ° and 65.42(5) °, respectively). This similarity is suggestive of $Cr(CO)_4$(PCN) complexes being good models for iminophosphine binding to both Cr(0) and Cr(III) centres.

It is also important that the bite angle of any Cr-iminophosphine complexes is similar to that of Cr(PNP) complexes. A strong link between the bite angle of PNP ligands and the trimerisation activity of the resulting catalytic system has been previously reported, with chelate rings displaying tight bite angles being the best catalytic precursors for ethylene

tetramerisation.[9] The P-C-N angle measured for complex **4.7** (~100 °) is very similar to that measured for $Cr(CO)_4(Ph_2PN(^iPr)PPh_2)$ reported by Wass *et al.* (~100 °),[5] indicating that the ligand **3.9** nicely mimics the tight bite angle displayed by PNP ligands.

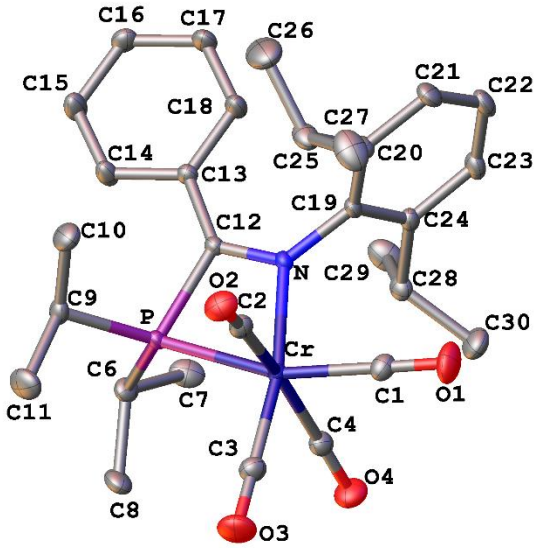

Figure 4.5: ORTEP representation of the molecular structure determined for **4.7**, with thermal ellipsoids set at 50 % probability level.

$Cr(CO)_4(Ph(P^iPr_2)C=N(2,6\text{-}^iPr_2C_6H_3))$ (4.7)		
Bond Lengths (Å)	Cr – P	2.3829(3)
	Cr – N	2.1425(9)
	Cr – C(1)	1.854(1)
	Cr – C(2)	1.893(1)
	Cr – C(3)	1.847(1)
	Cr – C(4)	1.895(1)
Bond Angles (°)	N – Cr – P	65.79(2)
	P – C(12) – N	100.48(6)

Table 4.4: Selected bond lengths (Å) and angles (°) determined for **4.7**.

Analysis of complex **4.7** by ^{13}C NMR spectroscopy reveals three doublet resonances in the carbonyl region of the spectrum (δ = 222 – 229 ppm). This is indicative of the three carbonyl environments expected for a $Cr(CO)_4(\kappa^2\text{-P,N})$ complex, confirming the bidentate coordination mode of complex **4.7** as that determined by X-ray crystallography. The ^{31}P NMR spectrum measured for complex **4.7** displays a major resonance at δ = 63.2 ppm, attributed to the product, but also a minor signal (~ 1% of the total phosphorus by integration of the spectrum) at δ = 83.1

ppm. The ^{31}P chemical shift of this minor product matches that found for the related κ^1-monodentate complex $Cr(CO)_5[Ph(P^iPr_2)C=N(2,6\text{-}^iPr_2C_6H_3)]$ (**4.8**), suggesting that the bidentate complex had spontaneously converted to its monodentate counterpart. In order to probe this change in more detail an external PPh_3 standard was added to the Young's NMR tube containing the sample of complex **4.7**, in order to quantify the conversion of the bidentate to the monodentate complex. The sample of complex **4.7** in $CDCl_3$ was left to stand for one week, after which 39 % of the starting complex had converted to the monodentate complex **4.8**, with no overall loss of phosphorus (relative to the PPh_3 standard). This κ^2- to κ^1- transformation requires the presence of additional CO, and it is hypothesised that the CO may be provided by trace amounts of the starting material $Cr(CO)_6$ present in the sample. This hypothesis was tested by the addition of excess $Cr(CO)_6$ to the previous NMR sample of complex **4.7,** followed by sonication of the reaction mixture, resulting in the sample changing colour from purple to yellow. ^{31}P NMR spectroscopic analysis of the NMR-scale reaction displayed complete conversion of the bidentate complex **4.7** to the monodentate counterpart, **4.8**, implying that residual $Cr(CO)_6$ may indeed be the cause of the decomposition of **4.7** to **4.8**.

IR spectroscopy was carried out to aid the characterisation of complex **4.7** (Table 4.5). The IR spectrum measured for the bidentate complex displays four carbonyl absorptions as expected for a complex with C_1 symmetry, confirming the solution state structure as matching the solid state structure determined by X-ray crystallography.

Complex	**ν C≡O[a] / cm^{-1}**			
4.7	1999	1900	1874	1859
[a] Spectrum obtained in DCM solution				

Table 4.5: The carbonyl stretching frequencies measured for complex **4.7**.

4.4.1.2 Characterisation of $Cr(CO)_5(Ph(P^iPr_2)C=N(2,6\text{-}^iPr_2C_6H_3))$ (4.8)

The yellow hexane solution isolated from the reaction of ligand **3.9** with $Cr(CO)_6$ was warmed and concentrated, before being left to cool and stand at room temperature for 16 hours. This led to the formation of yellow crystals of complex **4.8**, which were isolated to yield the compound in a reasonable yield (40 %). The complex was fully characterised by NMR spectroscopy, mass spectrometry and elemental analysis.

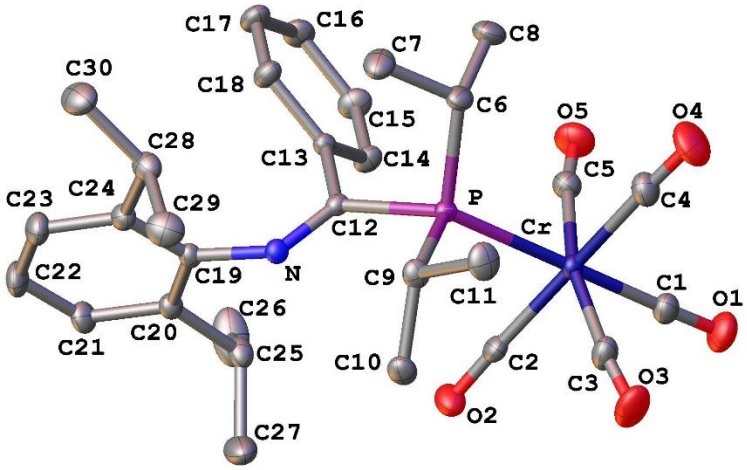

Figure 4.6: ORTEP representation of the molecular structure determined for **4.8**, with thermal ellipsoids set at 50 % level.

The crystals grown of complex **4.8** ($Cr(CO)_5(Ph(P^iPr_2)C{=}N(2,6\text{-}^iPr_2C_6H_3))$) were of suitable quality for X-ray crystallographic analysis, and the molecular structure determined (Figure 4.6) displays the iminophosphine ligand bound to the chromium centre in a monodentate coordination mode, with the complex adopting a distorted octahedral structure about Cr. Selected bond lengths (Å) and angles (°) measured for **4.8** are given in Table 4.6. Upon inspection of the Cr-C bond lengths the *trans* influence of the phosphine can be seen, with the Cr-C bond *trans* to the phosphine donor having the shortest of the five Cr-C bonds.

$Cr(CO)_5(Ph(P^iPr_2)C{=}N(2,6\text{-}^iPr_2C_6H_3))$ (4.8)		
Bond Lengths (Å)	Cr – P	2.4431(4)
	Cr – C(1)	1.864(1)
	Cr – C(2)	1.907(1)
	Cr – C(3)	1.900(1)
	Cr – C(4)	1.895(1)
	Cr – C(5)	1.904(1)
Bond Angles (°)	P – C(12) – N	115.80(7)

Table 4.6: Selected bond lengths (Å) and angles (°) determined for **4.8**

IR spectroscopy was also used to characterise complex **4.8** (Table 4.7). This revealed three absorption signals in the carbonyl region of the IR spectrum, as is expected for a complex with C_{4v} symmetry such as the monodentate complex $Cr(CO)_5(\kappa^1\text{-}Ph(P^iPr_2)C{=}N(2,6\text{-}^iPr_2C_6H_3))$ (**4.8**). This therefore supports the previous data gathered for compound **4.8** existing as a monodentate complex.

Complex	ν C≡O[a] / cm^{-1}		
4.7	2061	1980	1935
[a] Spectrum obtained in DCM solution			

Table 4.7: The carbonyl stretching frequencies measured for complex **4.8**.

Consistent with the X-ray structure, the ^{13}C NMR spectrum of complex **4.8** displays two resonances in the carbonyl region (δ = 221.3 (d), 217.8 (d) ppm), both of which are doublets, representative of two carbonyl environments (*trans*-P-Cr-*C*O and *trans*-O*C*-Cr-*C*O). These data compare well with those determined in the ^{13}C NMR spectra of the monodentate Cr(CO)$_5$(PNE) complexes reported in Chapter 2 (*e.g.* Cr(CO)$_5$(PNN) (**2.4**) δ_{CO} = 221.3 (d), 216.9 (d) ppm).

During the course of the reaction between Cr(CO)$_6$ and ligand **3.9** it was observed that the ratio of mono-:bi-dentate products (**4.8**:**4.7**) in the reaction solution did not change. It is apparent that the monodentate product, **4.8**, is preferentially formed in the reaction, with the products forming in a 2:1 ratio of mono-:bi-dentate species (as measured by integration of the ^{31}P[^{1}H] NMR spectrum). Hence, it is suggested that the monodentate complex **4.8** is the more thermodynamically stable product of the two complexes.

4.4.2 Synthesis of Cr(CO)$_4$(Ph(P^{i}Pr$_2$)C=N(2,6-Me$_2$C$_6$H$_3$)) (4.9) and Cr(CO)$_5$(Ph(P^{i}Pr$_2$)C=N(2,6-Me$_2$C$_6$H$_3$)) (4.10)

The reaction between Cr(CO)$_6$ and ligand **3.10** was carried out using the same method as reported in Section 4.4.1. The reaction mixture was heated at reflux for 24 hours, during which time the solution turned purple (Scheme 4.6). Analysis of the resulting solution by ^{31}P NMR spectroscopy displayed two new signals (2:1 ratio), indicative of the formation of two products. The crude product mixture was isolated as a purple residue, the majority of which was dissolved in hot hexane, and the resulting solution was isolated by filtration (Solution A). The residual purple solid was subsequently dissolved in a minimum amount of hot hexane, yielding a second solution of the reaction product (Solution B). From these two solutions the complexes **4.9** and **4.10** were isolated.

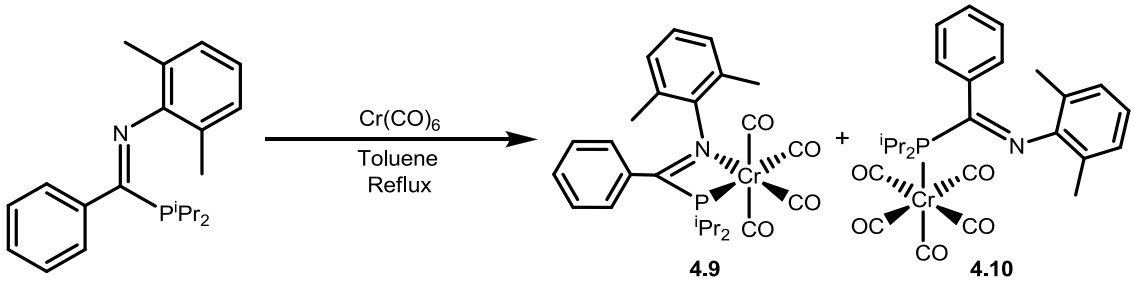

Scheme 4.6: Synthesis of **4.9** and **4.10** by heating iminophosphine **3.10** with Cr(CO)$_6$ at reflux in toluene

4.4.2.1 Characterisation of $Cr(CO)_4(Ph(P^iPr_2)C=N(2,6\text{-}Me_2C_6H_3))$ (4.9)

Upon cooling of the hot hexane solutions A and B, purple crystals formed from both mixtures and, in each case, the crystals were isolated to yield **4.9** as a purple crystalline solid in a poor yield (6 %). The purple crystals grown were of suitable quality for analysis by X-ray crystallography, allowing the molecular structure of **4.9** to be determined (Figure 4.7). Analysis of **4.9** by NMR spectroscopy confirmed the structure as being $Cr(CO)_4(Ph(P^iPr_2)C=N(2,6\text{-}Me_2C_6H_3))$. Unfortunately, due to the air-sensitive nature of the complex mass spectrometry and elemental analysis yielded inconclusive results. Inspection of the ^{13}C NMR spectrum of complex **4.9** shows three carbonyl signals, indicating three carbonyl environments, as expected for the bidentate $Cr(CO)_4(Ph(P^iPr_2)C=N(2,6\text{-}Me_2C_6H_3))$ complex.

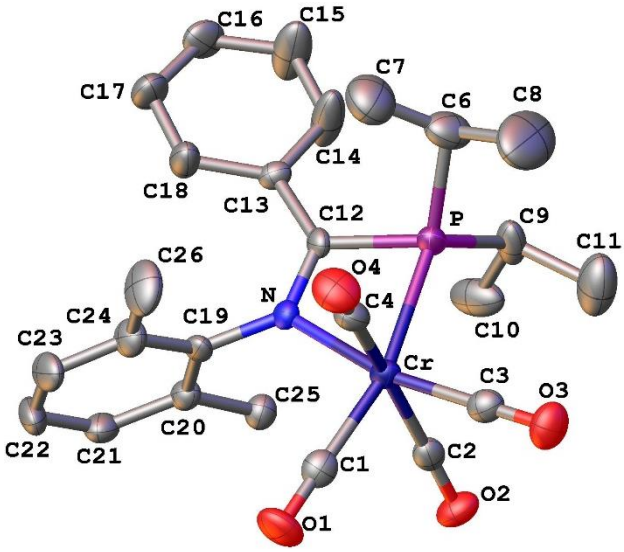

Figure 4.7: ORTEP representation of the molecular structure determined for **4.9**, with thermal ellipsoids set at 50 % level.

$Cr(CO)_4(Ph(P^iPr_2)C=N(2,6\text{-}Me_2C_6H_3))$ (4.9)		
Bond Lengths (Å)	Cr – P	2.384(2)
	Cr – N	2.161(5)
	Cr – C(1)	1.851(7)
	Cr – C(2)	1.886(7)
	Cr – C(3)	1.840(7)
	Cr – C(4)	1.891(7)
Bond Angles (°)	N – Cr – P	65.7(1)
	P – C(12) – N	103.0(4)

Table 4.8: Selected bond lengths (Å) and angles (°) measured for complex **4.9**.

The molecular structure determined for **4.9** displays the iminophosphine ligand bound to chromium in a bidentate fashion, consistent with the previous spectroscopic analyses. A selection of relevant bond lengths (Å) and angles (°) is displayed in Table 4.8. The P-C(12)-N bite angle is measured to be 103.0(4) °, comparable to that found for **4.7** as well as to the values reported for $Cr(CO)_4$(PNP) complexes by Wass *et al*. (~100 °).[5] The bite angle is also very similar to that found for the $CrCl_3$(THF)(PCN) complexes reported in Section 4.2 (~104 °), suggesting that the $Cr(CO)_4$(PCN) complexes are good structural models for investigating ethylene oligomerisation precursor Cr(III)-iminophosphine complexes. The differing *trans* influences of the phosphine and imine groups is apparent in the Cr-C bond lengths, matching the expected sequence ($Cr\text{-}C_{trans\text{-}CO}$ > $Cr\text{-}C_{trans\text{-}P}$ > $Cr\text{-}C_{trans\text{-}N}$).

Interestingly, it was found that when a solution of complex **4.9** in dry $CDCl_3$ was left in a sealed tube to stand for 48 hours under an N_2 atmosphere, a small amount (~10 %, measured by ^{31}P NMR spectroscopy) of the product was seen to convert to the monodentate complex **4.10** ($Cr(CO)_5(Ph(P^iPr_2)C{=}N(2,6\text{-}Me_2C_6H_3))$) by ^{31}P NMR spectroscopic analysis (Scheme 4.7). Upon analysis of the $CDCl_3$ solution of **4.9** by ^1H NMR spectroscopy, a series of signals matching the complex **4.10** were observed (Figure 4.8, α-δ), demonstrating that the bidentate complex is capable of converting to its monodentate analogue, **4.10**. This phenomenon will be further investigated in Section 4.4.5. It is assumed the mechanism of this conversion is the same as that previously observed and investigated for **4.7**, namely the decomposition of small amounts of unreacted $Cr(CO)_6$ releasing CO, which subsequently reacts with the bidentate complex to yield its monodentate counterpart (Section 4.4.1.1).

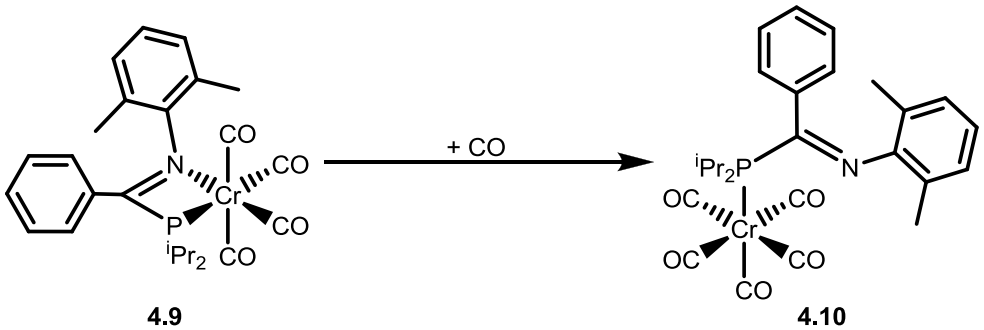

4.9 **4.10**

Scheme 4.7: Conversion of the bidentate complex **4.9** to the monodentate **4.10** observed by NMR spectroscopy.

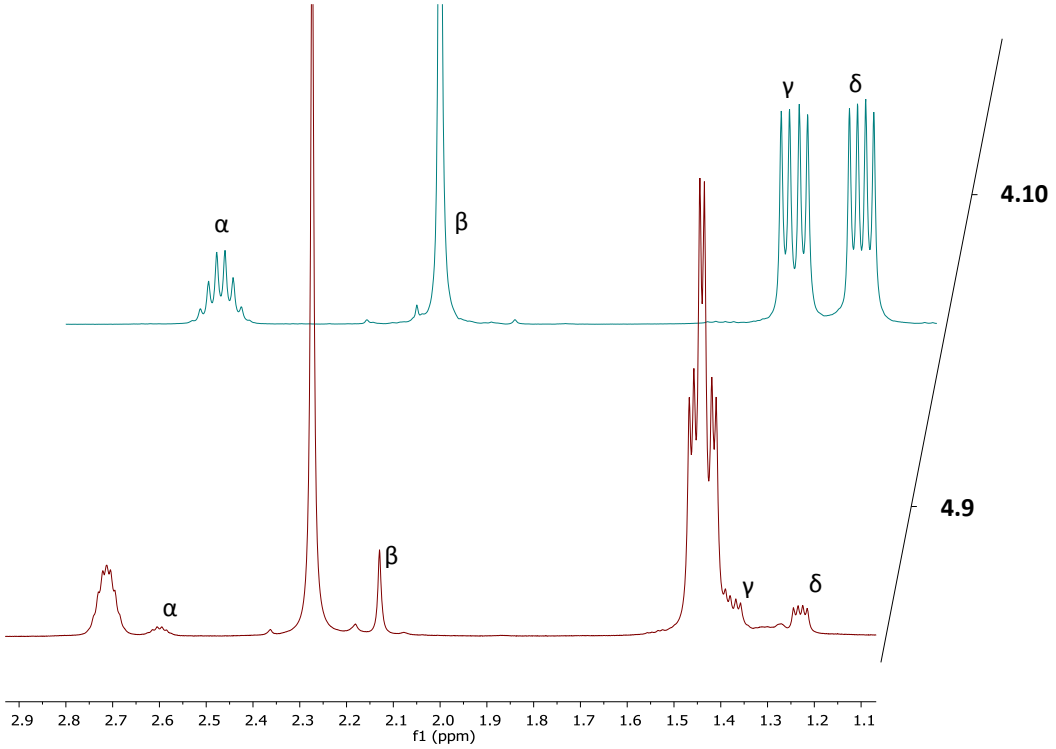

Figure 4.8: An excerpt from the ^{1}H NMR spectra of **4.10** (top) and **4.9** (bottom) ($CDCl_3$, 700 MHz).

IR spectroscopy was used to measure the carbonyl stretching frequencies of complex **4.9** (Table 4.9). The IR spectrum of complex **4.9** displays four carbonyl absorption bands, corresponding to the complex exhibiting a bidentate $Cr(CO)_4(\kappa^2\text{-}Ph(P^iPr_2)C{=}N(2,6\text{-}Me_2C_6H_3))$ structure. The C-O stretching frequencies are similar to those measured by Wass *et al.* for their $Cr(CO)_4(k^2\text{-PNP})$ complexes indicating that the iminophosphine ligand has similar coordinative properties to the PNP ligands reported by Wass.[5]

Complex	**ν C≡O[a] / cm^{-1}**			
4.9	2000	1899	1874	1858
[a] Spectrum obtained in DCM solution				

Table 4.9: The carbonyl stretching frequencies measured for complex **4.9**.

4.4.2.2 Characterisation of $Cr(CO)_5(Ph(P^iPr_2)C{=}N(2,6\text{-}Me_2C_6H_3))$ (4.10)

Of the two hexane solutions (A and B, Section 4.4.2) isolated from the reaction of $Cr(CO)_6$ with $Ph(P^iPr_2)C{=}N(2,6\text{-}Me_2C_6H_3)$ (ligand **3.10**), solution B was found to contain $Cr(CO)_5(Ph(P^iPr_2)C{=}N(2,6\text{-}Me_2C_6H_3))$ (**4.10**). Solution B was concentrated under vacuum and warmed, before being left to slowly cool. After 16 hours large yellow crystals formed, which were isolated to yield the other product of the reaction between $Cr(CO)_6$ and the ligand **3.10**, complex **4.10**, in a reasonable yield (43 %). The crystals grown were suitable for X-ray crystallographic analysis, allowing the molecular structure to be determined (Figure 4.9). The identity of the product was confirmed by NMR spectroscopy, mass spectrometry and elemental

analysis. Analysis of **4.10** by ^{13}C NMR spectroscopy reveals two characteristic resonances in the carbonyl region (δ = 221.5, 218.0 ppm), matching the two expected carbonyl environments for a $Cr(CO)_5(PCN)$ complex. Both the ^{1}H and ^{13}C NMR spectra were fully assigned with the aid of HSQC and HMBC NMR spectroscopic experiments. IR spectroscopy was carried out to reveal the complex **4.10** exhibits three carbonyl stretching frequencies (Table 4.10), indicating a monodentate complex with C_{4v} symmetry, as previously suggested by ^{13}C NMR spectroscopy.

Complex	**ν C≡O[a] / cm^{-1}**		
4.7	2060	1980	1934
[a] Spectrum obtained in DCM solution			

Table 4.10: The carbonyl stretching frequencies measured for complex **4.10**.

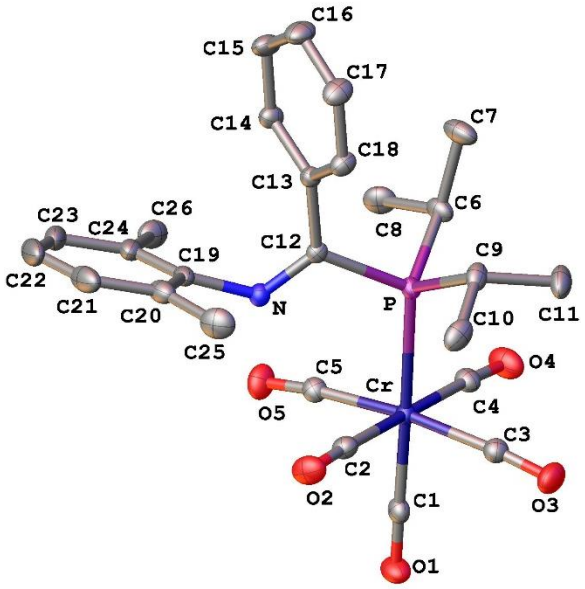

Figure 4.9: ORTEP representation of the molecular structure determined for **4.10**, with thermal ellipsoids set at 50 % level.

$Cr(CO)_5(Ph(P^iPr_2)C=N(2,6\text{-}Me_2C_6H_3))$ (4.10)		
Bond Lengths (Å)	Cr – P	2.4102(4)
	Cr – C(1)	1.863(1)
	Cr – C(2)	1.910(1)
	Cr – C(3)	1.888(1)
	Cr – C(4)	1.894(1)
	Cr – C(5)	1.901(1)
Bond Angles (°)	P – C(12) – N	114.27(8)

Table 4.11: Selected bond lengths (Å) and angles (°) for **4.10**.

Figure 4.9 shows the structure of **4.10** in which the chromium adopts a distorted octahedral configuration, with the iminophosphine ligand bound only through the phosphine donor group. The Cr-C(1) bond length in **4.10** is shorter than the other Cr-C bonds, due to the *trans*-influence of the phosphine donor *trans* to the Cr-C(1) bond. The P-Cr bond length, and P-C(12)-N bond angle are both comparable to those determined for the monodentate complex **4.8** previously reported (Section 4.4.1.2).

4.4.3 Analysis of the imine bond in $Cr(CO)_{6-n}(\kappa^n\text{-}Ph(P^iPr_2)C{=}N(R_2C_6H_3)$ (R = ^{i}Pr, Me) complexes

In this investigation a series of four $Cr(CO)_{6-n}(\kappa^n$-PCN) complexes have been synthesised and isolated, displaying both κ^1-mono- and κ^2-bi-dentate coordination modes. This allows for the rationalisation of the effect of imine-metal bonding on the imine bond, by comparison of the C=N bond properties in the mono- and bi-dentate complexes. The bonding between imine nitrogens and metals can be thought of as having two components: *a)* σ-donation from the nitrogen lone pair to the metal (Figure 4.10 *a*) and *b)* π-acceptance of electrons from metal d-orbitals into the imine π* anti-bonding orbitals (Figure 4.10 *b*). The π-acceptor ability of the imine is dependent upon the type of imine in question. For unconjugated imines it is thought that the electron acceptance of the π* anti-bonding orbitals is not significant, based on observations of ligand field strengths for first row transition metal-imine complexes.[22] However, if the imine is part of a larger conjugated system (*e.g.* the iminophosphine ligands in this investigation) the π-back donation is significant, and is thought to be the basis of many metal-to-ligand charge transfer complexes.[23]

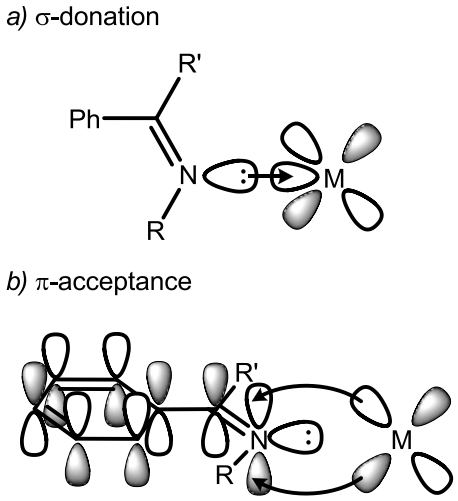

Figure 4.10: A depiction of the bonding between a conjugated imine and a metal.

It is clear by comparison of the mono- and bi-dentate complexes of iminophosphine ligands that the imine group is a π-acceptor (Table 4.12). Upon formation of the Cr-N bond (*i.e.*

conversion of a mono- to bi-dentate Cr(PCN) complex) the C=N imine bond is observed to weaken, due to a lowering of the IR bond stretching frequency, and a lengthening of the C=N bond. It is assumed that this change is due to donation of electrons from chromium into the imine π* anti-bonding orbitals.

Complex	Formula	ν C=N (cm^{-1})[a]	^{13}C δ *C*=N (ppm)[b]	C=N Bond Length (Å)
4.8	$Cr(CO)_5(\kappa^1\text{-}Ph(P^iPr_2)C{=}N(^iPr_2C_6H_3))$	1584	175.6	1.277(1)
4.7	$Cr(CO)_4(\kappa^2\text{-}Ph(P^iPr_2)C{=}N(^iPr_2C_6H_3))$	1532	185.0	1.305(1)
4.10	$Cr(CO)_5(\kappa^1\text{-}Ph(P^iPr_2)C{=}N(Me_2C_6H_3))$	1587	176.0	1.277(1)
4.9	$Cr(CO)_4(\kappa^2\text{-}Ph(P^iPr_2)C{=}N(Me_2C_6H_3))$	1536	184.9	1.291(8)
[a] Measured in DCM solution [b] 176 MHz, $CDCl_3$				

Table 4.12: Selected data for the imine bond in $Cr(CO)_{6-n}(\kappa^n\text{-}Ph(P^iPr_2)C{=}N(R_2C_6H_3)$ (R = ^{i}Pr, Me) complexes.

It has been previously mentioned that the bidentate $Cr(CO)^4(\kappa^2$-PCN) complexes isolated (**4.7, 4.9**) are both intensely purple coloured, compared to the pale yellow colour of their monodentate counterparts. It is suggested that this strong colour is due to charge transfer between the metal and the conjugated imine group, but further investigation is required to deduce the precise nature of this electronic transfer.

4.4.4 High-temperature reaction of $Cr(CO)_6$ and $Ph(P^iPr_2)C{=}N(2,6\text{-}^iPr_2C_6H_3)$ (3.9)

So far it has been observed that reactions between $Cr(CO)_6$ and iminophosphine ligands yield mixtures of mono- and bi-dentate products, with the monodentate products being strongly favoured (9:1 ratio). With a view to enhancing the formation of the bidentate products the same synthetic procedure was attempted at a higher temperature, something necessitating the use of a solvent with a higher boiling point. Hanton *et al.* have reported the use of diglyme as a solvent in the synthesis of their $Cr(CO)_4$(PNP) complexes, which allows the reaction to be heated to 162 °C, dramatically increasing the rate of reaction compared to when toluene is used.[7]

Consequently, a solution of ligand **3.9** and $Cr(CO)_6$ was heated at reflux in diglyme for 16 hours. The resulting crude reaction mixture was analysed by ^{31}P NMR spectroscopy, which displayed only one resonance with a chemical shift representative of the free ligand, **3.9**. It is suggested that the high reaction temperature and long reaction time used causes the decomposition of $Cr(CO)_6$, rather than the complexation reaction as desired.

4.4.5 Investigating the hemilability of $Cr(CO)_{(n-6)}(\kappa^n$-PCN) complexes

In the first report of PNP ligands being used as ligands in highly active ethylene trimerisation systems, it was suggested that the *ortho*-OMe groups present on the (Ar-*o*-OMe)$_2$PN(Me)P(Ar-*o*-OMe)$_2$ ligands were vital for the activity of the system due to the potential for the OMe groups to behave as pendant donors to the Cr centre.[24] This variable coordinative behaviour was further investigated by Bercaw and Labinger *et al*., who successfully proved that PNP$^{o\text{-OMe}}$ ligands were capable of adopting both bi- and *tri*-dentate coordination modes with chromium species (Scheme 4.8), something supporting the argument that variable coordination of the PNP ligand is important in the ethylene trimerisation catalytic cycle.[2] It is therefore of interest to investigate whether the iminophosphine ligands synthesised in this investigation may be capable of exhibiting similar hemi-labile behaviour.

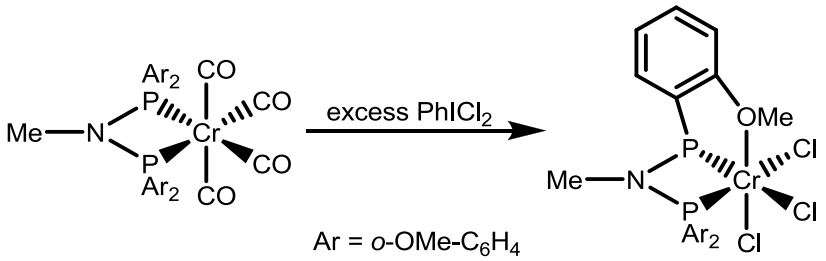

Scheme 4.8: Oxidation of a bidentate Cr^0(PNP) complex to a tridentate Cr^{III}(PNP) complex reported by Labinger and Bercaw *et al.*[2]

In Section 4.4.2.1 it has been mentioned that **4.7** is capable of converting to **4.8** (~10 %) when left to stand in solution, presumably due to small amounts of the starting complex decomposing to release the necessary CO. This conversion hints at the possibility that PCN ligands may exhibit hemilabile coordination properties with chromium in solution. In order to further investigate this possibilty an NMR-scale reaction was carried out between $Cr(CO)_6$ and **3.9** in diglyme. After heating at 140 °C for four hours, the solution turned yellow and subsequent analysis by ^{31}P NMR spectroscopy displayed a single resonance (δ = 83.1 ppm), corresponding to the formation of the monodentate complex **4.8**.

The process of heating and analysis of the reaction was repeated, but no further change in the reaction was observed by ^{31}P NMR spectroscopy. Unlike the previous reaction of $Cr(CO)_6$ with Ph(P^{i}Pr$_2$)C=N(2,6-^{i}Pr$_2$C$_6$H$_3$) (Section 4.4.1), no formation of the bidentate complex was observed. During the formation of complex **4.10** CO is released, creating a positive pressure of CO in the sealed NMR tube, and hindering the loss of further CO to yield the bidentate $Cr(CO)_4$(PCN) product.[25]

To aid the formation of the bidentate product, the NMR tube was placed under vacuum, to help remove CO from solution. The reaction was again heated to 140 °C for four hours, which

resulted in the solution turning purple. Analysis of the purple solution by ^{31}P NMR spectroscopy revealed the formation of a second product, with a chemical shift representative of the bidentate species, **4.7** (δ = 63.2 ppm). The tube was again placed under vacuum, and heated for four hours. Subsequently, the ^{31}P NMR spectrum showed the resonance associated with **4.7** had increased in intensity relative to the **4.8** signal, demonstrating that the removal of CO from the atmosphere favoured the production of the bidentate species.

For a ligand to be truly hemilabile, variable coordination must be reversible. To test whether the $Cr(CO)_{(n-6)}(\kappa^n$-PCN) system is reversible, the NMR tube containing the reaction mixture was placed under an atmosphere of CO. The tube was gently heated (50 °C), and the solution was observed to change from purple to yellow. Analysis of the reaction by ^{31}P NMR spectroscopy showed the disappearance of the bidentate complex **4.7**, leaving only a single resonance corresponding to **4.8** remaining. This successfully demonstrates the coordination of **3.9** with Cr(0) is reversible, and therefore iminophosphine **3.9** can be described as a hemilabile ligand with Cr(0) (Scheme 4.9).

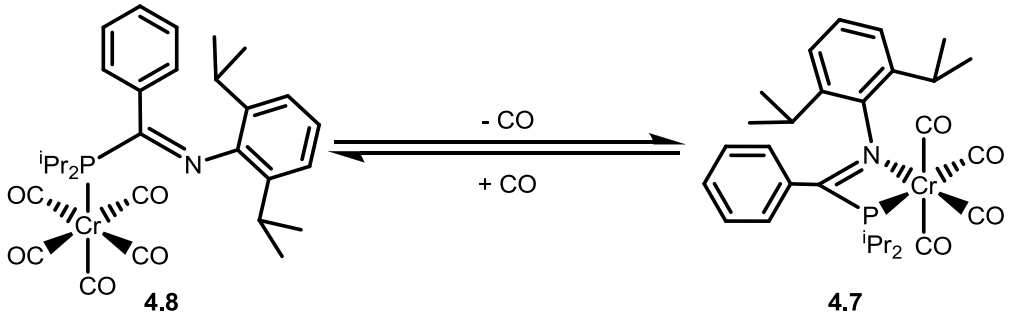

4.8 **4.7**

Scheme 4.9: The reversible reaction between **4.8** and **4.7**.

4.5 Summary and Conclusions

In this chapter the coordination chemistry of a series of iminophosphine ligands with chromium has been investigated. Coordination experiments have been carried out with Cr(0), Cr(II) and Cr(III) species and a range of chromium-iminophosphine complexes have been successfully isolated and characterised (Scheme 4.10).

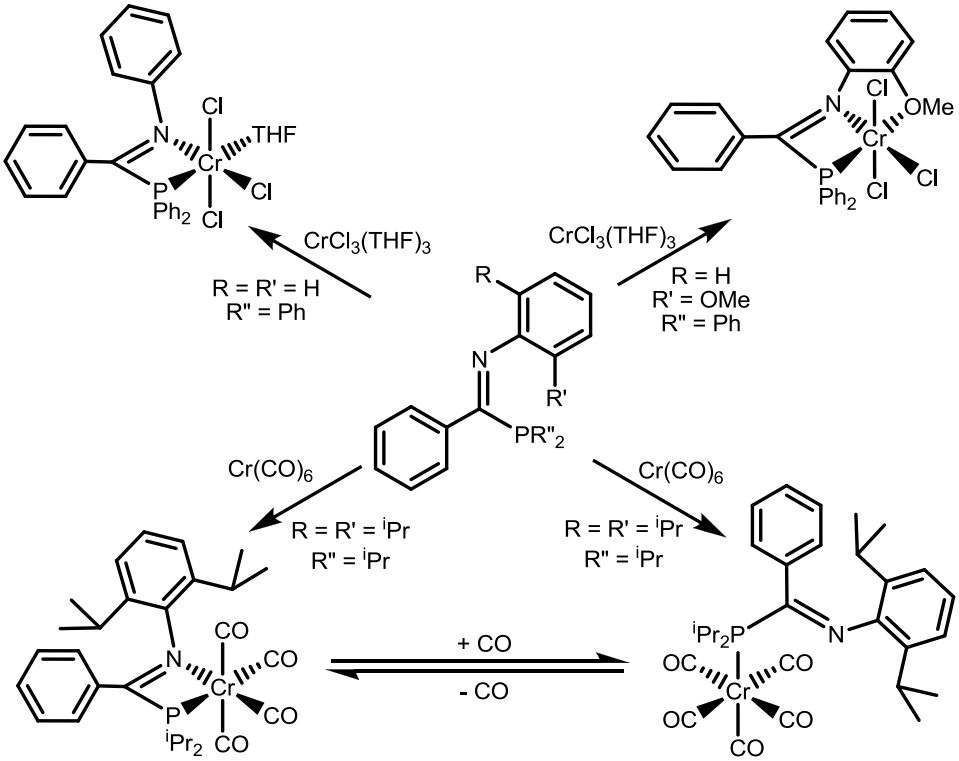

Scheme 4.10: Summary of Cr-PCN complexes isolated in Chapter 4.

A selection of Cr(III)-iminophosphine complexes were synthesised (**4.1**-**4.6**), using $CrCl_3(THF)_3$ as the chromium source. The complexes synthesised were all characterised by elemental analysis, and the magnetic susceptibilities of the complexes were measured using the Evans' NMR spectroscopic method. It was demonstrated that **4.1**, **4.2** and **4.4**-**4.6** exist as $CrCl_3(THF)(PCN)$ complexes with the iminophosphine ligands binding in a κ^2-P,N bidentate coordination mode to the chromium centre from the elemental composition of the products. This conclusion is supported by the molecular structures determined for **4.1** and **4.2**, which confirm the complexes adopting the structures described above. The molecular structures of **4.1** and **4.2** suggest that the Cr(III)-iminophosphine complexes have P-C-N bite angles comparable with Cr(III)-PNP complexes (103 – 106 °). Analysis of complex **4.3** is indicative of the iminophosphine ligand adopting a κ^3-P,N,O tridentate coordination mode, similar to structures of Cr(III)-PNP^{OMe} complexes reported by Bercaw and Labinger *et al*.[3] From these results it is apparent that structurally, Cr(III)-(PCN) complexes appear to be able to accurately mimic the

structure of Cr(III)-PNP complexes, and are a good candidate to replicate the activity and selectivity of PNP-based ethylene *tri*- and *tetra*-merisation systems.

Attempts were also made to synthesise Cr(II)-iminophosphine complexes. Upon reaction of $CrCl_2(THF)_2$ with **3.10** it was found that $CrCl_3(THF)_3$ crystallised out of the reaction mixture, demonstrating that the Cr(II) had been oxidised to Cr(III). It is suggested that this may be caused by disproportionation of Cr(II) to a Cr(I)-PCN dimer and $CrCl_3(THF)_3$, but no firm conclusions have been reached as to the identity of the other products of this reaction.

In order to further probe the reactivity of iminophosphines with chromium complexes, reactions between the ligands **3.9** and **3.10** and $Cr(CO)_6$ were carried out. From these two reactions four complexes (**4.7**-**4.10**) were isolated, the mono- and bi-dentate $Cr(CO)_5$(PCN) and $Cr(CO)_4$(PCN) complexes, respectively. All four of the complexes were characterised by X-ray crystallography and NMR spectroscopy. Complexes **4.8** and **4.10** were also characterised by mass spectrometry and elemental analyses. It was found that the monodentate complexes were favoured in the reactions between $Cr(CO)_6$ and iminophosphine ligands, giving a 9:1 ratio of mono- to bi-dentate product (measured by ^{31}P NMR spectroscopy). The structures of **4.7** and **4.10** both showed strong similarities with structures determined for $Cr(CO)_4$(PNP) complexes isolated by Wass *et al.*[5] Finally, it was successfully proven that **4.7** and **4.8** are capable of displaying hemilabile behaviour in solution, alternating between mono- and bi-dentate coordination modes upon the removal and addition of CO to the reaction.

4.6 References

(1) McGuinness, D. S. *Chem. Rev.* **2011**, *111*, 2321.
(2) Agapie, T.; Day, M. W.; Henling, L. M.; Labinger, J. A.; Bercaw, J. E. *Organometallics* **2006**, *25*, 2733.
(3) Agapie, T.; Schofer, S. J.; Labinger, J. A.; Bercaw, J. E. *J. Am. Chem. Soc.* **2004**, *126*, 1304.
(4) Tekkaya, A.; Özkar, S. *J. Organomet. Chem.* **1999**, *590*, 208.
(5) Bowen, L. E.; Haddow, M. F.; Orpen, A. G.; Wass, D. F. *Dalton Trans.* **2007**, 1160.
(6) Sydora, O. L.; Carney, M. J.; Small, B. L.; Hutshison, S.; Gee, J. C.; WO 2011/082192 (Chevron Phillips Chemical Company LP), December 29, 2011.
(7) Rucklidge, A. J.; McGuinness, D. S.; Tooze, R. P.; Slawin, A. M. Z.; Pelletier, J. D. A.; Hanton, M. J.; Webb, P. B. *Organometallics* **2007**, *26*, 2782.
(8) McGuinness, D. S.; Brown, D. B.; Tooze, R. P.; Hess, F. M.; Dixon, J. T.; Slawin, A. M. Z. *Organometallics* **2006**, *25*, 3605.
(9) Bollmann, A.; Blann, K.; Dixon, J. T.; Hess, F. M.; Killian, E.; Maumela, H.; McGuinness, D. S.; Morgan, D. H.; Neveling, A.; Otto, S.; Overett, M.; Slawin, A. M. Z.; Wasserscheid, P.; Kuhlmann, S. *J. Am. Chem. Soc.* **2004**, *126*, 14712.
(10) Yang, Y.; Gurnham, J.; Liu, B.; Duchateau, R.; Gambarotta, S.; Korobkov, I. *Organometallics* **2014**, *33*, 5749.
(11) Kauffman, G. B. *J. Chem. Educ.* **1977**, *54*, 86.
(12) McGuinness, D. S.; Overett, M.; Tooze, R. P.; Blann, K.; Dixon, J. T.; Slawin, A. M. Z. *Organometallics* **2007**, *26*, 1108.
(13) Overett, M. J.; Blann, K.; Bollmann, A.; de Villiers, R.; Dixon, J. T.; Killian, E.; Maumela, M. C.; Maumela, H.; McGuinness, D. S.; Morgan, D. H. *J. Mol. Catal. A: Chem.* **2008**, *283*, 114.
(14) Evans, D. F. *J. Chem. Soc.* **1959**, 2003.
(15) Loliger, J.; Scheffold, R. *J. Chem. Educ.* **1972**, *49*, 646.
(16) Schofer, S. J.; Day, M. W.; Henling, L. M.; Labinger, J. A.; Bercaw, J. E. *Organometallics* **2006**, *25*, 2743.
(17) Temple, C. N.; Gambarotta, S.; Korobkov, I.; Duchateau, R. *Organometallics* **2007**, *26*, 4598.
(18) Bhaduri, S.; Mukhopadhyay, S.; Kulkarni, S. A. *J. Organomet. Chem.* **2009**, *694*, 1297.
(19) Turki, T.; Guerfel, T.; Bouachir, F. *Inorg. Chem. Commun.* **2006**, *9*, 1023.
(20) Kohler, F. H.; Prossdorf, W. *Z. Naturforsch. B* **1977**, *32*, 1026.
(21) Balakrishna, M. S.; Prakasha, T. K.; Krishnamurthy, S. S.; Siriwardane, U.; Hosmane, N. S. *J. Organomet. Chem.* **1990**, *390*, 203.
(22) Curtis, N. F. *Coord. Chem. Rev.* **1968**, *3*, 3.
(23) Budzelaar, P. H. M.; de Bruin, B.; Gal, A. W.; Wieghardt, K.; van Lenthe, J. H. *Inorg. Chem.* **2001**, *40*, 4649.
(24) Carter, A.; Cohen, S. A.; Cooley, N. A.; Murphy, A.; Scutt, J.; Wass, D. F. *Chem. Commun.* **2002**, 858.
(25) Atkins, P.; de Paula, J. *Physical Chemistry*; OUP Oxford, 10th edition, **2014**, p 255.

Chapter 5:

The Effects of Iminophosphine Ligands in Selective Ethylene Oligomerisation Catalysis

5.1 Introduction

Since the discovery of the excellent activities and selectivities achieved by Cr-PNP-derived systems for selective ethylene *tri*- and *tetra*-merisation catalysis,[1] a huge variety of PNP ligand variants have been synthesised and tested in such reactions.[2] As well as PNP-based systems, a range of alternative selective catalytic oligomerisation processes have been reported in the patent literature by industry, from companies attempting to compete with the already commercialised *tri*- and *tetra*-merisation processes of Sasol[3] and Phillips[4,5] ethylene tetramerisation system. A brief summary of some of these patented processes is given in Table 5.1.

System	Catalyst precursor	Activity (mol/mol TM h^{-1})*	Polymer (wt %)	Liquid fraction selectivity to 1-hexene (wt %)
Sabic Linde [6] Cr-PNPN(H)	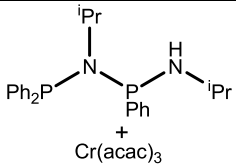	83,300	0.3	93.9
Sasol [3] Cr-PNP(*ortho*-alkyl-Ph)	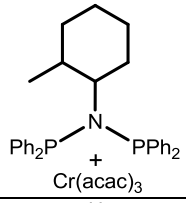	> 10,000,000	1 – 2	93
Sasol [7] Cr-SNS	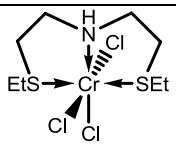	255,000	< 1	98
Phillips [4,5] Cr-pyrrole	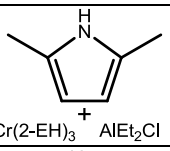	290,000	1.2	93
Mitsubishi-Phillips [4,5] Cr-pyrrole	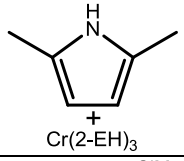	1,750,000	0.04	95
DPI [8] Ti-Arene^Bz	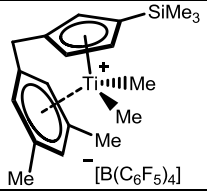	239,000	0.4	98
Tosoh [4] Cr-maleimide	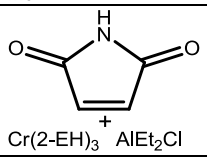	516,000	1.5	81
Mitsui [9] Ti-Phen-Im	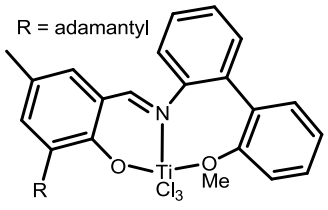	12,000,000	0.4	92

Table 5.1: Activities and extent of polymer formation for selected published ethylene *tri-* and *tetra-*merisation systems.

* All activities calculated based upon moles of ethylene converted to oligomer and polymer

Recently, new ligands have been developed for use in ethylene oligomerisation processes based around mixed donor bidentate P,N scaffolds, in attempts to discover alternative systems that are not covered by the wealth of patent literature surrounding PNP-based initiators (see Section 1.2.1.2). One of the most successful examples of P,N ligands in such applications was published by workers from Chevron Phillips, using a novel class of phosphinoamidine compound (Figure 5.1, *a*).[10] It was found that the influence of the phosphinoamidine ligands on ethylene oligomerisation systems could be tuned and that the 1-hexene to 1-octene ratio of the system could be changed from 140 to 1.5 (C_6:C_8) purely by altering the steric properties of the P,N framework. It was also shown that the presence of a pendant donor N group (giving rise to a κ^3-P,N,N coordination mode) entirely switched off the catalytic activity of the ethylene oligomerisation system, instead giving a low activity polymerisation process (Figure 5.2).

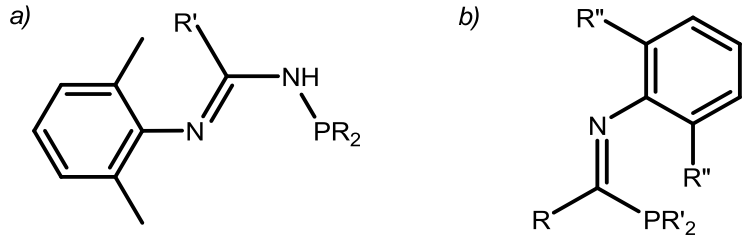

Figure 5.1: *a)* The phosphinoamidine scaffold developed by Chevron Phillips for use in ethylene *tri-* and *tetra*-merisation systems.[10] *b)* The iminophosphine ligands scaffold synthesised in this thesis.*

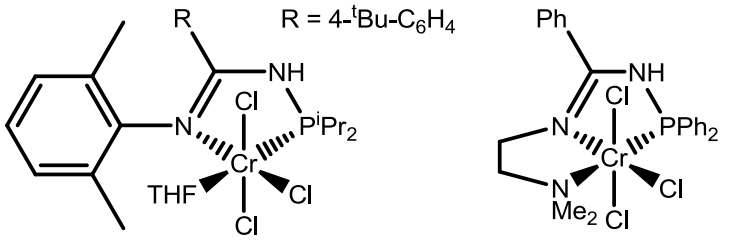

Activity = 1,052,000 g/g Cr h^{-1}
1-Hexene = 93.6 wt %
1-Octene = 0.9 wt %
Polyethylene = trace

Activity = 0 g/g Cr h^{-1}
1-Hexene = 0 wt %
1-Octene = 0 wt %
Polyethylene = 1.2 g

Figure 5.2: Bidentate vs. tridentate phosphinoamidine based ethylene trimerisation systems reported by Sydora *et al.*[10]

The iminophosphine ligands synthesised in this thesis (Figure 5.1, *b*) share structural similarities with the phosphinoamidine compounds developed by Chevron Phillips (Figure 5.1, *a*), in that both contain phosphine and imine donor groups that are capable of binding to a Cr(III) centre in a bidentate κ^2-P,N coordination mode. The PCN compounds reported in this thesis have also been shown to mimic the coordination of PNP ligands with Cr(III), namely adopting

* The iminophosphines synthesised may be able to adopt both *E* and *Z* configurations around the imine bond, a phenomena which has been previously discussed in Section 3.4. For simplicity, all iminophosphines will be drawn as the *Z* isomer in this chapter.

four-membered chelate rings with tight bite angles comparable to the previously reported Cr^{III}(PNP) complexes (Section 4.2). These similarities suggest that iminophosphines could yield highly active Cr-PCN based ethylene *tri*- and *tetra*-merisation systems.

5.1.1 Catalyst testing conditions

This chapter reports and discusses the catalytic testing data that has been gathered on the use of iminophosphine compounds as ligands in selective chromium-mediated ethylene oligomerisation catalysis. The reaction conditions used for primary screening of the PCN ligands in these oligomerisation systems were based upon those widely used in the field of ethylene *tri*- and *tetra*-merisation catalysis, namely using chlorobenzene as a solvent, with 500 equivalents of MMAO-3A as an activator (Scheme 5.1).[11] These conditions were subsequently optimised with the most promising ligand-metal combinations, with the results of these latter tests being discussed in Section 5.5. The catalytic testing protocol used for all the testing in this thesis is described in detail below.

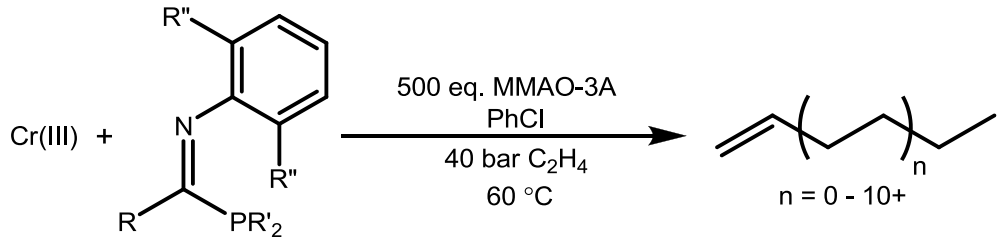

Scheme 5.1: Ethylene oligomerisation catalysis conditions used in the screening of iminophosphine ligands in this thesis.

All of the catalyst testing carried out was undertaken in collaboration with Dr M. J. Hanton and Dr D. M. Smith at Sasol Technology UK. Unless otherwise stated, the catalytic tests were carried out using a semi-batch process in a 250 mL steel autoclave. The autoclave was filled with 70 mL solvent before being charged with the catalyst precursors. Four methods of generating the active catalyst have been studied in this investigation:

- **Method A**: The autoclave was charged with the relevant chromium and ligand starting materials, before stirring for 5 minutes and subsequently adding the activator. The autoclave was then pressurised with ethylene, starting the catalysis.
- **Method B**: The desired ligand and chromium source were combined in a Schlenk flask in solvent and stirred for 5 minutes, prior to addition of the aluminium activator. The resulting activated catalyst solution was allowed to stir for a further minute before being transferred to the autoclave *via* syringe. The autoclave was subsequently pressurised with ethylene.

- **Method C**: The desired ligand and chromium source were combined in a Schlenk flask in solvent and stirred for 18 hours, prior to addition of the aluminium activator. The activated catalyst solution was allowed to stir for a further minute before being transferred to the autoclave *via* syringe. The autoclave was subsequently pressurised with ethylene.
- **Method D**: The autoclave was purged with argon (10 bar), rather than ethylene, before being charged with the relevant chromium and ligand starting materials and stirred for 5 minutes. Subsequently, the catalyst activator was added and the autoclave pressurised with ethylene to initiate the reaction.

For all of the catalytic reactions the ethylene uptake was monitored through the use of a mass-flow meter. The use of a mass-flow meter meant that the point at which the catalyst "died" was apparent, and the reaction could be terminated once the ethylene uptake had stopped. For all tests undertaken in this chapter, the activity of the catalyst system is reported as the amount of ethylene consumed by the reaction per mole of chromium per hour (mol/mol Cr h^{-1}).

In order to provide a point of comparison for all the catalytic systems tested, a series of control runs were carried out. Each of the reactions was initiated using the *in situ* activation protocol (method **A**), with the following precursors:

- $Cr(acac)_3$ and MMAO-3A (no ligand), activated *in situ* (run **1**, appendix 7.4.2).
- $CrCl_3(THF)_3$ and MMAO-3A (no ligand), activated *in situ* (run **2**, appendix 7.4.2).
- Only MMAO-3A (run **3**, appendix 7.4.2).
- Iminophosphine **3.9** and MMAO-3A (no chromium), activated *in situ* (run **4**, appendix 7.4.2).

The two control runs carried out using only chromium and MMAO-3A yielded polymerisation systems (>90 wt % polymer production), while the MMAO-3A control run gave a low activity (1,500 mol/mol Cr h^{-1}) non-selective oligomerisation reaction. The final control test combining the iminophosphine with MMAO-3A gave results essentially identical to the run using only MMAO-3A, suggesting that the ligand alone does not promote catalysis.

Unfortunately, due to the time-consuming nature of the catalytic testing carried out, only a limited number of repeat runs could be undertaken to calculate the error of the system, and so precise error bars have not been generated. However, extensive testing within Sasol has shown the error of the equipment used for the catalytic runs, and in the subsequent analysis is approximately ±5 %, and it is assumed that the error is the same for this investigation.

5.1.1.1 Variation of ethylene pressure to maintain constant ethylene concentration in solution at varying reaction temperatures

In this thesis studies have been carried out to investigate the effect of varying temperature upon Cr-iminophosphine-based ethylene oligomerisation catalysts. It is well known that the solubility of gases in liquids varies with temperature, and so there is a risk that upon altering the temperature of the catalysis reactions the amount of ethylene in solution will change, therefore adding another variable to the reaction.[12] In order to combat this, the ethylene pressure was adjusted with temperature in order to maintain a constant ethylene concentration of 4.2 mol L^{-1} and, hence, consistency during tests in which the effect of temperature upon catalysis was under investigation.* Table 5.2 shows the reaction temperatures used, and the corresponding ethylene pressures.

Reaction temperature (°C)	Ethylene pressure (bar)
20	20
40	30
50	36
60	40
70	44.5
80	49
90	55
100	60

Table 5.2: Table of reaction temperatures and corresponding ethylene pressures used in order to keep a constant ethylene concentration in solution of 4.2 mol L^{-1}. * The values used are based on calculations carried out in-house by Sasol Technology.

5.1.1.2 Presence of oxygen as a catalyst additive

It has recently been reported by workers from Sasol that the presence of oxygen is vital for ethylene *tri*- and *tetra*-merisation systems to successfully operate, something that hitherto has not been reported or described for this system or other oligomerisation systems.[13] Here, Sasol demonstrated that for a range of initiators both catalyst activity and the extent of polymer formation vary dramatically in the presence of small amounts (~0.1-1 ppm) of O_2 or non-metal oxygen-containing additives (*e.g.* SO_2). For Sasol's catalyst systems it was shown that in the absence of oxygen ethylene oligomerisation was switched off, and instead the systems behaved as low activity polymerisation catalysts. Together, this demonstrates that a certain level of

* Values used were based on calculations carried out in-house by Sasol Technology.

oxygen is necessary for selective *tri*-/*tetra*-merisation to occur with the Sasol systems. However, it was proven that the presence of larger amounts of oxygen (*e.g.* >1 ppm) also inhibits oligomerisation, again yielding primarily polymer-producing systems. The precise oxygen concentration "sweet spot" is generally between 0.1 and 1 ppm of O_2, with the optimum value varying slightly between the various different ethylene oligomerisation systems reported previously. Based on this discovery, all catalysis testing in this thesis has been carried out using an ethylene feed measured to contain 0.6 ppm O_2,[*] unless otherwise stated. The optimisation of the oxygen dosing used in Cr-iminophosphine-based ethylene oligomerisation systems has been carried out, and is described in Section 5.5.6.

[*] The O_2 level was determined *via* measurement of the gas stream using a GPR-1200 oxygen meter from Advanced Instruments Inc., which had been freshly calibrated with 10 ppm O_2 stock gas.

5.2 Initial Screening of the Performance of Iminophosphine Ligand 3.1

The behaviour of iminophosphine **3.1** (Figure 5.3) in ethylene oligomerisation systems was investigated. Initially, the reaction conditions were based upon those used in the trimerisation system reported by Bercaw *et al.*[11] (Scheme 5.1).

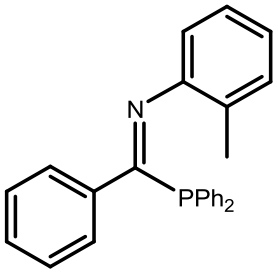

Figure 5.3: Structure of iminophosphine **3.1**

Subsequently, systematic modifications were made in order to derive the optimal conditions for these new ligands based on literature reports of comparable systems and their catalytic screening studies.[14-17] The parameters altered were:

Cr(III) source

- $CrCl_3(THF)_3$
- $Cr(acac)_3$

Activation method

- *In situ* (Method **A**)
- Pre-activation (Method **B**)
- Extended pre-activation (Method **C**)

Temperature

- 20 °C
- 60 °C
- 100 °C

Activator

- MMAO-3A
- PMAO-IP
- TEA/borate

Once the optimal conditions for ethylene oligomerisation have been elucidated for this ligand, these conditions can be applied to screening a wider library of iminophosphine ligands. The effect of altering the catalysis conditions upon the activity and selectivity of the Cr(III)-**3.1** based system is discussed below (Sections 5.2.1-5.2.4).

5.2.1 Effect of varying chromium sources

Initial tests were undertaken to explore the effect of the Cr(III) source upon the performance of PCN-based oligomerisation catalysis. Two commonly used Cr(III) sources were compared, $Cr(acac)_3$ and $CrCl_3(THF)_3$. In order to evaluate the performance of these two Cr-containing complexes, the iminophosphine ligand **3.1** was used, and the conditions employed were those described in Scheme 5.1. Selected data for the systems derived from the two different metal precursors are compared in Graph 5.1.

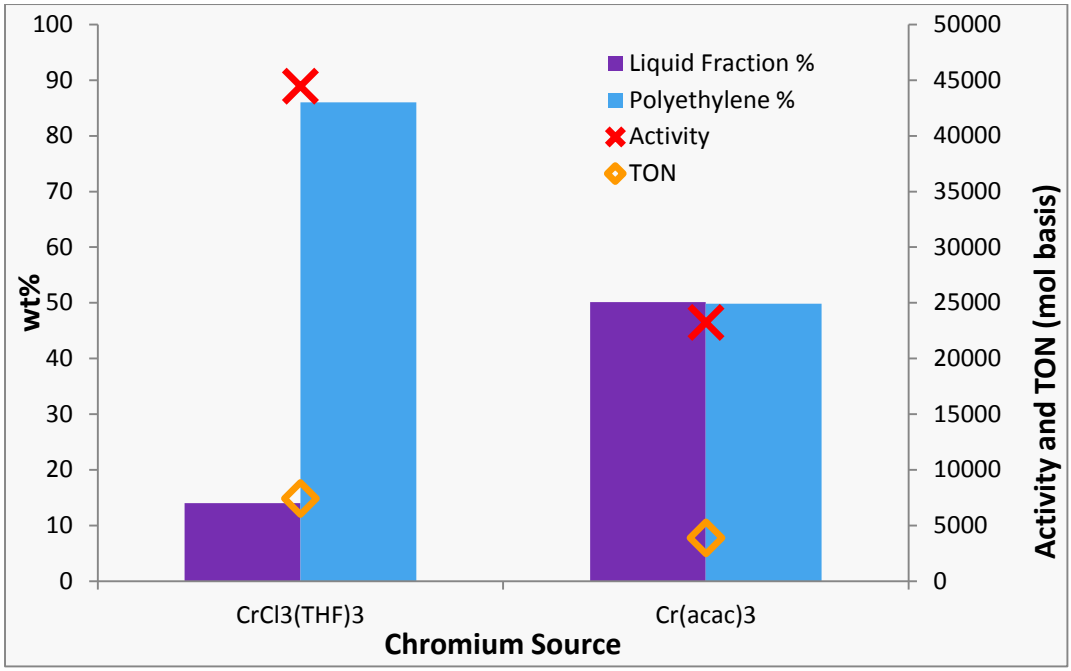

Graph 5.1: Comparison of ethylene oligomerisation performance with either $Cr(acac)_3$ or $CrCl_3(THF)_3$, and iminophosphine **3.1**. Conditions: 5 µmol Cr, 1.2 eq. ligand, 500 eq. MMAO-3A, 70 mL PhCl, 60 °C, 40 bar C_2H_4, activation method **A**.

Notably, the $CrCl_3(THF)_3$ and $Cr(acac)_3$ precursors give significant differences in activity and turn-over-number (TON), with $CrCl_3(THF)_3$ giving almost double the activity of the $Cr(acac)_3$ derived system. This difference is similar to that observed in the work described in Chapter 2 for the PNE-based ethylene oligomerisation systems, with $CrCl_3(THF)_3$ giving a four-fold greater activity compared to that with the $Cr(acac)_3$-based system. However, along with this greater activity achieved with $CrCl_3(THF)_3$, the data in Graph 5.1 show that the $CrCl_3(THF)_3$-derived system significantly favours polymer formation when compared to the $Cr(acac)_3$ system. Conseqently, despite the increased activity of the $CrCl_3(THF)_3$ system, the $Cr(acac)_3$-based run gave a larger absolute mass of oligomer product ($Cr(acac)_3$ system: 0.272 g oligomer, $CrCl_3(THF)_3$ system: 0.145 g oligomer). This observation again matches with the data obtained from the PNE-based oligomerisation system derived from these two Cr(III) sources discussed in Chapter 2.

In terms of the liquid fraction selectivities measured for the $Cr(acac)_3$ and $CrCl_3(THF)_3$ iminophosphine-based systems very little difference was observed. This is suggestive of a similar oligomerisation mechanism occurring in both processes, but the use of $CrCl_3(THF)_3$ favours the production of a highly active polymerisation species under the reaction conditions used. On considering the data together, it was decided that all further testing be carried out using $Cr(acac)_3$ as a chromium source, due to the lower degree of polymer formation.

5.2.2 Effects of varying the activation protocol upon catalysis

Three different activation protocols were tested for the ethylene oligomerisation systems derived from $Cr(acac)_3$ and iminophosphine **3.1**. The protocols tested were initially based upon those reported by Chevron Phillips for their phosphinoamidine-based ethylene oligomerisation systems.[15] The three activation methods tested were methods **A**-**C** (*in situ*, pre-activation and extended pre-activation respectively)*, and their effects upon catalysis are compared in Graph 5.2.

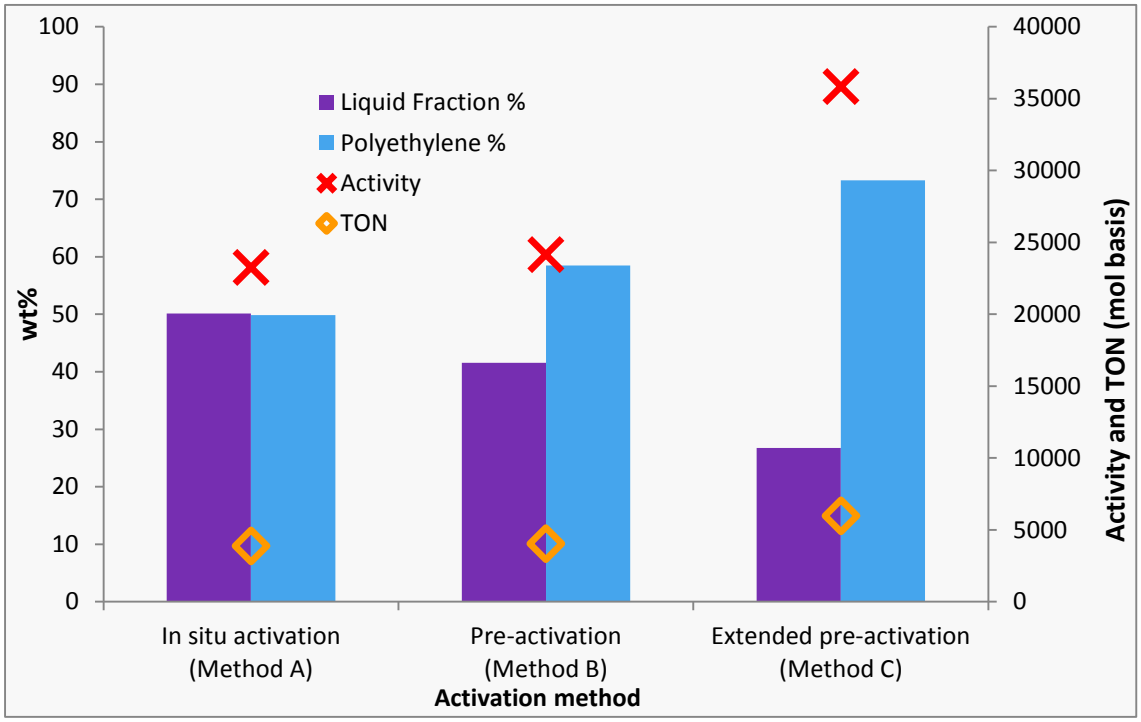

Graph 5.2: Comparison of ethylene oligomerisation performance for *in situ* (Method **A**) activated, pre-activated (Method **B**) and extended pre-activated (Method **C**) systems using iminophosphine **3.1**. Conditions: 5 µmol $Cr(acac)_3$, 1.2 eq. ligand, 500 eq. MMAO-3A, 70 mL PhCl, 60 °C, 40 bar C_2H_4.

From the data in Graph 5.2 it is clear that the method of catalyst activation has a significant effect upon the catalytic behaviour of the resulting oligomerisation system. Both the TON and activities of the systems formed using the *in situ* and pre-activated approach (Methods **A** and **B**) are identical (within error). However, the difference observed between the *in situ* (**A**) and pre-activated (**B**) systems vis-à-vis polymer formation is significant, with the *in situ* activated system producing less polymer than the pre-activated system. Notably, analysis of the liquid

* i) Method **A** (*in situ* activation): the autoclave was charged with starting materials, before MMAO-3A was added and pressurised with ethylene. ii) Method **B** (pre-activation): the starting materials were mixed in a Schlenk flask for 5 minutes, before MMAO-3A was added and stirred for 1 minute; the resulting initiator solution was transferred to the autoclave, which was subsequently pressurised with ethylene. iii) Method **C** (extended pre-activation): an analogous procedure to the pre-activation was used, except the starting materials were mixed in a Schlenk flask for 18 hours.

fraction showed that of the two methods, the pre-activated system (Method B) offers the better selectivity towards 1-hexene and 1-octene (46 and 24 wt %, respectively).

When the "extended pre-activation" (Method **C**) protocol was used an increase in activity (as measured by the ethylene uptake of the system) was observed, coupled with an increase in polymer formation. This is suggestive of the increase in activity being solely due to polymer formation, rather than increased oligomer formation as desired.

Overall, this suggests that the pre-activation protocol (Method **B**) is optimal for ethylene *tri*- and *tetra*-merisation using the new iminophosphine-based oligomerisation systems. Therefore it was decided that the pre-activation method (Method **B**) would be used for further ligand screening.

5.2.3 Effect of varying reaction temperature upon catalysis with iminophosphine 3.1

The effect of temperature upon the catalytic performance of the $Cr(acac)_3$-**3.1** based system was explored with ethylene oligomerisation runs carried out at 20, 60 and 100 °C. As the temperature of the reaction was altered, the ethylene pressure was changed in order to maintain a constant ethylene concentration in solution of 4.2 mol L^{-1}, as described in Section 5.1.1.1.

The activity of the ethylene oligomerisation system increases with temperature, in a roughly exponential fashion. In contrast to the temperature-activity relationship observed, the extent of polymer formation follows a more complex trend with respect to temperature. The data in Graph 5.3 show reactions undertaken at 60 °C give the largest oligomer vs. polymer ratio (0.7) formation, with the runs carried out at 20 °C and 100 °C both giving considerably worse oligomer:polymer ratios (0.4 and 0.07, respectively).

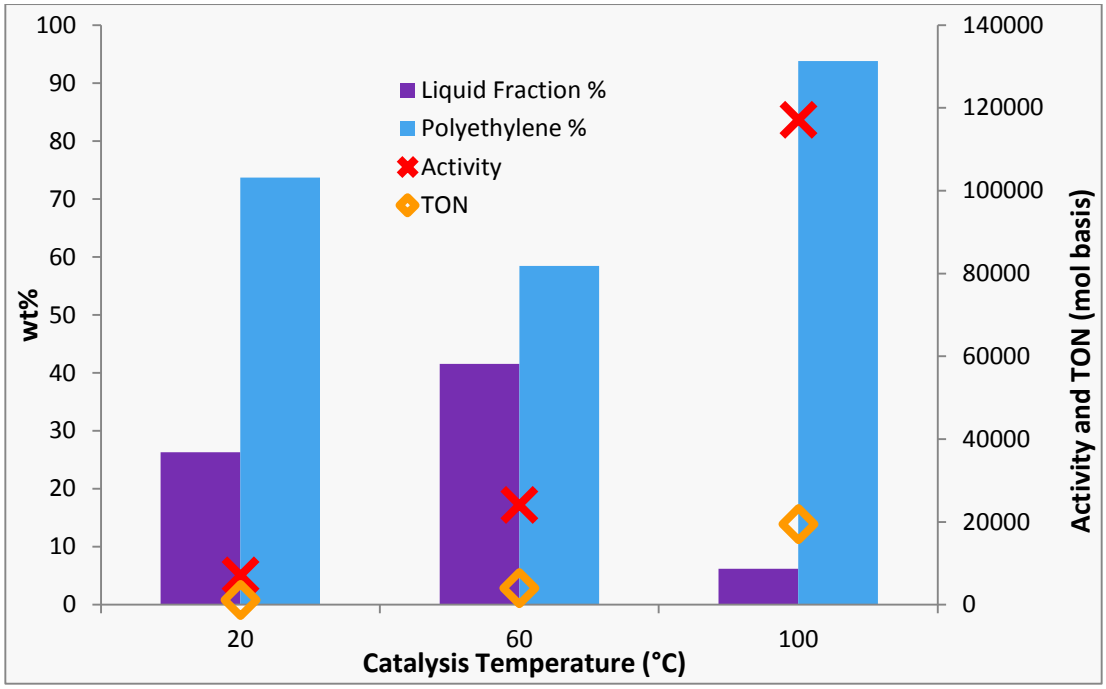

Graph 5.3: Comparison of ethylene oligomerisation performance at 20 °C, 60 °C and 100 °C using iminophosphine **3.1**. Conditions: 5 µmol $Cr(acac)_3$, 1.2 eq. ligand, 500 eq. MMAO-3A, 70 mL PhCl, 40 bar C_2H_4, activation method B.

Detailed analysis of the products in the liquid fraction reveal that for the reaction performed at 20 °C only butene and hexene (as well as polymer) were produced, something similar to the control run carried out with only MMAO-3A and ligand (as described in Section 5.1.1). From the control run carried out it is clear that aluminium species in the reaction are capable of carrying out ethylene oligomerisation, and it is suggested that the products formed in the run carried out at 20 °C are primarily formed by this aluminium-mediated oligomerisation process. It is thought at 20 °C very little chromium-based oligomerisation occurs, as indicated by the lack of higher molecular weight olefins produced at this low temperature.

Previous studies of Cr(PNP)-mediated ethylene *tri-* and *tetra*-merisation systems have found that increased reaction temperatures can favour the production of 1-hexene over 1-octene.[18] This increase in hexene formation with temperature is due to an increased rate of decomposition of the metallacycloheptane intermediate in the metallacyclic mechanism, producing more 1-hexene (Scheme 5.2). Despite this prediction, upon increasing the catalysis temperature from 60 °C to 100 °C using the new PCN ligands, the octene:hexene (OTH) ratio increased (from 0.17 to 0.53, respectively). It is thought that this result may be due to the large uncertainty associated with analysing small amounts of oligomer product, therefore should be treated as tenuous.

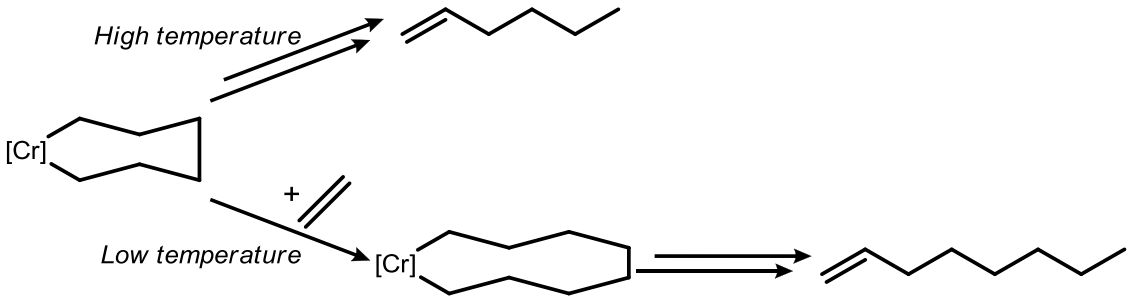

Scheme 5.2: Comparison of the proposed high temperature and low temperature behaviour of a metallacyclic ethylene *tri*-/*tetra*-merisation mechanism.

The catalytic run carried out at 60 °C has been shown to give the best performance with regard to oligomer formation, despite being less active than when the system was operated at 100 °C. Based on this, further catalytic screening runs were carried out at 60 °C.

5.2.4 Effect of varying the aluminium activator upon ethylene oligomerisation catalysis

All of the screening runs reported so far in this thesis have utilised MMAO-3A (modified methylaluminoxane) as the activator, but a wide selection of activators have been used in previously reported selective ethylene oligomerisation systems, including various alkylaluminoxanes, and alkyl aluminiums in combination with weakly coordinating anions (*e.g. tetrakis*(pentafluorophenyl)borate).[19] Furthermore, it has been previously reported that the presence of free alkyl aluminium species in MAO activators can alter the catalytic activity of polymerisation systems.[20] The MMAO-3A used in this investigation has been measured to contain relatively high amounts of free $AlMe_3$ (42 %).[21] In order to probe the effect of free $AlMe_3$ upon catalysis, PMAO-IP (polymethylaluminoxane – improved performance) was tested as an activator, since this reagent has been analysed and found to contain a reduced amount of free $AlMe_3$ (24 %).[21,22] The data in Graph 5.4 show that the catalytic system activated with PMAO-IP gave nearly entirely polymer (98 wt %), but generated a system that was more than an order of magnitude more active than the comparable MMAO-3A-activated system. This difference in both activity and polymer formation found on replacing MMAO-3A with PMAO-IP suggests that the latter co-catalyst promotes the formation of a highly active polymer-forming Cr species, rather than the desired oligomerisation species. Therefore, it is clear that free $AlMe_3$ present in MMAO-3A aids the Cr-mediated oligomerisation reaction, and it is suggested that $AlMe_3$ has a multi-faceted role in Cr-iminophosphine based catalytic systems. Overall, since the use of PMAO-IP gave significantly increased polymer formation, no further tests with this activator were carried out.

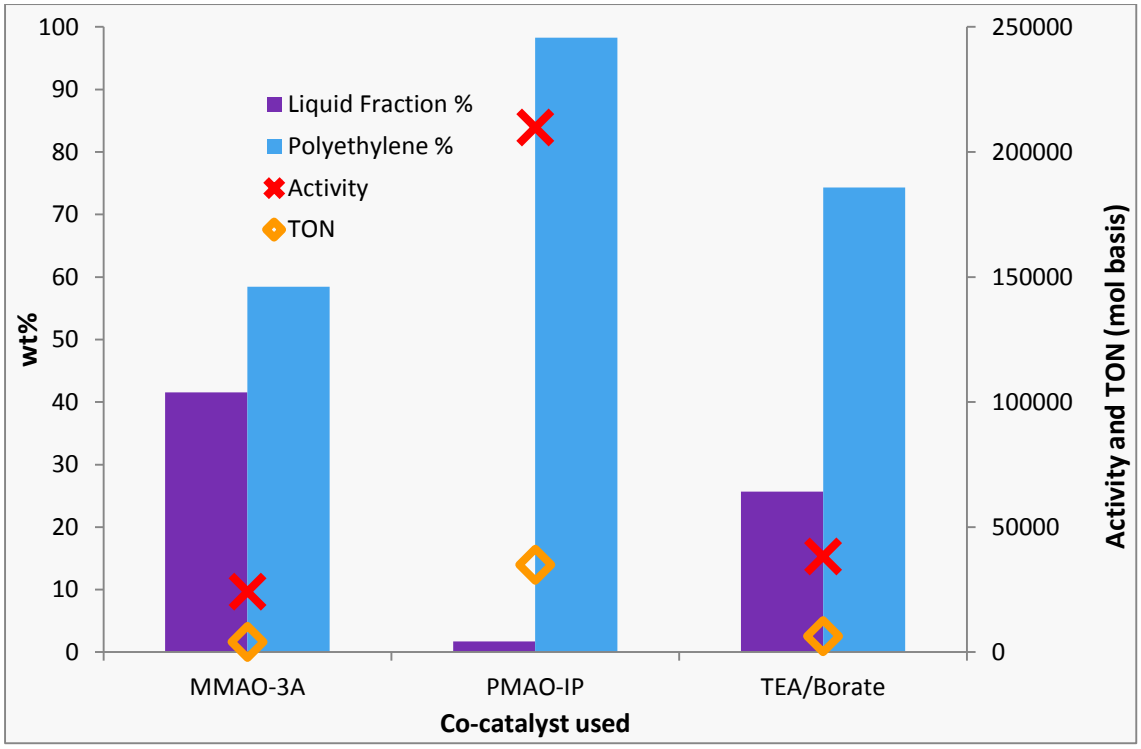

Graph 5.4: Comparison of ethylene oligomerisation performance of systems activated with MMAO-3A, PMAO-IP and TEA/Borate, using iminophosphine **3.1** and $Cr(acac)_3$. Conditions: 5 µmol $Cr(acac)_3$, 1.2 eq. ligand, 70 mL PhCl, 60 °C, 40 bar C_2H_4, activation method B.

In addition to alkylaluminoxane-based co-catalysts, such as MMAO-3A, a combination of TEA and *tetrakis*(pentafluorophenyl)borate (TEA/borate) was also tested in conjunction with $Cr(acac)_3$/(**3.1**). Previous work from Sasol has demonstrated that the use of this mixed TEA/borate activator package lowers the degree of polymer formation of selective ethylene oligomerisation systems.[17] However, this was not found to be the case with the PCN-based oligomerisation systems. Indeed, when TEA/borate was used to activate the Cr-iminophosphine catalytic systems, it was found that the extent of polymer formation increased, albeit accompanied by a small increase in activity of the catalyst, compared to the MMAO-3A activated system (from 24,000 to 38,000 mol /mol Cr h^{-1}). It is clear that the TEA/borate activator package offers no advantages in terms of catalytic performance, and is harder to use and more expensive than MMAO-3A. Therefore, only MMAO-3A was used in the further catalytic tests performed.

5.3 Use of Pre-formed Cr(III)-iminophosphine Complexes as Catalyst Precursors

The work reported in Section 5.2 demonstrates that the $Cr(acac)_3$-**3.1** based systems tested do not display selective ethylene *tri*- or *tetra*-merisation behaviour. In order to further investigate the potential of iminophosphine-based systems for ethylene oligomerisation a series of catalytic tests were carried out using pre-formed Cr(III)-PCN complexes, whose synthesis was described in Chapter 4 (Section 4.2). Previous work by Chevron Phillips has shown that the difference in catalytic activity of oligomerisation systems utilising pre-formed Cr-ligand complexes and analogous complexes formed *in situ* can be dramatic. The Chevron Phillips group demonstrated that their pre-formed catalyst precursors give excellent *tri*- and *tetra*-merisation systems, while the analogous systems generated *in situ* yield almost inactive ethylene oligomerisation catalysts.[15] Consequently, the screening of pre-formed Cr-PCN complexes in selective ethylene oligomerisation systems was carried out, based on literature reports of comparable systems and their catalytic screening studies to explore the effect of the following variables: [15,4,23,17]

Activation Method

- *In situ* (Method **A**)
- Pre-activation (Method **B**)
- Extended pre-activation (Method **C**)
- *In situ* (argon atmosphere) (Method **D**)

Temperature

- 40 °C
- 60 °C
- 80 °C
- 100 °C

Complex

- $CrCl_3(THF)(Ph(PPh_2)C{=}NPh)$ (**4.1**)
- $CrCl_3(THF)(Ph(PPh_2)C{=}N(2\text{-}MeC_6H_4)$ (**4.2**)
- $CrCl_3(Ph(PPh_2)C{=}N(2\text{-}MeOC_6H_4)$ (**4.3**)
- $CrCl_3(THF)(Ph(P^iPr_2)C{=}N(2\text{-}MeC_6H_4)$ (**4.4**)

Activator

- MMAO-3A
- PMAO-IP
- TEA/borate
- TEA/$[Oct_4N[Cl]$

5.3.1 Effect of varying catalyst activation method upon catalysis using preformed Cr-iminophosphine complexes

A series of different activation methods were screened utilising complex **4.2** as the catalyst precursor.* The data in Graph 5.5 show that the choice of activation method used has a significant effect on the behaviour of the process. It is apparent that the main difference is between the pre-activated (Methods **B** and **C**) and *in situ* activated systems (Methods **A** and **D**), with both the *in situ* activated systems giving higher activities and lower oligomer formation than the pre-activated catalyst systems.

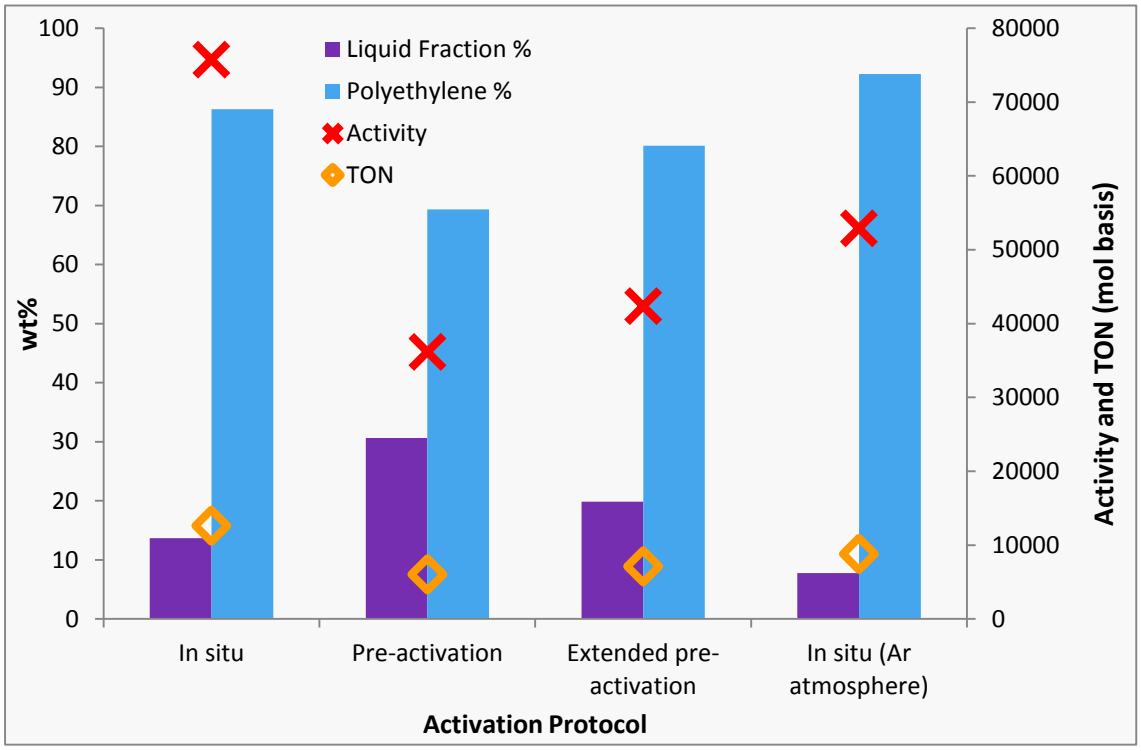

Graph 5.5: Comparison of ethylene oligomerisation performance of systems activated using the *in situ* (**A**), pre-activation (**B**), extended pre-activation (**C**), and *in situ* (Ar atmosphere) protocols (**D**), with complex **4.2**. Conditions: 5 µmol Cr, 500 eq. MMAO-3A, 70 mL PhCl, 60 °C, 40 bar C_2H_4.

When comparing the two *in situ* activated catalyst runs (Methods **A** and **D**), the system activated under an atmosphere of ethylene (Method **A**) gave both improved activity and lower polymer formation relative to the comparable system generated under an atmosphere of argon (Method **D**). Based on these observations, it is suggested that the presence of ethylene during activation favours the formation of, and may stabilise, the active catalytic species in the reaction.

The two pre-activated catalyst systems using complex **4.2** (Method **B** and Method **C**) give remarkably similar catalytic performance, with the difference in activities of the systems

* See Section 5.1.1 for description of catalyst activation Methods **A**-**D**

deemed to be within the error of the process. The run utilising the standard pre-activation protocol (Method **B**) yielded the largest oligomer fraction, and therefore this activation method was judged to be the best protocol to favour ethylene oligomerisation. Based on this observation, all subsequent tests were carried out using the pre-activation method of catalyst activation (Method **B**).

5.3.2 Effect of varying temperature upon catalysis using preformed Cr-iminophosphine complexes

Once the optimal catalyst activation protocol had been established, the effect of temperature on the catalytic performance of preformed Cr-PCN complex-based ethylene oligomerisation was investigated using complex **4.2** as a precursor; the results are presented in Graph 5.6. The trend of increasing catalyst activity with increased operating temperature observed matches that demonstrated by previous studies of selective ethylene oligomerisation systems carried out at varying temperatures.[18] As with the previous temperature screening study for *in situ*-generated systems (Section 5.2.3), the increase in reaction temperature is also mirrored by a decrease in oligomer formation, and an increase in the amount of undesirable polymer produced.

Interestingly, the change in reaction temperature employed does not have the predicted effect of decreasing the OTH ratio across the range of temperatures explored, as previously demonstrated for Cr(PNP)-based systems reported by Wasserceid *et al.*[18] Analysis of the liquid fraction products shows that the run performed at 80 °C gives the largest OTH ratio (7.8). It is likely that this unusual result is due to the inherent error associated with analysing very small amounts of oligomer products formed, and the result should be treated as tenuous at best. Overall it was judged that the reaction at 60 °C gave the optimal performance with regard to minimising polymer formation, while maximising catalytic activity of the system, and so subsequent tests were carried out at this temperature.

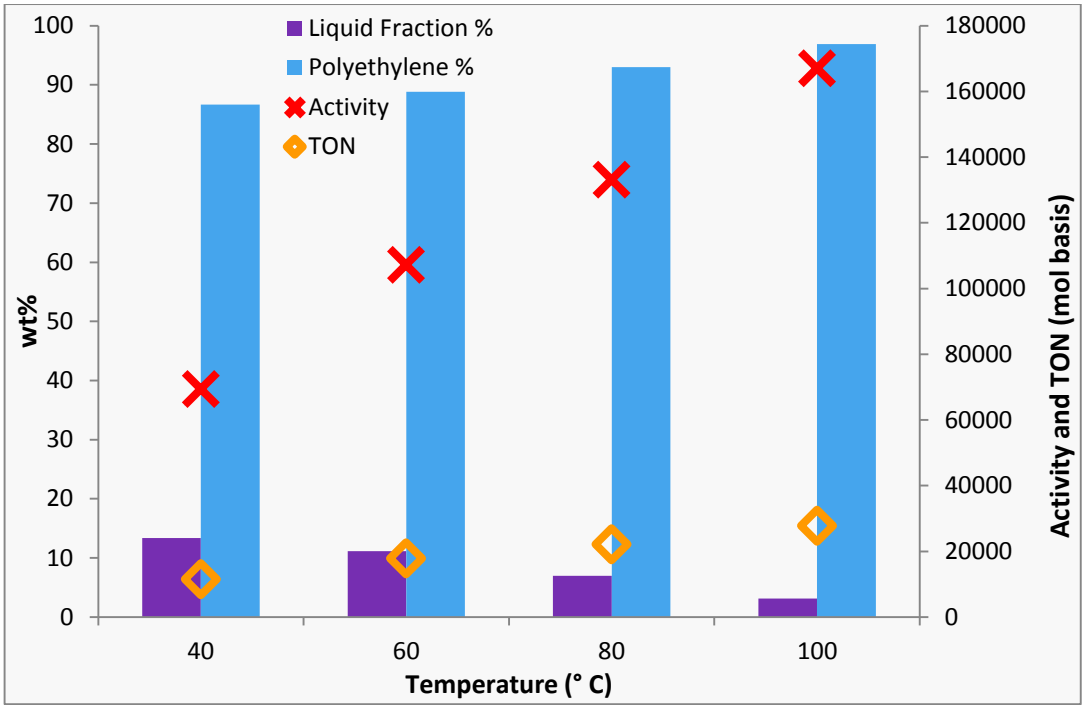

Graph 5.6: Comparison of ethylene oligomerisation performance of reactions run at 40, 60, 80 and 100 °C, using complex **4.2**. Conditions: 5 µmol Cr, 500 eq. MMAO-3A, 70 mL PhCl, 40 bar C_2H_4, activation method **B**.

5.3.3 Effect of varying the co-catalyst upon catalysis using preformed Cr-iminophosphine complexes

In order to provide a comparison of the pre-formed Cr-PCN complexes with the analogous *in situ*-formed complexes in ethylene oligomerisation, the effect of catalyst activator was probed for the former, mirroring the study carried out in Section 5.2.4. Four activator packages have been tested; MMAO-3A, PMAO-IP, TEA/Borate and TEA/[Oct_4N][Cl]. One of the primary reasons for testing TEA/borate and TEA/[Oct_4N][Cl] as activator packages is that they are known to reduce polymer formation in Cr(PNP)-based oligomerisation systems.[17] When applied to Cr-PCN complex-based systems in this investigation, both TEA/borate and TEA/[Oct_4N][Cl] activators were observed to lower the extent of polymer formation of the process, relative to using the traditional MMAO-3A activator. The disadvantage found when these TEA co-catalyst packages were tested with the preformed Cr-PCN complexes was that a significant reduction in catalyst activity was observed, compared with systems activated with MMAO-3A, thus limiting the utility of these systems which were dropped from further testing programmes. Upon changing the catalyst activator from MMAO-3A to PMAO-IP, the catalytic activity of the resulting system was seen to increase slightly, but a greater degree of polymer formation was also observed. This detrimental effect on polymer production caused by activation of the system with PMAO-IP leads to the conclusion that MMAO-3A remains the best

co-catalyst for use in activating Cr-iminophosphine based ethylene oligomerisation systems, as was the case for the *in situ*-generated systems (Section 5.2.4).

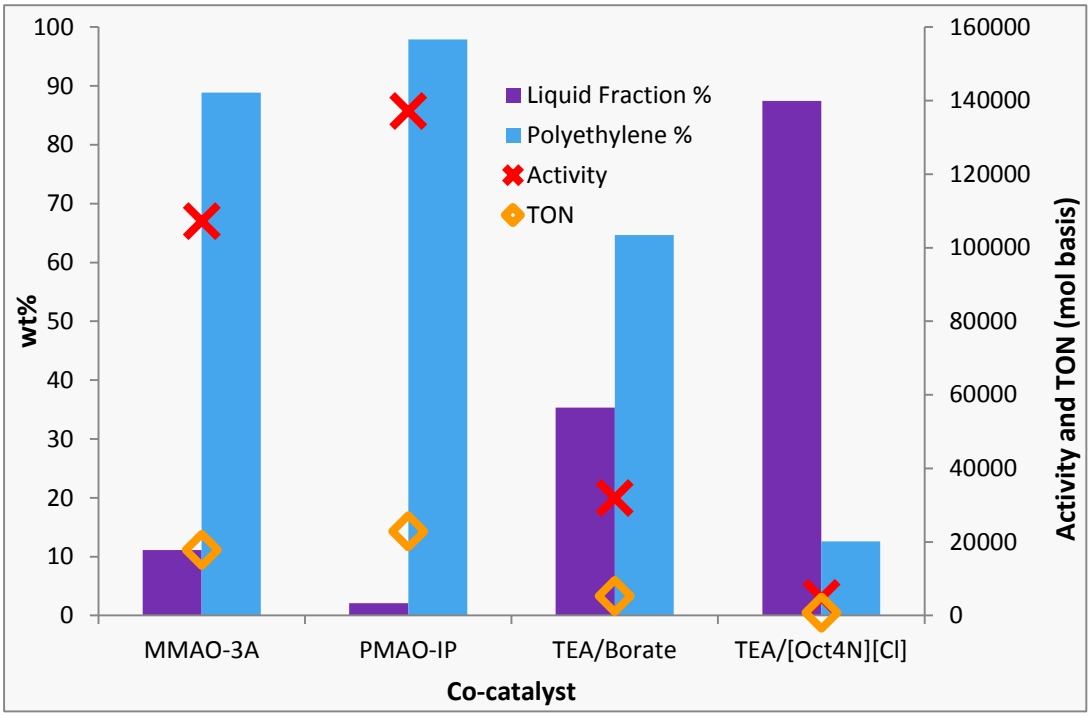

Graph 5.7: Comparison of ethylene oligomerisation systems activated with the co-catalyst packages MMAO-3A, PMAO-IP, TEA/Borate and TEA/[Oct_4N][Cl], using complex **4.4**. Conditions: 5 µmol Cr, 70 mL PhCl, 60 °C, 40 bar C_2H_4, activation method **B**.

5.3.4 Application of polymer minimisation techniques to ethylene oligomerisation systems using preformed Cr-iminophosphine complexes

Recent developments from Sasol for their Cr(PNP)-based *tri*- and *tetra*-merisation processes have demonstrated the ability of $ZnEt_2$ to help minimise the formation of polymer reducing in ethylene oligomerisation systems.[24] It is thought that zinc acts as a classical chain-transfer agent ("chain transfer to metal") towards the polymer-forming species in the reaction, hence preventing the growth of long polymer chains in the reaction (Scheme 5.3).[25] Following chain transfer of the polymer chain from the active Cr-centre to the alkylated zinc, the Zn-polymer can undergo chain termination to yield oligomer and a new zinc centre ready to undergo further chain transfer reactions.

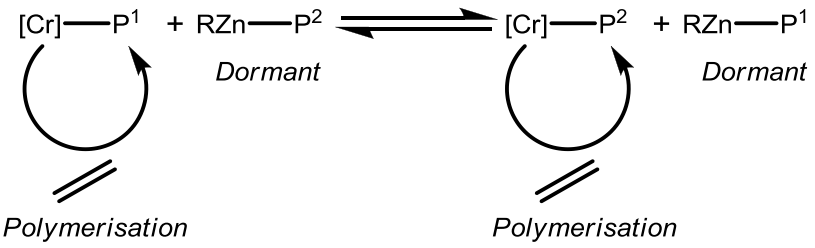

Scheme 5.3: Catalysed chain growth (CCG) mechanism, modified from Gibson *et al.*[25]

In another recent publication concerning attempts to reduce the extent of polymer formation in oligomerisation processes, Chevron Philips detailed the use of H_2 (another classical chain transfer agent[26]) with their Cr-phosphinoamidine-based system.[15] In this study it is thought that the presence of H_2 aids chain termination of polymer-forming species, hence limiting ethylene polymerisation in the reaction.

As well as lowering the extent of polymer formation in the catalytic reaction, it is suggested that the presence of $ZnEt_2$ and H_2 in ethylene oligomerisation systems lowers the molecular weight of the polymer produced. This is advantageous when developing a process for commercialisation, as lower molecular weight polyethylene is less likely to foul large-scale reactors. Due to the highly beneficial nature of $ZnEt_2$ and H_2 in previously published *tri*- and *tetra*-merisation systems, the effect of these additives upon Cr-iminophosphine-based processes was investigated. Screening runs were carried out in which H_2 and $ZnEt_2$ were added to the catalyst system, using pre-formed Cr-PCN complexes; the results from these studies are compared in Graph 5.8.*

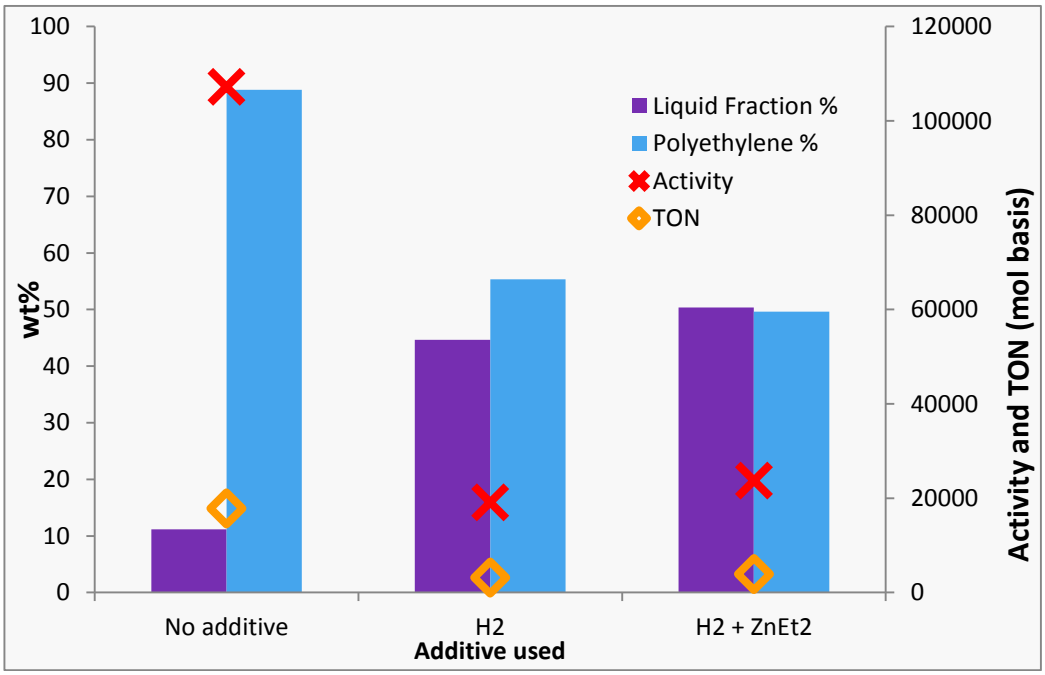

Graph 5.8: Comparison of ethylene oligomerisation performance of systems using no additives (standard), H_2 and H_2 + $ZnEt_2$, with complex **4.4**. Conditions: 5 µmol Cr, 500 eq. MMAO-3A, 70 mL PhCl, 60 °C, 40 bar C_2H_4, activation method **B**.

As expected, the presence of H_2 by itself and a combination of H_2 and $ZnEt_2$ both reduce the extent of polymer formation of the catalytic system, but at the expense of catalytic activity in both cases, which is reduced fivefold (compared to a "standard" run with no H_2 or $ZnEt_2$). This

* $ZnEt_2$ was added to the reaction as a solution prior to the activation of the pre-catalyst. H_2 gas was added to the headspace of the reactor prior to addition of the activated pre-catalyst solution.

reduction of activity upon addition of H_2 to the system contrasts with the results reported by Chevron Phillips, in which their Cr-phosphinoamidine systems displayed both increased activity and lower polymer formation when H_2 was added.[15] Comparison of the mass of liquid fraction produced by all three systems shows they yielded similar amounts of oligomer (0.20-0.28 g), regardless of the presence of H_2 or $ZnEt_2$. It is therefore suggested that the reduction of catalytic activity of the Cr(PCN)-oligomerisation systems brought about by addition of $ZnEt_2$ and H_2 is due to the inhibition of the Cr-mediated polymerisation process in the reaction, rather than altering the oligomerisation reaction occurring. This is suggestive of there being two non-interconverting Cr-species, one which mediates polymerisation, and the other giving rise to oligomerisation. Overall, since the addition of H_2 or $H_2/ZnEt_2$ gives rise to a significant reduction in catalytic activity, their use was not explored further with Cr(PCN) complexes.

5.3.5 Effect of varying the iminophosphine ligand upon catalysis using preformed Cr-iminophosphine complexes

The final variable explored in the screening of preformed Cr-PCN complexes for ethylene oligomerisation was the iminophosphine ligand itself. Four of the Cr-iminophosphine complexes synthesised in Chapter 4 (**4.1**-**4.4**, Figure 5.4) were tested as catalyst precursors in ethylene oligomerisation systems using the conditions described in Scheme 5.1, and the results are compared in Graph 5.9.

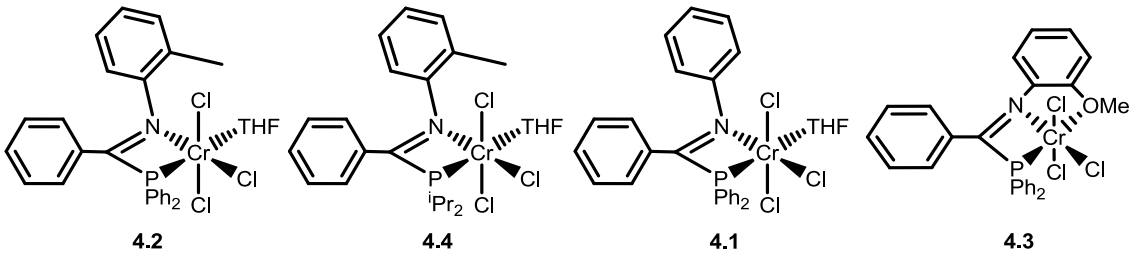

4.2 **4.4** **4.1** **4.3**

Figure 5.4: Cr-iminophosphine complexes tested as catalyst precursors in ethylene oligomerisation systems

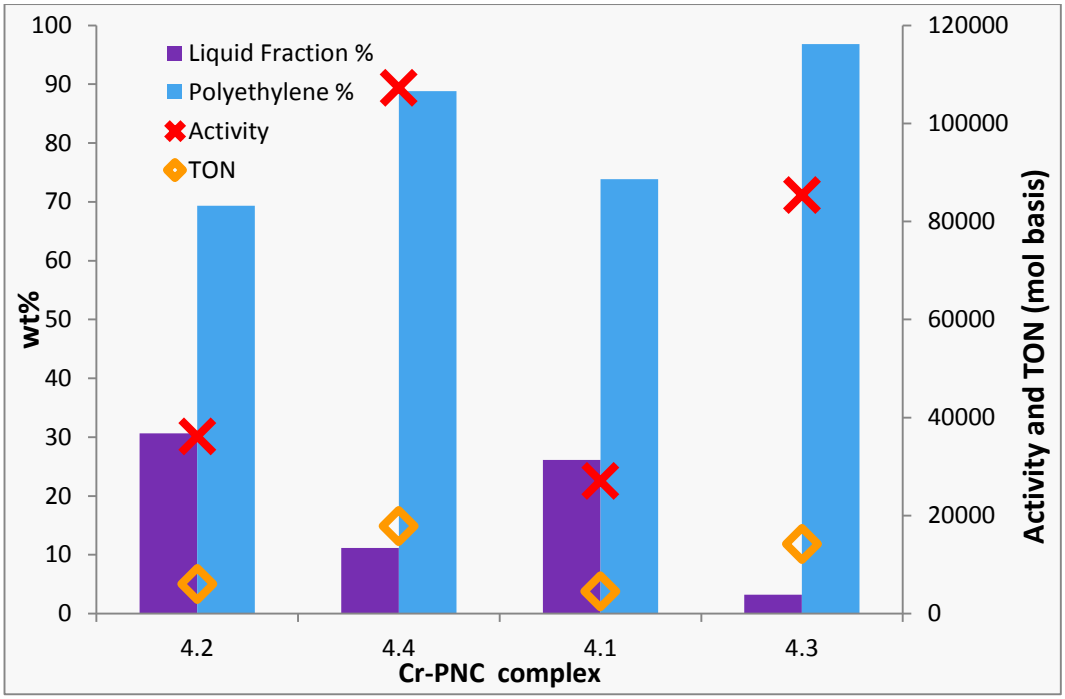

Graph 5.9: Comparison of ethylene oligomerisation performance of systems using complexes **4.1**-**4.4** as catalyst precursors. Conditions: 5 µmol Cr, 500 eq. MMAO-3A, 70 mL PhCl, 60 °C, 40 bar C_2H_4, activation method **B**.

Unfortunately, it was found that none of the precursor complexes **4.1**-**4.4** afforded oligomerisation systems that produced more oligomer than polymer (Graph 5.9). All four of the pre-formed Cr-PCN catalyst precursors tested yielded systems with reactivity broadly similar to that of the analogous systems based on Cr-PCN catalytic precursors generated *in situ* (Section 5.4). However, a number of differences in catalytic activity and extent of polymer formation between the varying pre-formed complexes tested have been found, and these are discussed below.

In this study the worst performing system with regard to liquid fraction formation is that derived from complex **4.3** ($CrCl_3(Ph(PPh_2)C{=}N\text{-}o\text{-}OMeC_6H_4)$), producing only 3 wt % liquid products, significantly less than for the other catalyst precursors tested. This is suggestive of the established κ^3-P,N,O tridentate ligand (Section 4.2.3 and Figure 5.5, *a*) not allowing the formation of an active ethylene oligomerisation species. This matches the observations of Sydora *et al.* of their phosphinoamidine scaffolds for use in ethylene *tri*- and *tetra*-merisation systems, in which the use of a tridentate ligand (Figure 5.5, *b*) resulted in a switching off of the catalytic activity of the resulting oligomerisation system.[10] Sydora *et al*. hypothesised that the abstraction of THF from their bidentate catalyst precursors is an important step in the formation of an active ethylene oligomerisation catalyst (Figure 5.6), a process which cannot occur with a tridentate $CrCl_3(\kappa^3\text{-L})$ complex. Consequently, it is thought that a similar THF-abstraction process

may occur in the formation of Cr-iminophosphine-based catalysts, which is not possible for complex **4.3**.

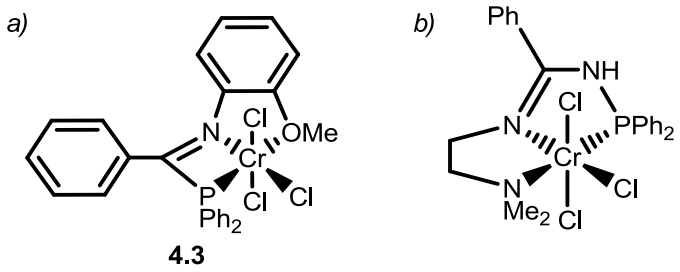

Figure 5.5: *a)* Structure of Cr(PCN) tridentate complex $CrCl_3(Ph(PPh_2)C{=}N\text{-}o\text{-}OMeC_6H_4)$ (**4.3**) *b)* Structure of Cr-phosphinoamidine complex published by Sydora *et al.*[15]

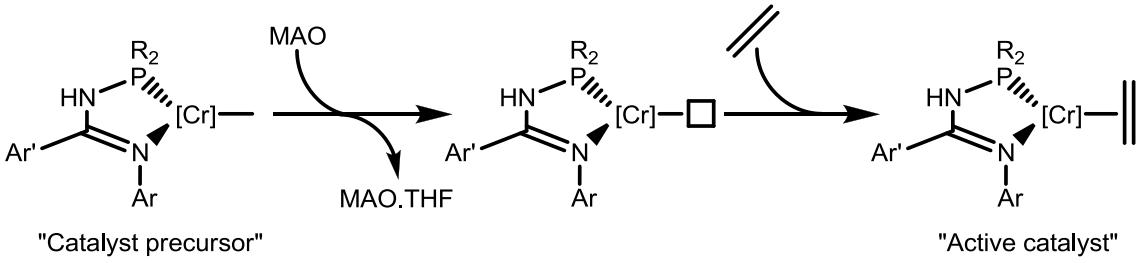

Figure 5.6: Suggested catalyst activation pathway for the Chevron Phillips phosphinoamidine-based oligomerisation system, going *via* a THF abstraction step.

In contrast to the results from the Cr(**4.3**)-based system, comparable polymer:oligomer ratios were observed for the systems utilising the three complexes **4.1**, **4.2** and **4.4** (polymer:oligomer ratios of 2.3-8.0, Graph 5.9). All three of these systems showed a link between increased catalytic activity and increasing polymer production, suggesting that the variations in activity observed are due changes in polymerisation activity, rather than differences in the oligomerisation behaviour of the systems. This link between activity and the extent of polymer formation is something that has been previously observed for the *in situ* formed Cr(PCN) oligomerisation systems (Section 5.2).

Overall, based on the four systems reported in this section (Section 5.3.5) it can be concluded that none of the complexes **4.1**-**4.4** yield selective ethylene oligomerisation catalysts upon activation. These tests carried out so far have only covered a small range of iminophosphine ligands, with limited variations in ligand structure. It is suggested that systems using iminophosphine ligands with significantly different steric and electronic properties may still yield highly active and selective ethylene oligomerisation systems. To this end, a wider range of ligand structures have been synthesised and tested in *in situ* formed catalytic systems, in combination with Cr(III) sources and varying activator packages.

5.4 Optimisation of Iminophosphine Ligand Structure for Selective Ethylene Oligomerisation Systems

The screening of iminophosphine ligands in ethylene oligomerisation systems reported so far in this thesis has been limited to a small selection of iminophosphine variants, none of which have shown reasonable selectivity towards oligomer products (>50 % oligomer). All of the PCN compounds tested in the previous sections (**3.1** and **4.1**-**4.4**) have performed in a reasonably similar fashion, something to be expected, perhaps, since each of the ligand variants explored had substituents with similar steric and electronic properties. It was therefore of interest to widen the scope of this investigation by screening iminophosphine compounds with a larger array of structural features. It was hoped that by varying the nature of the substituents at the phosphine, imine and carbon-backbone moieties, relationships between structure and catalytic activity could be drawn, therefore allowing the iminophosphine scaffold to be tuned and optimised.

The conditions used for the subsequent ethylene oligomerisation screening of the ligands **3.2**-**3.26** were those described in Section 5.2, namely using 5 µmol $Cr(acac)_3$ and 1.2 equivalents of ligand pre-activated (activation method **B**), 500 equivalents of MMAO-3A, and a reaction temperature of 60 °C. The data in Graph 5.10 summarises the activity and extent of polymer formation for these screening runs utilising iminophosphines **3.2**-**3.26** (displayed in Figure 5.7).

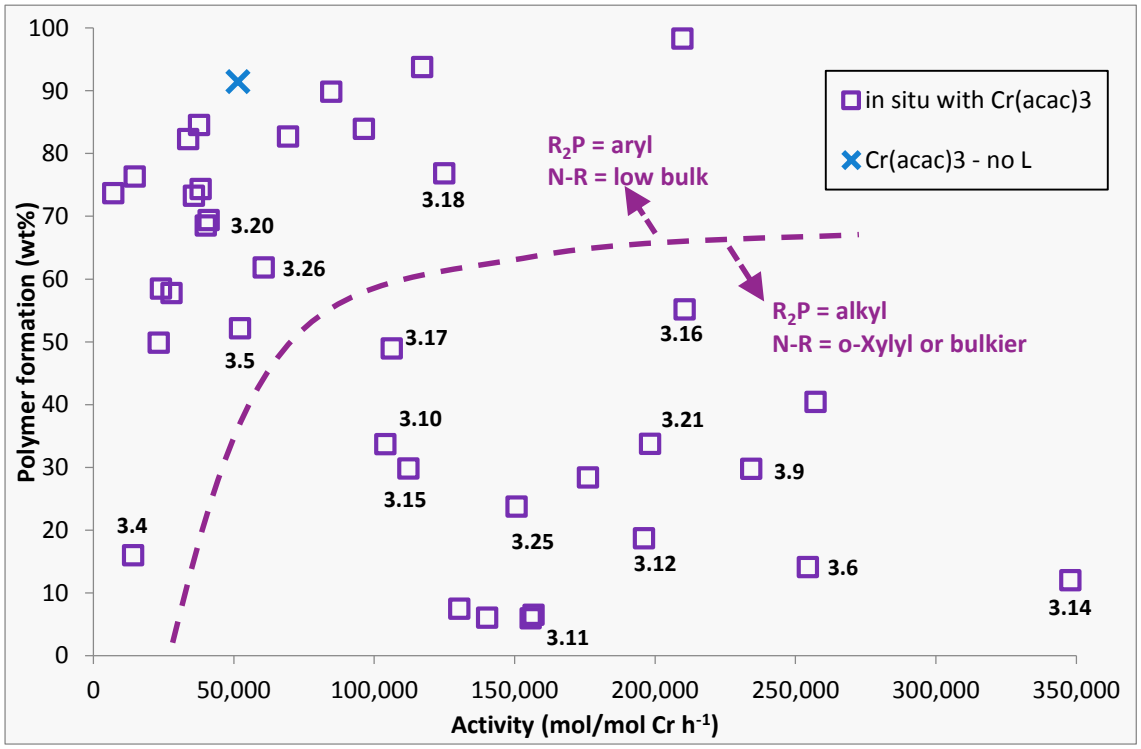

Graph 5.10: Comparison of activity and extent of polymer formation for the screening of PCN-based ethylene oligomerisation systems using ligands **3.1**-**3.26**. Catalytic conditions: 5 µmol $Cr(acac)_3$, 1.2 eq. PCN ligand, 500 eq. MMAO-3A, 60 °C, 40 bar ethylene.

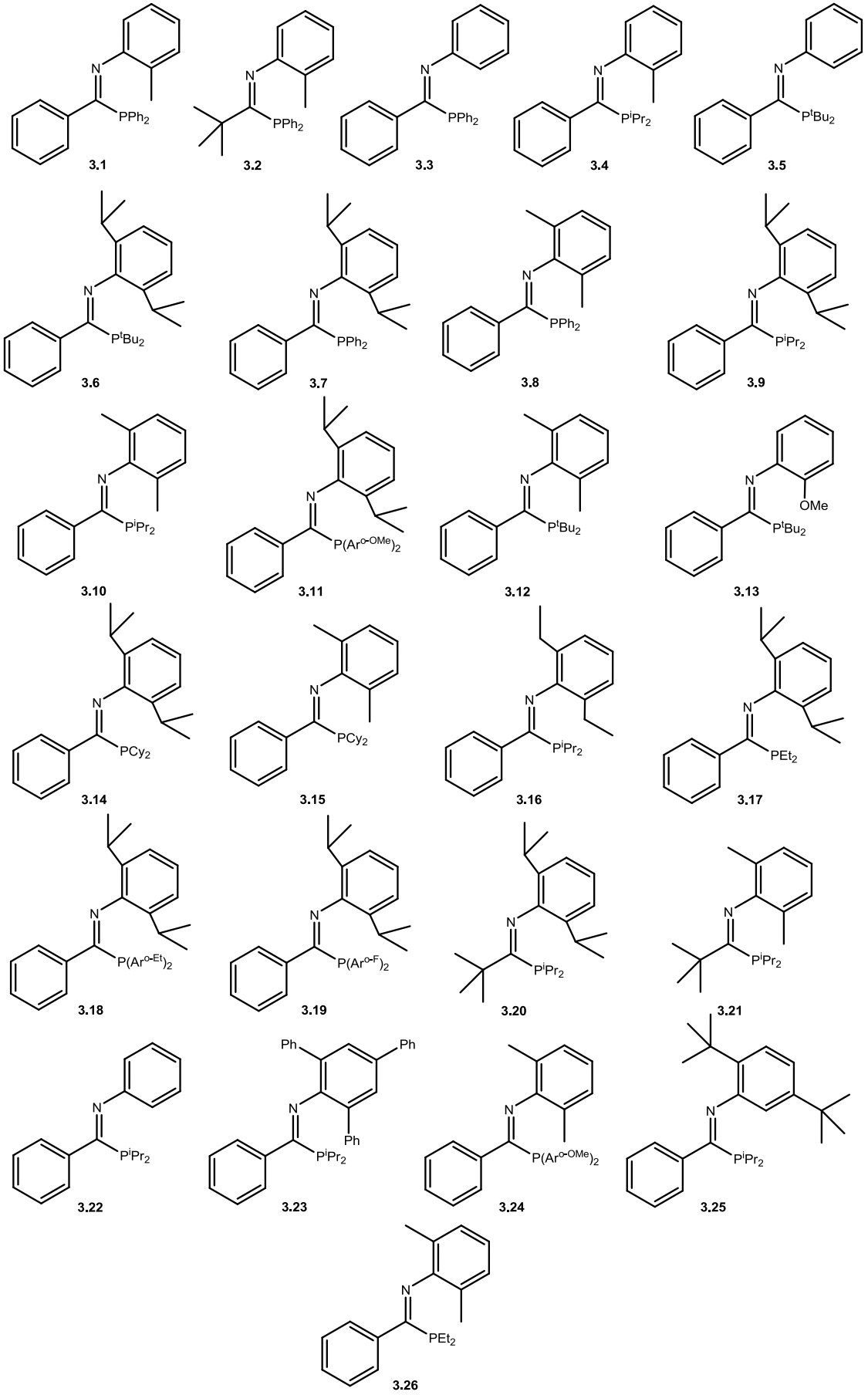

Figure 5.7: The library of iminophosphine ligands **3.1**-**3.26** synthesised in this investigation

From the data displayed in Graph 5.10, it is apparent that certain Cr-iminophosphine combinations are capable of giving highly active ethylene oligomerisation systems. In the screening runs carried out it was found that catalytic activities of 350,000 mol/mol Cr h^{-1} could be achieved (**3.14**), with the levels of polymer production being reduced to 6 % (**3.11**), comparable to Sasol's first Cr(PNP)-based ethylene tetramerisation process (506,000 mol/mol Cr h^{-1}, 1.1 % polymer).[27] In addition to these high activities and comparatively low degrees of polymer formation, it was demonstrated that Cr-iminophosphine catalytic systems were capable of giving very high liquid fraction selectivities towards combined 1-hexene and 1-octene formation *e.g.* up to 98 % 1-C_6+1-C_8 (**3.9**). Based upon the iminophosphine ligand screening results a number of trends can be drawn relating ligand structure to the performance of a specific compound in selective ethylene oligomerisation systems, and these correlations will be discussed in the following section.

5.4.1 Effect of varying the iminophosphine phosphine substituent on ethylene oligomerisation catalysis

Iminophosphine ligands have been synthesised with a range of phosphine substituents, covering differing steric and electronic parameters (P-alkyl and P-aryl groups). In order to compare the effects of varying the nature of the substituents at phosphorus the N-aryl and C-backbone substituents were kept the same. Initially N-2,6-$^{i}Pr_2C_6H_4$ was used, followed by a smaller set of tests using the N-2,6-$Me_2C_6H_4$ substituted ligand variants. For all of the iminophosphines tested in this section a phenyl C-backbone substituent was used. Due to the difficulty in separating the electronic and steric effects of P-alkyl and P-aryl substituents (see Section 3.3.3) it is not possible to directly compare P-alkyl and P-aryl phosphines. Rather, trends have been observed between iminophosphines within these two groups.

5.4.1.1 Comparison of catalytic systems using iminophosphines with alkyl-substituted phosphines

In Section 3.3.3.1 the percentage buried volume of iminophosphine compounds with varying alkyl substituents was calculated in an attempt to quantify the steric bulk of iminophosphines with different phosphine groups. The trend in $\%V_{bur}$ calculated for the iminophosphine compounds shown in Figure 5.8, indicates that the increase in $\%V_{bur}$ matches with the expected increase in steric bulk of the P-alkyl groups. It has been observed that there is a general decrease in extent of polymer formation of the catalytic systems with increasingly bulky P-alkyl groups, correlating with the calculated increase in $\%V_{bur}$ of the ligands. The $|^1J_{P\text{-}Se}|$ values for the selenide derivatives of the iminophosphines **3.26**, **3.8**, **3.10** and **3.12** were determined (Section 3.3.3.3), allowing for the catalytic behaviour of the systems using these ligands to be compared with the donor properties of the phosphine groups. Interestingly, no

correlation between the $|^1J_{P\text{-}Se}|$ couplings of the P-alkyl substituted iminophosphines and the catalytic activities or extent of polymer formation of the relevant processes is observed. Similarly, no link between the measured ν_{CN} values for the iminophosphines (see Section 3.3.3.2) and the behaviour of the related catalytic systems has been found. This suggests that the differing behaviour of the various P-alkyl-substituted phosphines in oligomerisation systems is primarily a steric effect.

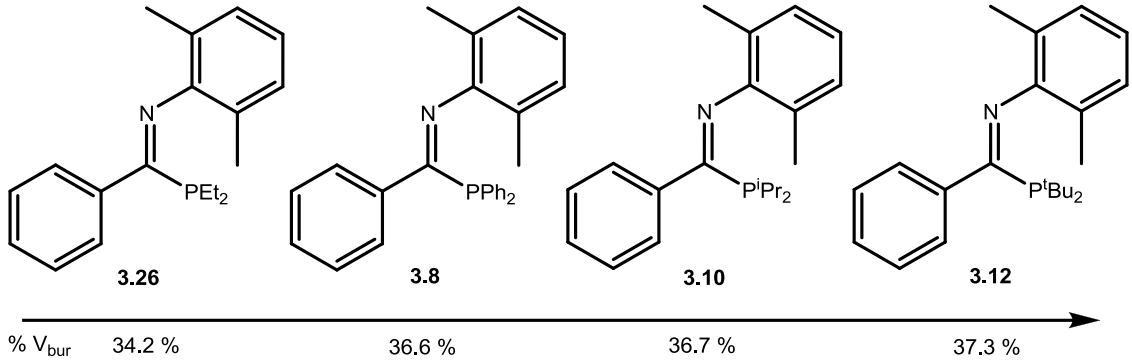

Figure 5.8: Variation in % V_{bur} for iminophosphine ligands **3.26**, **3.8**, **3.10** and **3.12**.

The activity and polymer/oligomer formation data for the catalytic runs using the iminophosphine compounds (2,6-^{i}Pr$_2$C$_6$H$_3$)N=C(Ph)PR$_2$ (R = Et, ^{i}Pr, Cy, ^{t}Bu) are displayed in Graph 5.11. Notably, these systems provide the first example of iminophosphine-based ethylene oligomerisation reactions producing more oligomer than polymer. Indeed, the reaction using compound **3.14** as the ligand gave some of the lowest levels of polymer production for all of the iminophosphines tested, just 12 wt %. More generally, the oligomerisation results show a correlation between increasing steric bulk of the PR_2 alkyl group and oligomer formation, suggesting that a bulky iminophosphine ligand is required to inhibit the formation of polymer (Graph 5.11). This is the converse of the results reported by Gibson *et al.* for their 2,6-*bis*(imino)pyridyl-based olefin polymerisation systems.[28] In this work it was shown that the use of bulky 2,6-*bis*(imino)pyridyl ligands favoured ethylene polymerisation (Figure 5.9, *i*), while using less sterically demanding ligands (Figure 5.9, *ii*) yielded primarily oligomeric products. Based on this, it is clear that the Cr-iminophosphine systems reported in this thesis and Gibson's Fe-2,6-*bis*(imino)pyridyl-based process initiate ethylene oligomerisation catalysis differently.

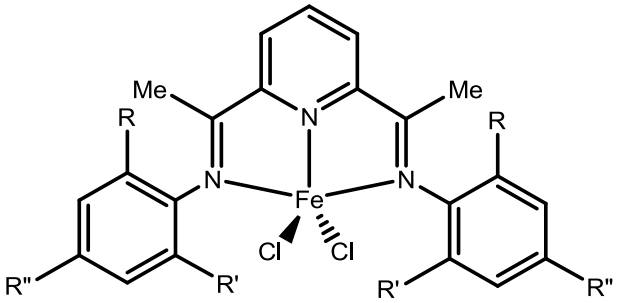

i) R = R' = ^{i}Pr, R'' = H
ii) R = H, R' = Me, R'' = Me

Figure 5.9: Fe-*bis*(imino)pyridyl precursor for olefin oligomerisation (*ii*) and polymerisation catalysts (*i*) reported by Gibson *et al.*[28]

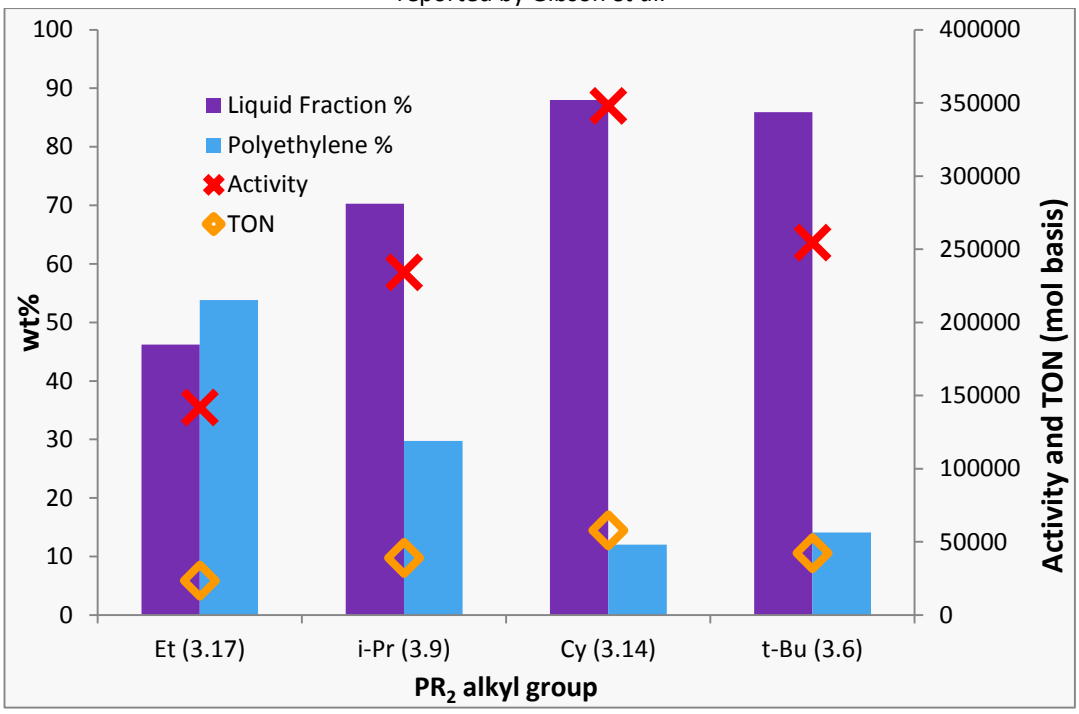

Graph 5.11: Comparison of catalytic activities and polymer/oligomer formation for ethylene oligomerisation systems utilising iminophosphine ligands with varying P-alkyl groups (alkyl = Et, ^{i}Pr, Cy, ^{t}Bu). Conditions: 5 µmol $Cr(acac)_3$, 1.2 eq. ligand, 500 eq. MMAO-3A, 70 mL PhCl, 60 °C, 40 bar C_2H_4, activation method **B**.

Upon increasing the steric bulk of the iminophosphine P-alkyl substituent from ethyl (**3.17**) to cyclohexyl (**3.14**) an increase in catalytic activity is observed, something paralleled by increasing oligomer formation. Changing the alkyl substituent from cyclohexyl to *tert*-butyl however, causes a decrease in activity. This matches with the hypothesis that oligomerisation reaction occurs *via* a metallacyclic process, in which increasing steric bulk beyond a certain limit would inhibit metallacycle expansion at the Cr centre, hence lowering catalytic activity and selectivity (Figure 5.10).

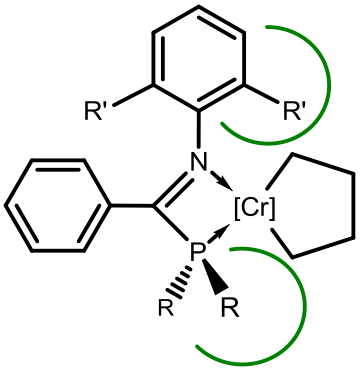

Figure 5.10: Depiction of the steric bulk imposed by an appropriately-substituted iminophosphine ligand upon a Cr-metallacycle.

Links between the steric bulk of the P-alkyl group and the oligomer selectivity of the catalytic system can also be drawn (Graph 5.12). Comparing the amounts of the various LAOs produced in each screening run shows that 1-hexene production increases, while formation of 1-octene is decreased with increasing steric bulk of the iminophosphine ligand used. The difference in OTH ratios between PEt_2 (2.1) and P^tBu_2 (0.0) shows that there is potential for the iminophosphine compounds to be tuned to mediate ethylene oligomerisation catalysis with defined 1-hexene and 1-octene production ratios, which is a highly attractive proposition. It is likely that the presence of bulky P-alkyl groups favours 1-hexene production due to the more sterically demanding phosphine group inhibiting the formation of the Cr-metallacyclononane intermediate required for the selective production of 1-octene. The excellent liquid fraction selectivities displayed by these PCN-based systems demonstrate that iminophosphine ligands are capable of giving highly selective Cr-mediated ethylene oligomerisation catalysis.

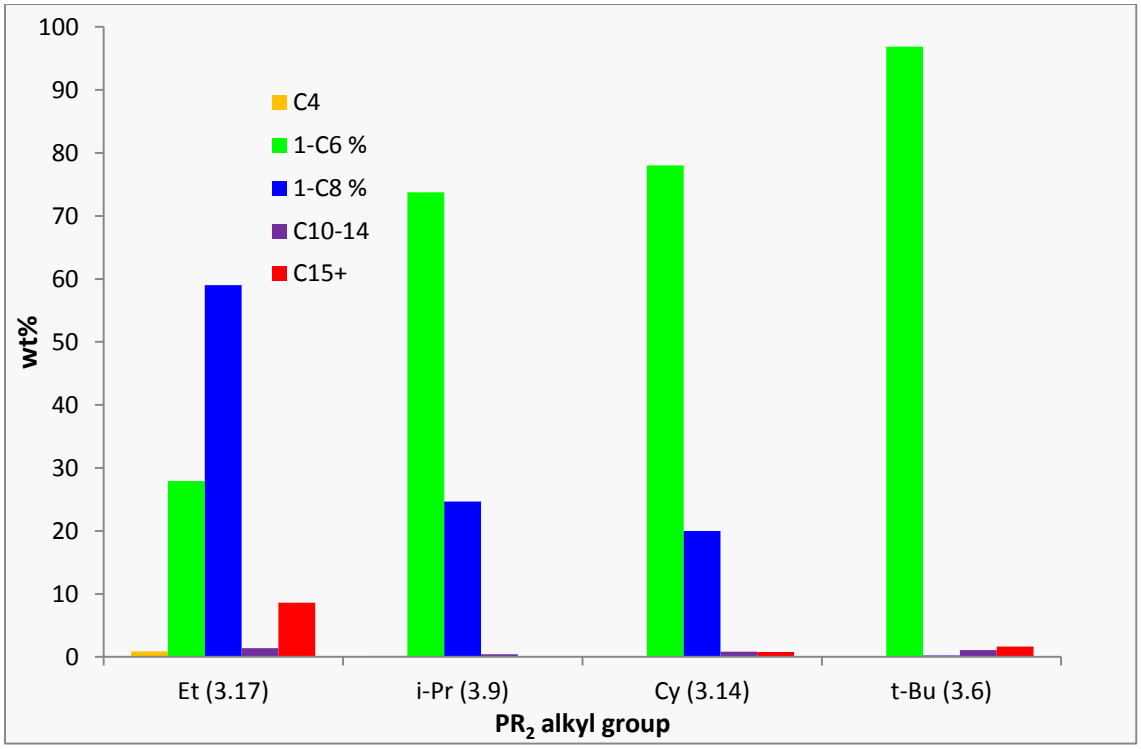

Graph 5.12: Comparison of liquid fraction oligomer selectivities for ethylene oligomerisation systems utilising iminophosphine ligands with varying P-alkyl groups (alkyl = Et, ^{i}Pr, Cy, ^{t}Bu). Conditions: 5 µmol $Cr(acac)_3$, 1.2 eq. ligand, 500 eq. MMAO-3A, 70 mL PhCl, 60 °C, 40 bar C_2H_4, activation method **B**.

5.4.1.2 Comparison of catalytic systems using iminophosphines with varying ortho-substituted aryl phosphines

In Chapter 3 the synthesis of a series of iminophosphine compounds with varying polar-aryl-substituted phosphine groups (**3.7**, **3.11**, **3.18**, **3.19**) was reported. The steric influence of these *ortho*-substituted aryl phosphines upon a metal centre is somewhat harder to quantify compared to alkyl phosphines, due to the ability of the aryl groups to rotate, altering the steric demands of the phosphine upon the metal. However, the presence of polar substituents on the aryl groups causes significant electronic differences in the donor properties of the aryl phosphine group. The electronic donor properties of the aryl phosphines have been quantified through the measurement of the $|^1J_{P\text{-}Se}|$ couplings of the phosphine-selenide analogues of the relevant iminophosphine compounds (Section 3.3.3.3), and the increasing $|^1J_{P\text{-}Se}|$ coupling values, and therefore decreasing donor ability, for a series of aryl-substituted phosphines are given in Figure 5.11.

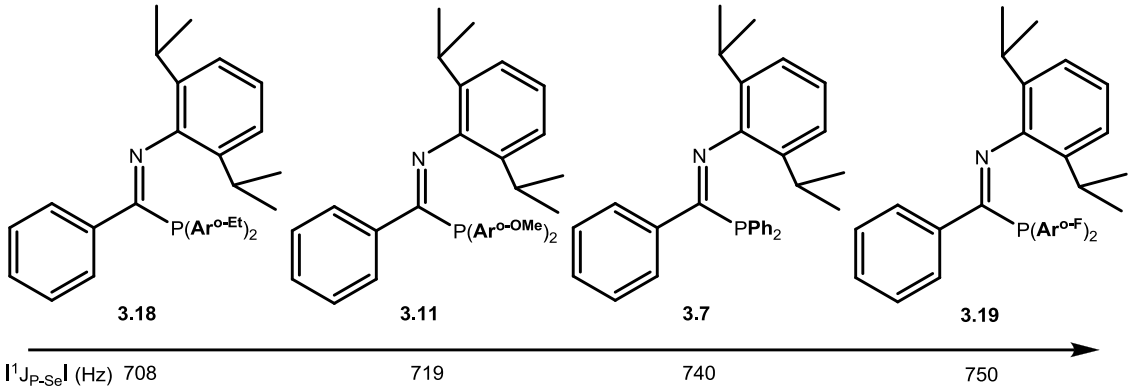

Figure 5.11: Variation in $|^1J_{P\text{-}Se}|$ values with various P-aryl substituents of iminophosphine compounds **3.7**, **3.11**, **3.18** and **3.19**)

The catalytic behaviour of iminophosphine-based ethylene oligomerisation systems utilising P-aryl-substituted iminophosphines can be compared with the donor ability of the phosphine group, as determined from the $|^1J_{P\text{-}Se}|$ values measured for the phosphines. A series of catalytic screening runs were carried out using the iminophosphines **3.7**, **3.11**, **3.18** and **3.19** (Figure 5.11), and the activity and resulting oligomer/polymer formation data are compared in Graph 5.13.

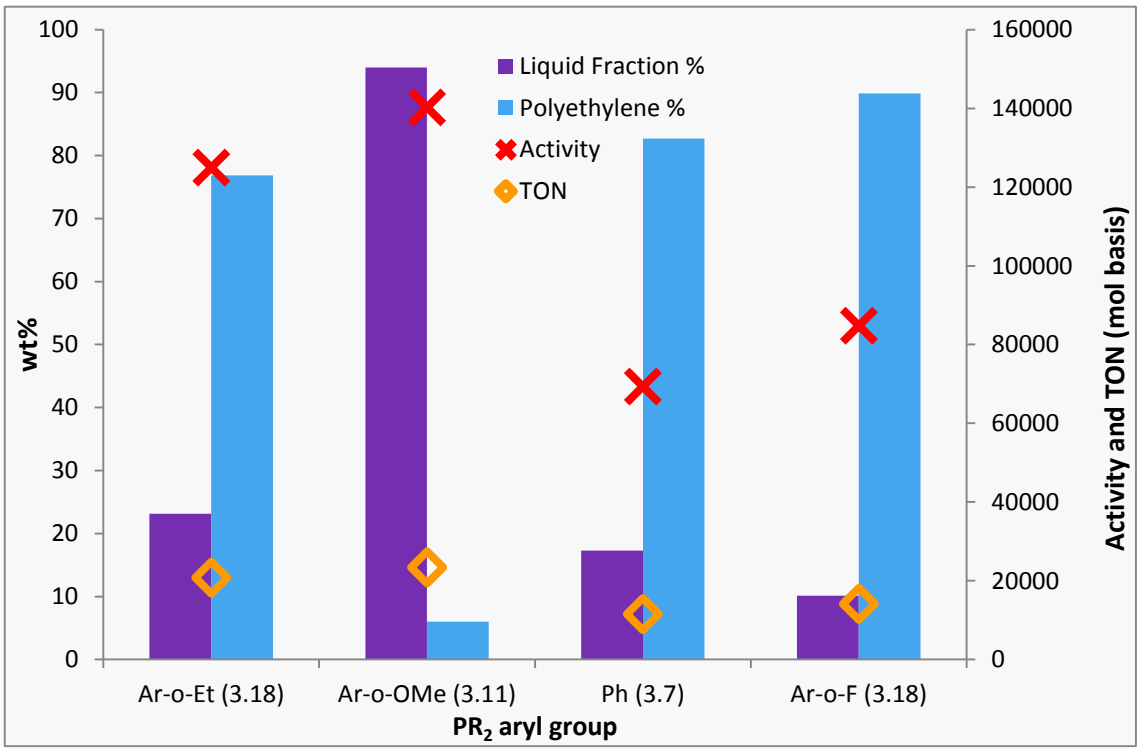

Graph 5.13: Comparison of catalytic activities and polymer/oligomer formation for ethylene oligomerisation systems utilising iminophosphine ligands with varying P-aryl groups (aryl = *o*-$OMeC_6H_4$, *o*-EtC_6H_4, Ph, *o*-FC_6H_4). Conditions: 5 µmol $Cr(acac)_3$, 1.2 eq. ligand, 500 eq. MMAO-3A, 70 mL PhCl, 60 °C, 40 bar C_2H_4, activation method **B**.

The data in Graph 5.13 highlight a large difference in catalytic behaviour between the systems utilising the various different aryl-substituted phosphine groups. Of the four tests

carried out, the test utilising the P(*o*-$OMeC_6H_4)_2$-substituted ligand (**3.11**) was the only run of the four polar-aryl-substituted phosphine systems to yield more oligomer than polymer product. It is suggested that this marked difference in reactivity of the P(*o*-$OMeC_6H_4)_2$-substituted system is due to the ability of the *ortho*-OMe group to act as a pendant donor towards the Cr-centre (analogous to that described by Bercaw *et al.* for Cr($PNP^{o\text{-}OMe}$) complexes),[29] a behaviour that the other P(aryl)$_2$-substituted ligands cannot emulate. Interestingly, this directly contradicts the results displayed by the catalytic system using complex **4.3**, in which the presence of an OMe donor group on the N-aryl-substituent was shown to switch off catalysis. It is suggested that this difference is caused by differing geometries of the P-*o*-$MeOC_6H_4$ group versus the N-*o*-$MeOC_6H_4$ group. In this thesis it has been suggested that the $Ph(PPh_2)C{=}N(2\text{-}MeOC_6H_4)$ ligand (bearing N-*o*-$MeOC_6H_4$) binds to chromium in a κ^3-*mer* coordination mode (Figure 5.12, *a*), while it is known that Cr($PNP^{o\text{-}OMe}$) complexes (bearing P-*o*-$MeOC_6H_4$), the PNP ligand binds in a κ^3-*fac* coordination mode (Figure 5.12, *b*) and thus is a geometric effect.[29] It is proposed that the P(*o*-$OMeC_6H_4)_2$-substituted iminophosphine (**3.11**) can adopt a κ^3-*fac* coordination mode, which yields an active ethylene oligomerisation system, compared to the κ^3-*mer* coordination of $Ph(PPh_2)C{=}N(2\text{-}MeOC_6H_4)$ (**3.27**) which blocks the formation of an active catalytic species.

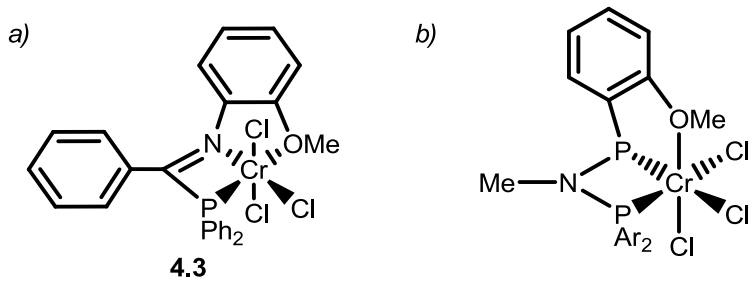

Figure 5.12: Comparison of the coordination modes of $Ph(PPh_2)C{=}N(2\text{-}MeOC_6H_4)$ (κ^3-*mer*, complex **4.3**) and $PNP^{o\text{-}OMe}$ (κ^3-*fac*) ligands.

If the P(*o*-$OMeC_6H_4)_2$ run is not included (due to the significantly different coordination chemistry of this system), then a correlation between decreasing phosphine basicity and decreasing oligomer formation is observed. By increasing the electron-withdrawing nature of the phosphine group, the catalytic system tends to be less active and produce more polymer. This agrees with the observation that P-alkyl-substituted iminophosphines tend to yield more active and selective ethylene oligomerisation systems than their P-aryl counterparts, due to their improved phosphine-donor ability (Section 5.4.1.1). It is suggested that the electronic character of the metal centre in catalysis (*i.e.* electron rich or electron poor) will have an impact upon the ease of oxidation of the chromium, and hence will alter the systems response to

oxygen, which is demonstrated to play a significant role in ethylene oligomerisation catalysis (see Section 5.5.6).

A link between the electronic properties of P-aryl-substituted iminophosphines and the liquid fraction selectivity of the resulting ethylene oligomerisation system is also apparent (Graph 5.14). A major difference in OTH ratio between the more electron donating systems (P(*o*-$EtC_6H_4)_2$- and P(*o*-$OMeC_6H_4)_2$-substituted phosphines **3.18** and **3.11**) and the more electron withdrawing systems (PPh_2- and P(*o*-$FC_6H_4)_2$-substituted phosphines **3.7** and **3.19**) is observed. The two systems bearing the relatively more electron donating phosphine substituents (P(*o*-$EtC_6H_4)_2$ (**3.18**) and P(*o*-$MeOC_6H_4)_2$ (**3.11**)) both yielded predominantly 1-hexene and 1-octene (92–97 % combined 1-C_6 + 1-C_8 selectivity). Upon changing the aryl phosphine groups to more electron-withdrawing groups (PPh_2- and P(*o*-$FC_6H_4)_2$-substituents) a significant increase in non-selective oligomer formation is observed (only producing 71-78 % combined 1-C_6 + 1-C_8), yielding significantly more C_{15+} oligomers. It is therefore concluded that the iminophosphines bearing electron-withdrawing P-aryl groups promote non-selective ethylene oligomerisation processes to a greater extent than their electron-donating P-aryl counterparts.

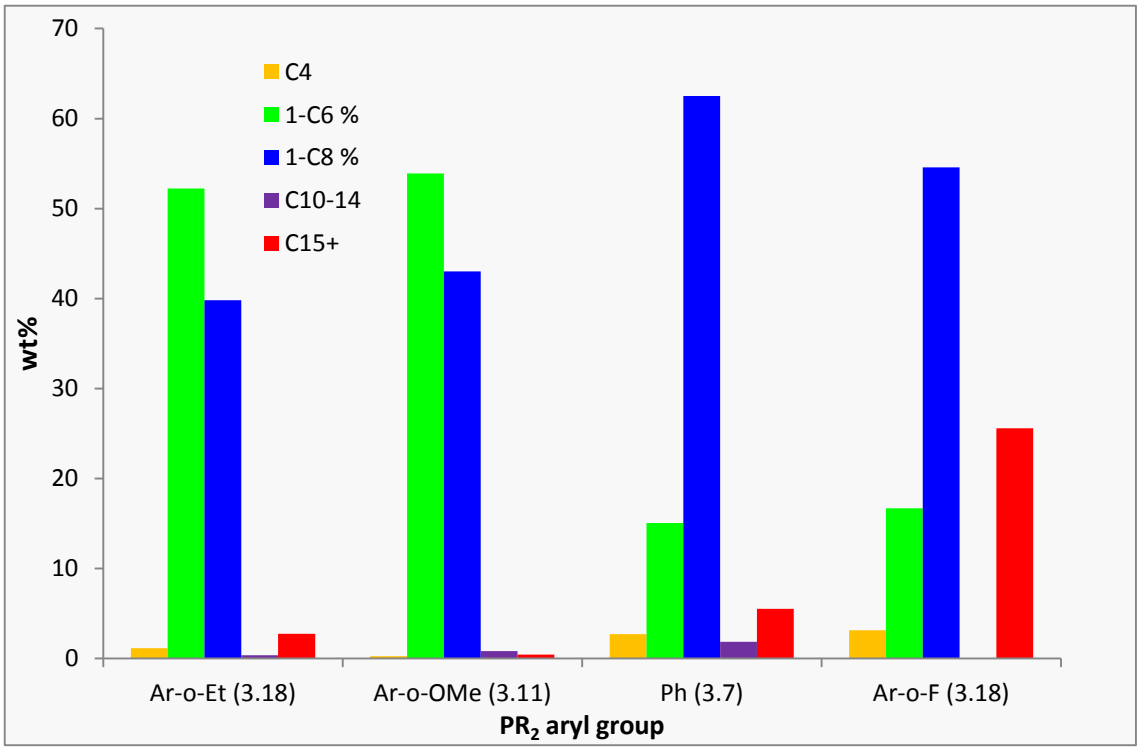

Graph 5.14: Comparison of liquid fraction oligomer selectivities for ethylene oligomerisation systems utilising iminophosphine ligands with varying P-aryl groups (aryl = o-$OMeC_6H_4$, o-EtC_6H_4, Ph, o-FC_6H_4). Conditions: 5 µmol $Cr(acac)_3$, 1.2 eq. ligand, 500 eq. MMAO-3A, 70 mL PhCl, 60 °C, 40 bar C_2H_4, activation method **B**.

It has been shown that the use of the P(*o*-$OMeC_6H_4)_2$-substituted iminophosphine **3.11** (Ph(P(*o*-$OMeC_6H_4)_2C$=N(2,6-$^iPr_2C_6H_3$)) in ethylene oligomerisation systems does yield a highly active and selective ethylene *tri*- and *tetra*-merisation catalyst, comparable to Cr(PNP)-based literature systems.[27] It is thought that the significantly different catalytic behaviour of the Cr(**3.11**)-based system, when compared to other P-aryl-substituted iminophosphines, is due to the ability of the *ortho*-OMe group to act as a pendant donor in the catalytic system, binding the ligand in a κ^3-*fac* coordination mode. This pendant donor coordination does not apply to the other P-aryl substituted compounds screened, all of which yield predominantly polymer-forming catalysts.

5.4.2 Effect of varying the iminophosphine N-aryl substituent upon ethylene oligomerisation catalysis

In addition to altering the phosphine substituent of the iminophosphine compounds in this investigation, the N-aryl substituent was also varied, allowing for the effect of the steric bulk around the N-donor group on catalysis to be probed. For this set of screening tests the iminophosphine scaffold used was (2,6-$R_2C_6H_3$)N=C(Ph)PiPr_2 (R = H, Me, Et, ^{i}Pr; **3.22**, **3.10**, **3.16** and **3.9,** respectively). The P-$^i Pr_2$ substituted variants were chosen due to the excellent performance found for ligands bearing this group in the previous phosphine variant screening study (Section 5.4.1). Upon comparison of the effects observed on changing the N-aryl substituents, a series of trends between steric bulk, activity and oligomer formation can be drawn (Graph 5.15).

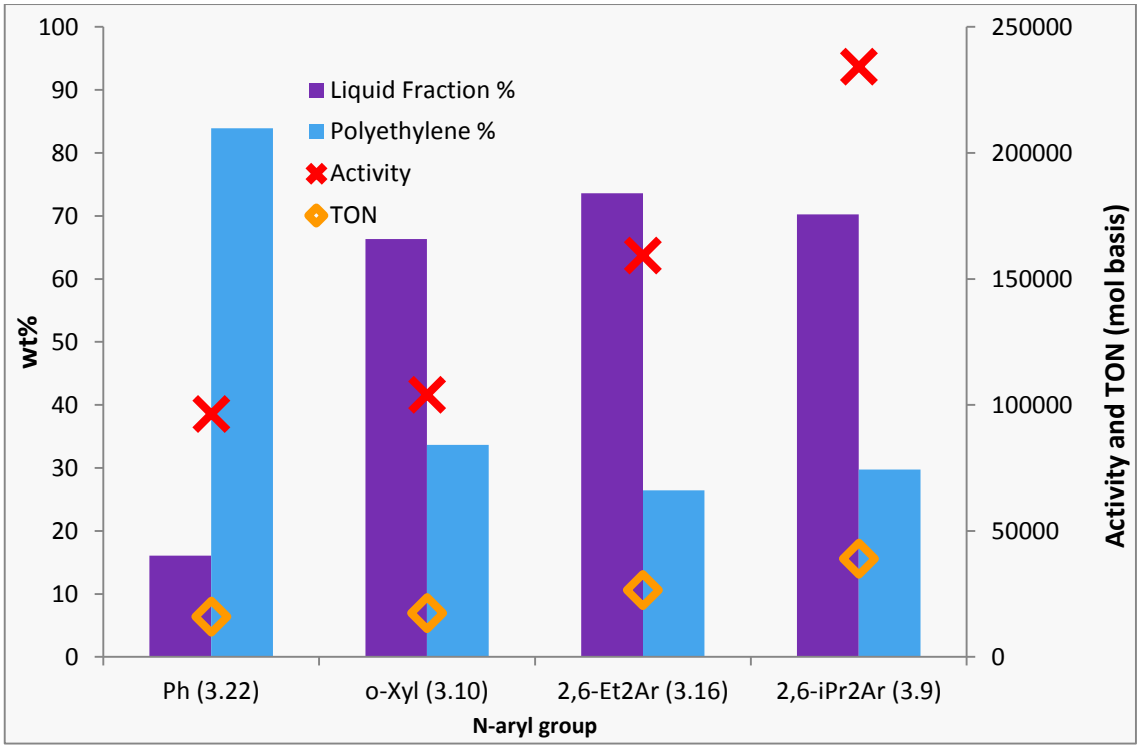

Graph 5.15: Comparison of catalytic activities and polymer/oligomer formation for ethylene oligomerisation systems utilising iminophosphine ligands with varying N-aryl groups (aryl = Ph, o-Xyl, 2,6-$Et_2C_6H_3$, 2,6-$^iPr_2C_6H_3$). Conditions: 5 µmol $Cr(acac)_3$, 1.2 eq. ligand, 500 eq. MMAO-3A, 70 mL PhCl, 60 °C, 40 bar C_2H_4, activation method **B**.

A clear correlation between steric bulk of the iminophosphine N-aryl substituent and activity of the resulting catalytic system is observed, with greater steric bulk increasing activity towards ethylene oligomerisation. This is similar to the trend observed for iminophosphines when the bulk of the P-alkyl substituents was increased (Section 5.4.1.1). However, compared to the trends found for the varying P-alkyl substituents, the link between N-aryl steric bulk and polymer/oligomer formation of the catalytic systems is not as clear cut. The N-Ph substituted iminophosphine (**3.22**) gives a primarily polymer producing system, while the other three ligands tested (**3.10**, **3.16** and **3.9**) all gave similar oligomer:polymer ratios (2.0 – 2.8). The presence of substituents in the *ortho* positions on the N-aryl group significantly alters the reactivity of the system, switching from polymerisation to oligomerisation.

Changing the steric bulk of the N-aryl group also has a major effect upon the liquid fraction selectivity of the catalytic system (Graph 5.16). On increasing the steric bulk of the *ortho*-aryl substituents, greater selectivity towards 1-hexene production is observed, while the formation of 1-octene is reduced. These observations match with the hypothesis that more bulky iminophosphine ligands inhibit the formation of the 9-membered metallacycle required to give 1-octene selectivity, therefore favouring ethylene trimerisation (Section 5.4.1.1). Notably, increasing the N-aryl steric bulk also reduces the formation of unwanted heavy oligomeric C_{15+} by-products, which is highly desirable for use in an industrial process.

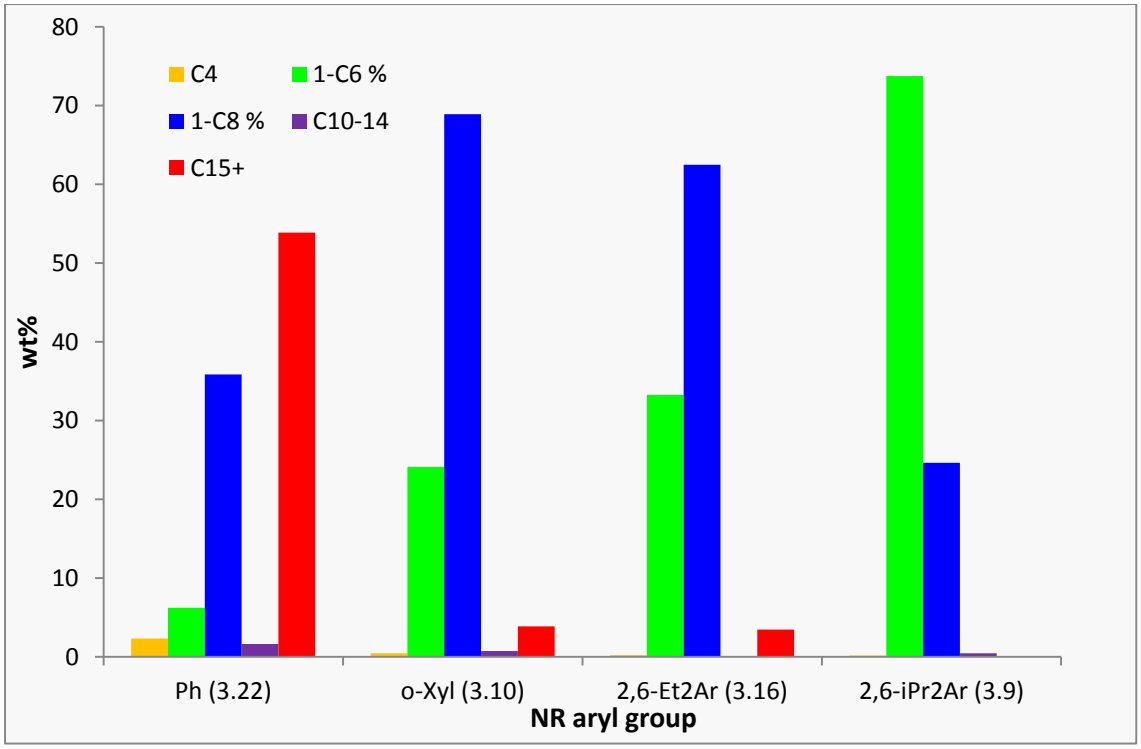

Graph 5.16: Comparison of liquid fraction oligomer selectivities for ethylene oligomerisation systems utilising iminophosphine ligands with varying N-aryl groups (aryl = Ph, o-Xyl, 2,6-$Et_2C_6H_3$, 2,6-$^{i}Pr_2C_6H_3$). Conditions: 5 µmol $Cr(acac)_3$, 1.2 eq. ligand, 500 eq. MMAO-3A, 70 mL PhCl, 60 °C, 40 bar C_2H_4, activation method **B**.

Screening runs with non-symmetrical imine N-aryl substituents were carried out, using ligand **3.1** (aryl = *ortho*-tolyl) and **3.25** (aryl = 2,5-$^{t}Bu_2C_6H_3$). Unsurprisingly, the N-*o*-tolyl system gave catalytic results very similar to those for the N-phenyl-substituted species, presumably due to the ability of the tolyl group to rotate away from the Cr centre, providing a similar steric presence as the N-phenyl species. The increased bulk of the N-2,5-$^{t}Bu_2C_6H_3$ iminophosphine (**3.25**) leads to the catalytic activity of this system being comparable to that achieved using the analogous N-2,6-$^{i}Pr_2C_6H_3$ derivative, albeit with more significant formation of C_{15+} oligomers and a lower activity. From these observations it is proposed that symmetrical and bulky N-aryl substituents are necessary for the formation of highly active iminophosphine-based ethylene *tri*- and *tetra*-merisation catalysts. Indeed, it has been shown that N-2,6-$^{i}Pr_2C_6H_3$ is the optimal imine N-substituent, offering both high activity (up to 234,000 mol/mol Cr h^{-1}) and *tri*- and *tetra*-merisation selectivity (98 % combined 1-hexene and 1-octene within the liquid fraction).

5.4.3 Effect of varying the iminophosphine C-backbone substituent on ethylene oligomerisation catalysis

Iminophosphines with various C-backbone substituents have been tested for their performance in ethylene oligomerisation systems. The effect of altering the C-substituent, from Ph to ^{t}Bu, upon catalysis was investigated using three ligand scaffolds (Figure 5.13); **R**(PPh_2)C=N(2-MeC_6H_4) (**3.1** and **3.2**), **R**(P^iPr_2)C=N(2,6-$Me_2C_6H_3$) (**3.10** and **3.21**) and **R**(P^iPr_2)C=N(2,6-$^iPr_2C_6H_3$) (**3.9** and **3.20**), where R = Ph, ^{t}Bu. The activity and oligomer/polymer formation results are compared in Graph 5.17.

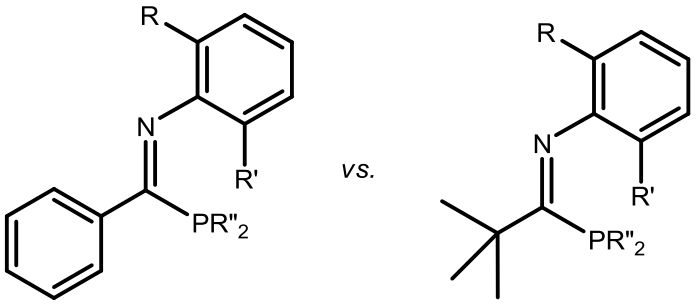

3.1: R = H, R' = Me, R" = Ph **3.2**: R = H, R' = Me, R" = Ph
3.10: R = R' = Me, R" = ^{i}Pr **3.21**: R = R' = Me, R" = ^{i}Pr
3.9: R = R' = ^{i}Pr, R" = ^{i}Pr **3.20**: R = R' = ^{i}Pr, R" = ^{i}Pr

Figure 5.13: The iminophosphine ligands bearing Ph and ^{t}Bu C-backbones tested in ethylene oligomerisation systems.

Changing the C-backbone substituent from Ph to ^{t}Bu affects both the steric and electronic properties of the iminophosphine ligands. It has been previously found that iminophosphines with ^{t}Bu backbone substituents have phosphine groups with stronger s-donor character (by measurement of $|^1J_{Se\text{-}P}|$ couplings of phosphine-selenides, Section 3.3.3.3), and weaker C=N bonds (measured by IR spectroscopy) than their Ph-substituted analogues. As well as differing electronic properties, there is a marked difference in the steric influence between ^{t}Bu and Ph groups. This means that, unfortunately, separating the steric and electronic effects of the C-backbone group with regard to their impact in catalytic systems is not trivial, and has not been carried out in this investigation. It is likely that the observed differences between the Ph and ^{t}Bu systems results from a combination of steric and electronic effects, but based upon the results obtained it is suggested that steric effects have the primary influence over catalytic behaviour.

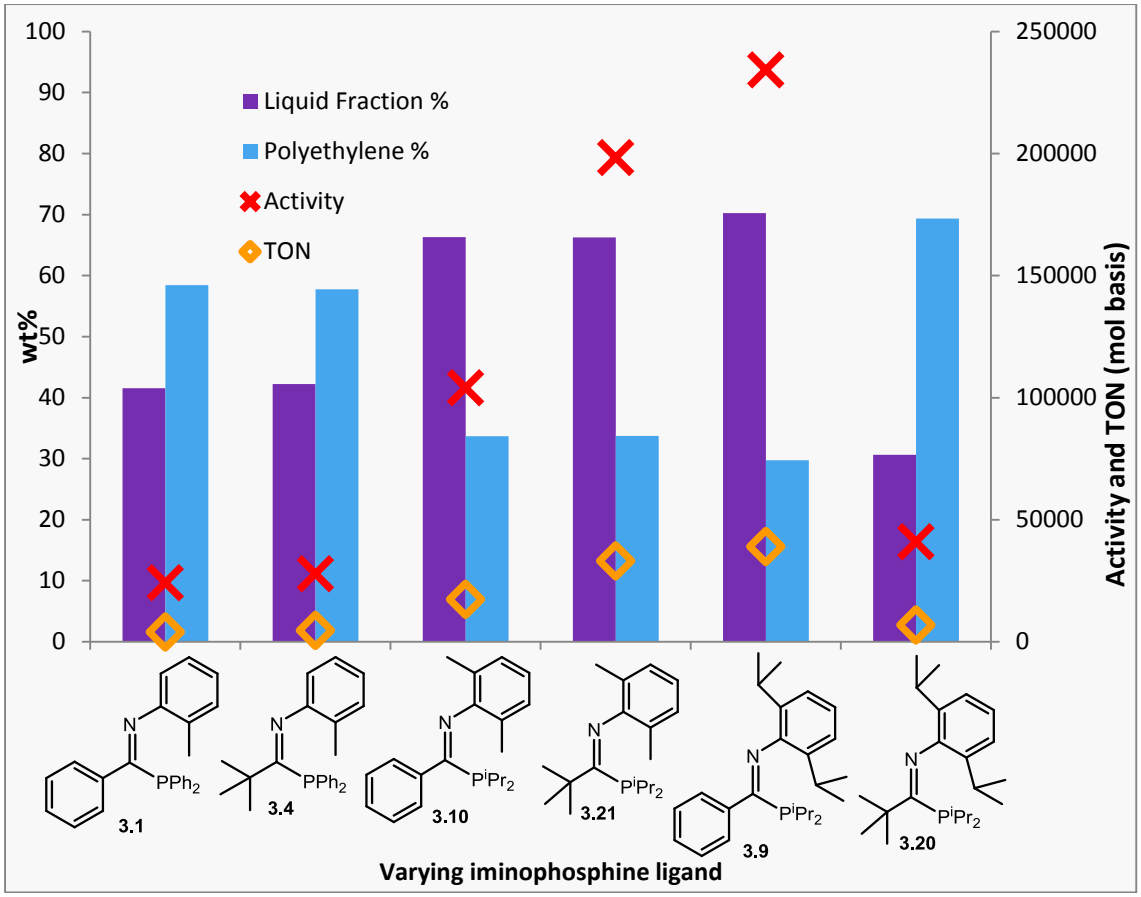

Graph 5.17: Comparison of catalytic activities and polymer/oligomer formation for ethylene oligomerisation systems utilising three iminophosphine scaffolds, each with varying C-substituents. Conditions: 5 µmol $Cr(acac)_3$, 1.2 eq. ligand, 500 eq. MMAO-3A, 70 mL PhCl, 60 °C, 40 bar C_2H_4, activation method **B**.

For each of the scaffolds investigated, the effect of changing the backbone upon catalysis varies, with the change in catalytic behaviour seemingly being dependant on the overall steric bulk of the ligand used. Upon changing the backbone of the **R**(PPh_2)C=N(2-MeC_6H_4) (**3.1** and **3.2**) scaffold from Ph to ^{t}Bu no change in catalytic activity or extent of oligomer formation was observed, as any differences are within the estimated error of the system (±5 %). When the performance of the systems with the **R**(P^iPr_2)C=N(2,6-$Me_2C_6H_3$) (**3.10** and **3.21**) ligands is compared, switching the backbone from ^{t}Bu to Ph is found to have little effect on the oligomer/polymer formation, but a jump in activity of the system is observed. The observed increase in activity caused by the ^{t}Bu group suggests that the more bulky backbone results in greater steric congestion around the Cr-centre, through forcing the N and P donor groups towards the metal (Figure 5.14), therefore promoting ethylene oligomerisation.

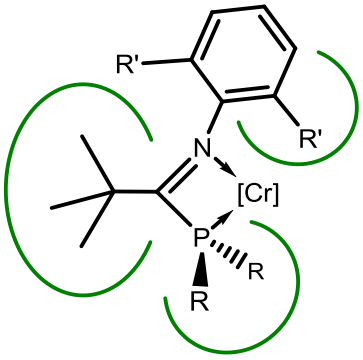

Figure 5.14: Influence of the ^{t}Bu-backbone group on the steric demands of an iminophosphine ligand on a Cr centre.

A similar steric effect upon oligomerisation catalysis was observed for bulky P-alkyl and N-aryl iminophosphines (Sections 5.4.1.1 and 5.4.2, respectively). Interestingly, the converse applies when the C-backbone is changed from Ph to ^{t}Bu for the **R**(P^{i}Pr$_2$)C=N(2,6-^{i}Pr$_2$C$_6$H$_3$) derivatives, causing both a large drop in activity, and a switch from oligomer to polymer production. For this highly bulky ^{t}Bu(P^{i}Pr$_2$)C=N(2,6-^{i}Pr$_2$C$_6$H$_3$) compound (**3.20**) it is hypothesised that too much steric bulk inhibits metallacycle formation at the Cr-centre in the catalytic system, halting selective oligomerisation activity. Overall, with regard to activity and oligomer production ligand **3.9** (Ph(P^{i}Pr$_2$)C=N(2,6-^{i}Pr$_2$C$_6$H$_3$)) still appears to be the optimal compound for ethylene oligomerisation.

Upon examining the effect of altering the C-backbone group on the oligomer liquid fraction selectivities, a similar trend to that observed for the change in catalytic activities is observed (Graph 5.18). Alteration of the C-substituent from Ph to ^{t}Bu on the **R**(PPh$_2$)C=N(2-MeC$_6$H$_4$) scaffold (**3.1** and **3.2**) does not cause a major change in product selectivity for these systems, with both the C-^{t}Bu (**3.2**) and C-Ph (**3.1**) variants giving essentially non-selective oligomer products. Both of the **R**(P^{i}Pr$_2$)C=N(2,6-Me$_2$C$_6$H$_3$) derivatives (**3.10** and **3.21**) yield systems that produce primarily 1-hexene and 1-octene, with the more sterically demanding C-^{t}Bu-substituted iminophosphine (**3.21**) giving products with a lower OTH ratio (compared to **3.10**), as has been observed for other systems with bulky ligands (Section 5.4.1.1). The same decrease in tetramerisation activity upon switching from C-Ph to C-^{t}Bu is displayed by the **R**(P^{i}Pr$_2$)C=N(2,6-^{i}Pr$_2$C$_6$H$_3$) compounds, again presumably due to the increased steric bulk around the Cr-centre as described for the **R**(P^{i}Pr$_2$)C=N(2,6-Me$_2$C$_6$H$_3$) system. The change of the C-backbone substituent on the **R**(P^{i}Pr$_2$)C=N(2,6-^{i}Pr$_2$C$_6$H$_3$) scaffold from Ph (**3.9**) to ^{t}Bu (**3.20**) also caused a significant increase in the production of C$_{15+}$ oligomers; consequently iminophosphine **3.20** (^{t}Bu(P^{i}Pr$_2$)C=N(2,6-^{i}Pr$_2$C$_6$H$_3$)) was not used in further optimisation studies, with **3.9** (Ph(P^{i}Pr$_2$)C=N(2,6-^{i}Pr$_2$C$_6$H$_3$)) remaining the optimal iminophosphine scaffold for ethylene *tri*- and *tetra*-merisation catalysis.

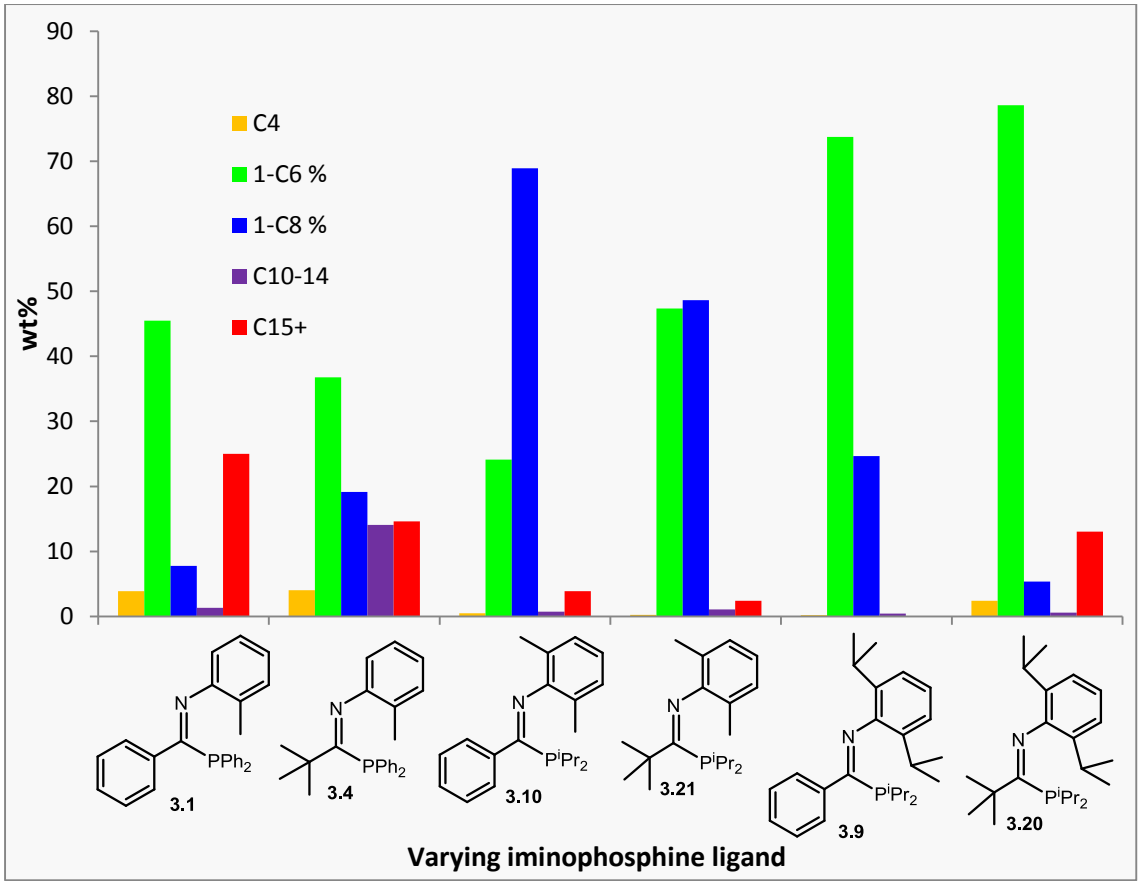

Graph 5.18: Comparison of liquid fraction oligomer selectivities for ethylene oligomerisation systems utilising three iminophosphine scaffolds, each with varying C-substituents. Conditions: 5 µmol $Cr(acac)_3$, 1.2 eq. ligand, 500 eq. MMAO-3A, 70 mL PhCl, 60 °C, 40 bar C_2H_4, activation method **B**.

5.5 Optimisation of the Catalytic Conditions Used for Iminophosphine-based Selective Ethylene Oligomerisation Systems.

5.5.1 Optimisation of ligand equivalents used in PCN ethylene oligomerisation systems

All of the iminophosphine-based oligomerisation tests reported so far in this thesis have used 1.2 equivalents of ligand relative to the chromium loading of the system. Previous studies of PNP-based trimerisation systems have shown this catalyst loading is not necessarily optimal. For example, in 2008 Jiang *et al.* reported that their "triple-site" (*i.e.* contains three PNP units capable of coordinating to a metal centre) PNP ligand, $N(C_2H_4N(PPh_2)_2)_3$ (Figure 5.15), gave the best ethylene oligomerisation performance at a Cr:L ratio of 2:1 (1.5 PNP units per chromium).[30] From their work, Jiang *et al.* concluded that an excess of PNP sites is required to give optimal catalytic conditions, in order to ensure that all Cr-sites are coordinated in the catalytic system.

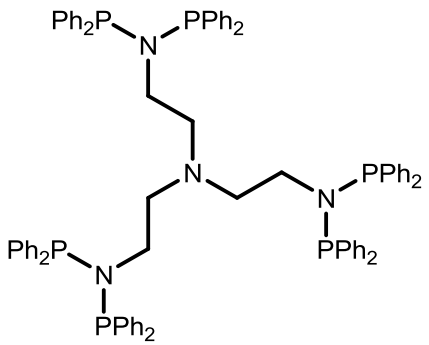

Figure 5.15: The "triple-site" PNP ligand ($(N(C_2H_4N(PPh_2)_2)_3)$) synthesised by Jiang *et al.*[30]

Based upon this study by Jiang *et al.* it was decided to probe the effect of the amount of PCN ligand present on the behaviour of iminophosphine-based catalytic systems. In this investigation the amount of iminophosphine used in the catalytic reaction was varied, while all the other parameters were kept constant. Tests were carried out with ligand loadings ranging from 0 to 2.4 equivalents, relative to chromium (Graph 5.19).

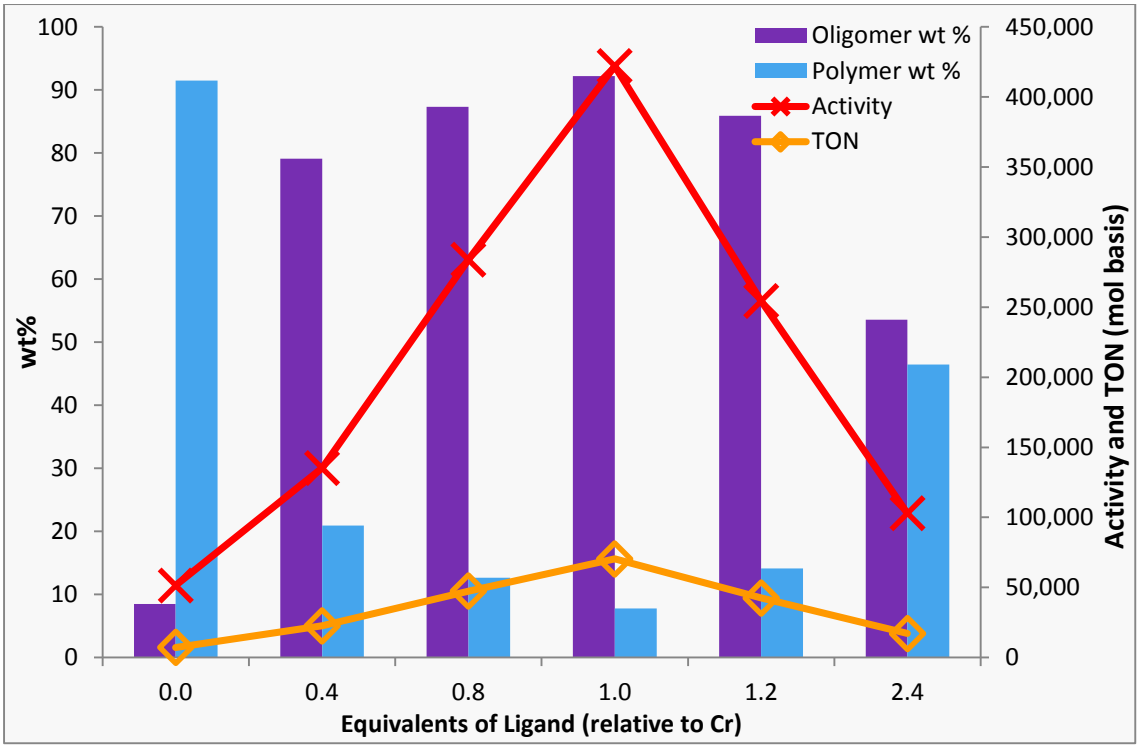

Graph 5.19: Comparison of ethylene oligomerisation systems using **3.6**, with 0, 0.4, 0.8, 1.0, 1.2 and 2.4 equivalents of ligand. Conditions: 5 µmol $Cr(acac)_3$, 500 eq. MMAO-3A, 70 mL PhCl, 60 °C, 40 bar C_2H_4, activation method B.

A significant influence of the amount of PCN ligand upon the behaviour of the catalyst was found affording a classical "volcano"-type activity plot (Graph 5.19). A clear optimal ratio is reached at 1 equivalent of ligand, giving rise to a system that gives both the least polymer, and the highest activity (422,000 mol/mol Cr h^{-1}, 8 % polymer). A major change in reactivity of the system occurs between 0 and 0.4 equivalents of iminophosphine, suggesting that even a small amount of ligand is capable of producing a highly active oligomerisation species, which competes with an active polymerisation species (**A**, Figure 5.16) that is responsible for the polymer formation in the blank run with no ligand present (*i.e.* 0.0 equivalents of ligand). The optimal performance of the catalytic system reached at 1.0 equivalent of ligand is presumably due to all of the chromium centres being bound to the ligands, yielding catalytically active species (**B**, Figure 5.16), hence resulting in improved oligomerisation activity.

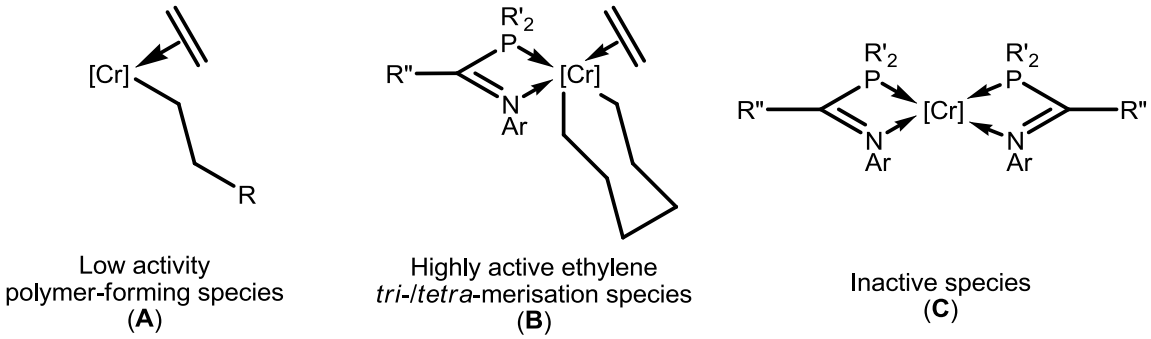

Figure 5.16: Proposed types of Cr species present in PCN ethylene oligomerisation systems at different L:Cr ratios

When the amount of ligand is increased above 1 equivalent, a sharp drop in catalytic activity occurs, accompanied by a rise in polymer formation. Upon addition of 2.4 equivalents of ligand to the system the extent of polymer formation increases to 46 %, and the activity drops to 103,000 mol/mol Cr h^{-1}. This decrease in catalyst performance with increased ligand loadings suggests that excess ligand inhibits oligomerisation catalysis, potentially through the formation of inactive Cr(ligand)$_2$ species (**C**, Figure 5.16). The formation of Cr(ligand)$_2$ species has been documented by Rosenthal *et al.* for their Cr(PNPN) complexes (Figure 5.17), suggesting that the formation of species such as **C** (Figure 5.16) may be possible.[31] However, Rosenthal *et al.* report that their Cr(PNPN) complexes can be used as catalyst precursors for ethylene trimerisation processes, unlike the hypothetical inactive Cr(PCN)$_2$ species depicted in Figure 5.16. Despite the similarities of the two systems, this comparison should be treated with caution, due to the significant differences between the PCN (L_2) and PNPN (LX) ligands. Furthermore, the PNPN ligands are capable of adopting a number of bidentate coordination modes, compared to the iminophosphine ligands which can only adopt a single bidentate P,N coordination mode.

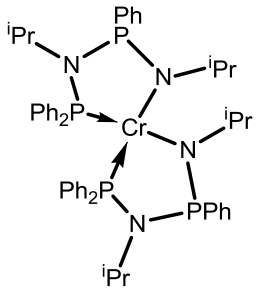

Figure 5.17: Cr(PNPN)$_2$ complex synthesised by Rosenthal *et al.*[31]

Analysis of the liquid fraction selectivities obtained from the iminophosphine-based oligomerisation systems with varying chromium:ligand ratios over the range 0-2.4 shows that there is little change in the oligomer product distribution as the number of equivalents of ligand is altered. This is suggestive of only one Cr(PCN) catalytic species (*e.g.* Figure 5.16, **B**) being responsible for the oligomerisation activity of the system. It is thought that the ligand

concentration is responsible for controlling the amount of this active species present in the catalytic system, hence giving rise to the variation in activity observed with varying Cr:ligand ratios (Graph 5.19).

From this narrow ligand equivalents study, it has been shown that PCN-based ethylene oligomerisation systems are most effective when a 1:1 ratio of chromium to iminophosphine is used. A similar effect was observed by Kuhlmann *et al.* for their *N*-cyclohexyl substituted PNP ligand ($Ph_2PN(C_6H_{10})PPh_2$).[3] In this work Kuhlmann reported that upon decreasing the Cr:PNP ratio from 1.5 to 1.0, the activity of the resulting catalyst increased threefold (from 1,370,000 mol/mol Cr h^{-1} to 3,987,000 mol/mol Cr h^{-1}), suggesting a similar active *tri-*/*tetra*-merisation species to that proposed here for the related PCN ligand, namely **B** (Figure 5.16). Based upon this report by Kuhlmann, and the findings in this thesis, a Cr:L ratio of 1.0 has been used in all further testing described in this report.

5.5.2 Conversion of catalyst screening conditions to industrially relevant conditions

The catalysis screening conditions used so far in this investigation have proved that iminophosphine-based ethylene oligomerisation systems are capable of promoting highly selective *tri-* and *tetra*-merisation. Despite this, these operating conditions used to test the PCN ligands in catalytic systems are not compatible with larger scale industrial settings for three primary reasons: *a)* chlorobenzene is not suitable for use as a solvent on a large scale, due to the potential for radical reactions to occur with chlorinated solvents, forming HCl; *b)* high Cr/ligand loadings are costly, and can give rise to high levels of product contamination; and *c)* the use of $Cr(acac)_3$ as a chromium source, due to its insolubility in alkane solvents. If iminophosphines are to be used on an industrial scale ethylene oligomerisation process, these factors must be changed to more industrially suitable conditions. To this end, a series of tests were carried out using ligand **3.9** ($Ph(P^iPr_2)C=N(2,6\text{-}^iPr_2C_6H_3)$), to develop catalytic reaction conditions for ethylene *tri-* and *tetra*-merisation that are industrially compatible.

In this context, reactions were carried out in which the Cr(III) source, the reaction solvent and the chromium loading of the catalytic system were systematically changed (Graph 5.20). Firstly, the Cr(III) source was switched from $Cr(acac)_3$ to Cr(2-ethylhexanoate)$_3$ ($Cr(2\text{-EH})_3$) (Graph 5.20, column i vs. column ii), something that caused the activity to halve, and the polymer formation to increase by a factor of four. Despite this decrease in catalyst performance, the selectivity of the system was retained, producing 97 % combined 1-hexene and 1-octene within the liquid fraction.

Following the change in Cr source, a test was run utilising methylcyclohexane (MCH) as the solvent, while using a $Cr(2\text{-EH})_3$/**3.9**/MMAO-3A initiator package. The use of MCH as a

solvent brings the Cr(PCN)-based catalytic systems into line with the operating conditions for the highly active Cr(PNP) systems reported by workers from Sasol.[32] Despite previous reports of Cr-based oligomerisation processes giving highly active oligomerisation catalysis, in this thesis the use of MCH was shown to further reduce the catalytic activity of the system at high Cr loadings (Graph 5.20, column iii). The catalytic activity was observed to reduce by a factor of four in MCH, compared to the analogous chlorobenzene system, giving an activity of just 25,000 mol/mol Cr h^{-1}.

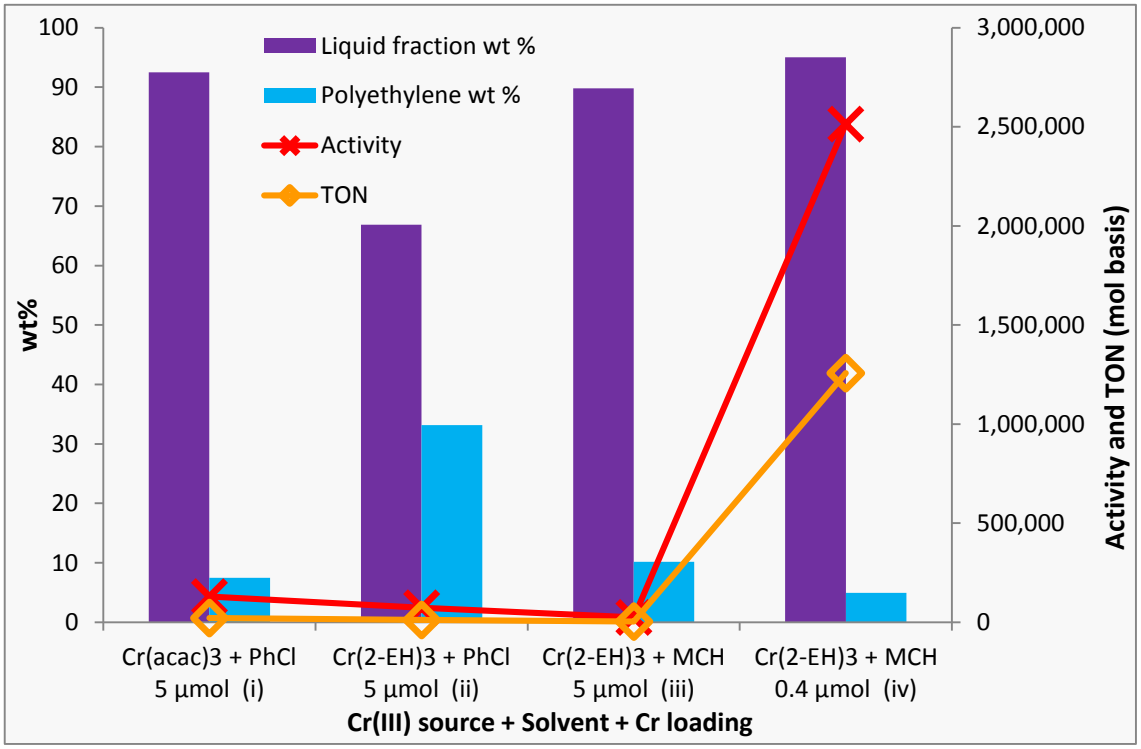

Graph 5.20: Comparison of ethylene oligomerisation systems using **3.9** with varying Cr(III) sources ($Cr(acac)_3$, $Cr(2\text{-}EH)_3$), solvents (PhCl and MCH) and Cr loadings (5 µmol and 0.4 µmol). Conditions: 1.0 eq. ligand, 500 eq. MMAO-3A, 70 mL solvent, 60 °C, 40 bar C_2H_4, activation method **B**.

Despite this poor result, one final run was carried out, in which the Cr(III) loading was reduced to industrially relevant levels (0.4 µmol Cr(III) in 70 mL solvent). Remarkably, this final run demonstrated an increased catalytic activity of two orders of magnitude compared to the previous test run using 5 µmol catalyst in MCH, yielding an activity of 2,500,000 mol/mol Cr h^{-1}, and the lowest polymer formation of all the runs carried out, only 5 % wt (Graph 5.20, column iv). This unprecedented jump in activity puts this iminophosphine-based ethylene oligomerisation system on a par with the best literature PNP-systems published by Wass *et al.* and Wasserscheid *et al.*[1,3] This increase in activity at low chromium loadings is thought to be due to a greater oxygen concentration, relative to the chromium concentration. It has been previously determined that in this reactor set up the ethylene feed used contained an oxygen concentration of 0.6 ppm. A recent patent from Sasol revealed that the presence of oxygen in

ethylene oligomerisation systems is vital, with catalytic activity of their Cr(PNP) tetramerisation systems varying dramatically based upon the amount of oxygen present in the reaction.[13] This oxygen dosing phenomena will be investigated in detail regarding Cr(PCN)-based systems in Section 5.5.6. Based on the dramatic increase in activity of the $Cr(2\text{-}EH)_3$/**3.9**-based system at 0.4 μmol catalyst loading, it was assumed that these small scale conditions used for catalysis are roughly optimal, therefore further optimisation of the system was based upon this $Cr(2\text{-}EH)_3$ in MCH catalytic system, utilising iminophosphine **3.9**.

5.5.3 Optimisation of reaction temperature of the PCN ethylene oligomerisation system

Previously, a small scale test was carried out to investigate the effect of temperature on a non-optimal iminophosphine-based ethylene oligomerisation system (Section 5.2.3). These tests revealed that 60 °C is roughly the optimal temperature for catalysis, but only three temperatures were tested, which gave only a rough picture of how temperature effects the catalytic process. Consequently, a more detailed set of tests were undertaken using the optimised conditions described in Section 5.5.1 and ligand **3.9** ($Ph(P^iPr_2)C{=}N(2,6\text{-}^iPr_2C_6H_3)$). Here, the reaction temperature was varied in 10 °C intervals between 50 and 90 °C, while the ethylene pressure was adjusted in order to maintain a constant ethylene concentration in solution (4.2 mol L^{-1}, as described in Section 5.1.1.1). The ensuing relationship between temperature and catalytic activity and oligomer/polymer formation is summarised in Graph 5.21.

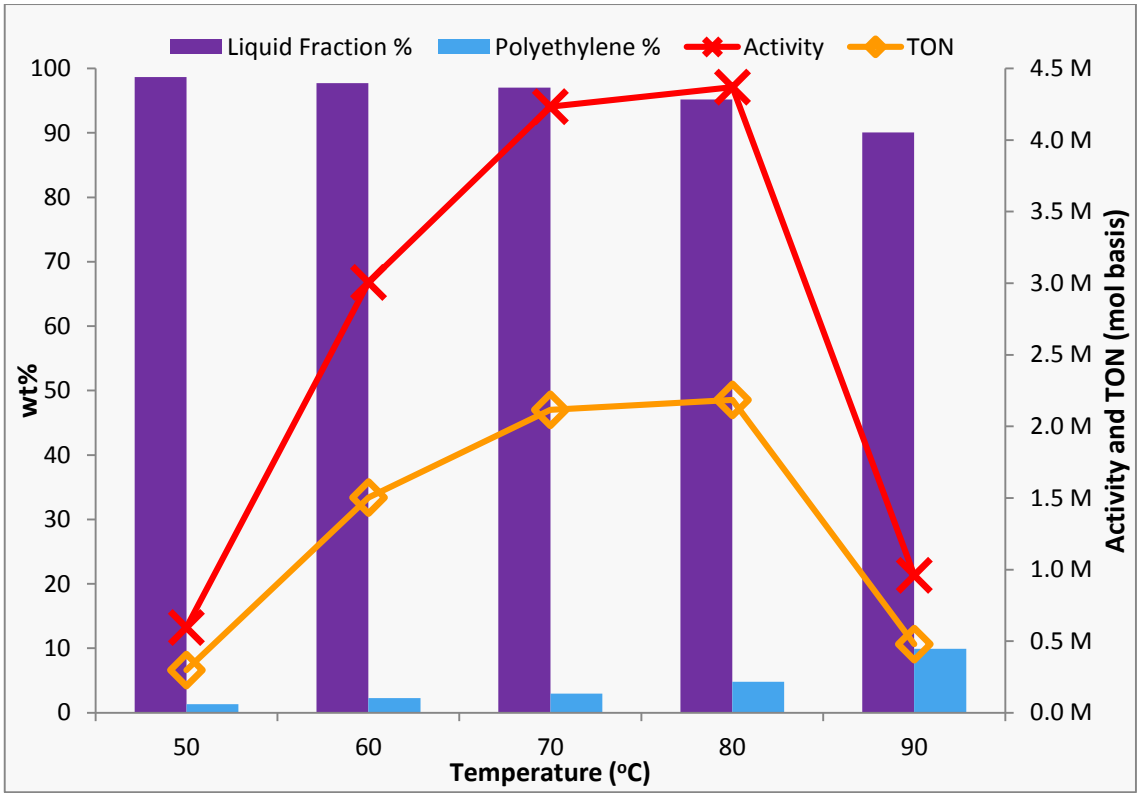

Graph 5.21: Comparison of ethylene oligomerisation systems utilising **3.9** at varying temperatures (50, 60, 70, 80 and 90 °C). Conditions: 0.4 µmol $Cr(2\text{-}EH)_3$, 1.0 eq. ligand, 500 eq. MMAO-3A, 70 mL MCH, activation method **B**.

A clear increase in catalytic activity is observed for runs undertaken between 50 and 80 °C, with the activity plateauing at temperatures around 70 °C. Upon increasing the temperature to 90 °C the activity sharply falls off, something suggestive of catalyst decomposition occurring at this elevated temperature. Upon increasing the reaction temperature from 50 to 80 °C the polymer formation of the catalytic systems also increases. A particular jump in polymer production between 80 and 90 °C is seen, with a doubling of the amount of polymer formed (from 5 – 10 %). It is assumed that the catalyst decomposition occurring at 90 °C results in the formation of a non-selective ethylene polymerisation species in the system, which gives rise to the increased polymer formation.

Analysis of the liquid fraction products from the catalysis at the varying temperatures displays the expected trend of increasing 1-hexene and decreasing 1-octene production with increasing temperature from 50 – 90 °C (Graph 5.22), an effect previously discussed in Section 5.2.3.[33] A small increase in the production of $C_{10\text{-}14}$ oligomers is also observed between 50 and 80 °C (from 0.4 – 2.8 %), suggestive of the system forming products resulting from greater oligomer incorporation at elevated temperatures. This increase in the range of oligomer by-products is relatively small and does not change the conclusion that 70 °C is likely to be the

optimum temperature for ethylene *tri*- and *tetra*-merisation catalysis to be carried out using iminophosphine compounds.

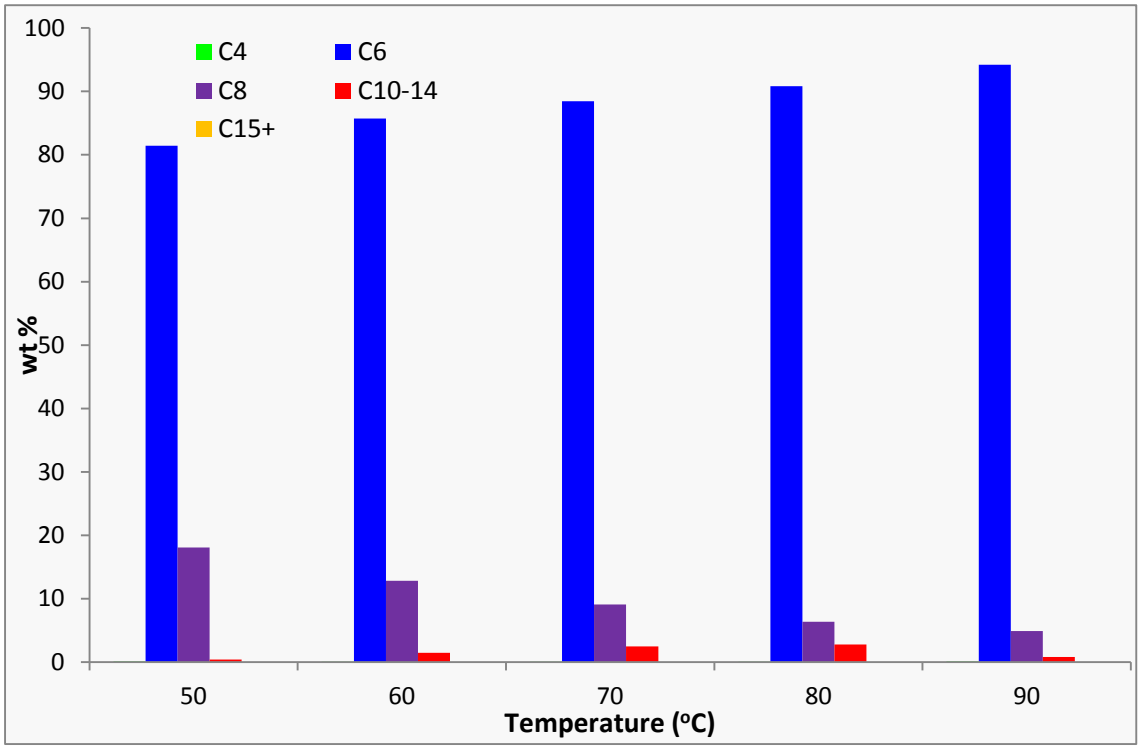

Graph 5.22: Comparison of liquid fraction selectivities of ethylene oligomerisation systems utilising **3.9** at varying temperatures (50, 60, 70, 80 and 90 °C). Conditions: 0.4 µmol $Cr(2\text{-}EH)_3$, 1.0 eq. ligand, 500 eq. MMAO-3A, 70 mL MCH, activation method **B**.

5.5.4 Optimisation of ethylene pressure for PCN ethylene oligomerisation systems

Until now it has been assumed that 40 bar of ethylene is the optimal pressure to carry out ethylene oligomerisation catalysis using iminophosphine ligands, based upon previous studies by Hanton *et al.* at Sasol.[34] Therefore it was decided to investigate the effect of varying ethylene pressure on the performance of iminophosphine-based oligomerisation systems. The reaction pressure was varied in roughly 5 bar intervals, with each run being undertaken at 70 °C, based on the results of the temperature optimisation study reported in Section 5.5.3. The influence of varying ethylene pressure on the catalytic activity, and polymer and oligomer formation of the oligomerisation system is displayed in Graph 5.23.

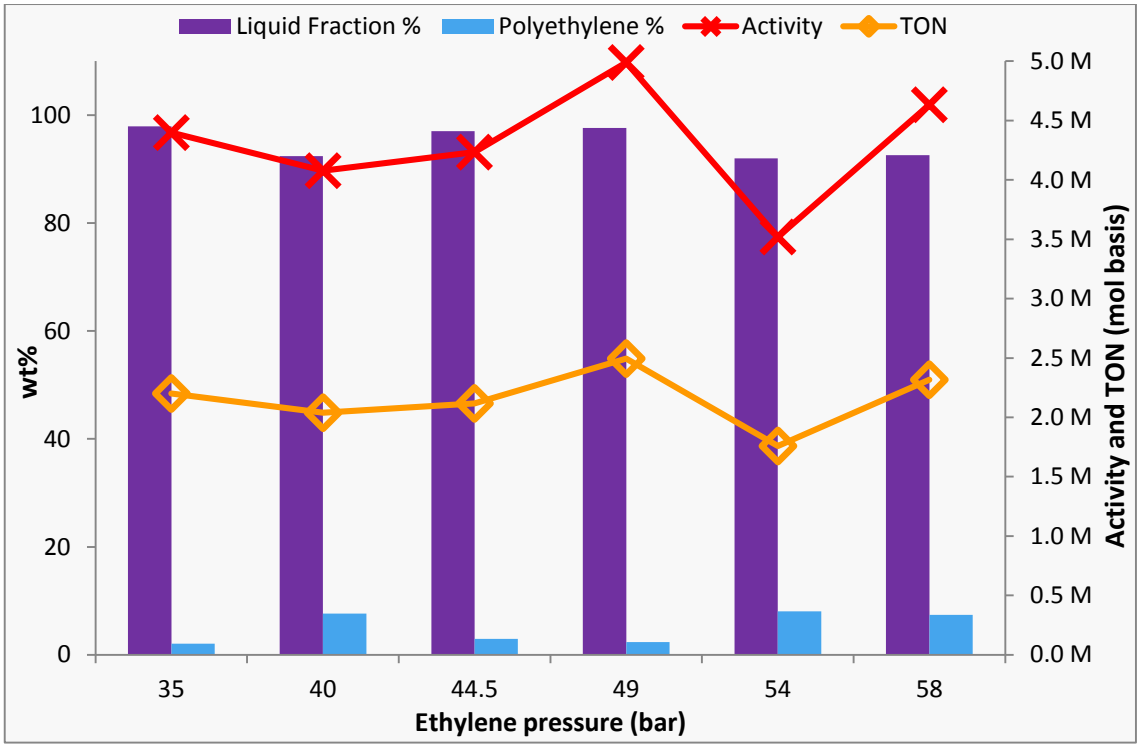

Graph 5.23: Comparison of catalytic activities and polymer/oligomer formation for ethylene oligomerisation systems utilising ligand **3.9** at 35, 40, 44.5, 49, 54 and 58 bar ethylene pressure. Conditions: 0.4 µmol $Cr(2\text{-}EH)_3$, 1.0 eq. ligand, 500 eq. MMAO-3A, 70 mL MCH, 60 °C, activation method **B**.

At first glance the data in Graph 5.23 show no continuous trend between 35 and 58 bar, due to the drop in activity, and increase in polymer formation, observed at 54 bar ethylene, a pressure that is above the critical pressure (P_c) of ethylene (50.4 bar).[35] Undertaking catalyst testing at above the P_c of ethylene can cause problems with the flow of ethylene into the reactor during the reaction,* hence it is suggested that the runs above this pressure cannot be directly compared with reactions at lower pressures. If the runs at above ethylene's P_c (54 and 58 bar) are discounted, a general increase in activity upon increasing the ethylene pressure from 40 to 49 bar is observed (giving rise to activities of up to 4,990,000 mol/mol Cr h^{-1} at 49 bar), matching the trends observed by Walsh *et al.* for their PNP-systems.[36] In contrast, no trend is seen between the C_2H_4 pressure and the degree of polymer formation, with all of the runs producing 2-8 % polymer.

Despite the lack of overall trend linking activity and polymer formation data with ethylene pressure, correlations between pressure and oligomer selectivity are apparent in the liquid fraction data (Graph 5.24). An increase in pressure correlates with an increase in 1-octene formation, and a decrease in the production of 1-hexene and C_{15+} oligomers. Together this is

* Problems are thought to be due to the irregularity of the flow of ethylene caused by the gas regulators used in the catalysis set up.

indicative of a metallacycle mechanism in which 1-hexene formation is a first order process (rather than a Cossee-Arlman-type process), while 1-octene formation is second order with respect to ethylene (Scheme 5.4). This matches the link between pressure and OTH ratio reported by Overett *et al.* concerning their Cr(PNP) ethylene tetramerisation systems.[37] In conclusion, it is apparent that 49 bar is the optimal ethylene pressure at which to run this iminophosphine-based selective ethylene oligomerisation system.

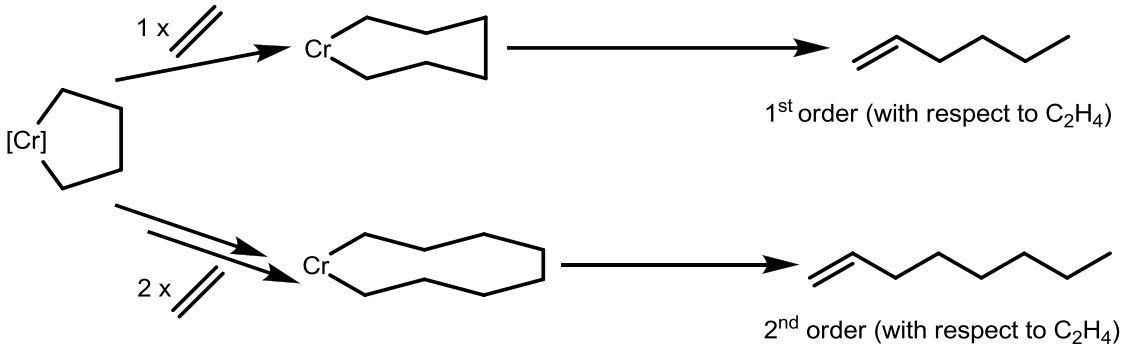

Scheme 5.4: Comparison of the 1st order ethylene trimerisation process, versus the 2nd order ethylene tetramerisation process (with respect to C_2H_4).

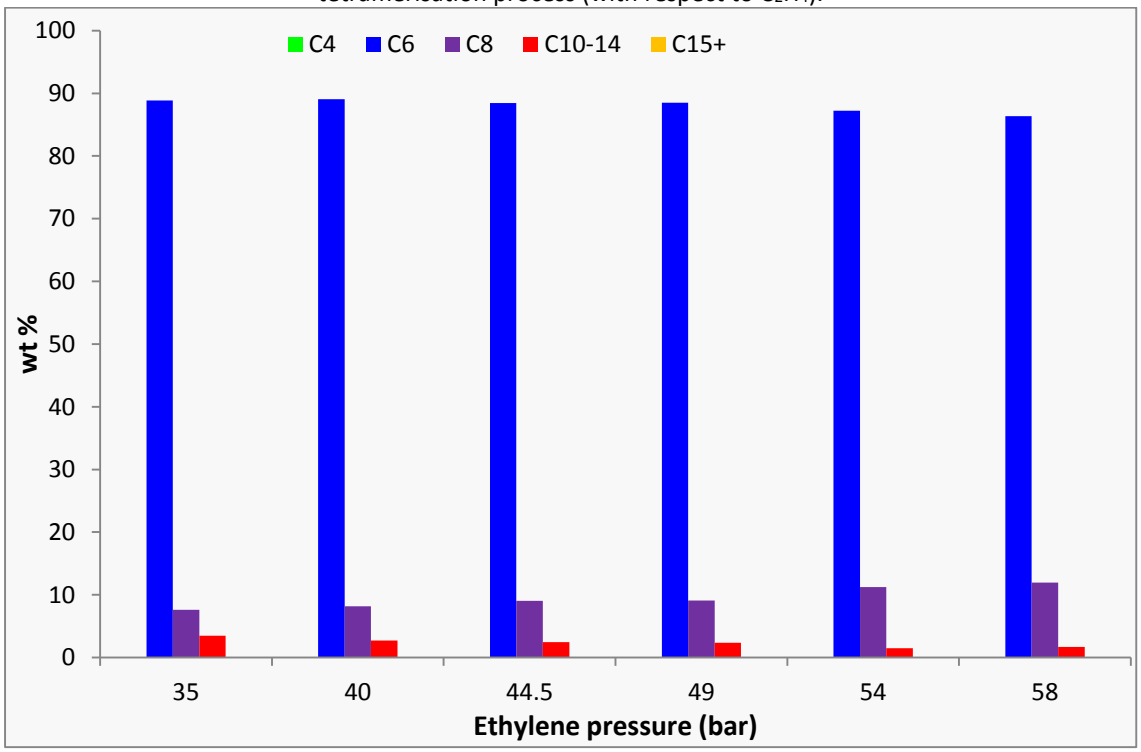

Graph 5.24: Comparison of liquid fraction selectivities for ethylene oligomerisation systems utilising ligand **3.9** at 35, 40, 44.5, 49, 54 and 58 bar ethylene pressure. Conditions: 0.4 µmol $Cr(2\text{-}EH)_3$, 1.0 eq. ligand, 500 eq. MMAO-3A, 70 mL MCH, 60 °C, activation method **B**.

5.5.5 Application of polymer minimisation techniques to ethylene oligomerisation systems under industrially relevant conditions

In order to further improve the performance of the iminophosphine-based oligomerisation systems a series of tests were carried out using various additives known to reduce polymer formation in ethylene oligomerisation processes. To this end, tests were carried out adding either H_2, or $ZnEt_2$, both of which are known to reduce the extent of polymer formation in ethylene oligomerisation processes; their use has been previously described in Section 5.3.4.[24] All of the catalysis testing described in this section was carried out by Dr David Smith of Sasol Technology UK, using a 1.2 L autoclave, using 210 mL MCH as solvent, while retaining all the other experimental procedures (Section 5.1). The runs were carried out under 40 bar ethylene pressure, at 60 °C with a Cr loading of 1.25 µmol and 1 equivalent of the iminophosphine **3.9**.

Three runs were carried out with varying amounts of H_2 added to the headspace of the reactor at the start of the reaction: 0, 0.5 and 2 bar H_2. The addition of hydrogen showed little effect on the activity of the catalytic systems (Graph 5.25). Similarly, no change in the amount of polymer formed was observed in the presence of 0.5 bar H_2 compared to the standard run with no H_2. Upon the addition of 2 bar H_2 to the catalytic system a slight decrease in catalytic activity was observed (from 3,600,000 to 3,300,000 mol/mol Cr h^{-1}) and, most surprisingly, the extent of polymer formation increased (from 3.6 to 6.2 %). This increase in polymer production with the addition of H_2 contradicts the results of previous experiments to minimise the extent of polymer formation using preformed Cr-iminophosphine catalyst precursors (Section 5.3.4), in which the extent of polymer formation almost halved when H_2 was added to the catalysis reaction. It is thought that the lack of polymer reduction observed upon the addition of H_2 to the Cr-**3.9**-based system may be due to the already low levels of polymer formation, meaning that any effect of H_2 upon the system is small, and hence lies within the error of the experimental setup.

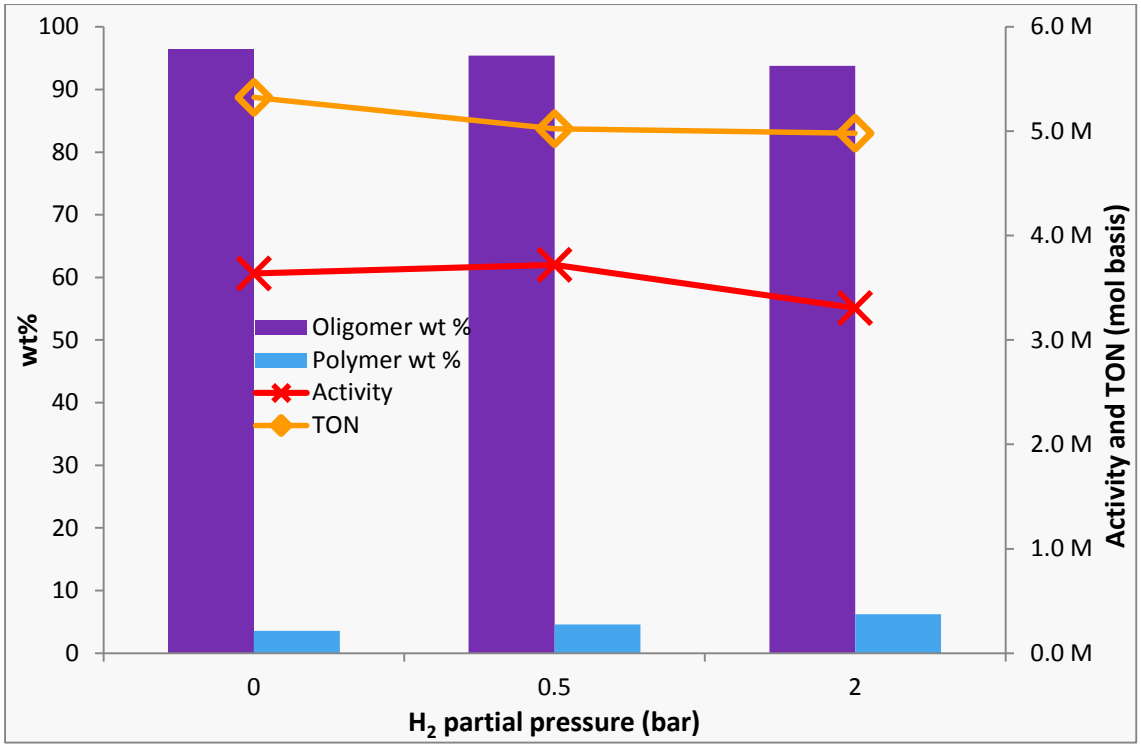

Graph 5.25: Comparison of catalytic activities and polymer/oligomer formation for ethylene oligomerisation systems utilising ligand **3.9**, with 0, 0.5 and 2 bar of H_2 added to the reaction. Conditions: 1.25 µmol $Cr(2\text{-}EH)_3$, 1.0 eq. ligand, 500 eq. MMAO-3A, 210 mL MCH, 60 °C, 40 bar C_2H_4, activation method **B**.

Since the addition of H_2 was not found to reduce the extent of polymer formation, instead the effect of $ZnEt_2$ on the ethylene PCN-based oligomerisation system was investigated. The role of $ZnEt_2$ as a chain transfer agent in ethylene oligomerisation reactions has been previously discussed (Section 5.3.4).[25] Four runs were carried out with varying amounts of $ZnEt_2$ added to the autoclave (0, 100, 200, and 400 equivalents), prior to the addition of the activated catalyst, and the data from these runs are compared in Graph 5.26. It is apparent that the addition of 100 equivalents of $ZnEt_2$ has succeeded in reducing the extent of polymer formation during catalysis, lowering the polymer weight percentage produced from 3.6 to 1.9 %. The addition of more than 100 equivalents of $ZnEt_2$ to the reaction had no further effect upon the extent of polymer production. However, it was found that the addition of 200 and 400 equivalents of $ZnEt_2$ did have an effect upon the activity of the catalytic system. The presence of 200 equivalents of $ZnEt_2$ gave an increase in catalytic activity (from 3,600,000 to 5,100,000 mol/mol Cr h^{-1}), while the addition of 400 equivalents of the organozinc species gave a marginally lower activity than the optimum system (4,500,000 mol/mol Cr h^{-1}). It is thought that this reduction in catalytic activity caused by 400 equivalents of zinc may be due to the zinc-catalysed chain transfer reaction competing with the Cr-mediated *tri*- and *tetra*-merisation process, hence reducing the overall oligomerisation activity of the system.

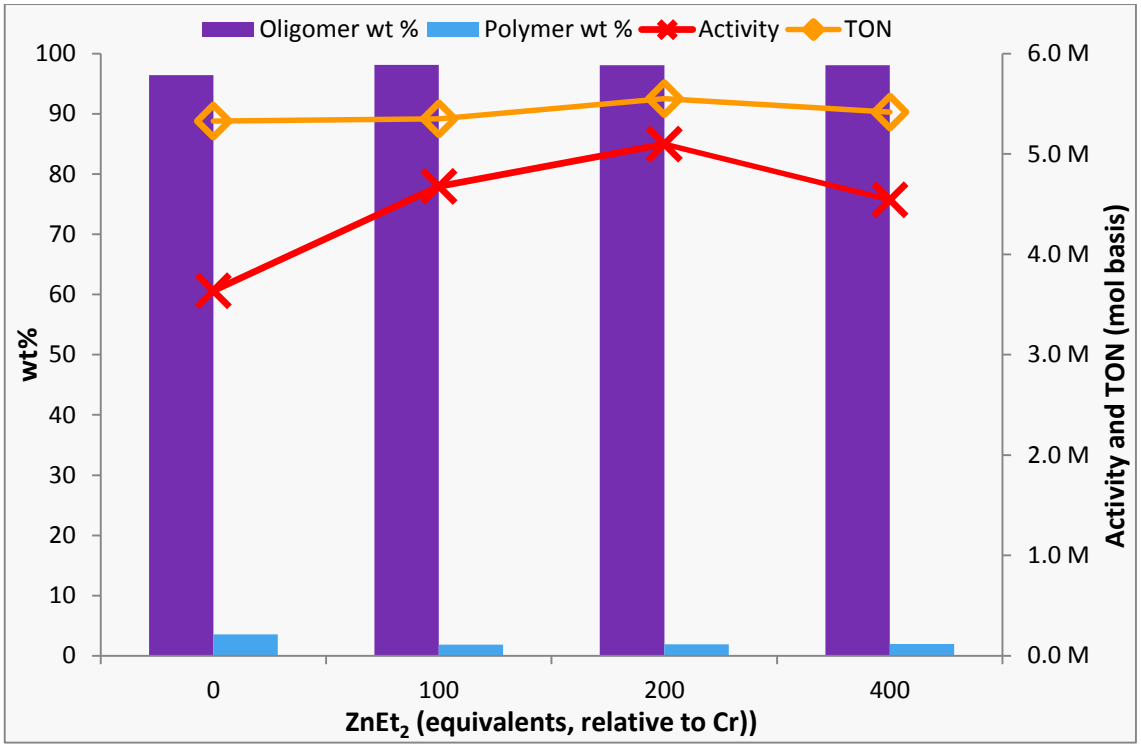

Graph 5.26: Comparison of ethylene oligomerisation systems using iminophosphine **3.9**, with varying amounts of $ZnEt_2$ added (0, 100, 200, and 400 equivalents, relative to Cr). Conditions: 1.25 µmol Cr(2-EH)$_3$, 1.0 eq. ligand, 500 eq. MMAO-3A, 210 mL MCH, 60 °C, 40 bar C_2H_4, activation method B.

It was found that the test run employing ligand **3.9** and 200 equivalents of $ZnEt_2$ (Graph 5.26) yielded the best catalytic performance achieved so far in this thesis, giving an activity of 5,100,000 mol/mol Cr h^{-1}, only 1.9 % polymer formation and a liquid fraction combined selectivity of 96 % towards production of 1-hexene and 1-octene. Analysis of the reaction liquid fraction shows that the presence of $ZnEt_2$ has no effect on the selectivity of the system, meaning that the addition of the zinc chain transfer agent only has positive effects on the system. These results make this iminophosphine-based selective ethylene *tri*- and *tetra*-merisation system arguably better than all of the *tri*- and *tetra*-merisation systems published in the literature, with the exception of Sasol's PNP-based tetramerisation process.[14,32]

5.5.6 Impact of O_2 upon catalysis for an industrially relevant system

It has recently been discovered by workers from Sasol that the presence of small amounts of oxygen (in the order of 0.1-1 ppm) are required for Cr-mediated ethylene *tri*- and *tetra*-merisation processes to function successfully.[13] Sasol have proven that when oxygen was completely excluded from a range of Cr-based ethylene oligomerisation systems no ethylene *tri*- and *tetra*-merisation activity was observed. So far during the investigations carried out in this thesis all of the small rig (250 mL autoclave) testing has been carried out using an ethylene feed containing 0.6 ppm O_2, while the large rig (1.2 L autoclave) tests were run with a constant flow of 0.66 ppm O_2. However, to further probe the effects of oxygen dosing upon

iminophosphine-based ethylene oligomerisation systems, a series of test runs were carried out using the optimised conditions described in Section 5.5.5, namely ($Cr(2\text{-}EH)_3$, ligand **3.9**, MCH solvent, 500 eq. MMAO-3A), with varying O_2 dosing levels. Tests were carried out using oxygen levels from 0.03 ppm to 1.4 ppm (Graph 5.27). These investigations of the effect of O_2 upon catalysis were carried out by Dr David Smith of Sasol Technology UK, using a 1.2 L autoclave.

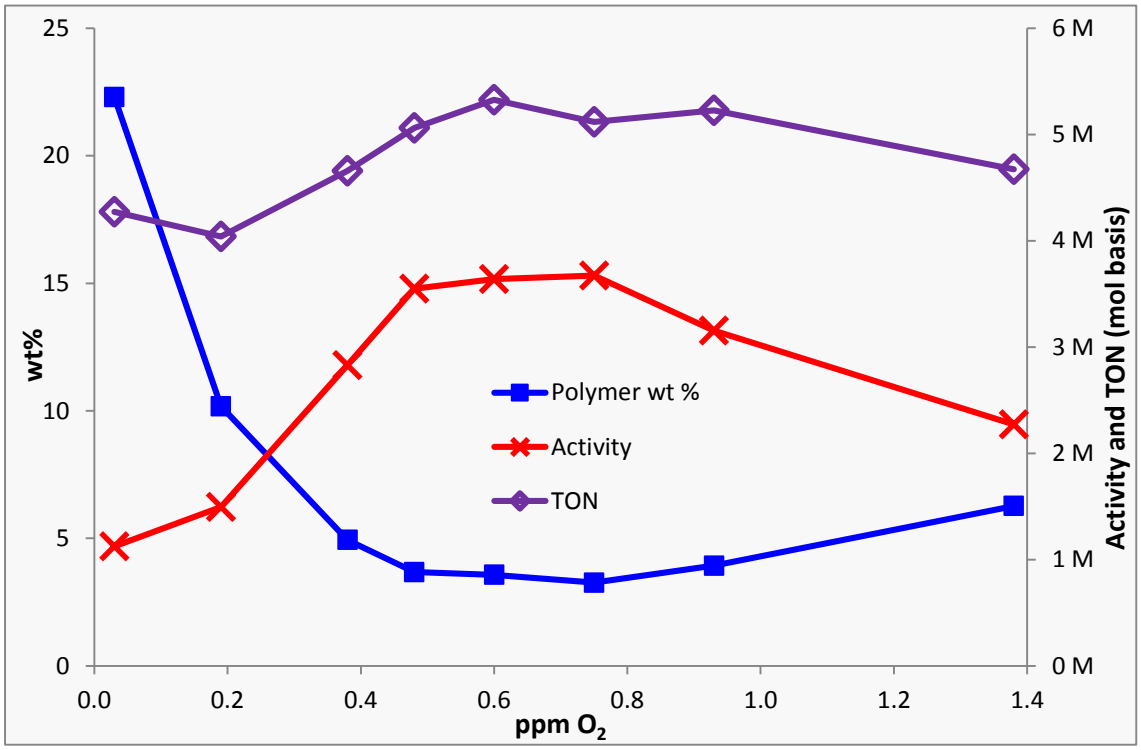

Graph 5.27: Comparison of ethylene oligomerisation systems using iminophosphine **3.9** and varying O_2 dosing levels (0.03, 0.19, 0.38, 0.48, 0.60, 0.75 and 1.38 ppm O_2). Conditions: 1.25 µmol $Cr(2\text{-}EH)_3$, 1.0 eq. ligand, 500 eq. MMAO-3A, 210 mL MCH, 60 °C, 40 bar C_2H_4, activation method **B**.

From the data presented in Graph 5.27 it is apparent that the level of oxygen dosing used during catalytic runs has a dramatic effect upon both the activity and the level of polymer formation of the Cr-iminophosphine oligomerisation system. Through addition of the correct amount of oxygen to the catalytic reaction the extent of polymer formation was reduced from 22 % (at 0.03 ppm O_2) to 3 % (0.75 ppm O_2). Simultaneously, the catalytic activity increased from 1,100,000 mol/mol Cr h^{-1} (at 0.03 ppm O_2) to 3,700,000 mol/mol Cr h^{-1} (0.75 ppm O_2). However, altering the concentration of oxygen present in the systems had little effect upon the liquid fraction selectivities, with all of the runs producing 78 - 83 % 1-hexene and 14 - 20 % 1-octene. Comparison of the performance of the iminophosphine-based oligomerisation catalyst with other systems published in the literature is difficult, due to there being no papers in which the phenomena of oxygen dosing is discussed. The 2012 patent in which the discovery of oxygen dosing is disclosed by Sasol does report oxygen dosing tests run with a selection of established ethylene *tri*- and *tetra*-merisation systems (Table 5.3).[13] In the patent it is revealed that the

presence of small amounts of oxygen is beneficial for all of the Cr-based systems tested, with all of the catalysts giving improved activities and lower extents of polymer formation upon addition of oxygen to the reaction. Interestingly, of the oligomerisation systems investigated by Sasol in their patent regarding oxygen dosing on ethylene *tri*- and *tetra*-merisation catalysts, only Sasol's PNP-based tetramerisation gives oligomerisation activities higher than those demonstrated for the PCN-based systems reported in this thesis.

System	Catalyst precursors	O_2 (ppm)	Activity (mol/mol Cr h^{-1})	Polymer (wt %)
BP Cr(PNP$^{o\text{-}OMe}$)	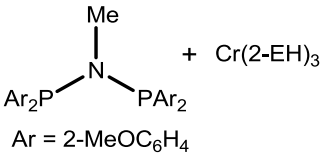	0.14 0.33	3,336,000 7,179,000	0.4 0.4
Cr(PNNP)	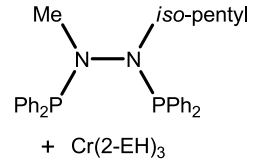	0.14 0.71	348,000 1,018,000	29.6 1.7
Sabic Linde PNPN(H)	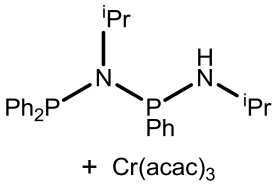	0.14 9.2	81,000 107,000	0.4 0.4
Chevron Phillips Cr(PNC=N)	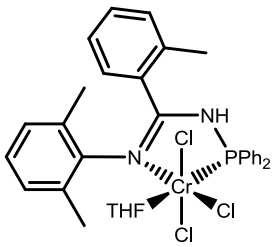	0.14 0.25	124,000 553,000	63.5 6.2
Iminophosphine **3.9**	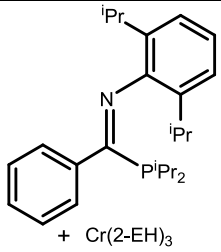	0.03 0.75	1,100,100 3,700,000	22 3

Table 5.3: Comparison of the effect of oxygen on selected ethylene *tri*- and *tetra*-merisation systems, and the Cr(**3.9**)-based system for comparison.

Since no detailed mechanistic study of the O_2-dosing effect was undertaken in this thesis no definite explanation of the role of oxygen in selective ethylene oligomerisation can be drawn. However, it is suggested that any oxygen present in the catalytic system is involved in redox processes with the chromium species. In order to attempt to understand the role of oxygen in

ethylene oligomerisation catalysis, firstly the formation and the oxidation state of the active catalytic species must be considered. A large amount of time and effort has been devoted by different research groups to elucidating the precise mechanism of Cr-based oligomerisation catalyst activation, and a detailed discussion of this can be found in Section 1.2.2.2. It is generally agreed that either a Cr(I) or Cr(II) centre is the starting point for the metallacycle mechanism, resulting in either a Cr(I)/(III) or a Cr(II)/(IV) coupled redox cycle, respectively.[2] A number of suggestions regarding the formation of these Cr(I) and Cr(II) active species from Cr(III) starting materials have been proposed. These include the dimerization of a $L_3Cr^{III}X_3$ starting material to yield a dimeric Cr(II) catalyst precursor (Scheme 5.5, **A**),[38] and the alkylation of a Cr(III) centre by alkyl aluminoxane reagents, followed by reductive elimination to yield an active Cr(I) centre (Scheme 5.5, **B**, **C**). A Cr(III) activation pathway similar to those in Scheme 5.5 has been suggested by Köhn *et al.*, albeit going *via* a dimeric Cr(III) species (Scheme 5.6) supporting a Cr(I)/(III) coupled catalytic cycle in ethylene oligomerisation.[39]

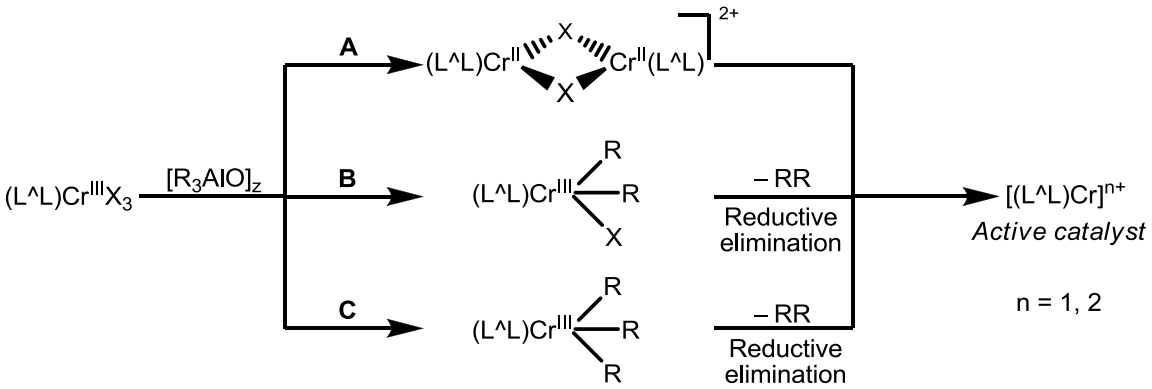

Scheme 5.5: Hypothesised alkylaluminium-mediated activation pathways (**A**-**C**) of Cr in an ethylene oligomerisation system.

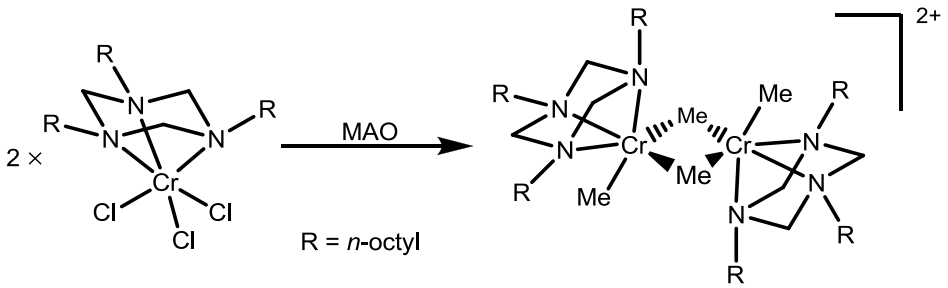

Scheme 5.6: Reaction of a L_3CrX_3 complex with MAO proposed by Köhn *et al.*[39]

Recently, further weight has been added to the argument for a Cr(I)/(III) coupled system by Britovsek and McGuinness *et al.* through both computational and experimental studies.[40] As well as studying the oxidation state, Britovsek and McGuinness investigated the difference between ethylene *tri-* and *tetra*-merisation mechanisms, suggesting that trimerisation is formed from a mono(ethylene) chromacyclopentane intermediate (Scheme 5.7, **A**), while a

bis(ethylene) chromacyclopentane species is responsible for the formation of 1-octene (Scheme 5.7, **B**).

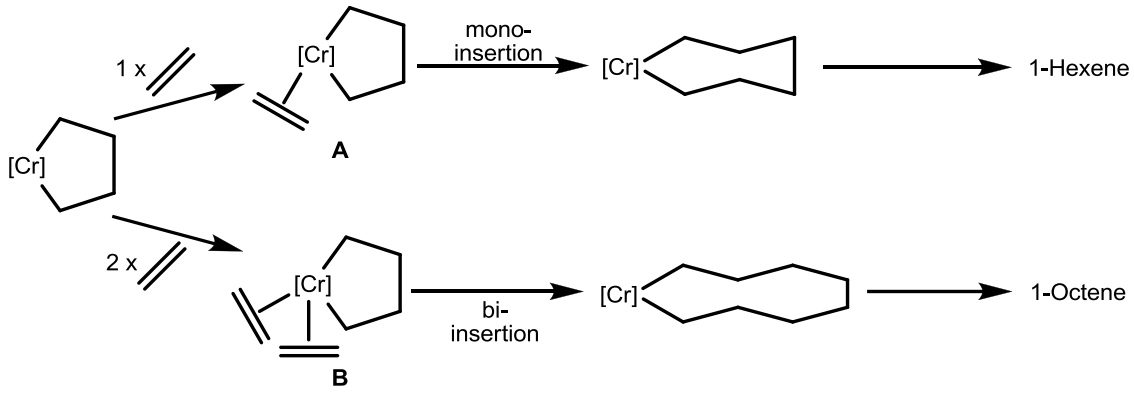

Scheme 5.7: The suggested ethylene *tri*- and *tetra*-merisation pathways reported by Britovsek and McGuinness et al.[40]

Once the oxidation state of the active catalytic chromium centre has been taken into account, the effect of oxygen upon oligomerisation can be considered. It is known that the role of oxygen is not catalytic, and it is not involved in a "one-off" activation step to achieve successful catalysis, as the reaction must be continuously fed with O_2 in order to retain catalytic activity. Therefore, it is proposed that oxygen is responsible for the oxidation of a continuously formed inactive, reduced Cr species, back to an active Cr-centre (Scheme 5.8). However, the precise mechanism of this reduction and oxidation process is currently unknown. It is suggested that the inactive reduced $Cr^{(n-1)+}$ species may be formed by the disproportionation of two Cr^{n+} centres, but no evidence has been found for this. It is clear that further work is required to investigate the role of oxygen in selective ethylene oligomerisation systems, but this is beyond the remit of this present investigation.

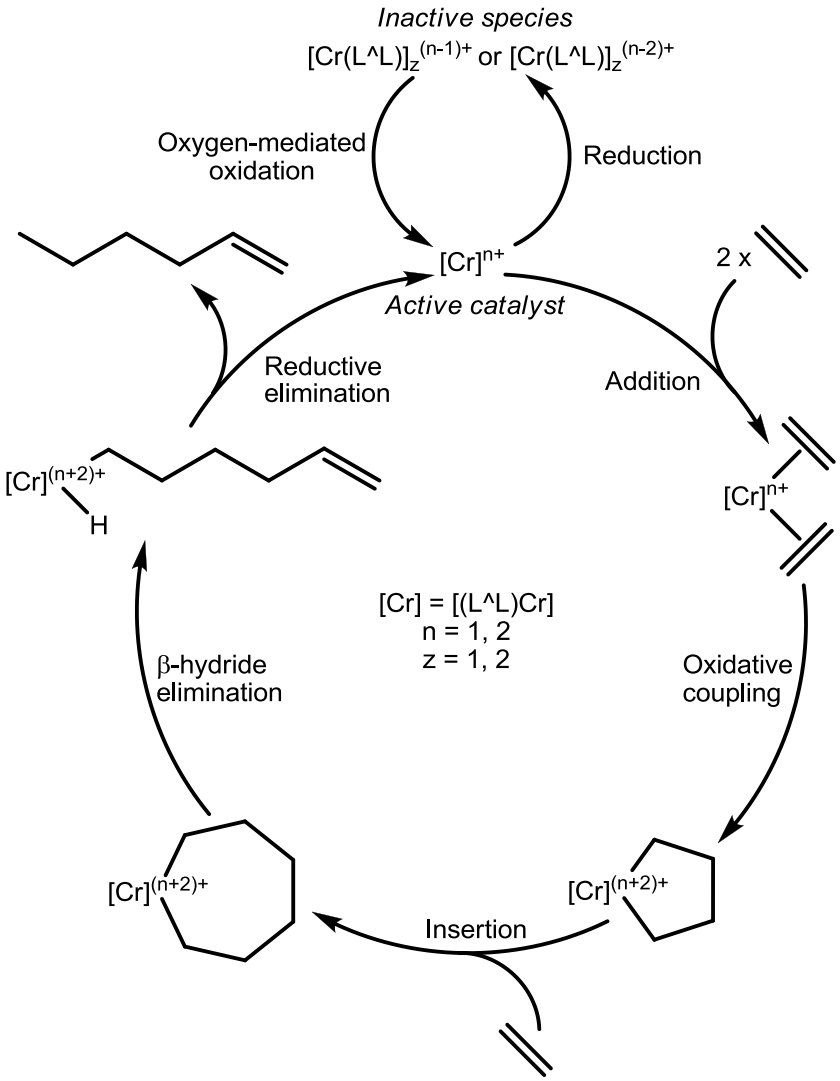

Scheme 5.8: The proposed mechanism of selective ethylene trimerisation, including the role of oxygen in maintaining the oxidation state of the active catalytic species.

5.5.7 Implementation of optimal conditions for selective ethylene oligomerisation

Having independently elucidated optimal catalysis conditions for Cr-iminophosphine-based ethylene *tri-* and *tetra*-merisation (Scheme 5.9), it was important to undertake a series of tests in which all of the optimal conditions were utilised simultaneously. A selection of the most promising ligands from the screening runs reported in Section 5.4 were tested and the data are compared in Graph 5.28. All of the runs in this sub-section were carried out by Dr David Smith of Sasol UK.

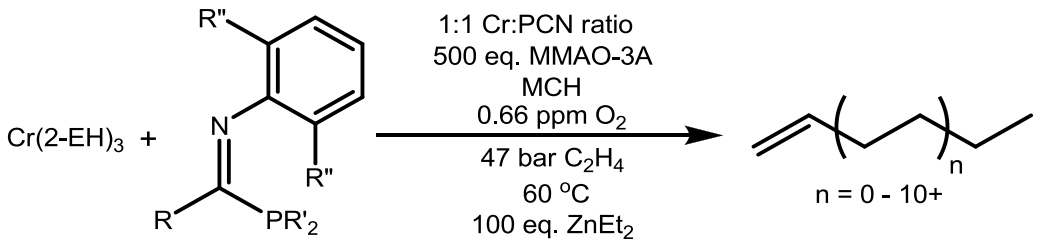

Scheme 5.9: Optimised conditions for a highly active and selective iminophosphine-based ethylene *tri-* and *tetra*-merisation process

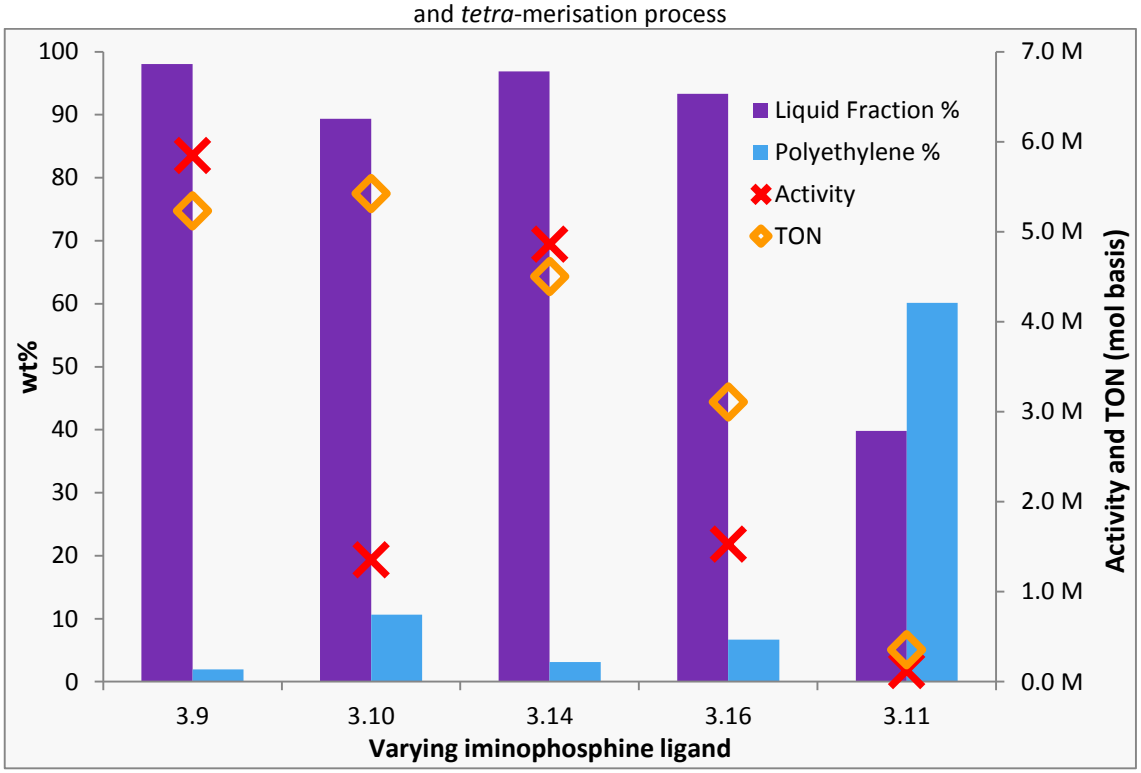

Graph 5.28: Comparison of optimised PCN-based ethylene oligomerisation systems with selected iminophosphine ligands (**3.9**, **3.10**, **3.14**, **3.16** and **3.11**). Conditions: 1.25 µmol $Cr(2\text{-}EH)_3$, 1.0 eq. ligand, 500 eq. MMAO-3A, 100 eq. $ZnEt_2$, 210 mL MCH, 60 °C, 40 bar C_2H_4, activation method **B**.

It is demonstrated that under these optimised conditions not all of the iminophosphine ligands tested (**3.10**, **3.14**, **3.16** and **3.11**) respond in the same way to those determined for compound **3.9**. The catalyst systems derived from ligands with P-alkyl substituents (**3.10**, **3.14**, and **3.16**) all responded well to the optimisation, each giving a roughly 10-fold increase in

activity (compared to the analogous non-optimised PhCl-based systems*) accompanied by a reduction in the extent of polymer formation by approximately two thirds. Interestingly, in tests using ligand **3.11** (Ph(P(2-MeOC$_6$H$_4$)$_2$)C=N(2,6-iPr$_2$C$_6$H$_3$)), bearing the polar (and potentially coordinating) *ortho*-OMe aryl phosphine groups, the degree of polymer formation was observed to *increase* using the "optimised" conditions (from 6 % to 60 % polymer), compared to levels from the earlier screening test using high catalyst loadings, and PhCl solvent.* However, the overall activity of the system did not show any significant change with the new "optimised" conditions. Consequently, it is proposed that the change in the degree of polymerisation is due to the change in solvent. In alkane solvent (*i.e.* MCH) it is proposed that the pendant donor *ortho*-OMe group binds to the Cr centre (yielding a tridentate Cr(κ^3-P,N,O-PCN) complex, **A** Scheme 5.10), due a lack of competition for binding from the solvent. By comparison, the tridentate coordination mode of the P(Ar-*o*-OMe)$_2$-PCN should be less favoured in the more polar chlorobenzene solvent, which is capable of coordinating to the Cr centre and blocking the catalytically inactive κ^3-P,N,O coordination mode (**B**, Scheme 5.10). This suggestion is supported by work from Carter, Cavell and Murphy *et al.* in which the coordination of arene groups to chromium in ethylene oligomerisation systems was observed by EPR spectroscopy.[41]

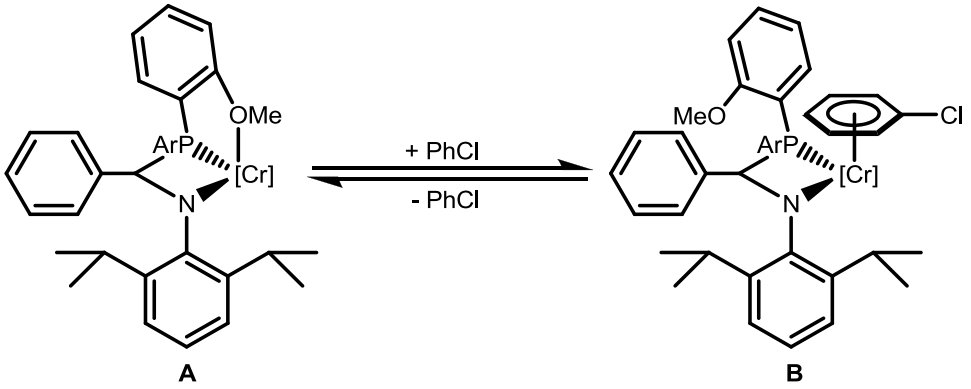

Scheme 5.10: The proposed variable coordination of iminophosphine 3.11 with Cr, in PhCl solvent.

5.5.7.1 Investigating catalyst deactivation of Cr-iminophosphine-based oligomerisation systems

For any catalytic process to be commerically viable the catalyst used must have a reasonable lifetime in order to reduce the amount of catalyst required for the process. It was therefore decided in investigate the catalyst lifetime of the Cr(**3.9**)-based oligomerisation system developed in this thesis. Two tests were carried out, one in which catalysis was run until the reaction vessel was filled with product (54 minutes), and the other reaction was stopped after just 12 minutes. The results are compared in Graph 5.29.

* "Non-optimised" screening conditions: 5 µmol Cr(acac)$_3$, 1.2 eq. ligand, 70 mL PhCl, 500 eq. MMAO-3A, 40 bar C_2H_4, 60 °C

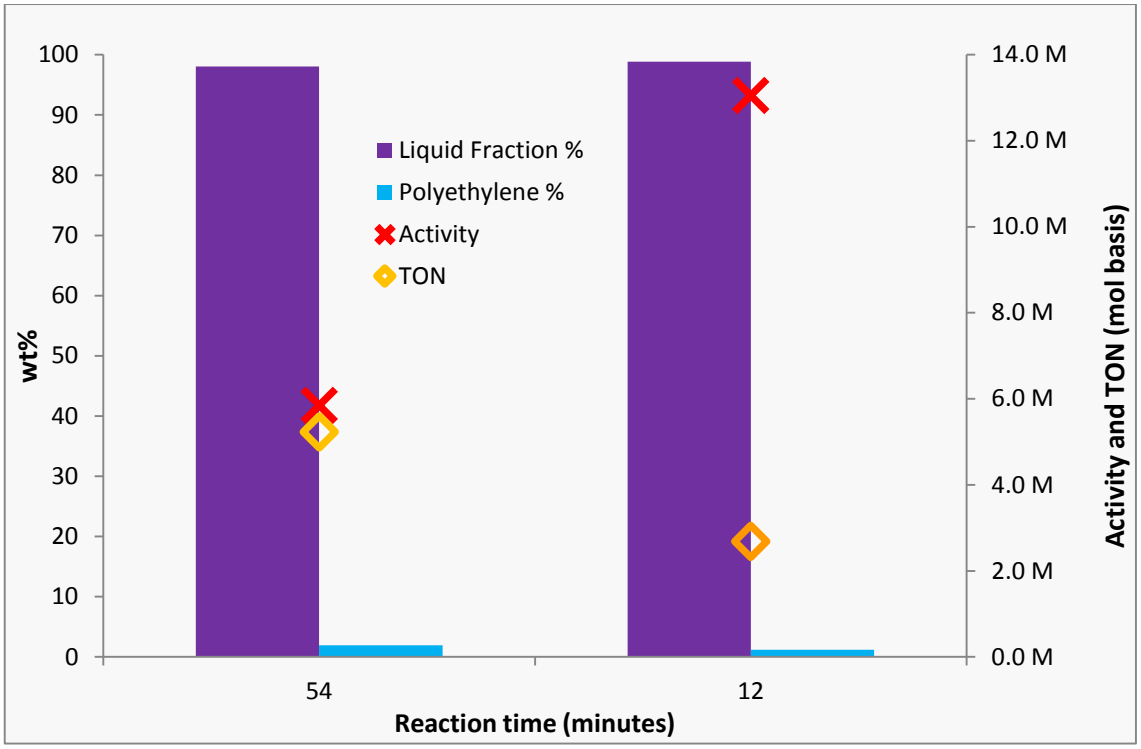

Graph 5.29: Comparison of ethylene oligomerisation performance of systems using iminophosphine **3.9**, with reactions run for 54 and 12 minutes. Conditions: 1.25 µmol $Cr(2\text{-}EH)_3$, 1.0 eq. ligand, 500 eq. MMAO-3A, 100 eq. $ZnEt_2$, 210 mL MCH, 60 °C, 40 bar C_2H_4, activation method **B**.

Upon extending the catalyst run time from 12 to 54 minutes the calculated activity is seen to halve, from 13,000,000 mol/mol Cr h^{-1} to 5,800,000 mol/mol Cr h^{-1}, indicating that significant catalyst deactivation is occurring during the longer run. In order to further probe this catalyst decomposition process, longer run times are required, something that has so far been limited by the volume of reactor available.

5.5.7.2 Comparisons of the iminophosphine-based ethylene oligomerisation process with previously patented systems

Overall, in this chapter it has been demonstrated that the catalytic system using **3.9** and the conditions described in Section 5.5 (*i.e.* 0.4 µmol $Cr(2\text{-}EH)_3$, 1 eq. **3.9**, 70 mL MCH, 500 eq. MMAO-3A, 49 bar C_2H_4, 70 °C, 0.6 ppm O_2 and 100 eq. $ZnEt_2$) performs as a highly successful ethylene *tri-*/*tetra*-merisation package, displaying catalytic activities and selectivities comparable with the best literature systems published to-date. For comparison of some of these patented systems with the iminophosphine-based process reported in this thesis, a selection of published ethylene trimerisation systems is summarised in Table 5.4. Interestingly, the Cr(iminophosphine) oligomerisation system discovered in this thesis is more active than the Mitsubishi-Phillips Cr(pyrrole) system, which was the first commercialised ethylene trimerisation process. This suggests that the novel Cr(iminophosphine) selective oligomerisation

system discovered in this thesis has potential to be patented, and potentially used on an industrial scale.

The main disadvantage with the novel Cr(iminophosphine) oligomerisation system is the relatively high levels of polymer formation exhibited. Even under optimised conditions, with the use of known polymer minimisation techniques (addition of $ZnEt_2$, Section 5.5.5), the oligomerisation process still produces nearly 2 % polymer products which is relatively high when compared to other patented systems (Table 5.4). The production of large amounts of polymer is highly detrimental to any oligomerisation process, due to potential for polymer to cause reactor fouling. However, only a short length of time has been spent developing the Cr(iminophosphine) oligomerisation process, and it is suggested that with further investigation and development, the extent of polymer formation of Cr(iminophosphine)-based oligomerisation systems could be reduced. It is hoped that with more detailed study of the catalytic behaviour of Cr(PCN) *tri*- and *tetra*-merisation process the catalyst package will be suitable for industrial-scale utilisation.

System	Catalyst precursor	Activity (mol/mol TM h^{-1})	Polymer (wt %)	Liquid fraction selectivity to 1-hexene (wt %)
Sabic Linde [6] Cr-PNPN(H)	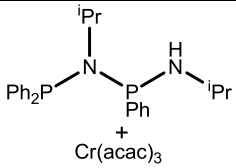	83,300	0.3	93.9
Sasol [3] Cr-PNP(*ortho*-alkyl-Ph)	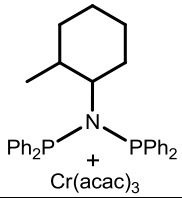	> 10,000,000	1 – 2	93
Sasol [7] Cr-SNS	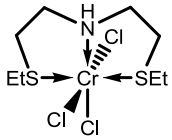	255,000	< 1	98
Phillips [4,5] Cr-pyrrole	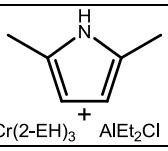	290,000	1.2	93
Mitsubishi-Phillips [4,5] Cr-pyrrole	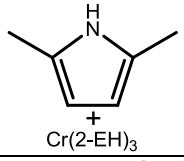	1,750,000	0.04	95
DPI [8] Ti-Arene^Bz	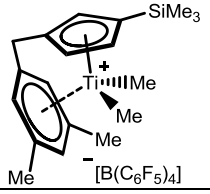	239,000	0.4	98
Tosoh [4] Cr-maleimide	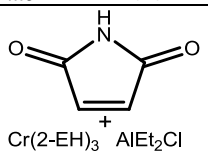	516,000	1.5	81
Mitsui [9] Ti-Phen-Im	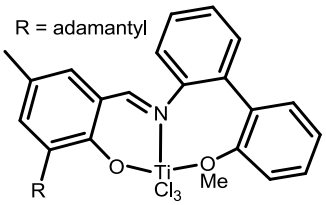	12,000,000	0.4	92
Iminophosphine **3.9**	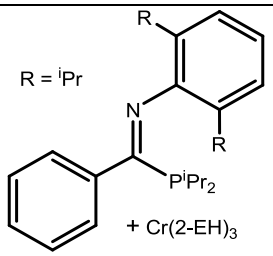	5,800,000	1.9	83

Table 5.4: Comparison of activities and polymer formation percentages for a selection of published ethylene trimerisation systems, including the Cr(PCN) system developed in this thesis.

5.6 Summary and Conclusions

This chapter has reported and discussed the properties of a wide range of iminophosphine-based ethylene oligomerisation systems tested. Initially, a range of catalytic reactions were carried out utilising ligand **3.1** ($Ph(PPh_2)C=N(2\text{-}MeC_6H_4)$) in order to probe a small range of preliminary catalytic conditions for use in screening further iminophosphine ligand variants, including the Cr source, the activator used, the activation method and the reaction temperature. From these tests it was apparent that systems using ligand **3.1** in combination with Cr(III) sources and MMAO-3A did not yield selective ethylene oligomerisation products, but rather gave primarily polymeric products (50 – 98 % polymer). Overall, it was found that the initial conditions used, a modified version of those reported by Bercaw *et al.*[11] and using $Cr(acac)_3$ as the Cr source, were the best tested in this small study, namely 5 µmol $Cr(acac)_3$, 1.2 equivalents of ligand, 500 equivalents MMAO-3A, 40 bar C_2H_4, 60 °C in 70 mL PhCl solvent using activation method **B** (pre-activation).

Due to the failure of the first catalytic systems tested to produce oligomer products, a series of preformed Cr-PCN complexes (**4.1** – **4.4**) were tested as catalyst precursors, based on the work of Sydora *et al.* in which it was demonstrated that their Cr-phosphinoamidine-based oligomerisation process required pre-formed complexes in order to generate active catalytic systems.[10] The complexes **4.1** – **4.4** were tested as components in ethylene oligomerisation packages with varying temperature, activation methods, co-catalysts and the application of potentially polymer-reducing additives. All of the catalyst systems gave primarily polymer as the product, and so could not be labelled as ethylene oligomerisation systems. Due to this failure to produce oligomeric products, no further investigation was carried out into the use of preformed Cr-PCN complexes as catalyst precursors.

A wider-ranging study was subsequently carried out to investigate the effect of the iminophosphine structure upon the behaviour of PCN-based oligomerisation processes. From these tests a number of strong correlations were found linking both the steric bulk and the electronic properties of the iminophosphine ligands to the activity, polymer formation and liquid fraction selectivity of the catalytic systems. It was demonstrated that, in general, the use of iminophosphines bearing bulky phosphine and N-aryl groups yielded the best catalytic performances, and also favoured the production of 1-hexene over 1-octene. Through optimisation of the ligand structure, systems were developed capable of yielding relatively high catalytic activities (350,000 mol/mol Cr h^{-1}, **3.14**) and low levels of polymer formation (6 %, **3.11**). More importantly, these new catalytic systems demonstrated remarkably high 1-hexene and 1-octene selectivities, up to 98 % combined 1-C_6 and 1-C_8 and an OTH ratio of 0.17,

employing ligand **3.9** . From these initial tests it was concluded that iminophosphine ligands demonstrated strong potential for use as ligands in highly active and selective ethylene *tri-*/*tetra*-merisation processes.

Based on the success of the ligand screening study (Section 5.4) investigating ligand structure, efforts were undertaken to further optimise the catalytic process used for ethylene oligomerisation. A study investigating the effect of the Cr:ligand ratio was carried out (Section 5.5.1), revealing that a 1:1 ratio of iminophosphine to chromium gave the optimal catalytic performance. Efforts were subsequently made to develop the oligomerisation process for use under conditions suitable for industry, *i.e.* using alkane solvents, low chromium concentrations, and low levels of polymer formation. Upon changing the reaction solvent and lowering the Cr concentration using ligand **3.9**, a dramatic increase in catalytic activity was observed (2,500,000 mol/mol Cr h^{-1}). Further optimisation was carried out, varying C_2H_4 pressure, reaction temperature, polymer minimising additives (*i.e.* $ZnEt_2$, H_2), and oxygen dosing levels, eventually yielding a fully optimised system capable of giving activities of 5,800,000 mol/mol Cr h^{-1}, 2 % polymer formation and 97 % combined selectivity towards 1-hexene and 1-octene formation (Figure 5.18).

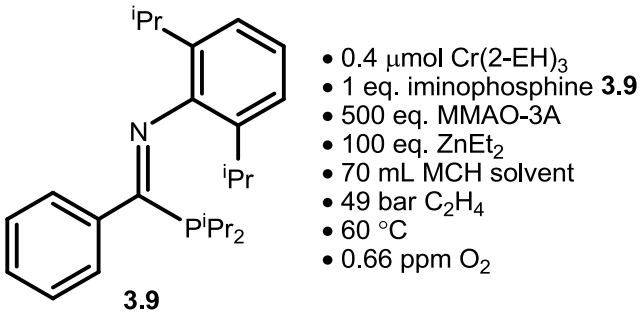

Figure 5.18: The optimal conditions derived for iminophosphine-based ethylene oligomerisation systems

These optimised catalysis conditions were applied to a selection of other promising systems, yielding similar improvements in activity and polymer formation. The optimised iminophosphine-based ethylene oligomerisation systems gave results comparable to, or better than, the majority of *tri-* and *tetra*-merisation systems published in the literature (*e.g.* Phillips commercialised Cr-pyrrole system with activities of 1,750,000 mol/mol Cr h^{-1}), with the exception of Sasol's PNP-tetramerisation process (capable of giving activities of >10,000,000 mol/mol Cr h^{-1}).

5.7 Future Work

This chapter has detailed the catalyst testing of a wide range of Cr(III)-based ethylene oligomerisation systems using iminophosphine ligands. The best systems developed gave catalytic activities comparable to some of the best previously reported systems in the patent literature (>5,000,000 mol/mol Cr h^{-1}), but these Cr(PCN)-based processes gave relatively high levels of polymer formation (2 %) and displayed significant catalyst deactivation during extended run times. It is suggested with further optimisation of the catalytic protocol used these issues could be overcome (*e.g.* through the use of alternative Al-based activator packages), giving a process that is truly competitive with Sasol's PNP-based tetramerisation process, the currently industry-leading selective ethylene oligomerisation system.

As well as additional optimisation of the catalytic protocol it is suggested that further alteration of the ligand structure may lead to other highly active and selective oligomerisation processes. In this thesis only a limited number of PR_2 groups have been tested, and ligands with only one of two C-backbone substituents have been trialled. It is easily conceivable that other ligand scaffolds with alternative C-backbone groups could promote *tri-* and *tetra*-merisation processes with better catalytic activities, or lower polymer yields. For example, C-backbone ether moieties, or fluorinated groups may yield significantly different behaviour in catalyst systems (Figure 5.19). It would therefore be of interest to synthesise a range of these iminophosphine compounds and submit these to the catalytic testing procedures detailed in this chapter.

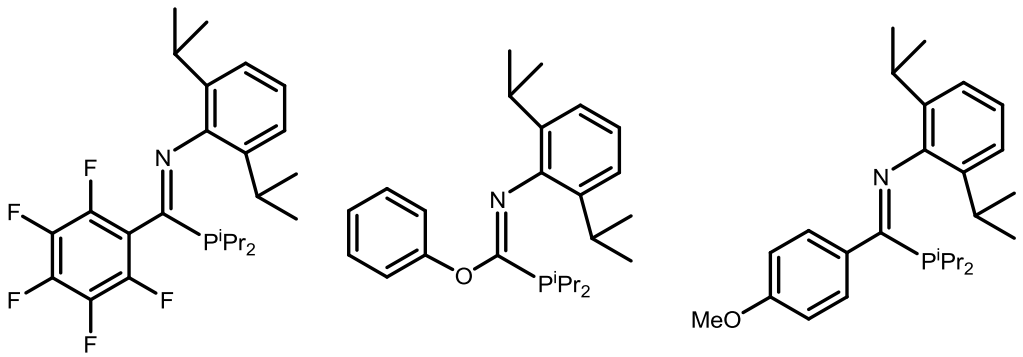

Figure 5.19: Examples of suggested ligands for future synthesis and testing in ethylene oligomerisation systems.

One particular catalyst activation method that was not studied in this thesis was the use of Cr(I) catalyst precursors, activated with alkyl aluminium reagents. It would be of interest in the future to synthesise $[Cr(CO)_4(\kappa^2\text{-PCN})]^+$ complexes with weakly coordination anions (*e.g.* Krossing's aluminate $[Al(OC(CF_3)_3)_4]$). This is in line with the work of Hanton *et al.* concerning their $[Cr(CO)_4(PNP)]^+$ complexes, which can be used to generate active oligomerisation catalysts

upon reaction with TEA (Scheme 5.11).[34] It is suggested that this alternative activation method for Cr(PCN)-based catalysis systems may aid in the reduction of polymer production by the systems, due to the lack of Cr(III) starting materials present, which have been shown in this thesis to catalyse ethylene polymerisation.

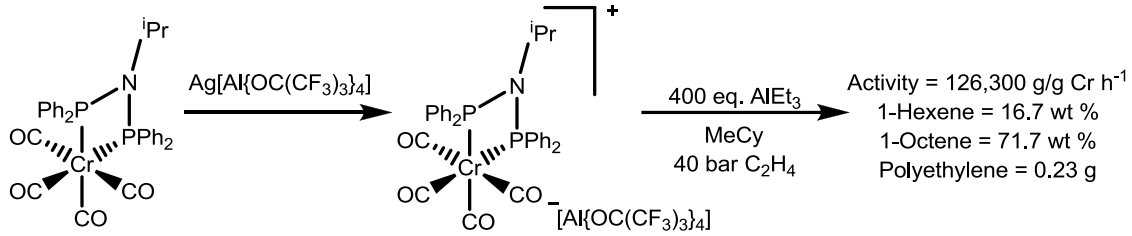

Scheme 5.11: Cr^{I}(PNP)-based ethylene tetramerisation system reported by Hanton *et al.*[34]

5.8 References

(1) Carter, A.; Cohen, S. A.; Cooley, N. A.; Murphy, A.; Scutt, J.; Wass, D. F. *Chem. Commun.* **2002**, 858.
(2) Agapie, T. *Coord. Chem. Rev.* **2011**, *255*, 861.
(3) Kuhlmann, S.; Blann, K.; Bollmann, A.; Dixon, J. T.; Killian, E.; Maumela, M. C.; Maumela, H.; Morgan, D. H.; Prétorius, M.; Taccardi, N.; Wasserscheid, P. *J. Catal.* **2007**, *245*, 279.
(4) Dixon, J. T.; Green, M. J.; Hess, F. M.; Morgan, D. H. *J. Organomet. Chem.* **2004**, *689*, 3641.
(5) Reagan, W. K. *Symp. Prepr. Conv. Light Olefins, Div. Pet. Chem., Am. Chem. Soc.* **1989**, *34*.
(6) Heinig, S.; Wöhl, A.; Müller, W.; Al-Hazmi, M. H.; Müller, B. H.; Peulecke, N.; Rosenthal, U. *ChemCatChem* **2014**, *6*, 514.
(7) McGuinness, D. S.; Wasserscheid, P.; Keim, W.; Morgan, D.; Dixon, J. T.; Bollmann, A.; Maumela, H.; Hess, F.; Englert, U. *J. Am. Chem. Soc.* **2003**, *125*, 5272.
(8) Otten, E.; Batinas, A. A.; Meetsma, A.; Hessen, B. *J. Am. Chem. Soc.* **2009**, *131*, 5298.
(9) Suzuki, Y.; Kinoshita, S.; Shibahara, A.; Ishii, S.; Kawamura, K.; Inoue, Y.; Fujita, T. *Organometallics* **2010**, *29*, 2394.
(10) Sydora, O. L.; Jones, T. C.; Small, B. L.; Nett, A. J.; Fischer, A. a.; Carney, M. J. *ACS Catal.* **2012**, *2*, 2452.
(11) Elowe, P. R.; McCann, C.; Pringle, P. G.; Spitzmesser, S. K.; Bercaw, J. E. *Organometallics* **2006**, *25*, 5255.
(12) Battino, R.; Clever, H. L. *Chem. Rev.* **1966**, *66*, 395.
(13) Hanton, M. J.; Smith, D. M.; Gabrielli, W.F.; Evans, S. J.; WO 2013/168103 A1 (Sasol Technology UK), 14 November 2014.
(14) McGuinness, D. S. *Chem. Rev.* **2011**, *111*, 2321.
(15) Sydora, O. L.; Carney, M. J.; Small, B. L.; Hutshison, S.; Gee, J. C.; WO 2011/082192 (Chevron Phillips Chemical Company LP), December 29, 2011.
(16) Wöhl, A.; Müller, W.; Peitz, S.; Peulecke, N.; Aluri, B. R.; Müller, B. H.; Heller, D.; Rosenthal, U.; Al-Hazmi, M. H.; Mosa, F. M. *Chem. Eur. J.* **2010**, *16*, 7833.
(17) McGuinness, D. S.; Overett, M.; Tooze, R. P.; Blann, K.; Dixon, J. T.; Slawin, A. M. Z. *Organometallics* **2007**, *26*, 1108.
(18) Kuhlmann, S.; Dixon, J. T.; Haumann, M.; Morgan, D. H.; Ofili, J.; Spuhl, O.; Taccardi, N.; Wasserscheid, P. *Adv. Synth. Catal.* **2006**, *348*, 1200.
(19) van Leeuwen, P. P. W. N. M.; Clément, N. D.; Tschan, M. J.-L. L.; Clement, N. D. *Coord. Chem. Rev.* **2011**, *255*, 1499.
(20) Reddy, S. S.; Sivaram, S. *Prog. Polym. Sci.* **1995**, *20*, 309.
(21) Akzo Nobel Product Data Sheet and Certificate of Analysis for MMAO-3A in heptanes 7 wt% . 'Active Al' content (mostly free AlR_3) 42%.
(22) Akzo Nobel Product Data Sheet and Certificate of Analysis for PMAO-IP in toluene 7 wt% . 'Active Al' content (mostly free AlR_3) 24%.
(23) Kuhlmann, S.; Paetz, C.; Hägele, C.; Blann, K.; Walsh, R.; Dixon, J. T.; Scholz, J.; Haumann, M.; Wasserscheid, P. *J. Catal.* **2009**, *262*, 83.
(24) Hanton, M. J.; Smith, D. M.; Gabrielli, W.F.; Kelly, M. W.; WO 2011/048527 A1 (Sasol Technology UK), 28 April 2011
(25) van Meurs, M.; Britovsek, G. J. P.; Gibson, V. C.; Cohen, S. A. *J. Am. Chem. Soc.* **2005**, *127*, 9913.
(26) Kissin, Y. V.; Rishina, L. A.; Vizen, E. I. *J. Polym. Sci. A* **2002**, *40*, 1899.

(27) Bollmann, A.; Blann, K.; Dixon, J. T.; Hess, F. M.; Killian, E.; Maumela, H.; McGuinness, D. S.; Morgan, D. H.; Neveling, A.; Otto, S.; Overett, M.; Slawin, A. M. Z.; Wasserscheid, P.; Kuhlmann, S. *J. Am. Chem. Soc.* **2004**, *126*, 14712.
(28) Britovsek, G. J. P.; Gibson, V. C.; McTavish, S. J.; Solan, G. A.; White, A. J. P.; Williams, D. J.; Kimberley, B. S.; Maddox, P. J. *Chem. Commun.* **1998**, 849.
(29) Agapie, T.; Schofer, S. J.; Labinger, J. A.; Bercaw, J. E. *J. Am. Chem. Soc.* **2004**, *126*, 1304.
(30) Mao, G.; Ning, Y.; Hu, W.; Li, S.; Song, X.; Niu, B.; Jiang, T. *Chin. Sci. Bull.* **2008**, *53*, 3511.
(31) Müller, B. H.; Peulecke, N.; Spannenberg, A.; Rosenthal, U.; Al-Hazmi, M. H.; Schmidt, R.; Wöhl, A.; Müller, W. *Organometallics* **2012**, *31*, 3695.
(32) Blann, K.; Bollmann, A.; de Bod, H.; Dixon, J. T.; Killian, E.; Nongodlwana, P.; Maumela, M. C.; Maumela, H.; McConnell, A. E.; Morgan, D. H.; Overett, M. J.; Prétorius, M.; Kuhlmann, S.; Wasserscheid, P. *J. Catal.* **2007**, *249*, 244.
(33) Müller, W.; Wöhl, A.; Peitz, S.; Peulecke, N.; Aluri, B. R.; Müller, B. H.; Heller, D.; Rosenthal, U.; Al-Hazmi, M. H.; Mosa, F. M. *ChemCatChem* **2010**, *2*, 1130.
(34) Rucklidge, A. J.; McGuinness, D. S.; Tooze, R. P.; Slawin, A. M. Z.; Pelletier, J. D. A.; Hanton, M. J.; Webb, P. B. *Organometallics* **2007**, *26*, 2782.
(35) Jahangiri, M.; Jacobsen, R. T.; Stewart, R. B.; McCarty, R. D. *J. Phys. Chem. Ref. Data* **1986**, *15*, 593.
(36) Walsh, R.; Morgan, D. H.; Bollmann, A.; Dixon, J. T. *Appl. Catal. A* **2006**, *306*, 184.
(37) Overett, M. J.; Blann, K.; Bollmann, A.; Dixon, J. T.; Haasbroek, D.; Killian, E.; Maumela, H.; McGuinness, D. S.; Morgan, D. H. *J. Am. Chem. Soc.* **2005**, *127*, 10723.
(38) Jabri, A.; Temple, C.; Crewdson, P.; Gambarotta, S.; Korobkov, I.; Duchateau, R. *J. Am. Chem. Soc.* **2006**, *128*, 9238.
(39) Köhn, R. D.; Haufe, M.; Kociok-Köhn, G.; Grimm, S.; Wasserscheid, P.; Keim, W. *Angew. Chem. Int. Ed.* **2000**, *39*, 4337.
(40) Britovsek, G. J. P.; McGuinness, D. S.; Wierenga, T. S.; Young, C. T. *ACS Catal.* **2015**, *5*, 4152.
(41) Carter, E.; Cavell, K. J.; Gabrielli, W. F.; Hanton, M. J.; Hallett, A. J.; McDyre, L.; Platts, J. A.; Smith, D. M.; Murphy, D. M. *Organometallics* **2013**, *32*, 1924.

Chapter 6:

Experimental Details

6.1 General Considerations

Unless stated otherwise, all manipulations were carried under an atmosphere of dry nitrogen using standard Schlenk line techniques or in a Saffron Scientific nitrogen-filled glovebox. All glassware was oven dried prior to use. Dry solvents were obtained from an Innovative Technologies SPS facility and degassed prior to use by freeze-pump-thaw cycles. Pentane and cyclohexane were dried over CaH_2 prior to distillation and degassing by freeze-pump-thaw cycles. Chlorobenzene was dried over P_2O_5 before being distilled and degassed by freeze-pump-thaw cycles. NMR spectroscopic solvents (benzene-d_6, toluene-d_8) were dried over CaH_2 prior to distillation and degassing. $CDCl_3$ was dried over P_2O_5 and subsequently distilled and degassed. NMR spectroscopic solvents were sourced from Apollo of Goss Scientific. All NMR-scale reactions were carried out using NMR tubes fitted with J. Young's taps.

$CrCl_3(THF)_3$ was prepared by literature methods and its purity verified by elemental analysis and IR spectroscopy.[1] Diphenylvinylphosphine, 1-(2-diphenylphosphino-ethyl)-4-methyl-piperazine, 1-(2-diphenylphosphino-ethyl)-morpholine,[2] piperidine-N-ethylene-diphenylphosphine,[3] diisopropylphosphine[4] and trimethylsilyl-diphenylphosphine[5] were prepared according to the literature and the purity partially assessed by $^{31}P\{^1H\}$ NMR spectroscopy. All other chemicals were obtained from Sigma Aldrich or Alfa Aesar and used without any further purification.

Solution-phase NMR spectra were collected on a Varian Mercury 400, Varian Inova 500, Varian VNMRS-700, Bruker Advance 400 or a Varian VNMRS-600 spectrometer at room temperature unless otherwise stated. All chemical shifts were referenced relative to residual solvent resonances (^1H, ^{13}C) or to external aqueous 85% H_3PO_4 (^{31}P). ^1H and ^{13}C NMR spectra were assigned with the aid of 2D COSY, HMBC and HSQC spectroscopic experiments.

Mass spectra were collected using a Waters Xevo QTOF equipped with an Atmospheric Solids Analysis Probe (ASAP). Elemental analyses were carried out by Stephen Boyer of London Metropolitan University.

All solid state IR spectra were recorded using a Perkin Elmer Paragon 1000 FT-IR spectrometer using a Golden Gate ATR cell and solution state IR spectra were collected using either a Nicolet Avatar or a Perkin Elmer UATR Two spectrometer between KBr discs. All deconvolutions of IR spectra were carried out using Origin (OriginLab, Northampton, MA). Of the IR spectroscopic data gathered for imines, only the C=N stretching frequencies are reported in this thesis due to the complexity of the data gathered.

GC-FID analyses were performed on an Agilent Technologies 6890N GC system equipped with PONA (50 m × 0.20 mm × 0.50 μm) and MDN-12 (60 m × 0.25 mm × 0.25 μm)

columns. All microwave reactions were carried out using a Biotage Initiator microwave reactor heating at a set temperature.

Ethylene oligomerisation catalysis experiments were carried out in 250 mL Buchi Miniclaves or in a 1.2 L Premex Pinto autoclave. Both were equipped with stainless steel vessels with integrated thermal-fluid jackets, internal cooling coils and mechanical mixing. Ethylene (Grade 4.5) was supplied by Linde and passed through oxygen and moisture scrubbing columns prior to use. The ethylene flow was measured using a Siemens Sitrans F C Massflo system (Mass 6000-Mass 2100). All catalytic testing was carried out at Sasol Technology UK, St Andrews with the assistance of Dr Martin Hanton and Dr David Smith.

DSC analysis of polyethylene was performed on a TA instruments DSC Q1000. The samples were heated from room temperature to 200 °C with a heating rate of 10 °C/min before cooling the sample to 50 °C at a rate of 10 °C/min. This cycle was repeated, and the data from the second cycle was used to determine the melting point of the polyethylene in question.

All laboratory work was undertaken adhering to standard safety protocols. A laboratory coat, safety glasses and gloves were worn at all times, while all experiments were carried out in an efficient fume-hood. All chemicals used were subjected to COSHH assessments. Solvents were disposed of in appropriate solvent waste containers following separation of waste streams. All metal residues were collected and separated according to metal. All highly reactive waste products were quenched appropriately before disposal.

6.2 Reaction of $CrCl_3(THF)_3$ with PNE Ligands

6.2.1 Reaction of $CrCl_3(THF)_3$ with 1-(2-diphenylphosphino-ethyl)-4-methyl-piperazine

A solution of PNN (0.190 g, 0.61 mmol) in toluene (15 mL) was slowly added to a solution of $CrCl_3(THF)_3$ (0.190 g, 0.50 mmol) in toluene (15 mL) and the resulting solution was seen to turn from purple to deep blue, along with the precipitation of a blue solid. The reaction mixture was heated to 80 °C for 16 hours before the solution was cooled and the solvent was removed by filtration to leave a blue solid product. The product was washed with hexane (2 × 10 mL) and dried under vacuum to give a pale blue powder (0.174 g). The paramagnetic nature of the product precluded NMR spectroscopic analysis. Elemental analysis was carried out, but gave inconclusive results, therefore the identity of the product could not be confirmed.

6.2.2 Preparation of chromium trichloride 1-(2-diphenylphosphino-ethyl)-morpholine tetrahydrofuran (2.1)

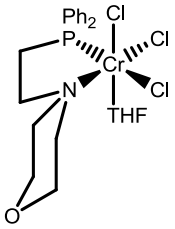

A solution of PNO (0.242 g, 0.81 mmol) in toluene (10 mL) was added dropwise to a solution of $CrCl_3(THF)_3$ (0.253 g, 0.67 mmol) in toluene (15 mL). The mixture instantly turned blue and a blue precipitate formed. The flask containing the PNO solution was washed through with more toluene (5 mL) before the reaction mixture was stored at –30 °C for 16 hours. The mixture was filtered to isolate a pale blue solid and a clear blue solution. The solution was concentrated under vacuum before being cooled to –30 °C again overnight, after which more blue precipitate formed. The precipitate was isolated by filtration and combined with the first batch of solid product to give the final product (258 mg, 73 % yield) (calc.: $C_{22}H_{29}Cl_3CrNO_2P$ C, 49.87; H, 5.71; N, 2.64. Found: C, 50.02; H, 5.83; N, 2.73)

6.2.3 Preparation of chromium trichloride piperidine-*N*-ethylene-diphenylphosphine tetrahydrofuran (2.2)

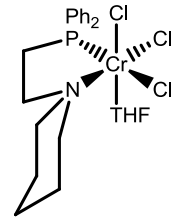

A solution of PNC (0.2 g, 0.67 mmol) in DCM (5 mL) was added dropwise to a solution of $CrCl_3(THF)_3$ (0.229 g, 0.61 mmol) in DCM (5 mL) and the resulting mixture instantly turned turquoise. The flask containing the PCN solution was washed with DCM (5 mL) and the washings were added to the reaction mixture. The resulting solution was stirred for one hour before the solvent was removed under reduced pressure to yield a turquoise solid, which was subsequently triturated with hexane (5 mL). The solid was isolated by filtration and further washed with hexane (2 × 5 mL) before being dried under vacuum to yield the title product as a turquoise solid (232 mg, 72 % yield) (calc.: $C_{23}H_{31}Cl_3CrNOP$ C, 52.34; H, 6.11; N, 2.65. Found: C, 52.21; H, 6.21; N, 2.73).

6.2.4 Preparation of triethylammonium 1-(2-diphenylphosphino-ethyl)-morpholine chromium tetrachloride (2.3)

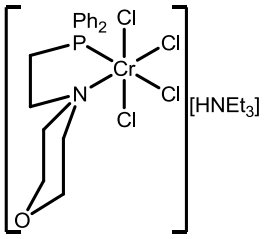

A Schlenk was charged with $CrCl_3(THF)_3$ (0.091 g, 0.24 mmol) and NEt_3.HCl (0.034 g, 0.24 mmol) before a solution of PNO (0.073 g, 0.24 mmol) in DCM (1 mL) was added. The solution instantly turned dark blue and, after standing for 20 minutes, dark blue crystals were observed to form. The solution was stored at –30 °C for 16 hours to maximise the yield of crystals. The solid was isolated by removal of the solvent and washed with hexane (3 × 1 mL) before being dried to give a blue crystalline product (0.104 g, 73% yield) suitable for X-ray crystallography. Elemental analysis was carried out, but gave inconclusive results, therefore the identity of the bulk product could not be confirmed.

6.3 Synthesis of $M(CO)_{(6-n)}(\kappa^n$-PNE) Complexes (M = Cr, Mo)

An analogous procedure to the reflux-based synthesis described by Wass *et al.* was followed to synthesise all chromium and molybdenum carbonyl complexes unless otherwise stated.[6]

6.3.1 Preparation of 1-(2-diphenylphosphino-ethyl)-4-methyl-piperazine chromium pentacarbonyl (2.4)

Method A: Reflux synthesis

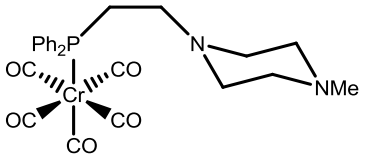

A solution of PNN (0.4 g, 1.28 mmol) in toluene (40 mL) was added to solid $Cr(CO)_6$ (0.376 g, 1.71 mmol). The solution was heated at reflux for 24 hours to give a clear yellow solution. This solution was cooled to 0 °C before being filtered, and the solution isolated. The toluene was removed under vacuum to give the product as a yellow viscous oil (yield 0.478 g, 74%), which solidified upon scraping resulting in a yellow powder. Crystals suitable for X-ray crystallography were obtained by leaving a concentrated solution of **2.4** in pentane to stand for 1 hour allowing for orange crystals to form. (calc.: $C_{24}H_{25}N_2O_5PCr$ C, 57.14; H, 5.00; N, 5.55. Found: C, 56.96; H, 4.91; N, 5.65).

^{1}H NMR (600 MHz, Benzene-d_6) δ ppm: 7.32 – 7.26 (m, 4H, *o*-C_6H_5), 6.93 – 6.92 (m, 6H, *m*/*p*-C_6H_5), 2.45 – 2.39 (m, 2H, PCH_2), 2.39 – 2.3 (m, 2H, PCH_2CH_2N), 2.23 – 2.16 (m, 4H, NCH_2CH_2NMe), 2.15 – 2.07 (m, 4H, $NCH_2CH_2NCH_3$), 2.01 (s, 3H, CH_3).

^{13}C{^{1}H} NMR (151 MHz, Benzene-d_6) δ ppm: 221.3 (d, $^2J_{PC}$ = 7 Hz, *trans*-PCrCO), 216.9 (d, $^2J_{PC}$ = 13 Hz, *trans*-CrCO), 136.3 (d, $^1J_{PC}$ = 36 Hz, *ipso*-PC_6H_5), 131.5 (d, $^2J_{PC}$ = 10 Hz, *o*-PC_6H_5), 129.7 (d, $^4J_{PC}$ = 2 Hz, *p*-PC_6H_5), 128.5 (d, $^3J_{PC}$ = 9 Hz, *m*-PC_6H_5), 55.0 (s, $NCH_2CH_2N\ CH_3$), 52.9 (d, $^2J_{PC}$ = 5 Hz, PCH_2CH_2N), 52.7 (s, $NCH_2CH_2NCH_3$), 45.8 (s, CH_3), 29.7 (d, $^1J_{PC}$ = 21 Hz, PCH_2).

^{31}P{^{1}H} NMR (162 MHz, Benzene-d_6) δ ppm 42.8 (s).

MS (ASAP$^+$) *m/z*: 505.1 ($[MH]^+$), 477.1 ($[M\text{-}CO]^+$), 448.1 ($[M\text{-}2(CO)]^+$), 364.1 ($[M\text{-}5(CO)]^+$), 311.2 ($[M\text{-}Cr(CO)_5]^+$).

IR (CH_2Cl_2): ν_{CO} = 2062 cm^{-1}, 1982 cm^{-1}, 1935 cm^{-1}.

Method B: Microwave synthesis

A 40 mL glass microwave vessel was charged with PNN (0.242 g, 0.775 mmol) and $Cr(CO)_6$ (0.222 g, 1.01 mmol) before adding toluene (20 mL). The vessel was sealed with a crimp-cap. Subsequently, the solution was heated to 140 °C using a microwave reactor for 4 hours, in which time the solution turned yellow. The solution was transferred into a Schlenk before cooling to 0 °C and filtering to remove excess $Cr(CO)_6$. The solvent was then removed under vacuum to give the product as a yellow viscous oil, which solidified upon scraping (0.377 g, 96% yield).

6.3.2 Preparation of 1-(2-diphenylphosphino-ethyl)-morpholine chromium pentacarbonyl (2.5)

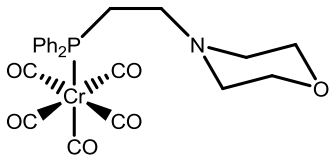

An analogous procedure to that used in the preparation of complex **2.4** was used, with PNO (0.482 g, 1.61 mmol) in toluene (40 mL), $Cr(CO)_6$ (0.425 g, 1.93 mmol) to yield a yellow oil that solidified upon scraping to give a yellow powder (0.71 g, 90%). Elemental analysis of the product produced inconclusive results.

^{1}H NMR (700 MHz, Benzene-d_6) δ ppm: 7.37 – 7.31 (m, 4H, *o*-C_6H_5), 7.01 – 6.96 (m, 6H, *m*-,-*p*-C_6H_5), 3.43 – 3.38 (m, 4H, NC_2H_4O), 2.43 – 2.37 (m, 2H, PCH_2), 2.35 – 2.29 (m, 2H, PCH_2CH_2N), 2.01 – 1.97 (m, 4H, NC_2H_4O).

^{13}C{^{1}H} NMR (176 MHz, Benzene-d_6) δ ppm 221.2 (d, $^2J_{PC}$ = 7 Hz, *trans*-PCr*C*O), 216.9 (d, $^2J_{PC}$ = 13 Hz, *trans*-Cr*C*O), 136.3 (d, $^1J_{PC}$ = 36 Hz, *ipso*-P*C*$_6H_5$), 131.5 (d, $^2J_{PC}$ = 10 Hz, *o*-P*C*$_6H_5$), 129.8 (d, $^4J_{PC}$ = 2 Hz, *p*-P*C*$_6H_5$), 128.5 (d, $^3J_{PC}$ = 9 Hz, *m*-P*C*$_6H_5$), 66.5 (s, O*C*H_2), 53.3 (d, $^2J_{PC}$ = 5 Hz, PCH_2CH_2N), 53.1 (s, NCH_2CH_2O), 29.3 (d, $^1J_{PC}$ = 21 Hz, P*C*H_2).

^{31}P{^{1}H} NMR (283 MHz, Benzene-d_6) δ ppm 43.5 (s).

MS (ASAP$^+$) *m/z*: 436.1 ([MH-2(CO)]$^+$), 379.0 ([M-4(CO)]$^+$), 351.1 ([M-5(CO)]$^+$).

IR (CH_2Cl_2): ν_{CO} = 2063 cm^{-1}, 1982 cm^{-1}, 1938 cm^{-1}.

6.3.3 Preparation of piperidine-*N*-ethylene-diphenylphosphine chromium tetracarbonyl (2.6)

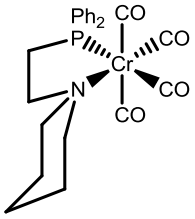

An analogous procedure to that used in the preparation of complex **2.4** was used initially, with PNC (0.456 g, 1.53 mmol) in toluene (40 mL), $Cr(CO)_6$ (0.439 g, 1.99 mmol) to yield a yellow oil. The oil was analysed by ^{31}P NMR spectroscopy, which showed that three products had formed ($^{31}P\{^1H\}$ NMR (162 MHz, C_6D_6) δ 58.3, 56.6, 42.4). The yellow oil was washed with hexane to leave a yellow oil insoluble in hexane. $^{31}P\{^1H\}$ NMR spectroscopic analysis showed this oil to contain one phosphorus-containing species. The product was isolated as yellow crystals following layering of a concentrated DCM solution of the product with hexane. The resulting crystals were suitable for X-ray diffraction (0.136 g, 19% yield). (calc.: $C_{23}H_{28}NO_4PCr$ C, 59.87; H, 5.24; N, 3.04. Found: C, 59.77; H, 5.14; N, 3.13).

^{1}H NMR (600 MHz, Benzene-d_6)) δ ppm: 7.70 – 7.65 (m, 4H, PC_6H_5), 7.10 – 7.06 (m, 4H, PC_6H_5), 7.02 – 6.99 (m, 2H, PC_6H_5), 2.95 – 2.88 (m, 2H, $NCH_2CH_2CH_2$), 2.26 – 2.21 (m, 2H, $NCH_2CH_2CH_2$), 2.07 – 1.98 (m, 2H, PCH_2CH_2N), 1.98 – 1.92 (m, 2H, PCH_2), 1.17 – 1.10 (m, 2H, $NCH_2CH_2CH_2$), 1.10 – 1.02 (m, 4H, $NCH_2CH_2CH_2$).

^{13}C{^{1}H} NMR (151 MHz, Benzene-d_6) δ ppm: 228.8 (d, $^2J_{PC}$ = 13 Hz, *trans*-PCr*C*O), 226.3 (d, $^2J_{PC}$ = 2.5 Hz, *trans*-NCr*C*O), 218.5 (d, $^2J_{PC}$ = 14 Hz, *trans*-Cr*C*O), 136.5 (d, $^1J_{PC}$ = 34 Hz, *ipso*-P*C*$_6$H$_5$), 131.3 (d, $^2J_{PC}$ = 11 Hz, *o*-P*C*$_6$H$_5$), 129.6 (d, $^4J_{PC}$ = 2 Hz, *p*-P*C*$_6$H$_5$), 128.5 (d, $^3J_{PC}$ = 9 Hz, *m*-P*C*$_6$H$_5$), 61.7 (s, N*C*H$_2$CH$_2$CH$_2$), 54.0 (s, PCH$_2$*C*H$_2$N), 25.3 (d, $^1J_{PC}$ = 16 Hz, P*C*H$_2$), 22.8 (s, NCH$_2$*C*H$_2$CH$_2$), 21.4 (s, NCH$_2$CH$_2$*C*H$_2$).

^{31}P{^{1}H} NMR (243 MHz, Benzene-d_6) δ ppm 57.1 (s).

IR (CH_2Cl_2): ν_{CO} = 2007 cm^{-1}, 1899 cm^{-1},* 1883 cm^{-1},* 1840 cm^{-1}.

MS (ASAP$^+$) *m/z*: 461.1 ([M]$^+$), 298.2 ([M-Mo(CO)$_4$]$^+$).

* Peak acquired by deconvolution of larger peak at 1888 cm^{-1}

6.3.4 Preparation of 1-(2-diphenylphosphino-ethyl)-4-methyl-piperazine molybdenum tetracarbonyl (2.7)

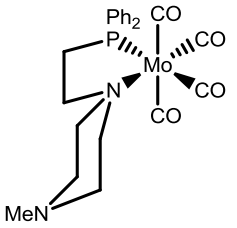

An analogous procedure to that used for the preparation of complex **2.4** was used initially, namely treating PNN (0.4 g, 1.28 mmol) in toluene (40 mL), with $Mo(CO)_6$ (0.405 g, 1.54 mmol) to yield a yellow solid product that was washed with hexane (5 mL) before being recrystallised from a concentrated solution of DCM by layering with hexane. This gave the product as yellow crystals suitable for X-ray diffraction (0.263 g, 39% yield). (calc.: $C_{23}H_{25}N_2O_4PMo$ C, 53.09; H, 4.84; N, 5.38. Found: C, 52.86; H, 5.06; N, 5.38).

^{1}H NMR (600 MHz, Benzene-d_6) δ ppm: 7.69 – 7.62 (m, 4H, PC_6H_5), 7.08 – 7.02 (m, 4H, PC_6H_5), 7.01 – 6.95 (m, 2H, PC_6H_5), 2.76 – 2.55 (m, 4H, $NCH_2CH_2NCH_3$), 2.23 – 2.15 (m, 2H, $NCH_2CH_2NCH_3$), 2.12 (s, 3H, CH_3), 2.04 – 1.95 (m, 2H, $NCH_2CH_2NCH_3$), 1.94 – 1.86 (m, 4H, PC_2H_4N).

^{13}C{^{1}H} NMR (151 MHz, Benzene-d_6 δ ppm: 221.4 (d, $^2J_{PC}$ = 9 Hz, *trans*-NMo*C*O), 216.3 (d, $^2J_{PC}$ = 33 Hz, *trans*-PMo*C*O), 208.4 (d, $^2J_{PC}$ = 9 Hz, *trans*-Mo*C*O), 136.0 (d, $^1J_{PC}$ = 34 Hz, *ipso*-PC_6H_5), 131.6 (d, $^2J_{PC}$ = 13 Hz, *o*-PC_6H_5), 129.8 (d, $^4J_{PC}$ = 2 Hz, *p*-PC_6H_5), 128.6 (d, $^3J_{PC}$ = 9 Hz, *m*-PC_6H_5), 61.0 (s, PCH_2CH_2N and $NCH_2CH_2NCH_3$), 52.6 (s, $NCH_2CH_2NCH_3$), 45.0 (s, CH_3), 24.7 (d, $^1J_{PC}$ = 17 Hz, PCH_2CH_2N).

^{31}P{^{1}H} NMR (243 MHz, Benzene-d_6) δ ppm 37.4 (s).

MS (ASAP$^+$) *m/z*: 523.1 ($[MH]^+$), 494.1 ($[M\text{-}CO]^+$), 466.1 ($[M\text{-}2(CO)]^+$), 311.2 ($[M\text{-}Mo(CO)_4]^+$).

IR (CH_2Cl_2): ν_{CO} = 2018 cm^{-1}, ν_{CO} = 1909cm^{-1},* ν_{CO} = 1889 cm^{-1},* ν_{CO} = 1846 cm^{-1}.

* Peak acquired by deconvolution of larger peak at 1902 cm^{-1}

6.3.5 Preparation of 1-(2-diphenylphosphino-ethyl)-morpholine molybdenum tetracarbonyl (2.8)

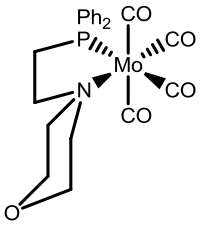

An analogous procedure to that used for the preparation of complex **2.4** was used initially, namely treating PNO (0.383 g, 1.28 mmol) in toluene (40 mL) with $Mo(CO)_6$ (0.405 g, 1.54 mmol) to yield a yellow solid product which was washed with hexane (5 mL) before being recrystallised from a concentrated DCM solution layered with hexane. This gave the product as yellow crystals suitable for X-ray diffraction (0.247 g, 38% yield). (calc.: $C_{22}H_{26}NO_5PMo$ C, 51.98; H, 4.56; N, 2.76. Found: C, 51.86; H, 4.48; N, 2.83).

^{1}H NMR (600 MHz, Benzene-d_6) δ ppm: 7.60 – 7.54 (m, 4H, PC_6H_5), 7.02 – 6.96 (m, 4H, PC_6H_5), 6.96 – 6.89 (m, 2H, PC_6H_5), 4.03 – 3.96 (m, 2H, NCH_2CH_2O), 3.34 – 3.28 (m, 2H, NCH_2CH_2O), 2.30 – 2.25 (m, 2H, NCH_2CH_2O), 1.93 – 1.78 (m, 4H, PC_2H_4N), 1.62 – 1.54 (m, 2H, NCH_2CH_2O).

^{13}C{^{1}H} NMR (151 MHz, Benzene-d_6) δ ppm: 221.0 (d, $^2J_{PC}$ = 8 Hz, *trans*-NMo*C*O), 216.0 (d, $^2J_{PC}$ = 33 Hz, *trans*-PMo*C*O), 208.1 (d, $^2J_{PC}$ = 9 Hz, *trans*-Mo*C*O), 136.0 (d, $^1J_{PC}$ = 34 Hz, *i*-PC_6H_5), 131.5 (d, $^2J_{PC}$ = 13 Hz, *o*-PC_6H_5), 129.9 (d, $^4J_{PC}$ = 2 Hz, *p*-PC_6H_5), 128.6 (d, $^3J_{PC}$ = 9 Hz, *m*-PC_6H_5), 64.8 (s, NCH_2CH_2O), 62.5 (d, $^2J_{PC}$ = 13 Hz, PCH_2CH_2N), 61.0 (s, NCH_2CH_2O), 24.2 (d, $^1J_{PC}$ = 17 Hz, PCH_2).

^{31}P{^{1}H} NMR (243 MHz, Benzene-d_6) δ ppm 37.4 (s).

MS (ASAP$^+$) *m/z*: 510.4 ($[MH]^+$), 481.0 ($[M\text{-}CO]^+$), 453.0 ($[M\text{-}2(CO)]^+$), 300.2 ($[MH\text{-}Mo(CO)_4]^+$).

IR (CH_2Cl_2): ν_{CO} = 2019 cm^{-1}, 1909 cm^{-1},* 1883 cm^{-1},* 1849 cm^{-1}.

* Peak acquired by deconvolution of a larger peak at 1903 cm^{-1}

6.3.6 Preparation of piperidine-*N*-ethylene-diphenylphosphine molybdenum tetracarbonyl (2.9)

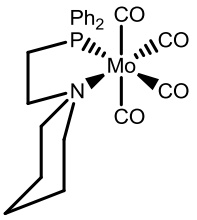

An analogous procedure to that used for the preparation of complex **2.4** was employed, treating PNC (0.371 g, 1.25 mmol) in toluene (40 mL) with $Mo(CO)_6$ (0.428 g, 1.62 mmol) to yield a yellow solid. Subsequently, the solid was washed with hexane (5 mL) before being recrystallised from a concentrated DCM solution layered with hexane, giving complex **2.7** as yellow crystals (0.307 g, 49% yield) (calc.: $C_{23}H_{25}NO_4PMo$ C, 54.55; H, 4.98; N, 2.77. Found: C, 54.51; H, 4.90; N, 2.87).

^{1}H NMR (700 MHz, Benzene-d_6) δ 7.70 – 7.64 (m, 4H, PC_6H_5), 7.08 – 7.03 (m, 4H, PC_6H_5), 7.01 – 6.96 (m, 2H, PC_6H_5), 2.81 – 2.74 (m, 2H, $NCH_2CH_2CH_2$), 2.11 – 2.02 (m, 2H, PCH_2CH_2N), 2.00 – 1.94 (m, 2H, PCH_2CH_2N), 1.85 – 1.79 (m, 2H, $NCH_2CH_2CH_2$), 1.70 – 1.57 (m, 2H, $NCH_2CH_2CH_2$), 1.28 – 1.23 (m, 1H, $NCH_2CH_2CH_2$), 1.18 – 1.10 (m, 2H, $NCH_2CH_2CH_2$), 0.94 – 0.86 (m, 1H, $NCH_2CH_2CH_2$).

^{13}C{^{1}H} NMR (176 MHz, Benzene-d_6) δ 221.6 (d, $^2J_{PC}$ = 8 Hz, *trans*-NMo*C*O), 216.4 (d, $^2J_{PC}$ = 33 Hz, *trans*-PMo*C*O), 208.5 (d, $^2J_{PC}$ = 9 Hz, *cis*-Mo*C*O), 136.1 (d, $^1J_{PC}$ = 34 Hz, *i*-P*C*$_6$H$_5$), 131.6 (d, $^2J_{PC}$ = 13 Hz, *o*-P*C*$_6$H$_5$), 129.8 (d, $^4J_{PC}$ = 2 Hz, *p*-P*C*$_6$H$_5$), 128.6 (d, $^3J_{PC}$ = 9 Hz, *m*-P*C*$_6$H$_5$), 61.9 (s, N*C*$H_2CH_2CH_2$), 58.6 (s, PCH_2CH_2N), 25.2 (d, $^1J_{PC}$ = 18 Hz, P*C*H_2CH_2N), 23.1 (s, $NCH_2CH_2CH_2$, 23.0 (s, $NCH_2CH_2CH_2$).

^{31}P{^{1}H} NMR (243 MHz, Benzene-d_6) δ ppm: 37.6 (s)**.**

MS (ASAP$^+$) *m/z*: 507.0 ([M]$^+$), 478.0 ([M−H−CO]$^+$), 298.2 ([MH−Mo(CO)$_4$]$^+$)**.**

IR (CH_2Cl_2) ν_{CO} = 2017 cm^{-1}, 1908 cm^{-1},* 1888 cm^{-1},* 1844 cm^{-1}.

* Peak acquired by deconvolution of larger peak at 1904 cm^{-1}

6.3.7 Decarbonylation Reactions

6.3.7.1 Decarbonylation of 1-(2-diphenylphosphino-ethyl)-4-methyl-piperazine chromium pentacarbonyl to 1-(2-diphenylphosphino-ethyl)-4-methyl-piperazine chromium tetracarbonyl (2.10)

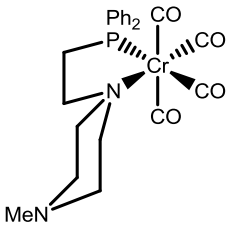

A round bottom flask was charged with a sample of complex **2.4** (0.110 g, 0.22 mmol) and TMNO (0.016 g, 0.22 mmol). The solids were dissolved in toluene (20 mL) and set to reflux. The progress of the reaction was monitored by $^{31}P\{^{1}H\}$ NMR spectroscopic analysis. After 54 hours the reaction was found to have stopped, and so the reaction mixture was cooled to room temperature and filtered to give a clear yellow solution. The solvent was removed under vacuum to give a viscous yellow oil. The oil was washed with hexane to leave the product as a yellow oil. $^{31}P\{^{1}H\}$ NMR analysis showed this to consist of a combination of two products. A concentrated DCM solution of the oil was layered with hexane to grow yellow crystals of the product (10 mg, 7% yield).

^{1}H NMR (700 MHz, Benzene-d_6) δ 7.69 – 7.63 (m, 4H, P-*m*-C_6H_5), 7.10 – 7.04 (m, 4H, P-*o*-C_6H_5), 7.02 – 6.97 (m, 2H, P-*p*-C_6H_5), 2.03 (s, 4H, N(CH_2)$_2$(CH_2)$_2$$NCH_3$), 1.87 (s, 2H, P$CH_2CH_2$N), 1.36 (s, 3H, N$CH_3$), 1.31 (s, 2H, P$CH_2CH_2$N), 0.97 – 0.87 (m, 4H, N(CH_2)$_2$(CH_2)$_2$$NCH_3$).

^{13}C{^{1}H} NMR (176 MHz, Benzene-d_6) δ 229.1 (d, $^{2}J_{PC}$ = 14 Hz, Cr(*C*O)$_4$), 226.7 (Cr(*C*O)$_4$), 218.9 (d, $^{2}J_{PC}$ = 14 Hz, Cr(*C*O)$_4$), 136.8 (d, $^{1}J_{PC}$ = 35 Hz, P-*i*-C_6H_5), 131.7 (d, $^{3}J_{PC}$ = 11 Hz, P-*m*-C_6H_5), 130.1 (d, $^{4}J_{PC}$ = 2 Hz, P-*p*-C_6H_5), 129.0 (d, $^{2}J_{PC}$ = 9 Hz, P-*o*-C_6H_5), 61.5 (N(CH_2)$_2$(CH_2)$_2$$NCH_3$), 51.2 (d, $^{2}J_{PC}$ = 33 Hz, PCH_2CH_2N), 45.6 (N(CH_2)$_2$(CH_2)$_2$$NCH_3$), 30.2 (N$CH_3$), 25.3 (d, $^{1}J_{PC}$ = 15 Hz, PCH_2CH_2N).

^{31}P{^{1}H} NMR (162 MHz, Benzene-d_6) δ ppm 55.8 (s).

6.3.7.2 Control reaction of 1-(2-diphenylphosphino-ethyl)-4-methyl-piperazine with TMNO

In an NMR tube a sample of PNN (0.025 g, 0.08 mmol) and TMNO (0.006 g, 0.08 mmol) were dissolved in DCM (0.7 mL). This was heated to 70 °C for 16 hours and the solution was seen to turn dark brown and brown precipitate formed. The progress of the reaction was monitored by $^{31}P\{^{1}H\}$ NMR spectroscopy, but no product was isolated.

6.4 Preparation of Chloroimines

A range of chloroimines were synthesised following a two-step preparation described by Budzelaar *et al.*[7] An example is given below.

i) Preparation of N-o-tolylbenzamide

A three-necked round bottom flask equipped with a dropping funnel and condenser was charged with DCM (160 mL) before triethylamine (11.97 g, 118 mmol) and *o*-toluidene (12.68 g, 118 mmol) were added. A solution of benzoyl chloride (16.63 g, 118 mmol) in DCM (40 mL) was then added dropwise to the amine solution. Upon completion of the addition the resulting solution was set to reflux for 1 hour, in which time the colour of the solution turned from red to orange. The solution was cooled and washed with distilled water (3 × 50 mL) before being dried over magnesium sulphate. The solvent was removed *in vacuo* and the resulting white solid product was washed with cold diethyl ether to yield the product as a white crystalline solid (22.61 g, 91% yield). The identity of the product was verified by ^{1}H NMR spectroscopy, matching with literature values.[8]

ii) Preparation of N-o-tolylbenzimidoyl chloride

Toluene (200 mL) was added to a two-necked round bottom flask before adding *N-o*-tolylbenzamide (22.61 g, 107 mmol), resulting in a slurry. Solid PCl_5 (22.29 g, 107 mmol) was added in small portions with vigorous stirring. Over the course of the addition HCl gas was evolved, and the slurry dissolved to leave a clear yellow solution. The solution was stirred for 16 hours before the volatile components were removed *in vacuo* to leave a crude orange oil. The final product was purified by vacuum distillation (1 mbar, 135°C) to yield the product as a yellow oil (21.31 g, 87% yield). The identity of the product was verified by ^{1}H NMR spectroscopy, matching with literature values.[8]

Compound	**^{t}Bu(Cl)C=N(2-MeC$_6$H$_4$)[9]**	**Ph(Cl)C=NPh[9]**	**Ph(Cl)C=N(2-MeOC$_6$H$_4$)[10]**
	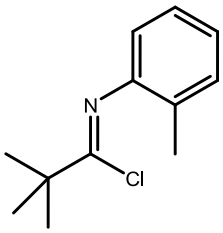	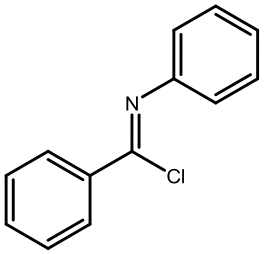	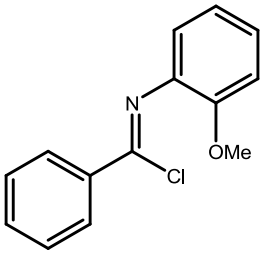
Distillation conditions used for purification	79-82 °C, 0.1 mbar	137-140 °C, 0.2 mbar	143-144 °C, 0.2 mbar
Yield (%)	82	88	90
Product appearance	Colourless oil	White crystalline solid	Yellow crystalline solid

Compound	**Ph(Cl)C=N(2,6-^{i}Pr$_2$C$_6$H$_3$)[11]**	**Ph(Cl)C=N(2,6-Me$_2$C$_6$H$_3$)[12]**	**Ph(Cl)C=N(2,6-Et$_2$C$_6$H$_3$)[12]**
	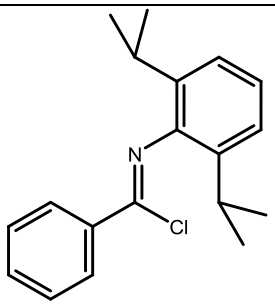	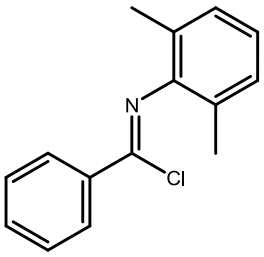	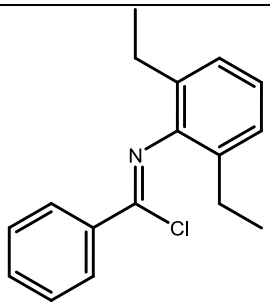
Distillation conditions used for purification	165-167 °C, 0.45 mbar	143-147 °C, 1 mbar	145-146 °C, 1 mbar
Yield (%)	90	90	85
Product appearance	Yellow crystalline solid	Pale yellow oil	Pale yellow oil

Compound	**Ph(Cl)C=N(2,4,6-$Ph_3C_6H_2$)**[*]	**^{t}Bu(Cl)C=N(2,6-$^{i}Pr_2C_6H_3$)**[13]	**^{t}Bu(Cl)C=N(2,6-$Me_2C_6H_3$)**[14]
	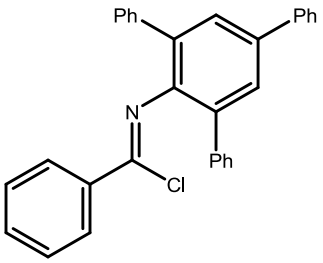	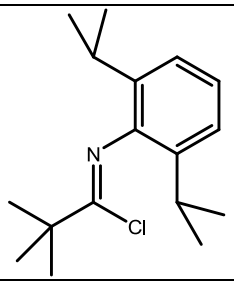	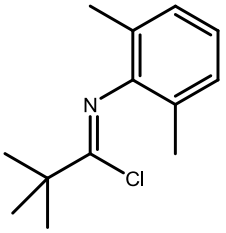
Distillation conditions used for purification	Crystallised from hot hexane	115-118 °C, 1 mbar	89-90 °C, 1 mbar
Yield (%)	65	77	89
Product appearance	White crystalline solid	Colourless oil	Colourless oil

Compound	**Ph(Cl)C=N(2,5-$^{t}Bu_2C_6H_3$)**[†]
	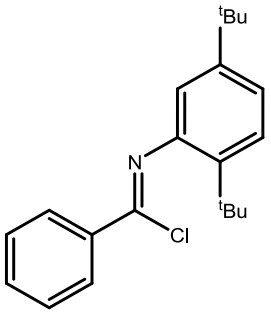
Distillation conditions used for purification	180 - 185 °C, 1 mbar
Yield (%)	Approx. 70 %[‡]
Product appearance	Extremely viscous clear yellow oil

[*] See Appendix 7.2.2 for characterisation
[†] See Appendix 7.2.1 for characterisation
[‡] Accurate yield could not be measured due to highly viscous nature of product

6.5 Preparation of Trimethylsilylphosphines

6.5.1 Preparation of trimethylsilyl-(diisopropyl)-phosphine

A flask was charged with diisopropylphosphine (9.629 g, 81.2 mmol) and THF (150 ml) before being cooled to – 78 °C. A solution of ^{n}BuLi (39.0 mL, 2.5 M solution in hexanes) in THF (30 mL) was then added dropwise. The solution was allowed to warm to room temperature and stirred for 1 hour before being cooled back to – 78 °C. TMSCl (13.40 mL, 0.106 mol) was added dropwise, causing a white precipitate to crash out of solution. The solution was left to warm to room temperature before the solvent was removed under vacuum, taking care not to remove the desired product as well. Pentane was added (10 mL) and the solution was isolated by filtration. The precipitate was washed with more pentane (3 × 10 mL) and the washings combined. The solvent was removed under reduced pressure to yield the title compound as a colourless oil (14.367 g, 93 % yield). The identity of the product was verified by $^{31}P\{^{1}H\}$ and ^{1}H NMR spectroscopy.[15]

6.5.2 Preparation of trimethylsilyl-(di-*tert*-butyl)-phosphine

A pre-weighed 2-necked round bottom flask was charged with di-*tert*-butylphosphine (10% wt solution in hexanes, 50 mL, 23 mmol). THF (15 mL) was added to the solution before cooling to 0 °C. A solution of ^{n}BuLi (2.5M solution in hexanes, 12 mL, 29.9 mmol) in THF (15 mL) was added dropwise to the flask, upon which the phosphine solution turned yellow. The solution was allowed to warm to room temperature and stirred for an hour before being cooled back to 0 °C. TMSCl (3.50 g, 32.2 mmol) was added dropwise to the phosphide solution to form a colourless solution and a white precipitate. The solvent was removed under vacuum and the product dissolved in hexane (20 mL) before filtering to remove the precipitate. The solid residue was washed with further hexane (2 × 10 mL). The hexane was removed under vacuum to isolate the product as a colourless oil (4.896 g, 97% yield). The identity of the product was verified by ^{1}H and $^{31}P\{^{1}H\}$ NMR spectroscopy.[16]

6.5.3 Preparation of trimethylsilyl-(dicyclohexyl)-phosphine

Dicyclohexylphosphine (10% wt soloution in hexanes, 60 mL, 22.2 mmol) was placed in a 2-necked round bottom flask along with THF (15 mL) before being cooled to 0 °C. ^{n}BuLi (2.5 M solution in hexanes, 11.6 mL, 28.9 mmol) was added dropwise to the phosphine solution and the colour of the solution turned to yellow along with the formation of a white precipitate. The solution was warmed to room temperature and stirred for an hour before being cooled back to 0 °C. TMSCl (3.379 g, 31.1 mmol) was added dropwise, which caused the solution to turn colourless and form a white precipitate. The solvent was removed under vacuum and hexane (10 mL) was added. The resulting mixture was filtered and the precipitate washed with further

hexane (3 × 5 mL) and the filtrate was collected. The solvent was removed *in vacuo* and the product was isolated as a colourless oil (5.490 g, 91 % yield). The identity of the product was verified by ^{1}H and $^{31}P\{^{1}H\}$ NMR spectroscopy, in agreement with literature values.[17]

6.5.4 Preparation of trimethylsilyl-(diethyl)-phosphine

Diethylphosphine (10 % wt solution in hexanes, 10.9 mmol) was added to a flask as well as THF (10 mL). The phosphine solution was cooled to 0 °C before a solution of ^{n}BuLi (2.5 M in hexanes, 5.24 mL, 13.1 mmol) and THF (10 mL) was added dropwise, upon which the solution turned yellow. The solution was left to warm to room temperature and stirred for an hour. The solution was then cooled to 0 °C and TMSCl was added dropwise to give a colourless solution and a white precipitate. The solution was warmed to room temperature before the solvent was removed under vacuum. The white solid residue was washed with pentane (3 × 10 mL) and the colourless filtrate was collected. The solvent was removed under vacuum to yield the product as a colourless oil (0.920 g, 51 % yield). The identity of the product was verified by ^{1}H and $^{31}P\{^{1}H\}$ NMR spectroscopy, in agreement with literature values.[18]

6.5.5 Preparation of trimethylsilyl-*bis*(ortho-fluoro)phenyl-phosphine

i. *Preparation of N,N-diethyl-bis(2-fluorophenyl)phosphinamine*

A solution of ^{n}BuLi (2.5M solution in hexanes, 18 mL, 45 mmol) and diethyl ether (150 mL) was put in a flask before being cooled to –78 °C. A solution of 1-bromo-2-fluorobenzene (7.875 g, 45 mmol) in diethyl ether (60 mL) was added dropwise to the cooled BuLi solution over the course of an hour. A solution of dichloro(diethylamino)phosphine (3.915 g, 22.5 mmol) in diethyl ether (30 mL) was then added dropwise to the cooled solution, while maintaining the temperature at –78 °C. Upon completion of the addition the solution was warmed to room temperature and the solvent removed under vacuum to isolate a colourless oil with the title compound as the primary product measured by $^{31}P\{^{1}H\}$ NMR spectroscopy (4.885 g, 74 % yield).

ii. *Preparation of chloro-bis(2-fluorophenyl)phosphine*

N,N-Diethyl-*bis*(2-fluorophenyl)phosphinamine was placed in a flask before being dissolved in diethyl ether (50 mL) and cooled to –78 °C. An HCl solution was added (2 M solution in diethyl ether, 33.3 mmol) dropwise causing the formation of a white precipitate. The solution was left to warm to room temperature and stirred for an hour before being filtered to remove the precipitate that had formed. The solvent was removed *in vacuo* to afford a colourless oil that was distilled under vacuum (85 °C, 0.1 mbar) to yield the product as a colourless oil (3.033 g, 71 % yield).

iii. *Preparation of trimethylsilyl-bis(ortho-fluoro)phenyl-phosphine*

A solution of chloro-*bis*(2-fluorophenyl)phosphine (3.033 g, 11.8 mmol) in diethyl ether (50 mL) was placed in a flask and cooled to 0 °C. A $LiAlH_4$ solution (1 M in diethyl ether, 17.7 mmol) was added dropwise, instantly forming a white precipitate. The solution was warmed to room temperature and stirred for an hour. The mixture was then cooled back to 0 °C and degassed H_2O (30 mL) added dropwise. The organic layer was extracted and the remaining aqueous fraction was washed with diethyl ether (3 × 20 mL). The organic washings were combined over $MgSO_4$ before the solvent was removed under vacuum to give the intermediate *bis*(2-fluorophenyl)phosphine as an oily white solid. The white residue was dissolved in THF (50 mL) and the resulting solution was cooled to –78 °C. ^{n}BuLi (2.5 M solution in hexanes, 11.8 mmol) was added dropwise instantly giving a colour change to blood red. The solution was left to stir at –78 °C for 30 minutes before TMSCl (1.923 g, 17.7 mmol) was added dropwise. The resulting yellow solution was warmed to room temperature before the solvent was removed under reduced pressure to give a white solid and a yellow oil. The oil was extracted by washing with hexane (3 × 10 mL) and the hexane was removed under vacuum to yield the crude product as a yellow oil. The crude product distilled under vacuum (110 °C, 0.1 mbar) to yield a colourless oil containing the title compound as the major product (81 % measured by $^{31}P\{^{1}H\}$ NMR spectroscopy) (1.856 g, 53 % yield). Elemental analysis was carried out, but due to the oily and highly air sensitive nature of the product gave inconclusive results.

^{1}H NMR (700 MHz, Benzene-d_6) δ 7.33 – 7.28 (m, 2H, 6-C_6H_4), 6.87 – 6.82 (m, 2H, 4-C_6H_4), 6.80 – 6.76 (m, 2H, 3-C_6H_4), 6.74 – 6.70 (m, 2H, 5-C_6H_4), 0.26 (dt, $^{2}J_{SiH}$ = 5 Hz, $^{3}J_{PH}$ = 1 Hz, 9H, Si(CH_3)$_3$).

$^{13}C\{^{1}H\}$ NMR (176 MHz, Benzene-d_6) δ 164.3 (dd, $^{1}J_{FC}$ = 243, $^{2}J_{PC}$ = 8 Hz, 2-C_6H_4), 136.2 (dd, *J* = 16, 5 Hz, 6-C_6H_4), 130.2 (d, *J* = 8 Hz, 4-C_6H_4), 124.6 (dd, *J* = 6, 3 Hz, 5-C_6H_4), 122.7 (td, *J* = 23, 2 Hz, 1-C_6H_4), 115.4 (d, *J* = 24 Hz, 3-C_6H_4), –0.6 (dt, *J* = 13, 3 Hz, Si(CH_3)$_3$).

$^{31}P\{^{1}H\}$ NMR (283 MHz, Benzene-d_6) δ –80.1 (t, $^{1}J_{SiP}$ = 19 Hz).

^{29}Si NMR (139 MHz, Benzene-d_6) δ 4.8 (dt, $^{1}J_{PSi}$ = 22 Hz, $^{4}J_{FSi}$ = 3 Hz).

MS (ASAP^{+}) *m/z*: 295.1 ([MH]$^{+}$), 311.1 ([MOH]$^{+}$).

6.5.6 Preparation of trimethylsilyl-*bis*(*ortho*-ethyl)phenyl-phosphine

i. Preparation of chloro-bis(ortho-ethyl)phenyl-phosphine

Magnesium turnings (9.19 g, 378 mmol) were added to a flask and heated under vacuum for one hour. The flask was cooled to room temperature before diethylether was added (200 mL). A solution of 1-bromo-2-ethylbenzene (14.00 g, 76 mmol) in diethyl ether (50 mL) was added dropwise before the resulting solution was heated at reflux for 2 hours. The solution was cooled and filtered to yield a clear orange solution of the Grignard reagent. In a separate flask PCl_3 (5.19 g, 38 mmol) and diethyl ether (100 mL) were added and cooled to –78 °C. The Grignard solution was then added dropwise to the phosphine, forming a cream precipitate. Upon completion of the addition the solution was warmed to room temperature and the solvent was removed under vacuum. The solid residue was washed with hexane (100 mL, 2 × 50 mL). The filtrate was isolated as a pale yellow solution before the solvent was removed under vacuum to yield the product as a yellow oil (8.458 g, 81 % yield). Upon analysis by $^{31}P\{^{1}H\}$ NMR spectroscopy it was revealed that the product contained both the chloro- and the bromo-species ($^{31}P\{^{1}H\}$ NMR δ (ppm): 73.0 (s, *P*Br, 46 %), 65.3 (s, *P*Cl, 54 %), consistent with the findings of Blann *et al.*[19]

ii. Preparation of bis(ortho-ethyl)phenyl-phosphine

The mixed chloro-/bromo-*bis*(ortho-ethyl)phenyl-phosphine (8.458 g, 30.6 mmol P) was dissolved in diethyl ether (140 mL) and the solution was cooled to –78 °C. A solution of $LiAlH_4$ (1 M solution in diethyl ether, 45.8 mmol) was added before the solution was warmed to room temperature. Upon warming a white precipitate formed. The solution was cooled to 0 °C and degassed H_2O was added dropwise. The organic phase was extracted and the remaining aqueous phase was washed with further diethyl ether (3 × 40 mL). The organic fractions were combined and dried over $MgSO_4$ and the mixture was filtered to isolate the phosphine solution. The solvent was removed under vacuum to yield the product as a pale yellow oil (5.536 g, 75% yield).

iii. Preparation of trimethylsilyl-bis(ortho-ethyl)phenyl-phosphine

A flask was charged with *bis*(ortho-ethyl)phenyl-phosphine (5.536 g, 22.8 mmol) and THF (100 mL) and cooled to –78 °C. ^{n}BuLi (2.5 M solution in hexanes, 27.4 mmol) was added dropwise instantly turning the solution red. The solution was allowed to warm to 0 °C and left to stir for one hour after which TMSCl (3.227 g, 29.7 mmol) was added dropwise leaving a pale brown solution. The solvent was removed *in vacuo* leaving a yellow oil and white precipitate. The oil was extracted from the precipitate by washing

with hexane (3 × 10 mL) and collecting the filtrate. The hexane was removed under reduced pressure to give a yellow oil, which was purified by vacuum distillation (108-111 °C, 0.1 mbar) giving the product as a colourless oil (4.926 g, 69 % yield). Elemental analysis was carried out, but due to the oily and highly air sensitive nature of the product the results were inconclusive.

^{1}H NMR (700 MHz, Benzene-d_6) δ 7.47 (dd, J = 8, 4 Hz, 2H, 4-C$_6H_4$), 7.12 – 7.06 (m, 4H, 3/6-C$_6H_4$), 6.98 – 6.93 (m, 2H, 5-C$_6H_4$), 3.05 (dqd, J = 15, 8, 2 Hz, 2H, CH_2CH$_3$), 2.84 (dq, J = 15, 8 Hz, 2H, CH_2CH$_3$), 1.19 (t, $^{3}J_{HH}$ = 8 Hz, 6H, CH$_2$CH_3), 0.23 (d, $^{2}J_{SiH}$ = 5 Hz, 9H, Si(CH_3)$_3$).

^{13}C{^{1}H} NMR (176 MHz, Benzene-d_6) δ 148.9 (d, $^{2}J_{PC}$ = 23 Hz, 2-C_6H$_4$), 135.6 (d, $^{4}J_{PC}$ = 2 Hz, 4-C_6H$_4$), 135.2 (d, $^{1}J_{PC}$ = 16 Hz, 1-C_6H$_4$), 129.2 (d, $^{3}J_{PC}$ = 5 Hz, 3-C_6H$_4$), 128.5 (6-C_6H$_4$), 125.9 (5-C_6H$_4$), 28.7 (d, $^{3}J_{PC}$ = 21 Hz, CH$_2$CH$_3$), 15.5 (d, $^{4}J_{PC}$ = 2 Hz, CH$_2$$CH_3$), -0.7 (d, $^{1}J_{SiC}$ = 13 Hz, Si(CH$_3$)$_3$).

^{31}P{^{1}H} NMR (283 MHz, Benzene-d_6) δ –77.8.

^{29}Si NMR (139 MHz, Benzene-d_6) δ 0.8 (d, $^{1}J_{PSi}$ = 20 Hz).

MS (ASAP^{+}) *m/z*: 315.2 ([MH]$^{+}$), 331.2 ([MOH]$^{+}$).

6.5.7 Preparation of trimethylsilyl-*bis*(*ortho*-methoxyphenyl)phosphine

i. Preparation of tris(ortho-methoxyphenyl)phosphine

Magnesium turnings (19.49 g, 800 mmol) were placed in a flask and heated under vacuum for an hour. The flask was cooled and diethyl ether was added (200 mL). A solution of 2-bromoanisole (93.12 g, 498 mmol) in diethyl ether (60 mL) was prepared and added dropwise to the magnesium suspension, causing the solution to gently reflux. Once the addition was complete the resulting mixture was heated at reflux for two hours. The solution was cooled and filtered to give a clear brown solution of the Grignard reagent. The Grignard reagent was added dropwise to a solution of PCl_3 (22.80 g, 166 mmol) in diethyl ether (150 mL) forming a beige precipitate. The solvent was removed under vacuum before degassed H_2O was added dropwise. The organic product was extracted by washing with DCM (4 × 100 mL), which was consequently removed under reduced pressure. The resulting crude product was purified in 3 batches by of recrystallisation from a minimum amount of hot MeCN and crystallised at 0 °C, yielding pale yellow crystals (31.015 g, 53 % yield).

ii. Attempted preparation of trimethylsilyl-bis(ortho-methoxyphenyl)phosphine from tris(ortho-methoxyphenyl)phosphine

A flask was charged with sodium (0.82 g, 35.5 mmol) before being cooled to – 78 °C. Ammonia (300 mL) was then condensed into the flask giving a blue solution. *tris*(*ortho*-Methoxyphenyl)phosphine (5.00 g, 14.2 mmol) was added to the ammonia solution as a solid and the mixture was stirred for four hours. The reaction vessel was then left to warm to room temperature, allowing the ammonia to evaporate. The resulting red solid was dissolved in THF (50 mL) and the solution filtered to afford a clear red solution. The solution was cooled to 0 °C and TMSCl (3.85 g, 35.5 mmol) was added dropwise. The solvent was removed under vacuum and the solid white residue was extracted with hexane (3 × 20 mL) to isolate the organic products. Analysis by $^{31}P[^{1}H]$ NMR spectroscopy revealed that 86% of the phosphine had converted to the *bis*(ortho-methoxyphenyl)phosphine species ($PH(2\text{-}MeOC_6H_4)_2$). It was decided to convert all of the product to the *bis*(ortho-methoxyphenyl)phosphine, and so HCl (1 M solution in diethyl ether, 2 moml) was added. The solvent was again removed under vacuum and the $PH(2\text{-}MeOC_6H_4)_2$ product was dissolved in a mixture of hot hexane/toluene and recrystallised at 0 °C to yield *bis*(ortho-methoxyphenyl)phosphine as a white solid (2.898 g, 83 % yield). The identity of the *bis*(ortho-methoxyphenyl)phosphine was confirmed by NMR spectroscopic analysis, in line with literature values.[20]

iii. Preparation of trimethylsilyl-bis(ortho-methoxyphenyl)phosphine from bis(ortho-methoxyphenyl)phosphine

bis(*ortho*-Methoxyphenyl)phosphine (2.066 g, 8.4 mmol) was placed in a flask and dissolved in THF (50 mL) before being cooled to 0 °C. A solution of ^{n}BuLi (2.M solution in hexanes, 12.6 mmol) was added dropwise to the cooled solution before leaving it to warm to room temperature and then stirred for an hour. The solution was cooled back to 0 °C and TMSCl (1.46 g, 13.4 mmol) was added dropwise. The solution was again allowed to warm to room temperature and stirred for an hour giving a pale yellow solution. The solvent was removed under vacuum, yielding a solid residue. The organic product was extracted from the lithium salt by washing with hexane (3 × 10 mL) before the solvent was removed from the filtrate under vacuum to yield the product as a white solid (2.368 g, 89 % yield). (calc.: $C_{17}H_{23}O_2PSi$, C, 64.12; H, 7.28; N, 0.0. Found: C, 63.94; H, 7.42; N, 0.0).

^{1}H NMR (700 MHz, Benzene-d_6) δ 7.47 – 7.42 (m, 2H, 4-C$_6H_4$), 7.09 (ddd, *J* = 8, 7, 2 Hz, 2H, P-6-C$_6H_4$), 6.78 (tt, *J* = 8, 2 Hz, 2H, 5-C$_6H_4$), 6.51 (dd, *J* = 8, 2 Hz, 2H, 3-C$_6H_4$), 3.25 (s, 6H, OCH_3), 0.26 (d, $^{2}J_{SiH}$ = 5 Hz, 9H, Si(CH_3)$_3$).

^{13}C{^{1}H} NMR (176 MHz, Benzene-d_6) δ 160.5 (d, $^{2}J_{PC}$ = 6 Hz, 2-C_6H$_4$), 136.3 (d, $^{4}J_{PC}$ = 20 Hz, 4-C_6H$_4$), 129.2 (6-C_6H$_4$), 125.0 (d, $^{1}J_{PC}$ = 20 Hz, 1-C_6H$_4$), 121.2 (d, $^{3}J_{PC}$ = 7 Hz, 5-C_6H$_4$), 110.0 (3-C_6H$_4$), 54.4 (OCH$_3$), 0.4 (d, *J* = 13 Hz, Si(CH$_3$)$_3$).

^{31}P{^{1}H} NMR (283 MHz, Benzene-d_6) δ –72.3.

^{29}Si NMR (139 MHz, Benzene-d_6) δ 2.1 (d, $^{1}J_{PSi}$ = 19 Hz).

MS (ASAP^{+}) *m/z*: 319.1 ([MH]$^{+}$), 335.1 ([MOH]$^{+}$).

6.6 Synthesis of Iminophosphines

6.6.1 Attempted synthesis of PhC(PPh_2)=NPh(*o*-Me) (3.1) from *N*-benzylidene-2-methylaniline and chlorodiphenylphosphine

A 2-neck round bottom flask was charged with *N*-benzylidene-2-methylaniline (0.645 g, 3.3 mmol) and placed under an atmosphere of nitrogen before adding toluene (20 mL) and triethylamine (0.334 g, 3.3 mmol). Chlorodiphenylphosphine (0.729 g, 3.3 mmol) was added dropwise to the flask and the resulting solution was heated to 80 °C. After two hours the solution was cooled and analysed by $^{31}P\{^{1}H\}$ NMR spectroscopy, which showed no reaction had occurred. The solution was heated back to 80 °C for a further 16 hours before the progress of the reaction was again checked by $^{31}P\{^{1}H\}$ NMR spectroscopy. Again it was shown that no reaction had occurred, and this method was abandoned.

6.6.2 Attempted synthesis of PhC(PPh_2)=NPh(*o*-Me) (3.1) from *N*-benzylidene-2-methylaniline and lithium diphenylphosphide

A sample of *N*-benzylidene-2-methylaniline (0.510 g, 2.6 mmol) was placed in a 2-neck round bottom flask and placed under an atmosphere of nitrogen. The aldimine was dissolved in THF (10 mL) before lithium diphenylphosphide was added (10 mL, 0.26 M solution in THF). The resulting solution was heated at reflux for 4 hours before being cooled to room temperature and analysed by $^{31}P\{^{1}H\}$ NMR spectroscopy, which showed that no reaction had occurred. The solution was heated back to reflux and left for 16 hours, after which time further $^{31}P\{^{1}H\}$ NMR spectroscopic analysis was carried out. This analysis also demonstrated that no reaction had occurred, and this method was abandoned.

6.6.3 Attempted synthesis of PhC(PPh_2)=NPh(*o*-Me) (3.1) from a nitrilium salt and diphenylphosphine

A Schlenk flask was charged with *N*-*o*-tolylbenzimidoyl chloride (0.518 g, 2.3 mmol) and DCM (15 mL) before being cooled to –78 °C. TMSOTf (0.501 g, 2.3 mmol) was added slowly to this solution while still cold and left to stir. After 15 minutes pyridine (0.178 g, 2.3 mmol) was added and the solution was allowed to warm to room temperature. Upon warming the solution was seen to change colour to yellow. The solution was stirred for 1 hour before diphenylphosphine was added (0.420 g, 2.3 mmol). The solution was again left to stir and a series of colour changes were observed. Initially, the solution changed from yellow to orange, to brown before changing back to yellow in 30 minutes. This colour changed again to orange before finally settling to red after 1 hour of stirring along with the formation of a precipitate. The solution was filtered to remove the precipitate and the solvent was removed *in vacuo* to

yield an orange solid. The orange solid was washed with diethyl ether and the resulting mixture was filtered to extract the yellow diethyl ether-soluble product from the white pyridinium triflate salt. The solvent was removed under reduced pressure and the crude product was isolated as an orange oil. Analysis by $^{31}P\{^{1}H\}$ NMR spectroscopy showed 11 products formed, all of which were subsequently found to be highly soluble in hexane. Due to the high solubility of the products all attempts at purification failed, and no product was isolated for further analysis.

6.6.4 Preparation of PhC(PPh_2)=NPh(*o*-Me) (3.1)

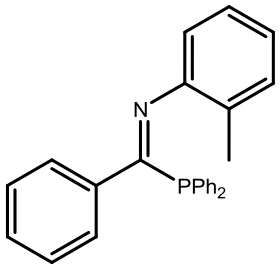

Solid PPh_3 (14.1 g, 54 mmol) was added to a three-neck round bottom flask before being placed under nitrogen and THF (200 mL) was added. Lithium (2 g, 285 mmol) was added and the solution was left to stir for 24 hours, after which time the solution turned deep red. The solution was filtered through celite to remove excess lithium and TMSCl (11.69 g, 108 mmol) was added. The solution was stirred for 2 hours and the colour changed to give a pale brown solution. The solvent was removed under vacuum to give a brown oil. The brown oil was dissolved in toluene (40 mL). In a separate Schlenk flask a sample of *N*-*o*-tolylbenzimidoyl chloride (12.32 g, 54 mmol) was dried by the repeated addition and removal of toluene under vacuum (3 × 5 mL) before dissolving in toluene (40 mL). This chloroimine solution was added to the lithiated phosphine solution along with more toluene (100 mL). The solution was set to reflux for 5 hours after which the completion of the reaction was verified by $^{31}P\{^{1}H\}$ NMR spectroscopy. The solvent was removed under reduced pressure to give a crude yellow solid product. The yellow solid was crystallised from a minimum amount of hexane to yield the product as a yellow crystalline solid (15.5 g, 76% yield). (calc.: $C_{26}H_{22}NP$ C, 82.30; H, 5.84; N, 3.69. Found: C, 82.22; H, 5.92; N, 3.79).

^{1}H NMR (700 MHz, Chloroform-*d*) δ 7.63 (s, 3H, C_6H_n), 7.52 (d, *J* = 8 Hz, 1H, C_6H_n), 7.35 (s, 6H, C_6H_n), 7.24 (d, *J* = 8 Hz, 1H, C_6H_n), 7.19 (s, 2H, C_6H_n), 7.11 (s, 3H, C_6H_n), 6.89 (s, 2H, C_6H_n), 6.70 (s, 0H, C_6H_n), 6.35 (s, 1H, C_6H_n), 2.22 (s, 3H, *o*-$CH_3C_6H_4$).

$^{13}C\{^{1}H\}$ NMR (176 MHz, Chloroform-*d*) δ 177.1 (d, $^{1}J_{PC}$ = 11 Hz, *C*=N), 150.5 (N-*i*-C_6H_4), 137.9 (d, $^{2}J_{PC}$ = 27 Hz, C-*i*-C_6H_5), 135.1 (d, J_{PC} = 19Hz, -C_6H_n), 134.3 (-C_6H_n), 134.0 (d, J_{PC} = 19 Hz, -C_6H_n), 130.0 (-C_6H_n), 129.2 (-C_6H_n), 128.8 (-C_6H_n), 128.6 (-C_6H_n), 128.3 (d, J_{PC} = 8 Hz, P-*i*-C_6H_5), 127.9 (-C_6H_n), 125.9 (-C_6H_n), 123.4 (-C_6H_n), 118.9 (-C_6H_n), 18.5 (*o*-$CH_3C_6H_4$).*

$^{31}P\{^{1}H\}$ NMR (162 MHz, Benzene-d_6) δ 8.2, – 2.2.†

MS (ASAP^{+}) *m/z*: 380.1 ($[MH]^{+}$), 194.0 ($[M\text{-}PPh_2]^{+}$).

IR (ATR): $\nu_{C=N}$ = 1588 cm^{-1}.

* ^{1}H and ^{13}C NMR spectra could not be fully assigned due to broadening of the signals, caused by hindered rotation of the phenyl groups.
† Two resonances due to presence of imine *E* and *Z* isomers in solution.

6.6.5 Preparation of ^{t}BuC(PPh$_2$)=NPh(*o*-Me) (3.2)

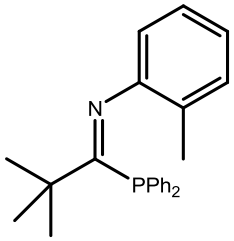

A Schlenk flask was charged with *N*-o-tolylpivalimidoyl chloride (10.37 g, 49 mmol), which was dried by the addition and removal of toluene under vacuum (3 × 10 mL) before adding toluene (50 mL). A separate Schlenk flask was charged with trimethylsilyl(diphenyl)phosphine (12.78 g, 49 mmol) before adding toluene (50 mL). Both the chloroimine and phosphine solutions were transferred to a three-neck round bottom flask and more toluene was added (200 mL) before the resulting solution was set to reflux for 4 hours over which time the colour changed from yellow to orange and a small amount of precipitate formed. The solution was cooled and the completion of the reaction was verified by ^{31}P{^{1}H} NMR spectroscopic analysis. The solution was filtered before the solvent was removed *in vacuo* to leave an orange oil. The oil was placed under vacuum for 16 hours before being recrystallized from a minimum amount of room temperature hexane at –30 °C to give a yellow crystalline solid (14.72 g, 84% yield). (calc.: $C_{24}H_{26}NP$ C, 80.20; H, 7.29; N, 3.90. Found: C, 80.12; H, 7.30; N, 3.92).

^{1}H NMR (700 MHz, Benzene-d_6) δ 7.39 – 7.34 (m, 4H, P-*o*-C_6H_5), 6.96 – 6.92 (m, 6H, P-*m*/*p*-C_6H_5), 6.73 – 6.70 (m, 1H, *o*-$CH_3C_6H_4$), 6.66 – 6.61 (m, 2H, *o*-$CH_3C_6H_4$), 6.61 – 6.57 (m, 1H, *o*-$CH_3C_6H_4$), 1.89 (s, 3H, $C_6H_4CH_3$), 1.40 (s, 9H, $C(CH_3)_3$).

^{13}C{^{1}H} NMR (176 MHz, Benzene-d_6) δ 180.0 (d, $^{1}J_{PC}$ = 59 Hz, *C*=N), 149.4 (s, N-*i*-C_6H_4), 135.8 (d, $^{1}J_{PC}$ = 13 Hz, P-*i*-C_6H_5), 134.5 (d, $^{2}J_{PC}$ = 20 Hz, P-*o*-C_6H_5), 130.0 (s, o_{CH}/*m*/*p*-C_6H_4), 128.6 (s, P-*m*-C_6H_5), 128.4 (s, P-*p*-C_6H_5), 125.7 (s, o_{CH}/*m*/*p*-C_6H_4), 125.6 (s, C-*i*-C_6H_4), 123.1 (s, o_{CH}/*m*/*p*-C_6H_4), 117.2 (s, o_{CH}/*m*/*p*-C_6H_4), 45.8 (d, $^{2}J_{PC}$ = 27 Hz, $C(CH_3)_3$), 29.3 (d, $^{3}J_{PC}$ = 6 Hz, $C(CH_3)_3$), 18.5 (d, $^{4}J_{PC}$ = 1 Hz, *o*-$CH_3C_6H_4$).

^{31}P{^{1}H} NMR (283 MHz, Benzene-d_6) δ –0.2.

MS (ASAP^{+}) *m/z*: 360.2 ($[MH]^{+}$).

IR (ATR): $\nu_{C=N}$ = 1611 cm^{-1}.

6.6.6 Preparation of $PhC(PPh_2)=NPh$ (3.3)

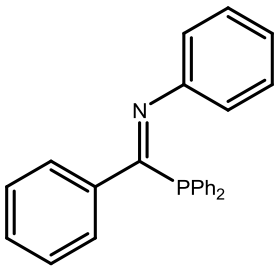

An analogous procedure to that used for the synthesis of compound **3.2** was undertaken with *N*-phenylbenzimidoyl chloride (8.62 g, 40 mmol) and trimethylsilyl(diphenyl)phosphine (10.33 g, 40mmol) in toluene (300 mL). The crude oil product was crystallised from hot hexane at –30 °C to give a yellow crystalline solid (12.71 g, 87% yield). (calc.: $C_{25}H_{20}NP$ C, 82.17; H, 5.52; N, 3.83. Found: C, 82.14; H, 5.61; N, 3.93).

^{1}H NMR (700 MHz, Benzene-d_6) δ 7.76 – 7.64 (m, 4H, -C_6H_5), 7.33 (s, 1H, -C_6H_5), 7.23 (d, J = 8 Hz, 1H, -C_6H_5), 7.07 (d, J = 8 Hz, 3H, -C_6H_5), 7.03 – 6.86 (m, 6H, -C_6H_5), 6.77 – 6.70 (m, 4H, -C_6H_5), 6.67 (d, J = 8 Hz, 1H, -C_6H_5).

^{13}C{^{1}H} NMR (176 MHz, Benzene-d_6) δ 178.5 (d, $^{1}J_{PC}$ = 13 Hz, *C*=N), 152.2 (d, $^{3}J_{PC}$ = 6 Hz, N-*i*-C_6H_5), 138.4 (d, $^{2}J_{PC}$ = 28 Hz, C-*i*-C_6H_5), 135.4 (d, $^{1}J_{PC}$ = 19 Hz P-*i*-C_6H_5), 134.9 (d, J_{PC} = 7 Hz, -C_6H_5), 134.2 (-C_6H_5), 129.4 (-C_6H_5), 128.8 (-C_6H_5), 128.6 (-C_6H_5), 128.6 (-C_6H_5), 123.6 (-C_6H_5), 121.2 (-C_6H_5), 119.5 (-C_6H_5).*

^{31}P{^{1}H} NMR (283 MHz, Benzene-d_6) δ 8.5, –3.2.†

MS (ASAP^{+}) *m/z*: 366.1 ([MH]$^{+}$), 180.1 ([M-PPh_2]$^{+}$).

IR (ATR): $\nu_{C=N}$ = 1587 cm^{-1}.

* ^{1}H and ^{13}C NMR spectra could not be fully assigned due to broadening of the signals, caused by hindered rotation of the phenyl groups.

† Two resonances due to presence of imine *E* and *Z* isomers in solution.

6.6.7 Preparation of PhC(P^iPr_2)=NPh(*o*-Me) (3.4)

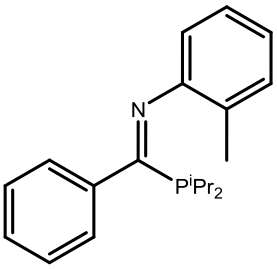

An analogous procedure to that used for the synthesis of compound **3.2** was carried out with *N*-*o*-tolylbenzimidoyl chloride (1.21 g, 5.3 mmol), trimethylsilyl(diisopropyl)phosphine (1.00 g, 5.3 mmol) in toluene (20 mL). The crude product was isolated as a viscous oil that was purified by vacuum distillation (0.2 mbar, 118-122 °C) to give a yellow oil (1.07 g, 65% yield). (calc.: $C_{20}H_{26}NP$ C, 77.14; H, 8.42; N, 4.50. Found: C, 77.03; H, 8.36; N, 4.58).

^{1}H NMR spectroscopic analysis showed the product still to have traces of the chloroimine starting material present (~12 %). This is thought to be due to both the starting *N*-*o*-tolylbenzimidoyl chloride and iminophosphine **3.4** have similar boiling points, hence are difficult to separate *via* distillation.

^{1}H NMR (600 MHz, Benzene-d_6) δ 7.31 (d, J = 7 Hz, 2H, -C_6H_n), 7.04 – 7.01 (m, 1H, -C_6H_n), 6.91 – 6.83 (m, 3H, -C_6H_n), 6.81 – 6.77 (m, 2H, -C_6H_n), 6.40 – 6.35 (m, 1H, -C_6H_n), 2.31 – 2.22 (m, 5H, P-CH(CH_3)$_2$, C_6H_4-CH_3), 1.26 (dd, $^2J_{PH}$ = 13, $^3J_{HH}$ =7 Hz, 6H, P-CH(CH_3)$_2$), 0.98 (dd, $^2J_{PH}$ = 13, $^3J_{HH}$ =7 Hz, 6H, P-CH(CH_3)$_2$).

^{13}C{^{1}H} NMR (151 MHz, Benzene-d_6) δ 178.1 (d, $^1J_{PC}$ = 23 Hz, *C*=N), 151.6 (d, $^3J_{PC}$ = 3 Hz, N-*i*-C_6H_4), 140.3 (d, $^2J_{PC}$ = 26.5 Hz, C-*i*-C_6H_5), 130.5 (-C_6H_n), 129.8 (-C_6H_n), 129.0 (-C_6H_n), 128.6 (-C_6H_n), 128.6 (-C_6H_n), 126.6 (-C_6H_n), 123.4 (-C_6H_n), 119.4 (-C_6H_n), 23.0 (d, $^1J_{PC}$ = 14 Hz, P-*C*H(CH_3)$_2$), 20.7 (d, $^2J_{PC}$ = 12 Hz, P-CH(*C*H_3)$_2$), 19.4 (d, $^2J_{PC}$ = 11 Hz, CH(*C*H_3)$_2$), 18.7 (C_6H_4-CH_3).*

^{31}P{^{1}H} NMR (162 MHz, Benzene-d_6) δ 26.7.

* ^{1}H and ^{13}C NMR spectra could not be fully assigned due to broadening of the signals, caused by hindered rotation of the phenyl groups.

6.6.8 Preparation of PhC(P^tBu_2)=NPh (3.5)

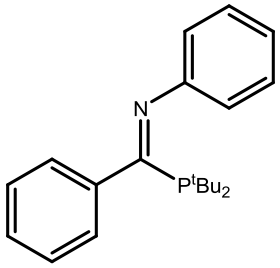

An analogous procedure to that used for the synthesis of compound **3.2** was carried out with *N*-*o*-phenylbenzimidoyl chloride (1.79 g, 8.3 mmol) and trimethylsilyl-*bis*(*tert*-butyl)phosphine (1.816 g, 8.3 mmol). The reaction solution was heated at reflux for 48 hours, after which $^{31}P\{^1H\}$ NMR spectroscopy showed the presence of 21% *bis*(tert-butyl)phosphine had formed. The toluene was then removed *in vacuo* and the residue was dissolved in chlorobenzene. More trimethylsilyl-*bis*(*tert*-butyl)phosphine was added (0.384 g, 1.76 mmol) was added to the reaction and the solution was set to reflux overnight. The solvent was removed under reduced pressure to leave the crude product as an orange oil. The crude product was purified by crystallisation from hot hexane to give the product as a yellow crystalline solid (2.150 g, 80 % yield). (calc.: $C_{21}H_{28}NP$ C, 77.51; H, 8.67; N, 4.30. Found: C, 77.38; H, 8.58; N, 4.39).

^{1}H NMR (700 MHz, Benzene-d_6) δ 7.41 – 7.37 (m, 2H, C-*o*-C_6H_5), 7.00 – 6.97 (m, 2H, N-*m*-C_6H_5), 6.90 – 6.85 (m, 2H, C-*m*-C_6H_5), 6.85 – 6.81 (m, 1H, C-*p*-C_6H_5), 6.79 – 6.75 (m, 1H, N-*p*-C_6H_5), 6.69 – 6.64 (m, 2H, N-*o*-C_6H_5), 1.35 (d, $^3J_{PH}$ = 12 Hz, 18H, P-C(CH_3)$_3$).

$^{13}C\{^1H\}$ NMR (176 MHz, Benzene-d_6) δ 179.6 (d, $^1J_{PC}$ = 31 Hz, *C*=N), 152.5 (d, $^3J_{PC}$ = 2 Hz, N-*i*-C_6H_5), 141.3 (d, $^2J_{PC}$ = 31 Hz, C-*i*-C_6H_5), 130.0 (d, $^3J_{PC}$ = 11 Hz, C-*o*-C_6H_5), 129.1 (N-*m*-C_6H_5), 128.8 (d, *J* = 1 Hz, C-*p*-C_6H_5), 128.0 (d, $^4J_{PC}$ = 1 Hz C-*m*-C_6H_5), 123.2 (N-*p*-C_6H_5), 120.6 (N-*o*-C_6H_5), 33.7 (d, $^1J_{PC}$ = 23 Hz, P-*C*(CH_3)$_3$), 30.4 (d, $^2J_{PC}$ = 13 Hz, P-C(*C*H_3)$_3$).

$^{31}P\{^1H\}$ NMR (283 MHz, Benzene-d_6) δ 45.0.

MS (ASAP$^+$) *m/z*: 326.2 ($[MH]^+$), 180.1 ($[M\text{-}P^tBu_2]^+$).

IR (ATR): $\nu_{C=N}$ = 1582 cm^{-1}.

6.6.9 Preparation of $PhC(PPh_2)=N(2,6\text{-}((CH_3)_2CH)_2C_6H_3)$ (3.7)

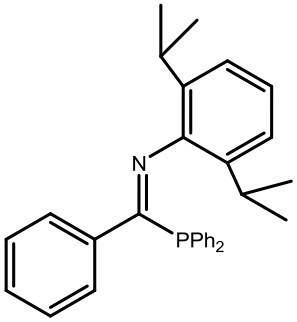

Two separate flasks were charged with trimethylsilyl-diphenylphosphine (2.982 g, 11.5 mmol) and N-(2,6-diisopropylphenyl)benzimidoyl chloride (3.461 g, 11.5 mmol), respectively, and chlorobenzene was added to both flasks (15 mL each). Both phosphine and chloroimine solutions were transferred into a 2-neck round bottom flask and both flasks were washed with further chlorobenzene (5 mL each). The resulting solution was heated at reflux for 3 hours, in which time the solution turned yellow. The solution was left to cool to room temperature before the solvent was removed under vacuum, giving the crude product as a yellow solid. The crude product was dissolved in hot hexane and cooled to 0 °C for 16 hours to crystallise the product. The product was isolated as yellow crystals (4.503 g, 87 % yield). (calc.: $C_{31}H_{32}NP$ C, 82.82; H, 7.17; N, 3.12. Found: C, 82.64; H, 7.26; N, 3.16).

^{1}H NMR (700 MHz, Chloroform-*d*) δ 7.52 (s, 4H, -C_6H_5), 7.31 (s, 8H, -C_6H_5), 7.11 (s, 3H, -C_6H_5), 7.00 – 6.92 (m, 3H, N-C_6H_3), 2.79 (hept, $^3J_{HH}$ = 7 Hz, 2H, P-CH(CH_3)$_2$), 1.00 (d, $^3J_{HH}$ = 7 Hz, 6H, P-CH(CH_3)$_2$), 0.94 (s, 6H, P-CH(CH_3)$_2$).

^{13}C{^{1}H} NMR (176 MHz, Chloroform-*d*) δ 174.9 (*C*=N), 147.2 (d, $^3J_{PC}$ = 7 Hz, N-*i*-C_6H_3), 138.2 (C-*i*-C_6H_5), 135.1 (d, $^4J_{PC}$ = 2 Hz, N-*o*-C_6H_3), 135.0 (-C_6H_5), 134.5 (d, J_{PC} = 7 Hz, -C_6H_5), 129.1 (-C_6H_5), 128.3 (d, J_{PC} = 8 Hz, -C_6H_5), 128.0 (-C_6H_5), 123.3 (N-*p*-C_6H_3), 122.8 (N-*m*-C_6H_3), 28.5 (P-*C*H(CH_3)$_2$), 23.7 (P-CH(*C*H_3)$_2$), 22.2 (P-CH(*C*H_3)$_2$).*

^{31}P{^{1}H} NMR (283 MHz, Chloroform-*d*) δ 9.3, –5.0.†

MS (ASAP$^+$) *m/z*: 450.2 ([MH]$^+$), 264.2 ([M-PPh_2]$^+$).

IR (ATR): $\nu_{C=N}$ = 1602 cm^{-1}.

* ^{1}H and ^{13}C NMR spectra could not be fully assigned due to broadening of the signals, caused by hindered rotation of the phenyl groups.
† Two resonances due to presence of imine *E* and *Z* isomers in solution.

6.6.10 Preparation of PhC(^{t}Bu$_2$)=N(2,6-((CH$_3$)$_2$CH)$_2$C$_6$H$_3$) (3.6)

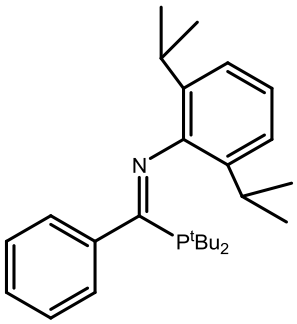

An analogous procedure to that used for the synthesis of iminophosphine **3.7** was carried out, using trimethylsilyl-*bis*(*tert*-butyl)phosphine (1.484 g, 6.8 mmol) and *N*-(2,6-diisopropylphenyl)benzimidoyl chloride (2.037 g, 6.8 mmol). The reaction solution was heated at reflux for 16 hours after which ^{31}P{^{1}H} NMR spectroscopy showed that 14 % of the starting material had converted to unwanted *bis*(*tert*-butyl)phosphine. Consequently, more trimethylsilyl-*bis*(*tert*-butyl)phosphine (0.207 g, 0.95 mmol) was added and the reaction was set back to reflux for 5 hours. The solution was allowed to cool to room temperature before the solvent was removed *in vacuo* giving an orange viscous oil as the product. The crude product was distilled under vacuum (150 °C, 0.1 mbar) to give the product as a yellow oil that crystallises upon scraping (1.633 g, 59 % yield). (calc.: $C_{27}H_{40}NP$ C, 79.17; H, 9.84; N, 3.42. Found: C, 78.98; H, 10.01; N, 3.55).

^{1}H NMR (600 MHz, Chloroform-*d*) δ 7.36 – 7.31 (m, 2H, C-*o*-C$_6$*H*$_5$), 7.18 – 7.14 (m, 3H, C-*m/p*-C$_6$*H*$_5$), 7.01 – 6.93 (m, 3H, N-*m/p*-C$_6$*H*$_3$), 2.97 (hept, $^3J_{HH}$ = 7 Hz, 2H, C$_6$H$_3$-C*H*(CH$_3$)$_2$), 1.31 (d, $^3J_{PH}$ = 12 Hz, 18H, P-C(C*H*$_3$)$_3$), 1.13 (d, $^3J_{HH}$ = 7 Hz, 6H, C$_6$H$_3$-CH(C*H*$_3$)$_2$), 0.84 (d, $^3J_{HH}$ = 7 Hz, 6H, C$_6$H$_3$-CH(C*H*$_3$)$_2$).

^{13}C{^{1}H} NMR (151 MHz, Chloroform-*d*) δ 177.9 (d, $^1J_{PC}$ = 29 Hz, *C*=N), 146.9 (d, $^3J_{PC}$ = 3 Hz, N-*i*-*C*$_6$H$_3$), 140.9 (d, $^2J_{PC}$ = 30 Hz, C-*i*-*C*$_6$H$_5$), 135.8 (d, $^4J_{PC}$ = 2 Hz, N-*o*-*C*$_6$H$_3$), 129.4 (d, $^3J_{PC}$ = 12 Hz, C-*o*-*C*$_6$H$_5$), 129.0 (C-*p*-*C*$_6$H$_5$), 127.8 (d, $^4J_{PC}$ = 2 Hz C-*m*-*C*$_6$H$_5$), 123.3 (N-*p*-*C*$_6$H$_3$), 123.1 (N-*m*-*C*$_6$H$_3$), 34.0 (d, $^1J_{PC}$ = 21 Hz P-*C*(CH$_3$)$_3$), 30.6 (d, $^2J_{PC}$ = 11.7 Hz P-C(*C*H$_3$)$_3$), 28.2 (C$_6$H$_3$-*C*H(CH$_3$)$_2$), 25.1 (C$_6$H$_3$-CH(*C*H$_3$)$_2$), 22.5 (C$_6$H$_3$-CH(*C*H$_3$)$_2$).

^{31}P{^{1}H} NMR (162 MHz, Chloroform-*d*) δ 49.5.

MS (ASAP$^+$) *m/z*: 410.3 ([MH]$^+$), 264.2 ([M-P^{t}Bu$_2$]$^+$).

IR (ATR): $\nu_{C=N}$ = 1580 cm^{-1}.

6.6.11 Preparation of $PhC(PPh_2)=N(2,6\text{-}(CH_3)_2C_6H_3)$ (3.8)

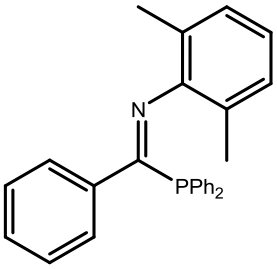

An analogous procedure to that used for the synthesis of **3.7** was carried out, using trimethylsilyl-diphenylphosphine (3.115 g, 12.1 mmol) and *N*-(2,6-dimethylphenyl)benzimidoyl chloride (2.939 g, 12.1 mmol). The reaction mixture was heated at reflux for 2 hours after which the reaction was allowed to cool to room temperature and the solvent was removed under vacuum to give the crude product as a yellow oil. The oil was dissolved in hot hexane and the resulting was solution slowly cooled to 0 °C and left overnight to give the reaction product as yellow crystals (8.856 g, 81 % yield). (calc.: $C_{27}H_{24}NP$ C, 82.42; H, 6.15; N, 3.56. Found: C, 82.32; H, 6.24; N, 3.61).

^{1}H NMR (700 MHz, Benzene-d_6) δ 7.87 – 7.59 (m, 4H, -C_6H_5), 7.49 – 7.37 (m, 2H, -C_6H_5), 7.10 – 6.94 (m, 6H, -C_6H_5), 6.86 – 6.64 (m, 6H, N-C_6H_3/C-C_6H_5), 2.06 (s, 6H, N-2,6-$(CH_3)_2C_6H_3$).

^{13}C{^{1}H} NMR (176 MHz, Benzene-d_6) δ 176.7 (*C*=N), 150.2 (N-*i*-C_6H_3), 139.7 (C-*i*-C_6H_5), 135.4 (-C_6H_n), 135.0 (d, *J* = 8 Hz -C_6H_n), 129.3 (-C_6H_n), 128.6 (d, $^{2}J_{PC}$ = 8 Hz, P-*i*-C_6H_5), 128.3 (-C_6H_n), 127.5 (-C_6H_n), 125.4 (N-*o*-C_6H_3), 123.2 (-C_6H_n), 18.9 (N-2,6-$(CH_3)_2C_6H_3$).*

^{31}P{^{1}H} NMR (283 MHz, Benzene-d_6) δ 8.8, 1.0.†

MS (ASAP^{+}) *m/z*: 394.2 ($[MH]^+$), 208.1 ($[M\text{-}PPh_2]^+$).

IR (ATR): $\nu_{C=N}$ = 1605 cm^{-1}.

* ^{1}H and ^{13}C NMR spectra could not be fully assigned due to broadening of the signals, caused by hindered rotation of the phenyl groups.

† Two resonances due to presence of imine *E* and *Z* isomers in solution.

6.6.12 Preparation of PhC(^{i}Pr$_2$)=N(2,6-((CH$_3$)$_2$CH)$_2$C$_6$H$_3$) (3.9)

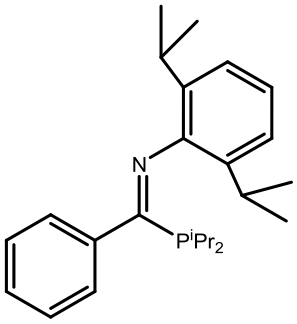

An analogous procedure to that used for the synthesis of **3.7** was carried out using trimethylsilyl-*bis*(*iso*-propyl)phosphine (2.284 g, 12.0 mmol) and *N*-(2,6-diisopropylphenyl)benzimidoyl chloride (3.598 g, 12.0 mmol). The reaction solution was heated at reflux for 28 hours after which analysis by ^{31}P{^{1}H} NMR spectroscopy showed 11 % of the starting phosphine had converted to *bis*(*iso*-propyl)phosphine. Consequently more trimethylsilyl-*bis*(*iso*-propyl)phosphine (0.251 g, 1.3 mmol) was added to the reaction mixture and the solution was set back to reflux. After 16 hours the solution was left to cool to room temperature and the solvent was removed under reduced pressure leaving the crude product as a yellow oil that spontaneously crystallised. The crude product was purified by crystallisation from hot hexane, which was slowly cooled to – 30 °C and left for 16 hours. The product was isolated by filtration as yellow crystals (2.955 g, 64 % yield). (calc.: $C_{25}H_{36}NP$ C, 78.70; H, 9.51; N, 3.67. Found: C, 78.51; H, 9.63; N, 3.73).

^{1}H NMR (700 MHz, Benzene-d_6) δ 7.47 (dt, J = 8, 1 Hz, 2H, C-*o*-C$_6$*H*$_5$), 7.06 – 6.99 (m, 3H, N-*m*,*p*-C$_6$*H*$_3$), 6.90 – 6.85 (m, 2H, C-*m*-C$_6$*H*$_5$), 6.85 – 6.81 (m, 1H, C-*p*-C$_6$*H*$_5$), 3.13 (hept, $^{3}J_{HH}$ = 7 Hz, 2H, C$_6$H$_3$-C*H*(CH$_3$)$_2$), 2.32 (heptd, $^{3}J_{HH}$ = 7 Hz, $^{2}J_{PH}$ = 3 Hz, 2H, P-C*H*(CH$_3$)$_2$), 1.33 (dd, $^{3}J_{PH}$ = 13 Hz, $^{3}J_{HH}$ = 7 Hz, 6H, P-CH(C*H*$_3$)$_2$), 1.23 (d, $^{3}J_{HH}$ = 7 Hz, 6H, C$_6$H$_3$-CH(C*H*$_3$)$_2$), 1.01 (dd, $^{3}J_{PH}$ = 13 Hz, $^{3}J_{HH}$ = 7 Hz, 6H, P-CH(C*H*$_3$)$_2$), 0.97 (d, $^{3}J_{HH}$ = 7 Hz, 6H, C$_6$H$_3$-CH(C*H*$_3$)$_2$).

^{13}C{^{1}H} NMR (176 MHz, Benzene-d_6) δ 177.8 (d, $^{1}J_{PC}$ = 22 Hz, *C*=N), 147.9 (d, $^{3}J_{PC}$ = 3 Hz, N-*i*-*C*$_6$H$_3$), 140.2 (d, $^{2}J_{PC}$ = 26 Hz, C-*i*-*C*$_6$H$_5$), 135.8 (d, $^{4}J_{PC}$ = 2 Hz, N-*o*-*C*$_6$H$_3$), 129.2 (d, $^{5}J_{PC}$ = 1 Hz, C-*p*-*C*$_6$H$_5$), 128.6 (d, $^{3}J_{PC}$ = 11 Hz, C-*o*-*C*$_6$H$_5$), 128.2 (d, $^{5}J_{PC}$ = 1 Hz, C-*m*-*C*$_6$H$_5$), 124.0 (N-*p*-*C*$_6$H$_3$), 123.4 (N-*m*-*C*$_6$H$_3$), 28.7 (C$_6$H$_3$-*C*H(CH$_3$)$_2$), 24.7 (C$_6$H$_3$-CH(*C*H$_3$)$_2$), 23.3 (d, $^{1}J_{PC}$ = 14 Hz, P-*C*H(CH$_3$)$_2$), 22.4 (C$_6$H$_3$-CH(*C*H$_3$)$_2$), 20.9 (d, $^{2}J_{PC}$ = 12 Hz, P-CH(*C*H$_3$)$_2$), 19.6 (d, $^{2}J_{PC}$ = 12 Hz, P-CH(*C*H$_3$)$_2$).

^{31}P{^{1}H} NMR (283 MHz, Benzene-d_6) δ 27.1.

MS (ASAP^{+}) *m/z*: 382.3 ([MH]$^{+}$), 338.2 ([M-^{i}Pr]$^{+}$), 264.2 ([M-P^{i}Pr$_2$]$^{+}$).

IR (ATR): $\nu_{C=N}$ = 1583 cm^{-1}.

6.6.13 Preparation of PhC(P^iPr_2)=N(2,6-$(CH_3)_2C_6H_3$) (3.10)

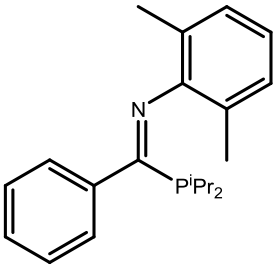

An analogous procedure to that used for the synthesis of **3.7** was carried out using trimethylsilyl-*bis*(*iso*-propyl)phosphine (1.892 g, 9.9 mmol) and *N*-(2,6-dimethylphenyl)benzimidoyl chloride (1.892 g, 9.9 mmol). The reaction was heated at reflux for 48 hours before analysis by $^{31}P\{^1H\}$ NMR spectroscopy showed that 10 % of the phosphine starting material had converted to *bis*(*iso*-propyl)phosphine. As a result more trimethylsilyl-*bis*(*iso*-propyl)phosphine (0.184 g, 0.96 mmol) was added to the reaction mixture and the solution was set back to reflux. After 16 hours the solution was allowed to cool to room temperature and the solvent was removed under vacuum. ^1H NMR spectroscopic analysis showed that the crude product still contained 12 % of the starting chloroimine, and so more trimethylsilyl-*bis*(*iso*-propyl)phosphine (0.227 g, 1.19 mmol) was added along with chlorobenzene (25 mL). The solution was again heated to reflux for 16 hours before being allowed to cool to room temperature. The solvent was then removed under vacuum yielding the crude product as an orange oil. The oil was purified by vacuum distillation (130 °C, 0.08 mbar) to give the product as a clear yellow oil that crystallised upon standing (2.436 g, 76 % yield). (calc.: $C_{21}H_{28}NP$ C, 77.51; H, 8.67; N, 4.30. Found: C, 77.47; H, 8.72; N, 4.34).

^1H NMR (700 MHz, Chloroform-*d*) δ 7.28 – 7.25 (m, 2H, C-*o*-C_6H_5), 7.24 – 7.21 (m, 1H, C-*p*-C_6H_5), 7.21 – 7.17 (m, 2H, C-*m*-C_6H_5), 6.89 (d, J = 8 Hz, 2H, N-*m*-C_6H_3), 6.79 (t, J = 8 Hz, 1H, N-*p*-C_6H_3), 2.25 (heptd, $^3J_{HH}$ = 7 Hz, $^2J_{PH}$ = 3 Hz, 3H, P-C*H*$(CH_3)_2$), 2.04 (s, 6H, 2,6-$(CH_3)_2C_6H_3$), 1.25 (dd, $^3J_{PH}$ = 13 Hz, $^3J_{HH}$ = 7 Hz, 6H, P-CH$(CH_3)_2$), 1.01 (dd, $^3J_{PH}$ = 13 Hz, $^3J_{HH}$ = 7 Hz, 6H, P-CH$(CH_3)_2$).

$^{13}C\{^1H\}$ NMR (176 MHz, Chloroform-*d*) δ 177.6 (d, $^1J_{PC}$ = 21 Hz, *C*=N), 150.2 (d, $^3J_{PC}$ = 4 Hz, N-*i*-C_6H_3), 140.5 (d, $^2J_{PC}$ = 26 Hz, C-*i*-C_6H_5), 129.1 (d, $^5J_{PC}$ = 1 Hz, C-*p*-C_6H_5), 128.0 (d, $^4J_{PC}$ = 1 Hz, C-*m*-C_6H_5), 127.9 (N-*m*-C_6H_3), 127.5 (d, $^3J_{PC}$ = 10 Hz, C-*o*-C_6H_5), 125.5 (d, $^4J_{PC}$ = 2 Hz, N-*o*-C_6H_3), 122.5 (N-*p*-C_6H_3), 22.8 (d, $^1J_{PC}$ = 12 Hz, P-*C*H$(CH_3)_2$), 20.9 (d, $^2J_{PC}$ = 12 Hz, P-CH$(CH_3)_2$), 19.4 (d, $^2J_{PC}$ = 11 Hz, P-CH$(CH_3)_2$), 18.9 (2,6-$(CH_3)_2C_6H_3$).

$^{31}P\{^1H\}$ NMR (283 MHz, Chloroform-*d*) δ 26.9.

MS (ASAP$^+$) *m/z*: 326.2 ($[MH]^+$), 208.1 ($[M\text{-}P^iPr_2]^+$).

IR (ATR): $\nu_{C=N}$ = 1600 cm^{-1}.

6.6.14 Preparation of PhC(P(2-(OCH$_3$)C$_6$H$_4$)$_2$)=N(2,6-((CH$_3$)$_2$CH)$_2$C$_6$H$_3$) (3.11)

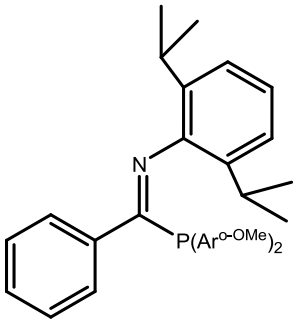

An analogous procedure to that used for the synthesis of **3.7** was carried out using trimethylsilyl-*bis*(*ortho*-methoxyphenyl)phosphine (1.033 g, 3.2 mmol) and *N*-(2,6-diisopropylphenyl)benzimidoyl chloride (0.973 g, 3.2 mmol). The reaction solution was heated at reflux for 16 hours, after which the solution turned yellow. The solution was left to cool to room temperature before the solvent was removed under vacuum to give a yellow oily residue. The yellow oil was dissolved in hot hexane before the solution was slowly cooled to 0 °C. After being left for 16 hours at 0 °C the product crystallised and the resulting yellow crystals were isolated by filtration (0.659 g, 40 % yield). (calc.: $C_{33}H_{36}NO_2P$ C, 77.77; H, 7.12; N, 2.75. Found: C, 77.63; H, 7.01; N, 2.69).

^{1}H NMR (700 MHz, Chloroform-*d,* 50 °C) δ 7.39 – 7.33 (m, 2H, P-(C$_6$*H*$_4$(OMe))$_2$), 7.29 – 7.24 (m, 2H, C-*o/m*-C$_6$*H*$_5$), 7.22 – 7.16 (m, 2H, P-(C$_6$*H*$_4$(OMe))$_2$), 7.09 – 7.03 (m, 3H, P-(C$_6$*H*$_4$(OMe))$_2$ and C-*p*-C$_6$*H*$_5$), 6.94 – 6.89 (m, 3H, N-C$_6$*H*$_3$), 6.83 (t, *J* = 7 Hz, 2H, C-*o/m*-C$_6$*H*$_5$), 6.79 – 6.74 (m, 2H, P-(C$_6$*H*$_4$(OMe))$_2$), 3.76 – 3.60 (m, 6H, (C$_6$H$_4$(OC*H*$_3$))$_2$), 2.85 (hept, $^3J_{HH}$ = 7 Hz, 2H, C$_6$H$_3$-C*H*(CH$_3$)$_2$), 0.92 (d, $^3J_{HH}$ = 7 Hz, 6H, C$_6$H$_3$-CH(C*H*$_3$)$_2$) 0.90 (d, $^3J_{HH}$ = 7 Hz, 6H, C$_6$H$_3$-CH(C*H*$_3$)$_2$).

^{13}C{^{1}H} NMR (151 MHz, Chloroform-*d*) δ 174.4 (*C*=N), 161.9 (*C*-OMe), 147.5 (d, $^3J_{PC}$ = 8 Hz, N-*i*-*C*$_6$H$_3$), 138.4 (P-*i*-(*C*$_6$H$_4$(OMe))$_2$), 135.5 (N-*o*-*C*$_6$H$_3$), 135.3 (C-*i*-*C*$_6$H$_5$), 130.8 (C-*o/m*-*C*$_6$H$_5$), 128.7 (P-*o/m/p*-(*C*$_6$H$_4$(OMe))$_2$), 128.1 (P-*o/m/p*-(*C*$_6$H$_4$(OMe))$_2$), 127.6 (C-*p*-*C*$_6$H$_5$), 123.0 (N-*p*-*C*$_6$H$_3$), 122.6 (N-*m*-*C*$_6$H$_3$), 120.9 (C-*o/m*-*C*$_6$H$_5$), 110.3 (P-*o/m/p*-(*C*$_6$H$_4$(OMe))$_2$), 55.6 (P(C$_6$H$_4$(O*C*H$_3$))$_2$), 28.2 (C$_6$H$_3$-*C*H(CH$_3$)$_2$), 23.8 (C$_6$H$_3$-CH(*C*H$_3$)$_2$), 22.4 (C$_6$H$_3$-CH(*C*H$_3$)$_2$).

^{31}P{^{1}H} NMR (243 MHz, Chloroform-*d*) δ –12.1, –24.7.*

MS (ASAP$^+$) *m/z*: 510.2 ([MH]$^+$), 264.2 ([M-(P-*o*-MeOC$_6$H$_4$)$_2$]$^+$).

IR (ATR): $\nu_{C=N}$ = 1584 cm^{-1}.

* Two resonances due to presence of imine *E* and *Z* isomers in solution.

6.6.15 Preparation of PhC(P^tBu_2)=N(2,6-$(CH_3)_2C_6H_3$) (3.12)

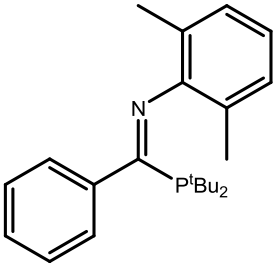

An analogous procedure to that used in the synthesis of **3.7** was carried out using *bis*(*tert*-butyl)-trimethylsilylphosphine (2.406 g, 11 mmol) and *N*-(2,6-dimethylphenyl)benzimidoyl chloride (2.685 g, 11 mmol). The solution was heated at reflux for 16 hours after which the solution was allowed to cool to room temperature and filtered to remove any precipitate. The solvent was then removed *in vacuo* to give a yellow/green oil. The oil was dissolved in hexane (10 mL) and the resulting solution was filtered to remove the green precipitate. The hexane was removed under vacuum and the resulting oil was vacuum distilled (130 °C, 0.1 mbar) to yield the product as a clear yellow oil which crystallised over a period of weeks at -30 °C (3.116 g, 80 % yield). (calc.: $C_{23}H_{32}NP$ C, 78.15; H, 9.12; N, 3.96. Found: C, 78.05; H, 9.06; N, 4.12).

^{1}H NMR (700 MHz, Chloroform-*d*) δ 7.29 (d, *J* = 8 Hz, 2H, C-*m*-C_6H_5), 7.19 (t, *J* = 7 Hz, 1H, C-*p*-C_6H_5), 7.15 (t, *J* = 7 Hz, 2H, C-*o*-C_6H_5), 6.87 (d, *J* = 7 Hz, 2H, N-*m*-C_6H_3), 6.77 (t, *J* = 7 Hz, 1H, N-*p*-C_6H_3), 2.04 (s, 6H, 2,6-$(CH_3)_2C_6H_3$), 1.30 (d, $^3J_{PH}$ = 12 Hz, 18H, C-$(CH_3)_3$).

^{13}C{^{1}H} NMR (176 MHz, Chloroform-*d*) δ 178.2 (d, $^1J_{PC}$ = 29 Hz, *C*=N), 150.0 (d, $^3J_{PC}$ = 3 Hz, N-*i*-C_6H_3), 141.7 (d, $^2J_{PC}$ = 30 Hz, C-*i*-C_6H_5), 129.1 (d, $^5J_{PC}$ = 1 Hz, C-*p*-C_6H_5), 128.6 (d, $^4J_{PC}$ = 11 Hz, C-*m*-C_6H_5), 128.0 (N-*m*-C_6H_3), 127.8 (d, $^3J_{PC}$ = 1 Hz, C-*o*-C_6H_5), 125.7 (d, $^4J_{PC}$ = 2 Hz, N-*o*-C_6H_3), 122.6 (N-*p*-C_6H_3), 33.9 (d, $^1J_{PC}$ = 21 Hz, *C*-$(CH_3)_3$), 30.7 (d, $^2J_{PC}$ = 12 Hz, C-$(CH_3)_3$), 19.2 (2,6-$(CH_3)_2C_6H_3$).

^{31}P{^{1}H} NMR (283 MHz, Chloroform-*d*) δ 48.7.

MS (ASAP$^+$) *m/z*: 354.2 ($[MH]^+$), 208.1 ($[M\text{-}P^tBu_2]^+$).

IR (ATR): $\nu_{C=N}$ = 1583 cm^{-1}.

6.6.16 Preparation of PhC(P^tBu_2)=N(2-(OCH_3)C_6H_4) (3.13)

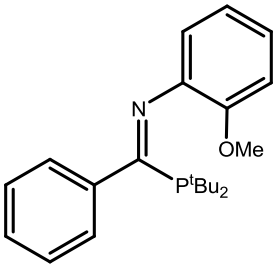

An analogous procedure to that used for the synthesis of **3.7** was carried out using *bis*(*tert*-butyl)-trimethylsilylphosphine (2.404 g, 11 mmol) and *N*-(2-orthomethoxyphenyl)benzimidoyl chloride (2.705 g, 11 mmol). The solution was set to reflux for 16 hours and the solution turned a brown colour. After 16 hours the solution was left to cool to room temperature and the solvent was removed under reduced pressure giving the crude product as a brown oil. The crude product was purified by vacuum distillation (135-140 °C, 0.1 mbar) and the product was isolated as a clear yellow/orange oil that crystallised upon scraping (3.090 g, 79 % yield). (calc.: $C_{22}H_{30}NOP$ C, 74.34; H, 8.51; N, 3.94. Found: C, 74.46; H, 8.63; N, 4.07).

^{1}H NMR (700 MHz, Chloroform-*d*) δ 7.27 (s, 2H, C-*o*-C_6H_5), 7.16 – 7.12 (m, 3H, C-*m,p*-C_6H_5), 6.88 (t, *J* = 8 Hz, 1H, N-*p*-C_6H_4), 6.75 (d, *J* = 8 Hz, 1H, N-2/5-C_6H_4), 6.73 (t, *J* = 8 Hz, 1H, N-3-C_6H_4), 6.45 (d, *J* = 8 Hz, 1H, N-2/5-C_6H_4), 3.66 (s, 3H, C_6H_4-*o*-OCH_3), 1.31 (d, $^3J_{PH}$ = 12 Hz, 18H, C-(CH_3)$_3$).

^{13}C{^{1}H} NMR (176 MHz, Chloroform-*d*) δ 179.9 (d, $^1J_{PC}$ = 31 Hz, *C*=N), 149.1 (N-*6*-C_6H_4), 142.3 (N-*i*-C_6H_4), 141.7 (d, $^2J_{PC}$ = 31 Hz, C-*i*-C_6H_5), 128.6 (C-*p*-C_6H_5), 128.5 (C-*o*-C_6H_5), 127.6 (C-*m*-C_6H_5), 123.6 (N-4-C_6H_4), 120.9 (N-3-C_6H_4), 119.9 (N-2/5-C_6H_4), 111.78 (N-2/5-C_6H_4), 55.7 (C_6H_4-*o*-OCH_3), 33.7 (d, $^1J_{PC}$ = 21.0 Hz, *C*-(CH_3)$_3$), 30.3 (d, $^2J_{PC}$ = 12.5 Hz, C-(*C*H_3)$_3$).

^{31}P{^{1}H} NMR (283 MHz, Chloroform-*d*) δ 45.0.

MS (ASAP$^+$) *m/z*: 356.2 ([MH]$^+$), 324.2 ([M-OMe]$^+$), 210.1 ([M-P^{t}Bu$_2$]$^+$).

IR (ATR): $\nu_{C=N}$ = 1602 cm^{-1}.

6.6.17 Preparation of PhC(PCy_2)=N(2,6-($(CH_3)_2CH)_2C_6H_3$) (3.14)

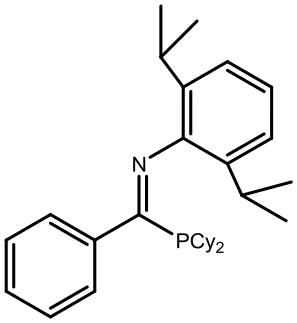

An analogous procedure to that used for the synthesis of **3.7** was carried out using *bis*(cyclohexyl)-trimethylsilylphosphine (2.47 g, 9.1 mmol) and *N*-(2,6-diisopropylphenyl)benzimidoyl chloride (2.738 g, 9.1 mmol). The reaction mixture was heated at reflux for 48 hours before the solution was cooled and the solvent removed under vacuum to give the crude product as a yellow oil. The oil was vacuum distilled (177-181 °C, 0.1 mbar) yielding the product as a clear yellow oil that slowly crystallised over a period of days to a yellow crystalline solid (2.826 g, 67 % yield). (calc.: $C_{31}H_{44}NP$ C, 80.65; H, 9.61; N, 3.03. Found: C, 80.77; H, 9.79; N, 3.07).

^{1}H NMR (700 MHz, Chloroform-*d*) δ 7.24 (d, *J* = 8 Hz, 2H, C-*o*-C_6H_5), 7.21 – 7.14 (m, 3H, C-*m,p*-C_6H_5), 7.00 – 6.96 (m, 2H, N-*m*-C_6H_3), 6.96 – 6.93 (m, 1H, N-*p*-C_6H_3), 2.85 (hept, $^3J_{HH}$ = 7 Hz, 2H, C_6H_3-C*H*$(CH_3)_2$), 2.06 (d, *J* = 14 Hz, 2H, P-C_6H_{11}), 2.02 (d, *J* = 19 Hz, 2H, P-C_6H_{11}), 1.77 (s, 2H, P-C_6H_{11}), 1.71 (d, *J* = 12 Hz, 4H, P-C_6H_{11}), 1.64 (d, *J* = 9 Hz, 2H, P-C_6H_{11}), 1.30 (d, *J* = 15 Hz, 2H, P-C_6H_{11}), 1.26 – 1.19 (m, 4H, P-C_6H_{11}), 1.14 (d, $^3J_{HH}$ = 7 Hz, 6H, C_6H_3-CH(C*H*$_3)_2$), 1.03 (s, 2H, P-C_6H_{11}), 0.88 (d, $^3J_{HH}$ = 7 Hz, 6H, C_6H_3-CH(C*H*$_3)_2$).

^{13}C{^{1}H} NMR (176 MHz, Chloroform-*d*) δ 177.0 (d, $^1J_{PC}$ = 17 Hz, *C*=N), 147.44 (N-*i*-C_6H_3), 139.8 (d, $^2J_{PC}$ = 27 Hz, C-*i*-C_6H_5), 135.5 (N-*o*-C_6H_3), 129.0 (d, $^5J_{PC}$ = 1 Hz, C-*p*-C_6H_5), 128.2 (d, $^3J_{PC}$ = 10 Hz, C-*o*-C_6H_5), 127.9 (d, $^4J_{PC}$ = 1 Hz, C-*m*-C_6H_5), 123.1 (N-*p*-C_6H_3), 122.9 (N-*m*-C_6H_3), 33.1 (d, J_{PC} = 12 Hz, P-C_6H_{11}), 30.4 (d, J_{PC} = 254 Hz, P-C_6H_{11}), 28.4 (C_6H_3-*C*H$(CH_3)_2$), 27.7 (d, J_{PC} = 35 Hz, P-C_6H_{11}), 26.6 (d, J_{PC} = 1 Hz, P-C_6H_{11}), 24.5 (C_6H_3-CH(*C*H$_3)_2$), 22.0 (C_6H_3-CH(*C*H$_3)_2$).

^{31}P{^{1}H} NMR (283 MHz, Chloroform-*d*) δ 18.5.

MS (ASAP$^+$) *m/z*: 462.3 ($[MH]^+$), 418.2 ($[M-^iPr]^+$), 264.2 ($[M-PCy_2]^+$).

IR (ATR): $\nu_{C=N}$ = 1585 cm^{-1}.

6.6.18 Preparation of PhC(PCy_2)=N(2,6-$(CH_3)_2C_6H_3$) (3.15)

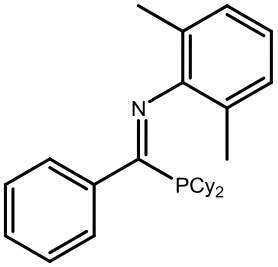

An analogous procedure to that used for the synthesis of **3.7** was carried out using *bis*(cyclohexyl)-trimethylsilylphosphine (2.109 g, 7.8 mmol) and *N*-(2,6-dimethylphenyl)benzimidoyl chloride (1.900 g, 7.8 mmol). The reaction solution was heated at reflux 24 hours before being allowed to cool to room temperature. The solvent was removed under vacuum leaving the crude product as an orange oil. The crude product was purified by vacuum distillation (180 °C, 0.1 mbar) to give the product as a clear orange oil that crystallised at -30 °C over a period of weeks (1.423 g, 45 % yield).* (calc.: $C_{27}H_{36}NP$ C, 79.96; H, 8.95; N, 3.45. Found: C, 79.85; H, 9.09; N, 3.49).

^{1}H NMR (700 MHz, Chloroform-*d*) δ 7.24 – 7.22 (m, 2H, C-*o*-C_6H_5), 7.22 – 7.19 (m, 1H, C-*p*-C_6H_5), 7.19 – 7.15 (m, 2H, C-*m*-C_6H_5), 6.90 – 6.86 (m, 2H, N-*m*-C_6H_3), 6.77 (t, *J* = 8 Hz, 1H, N-*p*-C_6H_3), 2.08 – 2.03 (m, 4H, P-C_6H_{11}), 2.01 (s, 6H, *o*-$CH_3C_6H_3$), 1.78 – 1.67 (m, 6H, P-C_6H_{11}), 1.67 – 1.61 (m, 2H, P-C_6H_{11}), 1.37 – 1.19 (m, 6H, P-C_6H_{11}), 1.17 – 1.08 (m, 2H, P-C_6H_{11}), 1.03 – 0.93 (m, 2H, P-C_6H_{11}).

^{13}C{^{1}H} NMR (176 MHz, Chloroform-*d*) δ 177.4 (d, $^1J_{PC}$ = 21 Hz, *C*=N), 150.3 (d, $^3J_{PC}$ = 4 Hz, N-*i*-C_6H_3), 140.7 (d, $^2J_{PC}$ = 27 Hz, C-*i*-C_6H_5), 129.1 (d, $^5J_{PC}$ = 1 Hz, C-*p*-C_6H_5), 127.9 (d, $^4J_{PC}$ = 1 Hz, C-*m*-C_6H_5), 127.8 (N-*m*-C_6H_3), 127.6 (d, $^3J_{PC}$ = 10 Hz, C-*o*-C_6H_5), 125.6 (d, $^4J_{PC}$ = 2 Hz, N-*o*-C_6H_3), 122.4 (N-*p*-C_6H_3), 32.6 (d, J_{PC} = 13 Hz, P-C_6H_{11}), 31.1 (d, J_{PC} = 10 Hz, P-C_6H_{11}), 29.5 (d, J_{PC} = 10 Hz, P-C_6H_{11}), 27.6 (dd, J_{PC} = 61, 10 Hz, P-C_6H_{11}), 26.6 (P-C_6H_{11}), 19.0 (*o*-$CH_3C_6H_3$).

^{31}P{^{1}H} NMR (283 MHz, Chloroform-*d*) δ 18.8.

MS (ASAP$^+$) *m/z*: 406.3 ([MH]$^+$), 208.1 ([M-PCy_2]$^+$).

IR (ATR): $\nu_{C=N}$ = 1586 cm^{-1}.

* Low yield due to inability to extract product from the reaction vessel, ^{31}P NMR spectroscopic analysis of the crude reaction mixture displayed 100 % conversion of starting material to product.

6.6.19 Preparation of PhC(P^iPr_2)=N(2,6-(CH_2CH_3)$_2$$C_6H_3$) (3.16)

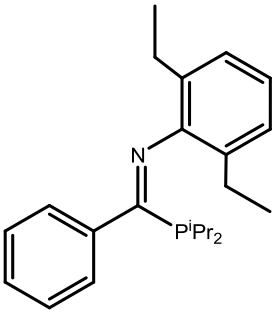

An analogous procedure to that used for the synthesis of **3.7** was carried out using *bis*(*iso*-propyl)-trimethylsilylphosphine (1.267 g, 6.7 mmol) and *N*-(2,6-diethylphenyl)benzimidoyl chloride (1.809 g, 6.7 mmol). The reaction solution was heated at reflux for 24 hours before being left to cool to room temperature. Analysis by $^{31}P\{^1H\}$ NMR spectroscopy showed that 10 % of the phosphine starting material had converted to *bis*(*iso*-propyl)phosphine, and so more *bis*(*iso*-propyl)-trimethylsilylphosphine (0.127 g, 0.67 mmol) was added. The solution was heated back to reflux for a further 24 hours, after which time the solution was let cool to room temperature and the solvent was removed under vacuum. The resulting crude product was distilled under vacuum (130-136 °C, 0.1 mbar) to yield the final product as a yellow oil (1.943 g, 82 % yield). (calc.: $C_{23}H_{32}NP$ C, 78.15; H, 9.12; N, 3.96. Found: C, 78.23; H, 9.19; N, 4.05).

^{1}H NMR (700 MHz, Chloroform-*d*) δ 7.25 – 7.22 (m, 2H, C-*o*-C_6H_5), 7.21 – 7.17 (m, 1H, C-*p*-C_6H_5), 7.17 – 7.12 (m, 2H, C-*m*-C_6H_5), 6.96 – 6.92 (m, 2H, N-*m*-C_6H_3), 6.91 – 6.86 (m, 1H, N-*p*-C_6H_3), 2.54 – 2.46 (m, 2H, P-C*H*$(CH_3)_2$), 2.27 – 2.16 (m, 4H, C_6H_3-(C*H*$_2$$CH_3$)$_2$), 1.23 (dd, $^3J_{PH}$ = 12 Hz, $^3J_{HH}$ = 7 Hz, 6H, P-CH(C*H*$_3$)$_2$), 1.11 (t, $^3J_{HH}$ = 8 Hz, 6H, C_6H_3-(CH_2C*H*$_3$)$_2$), 1.00 (dd, $^3J_{PH}$ = 12 Hz, $^3J_{HH}$ = 7 Hz, 6H, P-CH(C*H*$_3$)$_2$).

^{13}C{^{1}H} NMR (176 MHz, Chloroform-*d*) δ 177.6 (d, $^1J_{PC}$ = 24 Hz, *C*=N), 148.9 (N-*i*-C_6H_3), 140.1 (d, $^2J_{PC}$ = 26 Hz, C-*i*-C_6H_5), 131.0 (N-*o*-C_6H_3), 129.1 (C-*p*-C_6H_5), 128.0 (C-*m*-C_6H_5), 127.7 (d, $^3J_{PC}$ = 10 Hz, C-*o*-C_6H_5), 125.5 (N-*m*-C_6H_3), 122.9 (N-*p*-C_6H_3), 24.7 (C_6H_3-(*C*$H_2$$CH_3$)$_2$), 22.9 (d, $^1J_{PC}$ = 12 Hz, P-*C*H$(CH_3)_2$), 20.9 (d, $^2J_{PC}$ = 12 Hz, P-CH(*C*H_3)$_2$), 19.5 (d, $^2J_{PC}$ = 12 Hz, P-CH(*C*H_3)$_2$), 13.8 (C_6H_3-(CH_2*C*H_3)$_2$).

^{31}P{^{1}H} NMR (283 MHz, Chloroform-*d*) δ 27.8.

MS (ASAP$^+$) *m/z*: 354.2 ([MH]$^+$), 236.1 ([M-P^iPr_2]$^+$).

IR (ATR): $\nu_{C=N}$ = 1584 cm^{-1}.

6.6.20 Preparation of PhC(PEt_2)=N(2,6-((CH_3)$_2$CH)$_2$$C_6H_3$) (3.17)

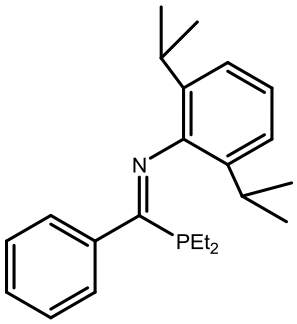

An analogous procedure to that used for the synthesis of **3.7** was carried out using *bis*(ethyl)-trimethylsilylphosphine (0.881 g, 5.4 mmol) and *N*-(2,6-diisopropylphenyl)benzimidoyl chloride (1.628 g, 5.4 mmol). The solution was heated at reflux for 16 hours before being left to cool to room temperature, after which the solvent was removed *in vacuo* yielding a brown oil. The oil was purified by vacuum distillation (135-140 °C, 0.1 mbar) to give the product as a yellow oil (1.600 g, 84 % yield). (calc.: $C_{23}H_{32}NP$ C, 78.15; H, 9.12; N, 3.96. Found: C, 78.26; H, 9.14; N, 4.07).

^{1}H NMR (700 MHz, Chloroform-*d*) δ 7.26 (s, 2H, C-*o*-C_6H_5), 7.22 (d, *J* = 11 Hz, 3H, C-*m/p*-C_6H_5), 7.03 – 6.99 (m, 2H, N-*m*-C_6H_3), 7.00 – 6.95 (m, 1H, N-*p*-C_6H_3), 2.91 – 2.85 (m, 2H, C_6H_3-C*H*-(CH_3)$_2$), 1.89 (s, 2H, P(C$H_2$$CH_3$)$_2$), 1.64 (dq, $^2J_{PH}$ = 15 Hz, $^3J_{HH}$ = 7 Hz, 2H, P(C$H_2$$CH_3$)$_2$), 1.18 (d, $^3J_{HH}$ = 7 Hz, 6H, C_6H_3-CH-(CH_3)$_2$), 1.16 – 1.08 (m, 6H, C_6H_3-CH-(CH_3)$_2$), 0.97 – 0.90 (m, 6H, P(CH_2CH_3)$_2$).

^{13}C{^{1}H} NMR (176 MHz, Chloroform-*d*) δ 178.8 (d, $^1J_{PC}$ = 16 Hz, *C*=N), 147.3 (N-*i*-C_6H_3), 138.1 (d, $^2J_{PC}$ = 19.4 Hz, C-*i*-C_6H_5), 135.5 (N-*o*-C_6H_3), 128.9 (C-*p*-C_6H_5), 128.1 (C-*m*-C_6H_5), 127.5 (d, $^3J_{PC}$ = 10 Hz, C-*o*-C_6H_5), 123.2 (N-*p*-C_6H_3), 122.8 (N-*m*-C_6H_3), 28.4 (C_6H_3-*C*H-(CH_3)$_2$), 24.1 (C_6H_3-CH-(*C*H_3)$_2$), 22.1 (C_6H_3-CH-(*C*H_3)$_2$), 16.6 (d, $^1J_{PC}$ = 10 Hz, P(*C*$H_2$$CH_3$)$_2$), 10.3 (d, $^2J_{PC}$ = 11 Hz, P(CH_2*C*H_3)$_2$).

^{31}P{^{1}H} NMR (283 MHz, Chloroform-*d*) δ 2.8.

MS (ASAP$^+$) *m/z*: 354.2 ([MH]$^+$), 264.2 ([M-PEt_2]$^+$).

IR (ATR): $\nu_{C=N}$ = 1585 cm^{-1}.

6.6.21 Preparation of PhC(P(2-(CH$_2$CH$_3$)C$_6$H$_4$)$_2$)=N(2,6-((CH$_3$)$_2$CH)$_2$C$_6$H$_3$) (3.18)

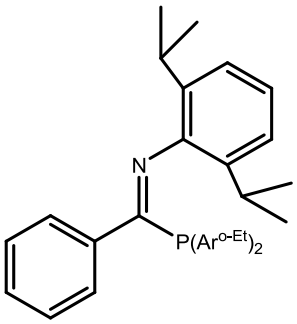

An analogous procedure to that used for the synthesis of **3.7** was carried out using *bis*(*ortho*-ethylphenyl)-trimethylsilylphosphine (1.951 g, 6.2 mmol) and *N*-(2,6-diisopropylphenyl)benzimidoyl chloride (1.860 g, 6.2 mmol). The solution was heated at reflux for 16 hours before being left to cool to room temperature. Analysis of the solution by ^{31}P{^{1}H} NMR spectroscopy displayed 8 % of the starting phosphine had converted to the *bis*(*ortho*-ethylphenyl)-phosphine by-product, and so more *bis*(*ortho*-ethylphenyl)-trimethylsilylphosphine (0.156 g, 0.5 mmol) was added to the reaction. The solution was heated back at reflux for 4 hours before being left to cool to ambient temperature. The solvent was then removed under vacuum to leave a yellow solid residue. The crude product was purified by crystallisation from hot hexane left to cool to room temperature. The yellow crystalline product was isolated by filtration (1.892 g, 60 % yield). (calc.: $C_{35}H_{40}NP$ C, 83.13; H, 7.97; N, 2.77. Found: C, 82.96; H, 8.14; N, 2.80).

^{1}H NMR (700 MHz, Chloroform-*d*) δ 7.33 (s, 2H, -C$_6$*H*$_n$), 7.27 – 7.22 (m, 2H, -C$_6$*H*$_n$), 7.22 – 7.17 (m, 4H, -C$_6$*H*$_n$), 7.11 – 7.08 (m, 3H, C-*o*-C$_6$*H*$_5$), 7.07 – 7.03 (m, 2H, -C$_6$*H*$_n$), 6.96 – 6.91 (m, 3H, N-*m*/*p*-C$_6$*H*$_3$), 3.03 (m, br, 4H, C$_6$H$_4$-C*H*$_2$CH$_3$), 2.75 (hept, $^{3}J_{HH}$ = 7 Hz, 2H, C$_6$H$_3$-C*H*-(CH$_3$)$_2$), 1.25 (s, 6H, C$_6$H$_4$-CH$_2$C*H*$_3$), 0.90 (d, $^{3}J_{HH}$ = 7 Hz, 6H, C$_6$H$_3$-CH-(C*H*$_3$)$_2$), 0.83 (s, 6H, C$_6$H$_3$-CH-(C*H*$_3$)$_2$).

^{13}C{^{1}H} NMR (176 MHz, Chloroform-*d*) δ 175.1 (d, $^{1}J_{PC}$ = 8 Hz, *C*=N), 149.9 (d, $^{1}J_{PC}$ = 26 Hz, P-*i*-*C*$_6$H$_4$), 147.2 (d, $^{3}J_{PC}$ = 6 Hz, N-*i*-*C*$_6$H$_3$), 138.3 (d, $^{2}J_{PC}$ = 29 Hz, C-*i*-*C*$_6$H$_5$), 135.3 (-*C*$_6$H$_n$), 135.3 (-*C*$_6$H$_n$), 132.6 (d, $^{2}J_{PC}$ = 5 Hz, P-2-*C*$_6$H$_4$), 129.4 (-*C*$_6$H$_n$), 129.0 (-*C*$_6$H$_n$), 128.3 (d, $^{2}J_{PC}$ = 6 Hz, P-6-*C*$_6$H$_4$), 128.1 (C-*o*-*C*$_6$H$_5$), 125.8 (-*C*$_6$H$_n$), 123.2 (-*C*$_6$H$_n$), 122.9 (N-*m*-*C*$_6$H$_3$), 28.5 (C$_6$H$_3$-*C*H-(CH$_3$)$_2$), 28.2 (d, $^{3}J_{PC}$ = 22 Hz, C$_6$H$_4$-*C*H$_2$CH$_3$), 23.9 (C$_6$H$_3$-CH-(*C*H$_3$)$_2$), 22.3 (C$_6$H$_3$-CH-(*C*H$_3$)$_2$), 15.8 (C$_6$H$_4$-CH$_2$*C*H$_3$).

^{31}P{^{1}H} NMR (283 MHz, Chloroform-*d*) δ –8.1.

MS (ASAP^{+}) *m/z*: 506.3 ([MH]$^{+}$).

IR (ATR): $\nu_{C=N}$ = 1584 cm^{-1}.

6.6.22 Preparation of PhC(P(2-F-C_6H_4)$_2$)=N(2,6-((CH_3)$_2$CH)$_2$$C_6H_3$) (3.19)

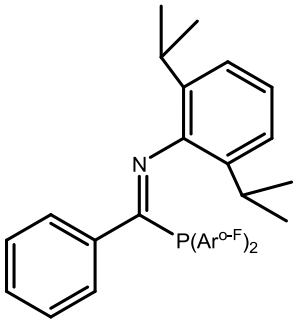

An analogous procedure to that used for the synthesis of **3.7** was carried out using *bis*(*ortho*-fluorophenyl)-trimethylsilyphosphine (1.352 g, 4.6 mmol) and *N*-(2,6-diisopropylphenyl)benzimidoyl chloride (1.377 g, 4.6 mmol). The solution was heated at reflux for 16 hours during which the solution turned an orange/brown colour. The solution was left to cool to room temperature and the solvent was removed under reduced pressure to yield an orange solid as the crude product. The crude product was dissolved in hot hexane and the solution filtered to remove traces of precipitate. The hot solution was concentrated and left to cool to room temperature. After 16 hours the product had crystallised and the yellow crystalline product was isolated by filtration (0.941 g, 42 % yield). (calc.: $C_{31}H_{30}F_2NP$ C, 76.68; H, 6.23; N, 2.88. Found: C, 76.81; H, 6.10; N, 3.02).

^{1}H NMR (700 MHz, Chloroform-*d*) δ 7.39 – 7.27 (m, 6H, P-*m/p*-C_6H_4F), 7.13 – 7.05 (m, 5H, C-C_6H_5), 7.03 – 6.98 (m, 2H, P-*o*-C_6H_4F), 6.97 – 6.90 (m, 3H, N-C_6H_3), 2.78 (hept, $^3J_{HH}$ = 6 Hz, 2H, C_6H_3-C*H*(CH_3)$_2$), 0.92 (d, $^3J_{HH}$ = 6 Hz, 6H, C_6H_3-CH(CH_3)$_2$), 0.88 (s, 6H, C_6H_3-CH(CH_3)$_2$).

^{13}C{^{1}H} NMR (176 MHz, Chloroform-*d*) δ 172.3 (*C*=N), 165.1 (dd, $^1J_{FC}$ = 244 Hz, $^1J_{PC}$ = 7 Hz, P-*i*-C_6H_4F), 146.9 (N-*i*-C_6H_3), 137.3 (d, $^2J_{PC}$ = 29 Hz, C-*i*-C_6H_5), 135.8 (d, J_{PC} = 15 Hz, P-*m/p*-C_6H_5), 135.5 (N-*o*-C_6H_3), 132.1 (P-*m/p*-C_6H_5), 129.3 (C-*o/m/p*-C_6H_5), 128.1 (C-*o/m/p*-C_6H_5), 127.9 (P-*m/p*-C_6H_5), 124.4 (C-*o/m/p*-C_6H_5), 123.4 (N-*p*-C_6H_3), 122.8 (N-*m*-C_6H_3), 120.4 (dd, $^2J_{PC}$ = 20 Hz, $^1J_{FC}$ = 11 Hz, *C*-F), 115.5 (dd, $^2J_{PC}$ = 24 Hz, $^3J_{FC}$ = 2 Hz, P-6-C_6H_4F), 28.3 (C_6H_3-*C*H(CH_3)$_2$), 23.7 (C_6H_3-CH(*C*H_3)$_2$), 22.1 (C_6H_3-CH(*C*H_3)$_2$).

^{31}P{^{1}H} NMR (283 MHz, Chloroform-*d*) δ –15.8.

MS (ASAP$^+$) *m/z*: 486.2 ([MH]$^+$), 264.2 ([M-(P-*o*-FC_6H_4)$_2$]$^+$).

IR (ATR): $\nu_{C=N}$ = 1597 cm^{-1}.

6.6.23 Preparation of ^{t}BuC($P^{i}Pr_2$)=N(2,6-$((CH_3)_2CH)_2C_6H_3$) (3.20)

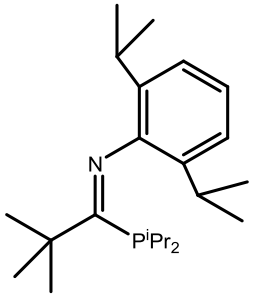

An analogous procedure to that used for the synthesis of **3.7** was carried out using *bis*(*iso*-propyl)-trimethylsilylphosphine (1.48 g, 7.8 mmol) and *N*-(2,6-diisopropylphenyl)pivalimidoyl chloride (2.176 g, 7.8 mmol). The solution was heated at reflux for 16 hours during which the solution turned yellow. The solution was left to cool to room temperature and filtered. The solvent was removed *in vacuo* to yield the crude product as a yellow oil which was distilled twice under vacuum (129-134 °C, 0.1 mbar) to yield the product as a clear yellow oil (1.674 g, 59 % yield). (calc.: $C_{23}H_{40}NP$ C, 76.41; H, 11.15; N, 3.87. Found: C, 76.23; H, 11.25; N, 3.96).

^{1}H NMR (600 MHz, Chloroform-*d*) δ 7.02 (d, *J* = 8 Hz, 2H, N-*m*-C_6H_3), 6.95 – 6.91 (m, 1H, N-*p*-C_6H_3), 2.76 (hept, $^{3}J_{HH}$ = 7 Hz, 2H, C_6H_3-C*H*$(CH_3)_2$), 2.18 (heptd, $^{3}J_{HH}$ = 7 Hz, $^{2}J_{PH}$ = 4 Hz, 2H, P-C*H*$(CH_3)_2$), 1.26 – 1.19 (m, 18H, C_6H_3/P-CH(C*H*$_3)_2$), 1.14 – 1.09 (m, 15H, C(C*H*$_3)_3$ / C_6H_3-CH(C*H*$_3)_2$).

^{13}C{^{1}H} NMR (151 MHz, Chloroform-*d*) δ 184.2 (d, $^{1}J_{PC}$ = 31 Hz, *C*=N), 147.7 (d, $^{3}J_{PC}$ = 3 Hz, N-*i*-C_6H_3), 132.8 (N-*o*-C_6H_3), 122.6 (N-*m*-C_6H_3), 122.0 (N-*p*-C_6H_3), 46.7 (d, $^{2}J_{PC}$ = 31 Hz, *C*$(CH_3)_3$), 28.7 (d, *J* = 9 Hz, C(*C*$H_3)_3$), 28.2 (Ph-*C*H$(CH_3)_2$), 24.9 (d, $^{1}J_{PC}$ = 14 Hz, P-*C*H$(CH_3)_2$), 24.7 (C_6H_3-CH(*C*H$_3)_2$), 22.3 (C_6H_3-CH(*C*H$_3)_2$), 21.9 (d, $^{2}J_{PC}$ = 20 Hz, P-CH(*C*H$_3)_2$), 19.2 (d, $^{2}J_{PC}$ = 10 Hz, P-CH(*C*H$_3)_2$).

^{31}P{^{1}H} NMR (243 MHz, Chloroform-*d*) δ 15.5.

MS (ASAP^{+}) *m/z*: 362.3 ([MH]$^{+}$), 244.2 ([M-P^{i}Pr$_2$]$^{+}$).

IR (ATR): $\nu_{C=N}$ = 1630 cm^{-1}.

6.6.24 Preparation of ^{t}BuC($P^{i}Pr_2$)=N(2,6-$(CH_3)_2C_6H_3$) (3.21)

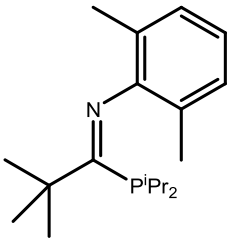

An analogous procedure to that used for the synthesis of **3.7** was carried out using *bis*(*iso*-propyl)-trimethylsilylphosphine (1.484 g, 7.8 mmol) and *N*-(2,6-dimethylphenyl)pivalimidoyl chloride (1.744 g, 7.8 mmol). The reaction mixture was heated at reflux for 16 hours after which the solution was allowed to cool to room temperature. The solution was filtered and the solvent removed to yield the crude product as a yellow oil. The oil was distilled under vacuum (115-120 °C, 0.1 mbar) to afford the product as a yellow oil which crystallised upon standing (1.568 g, 65 % yield). (calc.: $C_{19}H_{32}NP$ C, 74.71; H, 10.56; N, 4.59. Found: C, 74.56; H, 10.69; N, 4.67).

^{1}H NMR (600 MHz, Chloroform-*d*) δ 6.93 (d, *J* = 8 Hz, 2H, N-*m*-C_6H_3), 6.78 (t, *J* = 8 Hz, 1H, N-*p*-C_6H_3), 2.21 (heptd, $^{3}J_{HH}$ = 7 Hz, $^{2}J_{PH}$ = 4 Hz, 2H, P-C*H*$(CH_3)_2$), 2.07 (s, 6H, 2,6-$(CH_3)_2C_6H_3$), 1.28 – 1.20 (m, 12H, P-CH-$(CH_3)_2$), 1.11 (s, 9H, C-$(CH_3)_3$).

^{13}C{^{1}H} NMR (151 MHz, Chloroform-*d*) δ 184.1 (d, $^{1}J_{PC}$ = 31 Hz, C=N), 150.3 (N-*i*-C_6H_3), 127.7 (N-*m*-C_6H_3), 122.4 (N-*o*-C_6H_3), 121.3 (N-*p*-C_6H_3), 46.2 (d, $^{2}J_{PC}$ = 31 Hz, *C*-$(CH_3)_3$), 28.2 (d, $^{3}J_{PC}$ = 9 Hz, C-$(CH_3)_3$), 24.8 (d, $^{1}J_{PC}$ = 14 Hz, P-*C*H-$(CH_3)_2$), 21.9 (d, $^{2}J_{PC}$ = 20 Hz, P-CH-$(CH_3)_2$), 19.4 (2,6-$(CH_3)_2C_6H_3$), 19.1 (d, $^{2}J_{PC}$ = 10 Hz, P-CH-$(CH_3)_2$).

^{31}P{^{1}H} NMR (243 MHz, Chloroform-*d*) δ 13.7.

MS (ASAP^{+}) *m/z*: 306.2 ($[MH]^{+}$).

IR (ATR): $\nu_{C=N}$ = 1636 cm^{-1}.

6.6.25 Preparation on PhC(P^iPr_2)=NPh (3.22)

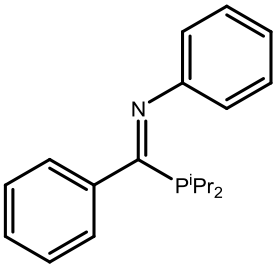

An analogous procedure to that used for the synthesis of **3.7** was carried out using *bis*(*iso*-propyl)-trimethylsilylphosphine (1.700 g, 8.93 mmol) and *N*-phenylbenzimidoyl chloride (1.926 g, 8.93 mmol). The reaction mixture was heated at reflux for 16 hours before the solution was allowed to cool to room temperature and filtered. The solvent was removed under reduced pressure to yield the crude product as a brown oil. The crude product was purified by vacuum distillation (115 - 127 °C, 0.1 mbar) to yield the title compound as a yellow oil that crystallised upon standing (2.157 g, 81 % yield). (calc.: $C_{19}H_{24}NP$ C, 76.74; H, 8.13; N, 4.71. Found: C, 76.87; H, 7.99; N, 4.79).

^{1}H NMR (700 MHz, Chloroform-*d*) δ 7.25 – 7.21 (m, 2H, C-*o*-C_6H_5), 7.19 (s, 3H, C-*m/p*-C_6H_5), 7.13 (t, *J* = 8 Hz, 2H, N-*o*-C_6H_5), 6.90 (t, *J* = 7 Hz, 1H, N-*p*-C_6H_5), 6.63 (d, *J* = 8 Hz, 2H, N-*m*-C_6H_5), 2.20 (heptd, $^3J_{HH}$ = 7 Hz, $^2J_{PH}$ = 3 Hz, 2H, P-C*H*$(CH_3)_2$), 1.20 (dd, $^3J_{PH}$ = 13 Hz, $^3J_{HH}$ = 7 Hz, 6H, P-CH(C*H*$_3)_2$), 1.01 (dd, $^3J_{PH}$ = 13 Hz, $^3J_{HH}$ = 7 Hz, 6H, P-CH(C*H*$_3)_2$).

^{13}C{^{1}H} NMR (176 MHz, Chloroform-*d*) δ 178.9 (d, $^1J_{PC}$ = 22 Hz, *C*=N), 152.4 (d, $^3J_{PC}$ = 4 Hz, N-*i*-C_6H_5), 139.7 (d, $^2J_{PC}$ = 27 Hz, C-*i*-C_6H_5), 128.8 (d, $^3J_{PC}$ = 9 Hz, C-*o*-C_6H_5), 128.7 (N-*o*-C_6H_5), 128.7 (C-*m/p*-C_6H_5), 128.0 (C-*m/p*-C_6H_5), 122.9 (N-*p*-C_6H_5), 120.6 (N-*m*-C_6H_5), 22.8 (d, $^1J_{PC}$ = 12.3 Hz, P-*C*H$(CH_3)_2$), 20.4 (d, $^2J_{PC}$ = 11 Hz, P-CH(*C*H$_3)_2$), 19.2 (d, $^2J_{PC}$ = 11 Hz, P-CH(*C*H$_3)_2$).

^{31}P{^{1}H} NMR (283 MHz, Chloroform-*d*) δ 26.6.

MS (ASAP$^+$) *m/z*: 298.2 ([MH]$^+$), 180.1 ([M-P^{i}Pr$_2$]$^+$).

IR (ATR): $\nu_{C=N}$ = 1587 cm^{-1}.

6.6.26 Preparation of PhC(P^iPr_2)=N(2,4,6-(Ph_3)C_6H_2) (3.23)

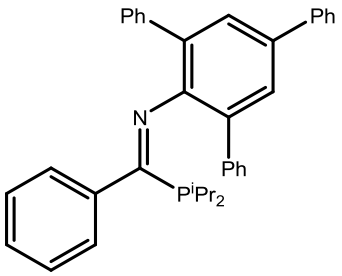

An analogous procedure to that used in the synthesis of **3.7** was carried out using *bis*(*iso*-propyl)-trimethylsilylphosphine (0.280 g, 1.47 mmol) and *N*-(2,4,6-(triphenyl)phenyl)benzimidoyl chloride (0.653 g, 1.47 mmol). The reaction mixture was heated at reflux for 16 hours, after which $^{31}P\{^1H\}$ NMR spectroscopic analysis revealed 35 % of the starting *bis*(*iso*-propyl)-trimethylsilylphosphine had converted to diisopropylphosphine. More *bis*(*iso*-propyl)-trimethylsilylphosphine was added to the reaction (98 mg, 0.5 mmol) before being heated back to reflux. After 16 hours the solution was left to cool to room temperature and the solvent was removed under vacuum. Hexane (10 mL) was added and warmed before filtering the mixture to yield a clear yellow solution. The hot solution was concentrated under reduced pressure before being left to cool and stand at room temperature for 72 hours in which time yellow crystals of the product formed. This process was repeated to acquire a second batch of yellow crystals which were combined with the first, giving the title product (393 g, 51 % yield). (calc.: $C_{37}H_{36}NP$ C, 84.54; H, 6.90; N, 2.66. Found: C, 84.41; H, 7.07; N, 2.67).

^{1}H NMR (600 MHz, Chloroform-*d*) δ 7.61 (d, *J* = 7.3 Hz, 2H, $C_6H_2(C_6H_5)_3$), 7.40 (s, 2H, $C_6H_2(C_6H_5)_3$), 7.38 (d, *J* = 7.9 Hz, 1H, $C_6H_2(C_6H_5)_3$), 7.33 – 7.23 (m, 12H, $C_6H_2(C_6H_5)_3$), 7.06 (t, *J* = 7.4 Hz, 1H, C-*p*-C_6H_5), 6.93 (t, *J* = 7.7 Hz, 2H, C-*m*-C_6H_5), 6.45 (d, *J* = 8 Hz, 2H, C-*o*-C_6H_5), 1.85 (heptd, $^3J_{HH}$ = 7 Hz, $^2J_{PH}$ = 4 Hz, 2H, P-C*H*$(CH_3)_2$), 0.96 (dd, $^3J_{PH}$ = 14 Hz, $^3J_{HH}$ = 7 Hz, 6H, P-CH(C*H*$_3)_2$), 0.64 (dd, $^3J_{PH}$ = 12 Hz, $^3J_{HH}$ = 7 Hz, 6H, P-CH(C*H*$_3)_2$).

$^{13}C\{^1H\}$ NMR (151 MHz, Chloroform-*d*) δ 179.9 (d, $^1J_{PC}$ = 20 Hz, *C*=N), 147.2 (N-*i*-C_6H_2), 140.6 (N-*o/p*-C_6H_2), 139.3 (d, $^2J_{PC}$ = 24 Hz, C-*i*-C_6H_5), 136.3 (C_6H_2-*i*-(C_6H_5)$_3$), 133.5 (C_6H_2-*i*-(C_6H_5)$_3$), 130.0 ($C_6H_2(C_6H_5)_3$), 128.9 ($C_6H_2(C_6H_5)_3$), 128.3 ($C_6H_2(C_6H_5)_3$), 128.1 (C-*p*-C_6H_5), 128.0 (N-*m*-C_6H_2), 127.5 (C-*m*-C_6H_5), 127.1 (d, $^3J_{PC}$ = 9 Hz, C-*o*-C_6H_5), 127.0 (C_6H_2-*i*-(C_6H_5)$_3$), 126.7 ($C_6H_2(C_6H_5)_3$), 22.8 (d, $^1J_{PC}$ = 12 Hz, P-*C*H$(CH_3)_2$), 20.5 (d, $^2J_{PC}$ = 12 Hz, P-CH(*C*H$_3)_2$), 19.1 (d, $^2J_{PC}$ = 10 Hz, P-CH(*C*H$_3)_2$).

$^{31}P\{^1H\}$ NMR (243 MHz, Chloroform-*d*) δ 31.5.

MS (ASAP$^+$) *m/z*: 526.2 ([MH]$^+$), 408.2 ([M-P^iPr_2]$^+$).

IR (ATR): $\nu_{C=N}$ = 1586 cm^{-1}.

6.6.27 Preparation of PhC(P(2-(OCH$_3$)C$_6$H$_4$)$_2$)=N(2,6-(CH$_3$)$_2$C$_6$H$_3$) (3.24)

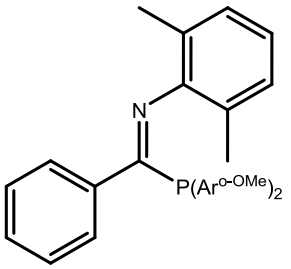

An analogous procedure to that used for the synthesis of **3.7** was carried out using trimethylsilyl-*bis*(*ortho*-methoxyphenyl)phosphine (0.660 g, 2.1 mmol) and *N*-(2,6-dimethylphenyl)benzimidoyl chloride (0.505 g, 2.1 mmol). The reaction mixture was heated at reflux for 16 hours, in which time the solution turned yellow. The solution was allowed to cool to room temperature and the solvent was removed under vacuum. The resulting oily solid was dissolved in a mixture of hot hexane and a small amount of MeCN before being left to cool. In 16 hours crystals of the product suitable for X-ray diffraction had grown (0.438 g, 46 % yield). (calc.: $C_{29}H_{28}NO_2P$ C, 76.80; H, 6.22; N, 3.09. Found: C, 76.77; H, 6.28; N, 3.19).

^{1}H NMR (700 MHz, Toluene-d_8, 70 °C) δ 7.64 (s, 2H, C-*o*-C$_6$*H*$_5$), 7.26 (s, 2H, P-5-C$_6$*H*$_4$), 7.03 (t, *J* = 9 Hz, 2H, P-3/4/6-C$_6$*H*$_4$), 6.90 (s, 3H, C-*m*/*p*-C$_6$*H*$_5$), 6.81 – 6.79 (m, 2H, N-*m*-C$_6$*H*$_3$), 6.76 – 6.73 (m, 1H, N-*p*-C$_6$*H*$_3$), 6.69 (t, *J* = 7 Hz, 2H, P-3/4/6-C$_6$*H*$_4$), 6.39 (s, 2H, P-3/4/6-C$_6$*H*$_4$), 3.19 (s, 6H, 2-C*H*$_3$O-C$_6$H$_4$), 2.07 (s, 6H, 2,6-(C*H*$_3$)$_2$C$_6$H$_3$).

^{13}C{^{1}H} NMR (176 MHz, Toluene-d_8, 70 °C) δ 176.1 (d, $^1J_{PC}$ = 35 Hz, *C*=N), 162.1 (d, $^2J_{PC}$ = 15 Hz, P-2-*C*$_6$H$_4$), 150.5 (d, $^3J_{PC}$ = 10 Hz, N-*i*-*C*$_6$H$_3$), 141.0 (C-*i*-*C*$_6$H$_5$), 135.6 (d, $^3J_{PC}$ = 12 Hz, P-5-*C*$_6$H$_4$), 130.8 (P-3/4/6-*C*$_6$H$_4$), 128.6 (C-*o*/*p*-C$_6$H$_5$), 128.1 (N-*m*-*C*$_6$H$_3$), 127.4 (C-*m*-C$_6$H$_5$), 125.9 (N-*o*-*C*$_6$H$_3$), 124.0 (d, $^1J_{PC}$ = 15 Hz, P-*i*-*C*$_6$H$_4$), 123.1 (N-*p*-*C*$_6$H$_3$), 121.2 (d, J_{PC} = 4 Hz, P-3/4/6-*C*$_6$H$_4$), 110.8 (P-3/4/6-*C*$_6$H$_4$), 54.9 (2-*C*H$_3$O-C$_6$H$_4$), 18.5 (d, $^5J_{PC}$ = 4 Hz, 2,6-(*C*H$_3$)$_2$C$_6$H$_3$).

^{31}P{^{1}H} NMR (202 MHz, Toluene-d_8) δ 9.3, –19.1.*

MS (ASAP$^+$) *m/z*: 454.2 ([MH]$^+$), 208.1 ([M-(P-*o*-MeOC$_6$H$_4$)$_2$]$^+$).

IR (ATR): $\nu_{C=N}$ = 1585 cm^{-1}.

* Two resonances due to imine E and Z isomers present in solution

6.6.28 Preparation of PhC(P^iPr_2)=N(2,5-($(CH_3)_3C$)C_6H_3) (3.25)

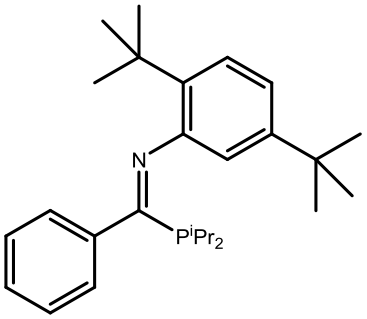

An analogous procedure to that used for the synthesis of **3.7** was carried out using *bis*(*iso*-propyl)-trimethylsilylphosphine (0.950 g, 4.99 mmol) and *N*-(2,5-di-*tert*-butylphenyl)benzimidoyl chloride (1.636 g, 4.99 mmol). The solution was set to reflux for 24 hours after which the solution was left to cool to room temperature and the solvent removed under vacuum, yielding the crude product as a viscous yellow oil. The crude product was purified by vacuum distillation (155 - 160 °C, 0.1 mbar) to give the product as a highly viscous oil (approx. 70% yield)* (calc.: $C_{27}H_{40}NP$ C, 79.17; H, 9.84; N, 3.42. Found: C, 79.26; H, 9.91; N, 3.48).

^{1}H NMR (700 MHz, Chloroform-*d*) δ 7.34 – 7.31 (m, 2H, C-*o*-C_6H_5), 7.28 (d, *J* = 8 Hz, 1H, N-3-C_6H_3), 7.25 – 7.22 (m, 2H, C-*m*-C_6H_5), 7.22 – 7.18 (m, 1H, C-*p*-C_6H_5), 6.90 (dd, *J* = 8, 2 Hz, 1H, N-4-C_6H_3), 6.13 (d, *J* = 2 Hz, 1H, N-6-C_6H_3), 2.38 (heptd, $^3J_{HH}$ = 7 Hz, $^2J_{PH}$ = 4 Hz, 2H, P-C*H*$(CH_3)_2$), 1.60 (s, 9H, 5-(CH_3)$_3$C-C_6H_3), 1.29 (dd, $^3J_{PH}$ = 14 Hz, $^3J_{HH}$ = 7 Hz, 6H, P-CH(C*H*$_3$)$_2$), 1.07 (dd, $^3J_{PH}$ = 12 Hz, $^3J_{HH}$ = 7 Hz, 6H, P-CH(C*H*$_3$)$_2$), 0.94 (s, 9H, 2-(CH_3)$_3$C-C_6H_3).

^{13}C{^{1}H} NMR (176 MHz, Chloroform-*d*) δ 177.3 (d, $^1J_{PC}$ = 19 Hz, *C*=N), 149.2 (d, $^3J_{PC}$ = 4 Hz, N-*i*-C_6H_3), 148.4 (N-2-C_6H_3), 140.5 (d, $^2J_{PC}$ = 26 Hz, C-*i*-C_6H_5), 139.2 (d, $^5J_{PC}$ = 2 Hz, N-5-C_6H_3), 128.3 (d, $^3J_{PC}$ = 9 Hz, C-*o*-C_6H_5), 128.2 (d, $^4J_{PC}$ = 1 Hz, C-*m*-C_6H_5), 128.2 (d, $^5J_{PC}$ = 1 Hz, C-*p*-C_6H_5), 125.6 (N-3-C_6H_3), 120.4 (N-6-C_6H_3), 119.9 (N-4-C_6H_3), 35.2 (5-(CH_3)$_3$*C*-C_6H_3), 33.9 (2-(CH_3)$_3$*C*-C_6H_3), 31.0 (2-(*C*H$_3$)$_3$C-C_6H_3), 30.5 (5-(*C*H$_3$)$_3$C-C_6H_3), 23.5 (d, $^1J_{PC}$ = 12 Hz, P-*C*H$(CH_3)_2$), 21.4 (d, $^2J_{PC}$ = 12Hz, P-CH(*C*H$_3$)$_2$), 19.9 (d, $^2J_{PC}$ = 10 Hz, P-CH(*C*H$_3$)$_2$).

^{31}P{^{1}H} NMR (283 MHz, Chloroform-*d*) δ 34.1.

MS (ASAP$^+$) *m/z*: 410.3 ([MH]$^+$), 292.2 ([M-P^{i}Pr$_2$]$^+$).

IR (ATR): $\nu_{C=N}$ = 1549 cm^{-1}.

* Not all of the product could not be removed from the flask due to the highly viscous nature of the compound, and a precise yield could not be measured.

6.6.29 Preparation of $PhC(PEt_2)=N(2,6\text{-}(CH_3)_2C_6H_3)$ (3.26)

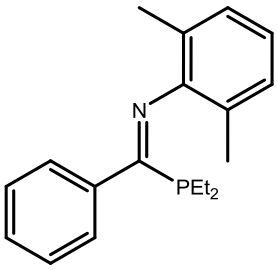

An analogous procedure to that used for the synthesis of **3.7** was carried out using *bis*(ethyl)-trimethylsilylphosphine (1.103 g, 6.8 mmol) and *N*-(2,6-dimethylphenyl)benzimidoyl chloride (1.657 g, 6.8 mmol). The solution was heated at reflux for 16 hours after which the solution was left to cool to room temperature. The solvent was removed under vacuum to give a brown oil as the crude product. The brown oil was distilled under vacuum (130-135 °C, 0.1 mbar) to yield the product as a clear yellow oil (1.542 g, 76 % yield). (calc.: $C_{19}H_{24}NP$ C, 76.74; H, 8.13; N, 4.71. Found: C, 76.82; H, 8.02; N, 4.79).

^{1}H NMR (700 MHz, Chloroform-*d*) δ 7.27 – 7.15 (m, 5H, C-*o/m/p*-C_6H_5), 6.93 – 6.86 (m, 2H, N-*m*-C_6H_3), 6.83 – 6.75 (m, 1H, N-*p*-C_6H_3), 2.02 (s, 6H, C_6H_3-$(CH_3)_2$), 1.91 – 1.82 (m, 2H, $P(CH_2CH_3)_2$), 1.67 – 1.59 (m, 2H, $P(CH_2CH_3)_2$), 1.17 – 1.05 (m, 6H, $P(CH_2CH_3)_2$).

^{13}C{^{1}H} NMR (176 MHz, Chloroform-*d*) δ 179.9 (*C*=N), 149.7 (N-*i*-C_6H_3), 138.8 (d, $^2J_{PC}$ = 27 Hz C-*i*-C_6H_5), 129.1 (C-*p*-C_6H_5), 128.2 (C-*o*-C_6H_5), 127.8 (N-*m*-C_6H_3), 126.8 (d, $^4J_{PC}$ = 9 Hz, C-*m*-C_6H_5), 125.6 (N-*o*-C_6H_3), 122.7 (N-*p*-C_6H_3), 18.6 (*o*-$(CH_3)_2C_6H_3$), 16.1 (d, $^1J_{PC}$ = 10 Hz, $P(CH_2CH_3)_2$), 10.0 (d, $^2J_{PC}$ = 10 Hz $P(CH_2CH_3)_2$).

^{31}P{^{1}H} NMR (162 MHz, Chloroform-*d*) δ 2.5.

MS (ASAP$^+$) *m/z*: 298.2 ($[MH]^+$), 208.1 ($[M\text{-}PEt_2]^+$).

IR (ATR): $\nu_{C=N}$ = 1588 cm^{-1}.

6.6.30 Synthesis of selenide derivatives of iminophosphine ligands and analysis of P-Se coupling constants

A Young's tap NMR tube was charged with a sample of iminophosphine ligand (10 – 30 mg) and an excess of grey selenium powder (10 – 20 mg). $CDCl_3$ (0.5 – 0.7 mL) was added and the reaction mixture was sonicated for at least 1 hour, after which time the reactions had gone to at least 60 % conversion. $^{31}P\{^1H\}$ NMR spectroscopy was used to analyse the products of the reaction, of which the data is listed below:

Label	Compound	$\lvert^1J_{P\text{-}Se}\rvert$ (Hz)[a]	^{31}P δ (ppm)
3.1(Se)	$PhC(SePPh_2)=N(2\text{-}MeC_6H_4)$	740	36.5
3.2(Se)	$^tBuC(SePPh_2)= N(2\text{-}MeC_6H_4)$	731[b]	34.6
3.3(Se)	$PhC(SePPh_2)=NPh$	742	36.4
3.5(Se)	$PhC(SeP^tBu_2)=NPh$	715	76.5
3.6(Se)	$PhC(SeP^tBu_2)=N(2,6\text{-}^iPr_2C_6H_3)$	705	77.3
3.7(Se)	$PhC(SePPh_2)=N(2,6\text{-}^iPr_2C_6H_3)$	740	36.0
3.8(Se)	$PhC(SePPh_2)=N(2,6\text{-}Me_2C_6H_3)$	738	36.2
3.9(Se)	$PhC(SeP^iPr_2)=N(2,6\text{-}^iPr_2C_6H_3)$	711	64.4
3.10(Se)	$PhC(SeP^iPr_2)=N(2,6\text{-}Me_2C_6H_3)$	710	64.1
3.11(Se)	$PhC(SeP(2\text{-}MeOC_6H_4)_2)=N(2,6\text{-}^iPr_2C_6H_3)$	719	21.4
3.12(Se)	$PhC(SeP^tBu_2)=NPh(2,6\text{-}Me_2C_6H_3)$	708	77.5
3.13(Se)	$PhC(SeP^tBu_2)=NPh(2\text{-}MeOC_6H_4)$	711	76.4
3.14(Se)	$PhC(SePCy_2)=N(2,6\text{-}^iPr_2C_6H_3)$	709	56.2
3.15(Se)	$PhC(SePCy_2)=N(2,6\text{-}Me_2C_6H_3)$	706	56.2
3.16(Se)	$PhC(SeP^iPr_2)=N(2,6\text{-}Et_2C_6H_3)$	709	63.9
3.17(Se)	$PhC(SePEt_2)=N(2,6\text{-}^iPr_2C_6H_3)$	703	43.0
3.18(Se)	$PhC(SeP(2\text{-}Et\text{-}C_6H_4)_2)=N(2,6\text{-}^iPr_2C_6H_3)$	708	30.1
3.19(Se)	$PhC(SeP(2\text{-}F\text{-}C_6H_4)_2)=N(2,6\text{-}^iPr_2C_6H_3)$	750	23.8
3.20(Se)	$^tBuC(SeP^iPr_2)=N(2,6\text{-}(2,6\text{-}^iPr_2C_6H_3)$	701	61.1
3.21(Se)	$^tBuC(SeP^iPr_2)=N(2,6\text{-}Me_2C_6H_3)$	702	60.2
3.22(Se)	$PhC(SeP^iPr_2)=NPh$	715	66.2
3.23(Se)	$PhC(SeP^iPr_2)=N(2,4,6\text{-}Ph_3C_6H_2)$	712	64.1
3.24(Se)	$PhC(SeP(2\text{-}MeOC_6H_4)_2)=N(2,6\text{-}Me_2C_6H_3)$	721	22.3
3.25(Se)	$PhC(SeP^iPr_2)=N(2,5\text{-}^tBu_2C_6H_3)$	707	65.5
3.26(Se)	$PhC(SePEt_2)=N(2,6\text{-}Me_2C_6H_3)$	701	43.3
3.27(Se)	$PhC(SePPh_2)=NPh(o\text{-}OMe)$	740	36.7

[a]162 MHz, $CDCl_3$; [b]81 MHz, $CDCl_3$

6.7 Synthesis of $CrCl_3(THF)(PCN)$ complexes

6.7.1 Preparation of $CrCl_3(THF)(PhC(PPh_2)=NPh)$ (4.1)

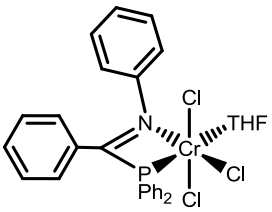

A flask was charged with $CrCl_3(THF)_3$ (0.363 g, 0.97 mmol), which was dissolved in toluene (20 mL). The solution was cooled to 0 °C before a solution of **3.3** (0.389 g, 1.07 mmol) in toluene (20 mL) was added dropwise. The reaction mixture was left to stir overnight, during which time a blue precipitate formed. The blue solid was isolated by filtration and washed with diethyl ether (2 × 5 mL) before being dried under vacuum to yield the title product (0.372 g, 64 % yield). Subsequently, crystals suitable for X-ray diffraction studies were grown of the complex by layering a concentrated DCM solution of the product with hexane. Analysis of the product by mass spectrometry was attempted, but gave inconclusive results, due to the non-volatile nature of the compound. (calc.: $C_{29}H_{28}Cl_3CrNOP$ C, 58.45; H, 4.74; N, 2.35. Found: C, 58.32; H, 4.76; N, 2.46).

6.7.2 Preparation of $CrCl_3(THF)(PhC(PPh_2)=N(2\text{-}MeC_6H_4))$ (4.2)

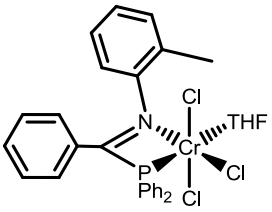

A sample of $CrCl_3(THF)_3$ (0.432 g, 1.2 mmol) was dissolved in toluene (40 mL) and cooled to 0 °C before a solution of **3.1** (0.525 g, 1.4 mmol) in toluene (20 mL) was added dropwise. The resulting solution was allowed to warm to room temperature and left to stir for 3 hours. The solution was concentrated under vacuum to 2/3 of the original volume, causing a green precipitate to form. The precipitate was isolated by filtration and washed with diethyl ether (2 × 5 mL) before being dried under vacuum to yield the product as a green solid (0.222 g, 30 % yield). Crystals suitable for X-ray diffraction studies were grown of the complex by layering a concentrated DCM solution of the product with hexane. Analysis of the product by mass spectrometry was attempted, but gave inconclusive results, due to the non-volatile nature of the compound. (0.372 g, 64 % yield). (calc.: $C_{30}H_{30}Cl_3CrNOP$ C, 59.08; H, 4.96; N, 2.30. Found: C, 59.16; H, 5.03; N, 2.32).

6.7.3 Preparation of $CrCl_3(Ph(PPh_2)C=N(2\text{-}MeOC_6H_4))$ (4.3)

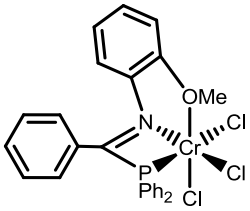

$CrCl_3(THF)_3$ (0.360 g, 0.96 mmol) was dissolved in toluene (20 mL) and cooled to 0 °C. A sample of $Ph(PPh_2)C=N(2\text{-}MeOC_6H_4)$ (0.456 g, 1.15 mmol) was dissolved in toluene (20 mL) and subsequently added dropwise to the $CrCl_3(THF)_3$ solution, causing the solution to turn dark green. The solution was allowed to warm to room temperature and

stirred for 2 hours, after which time the solution was concentrated under vacuum. A brown solid precipitated out of solution, which was isolated by filtration, washed with diethyl ether (2 × 5 mL) and dried under vacuum to yield the product as a brown solid (0.150 g, 30 % yield). Analysis of the product by mass spectrometry was attempted, but gave inconclusive results, due to the non-volatile nature of the compound. (calc.: $C_{26}H_{22}Cl_3CrNOP$ C, 56.39; H, 4.00; N, 2.53. Found: C, 56.43; H, 3.99; N, 2.61).

6.7.4 Preparation of $CrCl_3(THF)(Ph(P^iPr_2)C{=}N(2\text{-}MeC_6H_4))$ (4.4)

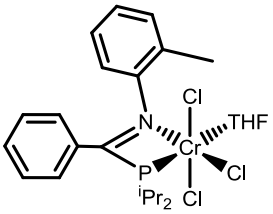

Samples of $CrCl_3(THF)_3$ (0.433 g, 1.16 mmol) and **3.4** (0.432 g, 1.39 mmol) were placed in separate flasks and dissolved in DCM (20 mL each). The ligand solution was added to the chromium solution and the reaction mixture was stirred for 1 hour. The solvent was removed under vacuum to yield a green solid. The green solid was washed with diethyl ether (2 × 15 mL) and hexane (2 × 10 mL) to yield the product as a pale blue powder (0.414 g, 66 % yield). Analysis of the product by mass spectrometry was attempted, but gave inconclusive results, due to the non-volatile nature of the compound. (calc.: $C_{24}H_{34}Cl_3CrNOP$ C, 53.20; H, 6.32; N, 2.58. Found: C, 53.04; H 6.15; N, 2.63).

6.7.5 Preparation of $CrCl_3(THF)(Ph(P^iPr_2)C{=}N(2,6\text{-}Me_2C_6H_3))$ (4.5)

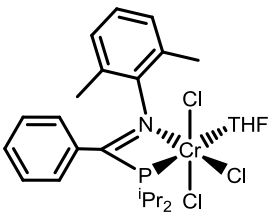

A pair of Schlenk flasks were charged with $CrCl_3(THF)_3$ (0.212 g, 0.57 mmol) and **3.10** (0.203 g, 0.62 mmol) respectively. Both starting materials were dissolved in DCM (5 mL each) and the ligand solution was added dropwise to the $CrCl_3(THF)_3$ solution, turning the resulting solution green. The solution was left to stir overnight before being filtered to remove any precipitate. The solvent was then removed under vacuum to give a green residue. The green solid was triturated with hexane (5 mL) before the solid was isolated by filtration. The solid was washed with further hexane (2 × 5 mL) and dried under vacuum to yield the title product (0.289 g, 90 % yield). Analysis of the product by mass spectrometry was attempted, but gave inconclusive results, due to the non-volatile nature of the compound. (calc.: $C_{25}H_{36}Cl_3CrNOP$ C, 54.02; H, 6.53; N, 2.52. Found: C, 53.97; H, 6.66; N, 2.43).

6.7.6 Preparation of $CrCl_3(THF)(Ph(P^iPr_2)C{=}N(2,6\text{-}^iPr_2C_6H_3))$ (4.6)

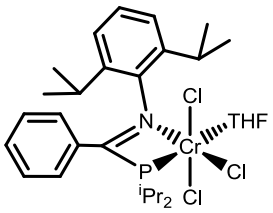

$CrCl_3(THF)_3$ (0.170 g, 0.45 mmol) and **3.9** (0.190 g, 0.50 mmol) were placed in separate Schlenk flasks and both dissolved in DCM (5 mL each). The ligand solution was added to the $CrCl_3(THF)_3$ solution *via* cannula transfer and the resulting reaction mixture was left to stir overnight. The solvent was removed *in vacuo* to yield a crude product as a green/brown residue. The solid was triturated with hexane (5 mL) and the solid isolated by filtration. The solid was washed with more hexane (2 × 5 mL) and dried under vacuum to yield the final product as a pale brown solid (0.224 g, 81 % yield). Analysis of the product by mass spectrometry was attempted, but gave inconclusive results, due to the non-volatile nature of the compound. (calc.: $C_{29}H_{44}Cl_3CrNOP$ C, 56.91; H, 7.25; N, 2.29. Found: C, 56.84; H, 7.34; N, 2.35).

6.8 Reaction of Cr(II) with a PCN Ligand

6.8.1 Reaction of $CrCl_2$ with iminophosphine 3.10

A flask was charged with $CrCl_2$ (0.094 g, 0.76 mmol) before THF was added (10 mL) and the resulting mixture was heated at reflux overnight, in which time the solution turned pale blue. The solution was allowed to cool to room temperature before a solution of **3.10** (0.274 g, 0.84 mmol) in THF (5 mL) was added and the solution wash heated back to reflux for 2 hours. The solution was again let cool to room temperature and filtered to yield a clear green solution. The solution was then warmed and concentrated under vacuum, before being left to cool and stand for 72 hours, in which time purple crystals formed. X-ray crystallographic analysis found these crystals to be $CrCl_3(THF)_3$. The crystals were isolated and the crystallisation process was repeated with the remaining solution, yielding the same $CrCl_3(THF)_3$ product. No further products were isolated from the solution. It is suggested that $CrCl_3(THF)_3$ formed through the disproportionation of the Cr(II) starting material, but no corresponding Cr(I) products were observed.

6.9 Reactions of PCN Ligands with $Cr(CO)_6$

6.9.1 Preparation of $Cr(CO)_4(Ph(P^iPr_2)C{=}N(2,6\text{-}^iPr_2C_6H_3))$ (4.7) and $Cr(CO)_5(Ph(P^iPr_2)C{=}N(2,6\text{-}^iPr_2C_6H_3))$ (4.8)

A flask was charged with $Cr(CO)_6$ (0.163 g, 0.74 mmol) and iminophosphine **3.9** (0.236 g, 0.62 mmol) and toluene was added (20 mL). The resulting mixture was heated at reflux for 72 hours, during which time the solution turned purple. The solution was allowed to cool to room temperature and the solvent removed under vacuum to give a solid purple residue. Hexane (7 mL) was added and the mixture was filtered to isolate a yellow solution and a purple solid.

6.9.1.1 Isolation and characterisation of $Cr(CO)_4(Ph(P^iPr_2)C{=}N(2,6\text{-}^iPr_2C_6H_3))$ (4.7)

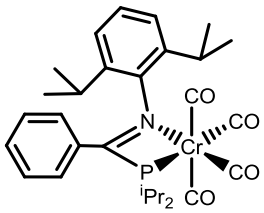

The purple solid was dissolved in a minimum amount of DCM and layered with hexane before being stored at 0 °C for 16 hours, forming purple crystals suitable for X-ray diffraction. The process was repeated with the remaining purple solution to yield a second batch of purple product (26 mg, 8 % yield), which analysis revealed to be the bidentate complex, $Cr(CO)_4(Ph(P^iPr_2)C{=}N(2,6\text{-}^iPr_2C_6H_3))$. Due to the air sensitive nature of the complex, successful elemental analysis could not be achieved. Mass spectrometry was attempted but yielded inconclusive results.

^{1}H NMR (700 MHz, Chloroform-*d*) δ 7.37 – 7.32 (m, 1H, C-*p*-C_6H_5), 7.25 – 7.22 (m, 1H, N-*p*-C_6H_3), 7.22 – 7.19 (m, 2H, C-*m*-C_6H_5), 7.19 – 7.15 (m, 2H, N-*m*-C_6H_3), 6.92 (d, *J* = 8 Hz, 2H, C-*o*-C_6H_5), 3.17 (hept, $^3J_{HH}$ = 7 Hz, 2H, C_6H_3-C*H*$(CH_3)_2$), 2.75 (heptd, $^2J_{PH}$ = 14 Hz, $^3J_{HH}$ = 7 Hz, 2H, P-C*H*$(CH_3)_2$), 1.49 (dd, $^3J_{PH}$ = 19 Hz, $^3J_{HH}$ = 7 Hz, 6H, P-CH(C*H*$_3)_2$), 1.41 (d, $^3J_{HH}$ = 7 Hz, 6H, C_6H_3-CH(C*H*$_3)_2$), 1.38 (dd, $^3J_{PH}$ = 15 Hz, $^3J_{HH}$ = 7 Hz, 6H, P-CH(C*H*$_3)_2$)), 0.82 (d, $^3J_{HH}$ = 7 Hz, 6H, C_6H_3-CH(C*H*$_3)_2$).

^{13}C{^{1}H} NMR (176 MHz, Chloroform-*d*) δ 229.3 (d, $^2J_{PC}$ = 12 Hz, *trans*-PCr(*C*O)), 225.5 (d, $^2J_{PC}$ = 3 Hz, *trans*-NCr(*C*O)), 222.3 (d, $^2J_{PC}$ = 13 Hz, *trans*-Cr(*C*O)), 185.0 (d, $^1J_{PC}$ = 18 Hz, *C*=N), 147.3 (d, $^3J_{PC}$ = 24 Hz, N-*i*-C_6H_3), 136.2 (N-*o*-C_6H_3), 133.3 (d, $^2J_{PC}$ = 5 Hz, C-*i*-C_6H_5), 132.3 (C-*p*-C_6H_5), 129.1 (C-*m*-C_6H_5), 128.9 (C-*o*-C_6H_5), 127.2 (N-*p*-C_6H_3), 125.0 (N-*m*-C_6H_3), 30.2 (d, $^1J_{PC}$ = 9 Hz, P-*C*H$(CH_3)_2$), 28.4 (C_6H_3-*C*H$(CH_3)_2$), 25.0 (C_6H_3-CH(*C*H$_3)_2$), 23.9 (C_6H_3-CH(*C*H$_3)_2$), 20.5 (d, $^2J_{PC}$ = 12 Hz, P-CH(*C*H$_3)_2$), 19.5 (d, $^2J_{PC}$ = 2.0 Hz, P-CH(*C*H$_3)_2$).

^{31}P{^{1}H} NMR (283 MHz, Chloroform-*d*) δ 63.2.

IR (CH_2Cl_2): ν_{CO} = 1999 cm^{-1}, 1900 cm^{-1}, 1874 cm^{-1}, 1859 cm^{-1}.

6.9.1.2 Isolation and characterisation of $Cr(CO)_5(Ph(P^iPr_2)C=N(2,6\text{-}^iPr_2C_6H_3))$ (4.8)

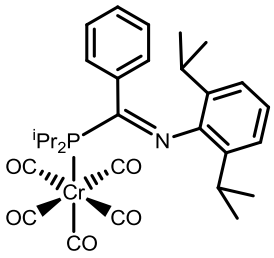

The yellow solution in hexane was also isolated and the solvent was removed under reduced pressure to yield a crude yellow solid. The solid was dissolved in a minimum amount of hot hexane and left to slowly cool and stand for 16 hours, during which time yellow crystals suitable for X-ray diffraction grew (146 mg, 40 % yield). Analysis demonstrated these yellow crystals were the monodentate complex, $Cr(CO)_5(Ph(P^iPr_2)C=N(2,6\text{-}^iPr_2C_6H_3)$. (calc.: $C_{30}H_{36}CrNO_5P$ C, 62.38; H, 6.98; N, 2.42. Found: C, 62.25; H, 6.94; N, 2.49).

^{1}H NMR (700 MHz, Chloroform-*d*) δ 7.23 – 7.19 (m, 3H, C-*m/p*-C_6H_5), 7.08 (dd, *J* = 8, 2 Hz, 2H, C-*o*-C_6H_5), 6.95 – 6.89 (m, 3H, N-*m/p*-C_6H_3), 2.89 (hept, $^3J_{HH}$ = 7 Hz, 2H, C_6H_3-C*H*$(CH_3)_2$), 2.66 – 2.58 (heptd, $^2J_{PH}$ = 14 Hz, $^3J_{HH}$ = 7 Hz, 2H, P-C*H*$(CH_3)_2$), 1.34 – 1.28 (m, 12H, P-CH(C*H*$_3)_2$), 1.11 (d, $^3J_{HH}$ = 7 Hz, 6H, C_6H_3-CH(C*H*$_3)_2$), 1.06 (d, $^3J_{HH}$ = 7 Hz, 6H, C_6H_3-CH(C*H*$_3)_2$).

^{13}C{^{1}H} NMR (176 MHz, Chloroform-*d*) δ 221.3 (d, $^2J_{PC}$ = 5 Hz, *trans*-PCr(*C*O)), 217.8 (d, $^2J_{PC}$ = 12 Hz, trans-Cr(*C*O)), 175.6 (d, $^1J_{PC}$ = 29 Hz, *C*=N), 145.8 (d, $^3J_{PC}$ = 15 Hz, N-*i*-C_6H_3), 137.6 (d, $^2J_{PC}$ = 21 Hz, C-*i*-C_6H_5), 135.3 (N-*o*-C_6H_3), 129.2 (C-*p*-C_6H_5), 128.1 (C-*m*-C_6H_5), 127.0 (d, $^3J_{PC}$ = 2 Hz, C-*o*-C_6H_5), 124.5 (N-*p*-C_6H_3), 122.9 (N-*m*-C_6H_3), 28.6 (C_6H_3-*C*H$(CH_3)_2$), 28.4 (d, $^1J_{PC}$ = 16 Hz, P-*C*H$(CH_3)_2$), 25.2 (C_6H_3-CH(*C*H$_3)_2$), 22.0 (C_6H_3-CH(*C*H$_3)_2$), 19.2 (P-CH(*C*H$_3)_2$), 18.3 (d, $^2J_{PC}$ = 3 Hz, P-CH(*C*H$_3)_2$).

^{31}P{^{1}H} NMR (283 MHz, Chloroform-*d*) δ 83.1.

MS (ASAP$^+$) *m/z*: 574.2 ([MH]$^+$), 382.3 ([MH-Cr(CO)$_5$)]$^+$), 264.2 ([M-Cr(CO)$_5$(P^{i}Pr$_2$)]$^+$).

IR (CH_2Cl_2): ν_{CO} = 2061 cm^{-1}, 1980 cm^{-1}, 1935 cm^{-1}.

6.9.2 Preparation of $Cr(CO)_4(Ph(P^iPr_2)C=N(2,6\text{-}Me_2C_6H_3))$ (4.9) and $Cr(CO)_5(Ph(P^iPr_2)C=N(2,6\text{-}Me_2C_6H_3))$ (4.10)

A flask was charged with $Cr(CO)_6$ (0.402 g, 1.8 mmol) and $Ph(P^iPr_2)C=N(2,6\text{-}Me_2C_6H_3)$ (0.495 g, 1.5 mmol) and toluene was added (40 mL). The mixture was heated to reflux for 24 hours after which the solution was cooled to 0 °C and filtered, giving a purple solution. The solvent was removed *in vacuo* to leave a purple residue.

6.9.2.1 Isolation and characterisation of $Cr(CO)_4(Ph(P^iPr_2)C=N(2,6\text{-}Me_2C_6H_3))$ (4.9)

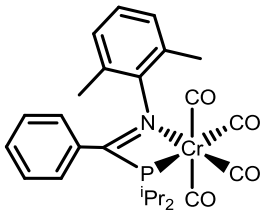

The majority of the purple solid was dissolved in hot hexane and the solution filtered and left to slowly cool. The remaining purple solid was separately dissolved in hot hexane and slowly cooled. Purple crystals formed in both flasks, and these were isolated by filtration and combined to yield the first product, the bidentate complex **4.9** (47 mg, 6 % yield). Due to the air sensitive nature of the complex successful elemental analysis data could not be obtained. Mass spectrometry was attempted, but yielded inconclusive results. The identity of complex **4.9** was confirmed by NMR spectroscopic analysis.

^{1}H NMR (700 MHz, Chloroform-*d*) δ 7.35 (t, *J* = 6.9 Hz, 1H, C-*p*-C_6H_5), 7.27 – 7.22 (m, 2H, C-*m*-C_6H_5), 7.01 (s, 3H, N-*m/p*-C_6H_3), 6.95 (d, *J* = 7.6 Hz, 2H, C-*o*-C_6H_5), 2.75 – 2.67 (m, 2H, P-C*H*-$(CH_3)_2$), 2.27 (s, 6H, N-Ph-$(CH_3)_2$), 1.51 – 1.39 (m, 12H, P-CH-$(CH_3)_2$).

^{13}C{^{1}H} NMR (176 MHz, Chloroform-*d*) δ 229.3 (d, $^2J_{PC}$ = 12 Hz, *trans*-PCr(*C*O)), 225.4 (*trans*-NCr(*C*O)), 222.5 (d, $^2J_{PC}$ = 12 Hz, *trans*-Cr(*C*O)), 184.9 (d, $^1J_{PC}$ = 18 Hz, *C*=N), 149.4 (d, $^3J_{PC}$ = 23 Hz, N-*i*-C_6H_3), 134.1 (d, $^2J_{PC}$ = 4 Hz, C-*i*-C_6H_5), 131.8 (C-*p*-C_6H_5), 129.4 (C-*m*-C_6H_5), 129.2 (N-*m*-C_6H_3), 127.2 (C-*o*-C_6H_5), 126.2 (N-*p*-C_6H_3), 125.9 (N-*o*-C_6H_3), 28.9 (d, $^1J_{PC}$ = 9 Hz, P-*C*H-$(CH_3)_2$), 20.0 (P-CH(CH$_3$)$_2$), 19.2 (N-C_6H_3(CH$_3$)$_2$).

^{31}P{^{1}H} NMR (283 MHz, Chloroform-*d*) δ 61.8.

IR (CH_2Cl_2): ν_{CO} = 2000 cm^{-1}, 1899 cm^{-1}, 1874 cm^{-1}, 1858 cm^{-1}.

6.9.2.2 Isolation and characterisation of $Cr(CO)_5(Ph(P^iPr_2)C=N(2,6\text{-}Me_2C_6H_3))$ (4.10)

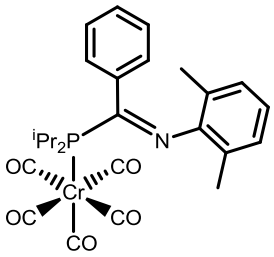

The solution isolated from the first hexane washing was heated and concentrated under vacuum before being left to slowly cool. After 16 hours large yellow crystals had formed which were suitable for X-ray diffraction (0.337 g, 43 % yield). Analysis showed this yellow product to be the monodentate $Cr(CO)_5(Ph(P^iPr_2)C=N(2,6\text{-}Me_2C_6H_3))$ complex. (calc.: $C_{26}H_{28}CrNO_5P$ C, 60.35; H, 5.45; N, 2.71. Found: C, 60.21; H, 5.50; N, 2.80).

^{1}H NMR (600 MHz, Chloroform-*d*) δ 7.25 – 7.20 (m, 3H, C-*m/p*-C_6H_5), 7.12 – 7.07 (m, 2H, C-*o*-C_6H_5), 6.85 – 6.80 (m, 2H, N-*m*-C_6H_3), 6.78 – 6.72 (m, 1H, N-*p*-C_6H_3), 2.60 (heptd, $^2J_{PH}$ = 14 Hz, $^3J_{HH}$ = 7 Hz, 2H, P-C*H*-$(CH_3)_2$), 2.13 (s, 6H, N-C_6H_3-$(CH_3)_2$), 1.37 (dd, $^3J_{PH}$ = 16 Hz, $^3J_{HH}$ = 7 Hz, 6H, P-CH$(CH_3)_2$), 1.23 (dd, $^3J_{PH}$ = 14 Hz, 7 Hz, $^3J_{HH}$ = 6H, P-CH$(CH_3)_2$).

^{13}C{^{1}H} NMR (151 MHz, Chloroform-*d*) δ 221.5 (d, $^2J_{PC}$ = 5 Hz, *trans*-PCr(*C*O)), 218.0 (d, $^2J_{PC}$ = 13 Hz *trans*-Cr(*C*O)), 176.0 (d, $^1J_{PC}$ = 30 Hz *C*=N), 149.2 (d, $^3J_{PC}$ = 17 Hz, N-*i*-C_6H_3), 138.3 (d, $^2J_{PC}$ = 17 Hz, C-*i*-C_6H_5), 129.3 (C-*p*-C_6H_5), 128.3 (C-*m*-C_6H_5), 128.1 (N-*m*-C_6H_3), 126.1 (C-*o*-C_6H_5), 124.8 (N-*o*-C_6H_3), 123.7 (N-*p*-C_6H_3), 27.9 (d, $^1J_{PC}$ = 15 Hz, P-*C*H$(CH_3)_2$), 19.7 (C_6H_3-CH-(*C*$H_3)_2$), 19.0 (P-CH(*C*$H_3)_2$), 18.2 (d, $^2J_{PC}$ = 4 Hz, (P-CH(*C*$H_3)_2$)).

^{31}P{^{1}H} NMR (243 MHz, Chloroform-*d*) δ 87.0.

MS (ASAP$^+$) *m/z*: 518.1 ([MH]$^+$), 489.1 ([M-CO]$^+$), 326.2 ([MH-$Cr(CO)_5$)]$^+$), 208.1 ([M-$Cr(CO)_5(P^iPr_2)$]$^+$).

IR (CH_2Cl_2): ν_{CO} = 2060 cm^{-1}, 1980 cm^{-1}, 1934 cm^{-1}.

6.9.3 Reaction of $Cr(CO)_6$ and $Ph(P^iPr_2)C=N(2,6\text{-}^iPr_2C_6H_3$ (3.9) in diglyme

A flask was charged with $Cr(CO)_6$ (69 mg, 0.31 mmol) and $Ph(P^iPr_2)C=N(2,6\text{-}^iPr_2C_6H_3$ (**3.9**) (99 mg, 0.026 mmol) before diglyme (8 mL) was added. The solution was heated at reflux for 16 hours before being allowed to cool to room temperature. Analysis by $^{31}P\{^1H\}$ NMR spectroscopy showed only free ligand present in solution, suggesting that the high temperature caused decomposition of the metal carbonyl starting material.

6.9.4 Study of iminophosphine ligand hemilability

$Cr(CO)_6$ (21 mg, 0.06 mmol) and $Ph(P^iPr_2)C=N(2,6\text{-}^iPr_2C_6H_3)$ (**3.9**) (30 mg, 0.05 mmol) were placed in a Young's NMR tube before diglyme (0.7 mL) was added along with a C_6D_6 lock-tube. The reaction mixture was heated to 165 °C for 4 hours, before being cooled and analysed by $^{31}P\{^1H\}$ NMR spectroscopy. The NMR spectrum showed a major signal representative of monodentate $Cr(CO)_5(Ph(P^iPr_2)C=N(2,6\text{-}^iPr_2C_6H_3))$ (**4.8**) and a minor signal matching the chemical shift of the free ligand (**3.9**). Subsequently, the reaction was heated back to reflux for a further 4 hours before cooling and analysing by ^{31}P NMR spectroscopy. This second NMR analysis showed no change from the first. The NMR tube was then placed and sealed under vacuum before being heated back to 165 °C causing the solution to turn purple. After 4 hours the reaction was allowed to cool to room temperature and analysed by $^{31}P\{^1H\}$ NMR spectroscopy, which displayed a signal at δ = 63.5 ppm, indicative of bidentate $Cr(CO)_4(Ph(P^iPr_2)C=N(2,6\text{-}^iPr_2C_6H_3))$ (**4.7**). The tube was placed under vacuum a second time and heated to 165 °C for a further 4 hours. After this time $^{31}P\{^1H\}$ NMR spectroscopy demonstrated an increase in the amount of $Cr(CO)_4(Ph(P^iPr_2)C=N(2,6\text{-}^iPr_2C_6H_3))$ (**4.7**) formed, relative to $Cr(CO)_5(Ph(P^iPr_2)C=N(2,6\text{-}^iPr_2C_6H_3))$ (**4.8**).

The atmosphere of the NMR tube was replaced with carbon monoxide (1 atm)and sealed. The reaction was gently heated and a colour change from purple to yellow was observed. $^{31}P\{^1H\}$ NMR spectroscopic analysis showed the signal at δ = 63.5 ppm had disappeared, showing the bidentate $Cr(CO)_4(Ph(P^iPr_2)C=N(2,6\text{-}^iPr_2C_6H_3))$ (**4.7**) had converted back to the monodentate $Cr(CO)_5(Ph(P^iPr_2)C=N(2,6\text{-}^iPr_2C_6H_3))$ (**4.9**) under an atmosphere of CO.

6.10 Attempts to Reduce Iminophosphines to Phosphinoamines

6.10.1 Attempted reduction of iminophosphine Ph(P^iPr_2)C=N(2,6-$^iPr_2C_6H_3$) (3.9) with $LiAlH_4$

A sample of Ph(P^iPr_2)C=N(2,6-$^iPr_2C_6H_3$) (**3.9**) (0.211 g, 0.55 mmol) was placed in a flask and dissolved in diethyl ether (7 mL). The resulting solution was cooled to 0 °C before $LiAlH_4$ (0.66 mL, 0.66 mmol, 1M solution in diethyl ether) was added. The solution was allowed to warm to room temperature and left to stir for an hour before $^{31}P\{^1H\}$ NMR spectroscopic analysis was undertaken, which revealed no reaction had occurred. The reaction was heated to reflux and after 16 hours was cooled before further $^{31}P\{^1H\}$ NMR spectroscopic analysis showed still no reaction had taken place with the phosphine. Solid $LiAlH_4$ (25 mg, 0.66 mmol) was added to the reaction mixture and the resulting mixture was again heated at reflux for 16 hours. The reaction was again allowed to cool and $^{31}P\{^1H\}$ NMR spectroscopic analysis undertaken still showed no sign of reaction. It was concluded that **3.9** cannot be reduced under the conditions used here with $LiAlH_4$.

6.10.2 Attempted reduction of Ph(P^iPr_2)C=N(2,6-$^iPr_2C_6H_3$) (3.9) with H_2 over Pd/C

A flask was charged with Pd/C (17 mg, 5 % wt Pd on C) before a solution of Ph(P^iPr_2)C=N(2,6-$^iPr_2C_6H_3$) (**3.9**) (169 mg, 0.44 mmol) in hexane (10 mL) was added. The reaction was placed under an atmosphere of H_2 (1 atm) and stirred for 16 hours, after which $^{31}P\{^1H\}$ NMR spectroscopic analysis revealed no reaction had taken place. It was concluded that more forcing conditions are required to reduce iminophosphine **3.9**.

6.11 Reactions of PCN Ligands with $AlMe_3$

6.11.1 Reaction of $Ph(P^iPr_2)C=N(2,6\text{-}^iPr_2C_6H_3)$ (3.9) with 1 equivalent of $AlMe_3$

A flask was charged with $Ph(P^iPr_2)C=N(2,6\text{-}^iPr_2C_6H_3)$ (**3.9**) (0.169 g, 0.44 mmol) and toluene was added (5 mL). A solution of $AlMe_3$ was added (0.22 mL, 0.44 mmol, 2M solution in toluene) and the reaction was stirred for an hour, after which analysis by $^{31}P\{^1H\}$ NMR spectroscopic analysis showed the formation of a new phosphorus species (δ = 18.3 ppm). The solvent was removed under vacuum before hot hexane was added and the resulting solution filtered. The solution spontaneously turned cloudy and a yellow oil that is insoluble in hexane precipitated out of solution. The remaining solution was isolated by filtration and $^{31}P\{^1H\}$ NMR spectroscopic analysis showed the presence of the starting material **3.9**. The oily product was found to be insoluble in hexane, therefore was dissolved in DCM (3 mL) and analysed by $^{31}P\{^1H\}$ NMR spectroscopy. NMR spectroscopic analysis showed three new signals (δ = 52.0, 47.4, 42.9 ppm), suggesting the product had decomposed into three new phosphorus-containing species. Ultimately no product could be isolated due to the highly unstable and reactive nature of the products formed.

This reaction was attempted a second time using **3.9** (0.179 g, 0.47 mmol) and $AlMe_3$ (0.23 mL, 0.47 mmol, 2M solution in toluene) in toluene (4 mL). The crude reaction mixture was concentrated by half under vacuum and the solution was stored at – 30 °C for 16 hours, but no product precipitated. After repeating this concentrating and cooling process still no product precipitated. This concentrated solution was layered with pentane and the mixture was stored in the freezer for a week after which an oily residue precipitated out of solution. The oily residue was isolated and dissolved In C_6D_6. Unfortunately the product was not pure enough for NMR spectroscopic analysis to provide conclusive evidence of composition.

6.11.2 Reaction of $Ph(P^iPr_2)C=N(2,6\text{-}^iPr_2C_6H_3)$ (3.9) with 2 equivalents of $AlMe_3$

A sample of $Ph(P^iPr_2)C=N(2,6\text{-}iPr_2C_6H_3)$ (**3.9**) (0.132 g, 0.35 mmol) was placed in a flask and dissolved in toluene (4 mL). A solution of $AlMe_3$ (0.35 mL, 0.69 mmol, 2M solution in toluene) was added and the reaction mixture was stirred overnight. Analysis by $^{31}P\{^1H\}$ NMR spectroscopy showed a new product formed (δ = 15.7 ppm). The solution was concentrated under vacuum and stored at – 30 °C for 16 hours. No precipitate formed and so the solution was further concentrated, and cooled again to – 30 °C for a further 16 hours. Again, no precipitate formed and so the entirety of the solvent was removed under reduced pressure to leave a yellow oil. This crude product was analysed by NMR spectroscopy but both $^{31}P\{^1H\}$ and ^1H NMR spectra showed an impure product that could not be characterised.

6.12 Reaction of PCN Ligands with Wilkinson's Catalyst

6.12.1 Reaction of $Ph(P^iPr_2)C=N(2,6\text{-}Me_2C_6H_3)$ (3.10) with $Rh(PPh_3)_3Cl$

A Young's NMR tube was charged with a sample of Wilkinson's Catalyst, $Rh(PPh_3)_3Cl$ (85 mg, 0.09 mmol) and $Ph(P^iPr_2)C=N(2,6\text{-}Me_2C_6H_3)$, (**3.10**) (30 mg, 0.09 mmol). Subsequently, C_6D_6 (0.7 mL) was added and the reaction mixture was heated to 60 °C. After four hours of heating analysis of the reaction by $^{31}P\{^1H\}$ NMR spectroscopic analysis revealed no reaction had taken place. The sample was left to stand for one month, after which further analysis by $^{31}P\{^1H\}$ NMR spectroscopy demonstrated all of the starting iminophosphine was present in the reaction. Based on this, it was concluded that under these conditions iminophosphine **3.10** does not react with Wilkinson's catalyst.

6.13 Evans' Method NMR Protocol

The magnetic susceptibilities of paramagnetic species in this thesis were measured using the Evans' NMR spectroscopic method.[21,22] A standard solution of the required sample (~20 mg) was prepared in DCM (2 mL). A portion of this solution (0.5 mL) was transferred into an NMR tube fitted with a Young's tap and containing a sealed capillary filled with d_2-DCM. The solvent was removed from the solution in the tube, before the remaining residue was dissolved in d_2-DCM (0.5 mL). The sample was analysed by ^{1}H NMR spectroscopy through comparison of the residual solvent resonance for the bulk solvent, and the standard present in the sealed capillary.

6.14 Ethylene Oligomerisation Catalysis Testing Protocols

Stock solutions of all catalyst precursors were prepared to the desired concentration using the relevant solvent. Stock solutions of catalyst additives were prepared in a similar fashion.

The catalytic tests used a semi-batch process in a 250 mL steel autoclave. Prior to use the autoclave was heated (130 °C) under vacuum for 1 hour, before cooling to reaction temperature and back-filled with ethylene (10 bar) and vented to 0 bar *via* the septa. Solvent (70 mL) was then added via syringe. The autoclave was again pressurised with ethylene (10 bar) and vented. The autoclave was charged with the relevant catalyst precursors, dependent upon the catalyst activation protocol used (Section 6.14.1). Subsequently, the autoclave was pressurised with ethylene and the pressure kept constant throughout the reaction by continuous addition of ethylene, which was monitored through the use of a mass-flow meter. Heating and cooling were applied to maintain a stable reaction temperature. Once ethylene uptake had ceased, or the set reaction time had expired the gas supply was closed and the reactor cooled to 5 °C. A portion of the gas was vented directly to a GC-FID instrument equipped with a gas-sampling loop. The remaining gas was slowly vented. Nonane (1 mL) was added to the reactor contents (as a GC internal standard). The reactor contents were quenched by addition of a mixture of 10% HCl (aq.) and toluene, before a sample of the organic phase was taken for GC-FID analysis. Any solid formed was collected, washed with acetone before being dried overnight and weighed. The solid products were subsequently analysed by DSC analysis.

6.14.1 Catalyst activation protocols

6.14.1.1 Method A – In situ activation

The autoclave was charged with the relevant chromium and ligand starting materials under an atmosphere of ethylene, before stirring for 5 minutes and subsequently adding the activator. The autoclave was then pressurised with ethylene, starting the catalysis.

6.14.1.2 Method B – Pre-activation

The desired ligand and chromium source were combined in a Schlenk flask and stirred for 5 minutes, prior to addition of the aluminium activator. The activated catalyst solution was allowed to stir for a further minute before being transferred to the autoclave *via* syringe. The autoclave was subsequently pressurised with ethylene.

6.14.1.3 Method C – Extended Pre-activation

The desired ligand and chromium source were combined in a Schlenk flask and stirred for 18 hours, prior to addition of the aluminium activator. The activated catalyst solution was

allowed to stir for a further minute before being transferred to the autoclave *via* syringe. The autoclave was subsequently pressurised with ethylene.

6.14.1.4 Method D – In situ (Ar atmosphere)

The autoclave was purged with argon (10 bar (rather than ethylene) before being charged with the relevant chromium and ligand starting materials and stirred for 5 minutes. Subsequently, the catalyst activator was added and the autoclave pressurised with ethylene to initiate the reaction.

6.14.2 Analysis of polyethylene

A range of analytical methods were attempted in order to characterise the polymer formed by the catalysis reactions in this thesis. It was found that the polymer by-products produced were only sparingly soluble in boiling chlorobenzene, limiting the analytical techniques possible.

Gel permeation chromatography (GPC) is widely used to measure the MW and polydispersity index (PDI) of polymers, including polyethylene samples.[23] Unfortunately, GPC relies upon the polymer sample being soluble, and therefore this analytical technique was ruled out. Similar solubility problems were encountered when attempting to undertake NMR spectroscopic analyses of the samples, due to the propensity of the polymers to form highly viscous gels when "dissolved" in boiling chlorobenzene or tetrachloroethane.

6.14.2.1 DSC analysis of polyethylene

In order to overcome the issues brought about by the limited solubility of the polymer samples, solid state techniques were turned to; in particular thermal analysis and differential scanning calorimetry (DSC).[24] The DSC protocol used was based upon methods reported by Cavallo and Basset *et al.*, and was carried out as follows:[25]

- DSC analysis of polyethylene was performed on a TA instruments DSC Q1000. The samples were heated from room temperature to 200 °C with a heating rate of 10 °C/min before cooling the sample to 50 °C at a rate of 10 °C/min. This cycle was repeated, and the data from the second cycle was used to determine the melting point and crystallisation point of the polyethylene in question.

All of the polyethylene samples analysed displayed melting points in the range 122.3-136.8 °C. Based on literature values, these melting points are indicative of high molecular weight polyethylene, but based on melting point alone no definitive characterisation can be made.[26]

As well as the crystallisation and melting temperatures of polyethylene, DSC analysis has been used to estimate the degree of crystallinity of polymer samples ($\%_{cryst}$).[25,26] The

thermogram under the final cooling cycle is representative of the heat of fusion (H_f) of the polymer, which is proportional to the crystallinity of the polymer. When this value is compared with the H_f for a sample of perfectly crystalline polyethylene (measured as 293.0 J/g, H_{std})[27] the degree of crystallinity can be calculated:

$$\left(\frac{\Delta H_f}{\Delta H_{std}}\right) \times 100 = \%_{cryst}$$

Based upon this equation, attempts were made to measure the crystallinity of a selection of the polymer samples produced in this investigation. Unfortunately, the data gathered showed large unexplained variations between samples. It is thought that this variation is due to the large uncertainty when measuring the H_f from the raw thermogram data. The polymer crystallisation curve is generally not a well-defined peak, and human judgement and error plays a significant role in deriving the heat of fusion for each sample. In this study it is concluded that the degree of human error is too great to give valid results, and to demonstrate this one worked example is given below (Figure 6.1).

Run 40:

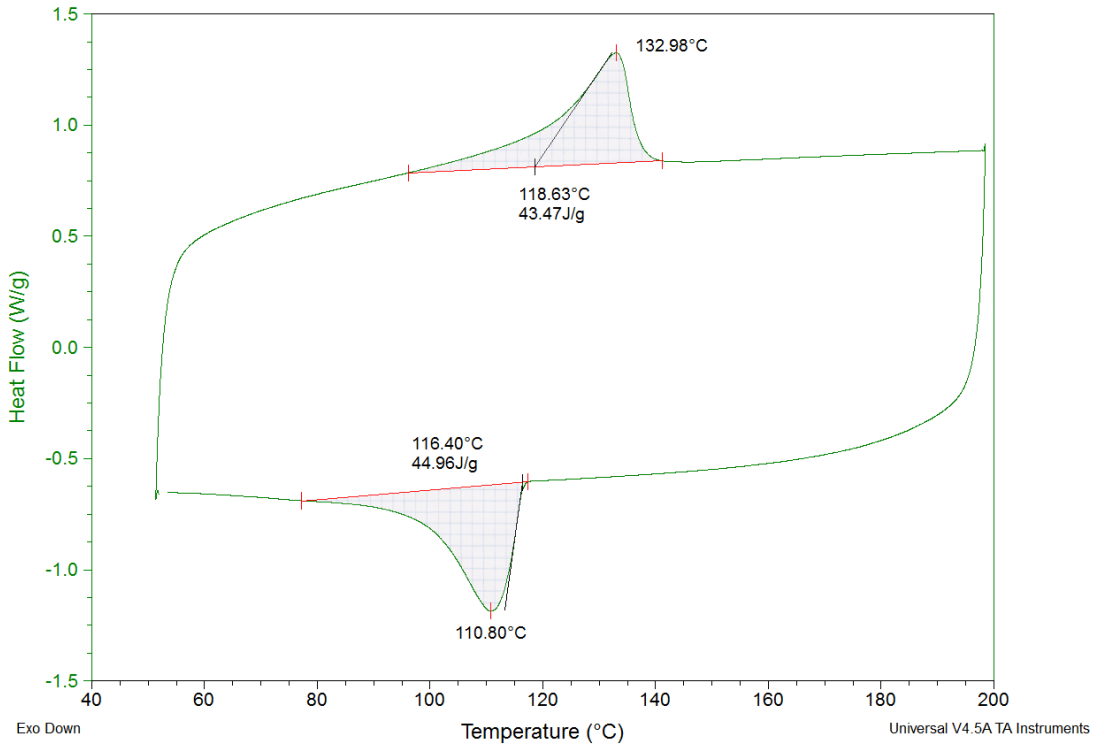

Figure 6.1: Thermogram of polymer sample isolated from ethylene oligomerisation run 40. Catalysis conditions: 0.4 µmol $Cr(2\text{-}EH)_3$, 1 eq. **3.9**, 70 mL MCH solvent, 40 bar C_2H_4, 60 °C, 0.6 ppm O_2.

ΔH_f = 44.96 J/g

$$\left(\frac{44.96}{293.0}\right) \times 100 = 15.5\ \%_{cryst}$$

This value of 15.5 % crystallinity measured for the polymer sample is considerably lower than that of 63.2 % reported by Atiqullah and Bercaw *et al.* for their sample of polyethylene produced by a vanadium-based polymerisation catalyst.[26] The low crystallinity value of the polymer produced in this thesis is suggestive of a branched polymer, but due to the questionable validity of these data no firm conclusions can be drawn.

6.15 References

(1) So, J. H.; Boudjouk, P. *Inorg. Chem.* **1990**, *29*, 1592.
(2) Anderson, C. E.; Apperley, D. C.; Batsanov, A. S.; Dyer, P. W.; Howard, J. A. K. *Dalton Trans.* **2006**, 4134.
(3) Anderson, C. E., PhD Thesis, University of Durham, 2007.
(4) Zhu, K.; Achord, P. D.; Zhang, X.; Krogh-Jespersen, K.; Goldman, A. S. *J. Am. Chem. Soc.* **2004**, *126*, 13044.
(5) Brisdon, A. K.; Herbert, C. J. *Chem. Commun.* **2009**, 6658.
(6) Bowen, L. E.; Charernsuk, M.; Hey, T. W.; McMullin, C. L.; Orpen, A. G.; Wass, D. F. *Dalton Trans.* **2010**, *39*, 560.
(7) Budzelaar, P. H. M.; Orpen, A. G.; van Oort, A. B. *Eur. J. Inorg. Chem.* **1998**, *10*, 1485.
(8) Chen, S.; Zhang, X.; Ma, H.; Lu, Y.; Zhang, Z.; Li, H.; Lu, Z.; Cui, N.; Hu, Y. *J. Organomet. Chem.* **2005**, *690*, 4184.
(9) Gao, G.-L.; Niu, Y.-N.; Yan, Z.-Y.; Wang, H.-L.; Wang, G.-W.; Shaukat, A.; Liang, Y.-M. *J. Org. Chem.* **2010**, *75*, 1305.
(10) Anderson, C. E.; Donde, Y.; Douglas, C. J.; Overman, L. E. *J. Org. Chem.* **2004**, *70*, 648.
(11) Nijhuis, C. a.; Jellema, E.; Sciarone, T. J. J.; Meetsma, A.; Budzelaar, P. H. M.; Hessen, B. *Eur. J. Inorg. Chem.* **2005**, *2005*, 2089.
(12) Rosenberg, M. L.; Langseth, E.; Krivokapic, A.; Gupta, N. S.; Tilset, M. *New J. Chem.* **2011**, *35*, 2306.
(13) Cowley, R. E.; Chiang, K. P.; Holland, P. L.; Adhikari, D.; Zuno-Cruz, F. J.; Cabrera, G. S.; Mindiola, D. J. *Inorganic Syntheses, Vol 35* **2010**, *35*, 13.
(14) Alonso, E.; Ramón, D. J.; Yus, M. *Tetrahedron* **1998**, *54*, 12007.
(15) Bailey, J. A.; Haddow, M. F.; Pringle, P. G. *Chem. Commun.* **2014**, *50*, 1432.
(16) Wolfsberger, W.; Burkart, W.; Bauer, S.; Hampp, A.; Wolf, J.; Werner, H. *Z. Naturforsch. B* **1994**, *49*, 1659.
(17) Lindner, E.; Merkle, R. D. *Z. Naturforsch. B* **1985**, *40*, 1580.
(18) Van Linthoudt, J. P.; Van den Berghe, E. V.; Van der Kelen, G. P. *Spectrochim. Acta A* **1980**, *36*, 17.
(19) Blann, K.; Bollmann, A.; Dixon, J. T.; Hess, F. M.; Killian, E.; Maumela, H.; Morgan, D. H.; Neveling, A.; Otto, S.; Overett, M. J. *Chem. Commun.* **2005**, 620.
(20) Budzelaar, P. H. M.; van Doorn, J. A.; Meijboom, N. *Recl. Trav. Chim. Pays-Bas* **1991**, *110*, 420.
(21) Evans, D. F. *J. Chem. Soc.* **1959**, 2003.
(22) Loliger, J.; Scheffold, R. *J. Chem. Educ.* **1972**, *49*, 646.
(23) Buffet, J.-C.; Turner, Z. R.; Cooper, R. T.; O'Hare, D. *Polymer Chemistry* **2015**, *6*, 2493.
(24) Wunderlich, B. In *Thermal Analysis of Polymeric Materials*; Springer Berlin Heidelberg: 2005, p 279.
(25) Chen, Y.; Credendino, R.; Callens, E.; Atiqullah, M.; Al-Harthi, M. A.; Cavallo, L.; Basset, J.-M. *ACS Catal.* **2013**, 1360.
(26) Atiqullah, M.; Winston, M. S.; Bercaw, J. E.; Hussain, I.; Fazal, A.; Al-Harthi, M. A.; Emwas, A. H. M.; Khan, M. J.; Hossaen, A. *Polymer Degrad. Stab.* **2012**, *97*, 1164.
(27) Wunderlich, B.; Czornyj, G. *Macromolecules* **1977**, *10*, 906.

Appendices

7.1 List of Compounds Synthesised and Associated Numbering Scheme

7.1.1 Chapter 2

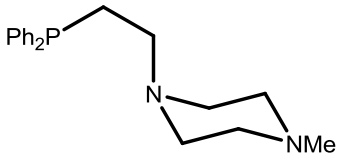

PNN

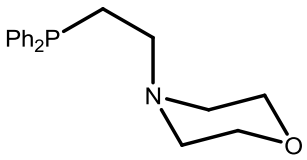

PNO

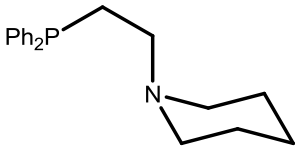

PNC

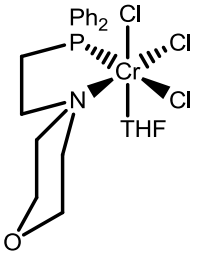

2.1

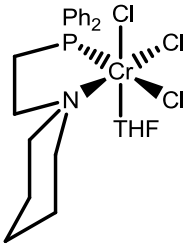

2.2

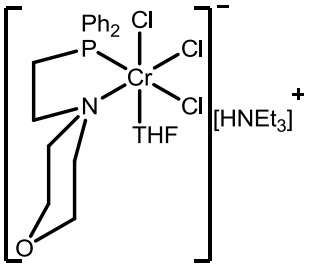

2.3

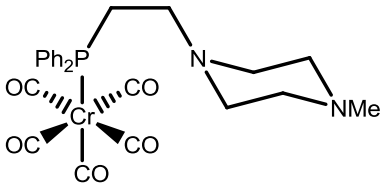

2.4

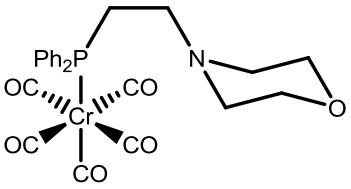

2.5

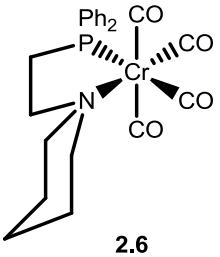

2.6

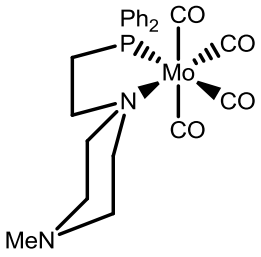

2.7

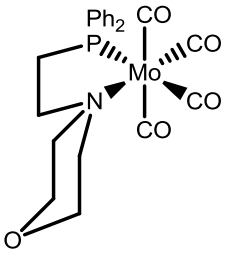

2.8

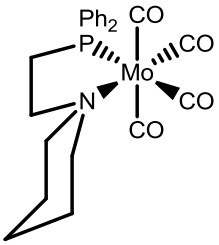

2.9

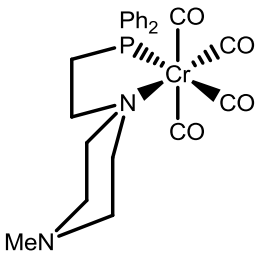

2.10

7.1.2 Chapter 3

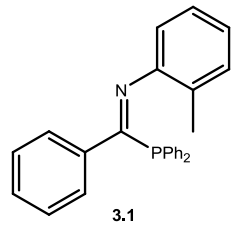

3.1

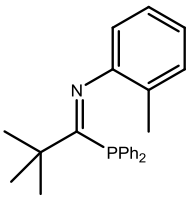

3.2

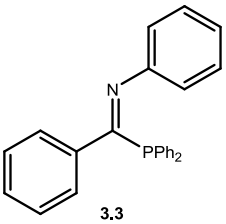

3.3

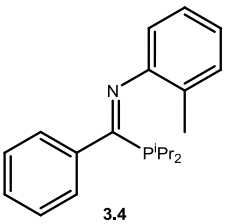

3.4

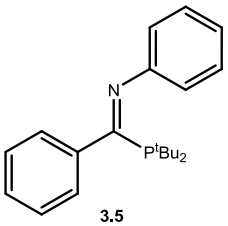

3.5

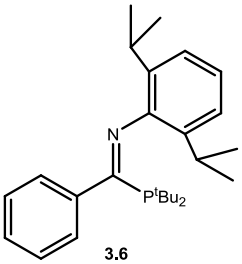

3.6

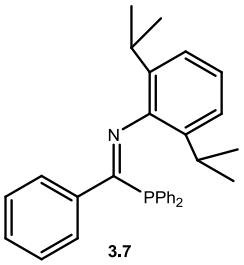

3.7

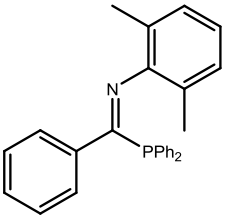

3.8

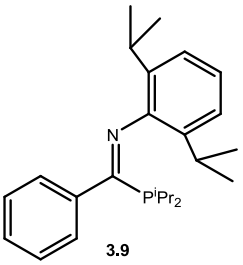

3.9

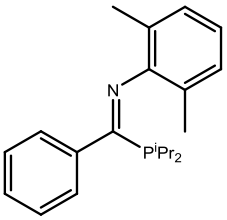

3.10

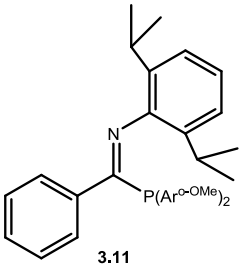

3.11

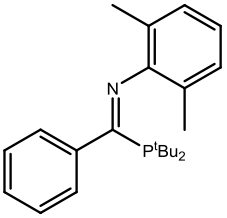

3.12

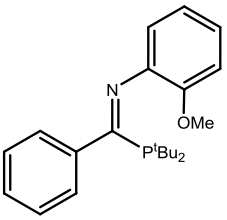

3.13

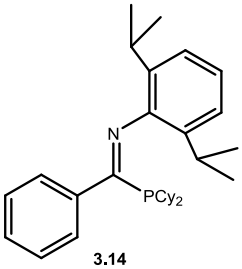

3.14

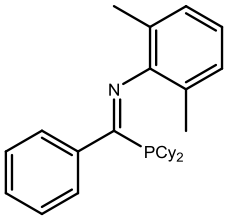

3.15

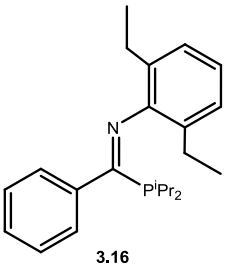

3.16

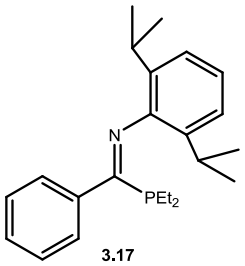

3.17

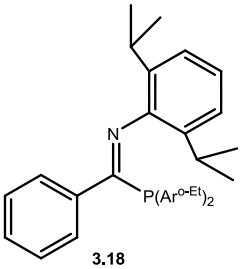

3.18

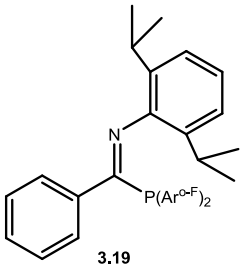

3.19

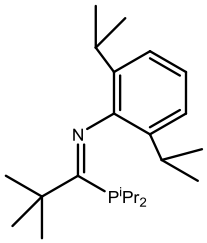

3.20

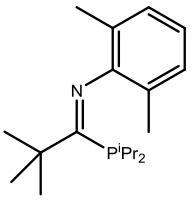

3.21

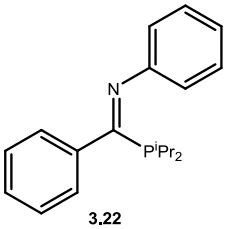

3.22

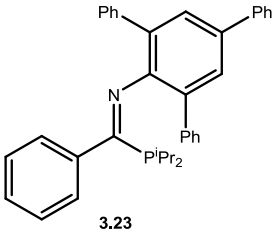

3.23

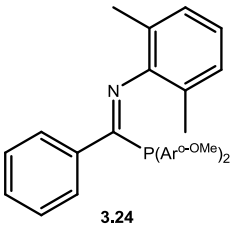

3.24

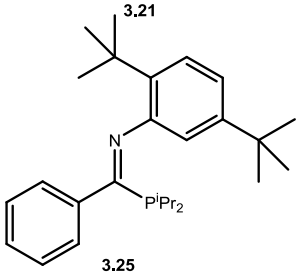

3.25

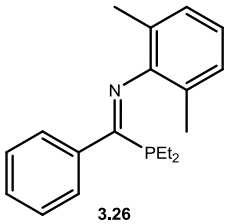

3.26

7.1.3 Chapter 4

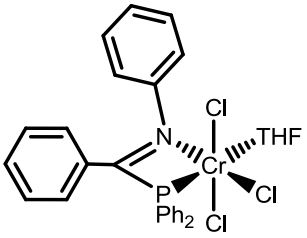

4.1

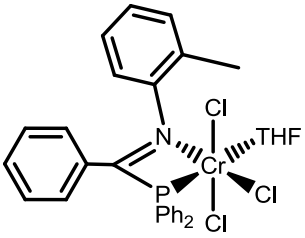

4.2

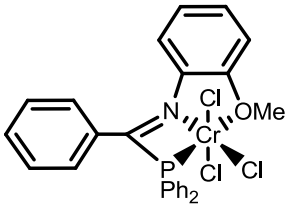

4.3

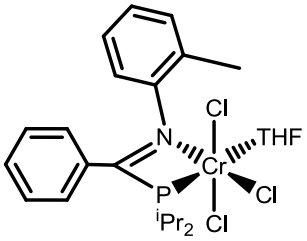

4.4

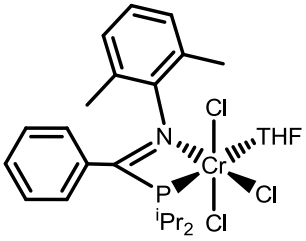

4.5

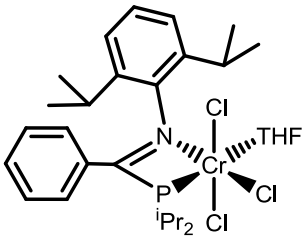

4.6

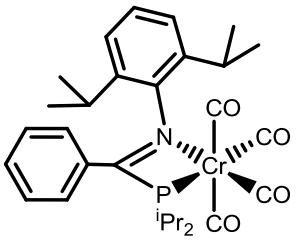

4.7

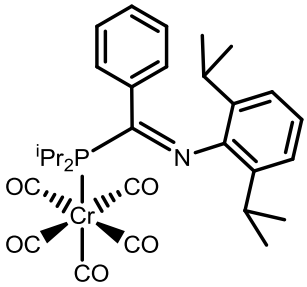

4.8

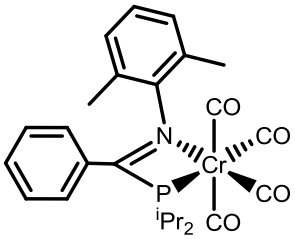

4.9

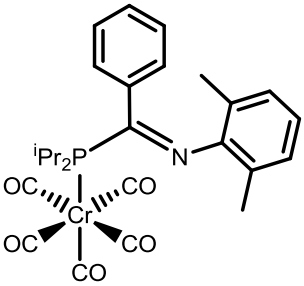

4.10

7.2 Characterisation Data for Chloroimines

7.2.1 Characterisation of Ph(Cl)C=N(2,5-$^{t}Bu_2C_6H_2$)

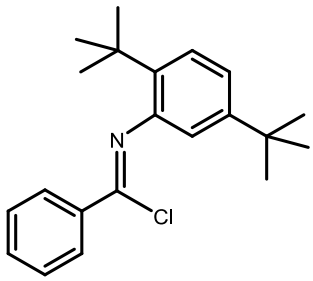

(calc.: $C_{21}H_{26}ClN$ C, 76.92; H, 7.99; N, 4.27. Found: C, 76.75; H, 8.16; N, 4.24).

^{1}H NMR (700 MHz, Chloroform-*d*) δ 8.25 (d, *J* = 8 Hz, 2H, C-*o*-C_6H_5), 7.58 (t, *J* = 8 Hz, 1H, C-*p*-C_6H_5), 7.53 (t, *J* = 8 Hz, 2H, C-*m*-C_6H_5), 7.40 (d, *J* = 8 Hz, 1H, N-3-C_6H_3), 7.21 (d, *J* = 8 Hz, 1H, N-4-C_6H_3), 6.86 (s, 1H, N-6-C_6H_3), 1.40 (s, 9H, 5-((CH_3)$_3$C)C_6H_3), 1.36 (s, 9H, 2-((CH_3)$_3$C)C_6H_3).

^{13}C NMR (176 MHz, Chloroform-*d*) δ 149.3 (N-5-C_6H_3), 145.9 (N-1-C_6H_3), 142.0 (*C*=N), 137.8 (N-2-C_6H_3), 135.8 (C-*i*-C_6H_5), 132.0 (C-*p*-C_6H_5), 129.6 (C-*o*-C_6H_5), 128.7 (C-*m*-C_6H_5), 126.0 (N-3-C_6H_3), 121.9 (N-4-C_6H_3), 118.9 (N-6-C_6H_3), 34.8 (2-((CH$_3$)$_3$*C*)C_6H_3), 34.5 (5-((CH$_3$)$_3$*C*)C_6H_3), 31.4 (2-((*C*H$_3$)$_3$C)C_6H_3), 30.0 (5-((*C*H$_3$)$_3$C)C_6H_3).

MS (ASAP^{+}) *m/z*: 328.2 ([MH]$^{+}$), 293.2 ([M-Cl]$^{+}$).

IR (ATR): $\nu_{C=N}$ = 1663 cm^{-1}.

7.2.2 Characterisation of Ph(Cl)C=N(2,4,6-$Ph_3C_6H_2$)

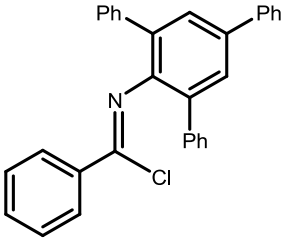

(calc.: $C_{31}H_{22}ClN$ C, 83.86; H, 4.99; N, 3.15. Found: C, 83.71; H, 5.15; N, 3.24).

^{1}H NMR (700 MHz, Chloroform-*d*) δ 7.72 – 7.67 (m, 4H, C_6H_n), 7.64 (s, 2H, C_6H_n), 7.50 – 7.47 (m, 4H, C_6H_n), 7.43 (t, *J* = 8 Hz, 2H, C_6H_n), 7.41 – 7.38 (m, 1H, C_6H_n), 7.35 – 7.32 (m, 1H, C_6H_n), 7.31 – 7.27 (m, 6H, C_6H_n), 7.24 – 7.21 (m, 2H, C_6H_n).*

^{13}C NMR (176 MHz, Chloroform-*d*) δ 144.1 (*C*=N), 143.1 (*i*-C_6H_n), 140.5 (*i*-C_6H_n), 139.9 (*i*-C_6H_n), 138.2 (*i*-C_6H_n), 135.3 (*i*-C_6H_n), 133.4 (C_6H_n), 131.8 (C_6H_n), 129.4 (C_6H_n), 129.2 (C_6H_n), 129.0 (C_6H_n), 128.5 (C_6H_n), 128.3 (C_6H_n), 128.1 (C_6H_n), 127.4 (C_6H_n), 127.2 (C_6H_n), 127.1 (C_6H_n).[1]

MS (ASAP$^+$) *m/z*: 444.2 ([MH]$^+$), 408.162 ([M-Cl]$^+$).

IR (ATR): $\nu_{C=N}$ = 1640 cm^{-1}.

[1] ^{1}H and ^{13}C NMR spectra could not be fully assigned due to complexity of the phenyl regions.

7.3 Experimental Data for Unsuccessfully Characterised Iminophosphines

7.3.1 Preparation of $PhC(PPh_2)=N(o\text{-}MeOC_6H_4)$ (3.27)

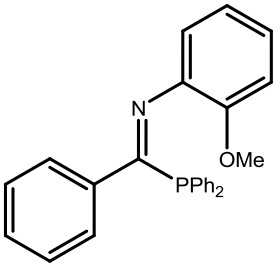

An analogous procedure to that used for the synthesis of compound **3.2** was carried out with *N*-(2-methoxyphenyl)benzimidoyl chloride (9.83 g, 40 mmol) and trimethylsilyl(diphenyl)phosphine (10.33 g, 40 mmol) in toluene (200 mL). The crude product was isolated as a viscous oil that could not be crystallised. The oil was purified by vacuum distillation aided by vigorous heating of the apparatus due to the high boiling point of the product, yielding the product as a viscous yellow oil. Unfortunately, vacuum distillation did not purify the product, hence no successful characterisation of the compound was achieved.

$^{31}P\{^{1}H\}$ NMR (162 MHz, C_6D_6) δ 8.19, -0.93.

7.3.2 Preparation of $^{i}PrC(P^{i}Pr_2)=N(2,6\text{-}((CH_3)_2CH)_2C_6H_3)$

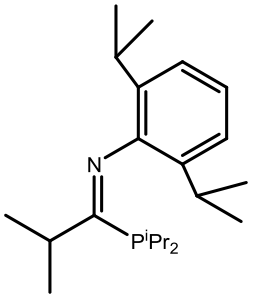

An analogous procedure to that used for the synthesis of **3.7** was carried out using *bis*(*iso*-propyl)-trimethylsilylphosphine (1.335 g, 7.0 mmol) and *N*-(2,6-diisopropylphenyl)isobutyrimidoyl chloride (1.865 g, 7.0 mmol). The reaction solution was heated at reflux for 16 hours after which the solution had turned yellow. The solution was allowed to cool to room temperature before the solvent was removed *in vacuo* to give the crude product as an orange oil. The oil was purified by vacuum distillation (105 - 113 °C, 0.1 mbar) to give the product as an orange oil (1.472 g, 61 % yield). (calc.: $C_{22}H_{38}NP$ C, 76.04; H, 11.02; N, 4.03. Found: C, 76.21; H, 11.16; N, 4.06).

Unfortunately, due to the complex nature of the NMR spectra acquired, no assignment of the resonances could be made and the product was not successfully characterised.

7.4 Catalysis Data Tables

7.4.1 Chapter 2

Run	Pre-catalyst	Time (mins)	TON (mol C_2H_4 /mol Cr)	Activity (mol C_2H_4 /mol Cr/h)	Liquid (wt %)	PE (wt %)	Total (g)	C_4 (wt %)	C_6 (wt %) (1-C_6)[d]	C_8 (wt %) (1-C_8)[d]	C_{10-14} (wt %)	C_{15+} (wt %)
1	$Cr(acac)_3$ + PNN[b]	5	968	11,614	24.5	75.5	0.27	19.9	58.2 (45.4)	21.9 (74.7)	0.0	0.0
2	$Cr(acac)_3$ + PNO[b]	5	1,100	13,196	27.1	72.9	0.31	25.8	51.2 (84.7)	23 (75.2)	0.0	0.0
3	$Cr(acac)_3$ + PNN[c]	5	979	11,747	22.1	77.9	0.28	19.3	53.4 (56.4)	27.3 (72.6)	0.0	0.0
4	$Cr(acac)_3$ + PNO[c]	5	1,105	13,262	24.2	75.8	0.31	22.5	50.8 (60.8)	26.7 (74.4)	0.0	0.0
5	$Cr(acac)_3$[b]	8	6,891	49,514	5.0	95.0	1.93	22.4	42.3 (74.2)	20.9 (59.2)	14.4	0.0
6	$CrCl_3(THF)_3$[b]	6	52,829	539,533	0.5	99.5	14.82	12.0	33.3 (16.8)	11 (41.2)	27.8	15.9
7	$CrCl_3(THF)_3$ + PNN[c]	8	5,114	40,886	1.9	98.2	1.44	17.1	54.9 (0.0)	28 (0.0)	0.0	0.0
8	$CrCl_3(THF)_3$ + PNO[c]	10	9,380	56,303	2.3	97.7	2.63	20.5	56.5 (30.9)	23 (49.8)	0.0	0.0
9	$CrCl_3(THF)_3$ + PNC[b]	10	25,785	154,710	1.0	99.0	7.23	12.3	44.1 (19.8)	16.1 (34.8)	21.1	6.4
10	$CrCl_3(THF)_3$ + PNC[c]	10	29,341	168,669	1.0	99.0	8.23	13.8	25.4 (26.2)	13.9 (32.0)	36.0	10.9

[a] General conditions: 10 µmol Cr, 12 µmol ligand, 500 eq MMAO-3A used in all runs; 40 bar ethene; 60 °C; 60 mL PhCl (solvent). [b] *In situ* catalyst activation (Method A). [c] Catalyst pre-activation (Method B) [d] Selectivity to α-olefin within carbon length fraction

7.4.2 Chapter 5

Run	Pre-catalyst[a]	Cr (µmol)	Ligand (eq.)	Time (min)	Activator {eq.}	Activation Method	O_2 (ppm)	T (°C)	C_2H_4 Pressure (bar)	TON (mol C_2H_4 /mol Cr)	Activity (mol C_2H_4 /mol Cr/h)	Liquid fraction (wt %)	PE fraction (wt %)	Total product mass (g)	C_4 {wt%} (1-C_4)	C_6 {wt%} (1-C_6)	C_8 {wt%} (1-C_8)	C_{10-14} {wt%}	C_{15+} {wt%}	Total-α 1-C_6 + 1-C_8 {wt%}
1	$Cr(acac)_3$	10	0	8	MMAO-3A {500}	A	0.60	60	40	7,000	51,000	9	91	2	17	26 (69)	16 (44)	27	14	25
2	$CrCl_3(THF)_3$	10	0	6	MMAO-3A {500}	A	0.60	60	40	53,000	541,000	1	99	15	10	34 (11)	7 (45)	34	16	7
3	none	5	0	12	MMAO-3A {500}	n/a	0.60	60	40	0	2,000	100	0	0	15	0 (0)	85 (9)	0	0	7
4	**3.9** - No Cr	0	6 µmol	10	MMAO-3A {500}	B	0.60	60	40	0	1,000	100	0	0	12	0 (0)	80 (64)	8	0	51
5	$CrCl_3(THF)_3$ + **3.1**	5	1.2	10	MMAO-3A {500}	A	0.60	60	40	7,000	44,000	14	86	1	7	21 (100)	28 (36)	5	39	32
6	$Cr(acac)_3$ + **3.1**	5	1.2	10	MMAO-3A {500}	A	0.60	60	40	4,000	23,000	50	50	1	4	40 (98)	19 (33)	3	33	46
7	$Cr(acac)_3$ + **3.1**	5	1.2	10	MMAO-3A {500}	B	0.60	60	40	4,000	24,000	42	58	1	4	46 (100)	24 (32)	1	25	53
8	$Cr(acac)_3$ + **3.1**	5	1.2	10	MMAO-3A {500}	C	0.60	60	40	6,000	36,000	27	73	1	4	19 (82)	24 (45)	15	38	26
9	$Cr(acac)_3$ + **3.1**	5	1.2	10	PMAO-IP {500}	B	0.60	60	40	35,000	210,000	2	98	5	6	31 (100)	62 (56)	0	0	66
10	$Cr(acac)_3$ + **3.1**	5	1.2	10	MMAO-3A {500}	B	0.60	20	20	1,000	7,000	26	74	0	7	0 (0)	93 (11)	0	0	11
11	$Cr(acac)_3$ + **3.1**	5	1.2	10	MMAO-3A {500}	B	0.60	100	60	20,000	117,000	6	94	3	11	37 (100)	51 (38)	0	0	57
12	$Cr(acac)_3$ + **3.2**	5	1.2	10	MMAO-3A {500}	B	0.60	60	40	5,000	28,000	42	58	1	4	40 (92)	27 (70)	14	15	56
13	$Cr(acac)_3$ + **3.3**	5	1.2	10	MMAO-3A {500}	B	0.60	60	40	7,000	40,000	32	68	1	7	20 (81)	19 (47)	17	38	25
14	$Cr(acac)_3$ + **3.1**	5	1.2	10	TEA/Borate {100/1.2}	B	0.60	60	40	6,000	38,000	26	74	1	2	17 (100)	21 (45)	9	52	26
15	$CrCl_3$(THF)(**3.1**)	5	n/a	10	MMAO-3A {500}	A	0.60	60	40	13,000	76,000	14	86	2	3	13 (100)	5 (60)	11	68	16
16	$CrCl_3$(THF)(**3.1**)	5	n/a	10	MMAO-3A {500}	B	0.60	60	40	6,000	36,000	31	69	1	3	16 (100)	5 (59)	11	65	19
17	$CrCl_3$(THF)(**3.1**)	5	n/a	10	MMAO-3A {500}	C	0.60	60	40	7,000	42,000	20	80	1	3	16 (100)	7 (56)	10	64	19
18	$CrCl_3$(THF)(**3.1**)	5	n/a	10	MMAO-3A {500}	D	0.60	60	40	9,000	53,000	8	92	1	7	8 (100)	16 (39)	35	34	14
19	$CrCl_3$(THF)(**3.4**)	5	n/a	10	MMAO-3A {500}	B	0.60	60	40	18,000	107,000	11	89	3	2	9 (59)	47 (92)	13	29	49
20	$CrCl_3$(THF)(**3.3**)	5	n/a	10	MMAO-3A {500}	B	0.60	60	40	5,000	27,000	26	74	1	6	11 (100)	8 (50)	14	61	15
21	$CrCl_3$(**3.27**)	5	n/a	10	MMAO-3A {500}	B	0.60	60	40	14,000	85,000	3	97	2	13	18 (60)	59 (21)	5	5	23
22	$CrCl_3$(THF)(**3.4**)	5	n/a	10	PMAO-IP {500}	B	0.60	60	40	23,000	137,000	2	98	3	0	5 (100)	66 (34)	24	5	27
23	$CrCl_3$(THF)(**3.4**)	5	n/a	10	TEA/Borate {100/1.2}	B	0.60	60	40	5,000	32,000	35	65	1	1	7 (26)	36 (39)	22	34	16
24	$CrCl_3$(THF)(**3.4**)	5	n/a	10	TEA/[Oct4N][Cl] {50/5}	B	0.60	60	40	1,000	5,000	87	13	0	12	13 (0)	61 (7)	2	12	4
25	$CrCl_3$(THF)(**3.4**) + H_2	5	n/a	10	MMAO-3A {500}	B	0.60	60	40	3,000	19,000	45	55	0	2	8 (58)	46 (68)	18	26	36
26	$CrCl_3$(THF)(**3.4**) + H_2 + DEZ	5	n/a	10	MMAO-3A {500}	B	0.60	60	40	4,000	24,000	50	50	1	2	6 (42)	25 (52)	38	29	15
27	$CrCl_3$(THF)(**3.4**)	5	n/a	10	MMAO-3A {500}	B	0.60	40	30	12,000	69,000	13	87	2	3	13 (43)	70 (79)	8	8	61
28	$CrCl_3$(THF)(**3.4**)	5	n/a	10	MMAO-3A {500}	B	0.60	80	50	22,000	133,000	7	93	3	3	7 (100)	56 (81)	0	34	53
29	$CrCl_3$(THF)(**3.4**)	5	n/a	10	MMAO-3A {500}	B	0.60	100	60	28,000	167,000	3	97	4	10	12 (100)	39 (75)	0	39	41
30	$Cr(acac)_3$ + **3.7**	5	1.2	10	MMAO-3A {500}	B	0.60	60	40	12,000	69,000	17	83	2	3	19 (81)	71 (88)	2	6	78
31	$Cr(acac)_3$ + **3.9**	5	1.2	10	MMAO-3A {500}	B	0.60	60	40	39,000	234,000	70	30	5	0	74 (99)	25 (98)	0	0	98
32	$Cr(acac)_3$ + **3.6**	5	1.2	10	MMAO-3A {500}	B	0.60	60	40	42,000	254,000	86	14	6	0	97 (100)	0 (91)	1	2	97
33	$Cr(acac)_3$ + **3.11**	5	1.2	10	MMAO-3A {500}	B	0.60	60	40	23,000	140,000	94	6	3	0	55 (99)	44 (98)	1	0	97
34	$Cr(acac)_3$ + **3.10**	5	1.2	10	MMAO-3A {500}	B	0.60	60	40	17,000	104,000	66	34	2	0	25 (97)	70 (98)	1	4	93
35	$Cr(acac)_3$ + **3.6**	5	2.4	10	MMAO-3A {500}	B	0.60	60	40	17,000	103,000	54	46	2	0	95 (100)	1 (85)	1	4	95
36	$Cr(acac)_3$ + **3.6**	5	1	10	MMAO-3A {500}	B	0.60	60	40	70,000	422,000	92	8	10	0	98 (100)	0 (94)	1	1	98
37	$Cr(2\text{-}EH)_3$ + **3.9**[c]	1.25	1	86	MMAO-3A {500}	B	0.48	60	40	5,061,000	3,548,000	96	4	177	0	83 (100)	14 (100)	3	0	96
38	$Cr(2\text{-}EH)_3$ + **3.11**	5	1.2	10	MMAO-3A {500}	B	0.60	60	40	12,000	73,000	67	33	2	1	52 (99)	46 (100)	1	1	96
39	$Cr(2\text{-}EH)_3$ + **3.11**[b]	5	1.2	10	MMAO-3A {500}	B	0.60	60	40	4,000	25,000	90	10	1	1	46 (98)	50 (99)	3	1	94
40	$Cr(2\text{-}EH)_3$ + **3.9**[b]	0.4	1	30	MMAO-3A {500}	B	0.60	60	40	1,257,000	2,514,000	95	5	14	0	86 (100)	13 (99)	2	0	98
41	$Cr(acac)_3$ + **3.6**	5	0.8	10	MMAO-3A {500}	B	0.60	60	40	47,000	284,000	87	13	7	0	96 (100)	1 (91)	1	2	97
42	$Cr(acac)_3$ + **3.6**	5	0.4	10	MMAO-3A {500}	B	0.60	60	40	23,000	135,000	79	21	3	0	95 (100)	3 (90)	1	1	97
43	$Cr(2\text{-}EH)_3$ + **3.9**[b]	0.4	1	30	MMAO-3A {500}	B	0.60	70	45	2,116,000	4,233,000	97	3	24	0	88 (100)	9 (100)	2	0	97
44	$Cr(2\text{-}EH)_3$ + **3.9**[b]	0.4	1	30	MMAO-3A {500}	B	0.60	50	36	297,000	594,000	99	1	3	0	81 (100)	18 (99)	0	0	99
45	$Cr(2\text{-}EH)_3$ + **3.9**[c]	1.25	1	228	MMAO-3A {500}	B	0.03	60	40	4,274,000	1,124,000	78	22	150	0	80 (100)	17 (100)	2	0	97
46	$Cr(2\text{-}EH)_3$ + **3.9**[c]	1.25	1	162	MMAO-3A {500}	B	0.19	59	40	4,039,000	1,493,000	90	10	142	0	78 (99)	20 (100)	2	0	97
47	$Cr(2\text{-}EH)_3$ + **3.9**[c]	1.25	1	99	MMAO-3A {500}	B	0.38	60	40	4,657,000	2,829,000	95	5	163	0	82 (100)	15 (100)	3	0	97
48	$Cr(2\text{-}EH)_3$ + **3.9**[c]	1.25	1	84	MMAO-3A {500}	B	0.75	60	40	5,120,000	3,674,000	97	3	180	0	83 (100)	14 (100)	3	0	96
49	$Cr(2\text{-}EH)_3$ + **3.9**[c]	1.25	1	99	MMAO-3A {500}	B	0.93	60	40	5,228,000	3,155,000	96	4	183	0	83 (100)	14 (100)	3	0	96
50	$Cr(2\text{-}EH)_3$ + **3.9**[c]	1.25	1	123	MMAO-3A {500}	B	1.38	60	40	4,673,000	2,271,000	94	6	164	0	83 (100)	14 (100)	3	0	96

Run	Pre-catalyst[a]	Cr (µmol)	Ligand (eq.)	Time (min)	Activator {eq.}	Activation Method	O_2 (ppm)	T (°C)	C_2H_4 Pressure (bar)	TON (mol C_2H_4 /mol Cr)	Activity (mol C_2H_4 /mol Cr/h)	Liquid fraction (wt %)	PE fraction (wt %)	Total product mass (g)	C_4 {wt%} (1-C_4)	C_6 {wt%} (1-C_6)	C_8 {wt%} (1-C_8)	C_{10-14} {wt%}	C_{15+} {wt%}	Total-α 1-C_6 + 1-C_8 {wt%}
51	Cr(2-EH)$_3$ + **3.9**[b]	0.4	1	30	MMAO-3A {500}	B	0.60	80	49	2,185,000	4,370,000	95	5	25	0	91 (100)	6 (100)	3	0	97
52	Cr(2-EH)$_3$ + **3.9**[b]	0.4	1	30	MMAO-3A {500}	B	0.60	90	55	480,000	960,000	90	10	5	0	94 (100)	5 (99)	1	0	99
53	Cr(2-EH)$_3$ + **3.9**[b]	0.4	1	30	MMAO-3A {500}	B	0.60	70	58	2,316,000	4,633,000	93	7	26	0	86 (100)	12 (100)	2	0	98
54	Cr(2-EH)$_3$ + **3.9**[b]	0.4	1	30	MMAO-3A {500}	B	0.60	70	54	1,759,000	3,518,000	92	8	20	0	87 (100)	11 (100)	1	0	98
55	Cr(2-EH)$_3$ + **3.9**[b]	0.4	1	30	MMAO-3A {500}	B	0.60	70	40	2,039,000	4,078,000	92	8	23	0	89 (100)	8 (100)	3	0	97
56	Cr(2-EH)$_3$ + **3.9**[b]	0.4	1	30	MMAO-3A {500}	B	0.60	70	35	2,199,000	4,399,000	98	2	25	0	89 (100)	8 (100)	3	0	96
57	Cr(2-EH)$_3$ + **3.9**[b]	0.4	1	30	MMAO-3A {500}	B	0.60	70	48	2,494,000	4,990,000	98	2	28	0	88 (100)	9 (100)	2	0	97
58	Cr(2-EH)$_3$ + **3.9**[b]	0.4	1	30	MMAO-3A {500}	B	0.60	60	40	1,503,000	3,005,000	98	2	17	0	86 (100)	13 (100)	1	0	98
59	Cr(2-EH)$_3$ + **3.9**	1.25	1	88	MMAO-3A {500}	B	0.60	60	40	5,326,000	3,638,000	96	4	187	0	82 (100)	15 (100)	3	0	97
60	Cr(2-EH)$_3$ + **3.9** + 0.5 bar H_2[c]	1.25	1	81	MMAO-3A {500}	B	0.66	61	40	5,025,000	3,719,000	95	5	176	0	82 (100)	15 (100)	3	0	97
61	Cr(2-EH)$_3$ + **3.9** + 2 bar H_2[c]	1.25	1	90	MMAO-3A {500}	B	0.66	60	40	4,980,000	3,306,000	94	6	175	0	83 (100)	14 (100)	3	0	96
62	Cr(2-EH)$_3$ + **3.9** + 100 DEZ[c]	1.25	1	69	MMAO-3A {500}	B	0.66	60	40	5,350,000	4,678,000	98	2	188	0	83 (100)	13 (100)	3	0	96
63	Cr(2-EH)$_3$ + **3.9** + 200 DEZ[c]	1.25	1	65	MMAO-3A {500}	B	0.67	60	40	5,551,000	5,099,000	98	2	195	0	84 (100)	13 (100)	3	0	96
64	Cr(2-EH)$_3$ + **3.9** + 400 DEZ[c]	1.25	1	72	MMAO-3A {500}	B	0.61	60	40	5,417,000	4,544,000	98	2	190	0	84 (100)	13 (100)	3	0	96
65	Cr(2-EH)$_3$ + **3.11** + 100 DEZ[c]	1.25	1	168	MMAO-3A {500}	B	0.62	60	41	354,000	126,000	40	60	12	0	57 (98)	40 (99)	1	1	96
66	Cr(2-EH)$_3$ + **3.9** + 100 DEZ[c]	1.25	1	54	MMAO-3A {500}	B	0.63	61	47	5,231,000	5,848,000	98	2	183	0	83 (100)	14 (100)	3	0	97
67	Cr(2-EH)$_3$ + **3.10** + 100 DEZ[c]	1.25	1	240	MMAO-3A {500}	B	0.89	60	47	5,424,000	1,355,000	89	11	190	0	38 (98)	59 (100)	3	0	96
68	Cr(acac)$_3$ + **3.14**	5	1.2	10	MMAO-3A {500}	B	0.60	60	40	58,000	348,000	88	12	8	0	78 (100)	20 (100)	1	1	98
69	Cr(acac)$_3$ + **3.16**	5	1.2	10	MMAO-3A {500}	B	0.60	60	40	27,000	159,000	74	26	4	0	34 (98)	62 (100)	0	3	96
70	Cr(acac)$_3$ + **3.17**	5	1.2	10	MMAO-3A {500}	B	0.60	60	40	24,000	142,000	46	54	3	1	30 (95)	60 (99)	1	9	87
71	Cr(acac)$_3$ + **3.20**	5	1.2	10	MMAO-3A {500}	B	0.60	60	40	7,000	41,000	31	69	1	2	79 (100)	5 (100)	1	13	84
72	Cr(acac)$_3$ + **3.21**	5	1.2	10	MMAO-3A {500}	B	0.60	60	40	33,000	198,000	66	34	5	0	48 (99)	49 (100)	1	2	96
73	Cr(acac)$_3$ + **3.19**	5	1.2	10	MMAO-3A {500}	B	0.60	60	40	14,000	85,000	10	90	2	3	17 (100)	55 (100)	0	26	71
74	Cr(acac)$_3$ + **3.18**	5	1.2	10	MMAO-3A {500}	B	0.60	60	40	21,000	125,000	23	77	3	1	56 (93)	40 (100)	0	3	92
75	Cr(2-EH)$_3$ + **3.14** + 100 DEZ[c]	1.25	1	56	MMAO-3A {500}	B	0.66	61	47	4,502,000	4,863,000	97	3	158	0	86 (100)	12 (100)	2	0	98
76	Cr(2-EH)$_3$ + **3.9** + 100 DEZ[c]	1.25	1	12	MMAO-3A {500}	B	0.75	64	41	2,683,000	13,052,000	99	1	94	0	85 (100)	13 (100)	2	0	97
77	Cr(2-EH)$_3$ + **3.16** + 100 DEZ[c]	1.25	1	122	MMAO-3A {500}	B	0.65	60	48	3,110,000	1,531,000	93	7	109	0	52 (99)	46 (100)	2	0	97
78	Cr(acac)$_3$ + **3.22**	5	1.2	10	MMAO-3A {500}	B	0.60	60	40	16,000	96,000	16	84	2	2	6 (100)	36 (100)	2	54	42

[a] 70 mL PhCl (solvent), 250 mL autoclave, unless otherwise stated. [b] 70 mL MCH (solvent), 250 mL autoclave. [c] 210 mL MCH (solvent), 1.2 L autoclave.

7.5 Crystallographic Data

Single crystal X-ray diffraction experiments were carried out using either a Bruker SMART 6000 CCD or a Siemens SMART 1000 CCD detector. A Mo-K_α radiation source was used (0.71073 Å) and all samples were cooled to 120 K for data collection using a Cryostream open-flow N_2 cryostat. Olex2 was used to process all data, with structures solved using SHELXS with Direct Methods and refined using SHELXL by Least Squares minimisation.[1,2] Non-hydrogen atoms were refined with anisotropic displacement parameters, with H atoms "riding" in idealised positions. All data (.cif) files are included on the CD accompanying this thesis.

[1] Dolomanov, O. V.; Bourhis, L. J.; Gildea, R. J.; Howard, J. A. K.; Puschmann, H. *J. Appl.Cryst.* **2009**, *42*, 339.

[2] Sheldrick, G. *Acta Cryst. A,* **2008**, *64*, 112.

$[CrCl_4(PNO)][HNEt_3]$ (2.3)	
Empirical formula	$C_{24}H_{38}Cl_4CrN_2OP$
Formula weight	595.33
Temperature/K	120
Crystal system	monoclinic
Space group	$P2_1/c$
a/Å	18.1351(10)
b/Å	10.4515(5)
c/Å	14.6903(7)
α/°	90
β/°	97.64(2)
γ/°	90
Volume/Å^3	2759.7(2)
Z	4
ρ_{calc}mg/mm^3	1.433
m/mm^{-1}	0.88
F(000)	1244
Crystal size/mm^3	0.19 × 0.06 × 0.01
2Θ range for data collection	2.26 to 50°
Index ranges	-21 ≤ h ≤ 21, -12 ≤ k ≤ 12, -17 ≤ l ≤ 17
Reflections collected	21982
Independent reflections	4867 [R(int) = 0.1078]
Data/restraints/ parameters	4867/0/304
Goodness-of-fit on F^2	0.81
Final R indexes [I>=2σ (I)]	R_1 = 0.0396, wR_2 = 0.0558
Final R indexes [all data]	R_1 = 0.1012, wR_2 = 0.0657
Largest diff. peak/hole / e Å^{-3}	0.36/-0.42

$Cr(CO)_5(PNN)$ (2.4)	
Empirical formula	$C_{24}H_{25}CrN_2O_5P$
Formula weight	504.43
Temperature/K	120
Crystal system	monoclinic
Space group	$P2_1/c$
a/Å	9.2063(13)
b/Å	16.898(2)
c/Å	16.031(2)
α/°	90
β/°	102.627(5)
γ/°	90
Volume/Å^3	2433.6(6)
Z	4
ρ_{calc}mg/mm^3	1.377
m/mm^{-1}	0.573
F(000)	1048
Crystal size/mm^3	0.6 × 0.45 × 0.35
2Θ range for data collection	3.54 to 59.96°
Index ranges	-12 ≤ h ≤ 12, -22 ≤ k ≤ 23, -22 ≤ l ≤ 22
Reflections collected	34017
Independent reflections	6931 [R(int) = 0.0194]
Data/restraints/ parameters	6931/1/291
Goodness-of-fit on F^2	1.043
Final R indexes [I>=2σ (I)]	R_1 = 0.0315, wR_2 = 0.0826
Final R indexes [all data]	R_1 = 0.0366, wR_2 = 0.0868
Largest diff. peak/hole / e Å^{-3}	0.52/-0.38

$Cr(CO)_4$(PNC) (2.6)	
Empirical formula	$C_{23}H_{24}CrNO_4P$
Formula weight	461.40
Temperature/K	120
Crystal system	monoclinic
Space group	$P2_1/c$
a/Å	10.7541(8)
b/Å	11.3845(7)
c/Å	18.5397(13)
α/°	90.00
β/°	99.017(8)
γ/°	90.00
Volume/Å^3	2241.8(3)
Z	4
ρ_{calc}mg/mm^3	1.367
m/mm^{-1}	0.610
F(000)	960.0
Crystal size/mm^3	0.4 × 0.31 × 0.25
2Θ range for data collection	3.84 to 69.98°
Index ranges	-17 ≤ h ≤ 17, -18 ≤ k ≤ 17, -29 ≤ l ≤ 28
Reflections collected	52009
Independent reflections	9571 [R(int) = 0.0236]
Data/restraints/ parameters	9571/0/271
Goodness-of-fit on F^2	1.040
Final R indexes [I>=2σ (I)]	R_1 = 0.0305, wR_2 = 0.0836
Final R indexes [all data]	R_1 = 0.0368, wR_2 = 0.0886
Largest diff. peak/hole / e Å^{-3}	0.59/-0.41

$Mo(CO)_4$(PNN) (2.7)	
Empirical formula	$C_{23}H_{25}N_2O_4PMo$
Formula weight	520.36
Temperature/K	120
Crystal system	monoclinic
Space group	$P2_1/c$
a/Å	11.5140(6)
b/Å	12.6476(6)
c/Å	15.5392(7)
α/°	90
β/°	93.208(7)
γ/°	90
Volume/Å^3	2259.34(19)
Z	4
ρ_{calc}mg/mm^3	1.53
m/mm^{-1}	0.683
F(000)	1064
Crystal size/mm^3	0.46 × 0.46 × 0.16
2Θ range for data collection	3.54 to 60°
Index ranges	-16 ≤ h ≤ 16, -17 ≤ k ≤ 17, -21 ≤ l ≤ 21
Reflections collected	41290
Independent reflections	6573 [R(int) = 0.0400]
Data/restraints/ parameters	6573/0/281
Goodness-of-fit on F^2	1.109
Final R indexes [I>=2σ (I)]	R_1 = 0.0401, wR_2 = 0.0935
Final R indexes [all data]	R_1 = 0.0471, wR_2 = 0.0979
Largest diff. peak/hole / e Å^{-3}	1.89/-0.60

$Mo(CO)_4$(PNO) (2.8)	
Empirical formula	$C_{22}H_{22}NO_5PMo$
Formula weight	507.32
Temperature/K	120
Crystal system	monoclinic
Space group	$P2_1/n$
a/Å	12.2238(7)
b/Å	12.7463(7)
c/Å	14.8458(8)
α/°	90
β/°	110.311(7)
γ/°	90
Volume/$Å^3$	2169.3(2)
Z	4
$\rho_{calc}mg/mm^3$	1.553
m/mm^{-1}	0.712
F(000)	1032
Crystal size/mm^3	0.38 × 0.28 × 0.15
2Θ range for data collection	3.74 to 60°
Index ranges	-17 ≤ h ≤ 17, -17 ≤ k ≤ 17, -20 ≤ l ≤ 20
Reflections collected	39889
Independent reflections	6321 [R(int) = 0.0399]
Data/restraints/ parameters	6321/0/328
Goodness-of-fit on F^2	1.066
Final R indexes [I>=2σ (I)]	R_1 = 0.0314, wR_2 = 0.0792
Final R indexes [all data]	R_1 = 0.0371, wR_2 = 0.0824
Largest diff. peak/hole / e $Å^{-3}$	1.48/-0.53

$Mo(CO)_4$(PNC) (2.9)	
Empirical formula	$C_{30}H_{32}MoNO_4P$
Formula weight	597.48
Temperature/K	120
Crystal system	monoclinic
Space group	$P2_1/n$
a/Å	13.3585(19)
b/Å	12.2799(16)
c/Å	17.261(2)
α/°	90.00
β/°	101.054(14)
γ/°	90.00
Volume/$Å^3$	2779.0(7)
Z	4
$\rho_{calc}g/cm^3$	1.428
μ/mm^{-1}	0.565
F(000)	1232.0
Crystal size/mm^3	0.2863 × 0.1954 × 0.1306
2Θ range for data collection/°	5.42 to 64.52
Index ranges	-18 ≤ h ≤ 19, -18 ≤ k ≤ 17, -25 ≤ l ≤ 25
Reflections collected	32283
Independent reflections	9028 [R_{int} = 0.0346, R_{sigma} = 0.0335]
Data/restraints/ parameters	9028/0/335
Goodness-of-fit on F^2	1.046
Final R indexes [I>=2σ (I)]	R_1 = 0.0279, wR_2 = 0.0609
Final R indexes [all data]	R_1 = 0.0342, wR_2 = 0.0640
Largest diff. peak/hole / e $Å^{-3}$	0.49/-0.63

$[Cr(CO)_4(PNN)]$ (2.10)	
Empirical formula	$C_{23}H_{25}CrN_2O_4P$
Formula weight	476.42
Temperature/K	120
Crystal system	monoclinic
Space group	$P2_1/c$
a/Å	11.4840(2)
b/Å	12.6038(3)
c/Å	15.3178(3)
α/°	90.00
β/°	92.5760(10)
γ/°	90.00
Volume/Å^3	2214.89(8)
Z	4
ρ_{calc}g/cm^3	1.429
μ/mm^{-1}	0.621
F(000)	992.0
Crystal size/mm^3	0.45 × 0.4 × 0.03
2Θ range for data collection/°	3.56 to 69.88
Index ranges	-18 ≤ h ≤ 18, -19 ≤ k ≤ 19, -24 ≤ l ≤ 24
Reflections collected	37987
Independent reflections	9336 [R_{int} = 0.0627, R_{sigma} = 0.0472]
Data/restraints/ parameters	9336/0/281
Goodness-of-fit on F^2	1.022
Final R indexes [I>=2σ (I)]	R_1 = 0.0401, wR_2 = 0.1066
Final R indexes [all data]	R_1 = 0.0579, wR_2 = 0.1149
Largest diff. peak/hole / e Å^{-3}	1.06/-0.97

$^tBu(OPPh_2)C=N(2\text{-}MeC_6H_4)$ (3.2-oxide)	
Empirical formula	$C_{24}H_{26}NO_{0.9}P$
Formula weight	373.83
Temperature/K	156
Crystal system	monoclinic
Space group	$P2_1/n$
a/Å	7.5244(6)
b/Å	16.5929(16)
c/Å	16.5331(17)
α/°	90
β/°	97.908(8)
γ/°	90
Volume/Å^3	2044.6(3)
Z	4
ρ_{calc}g/cm^3	1.214
μ/mm^{-1}	0.147
F(000)	797.0
Crystal size/mm^3	0.5 × 0.23 × 0.12
2Θ range for data collection/°	3.494 to 60.002
Index ranges	-10 ≤ h ≤ 10, -23 ≤ k ≤ 23, -23 ≤ l ≤ 23
Reflections collected	27872
Independent reflections	5972 [R_{int} = 0.0357, R_{sigma} = 0.0281]
Data/restraints/ parameters	5972/0/252
Goodness-of-fit on F^2	1.009
Final R indexes [I>=2σ (I)]	R_1 = 0.0391, wR_2 = 0.0985
Final R indexes [all data]	R_1 = 0.0538, wR_2 = 0.1077
Largest diff. peak/hole / e Å^{-3}	0.45/-0.33

$Ph(P^iPr_2)C=N(2\text{-}MeC_6H_4)$ (3.4)	
Empirical formula	$C_{20}H_{26}NP$
Formula weight	311.39
Temperature/K	120
Crystal system	monoclinic
Space group	C2/c
a/Å	11.8903(6)
b/Å	11.5015(4)
c/Å	27.0719(12)
α/°	90
β/°	101.613(11)
γ/°	90
Volume/Å^3	3626.5(3)
Z	8
ρ_{calc}mg/mm^3	1.141
m/mm^{-1}	0.149
F(000)	1344.0
Crystal size/mm^3	0.2 × 0.1 × 0.05
2Θ range for data collection	3.072 to 59.99°
Index ranges	-16 ≤ h ≤ 16, -16 ≤ k ≤ 16, -38 ≤ l ≤ 38
Reflections collected	24930
Independent reflections	5305 [R(int) = 0.0568]
Data/restraints/ parameters	5305/0/209
Goodness-of-fit on F^2	1.007
Final R indexes [I>=2σ (I)]	R_1 = 0.0401, wR_2 = 0.0986
Final R indexes [all data]	R_1 = 0.0608, wR_2 = 0.1059
Largest diff. peak/hole / e Å^{-3}	0.41/-0.20

$Ph(P(2\text{-}MeOC_6H_4)_2)C=N(2,6\text{-}Me_2C_6H_4)$ (3.24)	
Empirical formula	$C_{29}H_{28}NO_2P$
Formula weight	453.49
Temperature/K	120
Crystal system	triclinic
Space group	P-1
a/Å	8.6534(8)
b/Å	9.6560(11)
c/Å	15.6276(15)
α/°	87.000(4)
β/°	78.346(4)
γ/°	68.938(3)
Volume/Å^3	1193.1(2)
Z	2
ρ_{calc}g/cm^3	1.262
μ/mm^{-1}	0.142
F(000)	480.0
Crystal size/mm^3	0.525 × 0.492 × 0.254
2Θ range for data collection/°	4.522 to 60.2
Index ranges	-12 ≤ h ≤ 12, -13 ≤ k ≤ 13, -21 ≤ l ≤ 22
Reflections collected	18204
Independent reflections	6965 [R_{int} = 0.0616, R_{sigma} = 0.0728]
Data/restraints/ parameters	6965/0/302
Goodness-of-fit on F^2	1.067
Final R indexes [I>=2σ (I)]	R_1 = 0.0788, wR_2 = 0.1942
Final R indexes [all data]	R_1 = 0.0920, wR_2 = 0.2050
Largest diff. peak/hole / e Å^{-3}	0.87/-0.42

$CrCl_3(THF)(Ph(PPh_2)C=NPh$ (4.1)	
Empirical formula	$C_{29}H_{28}Cl_3CrNOP$
Formula weight	595.84
Temperature/K	120
Crystal system	orthorhombic
Space group	$P2_12_12_1$
a/Å	10.71436(16)
b/Å	16.0811(3)
c/Å	16.2406(3)
α/°	90
β/°	90
γ/°	90
Volume/$Å^3$	2798.22(8)
Z	4
$\rho_{calc}mg/mm^3$	1.414
m/mm^{-1}	0.776
F(000)	1228.0
Crystal size/mm^3	0.22 × 0.17 × 0.07
2Θ range for data collection	5.066 to 64.45°
Index ranges	-16 ≤ h ≤ 15, -24 ≤ k ≤ 23, -24 ≤ l ≤ 24
Reflections collected	36512
Independent reflections	9143[R(int) = 0.0366]
Data/restraints/ parameters	9143/1/333
Goodness-of-fit on F^2	1.069
Final R indexes [I>=2σ (I)]	R_1 = 0.0337, wR_2 = 0.0786
Final R indexes [all data]	R_1 = 0.0390, wR_2 = 0.0828
Largest diff. peak/hole / e $Å^{-3}$	0.48/-0.38

$CrCl_3(THF)(Ph(PPh_2)C=N(2\text{-}MeC_6H_4)$ (4.2)	
Empirical formula	$C_{31}H_{32}Cl_5CrNOP$
Formula weight	694.79
Temperature/K	120
Crystal system	monoclinic
Space group	$P2_1/c$
a/Å	16.2819(6)
b/Å	9.5738(4)
c/Å	20.9685(9)
α/°	90
β/°	103.098(11)
γ/°	90
Volume/$Å^3$	3183.5(2)
Z	4
$\rho_{calc}mg/mm^3$	1.450
m/mm^{-1}	0.855
F(000)	1428.0
Crystal size/mm^3	0.2 × 0.04 × 0.01
2Θ range for data collection	3.988 to 55°
Index ranges	-21 ≤ h ≤ 21, -12 ≤ k ≤ 12, -27 ≤ l ≤ 27
Reflections collected	33755
Independent reflections	7322[R(int) = 0.0716]
Data/restraints/ parameters	7322/3/379
Goodness-of-fit on F^2	0.907
Final R indexes [I>=2σ (I)]	R_1 = 0.0360, wR_2 = 0.0759
Final R indexes [all data]	R_1 = 0.0651, wR_2 = 0.0837
Largest diff. peak/hole / e $Å^{-3}$	0.49/-0.37

$Cr(CO)_4Ph(P^iPr_2)C=N(2,6\text{-}^iPr_2C_6H_3)$ (4.7)	
Empirical formula	$C_{29}H_{36}CrNO_4P$
Formula weight	545.56
Temperature/K	120
Crystal system	monoclinic
Space group	$P2_1/n$
a/Å	11.79138(14)
b/Å	14.69577(18)
c/Å	16.3394(2)
α/°	90
β/°	94.4771(11)
γ/°	90
Volume/Å^3	2822.70(6)
Z	4
ρ_{calc}g/cm^3	1.284
μ/mm^{-1}	0.495
F(000)	1152.0
Crystal size/mm^3	0.6323 × 0.4741 × 0.3061
2Θ range for data collection/°	3.732 to 64.944
Index ranges	-17 ≤ h ≤ 16, -22 ≤ k ≤ 21, -24 ≤ l ≤ 23
Reflections collected	53488
Independent reflections	9401 [R_{int} = 0.0318, R_{sigma} = 0.0209]
Data/restraints/ parameters	9401/0/341
Goodness-of-fit on F^2	1.032
Final R indexes [I>=2σ (I)]	R_1 = 0.0310, wR_2 = 0.0815
Final R indexes [all data]	R_1 = 0.0367, wR_2 = 0.0853
Largest diff. peak/hole / e Å^{-3}	0.45/-0.35

$Cr(CO)_5Ph(P^iPr_2)C=N(2,6\text{-}^iPr_2C_6H_3)$ (4.8)	
Empirical formula	$C_{30}H_{36}CrNO_5P$
Formula weight	573.57
Temperature/K	120
Crystal system	monoclinic
Space group	$P2_1/n$
a/Å	10.12630(15)
b/Å	23.3526(4)
c/Å	12.62634(19)
α/°	90
β/°	98.4258(14)
γ/°	90
Volume/Å^3	2953.58(8)
Z	4
ρ_{calc}g/cm^3	1.290
μ/mm^{-1}	0.479
F(000)	1208.0
Crystal size/mm^3	0.642 × 0.4515 × 0.2662
2Θ range for data collection/°	4.424 to 64.696
Index ranges	-14 ≤ h ≤ 14, -34 ≤ k ≤ 35, -18 ≤ l ≤ 17
Reflections collected	46323
Independent reflections	9651 [R_{int} = 0.0348, R_{sigma} = 0.0212]
Data/restraints/ parameters	9651/0/359
Goodness-of-fit on F^2	1.070
Final R indexes [I>=2σ (I)]	R_1 = 0.0335, wR_2 = 0.0878
Final R indexes [all data]	R_1 = 0.0372, wR_2 = 0.0901
Largest diff. peak/hole / e Å^{-3}	0.53/-0.44

$Cr(CO)_4Ph(P^iPr_2)C=N(2,6\text{-}Me_2C_6H_3)$ (4.9)	
Empirical formula	$C_{25}H_{28}CrNO_4P$
Formula weight	489.45
Temperature/K	120
Crystal system	orthorhombic
Space group	$P2_12_12_1$
a/Å	10.0194(8)
b/Å	14.8755(12)
c/Å	33.308(2)
α/°	90
β/°	90
γ/°	90
Volume/Å^3	4964.3(7)
Z	8
ρ_{calc}g/cm^3	1.310
μ/mm^{-1}	0.555
F(000)	2048.0
Crystal size/mm^3	0.22 × 0.2 × 0.03
2Θ range for data collection/°	3.672 to 50
Index ranges	-11 ≤ h ≤ 11, -17 ≤ k ≤ 17, -39 ≤ l ≤ 39
Reflections collected	41354
Independent reflections	8695 [R_{int} = 0.0876, R_{sigma} = 0.0701]
Data/restraints/ parameters	8695/6/573
Goodness-of-fit on F^2	1.017
Final R indexes [I>=2σ (I)]	R_1 = 0.0525, wR_2 = 0.1132
Final R indexes [all data]	R_1 = 0.0788, wR_2 = 0.1269
Largest diff. peak/hole / e Å^{-3}	0.66/-0.39

$Cr(CO)_5Ph(P^iPr_2)C=N(2,6\text{-}Me_2C_6H_3)$ (4.10)	
Empirical formula	$C_{26}H_{28}CrNO_5P$
Formula weight	517.46
Temperature/K	120
Crystal system	monoclinic
Space group	$P2_1/c$
a/Å	8.49510(14)
b/Å	15.4117(3)
c/Å	19.9673(4)
α/°	90
β/°	99.7804(17)
γ/°	90
Volume/Å^3	2576.20(8)
Z	4
ρ_{calc}g/cm^3	1.334
μ/mm^{-1}	0.542
F(000)	1080.0
Crystal size/mm^3	0.4286 × 0.2752 × 0.2119
2Θ range for data collection/°	4.14 to 64.674
Index ranges	-12 ≤ h ≤ 12, -21 ≤ k ≤ 21, -29 ≤ l ≤ 29
Reflections collected	48933
Independent reflections	8600 [R_{int} = 0.0427, R_{sigma} = 0.0260]
Data/restraints/ parameters	8600/0/319
Goodness-of-fit on F^2	1.044
Final R indexes [I>=2σ (I)]	R_1 = 0.0321, wR_2 = 0.0819
Final R indexes [all data]	R_1 = 0.0394, wR_2 = 0.0863
Largest diff. peak/hole / e Å^{-3}	0.41/-0.45

7.6 IR Deconvolution Tables

$Cr(CO)_4(PNC)$ (2.6)			
Model	Gauss		
Equation	y=y0 + (A/(w*sqrt(PI/2)))*exp(-2*((x-xc)/w)^2)		
Reduced Chi-Sqr	0.39806		
Adj. R-Square	0.99735		
		Value	**Standard Error**
Peak1(B)	**y0**	99.75807	0.04251
Peak1(B)	**xc**	2006.47427	0.04511
Peak1(B)	**w**	5.97002	0.09244
Peak1(B)	**A**	-133.36109	1.8712
Peak1(B)	**sigma**	2.98501	
Peak1(B)	**FWHM**	7.02916	
Peak1(B)	**Height**	-17.82352	
Peak2(B)	**y0**	99.75807	0.04251
Peak2(B)	**xc**	1899.17463	0.77944
Peak2(B)	**w**	17.95517	0.59478
Peak2(B)	**A**	-466.87494	76.82773
Peak2(B)	**sigma**	8.97758	
Peak2(B)	**FWHM**	21.14059	
Peak2(B)	**Height**	-20.7468	
Peak3(B)	**y0**	99.75807	0.04251
Peak3(B)	**xc**	1882.92974	0.86632
Peak3(B)	**w**	22.03086	0.78887
Peak3(B)	**A**	-937.84466	77.92445
Peak3(B)	**sigma**	11.01543	
Peak3(B)	**FWHM**	25.93936	
Peak3(B)	**Height**	-33.96562	
Peak4(B)	**y0**	99.75807	0.04251
Peak4(B)	**xc**	1840.23208	0.079
Peak4(B)	**w**	21.59051	0.17626
Peak4(B)	**A**	-645.13374	4.90622
Peak4(B)	**sigma**	10.79526	
Peak4(B)	**FWHM**	25.42088	
Peak4(B)	**Height**	-23.84113	

$Mo(CO)_4(PNN)$ (2.7)			
Model	Gauss		
Equation	y=y0 + (A/(w*sqrt(PI/2)))*exp(-2*((x-xc)/w)^2)		
Reduced Chi-Sqr	2.49616		
Adj. R-Square	0.99557		
		Value	**Standard Error**
Peak1(B)	**y0**	103.14396	0.09466
Peak1(B)	**xc**	2017.92723	0.05666
Peak1(B)	**w**	6.3283	0.11561
Peak1(B)	**A**	-289.18407	4.72078
Peak1(B)	**sigma**	3.16415	
Peak1(B)	**FWHM**	7.451	
Peak1(B)	**Height**	-36.46093	
Peak2(B)	**y0**	103.14396	0.09466
Peak2(B)	**xc**	1908.55965	0.0633
Peak2(B)	**w**	21.12604	0.12661
Peak2(B)	**A**	-1670.103	8.46926
Peak2(B)	**sigma**	10.56302	
Peak2(B)	**FWHM**	24.87401	
Peak2(B)	**Height**	-63.07617	
Peak3(B)	**y0**	103.14396	0.09466
Peak3(B)	**xc**	1889.15707	0.0823
Peak3(B)	**w**	20.3073	0.17588
Peak3(B)	**A**	-1327.1013	10.18364
Peak3(B)	**sigma**	10.15365	
Peak3(B)	**FWHM**	23.91002	
Peak3(B)	**Height**	-52.14252	
Peak4(B)	**y0**	103.14396	0.09466
Peak4(B)	**xc**	1846.54094	0.09085
Peak4(B)	**w**	25.1837	0.20057
Peak4(B)	**A**	-1549.69217	11.24235
Peak4(B)	**sigma**	12.59185	
Peak4(B)	**FWHM**	29.65154	
Peak4(B)	**Height**	-49.09825	

$Mo(CO)_4(PNO)$ (2.8)			
Model	Gauss		
Equation	y=y0 + (A/(w*sqrt(PI/2)))*exp(-2*((x-xc)/w)^2))		
Reduced Chi-Sqr	3.48867		
Adj. R-Square	0.99674		
		Value	**Standard Error**
Peak1(B)	**y0**	100.66239	0.12562
Peak1(B)	**xc**	2019.08477	0.04137
Peak1(B)	**w**	6.5032	0.08495
Peak1(B)	**A**	-489.42188	5.81371
Peak1(B)	**sigma**	3.2516	
Peak1(B)	**FWHM**	7.65693	
Peak1(B)	**Height**	-60.04769	
Peak2(B)	**y0**	100.66239	0.12562
Peak2(B)	**xc**	1908.86758	0.58068
Peak2(B)	**w**	23.15147	0.5493
Peak2(B)	**A**	-2458.46738	127.29289
Peak2(B)	**sigma**	11.57574	
Peak2(B)	**FWHM**	27.25877	
Peak2(B)	**Height**	-84.7278	
Peak3(B)	**y0**	100.66239	0.12562
Peak3(B)	**xc**	1888.07312	0.59583
Peak3(B)	**w**	20.34864	0.65362
Peak3(B)	**A**	-1594.74843	130.3245
Peak3(B)	**sigma**	10.17432	
Peak3(B)	**FWHM**	23.95869	
Peak3(B)	**Height**	-62.53121	
Peak4(B)	**y0**	100.66239	0.12562
Peak4(B)	**xc**	1849.23486	0.09439
Peak4(B)	**w**	25.86015	0.20834
Peak4(B)	**A**	-2424.04996	18.38712
Peak1(B)	**y0**	100.66239	0.12562
Peak1(B)	**xc**	2019.08477	0.04137
Peak1(B)	**w**	6.5032	0.08495

$Mo(CO)_4(PNC)$ (2.9)			
Model	Gauss		
Equation	y=y0 + (A/(w*sqrt(PI/2)))*exp(-2*((x-xc)/w)^2)		
Reduced Chi-Sqr	3.97026		
Adj. R-Square	0.99559		
		Value	**Standard Error**
Peak1(B)	**y0**	97.37958	0.08362
Peak1(B)	**xc**	2017.1887	0.05055
Peak1(B)	**w**	6.93443	0.10223
Peak1(B)	**A**	-470.4802	4.96585
Peak1(B)	**sigma**	3.46721	
Peak1(B)	**FWHM**	8.16467	
Peak1(B)	**Height**	-54.13407	
Peak2(B)	**y0**	97.37958	0.08362
Peak2(B)	**xc**	1908.3159	0.08384
Peak2(B)	**w**	21.82788	0.16682
Peak2(B)	**A**	-1952.229	9.72163
Peak2(B)	**sigma**	10.91394	
Peak2(B)	**FWHM**	25.70037	
Peak2(B)	**Height**	-71.36071	
Peak3(B)	**y0**	97.37958	0.08362
Peak3(B)	**xc**	1887.5165	0.09075
Peak3(B)	**w**	22.49846	0.18607
Peak3(B)	**A**	-1909.369	9.83487
Peak3(B)	**sigma**	11.24923	
Peak3(B)	**FWHM**	26.48991	
Peak3(B)	**Height**	-67.71379	
Peak4(B)	**y0**	97.37958	0.08362
Peak4(B)	**xc**	1844.4176	0.08493
Peak4(B)	**w**	26.81378	0.13351
Peak4(B)	**A**	-2305.999	10.56689
Peak4(B)	**sigma**	13.40689	
Peak1(B)	**y0**	97.37958	0.08362
Peak1(B)	**xc**	2017.1887	0.05055

7.7 Example % V_{bur} Calculation

7.7.1 $Ph(PPh_2)C{=}N(2,6\text{-}Me_2C_6H_3)$ (3.8)

Samb*V*ca @ MoLNaC
Results page

```
 ---------------------------------------------------
 |                                 |
 |          S A M B V C A          |
 |                                 |
 |       Buried Volume in Salerno  |
 |                                 |
 | http://www.molnac.unisa.it/OM-tools/SambVca  |
 |                                 |
 |  L. Cavallo et al. email: lcavallo@unisa.it  |
 |                                 |
 ---------------------------------------------------
```

Molecule from input :

Molecule from input :

Molecule Name

Number of atoms : 53
Atom that is coordinated : 1
Atoms that define the axis : 3
ID of these atoms : 2 13 25

Radius of sphere (Angs) : 3.500
Distance from sphere (Angs) : 2.100
Mesh step (Angs) : 0.050
H atoms omitted in the V_bur calculation

Cartesian coordinates from input :

P	0.00000	0.00000	0.00000
C	1.88320	0.13500	0.13100
C	2.53340	0.31270	-1.10760
C	2.65420	0.10720	1.30590
C	3.92590	0.43600	-1.17410
H	1.94800	0.35900	-2.02250
C	4.04960	0.24550	1.23620
H	2.15920	-0.00880	2.26140
C	4.68970	0.40430	0.00140
H	4.40990	0.56600	-2.13770
H	4.63290	0.22800	2.15260
H	5.76970	0.50890	-0.04630
C	-0.24690	-1.85400	-0.36140
C	-1.39330	-2.24190	-1.07600
C	0.67160	-2.83470	0.04830
C	-1.62590	-3.59420	-1.36400
H	-2.10170	-1.49000	-1.41060
C	0.44190	-4.18550	-0.24660
H	1.56800	-2.54760	0.58870
C	-0.70870	-4.56870	-0.94980
H	-2.51650	-3.88170	-1.91520
H	1.16050	-4.93510	0.07210

H	-0.88490	-5.61570	-1.17770
N	0.00000	0.00000	2.81930
C	-0.75210	0.00000	1.77800
C	-2.24850	-0.03710	1.76250
C	-2.96000	-0.93160	2.58810
H	-2.42150	-1.60850	3.24030
C	-4.35800	-0.96090	2.56530
H	-4.89000	-1.66070	3.20240
C	-5.06990	-0.09290	1.72560
H	-6.15530	-0.11440	1.71330
C	-4.37350	0.79950	0.90020
H	-4.91680	1.47580	0.24730
C	-2.97370	0.82060	0.90930
H	-2.44090	1.51020	0.26360
C	-0.40740	0.00000	4.18760
C	-0.17790	-1.17410	4.94570
C	-0.48230	-1.15760	6.31490
H	-0.32060	-2.05940	6.89970
C	-0.97390	-0.00200	6.93270
H	-1.19790	-0.00340	7.99510
C	-1.15820	1.15940	6.17610
H	-1.51990	2.06570	6.65450
C	-0.87840	1.18650	4.79990
C	0.38270	-2.41460	4.28850
H	1.33710	-2.20080	3.79170
H	0.54820	-3.20370	5.02900
H	-0.28550	-2.81510	3.51450
C	-1.04960	2.46360	4.00730
H	-1.88310	2.39900	3.29700
H	-0.14850	2.69770	3.42690
H	-1.25000	3.30560	4.67740

Atoms and radius in the parameter file

H	1.29
C2	1.99
C3	1.99
C	1.99
N2	1.81
N3	1.81
N	1.81
O	1.78
F	1.72
Si	2.45
P	2.11
S	2.10
Cl	2.05
As	2.17
Br	2.16
I	2.31

Coordinates scaled to put the metal at the origin

P	0.74985	-1.45781	1.31245
C	2.63305	-1.32281	1.44345
C	3.28325	-1.14511	0.20485
C	3.40405	-1.35061	2.61835
C	4.67575	-1.02181	0.13835
H	2.69785	-1.09881	-0.71005
C	4.79945	-1.21231	2.54865
H	2.90905	-1.46661	3.57385
C	5.43955	-1.05351	1.31385
H	5.15975	-0.89181	-0.82525
H	5.38275	-1.22981	3.46505
H	6.51955	-0.94891	1.26615
C	0.50295	-3.31181	0.95105
C	-0.64345	-3.69971	0.23645
C	1.42145	-4.29251	1.36075
C	-0.87605	-5.05201	-0.05155
H	-1.35185	-2.94781	-0.09815
C	1.19175	-5.64331	1.06585
H	2.31785	-4.00541	1.90115
C	0.04115	-6.02651	0.36265
H	-1.76665	-5.33951	-0.60275
H	1.91035	-6.39291	1.38455
H	-0.13505	-7.07351	0.13475
N	0.74985	-1.45781	4.13175
C	-0.00225	-1.45781	3.09045
C	-1.49865	-1.49491	3.07495
C	-2.21015	-2.38941	3.90055
H	-1.67165	-3.06631	4.55275
C	-3.60815	-2.41871	3.87775
H	-4.14015	-3.11851	4.51485
C	-4.32005	-1.55071	3.03805
H	-5.40545	-1.57221	3.02575
C	-3.62365	-0.65831	2.21265
H	-4.16695	0.01799	1.55975
C	-2.22385	-0.63721	2.22175
H	-1.69105	0.05239	1.57605
C	0.34245	-1.45781	5.50005
C	0.57195	-2.63191	6.25815
C	0.26755	-2.61541	7.62735
H	0.42925	-3.51721	8.21215
C	-0.22405	-1.45981	8.24515
H	-0.44805	-1.46121	9.30755
C	-0.40835	-0.29841	7.48855
H	-0.77005	0.60789	7.96695
C	-0.12855	-0.27131	6.11235
C	1.13255	-3.87241	5.60095
H	2.08695	-3.65861	5.10415
H	1.29805	-4.66151	6.34145
H	0.46435	-4.27291	4.82695
C	-0.29975	1.00579	5.31975
H	-1.13325	0.94119	4.60945
H	0.60135	1.23989	4.73935
H	-0.50015	1.84779	5.98985
XX	0.00000	0.00000	0.00000

Results : Volumes in Angs^3

Results : Volumes in Angs^3

N of voxels examined : 1436277
Volume of voxel : 0.125E-03

V Free	V Buried	V Total	V Exact
113.844	65.691	179.535	179.594

%V_Free	%V_Bur	% Tot/Ex
63.411	36.589	99.967

The %V_Bur of your molecule is: 36.6

7.8 List of Seminars Attended

Green chemistry and the biorefinery
Prof. James Clark, University of York
19th October 2011

Novel lightweight hydrogen storage materials
Prof. Bill David, RAL
2nd November 2011

Harvesting solar energy in photo-electrochemical cells
Prof. Leone Spiccia , Monash University
9th November 2011

Catalysis on the edge
Presented by Prof. Robert Tooze , Sasol
23rd November 2011

360 degree chemistry – Using tubes in synthesis
Dr. Ian Baxendale, University of Cambridge
29th November 2011

Phosphine-borane stabilised carbanions – Bulky ligands of the future?
Dr. Keith Izod, Newcastle University
6th December 2011

Metal-organo cooperative catalysis: Asymmetric hydrogenation with achiral metal catalysts
Prof. Jianliang Xiao, University of Liverpool
7th December 2011

Catalysts made of Earth-abundant elements for making C-C and H-H bonds
Prof. Xile Hu, Ecole Polytechnique Federal de Lausanne
17th January 2012

New Copper Catalyzed Reactions
Dr. Matthew Gaunt, University of Cambridge
1st February 2012

Chiral metal compounds in catalysis and medicine
Prof. Peter Scott, University of Warwick
28th February 2012

Catalysts by Design. A Case Study of Arylamine Synthesis
Prof. John F. Hartwig, University of California, Berkeley.
14th May 2012

Selective Functionalization of Aryl and Alkyl C-H Bonds
Prof. John F. Hartwig, University of California, Berkeley.
15th May 2012

Making Sense of Copper-Catalyzed Coupling Reactions
Prof. John F. Hartwig, University of California, Berkeley
16th May 2012

Metal catalysts for the activation of renewable resources to make polymers
Dr. Charlotte Williams, Imperial College London
7th November 2012

Surfaces for Regenerative Medicine
Prof. Robert Short, University of South Australia
10th January 2013

Organometallic chemistry in the solid–state
Prof. Andrew Weller, University of Oxford
16th January 2013

Chemistry on a background - new orders in simple solids
Prof. J Paul Attfield, University of Edinburgh
23rd January 2013

Sustainable Synthesis: Developing C-N and C-O Bond Forming Reactions
Dr Leoni Pennington, University of California Santa Barbara
12th February 2013

The physical chemistry of heterogeneous catalysis
Prof. Ken Waugh, University of Manchester
5th March 2013

Self-assembly and host-guest chemistry of polyhedral coordination cages
Prof. Michael Ward, University of Sheffield
1st May 2013

Preventing and Curing Infectious Disease: Carbohydrate Vaccines and Continuous Flow Synthesis
Prof. Dr. Peter H. Seeberger, Max Planck Institute of Colloids and Interfaces
14th May 2013

Borenium Cations: Versatile Reagents for Borylation of π-nucleophiles
Dr Mike Ingleson, University of Manchester
29th October 2013

Making Polymers Swim
Prof Tony Ryan, University of Sheffield
6th November 2013

Designing Heterogeneous Catalysts for Sustainable Chemistry
Prof Karen Wilson, Aston University
12th November 2013

Ionic Liquids in Whole Cell Biocatalysis
Prof Gill Stephens, University of Nottingham
4th December 2013

Redox and Functionalisation Reactions of the Uranyl Ion; in Pursuit of Transition Metal Oxo Chemistry
Prof Polly Arnold, University of Edinburgh
19th February 2014

Switchable Solvents
Prof Philip Jessop, Queen's University
12th March 2014

From Triple Bonds to Reactive Intermediates
Prof Kit Cummins, MIT
14th April 2014

Activation of Alkynes with $B(C_6F_5)_3$: Applications in Organic Synthesis
Dr Rebecca Melen, University of Toronto
24th April 2014

Controlled Polymer Synthesis with Olefin Metathesis
Prof Bob Grubbs, Caltech
16th May 2014

Design and Synthesis of Smart Polymer Materials for Applications in Bionanotechnology and Biomedicine
Prof Bridgitte Voit, TU Dresen
29th May 2014

The Physical Chemistry of Heterogeneous Catalysis: The Oxidation of Ethylene to Ethylene Oxide
Prof Ken Waugh
22nd July 2014

Organo-Lanthanide Molecular Magnets
Dr Richard Layfield, University of Manchester
2nd September 2014

Ionic Mo- W- and Ru- Based Olefin Metathesis Catalysts: Access to C-C Coupling Reactions Under Biphasic (Supported) Conditions
Prof Michael Buchmeiser, University of Stuttgart
6th October 2014

Interstitial Nitrides: Reservoirs of Activated Nitrogen?
Dr Justin Hargreaves, University of Glasgow
25th November 2014

Development of *in situ* Methods to Study Gas and Liquid Phase Heterogeneously Catalysed Reactions
Dr Chris Hardacre, Queen's University Belfast
28th January 2015

π-Conjugated Organophosphorus Oligomers for Optoelectronic Applications
Prof Muriel Hissler, Institute des Sciences Chimique de Rennes
18th February 2015

Ruthenium and Iridium Catalysts Equipped with a Bifunctional Phosphinesulfonate Ligand: Applications in Catalytic Reactions Involving Hydrogen Transfer
Christian Bruneau, Université de Rennes1
24th February 2015